Sustainable Approaches towards C-X (-N, -C, -O) Bond Formation Reactions in Organic Synthesis

By

SUDIP SAU

CHEM11201704027

National Institute of Science Education and Research Bhubaneswar, Odisha –752050

A thesis submitted to the
Board of Studies in Chemical Sciences
In partial fulfillment of requirements
for the Degree of

DOCTOR OF PHILOSOPHY

of

HOMI BHABHA NATIONAL INSTITUTE

June, 2022

Homi Bhabha National Institute[1]

Recommendations of the Viva Voce Committee

As members of the Viva Voce Committee, we certify that we have read the dissertation prepared by **Sudip Sau** entitled **"Sustainable Approaches towards C-X (-N, -C, -O) Bond Formation Reactions in Organic Synthesis"** and recommend that it may be accepted as fulfilling the thesis requirement for the award of Degree of Doctor of Philosophy.

Chairman – Prof. A. Srinivasan		**Date:** 14.11.'22
Guide/Convener- Dr. Prasenjit Mal		**Date:** 14/11/22
Examiner- Prof. Subhendu Sekhar Bag		**Date:** 14/11/2022
Member 1- Dr. Sudip Barman		**Date:** 14/11/22
Member 2- Dr. Subhadip Ghosh		**Date:** 14/11/22
Member 3- Dr. Shantanu Pal		**Date:** 14/11/22

Final approval and acceptance of this thesis is contingent upon the candidate's submission of the final copies of the thesis to HBNI.

I/We hereby certify that I/we have read this thesis prepared under my/our direction and recommend that it may be accepted as fulfilling the thesis requirement.

Date: 14.11.2022

Place: NISER, Bhubaneswar

(Dr. Prasenjit Mal)

Guide

Dr. Prasenjit Mal
Associate Professor
School of Chemical Sciences
National Institute of Science Education & Research
Jatni, Bhubaneswar-752050, Odisha, India

[1] This page is to be included only for final submission after successful completion of viva voce.

STATEMENT BY AUTHOR

This dissertation has been submitted in partial fulfillment of requirements for an advanced degree at Homi Bhabha National Institute (HBNI) and is deposited in the Library to be made available to borrowers under the rules of the HBNI.

Brief quotations from this dissertation are allowable without special permission, provided that accurate acknowledgment of the source is made. Requests for permission for extended quotation from or reproduction of this manuscript in whole or in part may be granted by the Competent Authority of HBNI when in his or her judgment the proposed use of the material is in the interests of scholarship. In all other instances, however, permission must be obtained from the author.

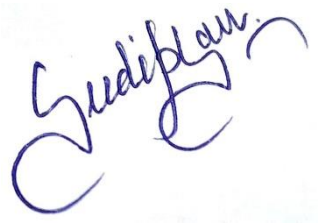

Sudip Sau

DECLARATION

I, hereby declare that the investigation presented in the thesis has been carried out by me. The work is original and has not been submitted earlier as a whole or in part for a degree / diploma at this or any other Institution / University.

Sudip Sau

List of Publications arising from the thesis: (# Pertaining to The Thesis)

Publications in Refereed Journal:

1. #**S. Sau,** A. Bose and P. Mal, *Asian J. Org. Chem.*, **2019,** *8*, 1854-1857.
2. #**S. Sau** and P. Mal, *Chem. Commun.*, **2021,** *57*, 9228-9231.
3. #**S. Sau** and P. Mal, *Eur. J. Org. Chem.*, **2022**, e202200425.
4. #**S. Sau** and P. Mal, *J. Org. Chem.*, **2022**, *87*, 14565-14579.
5. **S. Sau**,† M. Pramanik,† A. Bal and P. Mal, *Chem. Rec.*, **2022,** *22*, e202100208. (†Equally contributed)
6. A. Bose, S. Maiti, **S. Sau** and P. Mal, *Chem. Commun.*, **2019**, *55*, 2066-2069.
7. M. Pramanik, A. Mathuri, **S. Sau**, M. Das and P. Mal, *Org. Lett.*, **2021**, *23*, 8088-8092.
8. A. Bose, **S. Sau** and P. Mal, *Eur. J. Org. Chem.*, **2019**, 4105-4109.
9. M. Das, D. Maity, T. K. Acharya, **S. Sau**, C. Giri, C. Goswami and P. Mal, *Dalton Trans.*, **2021**, *50*, 3027-3036.
10. A. Mandal, P. Swain, B. Nath, **S. Sau** and P. Mal, *CrystEngComm*, **2019**, *21*, 981-989.
11. A. Mandal, A. Choudhury, **S. Sau**, P. K. Iyer and P. Mal, *J. Phys. Chem. C*, **2020**, *124*, 6544-6553.

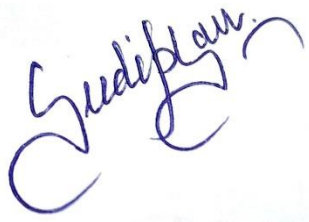

Sudip Sau

CONFERENCE AND PRESENTATIONS

1. **Poster Presentation:** International Conference on Chemistry for Human Development (ICCHD-2020); Kolkata, India on (9-11)th January, 2020. Title: "Intramolecular C(sp^3)-H Imination towards Benzimidazoles using Iodine Reagents".
2. **Poster Presentation:** International Virtual Conference on "The Present and Future of Excellence in Organic Synthesis" (PFEOS-2021); India on (7-8)th January, 2021. Title: "Metal-free Regioselective C_5 or C_7 Mono-nitration of Indolines using *tert*-Butyl Nitrite".
3. **Poster Presentation (Virtual):** 27th CRSI-National Symposium Chemistry, Kolkata, India on (26-29)th September, 2021. Title: "*tert*-Butyl Nitrite mediated Nitrative Cyclization of Aryl Alkynoates: An Access to 3-Nitro Coumarins".
4. **Mini Oral Presentation (Virtual):** Emerging Infectious Diseases & Therapeutc Strategies (MedChem 2021); IIT Madras, India on December 1-3, 2021. Title: Nitrative and chlorinative cyclization of aryl alkynoates: "Access to 3-nitro coumarins and 3-chloro coumarins".
5. **Oral Presentation (Virtual):** National Conference on Recent Advances in Heterocyclic Chemistry (RAHC-2022); Ravenshaw University, India on (15-16)th January, 2022. Title: "Sustainable strategies for nitrative and chlorinative cyclization of aryl alkynoates: An access to 3-nitro coumarins and 3-chloro coumarins".

Sudip Sau

Dedicated
To
My Grandparents,
Parents
&
Sister

ACKNOWLEDGEMENTS

I owe an unfathomable sense of gratitude to everybody who supports me throughout my work. I am sincerely thankful for their valuable guidance and constructive suggestions during the work. I am grateful to them for expressing their enlightening views and innovative idea to stabilize the work.

First of all, from the core of my heart, I would like to convey my earnest gratitude to my mentor Dr. Prasenjit Mal for his constant support, valuable guidance, and prompt suggestions throughout my research career. His judicious advice, scholarly presentation, meticulous inspection, and on-time activity have helped me to accomplish my research work to a great extent. I also want to express my gratitude to Prof. Alagar Srinivasan, Dr. Sudip Barman, Dr. Subhadip Ghosh, and Dr. Shantanu Pal (IIT Bhubaneswar), who stand for the doctoral committee.

My sincere thanks also go to Prof. Sudhakar Panda, Director, NISER, for providing nice institutional infrastructure and, of course, Department of Atomic Energy (DAE) India, for financial support. It is my great privilege to thank Dr. Sharanappa Nembenna (Chairperson of SCS), Dr. Himansu Sekhar Biswal (Former-Chairperson of SCS). I would also like to thank all other faculty members and staff profusely. I am also greatly obliged to Prof. Alagar Srinivasan, Dr. Prasenjit Mal, Dr. Nagendra K. Sharma, Dr. Moloy Sarkar, Dr. Chidambaram Gunanathan, Dr. Upakarasamy Lourderaj who taught me in the coursework during the Ph.D. program.

I express my warm thanks to my lab mates Dr. Debdeep Maity, Dr. Saikat Maiti, Dr. Anima Bose, Dr. Khokan Choudhuri, Dr. Toufique Alam, Dr. Ankita Bal, Dr. Milan Pramanik, Dr. Anupam Manna, Dr. Amarchand Parida, Dr. Arkalekha Mandal, Dr. Monojit Das, Shyamal Kanti Bera, Ashis Mathuri, Tarun Kumar Dinda, Buddhadev Pal, Rosalin Bhanja, Pravat Nayek, Sathi Sahoo,

Shraddha, Keshab, Prabhu, Sunil, Himangshu, Vrittik, Keshav, Abhishek, Chandan, uday, Soumyashree, Ankit, Supratim and Kushal for their constant encouragement, cheerful company and thoughtful discussions.

I thank all my NISER friends, especially Ranjit Mishra, Rajib Samanta, Shyam Kumar Banjare, Deepak Kumar Panda, Chinmay Kumar Jena, N. Preeyanka, Akshay Kumar Sahu for sharing frustration and happy moments.

I am also fortunate to have my bosom friends Liza Patra, Sambit Pradhan for being with me during this journey.

I wish to express my special admiration and love for my sister Ms. Sutapa Sau, who has always been a source of my strength, inspiration, and my achievements throughout my career endeavor.

I also like to convey sincere tribute to my grandparents (Late Jagannath Sau and Smt. Chabi Sau) for their unconditional love, affection and encouragement.

Last but not the least, from the bottom end of my heart, I would like to convey my deep sense of gratitude to my beloved parents (Mr. Dilip Sau and Mrs. Chhaya Sau) for bringing me into this world, for their constant support, unmatchable love, faith, affection, and encouragement all through the years, all the time, all the moment.

Above all, I thank the Almighty for showing me the right path always.

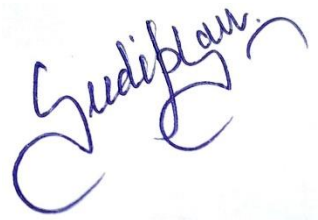

....*Sudip Sau*

CONTENTS

SUMMARY

Finding sustainable and step-economic strategies for the synthesis and functionalization of organic compounds has recently become an important topic of research in synthetic organic chemistry. To achieve environmentally benign methods, chemists have rendered unremitting efforts to replace toxic metal-based reagents and harsh reaction conditions with mild and metal-free reagents. In this regard, our major focus of this thesis is to introduce mild and sustainable protocols for C-X (-N, -C, -O) bond formation reactions towards the synthesis and functionalization of heterocycles. According to that, various strategies like utilization of the multitasking reagent *tert*-Butyl Nitrite (TBN) and implementation of visible-light photocatalysis were adopted. Regioselective C_5- or C_7-mono-niration of indolines was achieved by implementing 1.2 equiv *tert*-Butyl Nitrite (TBN) as a sole nitrating agent at 60 ^oC in acetonitrile within 6 h. In continuation, we explored a mild and convenient approach toward synthesis of 3-nitro coumarins, using 4.0 equiv of *tert*-Butyl Nitrite (TBN) at 120 ^oC in DMSO within a time-period of 36 h. Experimental results suggested that the reaction proceeded through a 5-exo-trig spirocyclization followed by ester migration. Next, we developed a protocol for C-H hydroxylation of quinoxalin-2(1*H*)-ones using 2.0 equiv of *tert*-Butyl Nitrite (TBN) as the sole reagent through *ipso*-substitution strategy. The reaction was accomplished in DMSO solvent, at 100 ^oC within 3 h and a library of quinoxalin-2,3-diones was synthesized. Control Experiment Suggested that water (from moisture) served as the oxygen source in the newly formed C_3-O bond. In addition, visible-light mediated regioselective oxygenation of quinoxalin-2(1*H*)-one was achieved with the use of 5 mol % of 9-mesityl-10-methylacridinium perchlorate as visible-light photocatalyst and O_2 has been utilized as a green oxidant.

LIST OF SCHEMES

LIST OF FIGURES

LIST OF TABLES

Page no

List of Abbreviations Used

Å	Angstrom
Ar	Aryl/Aromatic
Ac	Acetyl
br	Broad
Bn	Benzyl
BHT	Butylated hydroxy toluene
^{o}C	Degree Celcius
Calcd	Calculated
cm	Centimeter
d	Doublet, Days
1,2-DCB	1,2-Dihloro benzene
DCE	1,2-Dichloroethane
DCM	Dichloromethane
dd	Doublet of a Doublet
DMF	*N*,*N*-Dimethyl Formamide
DMSO	Dimethyl Sulfoxide
Equiv	Equivalent
ESI-TOF	Electrospray ionization time-of-flight
Et	Ethyl
EtOAC	Ethyl Acetate
EtOH	Ethyl Alcohol

g	Grams
h	Hours
HRMS	High-Resolution Mass Spectrometry
H_2O	Water
Hz	Hertz
IR	Infrared
$K_2S_2O_8$	Potassium persulfate
MeCN	Acetonitrile
mp	Melting point
Me	Methyl
Min	Minutes
mL	Milliliter
mmol	Millimole
mol	Mole
M	Molar
m	Multiplet
MS	Mass Spectra, Molecular Sieves
M/Z	Mass to charge ratio
nm	Nanometer
NMR	Nuclear Magnetic Resonance
[O]	Oxidation
O_2	Oxygen
OBn	Benzyloxy
OMe	Methoxy
Py	Pyridine
Ph	Phenyl
rt	Room Temperature
s	Singlet, Seconds
t	*Tert*
TBN	*tert*-Butyl nitrite
THF	Tetrahydrofuran

TLC	Thin Layer Chromatography
Ts	*p*-Toluenesulfonyl
TFA	Trifluoroacetic acid
XRD	X-ray diffraction
XRD	X-Ray Diffraction

CHAPTER 1

Introduction to *tert*-Butyl Nitrite and Visible-light Photocatalysis with their Applications

1.1 ABSTRACT

This chapter highlights the basic introduction to *tert*-Butyl Nitrite (TBN), its activity, and its synthetic utility. TBN-mediated applications such as nitro radical triggered reactions, nitrosation, oximation, diazotization, and miscellaneous are summarized. In the second part, a basic introduction to visible light photocatalysis and visible light-mediated oxygenation reactions has been discussed. Finally, the chapter is closed with a brief outline of the research focus of the current thesis.

1.2 INTRODUCTION

C-C and C-H bonds are the most common classes of bonds found in the skeletons of organic compounds. Along with this, C-hetero bonds like C-N and C-O bonds are also significantly important due to their abundance in numerous organic compounds prevalent in nature. In addition, they are synthetically important in the areas like pharmaceutics, agrochemical industry, material science, bacteriocides, insecticides, etc.

Our planet is continuously facing critical challenges due to contamination from distinctive perspectives like toxic and hazardous chemicals used in the chemical industries. Therefore, finding the sustainable and step-economic strategies for the synthesis and functionalization of organic

compounds is highly recommended to minimize global pollution. Transition metal-catalyzed C-N, C-C, and C-O bond formation reactions have become an important toolbox in organic synthesis. Catalysis.[1-6] But, in metal-catalyzed reactions, there are drawbacks, limitations, and challenges. Firstly, transition metal catalysts and ligands are expensive and tricky to prepare. Second, most of the transition metals are toxic. Therefore, the implementation of transition metal catalysts in reaction does not hold the sustainability of the reaction condition. In addition, it is challenging to remove trace amounts of metal catalysts from the reaction. Therefore, transition metal-catalyzed approaches are not compatible with pharmaceutical industries. Moreover, most importantly, many transition metals are air and moisture sensitive, and accordingly, they require an inert reaction environment. Parallelly, the requirement of co-catalyst and additives make the procedure strenuous. In this regard, synthetic chemists have rendered relentless efforts to replace toxic metal-based reagents and harsh reaction conditions with mild, sustainable, and convenient protocols by implementing mild and metal-free reagents. Therefore, herein we have showcased mild and sustainable protocols for C-N, C-C, and C-O bond formation reactions. The examples are classified into two main categories: i) *tert*-Butyl Nitrite and its applications in C-N, C-C, and C-O bond formation reactions ii) Visible-light photocatalysis and its application in oxygenation reactions.

1.3 *tert*-BUTYL NITRITE (TBN)

In the last two decades, tert-Butyl Nitrite (TBN) has been admired as a versatile reagent[7, 8] in organic synthesis. According to its distinct and unique structural features, it behaves differently depending upon the structure of reactants and reaction conditions.[7, 8] Parallelly, TBN is mild and metal-free, easily soluble in organic solvents, easy to handle, and inexpensive. In addition, no

acidic waste is generated during the reaction course with the involvement of TBN, only non-toxic *tert*-butanol is generated as a side product (Figure 1.1).[7, 8]

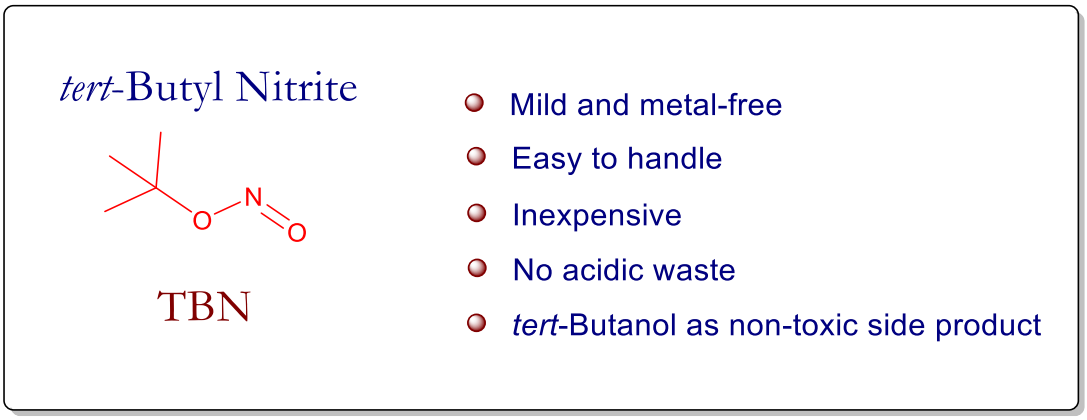

Figure 1.1. Structure of *tert*-Butyl Nitrite and its advantages.

1.3.1 RADICAL GENERATION FROM TBN

In presence of heat, due to thermolysis, TBN furnishes •NO and *t*-BuO• radicals. •NO radical in presence of aerial oxygen is converted into •NO_2 radical[7, 8] (Figure 1.2, path a). In another pathway, TBN can capture dioxygen directly and generate •NO_2 radical (Figure 1.2, path b). In another minor and secondary pathway (Figure 1.2, path c), TBN can react with water and acid present in the system and result in the formation of HNO_2. Next disproportionation of HNO_2 lead to the formation of •NO and •NO_2 radicals.[7] These radicals generated by TBN can trigger a wide array of reactions in organic synthesis. For its key advantages and as well as its inherent property towards radical generation, utilization of TBN in organic synthesis has become very popular.[7, 8]

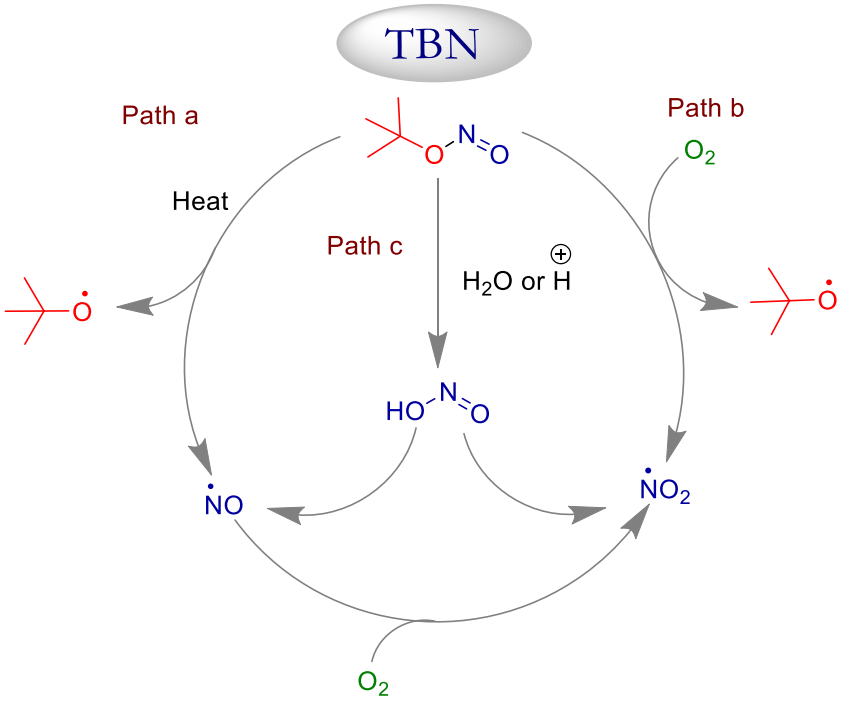

Figure 1.2. Radical generation from *tert*-Butyl Nitrite

1.3.2 TBN A "MULTITASKING REAGENT"

Radicals generated from TBN can be utilized in numerous chemical transformations like diazotization, nitrosation, oximation, etc (Figure 1.3).[7, 8] Parallelly, $^{\bullet}NO_2$ radical generated from TBN can successfully trigger nitration and different aerobic oxidation reactions under mild conditions. Therefore it has also gained popularity as an excellent nitrating agent. Apart from that TBN can be utilized as *N*-synthon in several reactions. Except for these examples, there are other miscellaneous applications of TBN, documented in the literatures. Therefore, for its extensive synthetic applications, it has been acknowledged as a multitasking reagent in organic synthesis.[8]

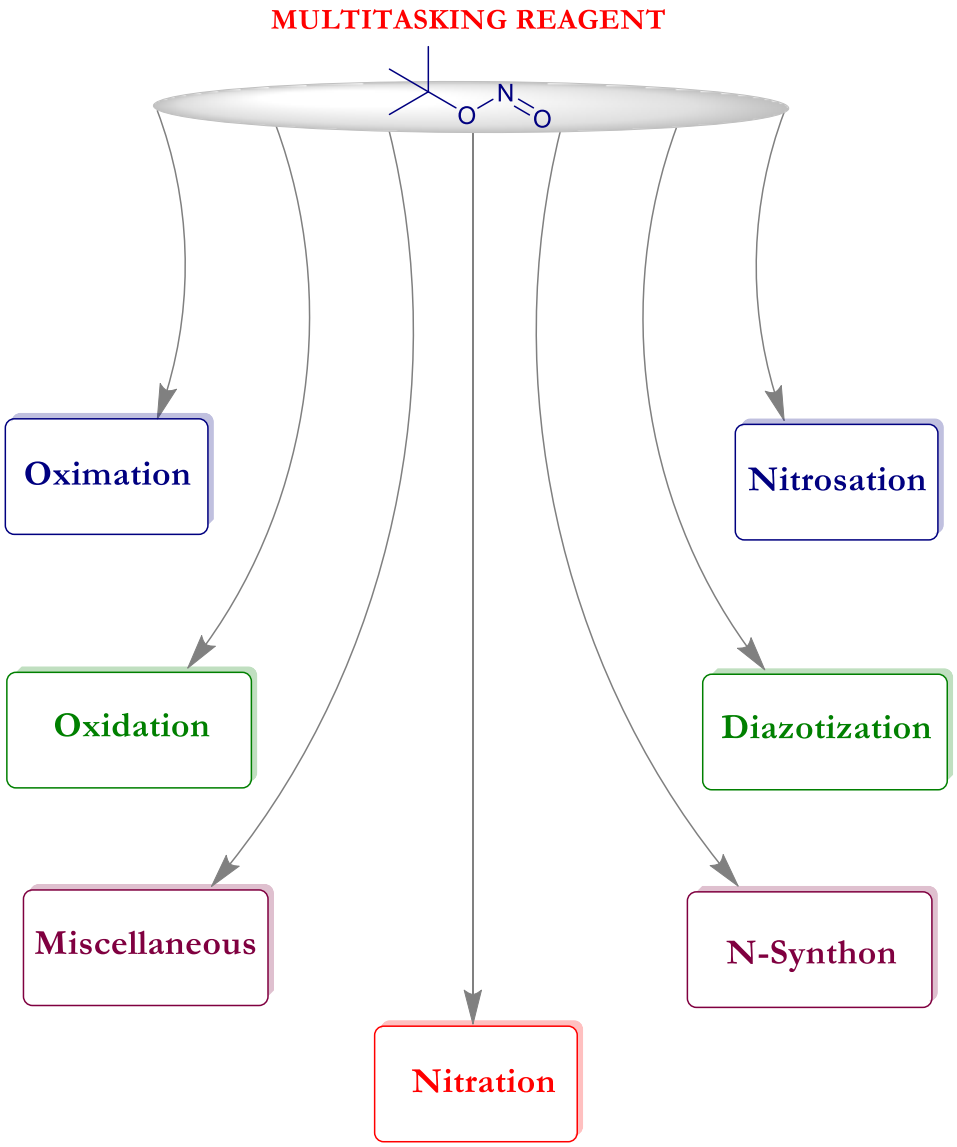

Figure 1.3. Different reactions mediated by TBN

1.3.3 IMPORTANCE OF NITRO COMPOUNDS & TBN MEDIATED NITRO RADICAL TRIGGERED REACTIONS

Nitro compounds are potential synthetic intermediate[9] in organic chemistry. In presence of suitable reaction conditions, nitro functionalities are easily convertible into their corresponding amine or diazo functionalities.[10, 11] From diazo compounds, different halo compounds can be synthesized

using Sandmeyer reaction. Parallelly, nitro compounds exhibit miscellaneous applications in the pharmaceutical industry.[12] For instance, nitro compounds such as metronidazole, and tinidazole are antibiotic and antiparasitic respectively. Flutamide and tolcapone are used for the treatment of prostate cancer and Parkinson's disease (Figure 1.4). Apart from these examples, there are miscellaneous examples of nitro-containing drugs.[12] So, the development of convenient and advantageous protocols for nitration reactions has always been an important topic in synthetic chemistry.

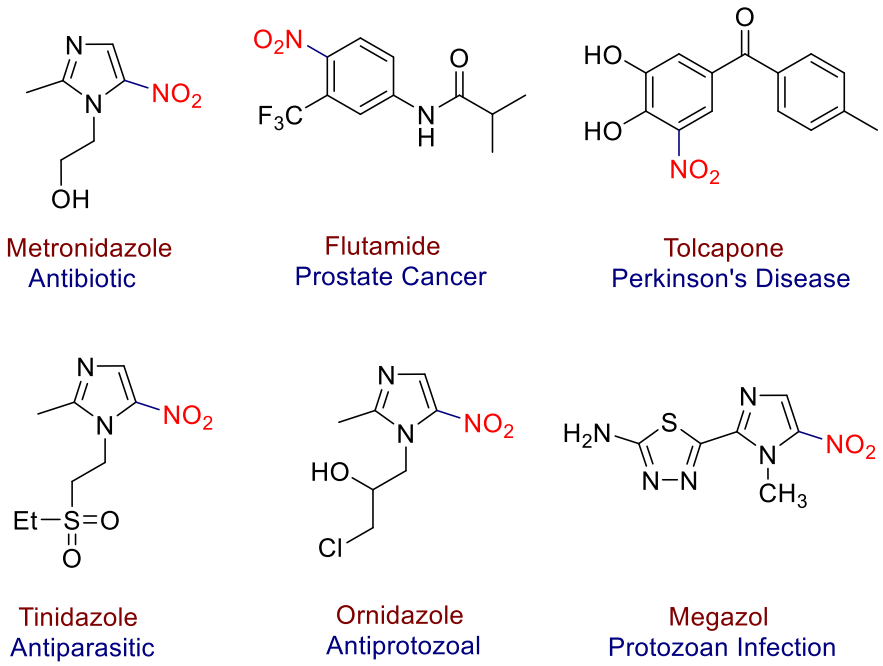

Figure 1.4. Pharmaceutical importance of nitro compounds

The classical method of nitration utilizes mixed acid and fuming nitric acids as a nitrating agent and follows an aromatic electrophilic substitution strategy. But the traditional method suffers from limitations such as the requirement of harsh reaction conditions, uncontrollable to mono-nitration, and problems in chemoselectivity. Parallelly, transition metal-catalyzed selective C-H nitration reactions[13] using Pd,[4] Fe,[14, 15] Rh,[5] Ru,[16] catalysts have also made significant development. Along

with this, metal nitrates[9] have been utilized for nitration reactions. But for the crucial advantages of TBN and its mild and metal-free nature, implementation of TBN in nitration reactions has become highly preferable compared to other nitrating agents.

Herein we have showcased TBN-mediated nitro radical triggered different reactions under mild and metal-free reaction conditions.

1.3.3.1 Chemoselective nitration of phenols

In 2009, Savinov's group disclosed a convenient nitration approach for phenols[17] by employing TBN as a nitro source (Scheme 1.1). This mild protocol manifested excellent chemoselectivity and high yields. Moreover, by applying this protocol, nitration of polymer-supported peptides can be carried out.

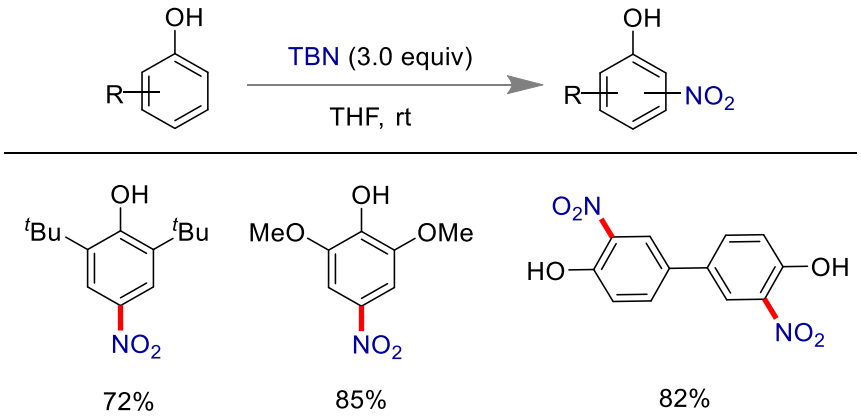

Scheme 1.1. Savinov's report on chemoselective nitration of phenols

1.3.3.2 Stereoselective nitration of olefins

In 2013, Maiti and coworkers disclosed a convenient and mild strategy for nitration of olefins[18] using TBN as the nitrating agent (Scheme 1.2). The protocol exhibited operational simplicity and

excellent *E*-selectivity. Using this methodology, a library of nitroolefins could be synthesized with diverse functionalities. The reaction followed a nitro radical-mediated pathway generated by TBN.

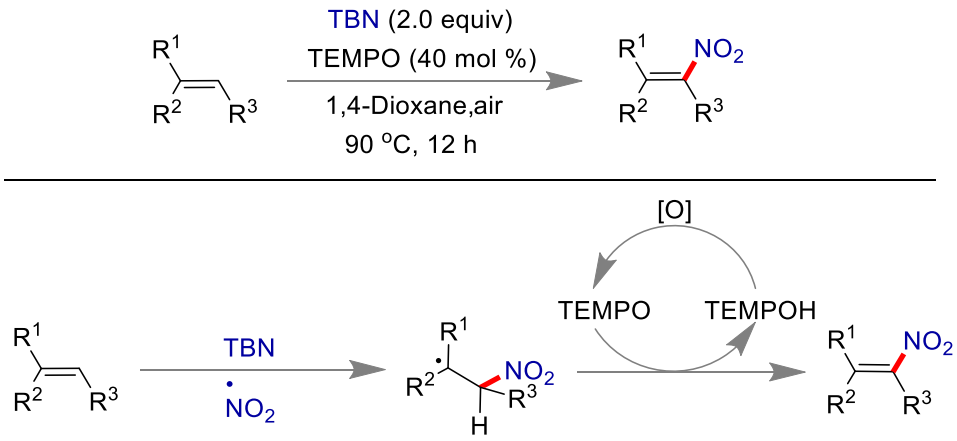

Scheme 1.2. Maiti's approach for stereoselective nitration of olefins

1.3.3.3 Nitroaminoxylation of alkynes

Nitroaminoxylation of alkynes[19] was explored by Maiti's group in 2014. By utilizing TBN as the nitrating agent and TEMPO, the conversion was achieved in high yields (Scheme 1.3). The protocol showed compatibility with a wide spectrum of functional groups and furnished broad substrate scopes. Control experiments suggested the involvement of a radical-mediated pathway in the reaction.

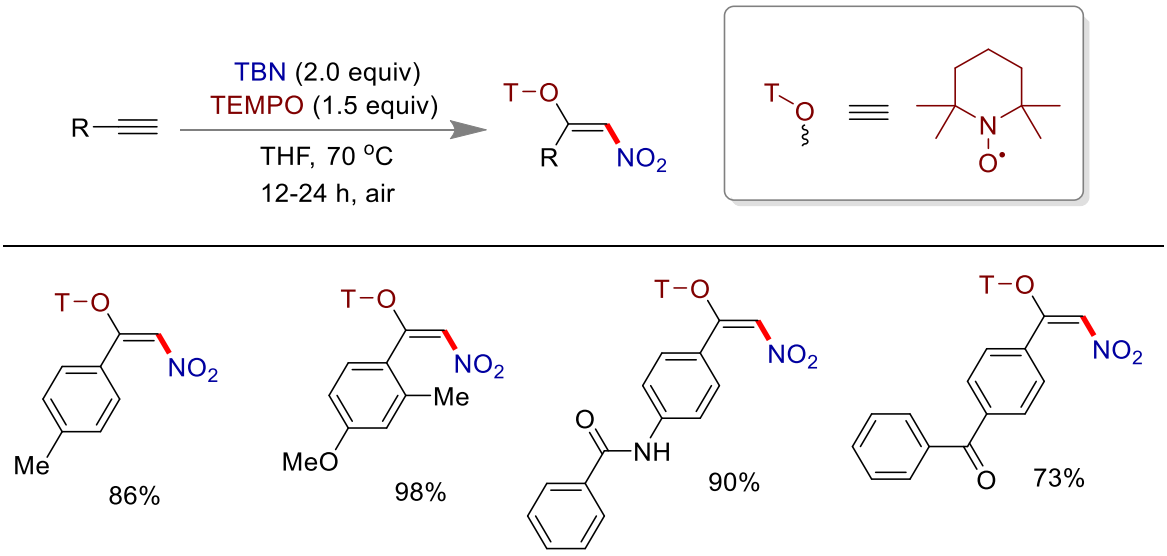

Scheme 1.3. Maiti's work on nitroaminoxylation of alkynes

1.3.3.4 Chemoselective nitration of aromatic sulfonamides

Arns and coworkers introduced a mono-nitration strategy for aromatic sulfonamides[20] with TBN as a sole nitrating agent without using any additive. The protocol revealed excellent chemoselectivity towards sulfonamide functionalized aryl systems (Scheme 1.4).

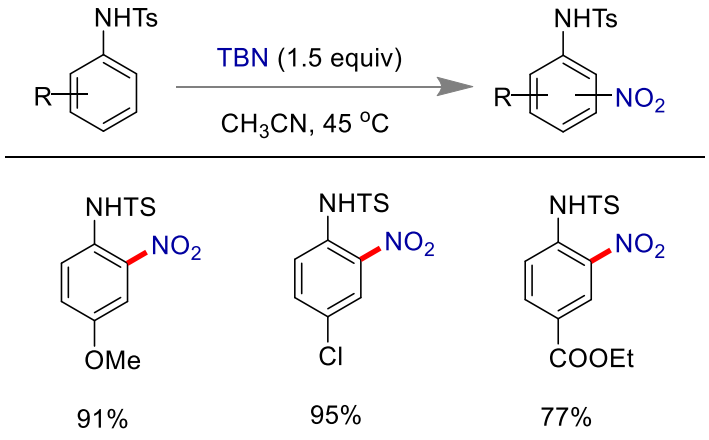

Scheme 1.4. Arn's approach toward chemoselective nitration of aromatic sulfonamides

1.3.3.5 Regioselective C-7 nitration of 8-aminoquinoline amides

Hajra's group demonstrated a reliable protocol for regioselective C-7 nitration of 8-aminoquinoline amides.[21]

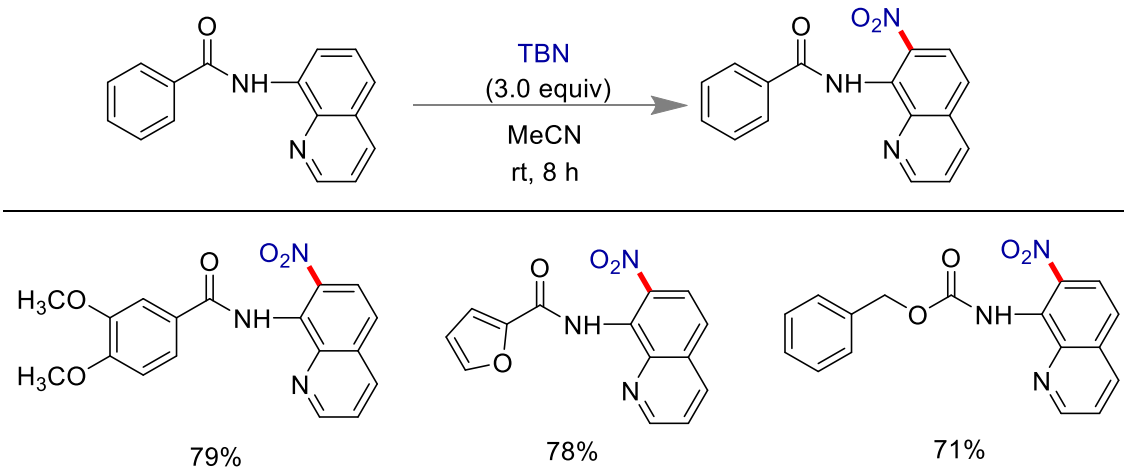

Scheme 1.5. Hajra's report on regioselective C-7 nitration of 8-aminoquinoline amides

The method excluded the use of any additive or catalyst except TBN as the only reagent (Scheme 1.5). The protocol was found to be efficient for various aryl, heteroaryl and aliphatic carboxamides and it presented high functional group compatibility.

1.3.3.6 Regioselective nitration of *N*-alkyl anilines

Kandasamy and co-workers reported a convenient approach toward regioselective nitration of *N*-alkyl anilines using TBN.[22] In this reaction, TBN served as a nitrosating agent as well as a nitrating agent (Scheme 1.6). Finally, denitrosation reaction could furnish *N*-alkyl nitro anilines. This protocol adopted a very mild reaction condition, any additive or catalyst was not required.

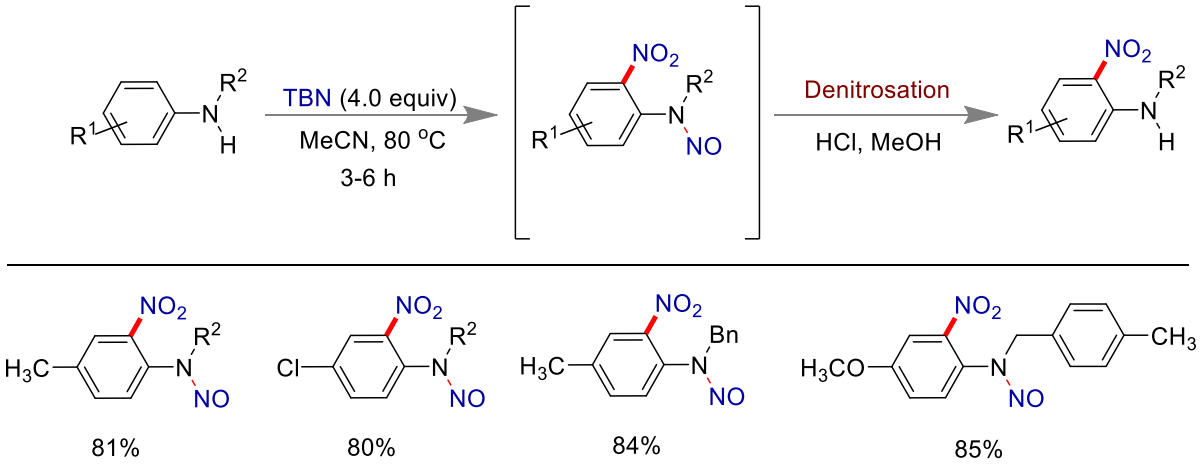

Scheme 1.6. Kandasamy's approach for regioselective nitration of *N*-alkyl anilines

1.3.3.7 Synthesis of 3-nitroquinoline *N*-oxide

In 2015, Li and co-workers established the synthetic protocol for regioselective C_3-nitration of quinoline *N*-oxides by employing TBN as both nitrating agent and oxidant[23] (Scheme 1.7). This eco-friendly nitration methodology offered excellent regioselectivity. Control experiments confirmed a radical-mediated pathway in the reaction course.

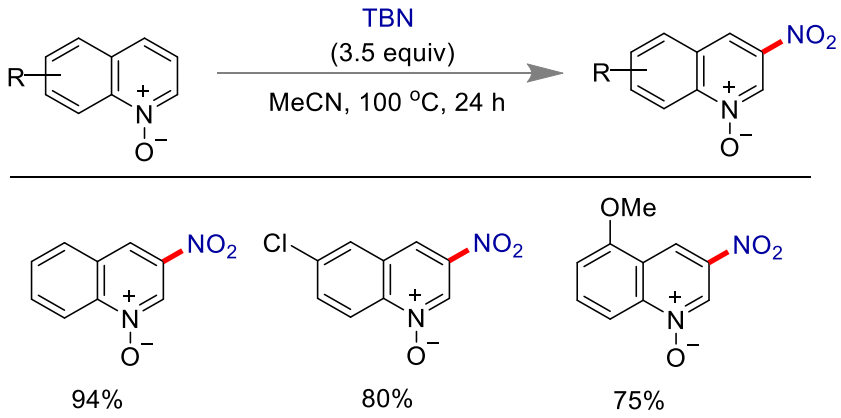

Scheme 1.7. Li's approach toward synthesis of 3-nitroquinoline *N*-oxide

1.3.3.8 *ipso*-Nitration of aryl boronic acid

An excellent *ipso*-Nitration strategy of aryl boronic acid was revealed by Beller et al. They executed the reaction using TBN in acid and additive-free conditions (Scheme 1.8).[24] According to the proposed mechanism, nitrosoarene was generated via inter or intramolecular activation of phenylboronic acid. Further oxidation of nitrosoarene resulted in the formation of the corresponding nitroarenes.

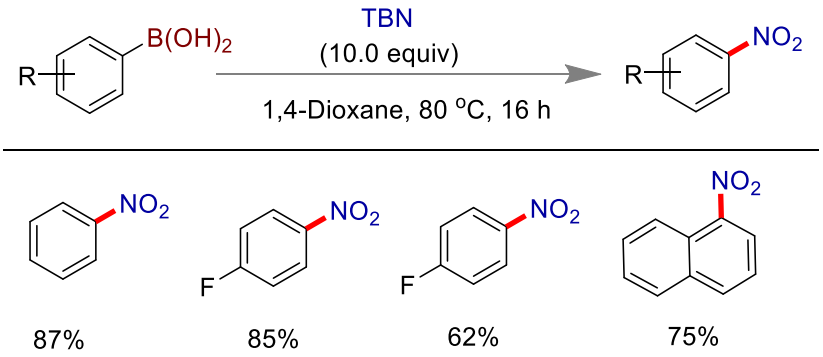

Scheme 1.8. Beller's work on *ipso*-Nitration of aryl boronic acid

1.3.3.9 Nitration of α,β-unsaturated carboxylic acids

Patel's group implemented TBN for nitration of α,β-unsaturated carboxylic acids.[25] This mild and metal-free protocol proceeded via nitro radical addition to α,β-unsaturated carboxylic acids followed by decarboxylation which led to the formation of the desired nitroalkenes (Scheme 1.9).

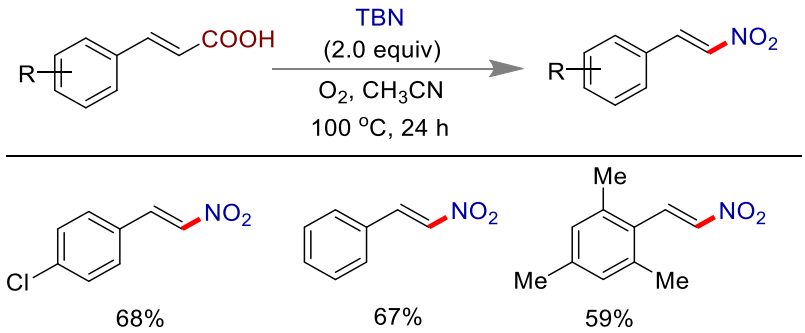

Scheme 1.9. Patel's report on Nitration of α,β-unsaturated carboxylic acids

1.3.3.10 Oxidative nitration of alkenes

Taniguchi and co-workers achieved a mild protocol for oxidative nitration of alkenes utilizing TBN and molecular oxygen (Scheme 1.10).[26] The methodology furnished good functional group tolerance and exhibited excellent regioselectivity.

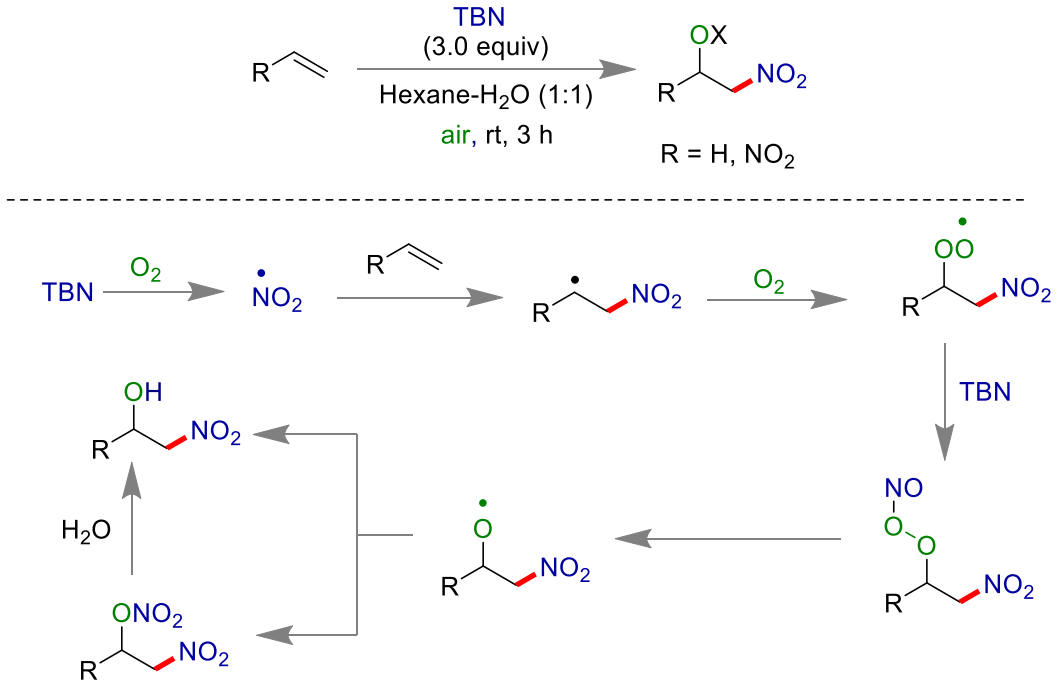

Scheme 1.10. Taniguchi's approach for oxidative nitration of alkenes

In this reaction, H_2O played a crucial role. In presence of H_2O, alkoxy-radical was quenched which led to the formation of β-nitro alcohol. Parallelly, in absence of H_2O, the alkoxy radical further reacted with $^{\bullet}NO_2$ radical and delivered the corresponding nitrated product.

1.3.3.11 Synthesis of β-nitrate esters

Guo's group disclosed a ring-opening reaction of 2-oxazolines using TBN as the sole reagent which gave access to β-nitrate esters.[27] The reaction was triggered by $^{\bullet}OONO$ radical which was

generated from •NO radical in the presence of oxygen. Finally, the abstraction of hydrogen from solvent 1,4-dioxane resulted in the formation of the desired product β-nitrate ester (Scheme 1.11). The methodology displayed high functional group tolerance and offered good to excellent yields.

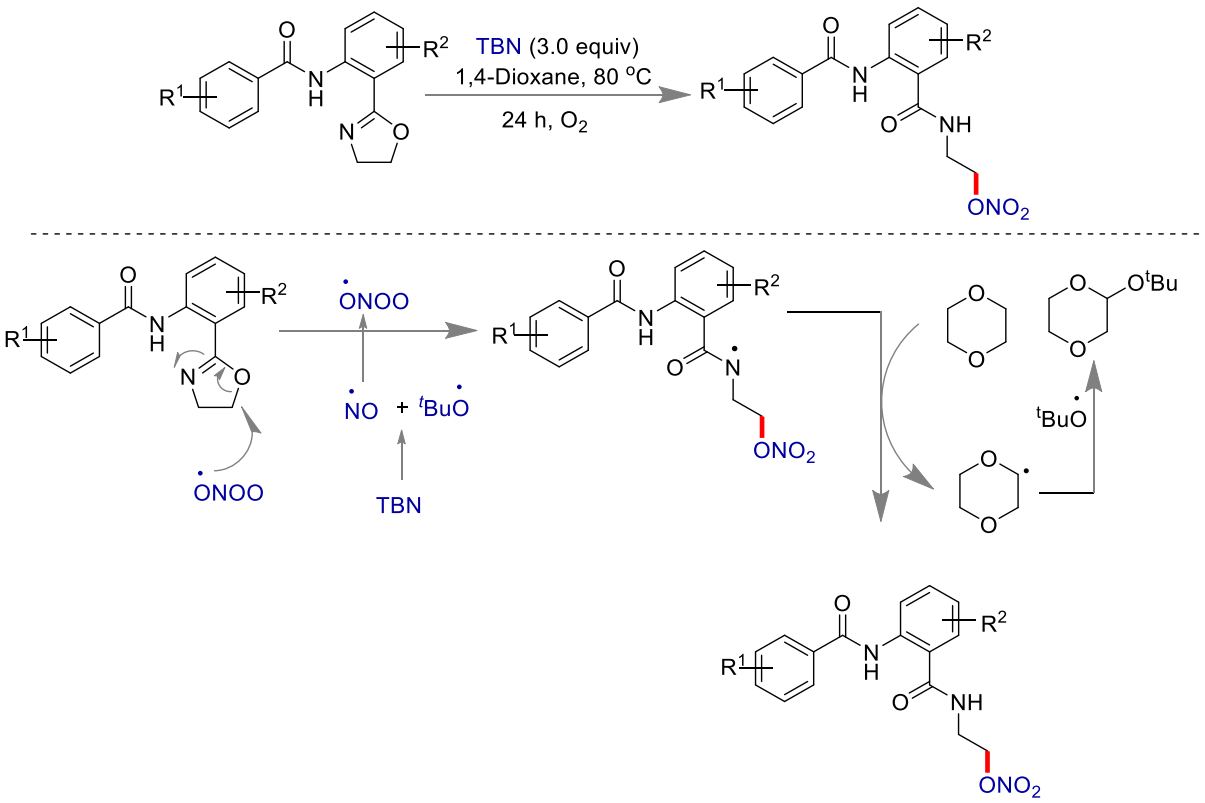

Scheme 1.11. Guo's report on synthesis of β-nitrate esters from 2-oxazolines

1.3.3.12 Nitrative spirocyclization of *N*-aryl propiolamides

Nitrative cyclization generally follows cascaded C-N and C-C bond formation reactions. With the successful implementation of TBN in different nitration reactions, it can also potentially trigger different nitrative cyclization reactions. Li's group demonstrated nitrative spirocyclization of *N*-aryl propiolamides using TBN, TEMPO, and water (Scheme 1.12).[28] As shown below, the reaction proceeded through a •NO_2 radical-mediated 5-exo-trig spirocyclization, followed by oxidation with TEMPO. Next, nucleophilic addition by water, followed by oxidation led to the formation of

the desired nitrated spirocycles. H_2O^{18} labeling experiment revealed that H_2O served as the oxygen source of the newly formed C=O bond in the nitrated spirocycle.

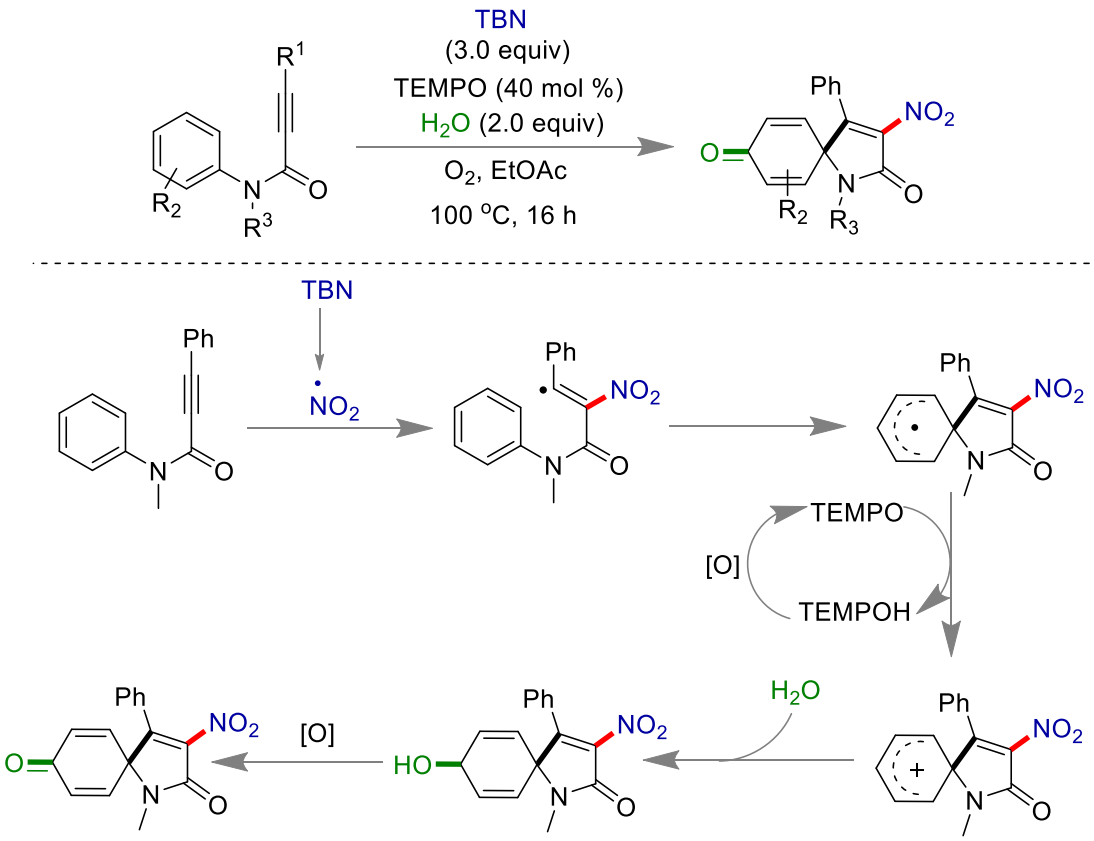

Scheme 1.12. Li's work on Nitrative spirocyclization of *N*-aryl propiolamides

1.3.3.13 Nitro-carbocyclization of activated alkenes

In 2013, Jiao's group explored TBN-promoted nitro-carbocyclization of activated alkenes in metal-free conditions.[29] This reliable protocol gave access to a library of nitrated oxindoles with satisfactory yields (Scheme 1.13) TBN-mediated nitration followed by intramolecular carbocyclization resulted in the desired product formation.

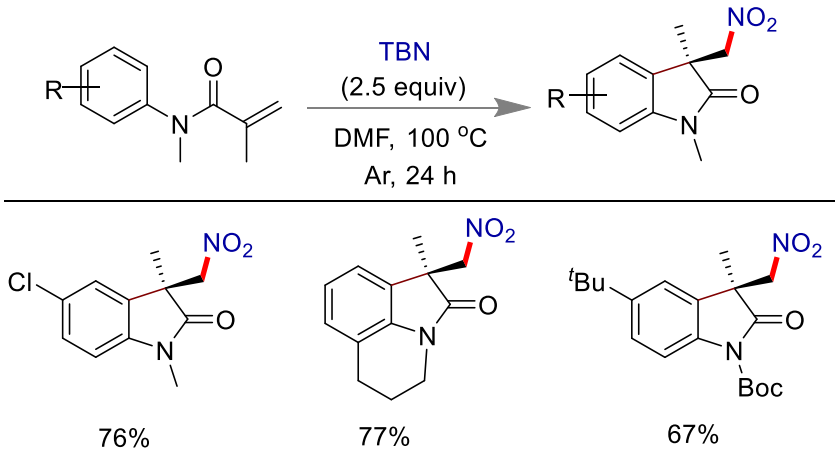

Scheme 1.13. Jiao's approach for nitro-carbocyclization of activated alkenes.

1.3.3.14 Cascaded nitrative cyclization of 1,7-enynes

TBN-mediated nitrative cyclization of 1,7-enynes[30] was disclosed by Li's group in 2014 (Scheme 1.14).

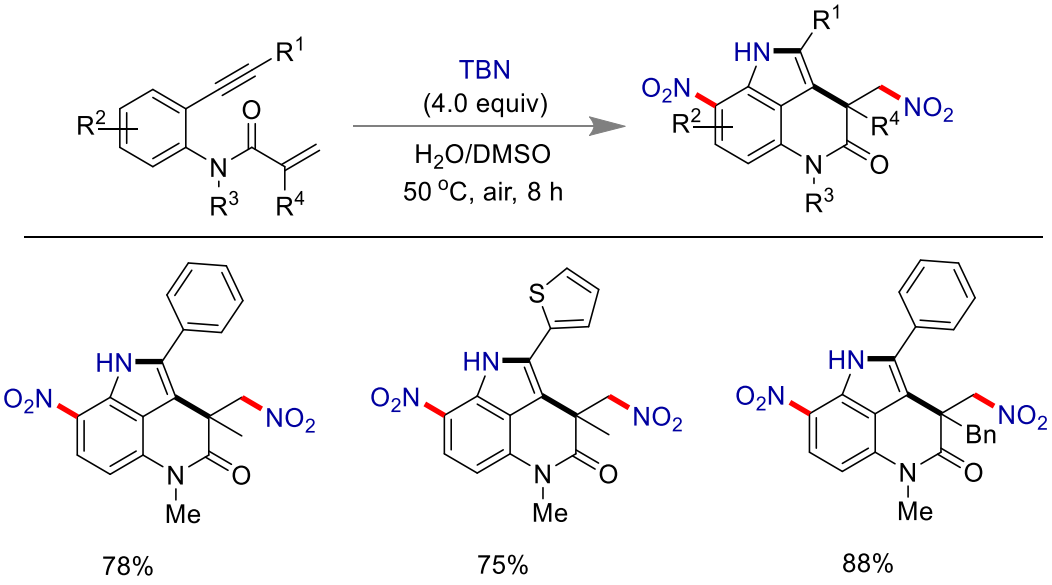

Scheme 1.14. Li's approach for nitrative cyclization of 1,7-enynes

This reaction manifested broad substrate scopes along with excellent functional group tolerance. In this protocol, TBN served as both nitro source and *N*-1 synthon.

1.3.3.15 Cascade reaction of allenynes

TBN mediated cascade reaction strategy for allenynes was revealed by Fan and co-workers.[31] As described below, the intermediate generated from [2+2] cycloaddition of alleynes, underwent $^{\bullet}NO_2$ radical addition and resulted in a nitro-containing radical intermediate which was then captured by TEMPO and led to the formation of another intermediate. Finally, N-O bond cleavage of TEMPO captured intermediate in the presence of $^{\bullet}NO$ radical, furnished nitrocyclobutane-fused naphthalene-1,2-diones (Scheme 1.15).

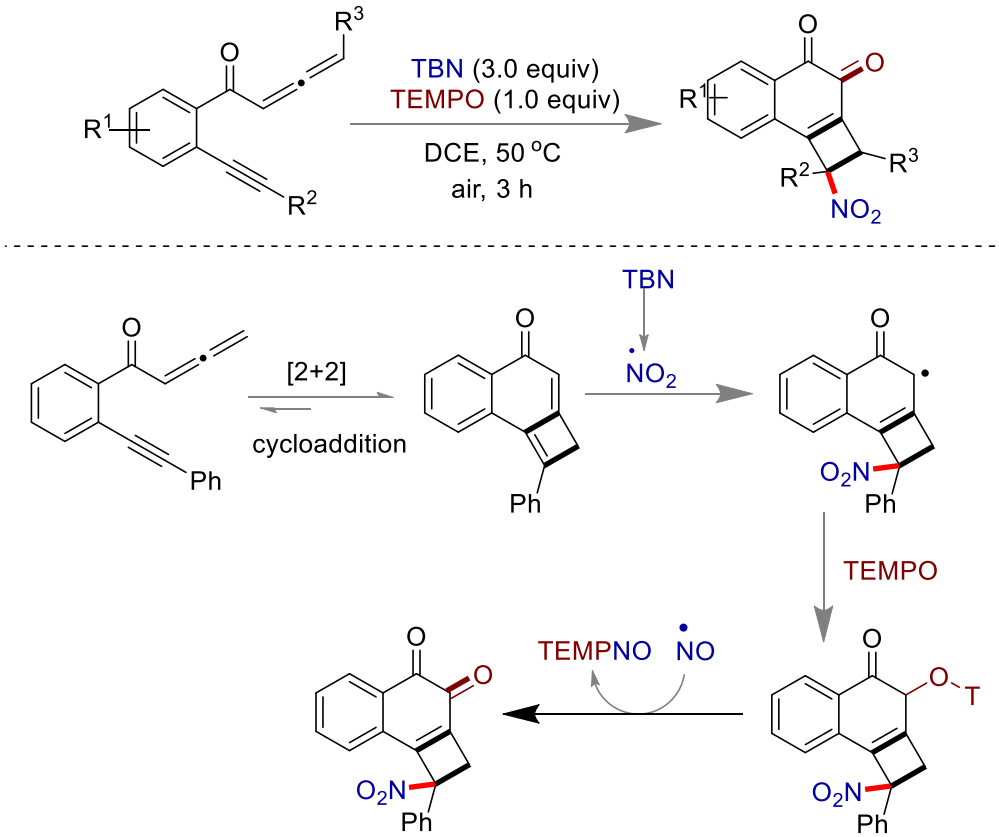

Scheme 1.15. Fan's report on TBN mediated cascade reaction of allenynes

1.3.3.16 Nitrative cyclization of 1-ethynyl-2-(vinyloxy)benzene

Li and co-workers have described nitrative cyclization of 1-Ethynyl-2-(vinyloxy)benzenes[32] employing TBN as the nitrating agent. As detailed below, $^{\bullet}NO_2$ radical generated from TBN triggered a nitrative cyclization in 1-Ethynyl-2-(vinyloxy)benzene which generated a nitro-containing radical intermediate. Next, dioxygen activation followed by peroxy bond cleavage and oxidation afforded the 1-[2-(Nitromethyl)benzofuran-3-yl]Ketones (Scheme 1.16).

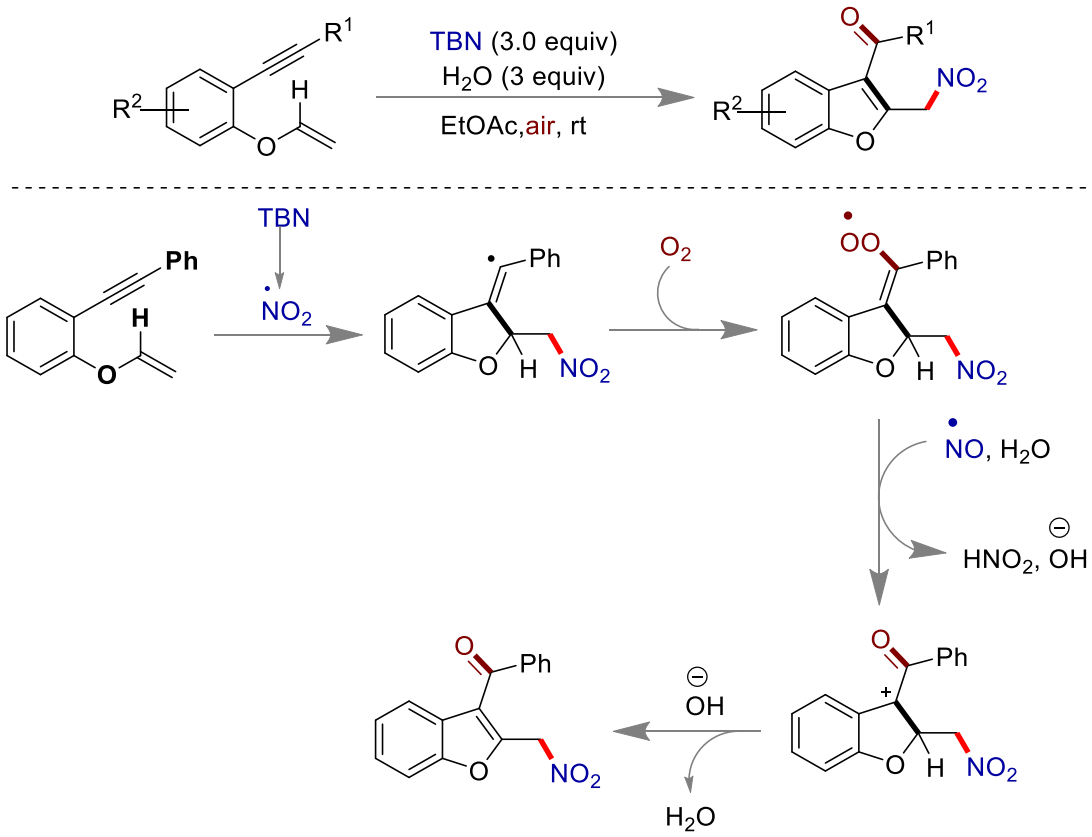

Scheme 1.16. Li's approach for nitrative cyclization of 1-Ethynyl-2-(vinyloxy)benzene

1.3.4 OTHER SYNTHETIC APPLICATIONS OF TBN

As previously discussed, along with different reactions triggered by nitro radicals, TBN can also be successfully implemented in other reactions like nitrosation, oximation, miscellaneous applications, and as *N*-synthon. Accordingly, this multitasking reagent has drawn the attention of synthetic organic chemists. Herein, we have briefly discussed some examples related to these reactions.

1.3.4.1 Nitrosation of secondary amines

In 2016, Kandasamy and co-workers reported a solvent-free protocol for nitrosation of secondary amines using TBN as a nitroso source (Scheme 1.17).[33] This metal-free strategy afforded *N*-nitrosoamines with high yields. Furthermore, acid labile groups such as *tert*-butyloxycarbonyl (Boc) and *tert*-butyldimethylsilyl (TBDMS) were well tolerated in this protocol.

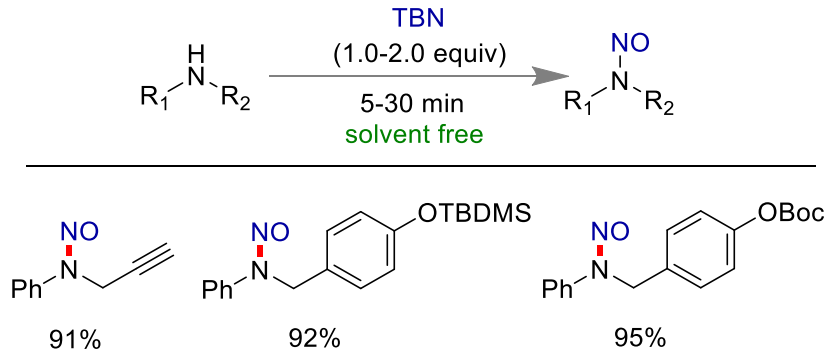

Scheme 1.17. Kandasamy's approach for nitrosation of secondary amines

1.3.4.2 Regioselective nitrosation of imidazo[1,2-a]pyridines

Regioselective C_3-nitrosation of imidazo[1,2-a]pyridines was explored by Hajra's group.[34] They executed the reaction in mild and metal-free conditions using TBN as the only reagent and the

reaction was achievable within a very short reaction time (Scheme 1.18). This methodology was also applicable for other heterocycles such as benzo[d]imidazo[2,1-b]thiazoles and imidazo[2,1-b]thiazoles.

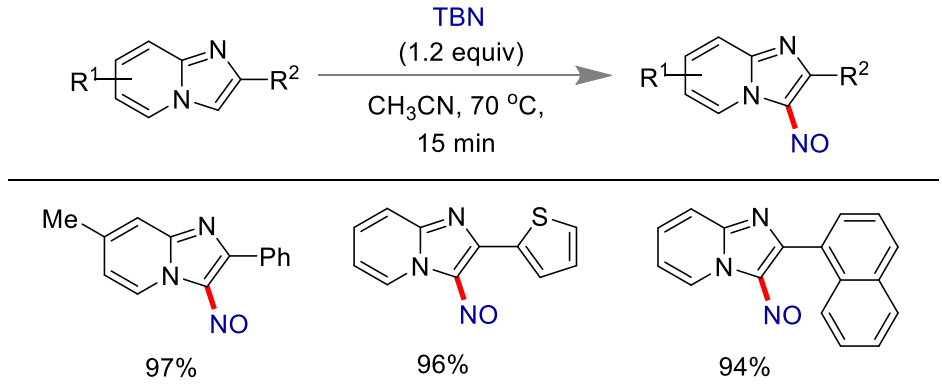

Scheme 1.18. Hajra's work on regioselective nitrosation of imidazo[1,2-a]pyridine

1.3.4.3 Transamidtion of secondary amides with amines

Kandasamy and co-workers introduced a TBN-mediated excellent approach toward transamidation of secondary amides with amines under metal and catalyst-free conditions (Scheme 1.19).[35] The protocol was compatible with various amines such as primary, secondary, cyclic, or cyclic amines. The reaction proceeded through a TBN-mediated nitrosation of secondary amides followed by amination with amines.

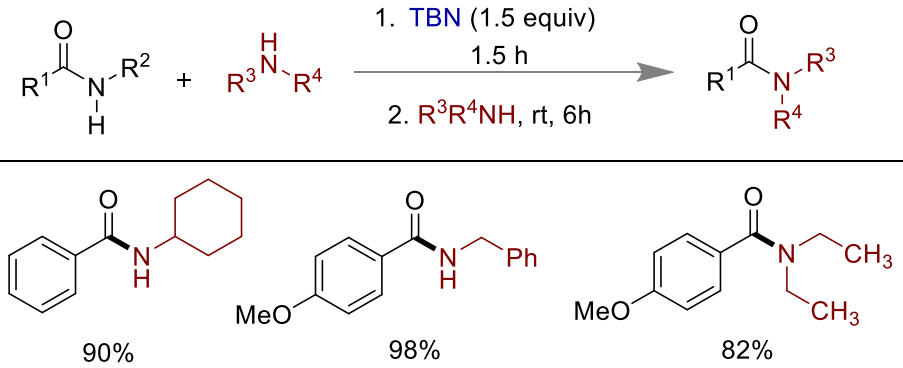

Scheme 1.19. Kandasamy's approach for transamidation of secondary amides with amines

1.3.4.4 Synthesis of isatin oximes from oxindoles

Liang's group introduced a sustainable approach for the synthesis of isatin oximes from oxindoles using TBN in water at room temperature.[36] TBN-mediated nitrosation followed by isomerization afforded the desired isatin oximes (Scheme 1.20). Mild reaction conditions, use of metal-free reagent, and H_2O as green solvent are the key advantages of the protocol.

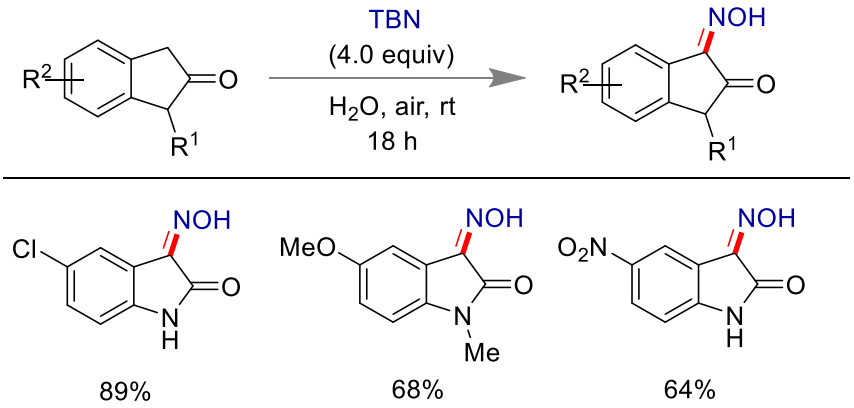

Scheme 1.20. Liang's approach to the synthesis of isatin oximes

1.3.4.5 Synthesis of isoxazolines and isoxazoles

Zhang demonstrated a strategy for TBN-mediated synthesis of isoxazolines and isoxazoles from methyl ketone and alkenes or alkynes.[37]

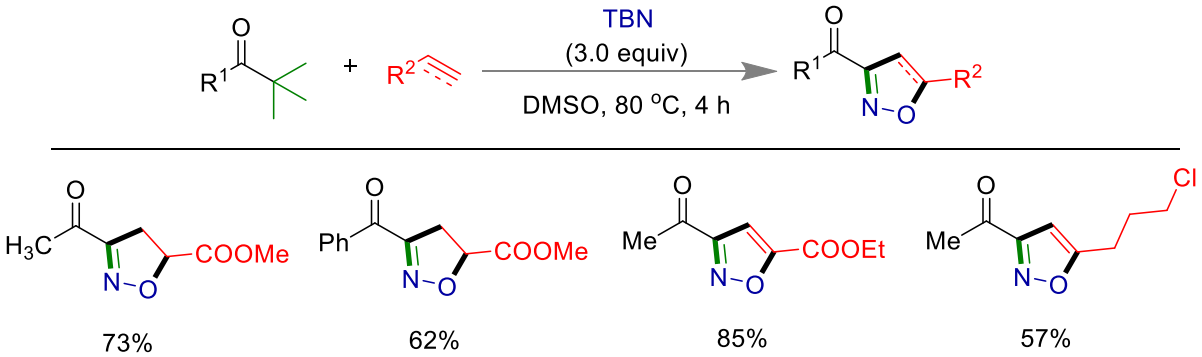

Scheme 1.21. Zhang's report on TBN mediated synthesis of isoxazolines and isoxazoles

According to the tentative mechanism as stated by the authors, a radical-mediated pathway was involved in the reaction (Scheme 1.21) First, methyl ketone underwent TBN-mediated nitrosation and then was further converted into acyl nitrile oxide intermediate in presence of *t*-BuO$^{\bullet}$ radical. Finally, the cycloaddition of acyl nitrile oxide intermediate with alkenes or alkynes resulted in the formation of oxazolines or oxazoles.

1.3.4.6 Direct C-H Arylation of (hetero)arenes with anilines

TBN-mediated diazotization approach was utilized in direct C-H Arylation of (hetero)arenes with anilines using ascorbic acid as an initiator (Scheme 1.22). This reaction was experienced and revealed by Carrilo's group.[38] According to the mechanistic pathway postulated by the authors, TBN-mediated diazotization of anilines resulted in the formation of arene diazonium intermediate which was then reduced by ascorbic acid to its corresponding aryl radical. Next, its subsequent homolytic aromatic substitution with (hetero)arene furnished C-C coupled product.

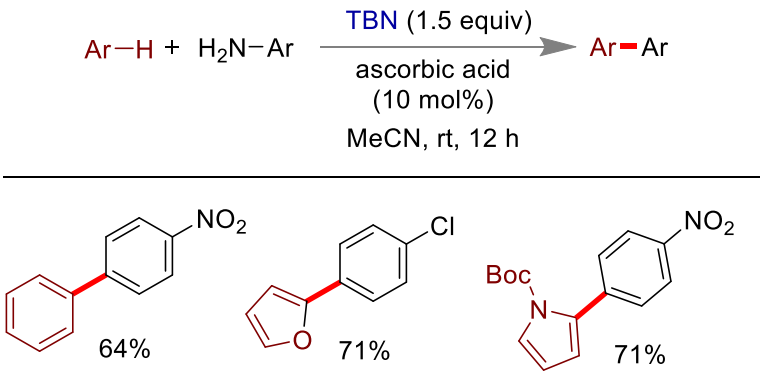

Scheme 1.22. Carrilo's work on direct C-H Arylation of (Hetero)arenes with Anilines

1.4 VISIBLE-LIGHT PHOTOCATALYSIS

Visible-light photocatalysis is one of the important cutting-edge tools for various chemical transformations in synthetic chemistry. Visible-light source is a clean, environment-friendly, and inexpensive energy source, parallelly, it is easy to handle. In addition, Visible-light photocatalytic reactions require ambient reaction conditions and are therefore easy to execute, and certainly, it is another major advantage of visible light photocatalysis in terms of sustainability. Therefore, it has become a trending topic in synthetic organic chemistry.

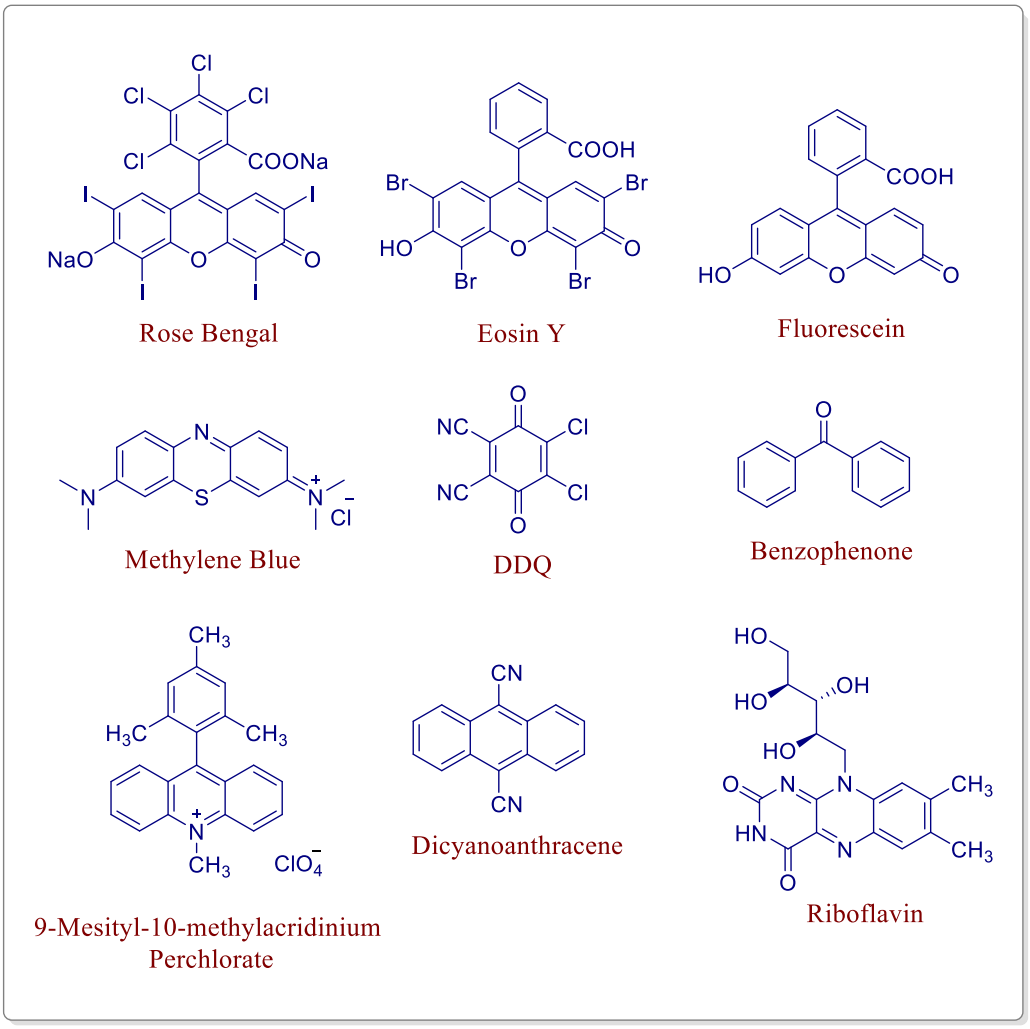

Figure 1.5. Common metal-free photocatalysts in organic synthesis

In visible-light-driven photocatalytic reactions, two categories of photocatalysts are generally employed. One is metal-based photocatalysts such as Ru and Ir-based photocatalysts[39, 40] and another is metal-free organic photocatalysts.[41, 42] Though metal-based photocatalysts have significantly extended their application, they are highly expensive and potentially toxic. Contrastingly, metal-free organic dyes are relatively non-toxic, inexpensive, and easy to handle. Commonly used metal-free photocatalysts are Rose Bengal, Eosin Y, Fluorescein, Methylene Blue, and 9-Mesityl-10-methyl-acridinium perchlorate, etc (Figure 1.5). Most of these photocatalysts have strong visible-light absorption, and a long excited-state lifetime, and are stable under photolytic conditions.

The inherent nature of photocatalyst is either to take part in a single-electron transfer process or to transfer energy to a substrate. Under visible-light irradiation, a photocatalyst absorbs light energy and gets promoted to its excited state which then participates in the oxidative-reductive or energy transfer process. During an oxidative cycle, an excited state photocatalyst (PC*) donates a single electron to an acceptor or substrate and itself gets oxidized. Next, the oxidized photocatalyst accepts one electron from the substrate or donor and returns to its ground state. Parallelly, in a reductive cycle, the excited state photocatalyst accepts an electron from a donor or substrate and itself gets reduced. Subsequently, the reduced photocatalyst transfers one electron to the substrate or acceptor and the photocatalyst is regenerated (Figure 1.6).

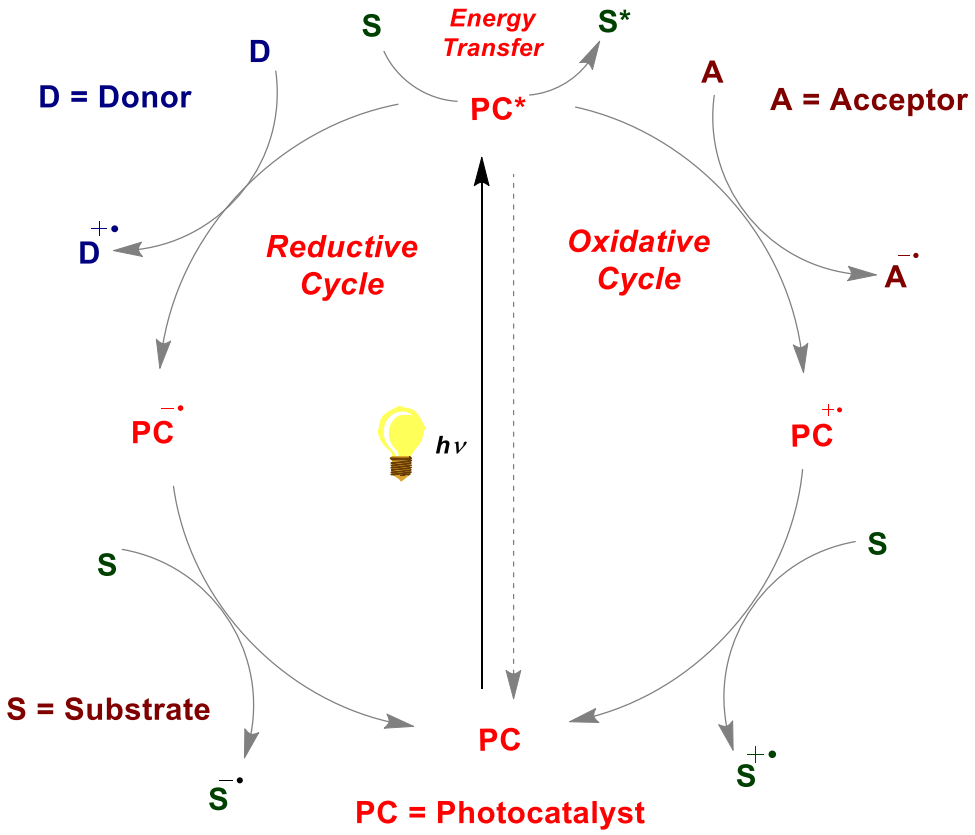

Figure 1.6. Catalytic cycle of a photocatalyst.

Visible-light photocatalysts have an intrinsic property to activate dioxygen. Accordingly, photoinduced oxygenation reaction using molecular oxygen as a green oxidant has become an important topic of research. Herein, we have summarized some recent examples of photocatalytic oxygenation reactions.

1.4.1 Photocatalytic oxygenation of benzylic sp^3 C-H bonds

Lei and co-workers reported visible-light promoted benzylic sp^3 C-H oxygenation using 9-Mesityl-10-methyl-acridinium perchlorate as visible-light photocatalyst under an O_2 atmosphere.[43] As shown below, under visible light irradiation the excited state photocatalyst underwent a single electron transfer with the benzylic sp^3 C-H compound, and corresponding radical cation was

generated and the photocatalyst was itself reduced. In the next step, the radical cation of the benzylic sp^3 C-H compound lost a proton and led to the corresponding radial which then reacted with a superoxide radical anion generated from electron transfer between O_2 and radical anion of the photocatalyst. Eventually, a hydroperoxide intermediate was generated which next lost a water molecule and delivered the desired product (Scheme 1.23). From control experiments, the authors have proved that the inserted oxygen molecule was exactly originated from dioxygen.

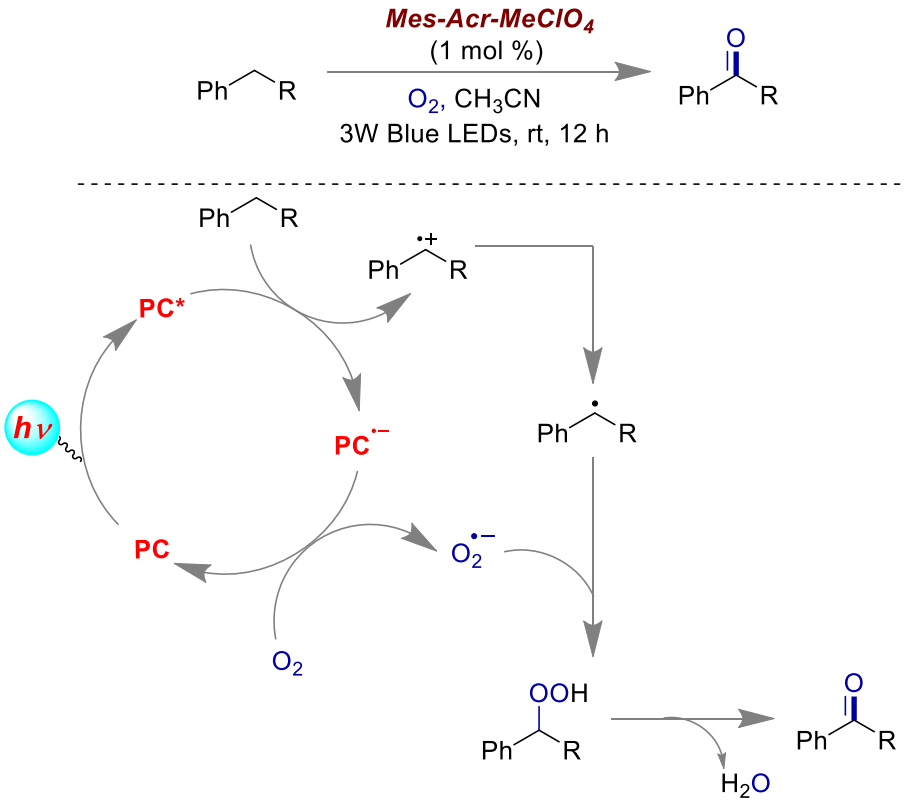

Scheme 1.23. Lei's approach for Photocatalytic oxygenation of benzylic sp^3 C-H bonds.

1.4.2 Photocatalytic aerobic oxidation of *N*-alkyl pyridinium salts

Fu's group introduced aerobic oxidation of *N*-alkyl pyridinium salts in presence of visible-light irradiation using Eosin Y as visible-light photocatalyst and Cs_2CO_3 as a base.[44] Ths protocol

adopted mild and environment-friendly reaction conditions and exhibited broad substrate scopes. The plausible mechanism illustrated by the authors is shown below. Under visible-light irradiation, Eosin Y was converted to its excited state and underwent a single electron transfer with *N*-alkyl pyridinium salt, and itself was oxidized. The single-electron transfer from *N*-alkyl pyridinium salt converted it into the corresponding radical which then reacted with molecular oxygen; eventually alkyldioxyl radical was generated. Following 1,3-hydrogen radical transfer in alkyldioxyl radical furnished another radical intermediate and that intermediate underwent another single electron transfer with the radical cation of the photocatalyst. Consequently, the photocatalyst was regenerated, and an oxygen-centered cation was formed. In presence of Cs_2CO_3, the oxygen-centered cation finally delivered the desired product (Scheme 1.24).

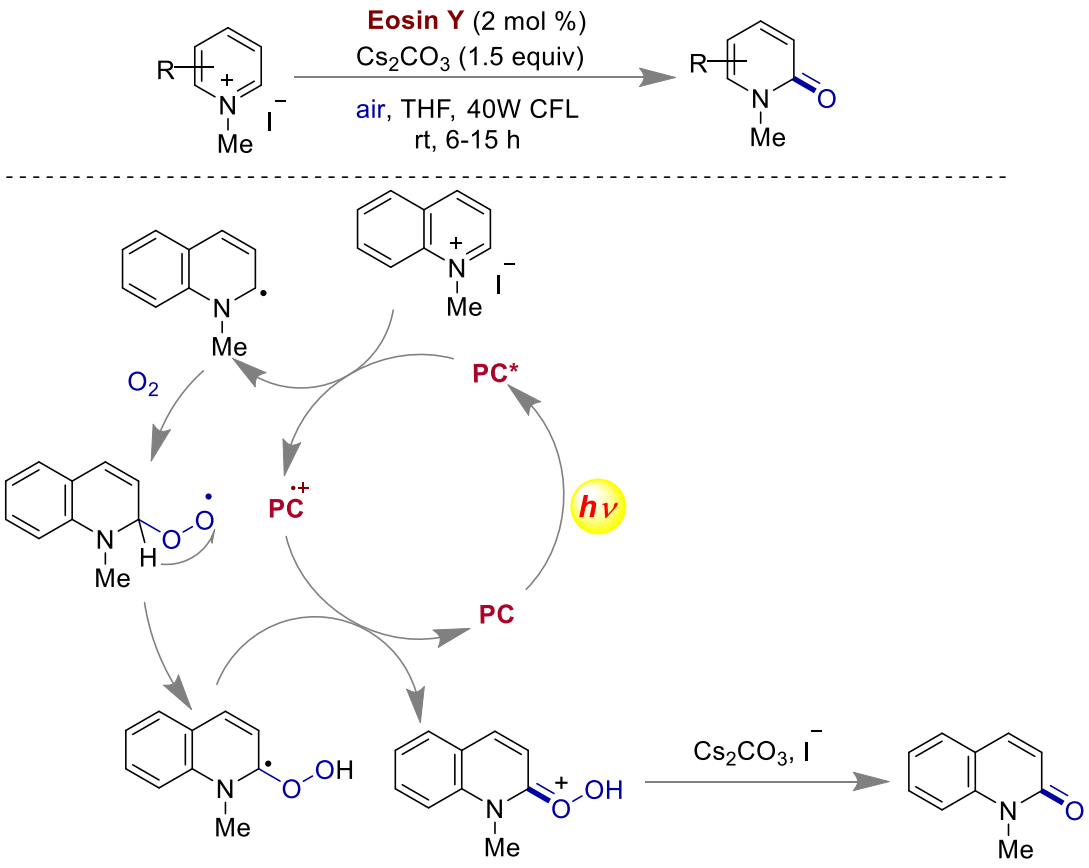

Scheme 1.24. Fu's report on photocatalytic oxidation of *N*-alkyl pyridinium salts using Eosin Y

1.4.3 Conversion of tertiary amines to amides using visible-light photocatalysis

Recently Das and co-workers disclosed photocatalytic conversion of tertiary amines to amides using Rose Bengal as a visible light photocatalyst, and DBN as a base under an O_2 atmosphere at room temperature.[45] According to the mechanistic pathway proposed by the authors; the excited state photocatalyst formed in presence of visible-light irradiation underwent a single electron transfer with a tertiary amine.

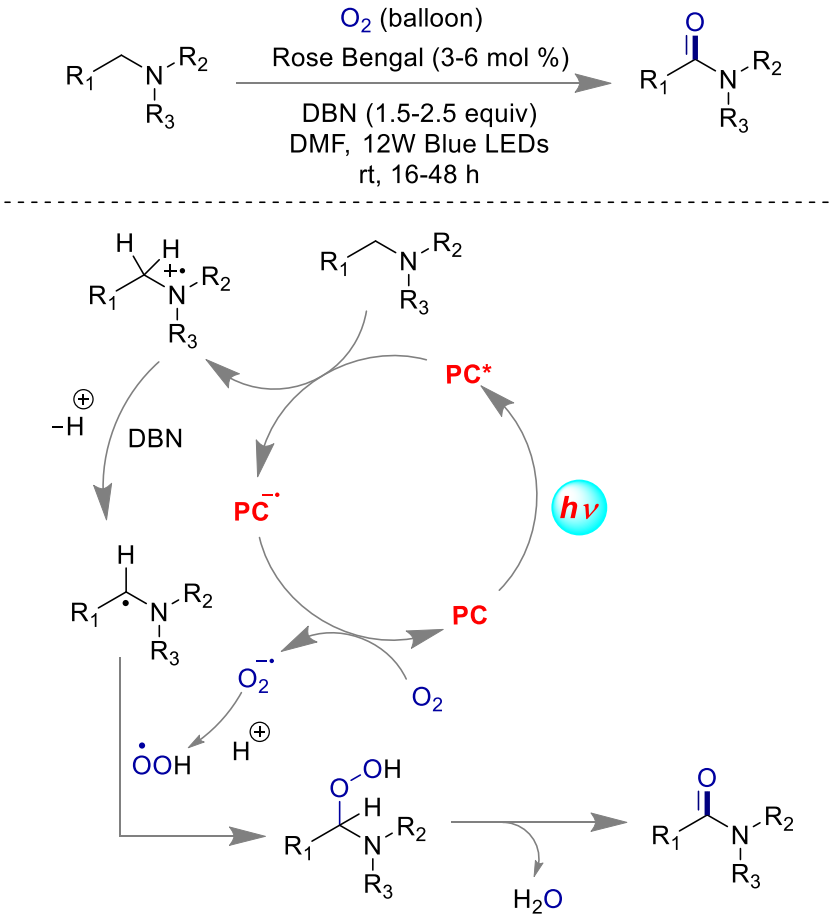

Scheme 1.25. Das's work on the conversion of tertiary amines to amides using visible-light photocatalysis

As a result, radical cation of the tertiary amine was generated and excited state photocatalyst was reduced to its corresponding radical anion. In the next step, DBN helped to deprotonate the radical cation of tertiary amine and resulted in its corresponding carbon-centered radical. Following, the radical anion of the photocatalyst produced a superoxide radical anion from molecular oxygen. Finally, peroxide radical generated from superoxide radical anion reacted with the carbon-centered radical intermediate of tertiary amine and delivered the corresponding amide via extrusion of a water molecule (Scheme 1.25). Control experiments performed by the authors also confirmed that the oxygen incorporated in the tertiary amine originated from molecular oxygen.

1.4.4 Visible-light mediated synthesis of 1,2-diketones from enaminones

Wen and co-workers demonstrated a photocatalytic strategy for 1, 2-diketone synthesis from enaminones utilizing Rose Bengal as a photocatalyst under an open-air atmosphere at room temperature (Scheme 1.26).[46]

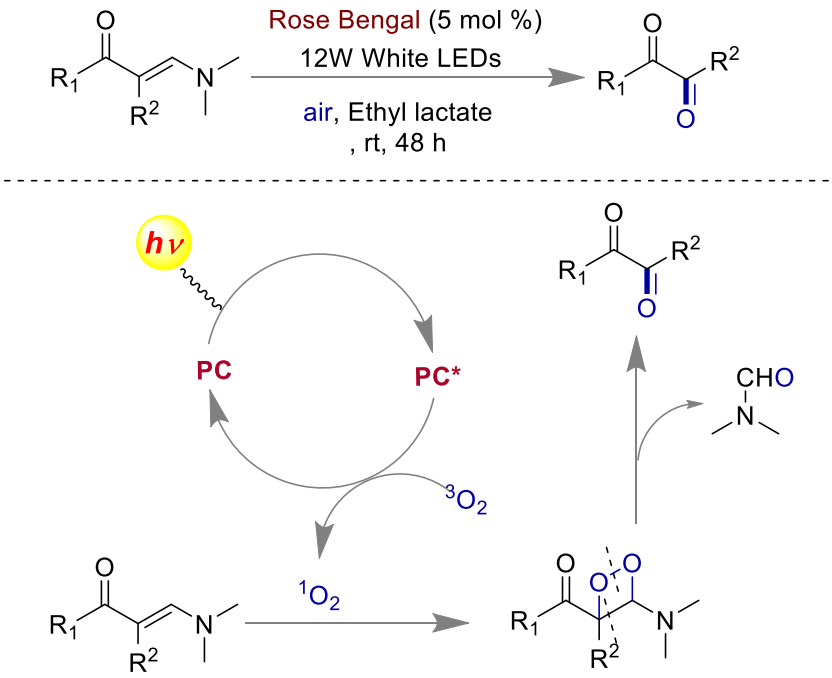

Scheme 1.26. Wen's approach for Photocatalytic synthesis of 1,2-diketones from enaminones

The authors have shown the tentative mechanistic pathway for the reaction (Scheme 1.26). The excited state photocatalyst was generated under visible-light irradiation and it helped in the conversion of triplet oxygen to singlet oxygen. Singlet oxygen then reacted with enaminone and delivered a peroxy intermediate. Finally, the automatic decomposition of the peroxide intermediate afforded 1,2-diketone.

1.5 OBJECTIVE

In summary, we have presented an overview of the multitasking reagent TBN and discussed its application in various C-N, C-C, and C-O bond formation reactions. Parallelly, we have outlined the overview of visible-light photocatalysis and its application in oxygenation reactions. The objective of this thesis is to develop sustainable strategies for C-N, C-C, and C-O bond formation reactions using TBN as the sole reagent under mild and metal-free conditions and to implement visible-light photocatalysis for oxygenation reaction (C-O bond formation) (Figure 1.7).

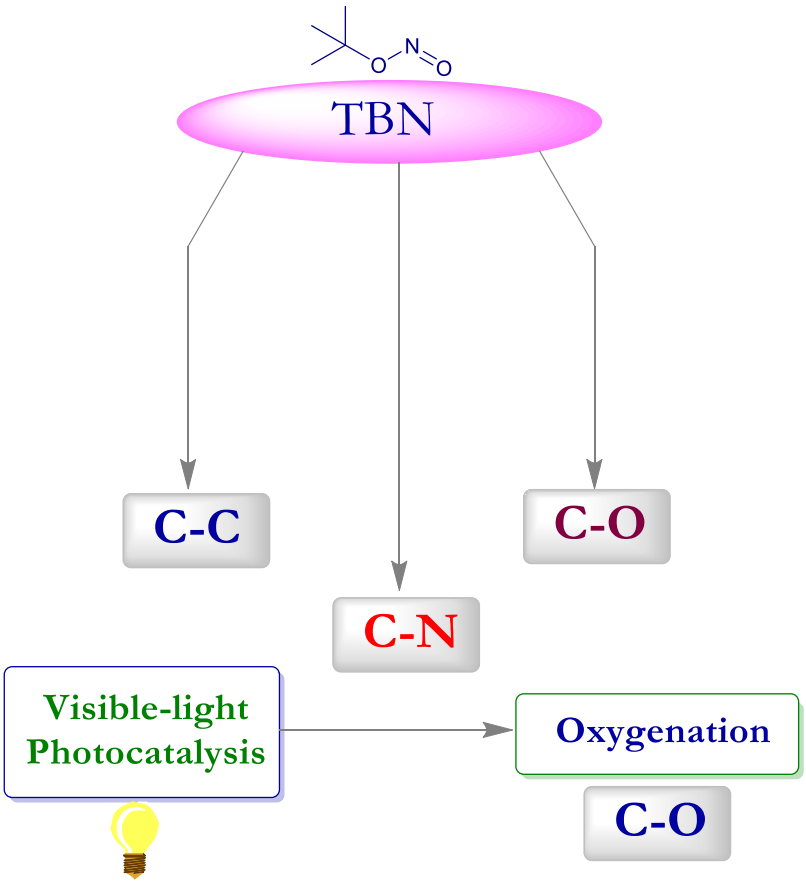

Figure 1.7. The objective of the present thesis at a glance

1.6 NOTES AND REFERENCES

1. S. Duan, Y. Xu, X. Zhang and X. Fan, *Chem. Commun.*, 2016, **52**, 10529-10532.

2. J. Dong, P. Liu and P. Sun, *J. Org. Chem.*, 2015, **80**, 2925-2929.

3. W. Liu and L. Ackermann, *Org. Lett.*, 2013, **15**, 3484-3486.

4. Y.-F. Liang, X. Li, X. Wang, Y. Yan, P. Feng and N. Jiao, *ACS Catal.*, 2015, **5**, 1956-1963.

5. F. Xie, Z. Qi and X. Li, *Angew. Chem. Int. Ed.*, 2013, **52**, 11862-11866.

6. S. K. Banjare, T. Nanda, B. V. Pati, G. K. D. Adhikari, J. Dutta and P. C. Ravikumar, *ACS Catal.*, 2021, **11**, 11579-11587.

7. X. Jia and P. Li, *Synthesis*, 2017, **50**, 711-722.

8. A. Dahiya, A. K. Sahoo, T. Alam and B. K. Patel, *Chem. Asian J.*, 2019, **14**, 4454-4492.

9. G. Yan and M. Yang, *Org. Biomol. Chem.*, 2013, **11**, 2554-2566.

10. G. Booth, in *"Nitro Compounds, Aromatic" in Ullmann's Encyclopedia of Industrial Chemistry*, Wiley-VCH, Weinheim, 2000, vol. 24.

11. N. Ono, in *The Nitro Group in Organic Synthesis*, John Wiley & Sons, Inc., 2002, DOI: 10.1002/0471224480.ch6, pp. 159-181.

12. K. Nepali, H.-Y. Lee and J.-P. Liou, *J. Med. Chem.*, 2019, **62**, 2851-2893.

13. G. M. Reddy, N. S. Rao and M. Hariharasarma, *Asian J. Org. Chem.*, 2017, **6**, 59-62.

14. Y. He, N. Zhao, L. Qiu, X. Zhang and X. Fan, *Org. Lett.*, 2016, **18**, 6054-6057.

15. V. Botla, D. V. Ramana, B. Chiranjeevi and M. Chandrasekharam, *ChemistrySelect*, 2016, **1**, 3974-3978.

16. Z. Fan, J. Ni and A. Zhang, *J. Am. Chem. Soc.*, 2016, **138**, 8470-8475.

17. D. Koley, O. C. Colón and S. N. Savinov, *Org. Lett.*, 2009, **11**, 4172-4175.

18. S. Maity, T. Naveen, U. Sharma and D. Maiti, *Org. Lett.*, 2013, **15**, 3384-3387.

19. U. Dutta, S. Maity, R. Kancherla and D. Maiti, *Org. Lett.*, 2014, **16**, 6302-6305.

20. B. Kilpatrick, M. Heller and S. Arns, *Chem. Commun.*, 2013, **49**, 514-516.

21. S. Mondal, S. Samanta and A. Hajra, *Adv. Synth. Catal.*, 2018, **360**, 1026-1031.

22. P. Chaudhary, S. Gupta, N. Muniyappan, S. Sabiah and J. Kandasamy, *J. Org. Chem.*, 2019, **84**, 104-119.

23. J. Zhao, P. Li, C. Xia and F. Li, *RSC Adv.*, 2015, **5**, 32835-32838.

24. X.-F. Wu, J. Schranck, H. Neumann and M. Beller, *Chem. Commun.*, 2011, **47**, 12462-12463.

25. B. A. Mir, S. Rajamanickam, P. Begum and B. K. Patel, *Eur. J. Org. Chem.*, 2020, **2020**, 2617-2625.

26. T. Taniguchi, A. Yajima and H. Ishibashi, *Adv. Synth. Catal.*, 2011, **353**, 2643-2647.

27. K. Qiao, X. Yuan, L. Wan, M.-W. Zheng, D. Zhang, B.-B. Fan, Z.-C. Di, Z. Fang and K. Guo, *Green Chem.*, 2017, **19**, 5789-5793.

28. X.-H. Yang, X.-H. Ouyang, W.-T. Wei, R.-J. Song and J.-H. Li, *Adv. Synth. Catal.*, 2015, **357**, 1161-1166.

29. T. Shen, Y. Yuan and N. Jiao, *Chem. Commun.*, 2014, **50**, 554-556.

30. Y. Liu, J.-L. Zhang, R.-J. Song, P.-C. Qian and J.-H. Li, *Angew. Chem. Int. Ed.*, 2014, **53**, 9017-9020.

31. T. Feng, Y. He, X. Zhang and X. Fan, *Adv. Synth. Catal.*, 2019, **361**, 1271-1276.

32. M. Hu, B. Liu, X.-H. Ouyang, R.-J. Song and J.-H. Li, *Adv. Synth. Catal.*, 2015, **357**, 3332-3340.

33. P. Chaudhary, S. Gupta, N. Muniyappan, S. Sabiah and J. Kandasamy, *Green Chem.*, 2016, **18**, 2323-2330.

34. K. Monir, M. Ghosh, S. Jana, P. Mondal, A. Majee and A. Hajra, *Org. Biomol. Chem.*, 2015, **13**, 8717-8722.

35. P. Sureshbabu, S. Azeez, P. Chaudhary and J. Kandasamy, *Org. Biomol. Chem.*, 2019, **17**, 845-850.

36. W.-T. Wei, W.-M. Zhu, W.-W. Ying, Y. Wu, Y.-L. Huang and H. Liang, *Org. Biomol. Chem.*, 2017, **15**, 5254-5257.

37. P. Dai, X. Tan, Q. Luo, X. Yu, S. Zhang, F. Liu and W.-H. Zhang, *Org. Lett.*, 2019, **21**, 5096-5100.

38. F. P. Crisóstomo, T. Martín and R. Carrillo, *Angew. Chem. Int. Ed.*, 2014, **53**, 2181-2185.

39. W.-J. Yoo and S. Kobayashi, *Green Chem.*, 2014, **16**, 2438-2442.

40. S. Sato, T. Morikawa, T. Kajino and O. Ishitani, *Angew. Chem. Int. Ed.*, 2013, **52**, 988-992.

41. A. Mishra, M. K. R. Fischer and P. Bäuerle, *Angew. Chem. Int. Ed.*, 2009, **48**, 2474-2499.

42. G. S. Selopal, H.-P. Wu, J. Lu, Y.-C. Chang, M. Wang, A. Vomiero, I. Concina and E. W.-G. Diau, *Scientific Reports*, 2016, **6**, 18756.

43. H. Yi, C. Bian, X. Hu, L. Niu and A. Lei, *Chem. Commun.*, 2015, **51**, 14046-14049.

44. Y. Jin, L. Ou, H. Yang and H. Fu, *J. Am. Chem. Soc.*, 2017, **139**, 14237-14243.

45. Y. Zhang, D. Riemer, W. Schilling, J. Kollmann and S. Das, *ACS Catal.*, 2018, **8**, 6659-6664.

46. S. Cao, S. Zhong, L. Xin, J.-P. Wan and C. Wen, *ChemCatChem*, 2015, **7**, 1478-1482.

CHAPTER 2

C-H Mono-Nitration of Indolines using *tert*-Butyl Nitrite

2.1 ABSTRACT

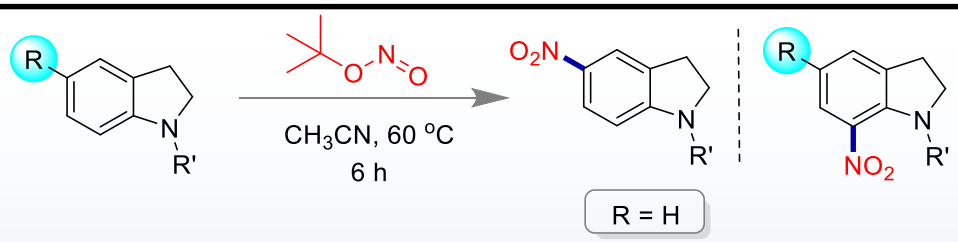

- *25 examples, up to 92 % yield*
- *metal free*
- *operationally simple*
- *excellent regioselectivity*
- *scalable*
- *mild condition*

A mild and regioselective C_5 or C_7 mono-nitration of indolines has been achieved by employing TBN (*tert*-butyl nitrite) as a sole nitrating agent in acetonitrile solvent within a reaction time of 6 h at 60 °C. The protocol excluded the use of any additive or external oxidant. Implementing this protocol a library of C_5- or C_7- mono-nitrated indolines has been synthesized. Excellent regioselectivity, good functional group tolerance, operational simplicity, and use of mild and metal-free reagent are the key advantages of this protocol.

2.2 INTRODUCTION

Nitro-group containing organic compounds are important synthetic blocks in synthetic chemistry. They furnish a wide array of potential applications in the areas fields of industries, pharmacology, agrochemicals, dyes, polymers, and so forth.[1, 2] So due to salient applications of nitro aryl moieties, the study of nitration chemistry has become an important topic over a century.[3] Moreover, nitro

functionalities are easily convertible into functional groups like amino, diazo, etc.[3, 4] In traditional synthesis, applying harsh reaction conditions[5], nitration reactions are carried out via aromatic electrophilic substitution by implementing reagents like HNO_3-H_2SO_4,[6] conc. HNO_3-mixed anhydrides,[7] nitronium tetrafluoroborate,[8] *N*-nitropyridinium salts, etc.[9] But these traditional method suffers from several drawbacks like lack of chemoselectivity, formation of a mixture of products, and chances of polynitration. Parallelly, template-based strategies involving transition metals have been introduced toward selective nitration reactions via aromatic electrophilic substitution. The notably used transition metals for selective C-H nitration reactions are Pd,[10] Fe,[11, 12] Rh,[13] Ru,[14,] etc. For instance, Maiti and co-workers introduced *ipso*-nitration reaction of aryl boronic acid using $Bi(NO_3)_3$ (Scheme 2.1).[15]

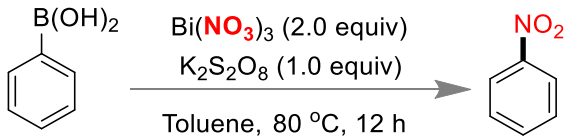

Scheme 2.1. Maiti's approach for *ipso*-nitration reaction of aryl boronic acid using $Bi(NO_3)_3$

Zhang's group disclosed Ru catalyzed C-H mono-nitration of arenes via ortho-metallation strategy (Scheme 2.2).[14]

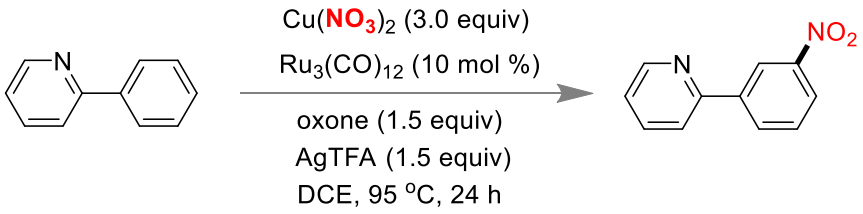

Scheme 2.2. Zhang's report on Ru-catalyzed C-H mono-nitration of arenes

Despite significant developments in transition-metal catalyzed C-H nitration, it holds disadvantages like the possibility of metal-toxicity, and contamination of metal into the product.

So the development of metal-free, mild, and greener protocols to replace toxic metal-based catalysts is always important and appreciable.

Over the last two decades, *tert*-Butyl Nitrite (TBN)[16-20] has emerged as an organic reagent with versatility and multitasking behavior.[21] This mild and metal-free reagent has been widely implemented for nitrosation,[22-24] oximation,[25] diazotization,[26], and miscellaneous applications. Parallelly, it is well recognized as an excellent mild nitrating agent. For instance, in 2009, Savinov's group reported regioselective nitration of phenols using TBN.[27] In 2013, Arns and co-workers disclosed TBN-mediated chemoselective nitration of aromatic sulfonamides.[28] Later, Hajra's group revealed regioselective C_7-nitration of 8-aminoquinoline amides using TBN as a nitro source.[29] Mal and co-workers introduced a weak interaction controlled strategy for regioselective mono-nitration of indolines using $Cu(NO_3)_2$ or $AgNO_3$ as a nitro source and $K_2S_2O_8$ as an oxidant (Scheme 2.3).[30]

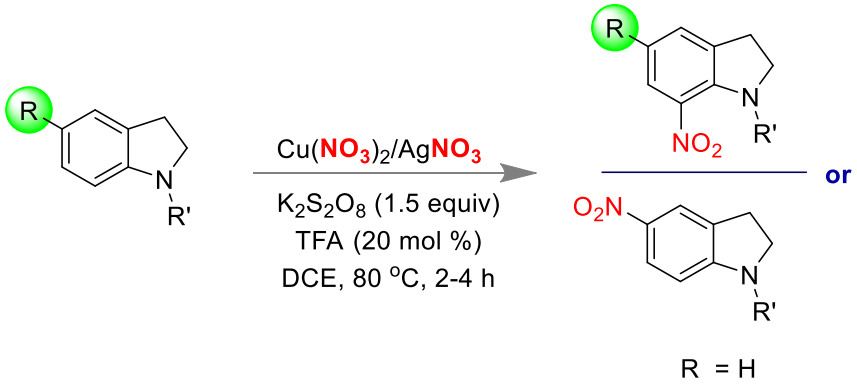

Scheme 2.3. Mal's approach for weak-interaction controlled mono-nitration of indolines

Next, our approach was to develop a mild and metal-free protocol for regioselective C_5-or C_7-mono-nitration of indolines using TBN as the sole nitrating reagent without using any additive, external oxidant, or metal catalyst (Figure 2.1).

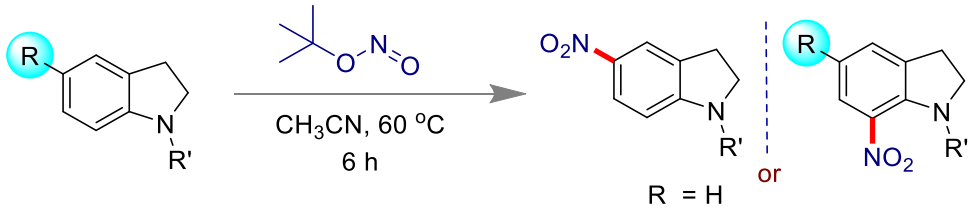

Figure 2.1. Our work on C_5-or C_7-mono-nitration of indolines using TBN

2.3 RESULT AND DISCUSSION

According to our hypothesis, we commenced our experiment with *N*-acetyl indoline (**1a**) as a model substrate to find the optimum condition for our reaction (Table 2.1). The reaction was performed with 1.5 equiv of TBN loading in DMSO solvent at 100 ^{o}C and after 6 h no product formation was observed (entry 1). Performing the reaction in solvents like DMF, EtOH, MeOH, and DCM also could not afford us any encouraging results (entry 2-5). When the reaction was performed in DCE at 70 ^{o}C with 1.5 equiv of TBN loading for 12 h reaction time; to our delight, our expected C_5-nitrated product (**2a**) was isolated with 59% yield (entry 6). Next, we executed the reaction in ACN at 80 ^{o}C for a reaction time of 12 hours; and the desired product was obtained with 80% yield (entry 7). Decreasing the amount of TBN loading, reaction temperature, and reaction time to 1.2 equiv, 60 ^{o}C, and 6 h respectively; resulted in the formation of **2a** with 92% yield (entry 8). After that, the reaction was executed at room temperature in ACN solvent for 12 hours and the formation of **2a** was experienced with 70% yield (entry 9). Furthermore, when the reaction was performed at 45 ^{o}C in ACN solvent; 83% of **2a** was afforded (entry 10). Next, we varied the amount of TBN loading to 1.1 equiv and 1.0 equiv respectively and as a result decrease in reaction yield was observed in both the cases (entry 11-12). So from the optimization study, the optimum condition for the reaction was experienced with 1.2 equiv of TBN loading in ACN at 60 ^{o}C with 6 h reaction period.

Table 2.1. Optimization of reaction conditions[a]

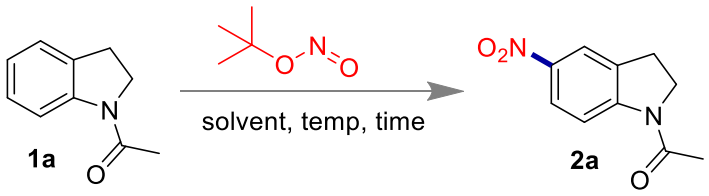

Entry	TBN (equiv)	Condition	Time (h)	Yield[b] (%)
1	1.5	DMSO, 100 ºC	6	NR[c]
2	1.5	DMF, 100 ºC	6	NR
3	1.5	EtOH, 80 ºC	6	NR
4	1.5	MeOH, 80 ºC	6	NR
5	1.5	DCM, RT	6	NR
6	1.5	DCE, 70 ºC	12	59
7	1.5	ACN, 80 ºC	12	80
8	**1.2**	**ACN, 60 ºC**	**6**	**92**
9	1.2	ACN, RT	12	70
10	1.2	ACN, 45 ºC	6	83
11	1.1	ACN, 60 ºC	6	76
12	1.0	ACN, 60 ºC	12	62

[a]Standard conditions: **1a** (0.248 mmol, 1.0 equiv), tert-butyl nitrite (0.297 mmol , 1.2 equiv) in 2 mL ACN was stirred at 60 ºC for 6 h. [b]Isolated yield. [c]No reaction.

Next, we explored the substrate scopes for the protocol with the achieved optimum condition (Figure 2.2). Substrates with N-acetyl, pivaloyl, and benzoyl protection, worked well under our optimum reaction condition and furnished the desired C_5-mono-nitrated products (**2a**-**2c**) in 68-92% yields. Indolines containing different sulfonyl protecting groups like tosyl, mesyl, benzene sulfonyl, and so forth delivered corresponding C_5-mono-nitrated products (**2d**-**2k**) in 65-84%

yields. Indolines with C_2 or C_3 substitution promptly participated in the reaction and the corresponding C_5-nitrated products (**2l-2p**) were obtained with 62-86% yields.

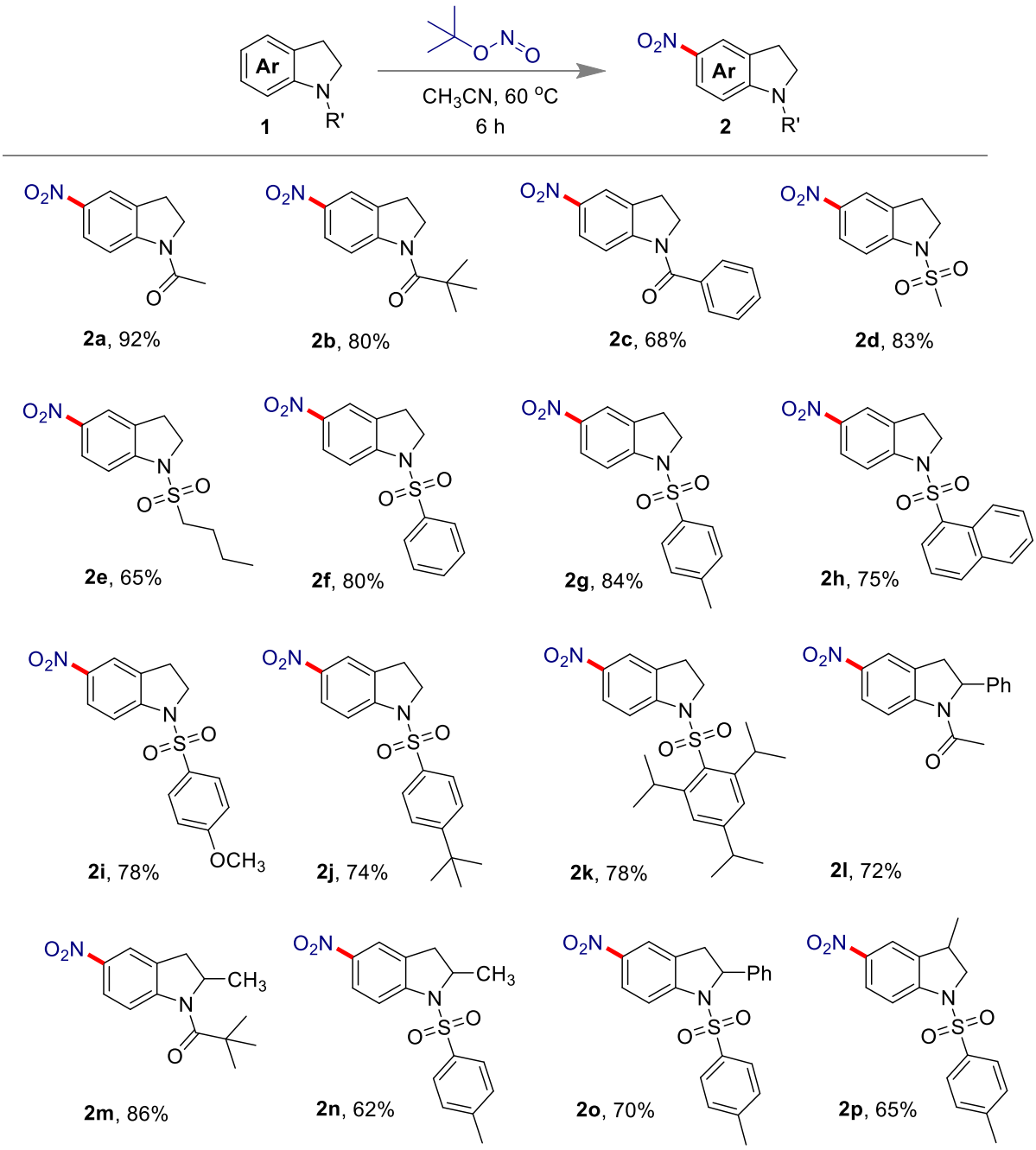

Figure 2.2. Scope for C_5-nitration of indolines

Next, we verified the scopes for C_7-nitration of indolines using starting compounds with blocked C_5-position (Figure 2.3). Indolines with electron-donating or electron-withdrawing at C_5-position underwent smooth conversion and provided C_7-nitrated products (**2q**-**2u**) in good yields.

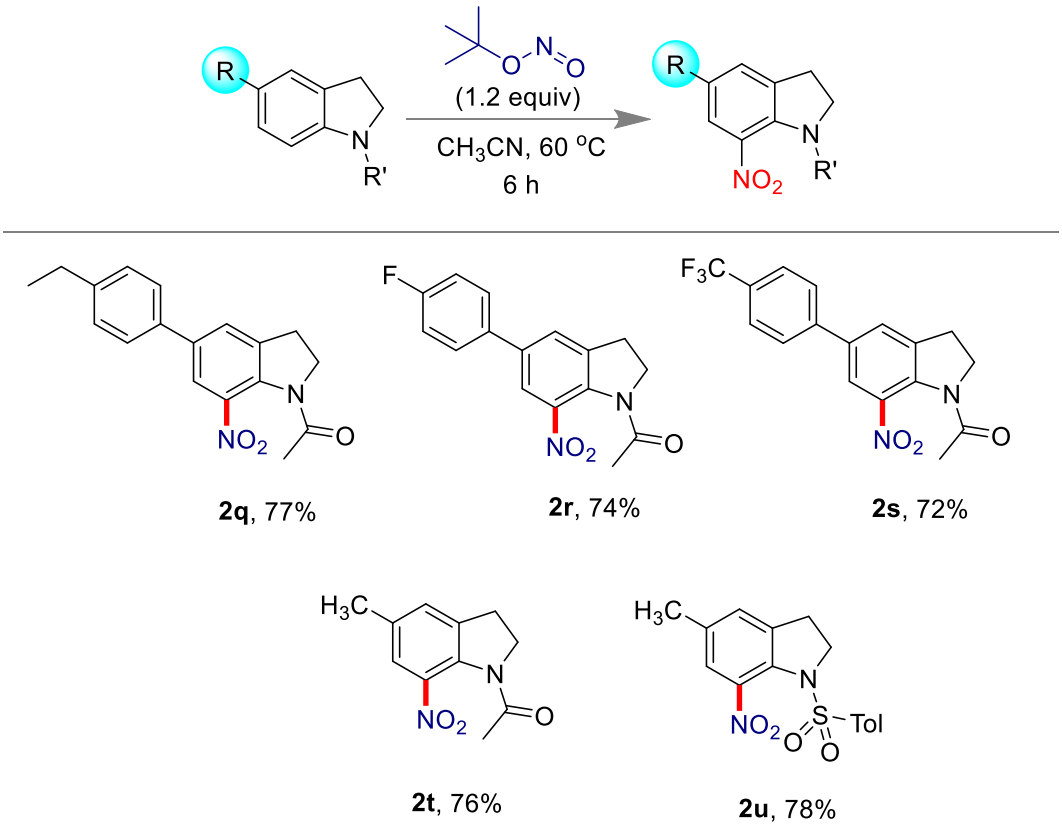

Figure 2.3. Scope for C_7-nitration on the C_5-substituted indolines.

To find the synthetic application of our protocol, the reaction was scaled up to 4.4 mmol and the desired product **2a** was isolated with 65% yield (Figure 2.4a).

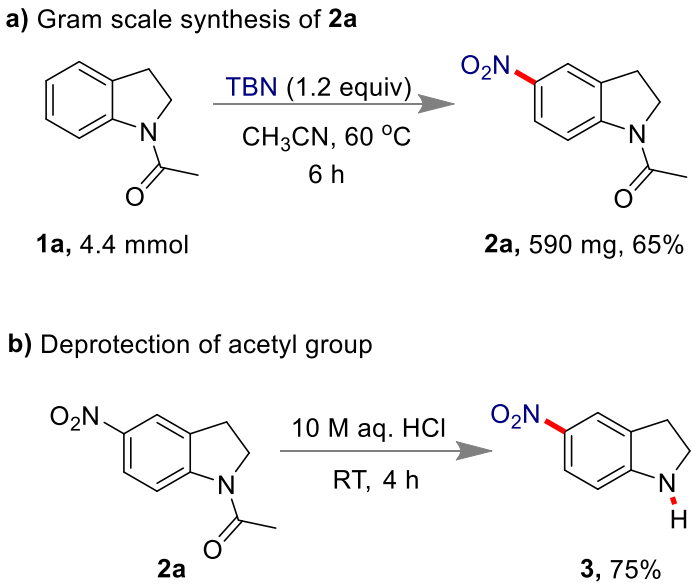

Figure 2.4. Synthetic applications.

Furthermore, deprotection of acetyl group of **2a** was carried out under an acidic medium, and the corresponding product 5-nitroindoline (**3**) was obtained within a 4 h reaction time in 75% yield (Figure 2.4b).

The radical scavenger experiments using 2,2,6,6-(tetramethylpiperidin-1-yl)oxyl (TEMPO) and butylated hydroxytoluene (BHT) were performed to understand the mechanism of the nitration protocol (Figure 2.5). The reaction was utterly hampered in the presence of TEMPO or BHT under optimum reaction conditions, indicating the involvement of a radical-mediated pathway in the reaction course.

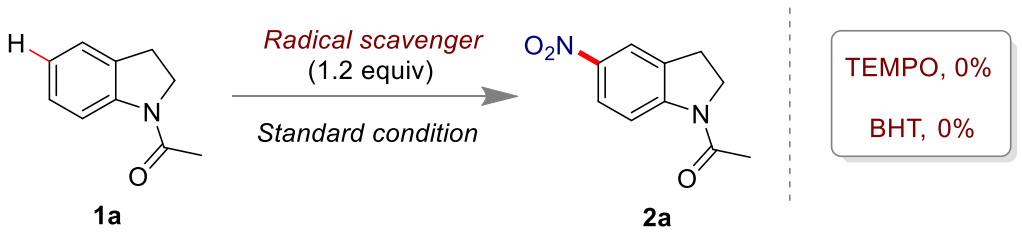

Figure 2.5. Control experiments with radical scavengers.

Based on literature reports and control experiments a tentative mechanism was depicted in (Figure 2.6). In the first step, due to homolytic cleavage under thermal condition; TBN generated *tert*-butyloxy radical and nitroso radical. Next, nitroso radical reacted with O_2 and resulted peroxynitrite radical intermediate (ONOO•) which then combined with another molecule of nitroso radical and led to the formation of unstable ONOONO intermediate. After that, unstable ONOONO intermediate promptly furnished nitro radicals through homolytic cleavage. Then *N*-protected indoline reacted with *tert*-butyloxy radical and furnished radical cation intermediate **5a** or **5a'.** Finally nitro radial reacted with **5a** or **5a'** to furnish **2** (C_5-nitrated product) and **2'** (C_7-nitrated product), respectively. The formation of **2** was more preferred over **2'** is possibly due to the effect of steric hindrance (Figure 2.6).

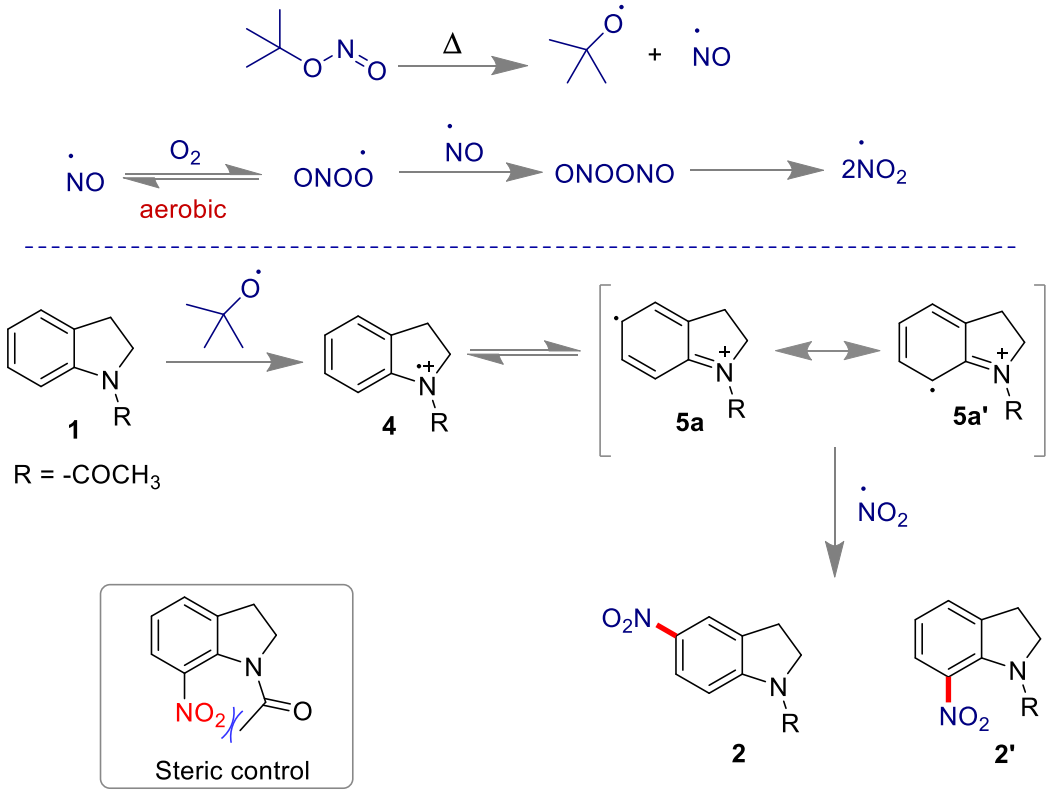

Figure 2.6. Plausible mechanism

2.4 CONCLUSION

In summary, we have developed a convenient protocol for regioselective C_5-or C_7-nitration of indolines by employing TBN as the sole nitrating agent. Applying this protocol, the use of any additive, external oxidant, or metal catalyst can be avoided. In addition, this protocol exhibits mild nature, scalability, operationally simplicity, and broad substrate scopes. We anticipate that this highly selective and efficient nitration methodology will offer direct access to various heterocyclic compounds of interest for applications in materials, making of complex molecules, and pharmaceutically important products.

2.5 EXPERIMENTAL SECTION

Instrumentation and Chemicals: Column chromatography was used for the purification of the compounds using silica gel (with mesh 100-200 or mesh 230-400) and hexane-ethyl acetate mixtures were used as eluent unless otherwise specified. Solvents were purchased from commercially available sources and used in the reaction without further purification. All NMR spectra were recorded in 400 MHz or 700 MHz instruments (Bruker) at room temperature (25 °C). The splitting of the NMR peaks (peak pattern) are represented by s: singlet; d: doublet; t: triplet; q: quartet; m: multiplet; dd: doublet of doublets; td: triplet of doublets; br s: broad singlet. Chemical shift values are reported in parts per million (ppm) with respect to residual trichloromethane (7.26 ppm for ^{1}H and 77.16 ppm for ^{13}C) and dimethyl sulfoxide (2.50 ppm for ^{1}H and 39.52 ppm for ^{13}C). The coupling constant values (*J*) are reported in hertz (Hz). A digital melting point apparatus was used to obtain the melting point of the compounds which were included in the characterization data without any correction. FT-IR spectra were recorded by making a thin film of the compounds on KBr pellets using dichloromethane and IR spectral data

are reported in wave number (cm^{-1}). High-resolution mass spectra (HR-MS) were recorded on an ESI-TOF (time of flight) mass spectrometer. The detailed procedure for the preparation of the starting materials and target molecule are described below.

Procedure for synthesis of 1-(5-Nitroindolin-1-yl)ethanone (2a). To an oven-dried sealed tube charged with a magnetic stirring bar and 1-(indolin-1-yl)ethanone (40 mg, 0.248 mmol, 1.0 equiv), *tert*-butyl nitrite (35 µL, 0.297 mmol, 1,2 equiv) in 2 mL acetonitrile solvent was stirred at 60 ºC for 6 h. After that, the reaction mixture was washed with dichloromethane and concentrated under reduced pressure. Purification through column chromatography (in 20% ethyl acetate/hexane) yielded 47 mg **2a** (92%).

Procedure for gram-scale synthesis: To an oven-dried sealed tube charged with a magnetic stirring bar and 1-(indolin-1-yl)ethanone (**1a**) (711 mg, 4.40 mmol, 1.0 equiv) , *tert*-butyl nitrite (630 µL, 5.28 mmol, 1.2 equiv) in 6.5 mL acetonitrile solvent was stirred at 60 ºC for 6 h. After 6 hours the reaction mixture was washed with dichloromethane and concentrated under reduced pressure and purification through column chromatography (in 20% ethyl acetate/hexane) yielded **2a** (590 mg, 65%).

Synthetic procedure of Nitro Indoline (3) (deprotection of acetyl group): In a round bottom flask, **2a** (45 mg, 0.218 mmol, 1.0 equiv) was taken and 2 mL of 10 M HCl was added to it. Then the mixture was allowed to stir at room temperature for 4 h. Then the reaction mixture was washed with 10% NaOH solution and the organic layer was extracted in dichloromethane, concentrated

under reduced pressure, and purification through column chromatography (30% ethyl acetate/hexane) yielded 5-nitro indoline[31] **3** in 75% yield (27 mg).

Synthesis of starting materials: Starting materials were prepared following the previous literature reported procedure.[31]

Synthetic Procedure for preparation of indolines from indoles: In a round bottom flask equipped with a magnetic stirring bar, 3-methyl indole (250 mg, 1.90 mmol, 1 equiv) was taken in 10 mL glacial acetic and cooled at 0 ^{o}C. Next $NaBH_3CN$ (716 mg, 11.4 mmol, 6.0 equiv) was added to it in small portions for 30 min and the temperature was maintained at 0 ^{o}C. After complete addition, the temperature was raised to room temperature and the reaction was continued for 3 h the progress of the reaction was monitored with TLC. After 3 h, the reaction mixture was quenched using 1 M NaOH solution at 0 ^{o}C. Next, the organic layer was extracted using DCM solvent. Finally, the collected organic layer was dried over Na_2SO_4 and concentrated under reduced pressure. Then we directly used the obtained crude product in the next step for *N*-protection.

Synthetic procedure for *N*-protected indolines: In a round bottom flask equipped with a magnetic stirring bar, indoline (200 mg, 1.68 mmol, 1.0 equiv) was taken in 10 mL dichloromethane and cooled at 0 ^{o}C. Next pyridine (173 mg, 2.18 mmol, 1.3 mmol) was added to it dropwise. Following, acetyl chloride (145 mg, 1.85 mmol, 1.1 equiv) was added to it dropwise manner and while adding the temperature was maintained at 0 ^{o}C. After that temperature was raised to room temperature and the reaction was continued for 2 h. After 2 h, the reaction was quenched with saturated NH_4Cl solution, and the organic layer was extracted with

dichloromethane. Then the combined organic layer was collected, dried over Na_2SO_4, and concentrated under reduced pressure. Finally, column purification of the crude mixture afforded the desired *N*-protected indoline.

Crystallographic Investigation

Good quality crystals for the compound **2h** were obtained by the slow evaporation of chloroform. The crystals data were collected with Bruker SMART D8 goniometer equipped with an APEX CCD detector and with an INCOATEC micro source (Cu-Kα radiation, λ = 0.71073 Å). SAINT+[32] and SADABS[33] were used to integrate the intensities and to correct the absorption respectively The structure was resolved by direct methods and refined on F^2 with SHELXL-97.[34]

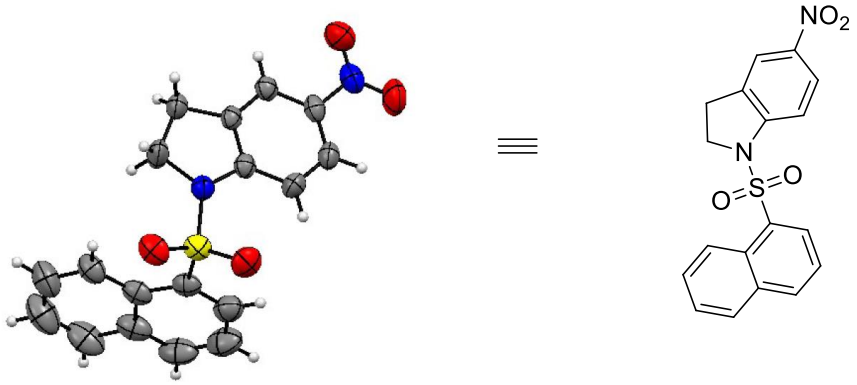

Fig. 2.7. Crystal structure of **2h**.

Crystallographic data for 2h.

CCDC number	1921496
Empirical formula	$C_{18}H_{14}N_2O_4S$
Formula weight	354.37
Temperature/K	298.88(12)
Crystal system	monoclinic

Space group	$P2_1/n$
a/Å	13.4846(2)
b/Å	7.53780(10)
c/Å	16.2029(3)
α/°	90
β/°	106.856(2)
γ/°	90
Volume/$Å^3$	1576.17(5)
Z	4
$\rho_{calc}g/cm^3$	1.493
μ/mm^{-1}	2.071
F(000)	736.0
Crystal size/mm^3	0.25 × 0.25 ×0.20
Radiation	CuKα (λ = 1.54184)
2Θ range for data collection/°	7.536 to 152.748
Index ranges	$-16 \leq h \leq 17$, $-9 \leq k \leq 9$, $-20 \leq l \leq 17$
Reflections collected	11881
Independent reflections	3259 [R_{int} = 0.0592, R_{sigma} = 0.0346]
Data/restraints/parameters	3259/0/226
Goodness-of-fit on F^2	1.088
Final R indexes [I>=2σ (I)]	R_1 = 0.0568, wR_2 = 0.1657
Final R indexes [all data]	R_1 = 0.0598, wR_2 = 0.1687
Largest diff. peak/hole / e $Å^{-3}$	0.23/-0.57

1-(5-Nitroindolin-1-yl)ethanone (2a).[31] R_f = 0.3 (20% ethyl acetate/hexane); yellow solid; yield 47 mg (92%); mp: 170-172 ºC; ^{1}H NMR (400 MHz, $CDCl_3$) δ 8.29 (d, *J* = 8.4 Hz, 1H), 8.12 (d, *J* = 8.4 Hz, 1H), 8.04 (s, 1H), 4.19 (t, *J* = 8.4 Hz, 2H), 3.29 (t, *J* = 8.4 Hz, 2H), 2.28 (s, 3H); ^{13}C

NMR (100 MHz, $CDCl_3$) δ 168.9, 143.0, 131.2, 127.6, 124.6, 123.7, 117.1, 48.9, 28.1, 24.3; IR (KBr) ϑ 3015, 2967, 1772, 1692, 1349, 1083, 792, 655 cm^{-1}.

2,2-dimethyl-1-(5-nitroindolin-1-yl)propan-1-one (2b).[31] R_f = 0.5 (25% ethyl acetate/hexane); light yellow solid; yield 165 mg (80%); mp: 122-124 ºC; ^1H NMR (400 MHz, $CDCl_3$) δ 8.28 (d, *J* = 9.2 Hz, 1H), 8.07 (dd, *J* = 9.2, 2.4 Hz, 1H), 8.00 (s, 1H), 4.35 (t, *J* = 8.4 Hz, 2H), 3.22 (t, *J* = 8.4 Hz, 2H), 1.37 (s, 9H); ^{13}C NMR (175 MHz, $CDCl_3$) δ 177.6, 150.5, 143.5, 132.1, 124.5, 120.0, 117.7, 50.3, 40.7, 28.7, 27.6; IR (KBr) ϑ 3032, 2953, 2861, 2742, 2512, 1653, 1322, 1055, 759 cm^{-1}.

5-Nitroindolin-1-yl(phenyl)methanone (2c).[31] R_f = 0.3 (20% ethyl acetate/hexane); yellow solid; yield 65 mg (68%); mp: 201-203 ºC; ^1H NMR (400 MHz, $CDCl_3$) δ 8.08 (s, 2H), 7.57 (d, *J* = 7.2 Hz, 2H), 7.54-7.46 (m, 3H), 4.19 (t, *J* = 8.4 Hz, 2H), 3.21 (t, *J* = 8.4 Hz, 2H); ^{13}C NMR (175 MHz, $CDCl_3$) δ 169.8, 148.5, 143.9, 136.0, 133.7, 131.2, 128.9, 127.2, 124.4, 120.7, 116.4, 51.4, 27.7; IR (KBr) ϑ 3050, 2990, 1790, 1530, 1325, 1025, 790, 680 cm^{-1}.

1-(Methylsulfonyl)-5-nitroindoline (2d).[31] R_f = 0.4 (25% ethyl acetate/hexane); light yellow solid; yield 64 mg (83%); mp: 137-139 ºC; ^1H NMR (400 MHz, $CDCl_3$) δ 8.13 (dd, *J* = 8.8, 1.6 Hz, 1H), 8.07 (s, 1H), 7.46 (d, *J* = 8.8 Hz, 1H), 4.13 (t, *J* = 8.4 Hz, 2H), 3.26 (t, *J* = 8.4 Hz, 2H), 2.99 (s, 3H); ^{13}C NMR (175 MHz, $CDCl_3$) δ 147.7, 143.9, 132.4, 125.2, 121.4, 112.5, 51.0, 36.3, 27.3; IR (KBr) ϑ 2850, 1540, 1363, 1035, 850, 752 cm^{-1}.

1-(Butylsulfonyl)-5-nitroindoline (2e). R_f = 0.3 (20% ethyl acetate/hexane); yellow solid; yield 66 mg (65%); mp: 110-112 ºC; ^{1}H NMR (400 MHz, $CDCl_3$) δ 8.12 (dd, *J* = 8.8, 2.0 Hz, 1H), 8.06 (s, 1H), 7.43 (d, *J* = 8.8 Hz, 1H), 4.16 (t, *J* = 8.4 Hz, 2H), 3.25 (t, *J* = 8.4 Hz, 2H), 3.15 – 3.10 (m, 2H), 1.88 – 1.80 (m, 2H), 1.50 – 1.40 (m, 2H), 0.93 (t, *J* = 7.2 Hz, 3H); ^{13}C NMR (175 MHz, $CDCl_3$) δ 148.0, 143.5, 132.2, 125.1, 121.4, 112.3, 51.0, 50.5, 27.3, 25.0, 21.7, 13.6; IR (KBr) ῡ 2930, 1625, 1545, 1370, 1090, 825, 735 cm^{-1}; HRMS (ESI-TOF) calcd for $C_{12}H_{17}N_2O_4S$ $[M+H]^+$ 285.0904, found 285.0877.

5-Nitro-1-(phenylsulfonyl)indoline (2f).[35] R_f = 0.4 (20% ethyl acetate/hexane); brown solid; yield 75 mg (80%); mp: 160-162 ºC; ^{1}H NMR (400 MHz, $CDCl_3$) δ 8.11 (dd, *J* = 8.8, 2.0 Hz, 1H), 7.94 (d, *J* = 0.8 Hz, 1H), 7.86 – 7.83 (m, 2H), 7.69 (d, *J* = 9.2 Hz, 1H), 7.62 (t, *J* = 7.6 Hz, 1H), 7.51 (t, *J* = 8.0 Hz, 2H), 4.04 (t, *J* = 8.8 Hz, 2H), 3.08 (t, *J* = 8.8 Hz, 2H); ^{13}C NMR (175 MHz, $CDCl_3$) δ 147.7, 143.8, 136.7, 134.1, 132.7, 129.6, 127.2, 124.9, 121.2, 113.3, 50.6, 27.2; IR (KBr) ῡ 3065, 2920, 1632, 1560, 1330, 1055, 945, 865, 740 cm^{-1}.

5-Nitro-1-tosylindoline (2g).[31] R_f = 0.3 (20% ethyl acetate/hexane); light yellow solid; yield 93 mg (84%); mp: 172-174 ºC; ^{1}H NMR (400 MHz, $CDCl_3$) δ 8.10 (dd, *J* = 8.8, 2.0 Hz, 1H), 7.94 (s, 1H), 7.72 (d, *J* = 8.4 Hz, 2H), 7.67 (d, *J* = 8.8 Hz, 1H), 7.29 (d, *J* = 8.4 Hz, 2H), 4.03 (t, *J* = 8.8 Hz, 2H), 3.07 (t, *J* = 8.8 Hz, 2H), 2.39 (s, 3H); ^{13}C NMR (175 MHz, $CDCl_3$) δ 147.8, 145.1, 143.7, 133.7, 132.7, 130.2, 127.3, 124.9, 121.1, 113.3, 50.6, 27.2, 21.7; IR (KBr) ῡ 2970, 1545, 1570, 1323, 1036, 990, 832 cm^{-1}.

1-(Naphthalen-1-ylsulfonyl)-5-nitroindoline (2h). R_f =0.6 (20% ethyl acetate hexane); brown solid, yield 70 mg (75%); mp: 170-172 ºC; ^{1}H NMR (400 MHz, $CDCl_3$) δ 8.65 (d, *J* = 7.6 Hz, 1H), 8.29 (d, *J* = 7.6 Hz, 1H), 8.14 – 8.07 (m, 2H), 7.97 – 7.92 (m, 2H), 7.63-7.55 (m,4H), 4.15 (t, *J* = 8.8 Hz, 2H), 3.07 (t, *J* = 8.8 Hz, 2H); ^{13}C NMR (175MHz, $CDCl_3$) δ 148.1, 143.6, 135.5, 134.6, 133.3, 132.3, 130.2, 129.3, 128.9, 128.8, 127.4, 124.9, 124.4, 124.3, 121.2, 113.2, 50.9, 27.3; IR (KBr) ῡ 3025, 2908, 1655, 1550, 1295, 1065, 762 cm^{-1}; HRMS (ESI-TOF) calcd for $C_{18}H_{15}N_2O_4S$ $[M+H]^+$ 355.0747, found 355.0705.

1-((4-Methoxyphenyl)sulfonyl)-5-nitroindoline (2i). R_f = 0.4 (30% ethyl acetate1/hexane) yellow solid; yield 57 mg (78%); mp: 168-170 ºC; ^{1}H NMR (400 MHz, $CDCl_3$) δ 8.12 (dd, *J* = 8.8, 2.0 Hz, 1H), 7.95 (s, 1H), 7.78 (d, *J* = 8.8 Hz, 2H), 7.68 (d, *J* = 9.2 Hz, 1H), 6.95 (d, *J* = 8.8 Hz, 2H), 4.02 (t, *J* = 8.8 Hz, 2H), 3.84 (s, 3H), 3.07 (t, *J* = 8.8 Hz, 2H); ^{13}C NMR (100 MHz, $CDCl_3$) δ 164.0, 147.9, 143.7, 132.7, 129.5, 128.2, 124.9, 121.2, 114.7, 113.2, 55.8, 50.6, 27.2; IR (KBr) ῡ 2965, 1673, 1568, 1228, 1013, 883, 662 cm^{-1}; HRMS (ESI-TOF) calcd for $C_{15}H_{15}N_2O_5S$ $[M+H]^+$ 335.0696, found 335.0666.

1-((4-(tert-butyl)phenyl)sulfonyl)-5-nitroindoline (2j). R_f = 0.3 (20% ethyl acetate/hexane); yellow solid; yield 81 mg (74%); mp: 165-167 ºC; ^{1}H NMR (700 MHz, $CDCl_3$) δ 8.11 (dd, *J* = 9.1, 2.1 Hz, 1H), 7.95 (s, 1H), 7.76 (d, *J* = 8.4 Hz, 2H), 7.69 (d, *J* = 9.1 Hz, 1H), 7.50 (d, *J* = 8.4 Hz, 2H), 4.04 (t, *J* = 9.1 Hz, 2H), 3.09 (t, *J* = 9.1 Hz, 2H), 1.30 (s, 9H); ^{13}C NMR (175 MHz, $CDCl_3$) δ 158.0, 147.9, 143.7, 133.7, 132.6, 127.2, 126.6, 124.9, 121.2, 113.1, 50.5, 35.4, 31.1, 27.2; IR (KBr) ῡ 3070, 1554, 1362, 1132, 1085, 790 cm^{-1}; HRMS (ESI-TOF) calcd for $C_{18}H_{20}N_2O_4SNa$ $[M+Na]^+$ 383.1036, found 383.1022.

5-Nitro-1-((2,4,6-triisopropylphenyl)sulfonyl)indoline (2k). R_f = 0.4 (30% ethyl aetate/hexane); yield 77 mg (78%); yellow solid; yield 79 mg (78%); mp: 150-152 ºC; ^{1}H NMR (400 MHz, $CDCl_3$) δ 8.08 – 8.05 (m, 1H), 8.01 (s, 1H), 7.34 (d, *J* = 8.8 Hz, 1H), 7.21 (s, 2H), 4.14-4.08 (m, 2H), 3.96 (t, *J* = 8.8 Hz, 2H), 3.15 (t, *J* = 8.8 Hz, 2H), 2.96-2.87 (m, 1H), 1.26 (d, *J* = 6.8 Hz, 6H), 1.20 (d, *J* = 6.8 Hz, 12H); ^{13}C NMR (175 MHz, $CDCl_3$) δ 154.5, 151.6, 148.8, 143.1, 131.8, 130.9, 124.9, 124.4, 121.1, 112.4, 49.9, 34.3, 29.5, 27.3, 24.7, 23.6; IR (KBr) ῡ 3020, 2880, 1640, 1510, 1355, 1072, 662 cm^{-1}; HRMS (ESI-TOF) calcd for $C_{23}H_{31}N_2O_4S$ $[M+H]^+$ 431.1999, found 431.1972.

1-(5-Nitro-2-phenylindolin-1-yl)ethanone (2l). R_f = 0.5 (30% ethyl acetate/hexane); yellow liquid; yield 60 mg (72%); ^{1}H NMR (400 MHz, $CDCl_3$) δ 8.20 (d, *J* = 8.8 Hz, 1H), 8.01 (s, 1H), 7.38 – 7.26 (m, 4H), 7.13 (d, *J* = 7.2 Hz, 2H), 5.51 (d, *J* = 9.2 Hz, 1H), 3.84 (dd, *J* = 16.4, 10.4 Hz, 1H), 3.08 (d, *J* = 16.4 Hz, 1H), 2.08 (s, 3H); ^{13}C NMR (175 MHz, $CDCl_3$) δ 170.5, 148.7, 144.2, 142.1, 129.6, 128.5, 125.1, 124.9, 120.8, 116.3, 64.5, 38.4, 24.4; IR (KBr) ῡ 2973, 2745, 2538, 1612, 1531, 1038, 705 cm^{-1}; HRMS (ESI-TOF) calcd for $C_{16}H_{15}N_2O_3$ $[M+H]^+$ 283.1077, found 283.1086.

2,2-Dimethyl-1-(2-methyl-5-nitroindolin-1-yl)propan-1-one (2m).[31] R_f = 0.6 (10% ethyl acetate/hexane); off white solid; yield 76 mg (86%); mp: 160-162 ºC; ^{1}H NMR (400 MHz, $CDCl_3$) δ 8.21 (d, *J* = 8.8 Hz, 1H), 8.17 – 8.12 (m, 1H), 8.09 (s, 1H), 5.01 – 4.93 (m, 1H), 3.37 (dd, *J* = 15.6, 7.6 Hz, 1H), 2.72 (d, *J* = 15.6 Hz, 1H), 1.40 (s, 9H), 1.30 (d, *J* = 6.3 Hz, 3H); ^{13}C NMR (175 MHz, $CDCl_3$) δ 177.4, 149.1, 143.9, 132.0, 124.4, 120.7, 118.7, 57.3, 41.2, 36.5, 28.5, 22.1; IR (KBr) ῡ 3105, 2935, 2854, 1516, 1352, 1129, 1046, 772 cm^{-1}.

2-Methyl-5-nitro-1-tosylindoline (2n).[36] R_f = 0.5 (20% ethyl acetate/hexane); yellow solid; yield 80 mg (62%); mp: 148-150 ºC; ^{1}H NMR (400 MHz, $CDCl_3$) δ 8.11 (dd, *J* = 9.2, 2.4 Hz, 1H), 7.92 (s, 1H), 7.69 (d, *J* = 9.2 Hz, 1H), 7.63 (d, *J* = 8.4 Hz, 2H), 7.23 (d, *J* = 8.4 Hz, 2H), 4.52-4.44 (m,1H), 3.11 (dd, *J* = 16.4, 9.6 Hz, 1H), 2.62 (dd, *J* = 16.4, 3.2 Hz, 1H), 2.37 (s, 3H), 1.49 (d, J = 6.4 Hz, 3H); ^{13}C NMR (175 MHz, $CDCl_3$) δ 147.1, 144.8, 144.4, 135.2, 132.3, 130.1, 126.9, 124.7, 121.3, 115.3, 59.8, 35.9, 23.6, 21.7; IR (KBr) ῡ 2965, 2725, 2535, 1612, 1526, 1395, 1237, 953 cm^{-1}.

5-Nitro-2-phenyl-1-tosylindoline (2o). R_f = 0.4 (20% ethyl acetate/hexane); yellow liquid; yield 55 mg (70%); ^{1}H NMR (400 MHz, $CDCl_3$) δ 8.18 (d, *J* = 8.8 Hz, 1H), 7.96 (s, 1H), 7.72 (d, *J* = 8.8 Hz, 1H), 7.50 (d, *J* = 8.4 Hz, 2H), 7.30-7.26 (m, 5H), 7.17 (d, *J* = 8.4 Hz, 2H), 5.49 (dd, *J* = 10.4, 3.2 Hz, 1H), 3.54 (dd, *J* = 16.4, 10.4 Hz, 1H), 3.04 (dd, *J* = 16.4, 3.2 Hz, 1H), 2.37 (s, 3H); ^{13}C NMR (100 MHz, $CDCl_3$) δ 144.8, 141.7, 135.3, 131.90, 131.8, 129.9, 129.0, 128.4, 127.2, 126.2, 125.1, 121.2, 114.3, 66.2, 37.8, 21.7; IR (KBr) ῡ 3018, 2695, 2433, 1590, 1433, 968, 672 cm^{-1}; HRMS (ESI-TOF) calcd for $C_{21}H_{19}N_2O_4S$ $[M+H]^+$ 395.1060, found 395.1075.

3-Methyl-5-nitro-1-tosylindoline (2p). R_f = 0.3 (20% ethyl acetate/hexane); brown solid; yield 43 mg (65%); mp: 124-126 ºC; ^{1}H NMR (400 MHz, $CDCl_3$) δ 8.12 (dd, *J* = 8.8, 2.0 Hz, 1H), 7.92 (d, *J* = 0.8 Hz, 1H), 7.72 (d, *J* = 8.0 Hz, 2H), 7.68 (d, *J* = 8.8 Hz, 1H), 7.29 (d, *J* = 8.0 Hz, 2H), 4.18 (t, *J* = 10.0 Hz, 1H), 3.54 (dd, *J* = 10.0, 6.8 Hz, 1H), 3.40 – 3.30 (m, 1H), 2.39 (s, 3H), 1.22 (d, *J* = 7.2 Hz, 3H); ^{13}C NMR (100 MHz, $CDCl_3$) δ 147.3, 145.2, 144.0, 137.8, 133.7, 130.2, 127.3,

125.1, 120.2, 113.5, 58.1, 34.2, 21.7, 19.7; IR (KBr) ῡ 3035, 2865, 2560, 1662, 1524, 1022, 714 cm^{-1}; HRMS (ESI-TOF) calcd for $C_{16}H_{17}N_2O_4S$ $[M+H]^+$ 333.0904, found 333.0911.

1-(5-(4-Ethylphenyl)-7-nitroindolin-1-yl)ethanone (2q).[31] R_f = 0.5 (20% ethyl acetate hexane); yellow solid; yield 18 mg (77%); mp: 140-142 ºC; ^{1}H NMR (400 MHz, $CDCl_3$) δ 7.84 (s, 1H), 7.62 (s, 1H), 7.47 (d, *J* = 8.4 Hz, 2H), 7.28 (d, *J* = 8.4 Hz, 2H), 4.27 (t, *J* = 8.0 Hz, 2H), 3.27 (t, *J* = 8.0 Hz, 2H), 2.70 (q, *J* = 7.6 Hz, 2H), 2.28 (s, 3H), 1.26 (t, *J* = 7.6 Hz, 3H); ^{13}C NMR (175 MHz, $CDCl_3$) δ 168.5, 144.6, 141.2, 138.5, 137.2, 136.1, 133.4, 128.8, 126.9, 126.9, 121.3, 50.4, 29.3, 28.7, 23.4, 15.7; IR (KBr) ῡ 2937, 2825, 2558, 1561, 1337, 1027, 715 cm^{-1}.

1-(5-(4-Fluorophenyl)-7-nitroindolin-1-yl)ethanone (2r).[31] R_f = 0.5 (15% ethyl acetate/hexane); yellow solid; yield 20 mg (74%); mp: 150-152 ºC; ^{1}H NMR (400 MHz, $CDCl_3$) δ 7.80 (s, 1H), 7.59 (s, 1H), 7.53-7.50 (m, 2H), 7.14 (t, *J* = 8.8 Hz, 2H), 4.28 (t, *J* = 8.0 Hz, 2H), 3.28 (t, *J* = 8.0 Hz, 2H), 2.29 (s, 3H); ^{13}C NMR (175 MHz, $CDCl_3$) δ 168.6, 163.0 (d, $^1J_{C\text{-}F}$ = 248 Hz), 141.2, 137.4, 135.0 (d, $^4J_{C\text{-}F}$ = 3.3 Hz), 128.8, 128.7, 128.1 (d, $^3J_{C\text{-}F}$ = 8 Hz), 127.0, 121.4, 116.2 (d, $^2J_{C\text{-}F}$ = 22 Hz), 50.4, 29.2, 23.4; IR (KBr) ῡ 2928, 2911, 2214, 1632, 1509, 1202, 1151, 805, 711 cm^{-1}.

1-(7-Nitro-5-(4-(trifluoromethyl)phenyl)indolin-1-yl)ethanone (2s). R_f = 0.2 (30% ethyl acetate/hexane); yield 41 mg (72%); mp: 190-192 ºC; ^{1}H NMR (400 MHz, $CDCl_3$) δ 7.86 (s, 1H), 7.71 (d, *J* = 8.4 Hz, 2H), 7.66 (d, *J* = 8.0 Hz, 3H), 4.30 (t, *J* = 8.0 Hz, 2H), 3.31 (t, *J* = 8.0 Hz, 2H), 2.30 (s, 3H); ^{13}C NMR (175 MHz, $CDCl_3$) δ 168.6, 142.2, 141.1, 137.8, 136.6, 134.4, 130.2 (q, $^2J_{C\text{-}F}$ = 32 Hz), 127.3, 127.2, 126.2 (q, $^3J_{C\text{-}F}$ = 3.6 Hz), 124.2 (q, $^1J_{C\text{-}F}$ = 272 Hz), 121.7, 50.4, 29.1,

23.4; IR (KBr) ῡ 2918, 2810, 2341, 1694, 1538, 1322, 1216, 1012, 931, 749 cm^{-1}; HRMS (ESI-TOF) calcd for $C_{17}H_{13}F_3N_2O_3Na$ $[M+Na]^+$ 373.0770, found 373.0750.

1-(5-Methyl-7-nitroindolin-1-yl)ethanone (2t). R_f = 0.3 (50% ethyl aetate/hexane); yellow solid; yield 70 mg (76%); mp: 175-177 ºC; ^{1}H NMR (400 MHz, $CDCl_3$) δ 7.40 (s, 1H), 7.21 (s, 1H), 4.19 (t, *J* = 8.0 Hz, 2H), 3.15 (t, *J* = 8.0 Hz, 2H), 2.34 (s, 3H), 2.21 (s, 3H); ^{13}C NMR (100 MHz, $CDCl_3$) δ 168.4, 140.6, 136.7, 135.0, 132.2, 129.6, 122.7, 50.2, 29.1, 23.3, 20.8; IR (KBr) ῡ 2935, 2840, 2625, 1531, 1325, 1032, 621 cm^{-1}; HRMS (ESI-TOF) calcd for $C_{11}H_{13}N_2O_3$ $[M+H]^+$ 243.0740, found 243.0746.

5-Methyl-7-nitro-1-tosylindoline (2u). R_f = 0.6 (20% ethyl acetate/hexane); yellow solid; yield 74 mg (78%); mp: 172-174 ºC; ^{1}H NMR (700 MHz, $CDCl_3$) δ 7.57 (d, *J* = 8.4 Hz, 3H), 7.25 (d, *J* = 8.4 Hz, 2H), 7.17 (s, 1H), 4.04 (t, *J* = 7.7 Hz, 2H), 2.56 (t, *J* = 7.7 Hz, 2H), 2.42 (s, 3H), 2.40 (s, 3H); ^{13}C NMR (175 MHz, $CDCl_3$) δ 144.8, 142.4, 139.9, 137.5, 134.5, 132.9, 130.0,129.9, 127.8, 123.9, 52.1, 29.1, 21.7, 21.0; IR (KBr) ῡ 2855, 2530, 1553, 1315, 1073, 931, 791 cm^{-1}; HRMS (ESI-TOF) calcd for $C_{16}H_{17}N_2O_4S$ $[M+H]^+$ 333.0904, found 333.0903.

5-Nitroindoline (3).[31] orange solid; yield 27 mg (75%); mp: 86-88 ºC; ^{1}H NMR (400 MHz, $CDCl_3$) δ 7.97 (dd, *J* = 8.8, 1.6 Hz, 1H), 7.92 (s, 1H), 6.46 (d, *J* = 8.8 Hz, 1H), 4.60 (s, 1H), 3.75 (t, *J* = 8.4 Hz, 2H), 3.10 (t, *J* = 8.4 Hz, 2H); ^{13}C NMR (100 MHz, $CDCl_3$) δ 157.6, 139.3,129.1, 126.2, 121.1, 106.2, 47.4, 28.4; IR (KBr) 3145, 2892, 2531, 1653, 1584, 1061, 819, 721, 634 cm^{-1}.

2.6 NOTES AND REFERENCES

1. K. Nepali, H.-Y. Lee and J.-P. Liou, *J. Med. Chem.*, 2019, **62**, 2851-2893.
2. P. Li and X. Jia, *Synthesis*, 2018, **50**, 711-722.
3. G. Booth, in *"Nitro Compounds, Aromatic" in Ullmann's Encyclopedia of Industrial Chemistry*, Wiley-VCH, Weinheim, 2000, vol. 24.
4. N. Ono, in *The Nitro Group in Organic Synthesis*, John Wiley & Sons, Inc., 2002, DOI: 10.1002/0471224480.ch6, pp. 159-181.
5. N. Ono, in *The Nitro Group in Organic Synthesis*, John Wiley & Sons, Inc., 2002, DOI: 10.1002/0471224480.ch2, pp. 3-29.
6. G. Koleva, B. Galabov, B. Hadjieva, H. F. Schaefer and P. v. R. Schleyer, *Angew. Chem. Int. Ed.*, 2015, **54**, 14123-14127.
7. G. Aridoss and K. K. Laali, *J. Org. Chem.*, 2011, **76**, 8088-8094.
8. G. A. Olah, A. Orlinkov, A. B. Oxyzoglou and G. K. S. Prakash, *J. Org. Chem.*, 1995, **60**, 7348-7350.
9. G. A. Olah, S. C. Narang, J. A. Olah and K. Lammertsma, *Proc. Natl. Acad. Sci. U. S. A.*, 1982, **79**, 4487-4494.
10. Y.-F. Liang, X. Li, X. Wang, Y. Yan, P. Feng and N. Jiao, *ACS Catal.*, 2015, **5**, 1956-1963.
11. Y. He, N. Zhao, L. Qiu, X. Zhang and X. Fan, *Org. Lett.*, 2016, **18**, 6054-6057.
12. V. Botla, D. V. Ramana, B. Chiranjeevi and M. Chandrasekharam, *ChemistrySelect*, 2016, **1**, 3974-3978.
13. F. Xie, Z. Qi and X. Li, *Angew. Chem. Int. Ed.*, 2013, **52**, 11862-11866.
14. Z. Fan, J. Ni and A. Zhang, *J. Am. Chem. Soc.*, 2016, **138**, 8470-8475.
15. S. Manna, S. Maity, S. Rana, S. Agasti and D. Maiti, *Org. Lett.*, 2012, **14**, 1736-1739.

16. S. Maity, T. Naveen, U. Sharma and D. Maiti, *Org. Lett.*, 2013, **15**, 3384-3387.

17. S. Mondal, S. Samanta and A. Hajra, *Adv. Synth. Catal.*, 2018, **360**, 1026-1031.

18. T. Taniguchi, A. Yajima and H. Ishibashi, *Adv. Synth. Catal.*, 2011, **353**, 2643-2647.

19. P. Chaudhary, S. Gupta, N. Muniyappan, S. Sabiah and J. Kandasamy, *J. Org. Chem.*, 2019, **84**, 104-119.

20. B. Kilpatrick, M. Heller and S. Arns, *Chem. Commun.*, 2013, **49**, 514-516.

21. A. Dahiya, A. K. Sahoo, T. Alam and B. K. Patel, *Chem. Asian J.*, 2019, **14**, 4454-4492.

22. P. Chaudhary, S. Gupta, N. Muniyappan, S. Sabiah and J. Kandasamy, *Green Chem.*, 2016, **18**, 2323-2330.

23. S. L. Yedage and B. M. Bhanage, *J. Org. Chem.*, 2017, **82**, 5769-5781.

24. K. Monir, M. Ghosh, S. Jana, P. Mondal, A. Majee and A. Hajra, *Org. Biomol. Chem.*, 2015, **13**, 8717-8722.

25. S. Prateeptongkum, I. Jovel, R. Jackstell, N. Vogl, C. Weckbecker and M. Beller, *Chem. Commun.*, 2009, DOI: 10.1039/b900326f, 1990-1992.

26. G. C. Senadi, B. S. Gore, W. P. Hu and J. J. Wang, *Org. Lett.*, 2016, **18**, 2890-2893.

27. D. Koley, O. C. Colón and S. N. Savinov, *Org. Lett.*, 2009, **11**, 4172-4175.

28. B. Kilpatrick, M. Heller and S. Arns, *Chem. Commun.*, 2013, **49**, 514-516.

29. S. Mondal, S. Samanta and A. Hajra, *Adv. Synth. Catal.*, 2018, **360**, 1026-1031.

30. A. Bose and P. Mal, *Chem. Commun.*, 2017, **53**, 11368-11371.

31. A. Bose and P. Mal, *Chem. Commun.*, 2017, **53**, 11368-11371.

32. SAINT+, Bruker AXS Inc., Madison, Wisconsin, USA, 1999 (Program for Reduction of Data collected on Bruker CCD Area Detector Diffractometer V. 6.02.)

33. SADABS, Bruker AXS, Madison, Wisconsin, USA, 2004

34. G. Sheldrick, *Acta Crystallogr. Sect. A*, 2008, **64**, 112-122.

35. K. Pandya, D. Dietrich, J. Seibert, J. C. Vederas and A. Odermatt, *Biorg. Med. Chem.*, 2013, **21**, 6274-6281.

36. Y. Yin and G. Zhao, *J. Fluorine Chem.*, 2007, **128**, 40-45.

Copies of ^{1}H and ^{13}C NMR Spectra of selected compounds

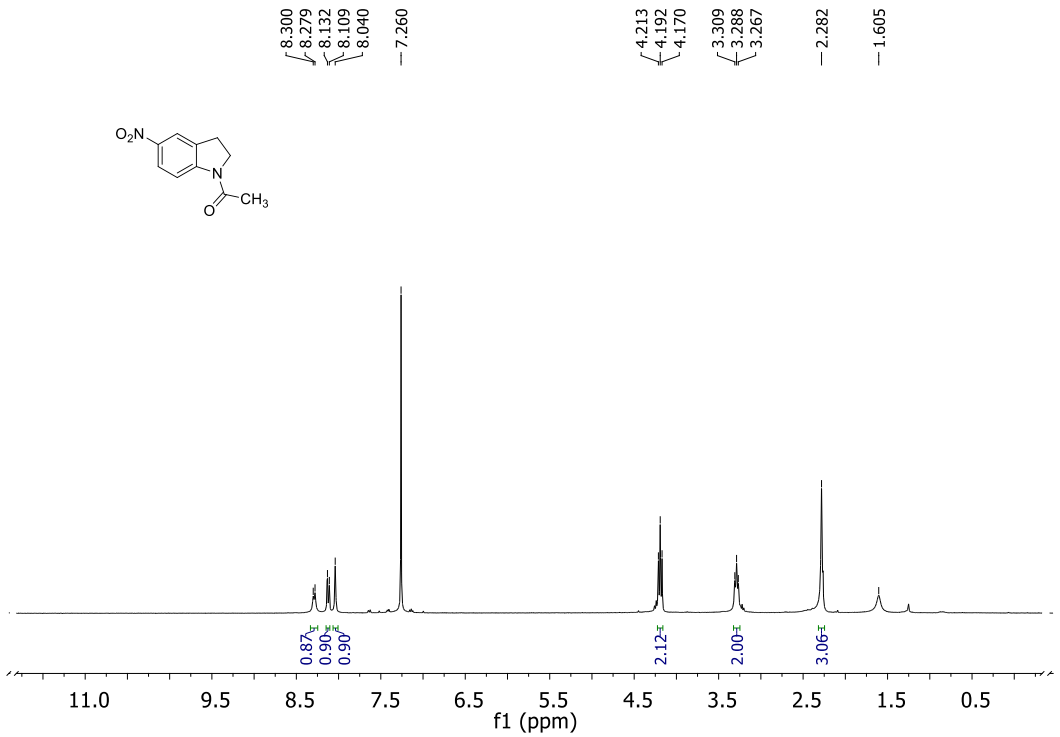

Figure 2.8. ^{1}H NMR of 1-(5-nitroindolin-1-yl)ethanone (**2a**)

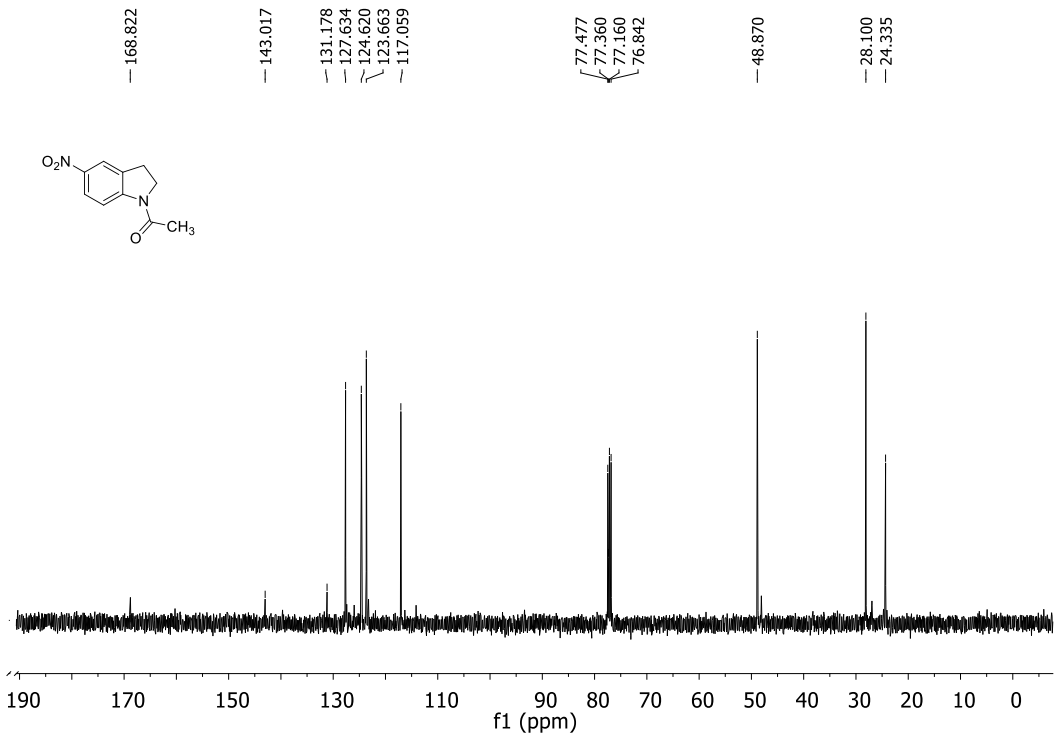

Figure 2.9. ^{13}C NMR of 1-(5-nitroindolin-1-yl)ethanone (**2a**)

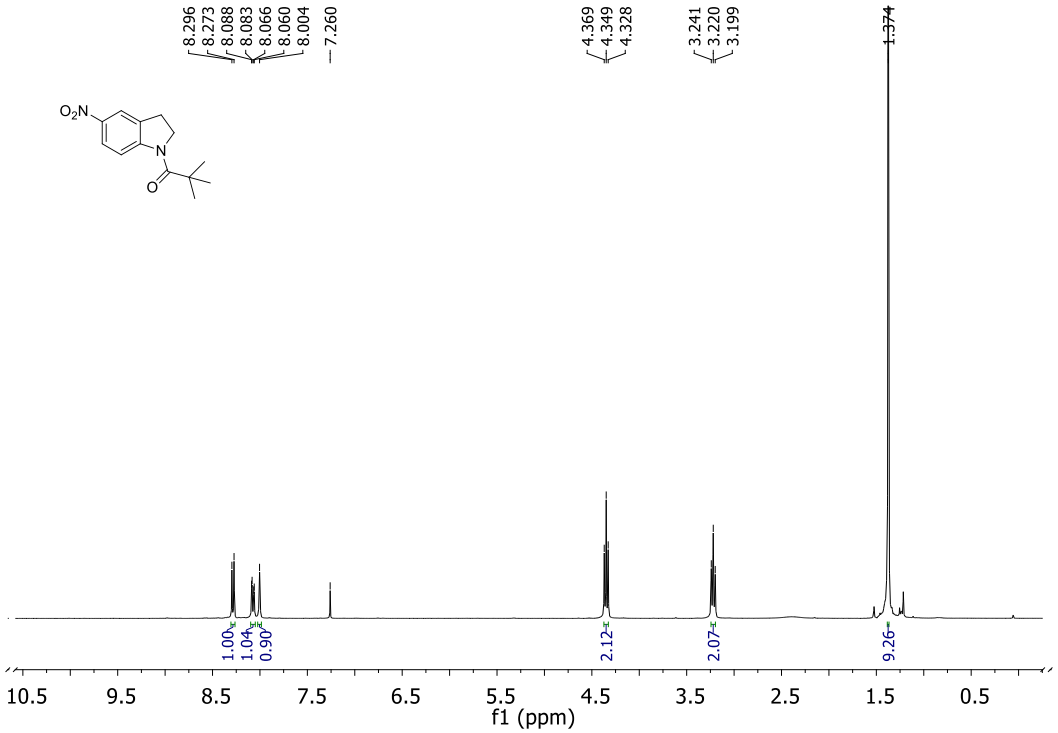

Figure 2.10. ^{1}H NMR of 2,2-dimethyl-1-(5-nitroindolin-1-yl)propan-1-one (**2b**)

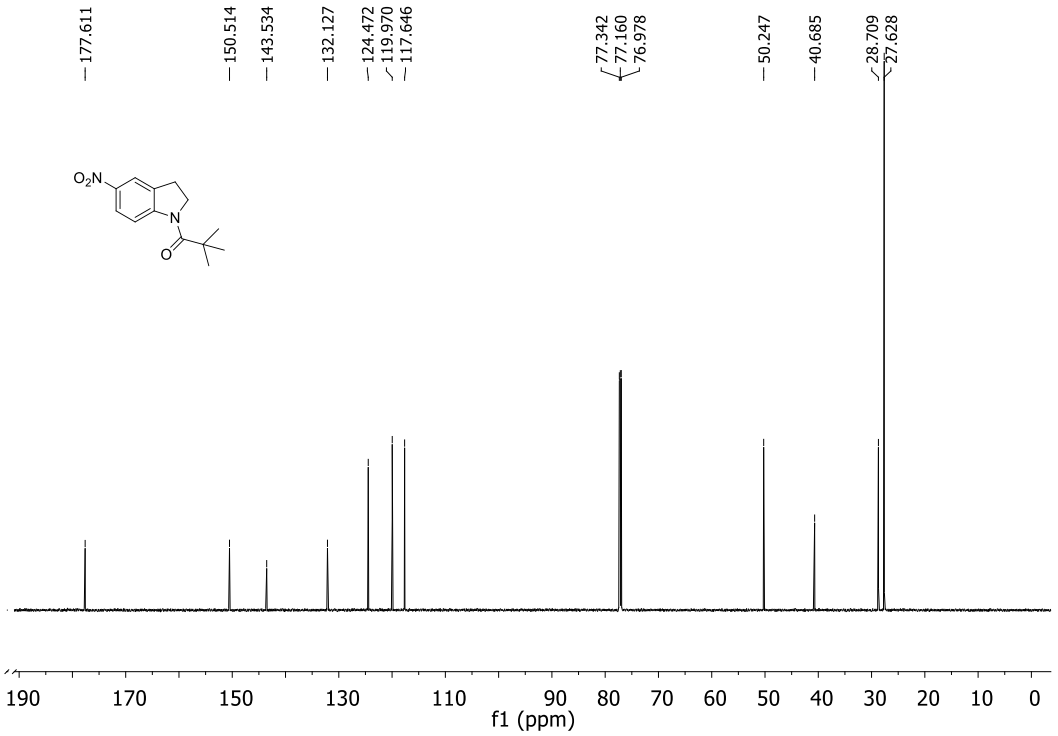

Figure 2.11. ^{13}C NMR of 2,2-dimethyl-1-(5-nitroindolin-1-yl)propan-1-one (**2b**)

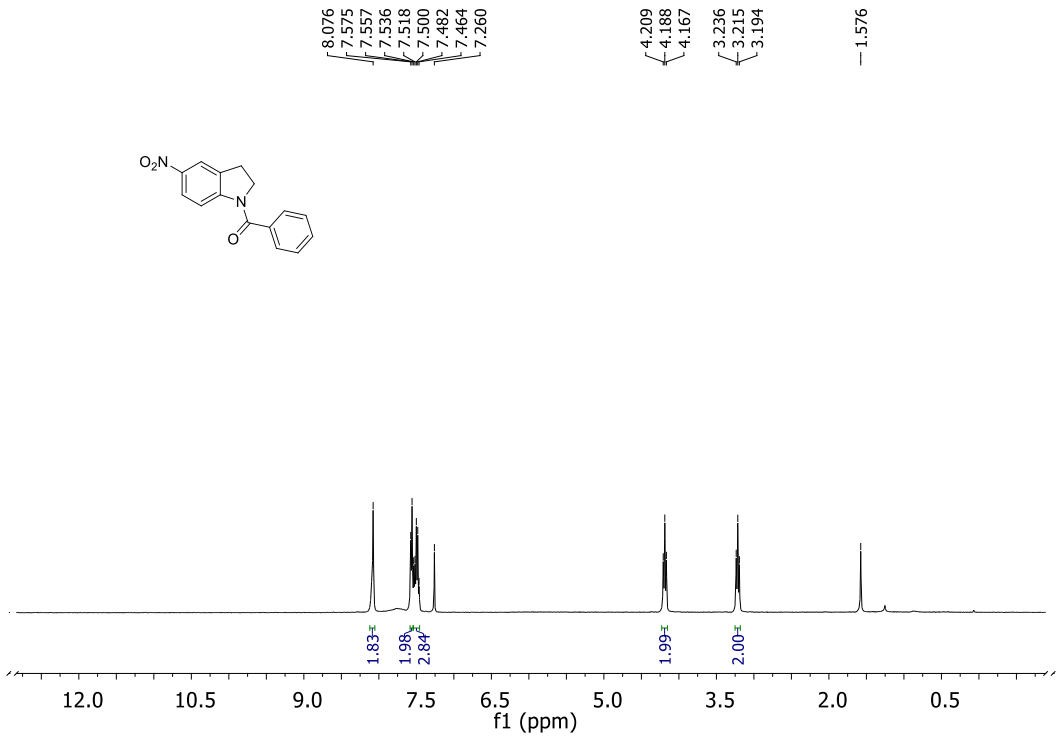

Figure 2.12. ^{1}H NMR of (5-nitroindolin-1-yl)(phenyl)methanone (**2c**)

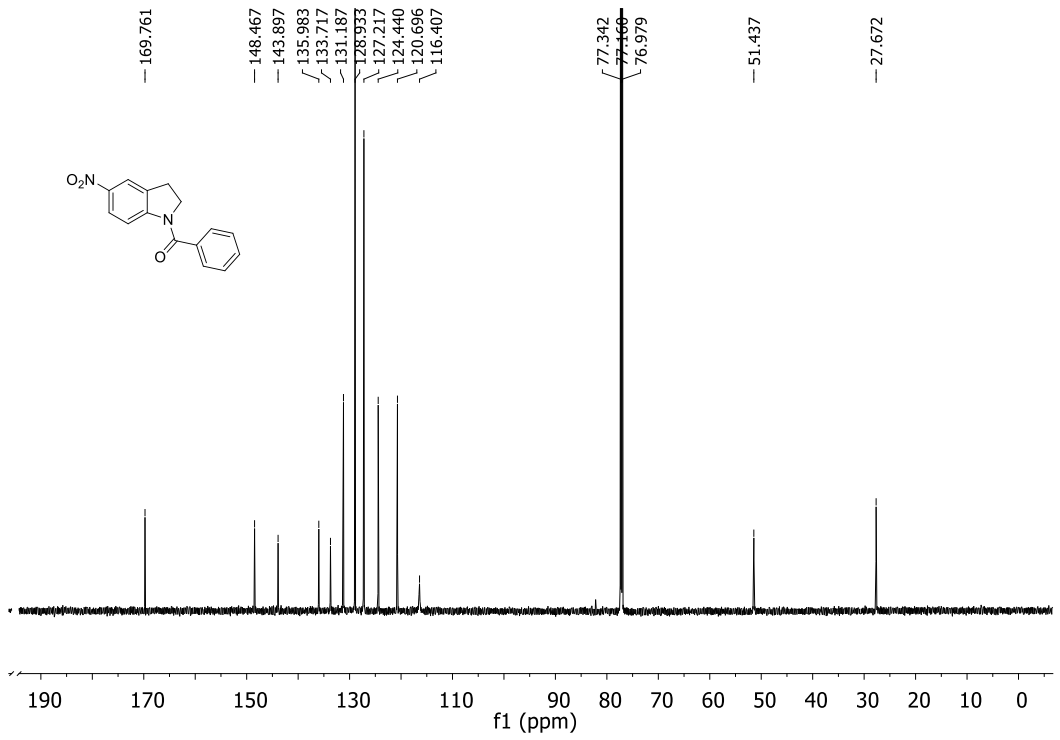

Figure 2.13. ^{13}C NMR of (5-nitroindolin-1-yl)(phenyl)methanone (**2c**)

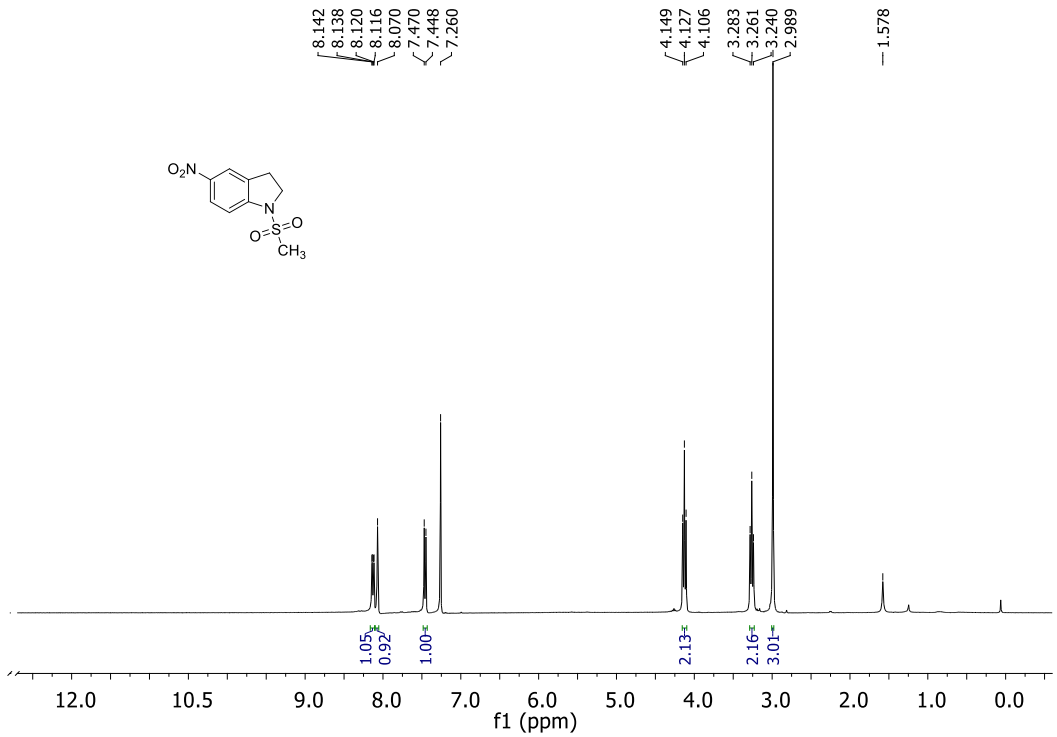

Figure 2.14. ^{1}H NMR of 1-(Methylsulfonyl)-5-nitroindoline (**2d**)

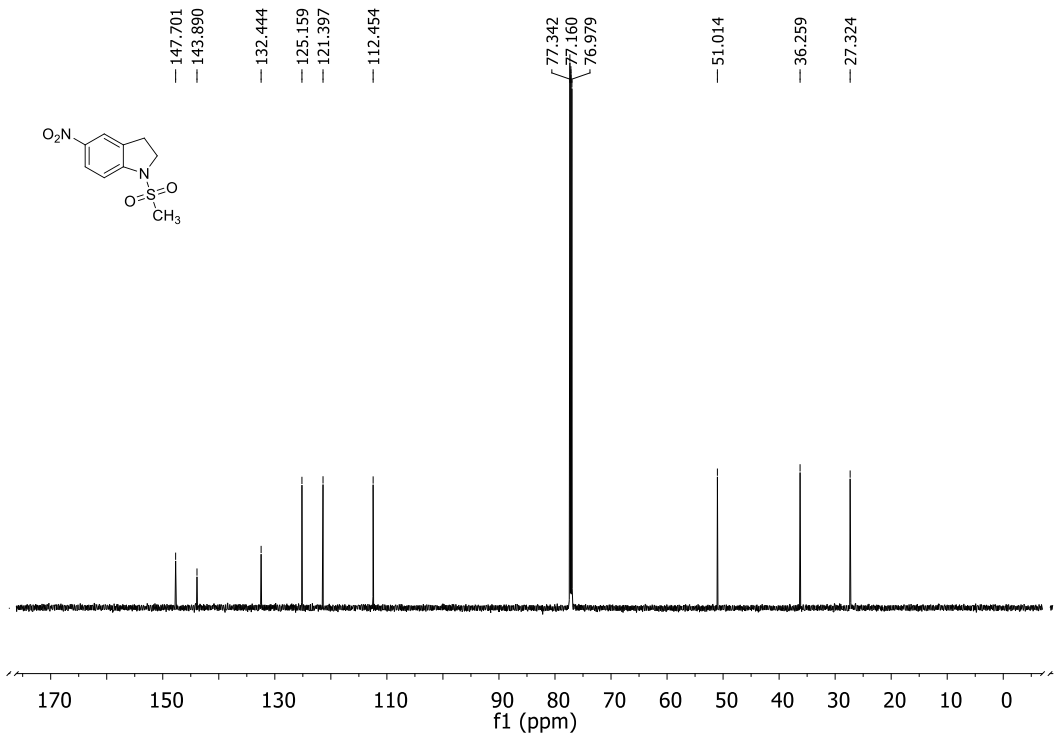

Figure 2.15. ^{13}C NMR of 1-(Methylsulfonyl)-5-nitroindoline (**2d**)

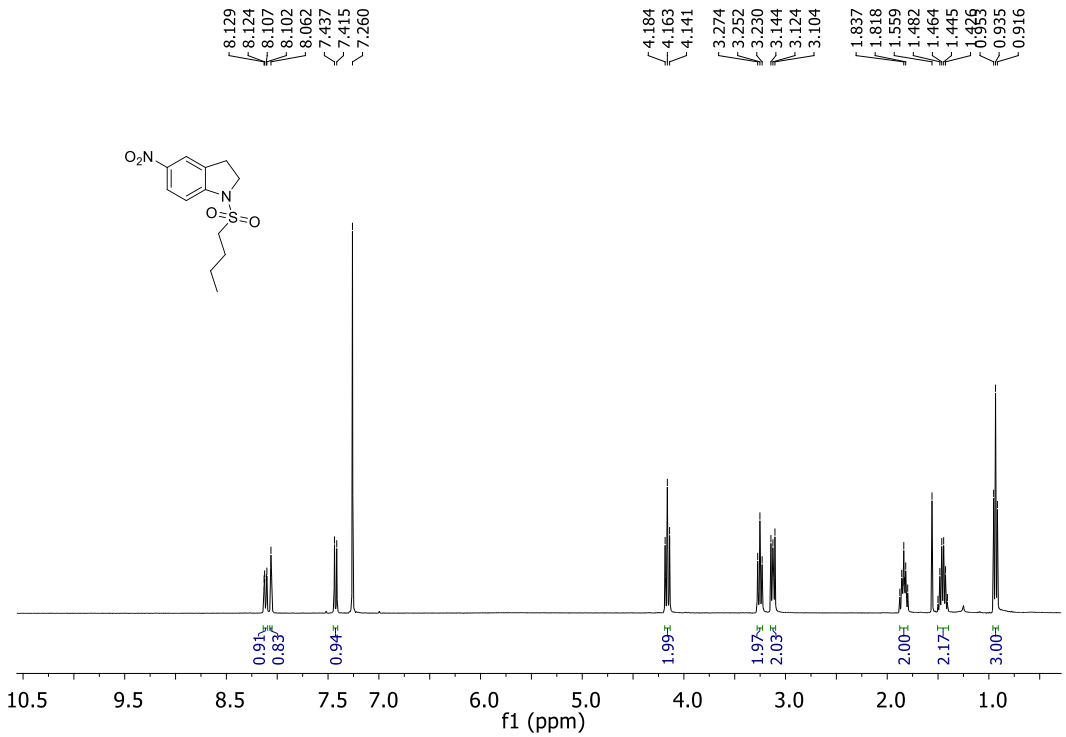

Figure 2.16. ^{1}H NMR of 1-(Butylsulfonyl)-5-nitroindoline (**2e**).

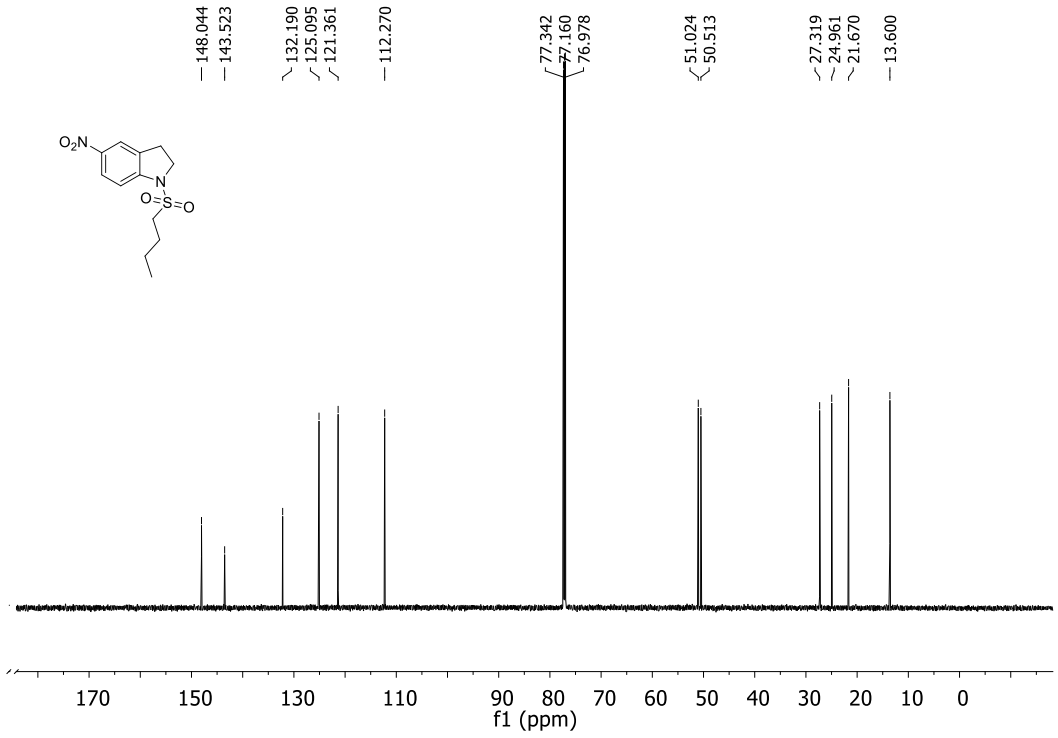

Figure 2.17. ^{13}C NMR of 1-(Butylsulfonyl)-5-nitroindoline (**2e**)

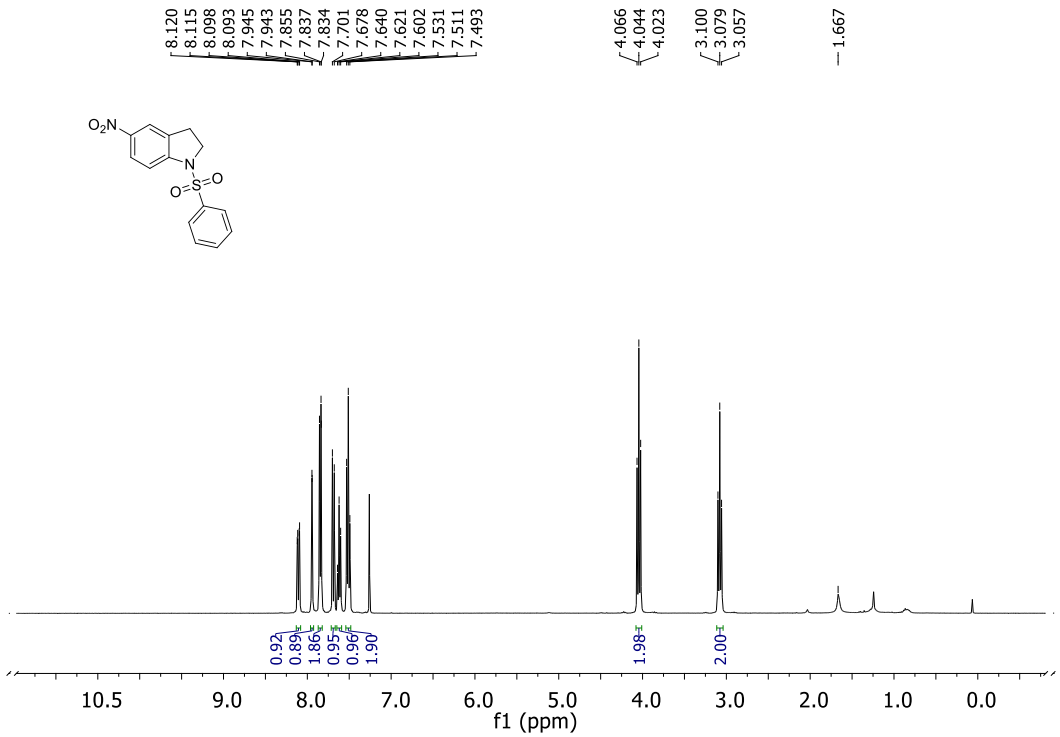

Figure 2.18. ^{1}H NMR of 5-Nitro-1-(phenylsulfonyl)indoline (**2f**)

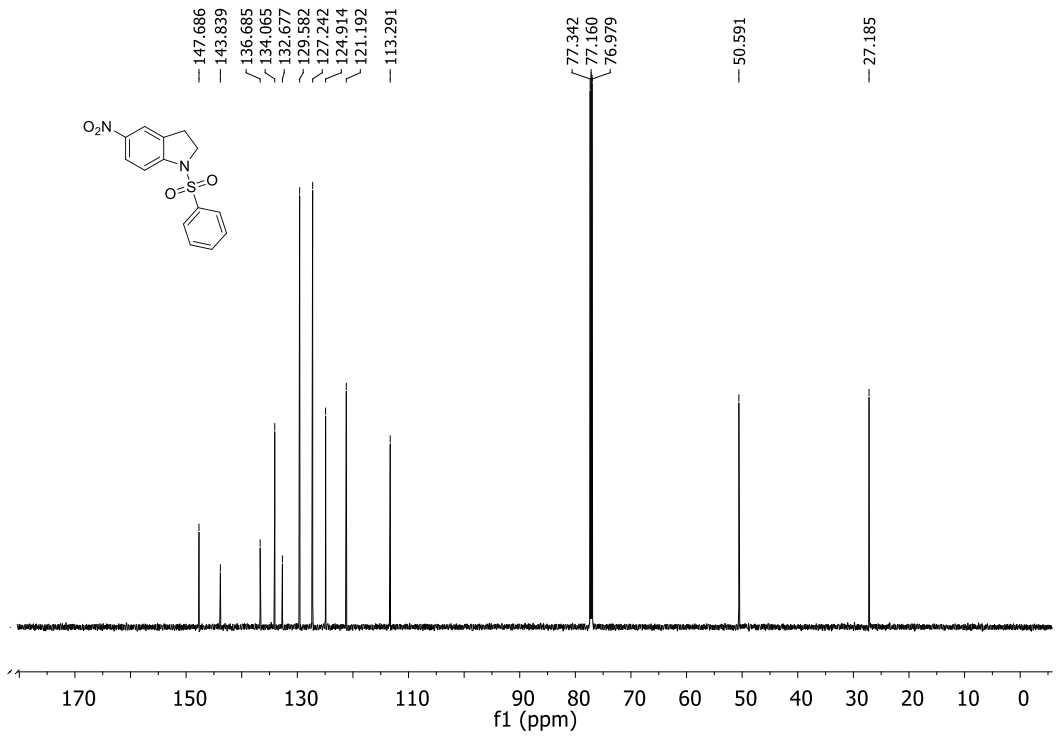

Figure 2.19. ^{13}C NMR of 5-Nitro-1-(phenylsulfonyl)indoline (**2f**)

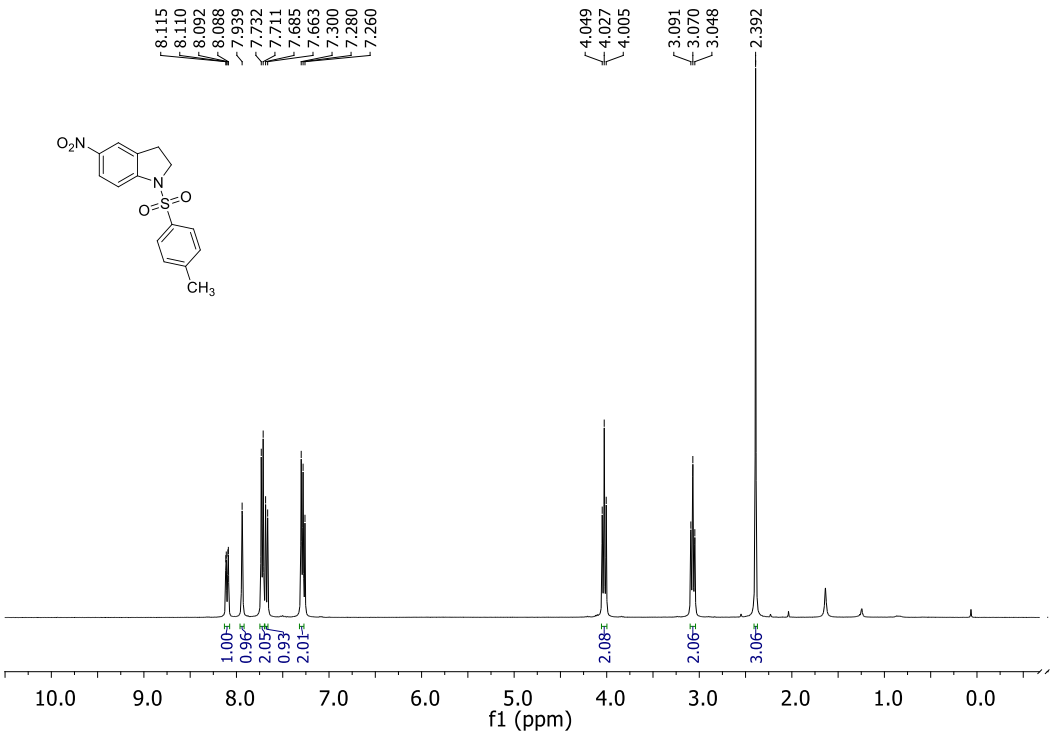

Figure 2.20. ^{1}H NMR of 5-Nitro-1-tosylindoline (**2g**)

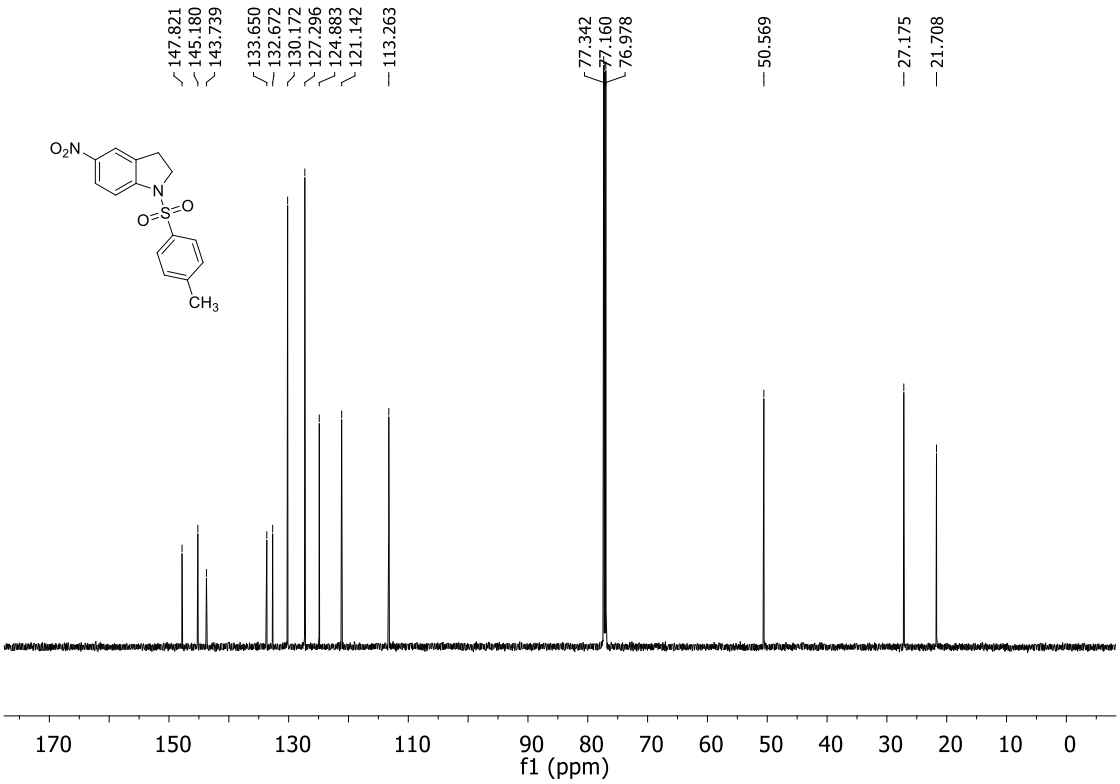

Figure 2.21. ^{13}C NMR of 5-Nitro-1-tosylindoline (**2g**)

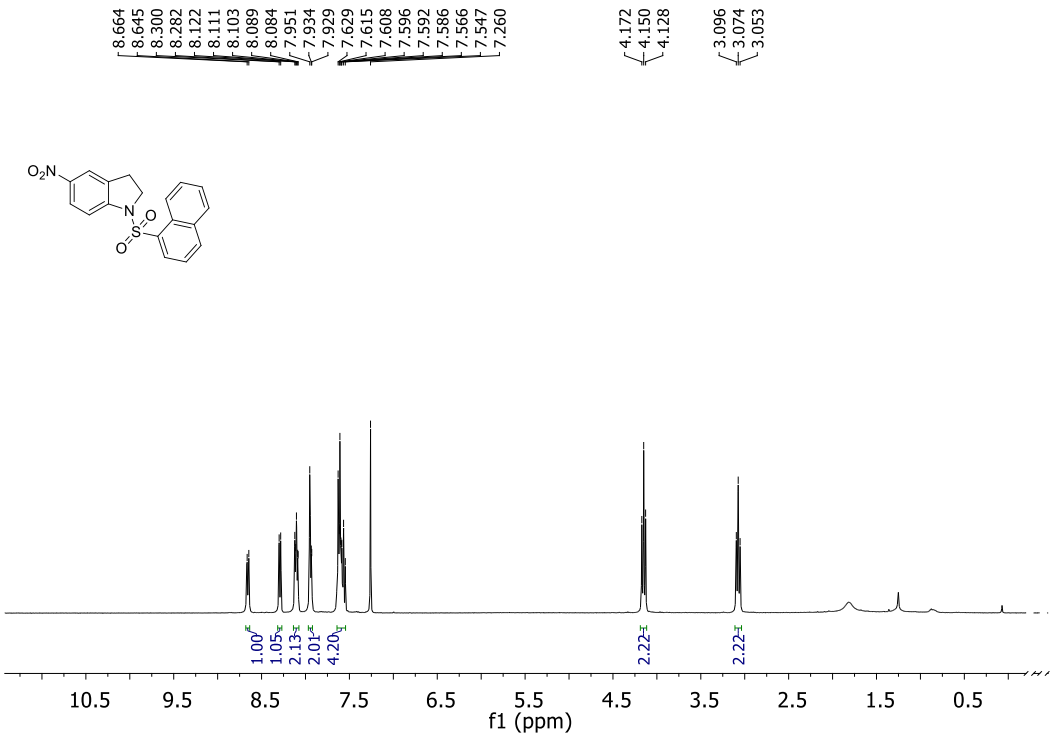

Figure 2.22. ^{1}H NMR of 1-(Naphthalen-1-ylsulfonyl)-5-nitroindoline (**2h**)

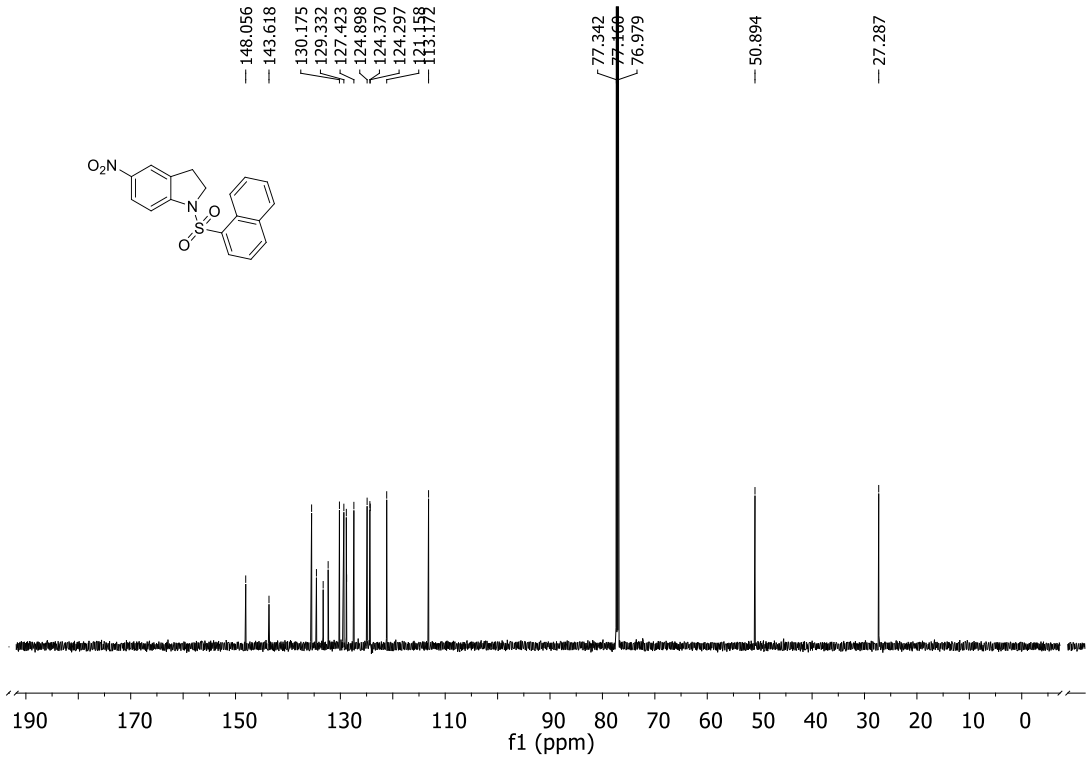

Figure 2.23. ^{13}C NMR of 1-(Naphthalen-1-ylsulfonyl)-5-nitroindoline (**2h**)

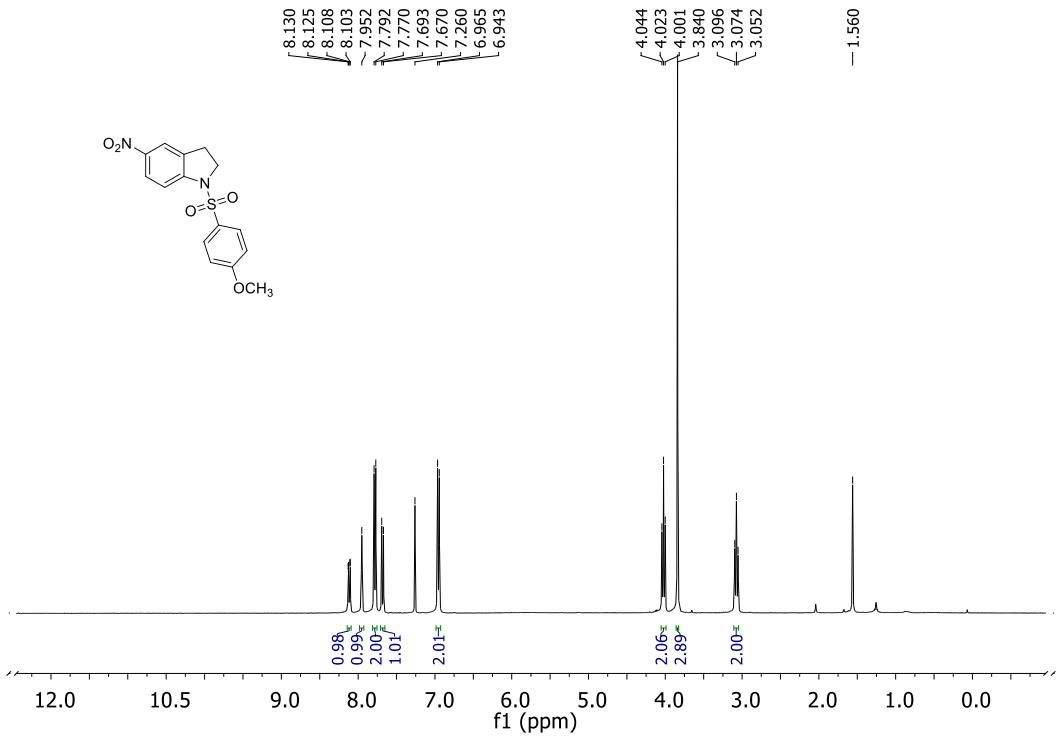

Figure 2.24. ^{1}H NMR of 1-((4-Methoxyphenyl)sulfonyl)-5-nitroindoline (**2i**)

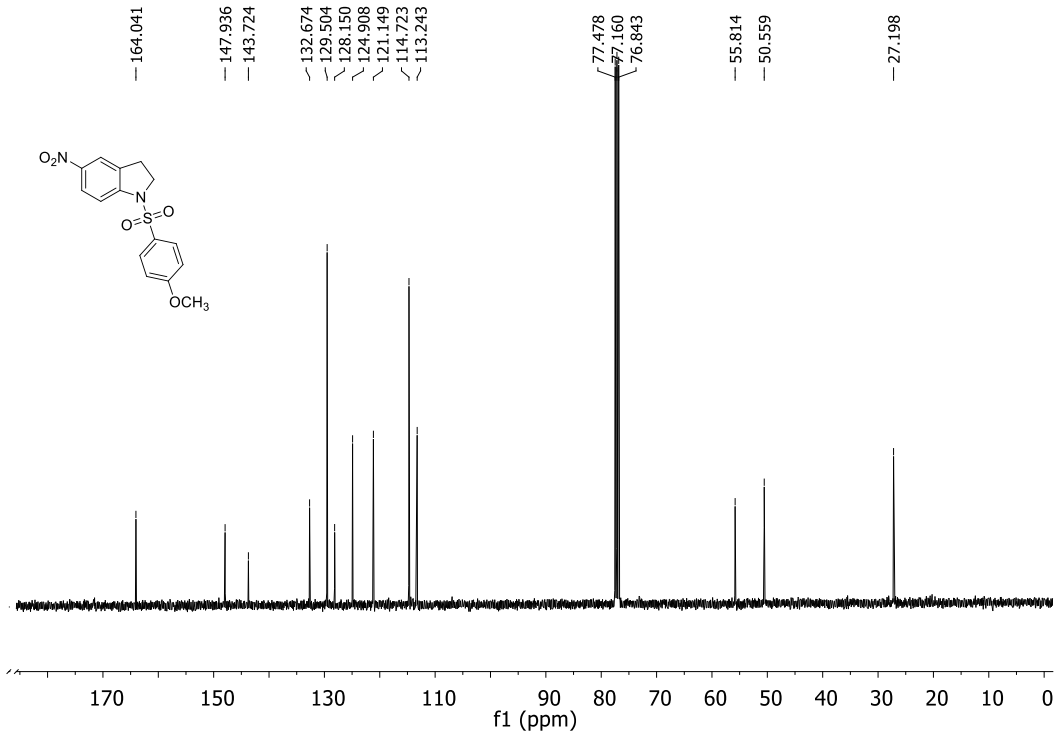

Figure 2.25. ^{13}C NMR of 1-((4-Methoxyphenyl)sulfonyl)-5-nitroindoline (**2i**)

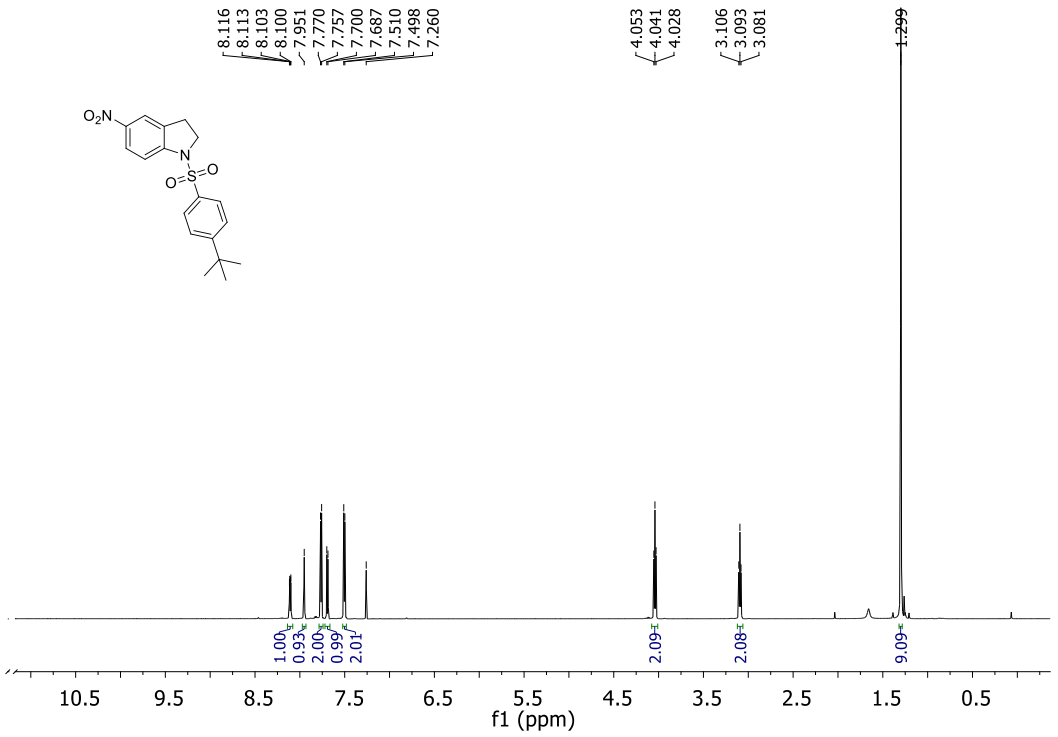

Figure 2.26. ^{1}H NMR of 1-((4-(tert-butyl)phenyl)sulfonyl)-5-nitroindoline (**2j**)

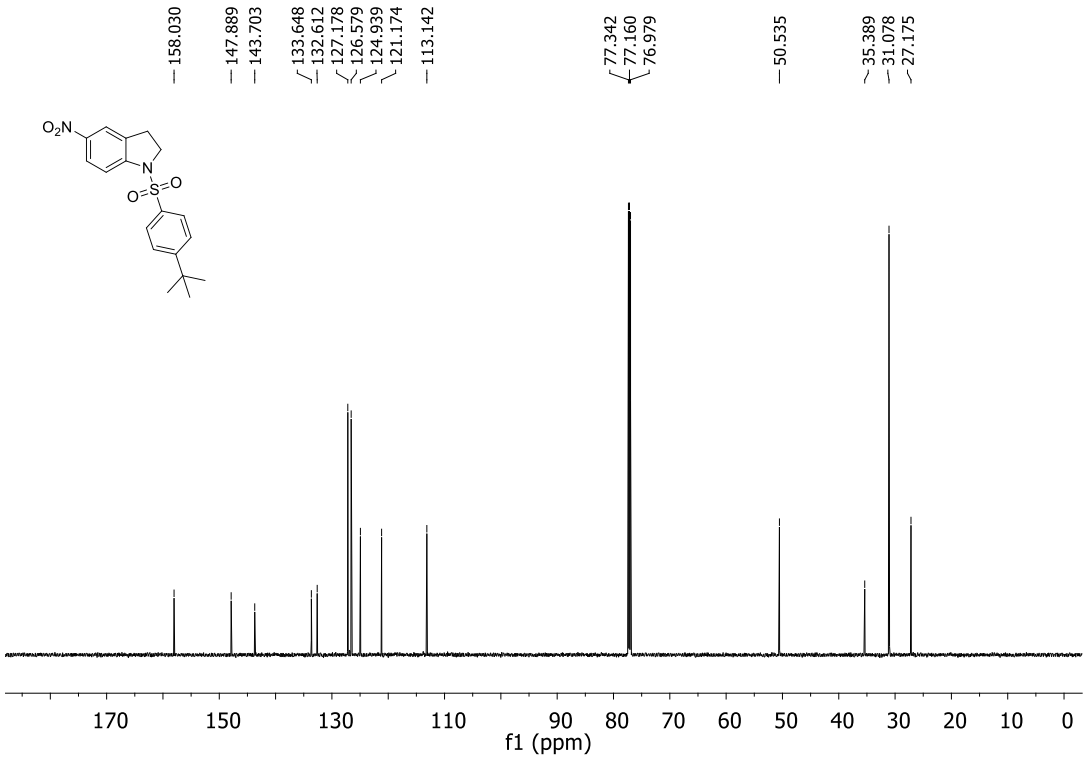

Figure 2.27. ^{13}C NMR of 1-((4-(tert-butyl)phenyl)sulfonyl)-5-nitroindoline (**2j**)

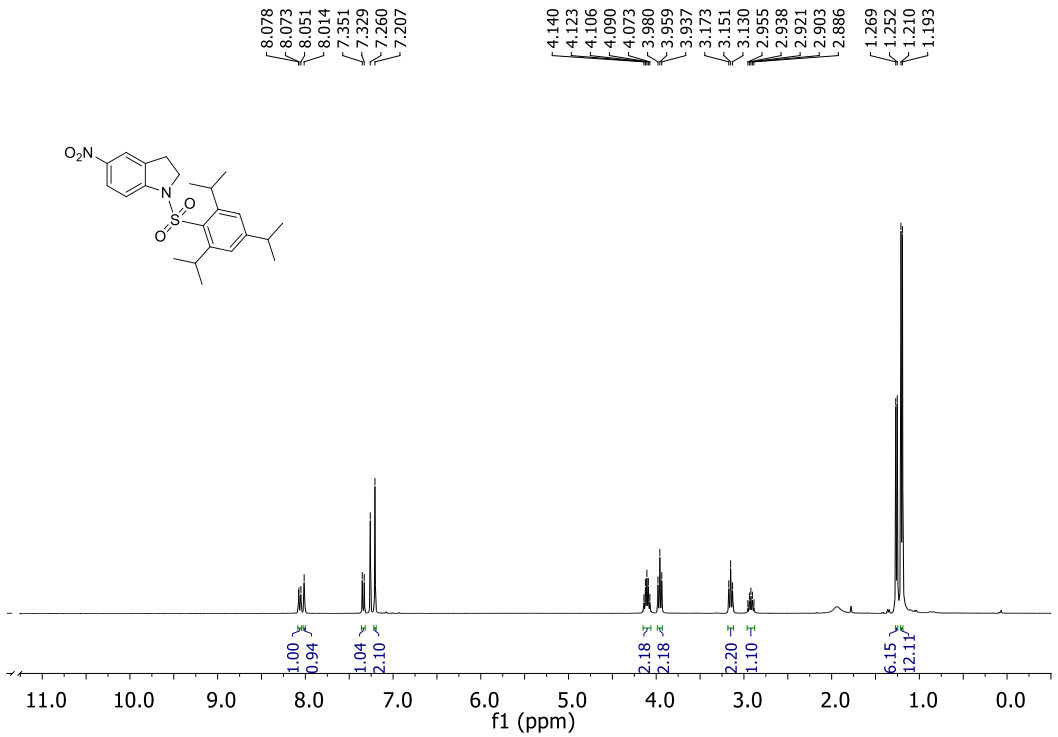

Figure 2.28. ^{1}H NMR of 5-Nitro-1-((2,4,6-triisopropylphenyl)sulfonyl)indoline (**2k**)

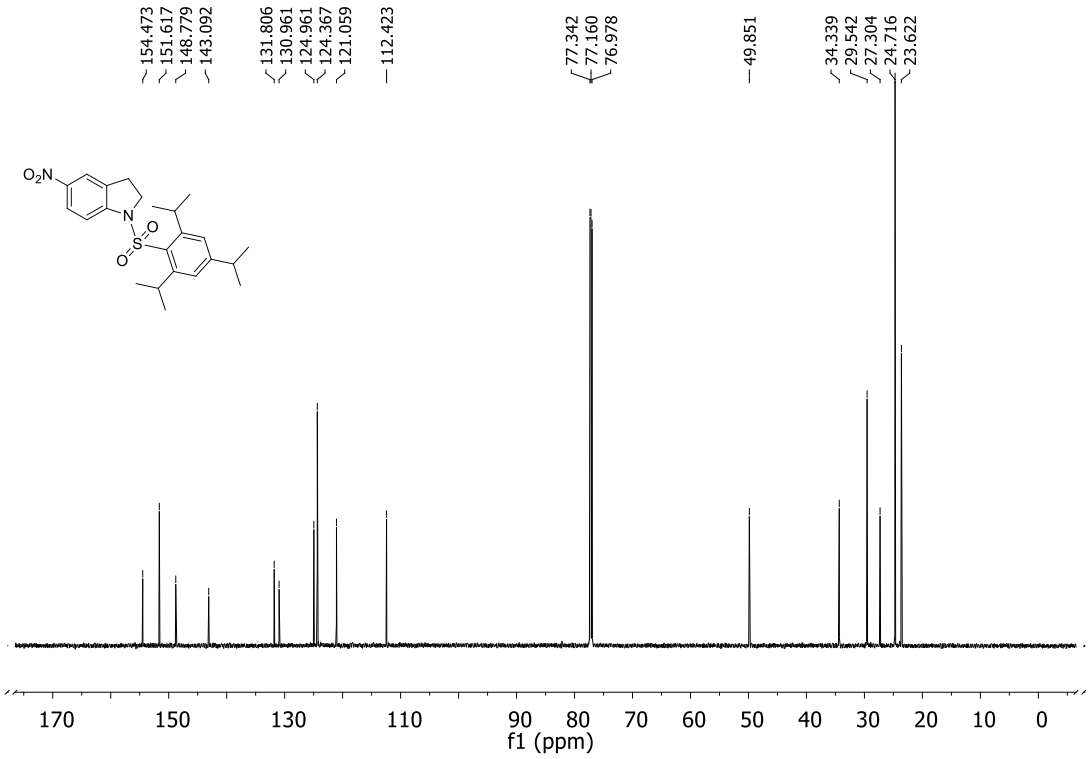

Figure 2.29. ^{13}C NMR of 5-Nitro-1-((2,4,6-triisopropylphenyl)sulfonyl)indoline (**2k**)

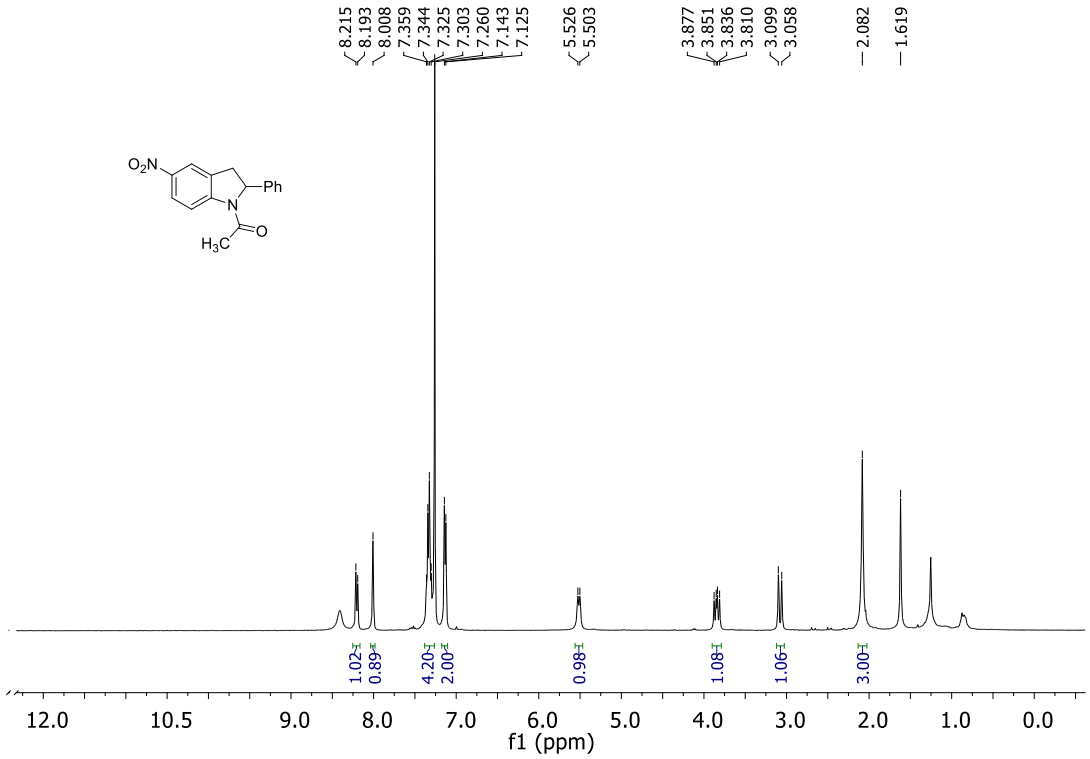

Figure 2.30. [1]H NMR of 1-(5-Nitro-2-phenylindolin-1-yl)ethanone (**2l**)

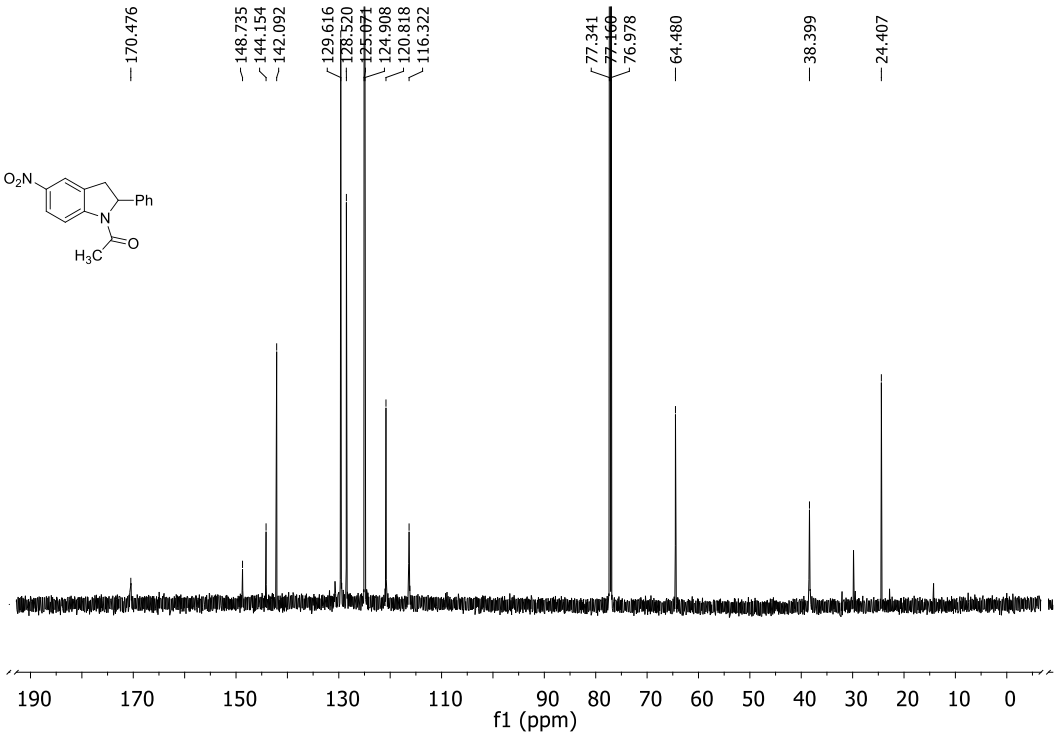

Figure 2.31.[13]C NMR of 1-(5-Nitro-2-phenylindolin-1-yl)ethanone (**2l**)

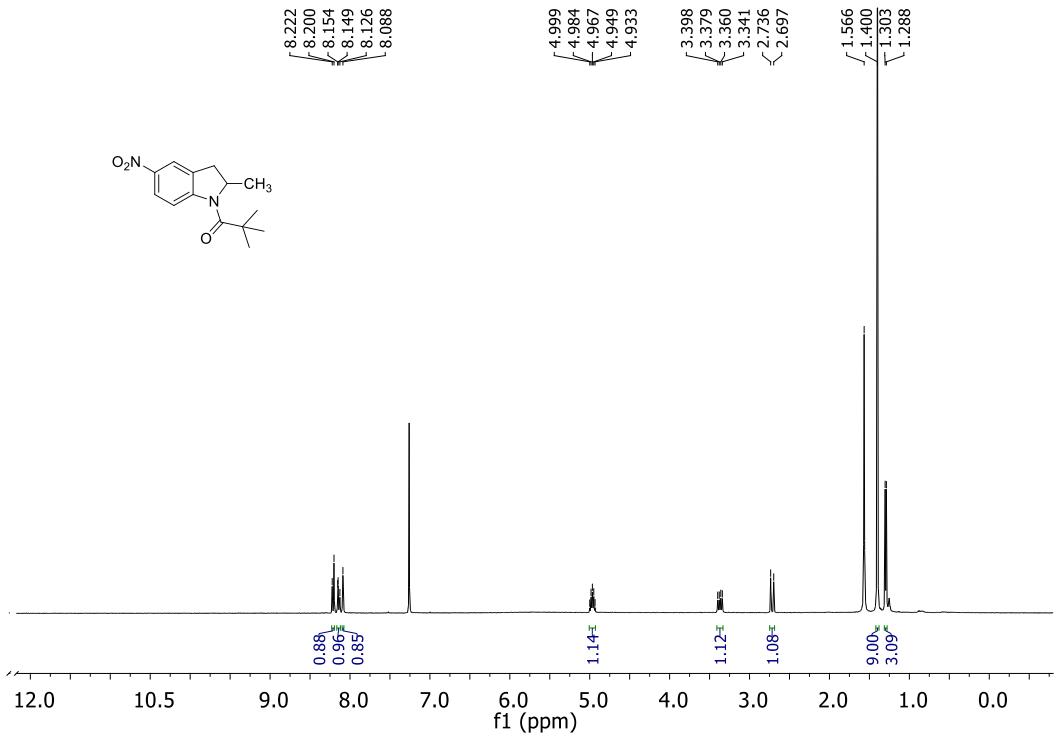

Figure 2.32. ^{1}H NMR of 2,2-dimethyl-1-(2-methyl-5-nitroindolin-1-yl)propan-1-one (**2m**)

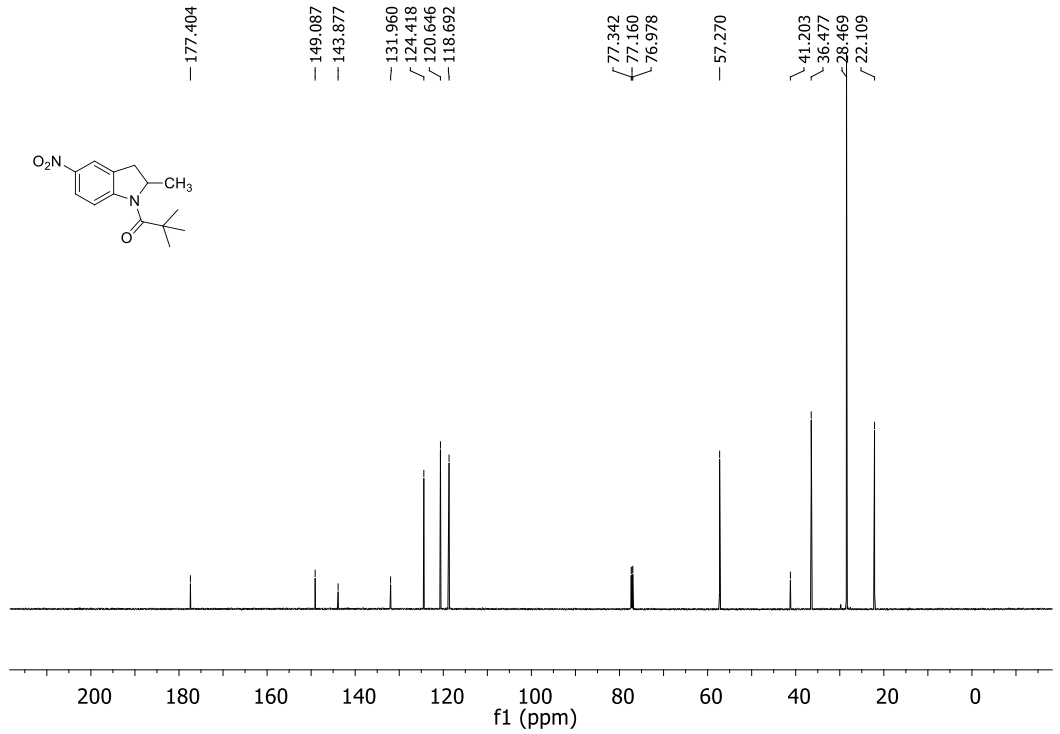

Figure 2.33. ^{13}C NMR of 2,2-dimethyl-1-(2-methyl-5-nitroindolin-1-yl)propan-1-one (**2m**)

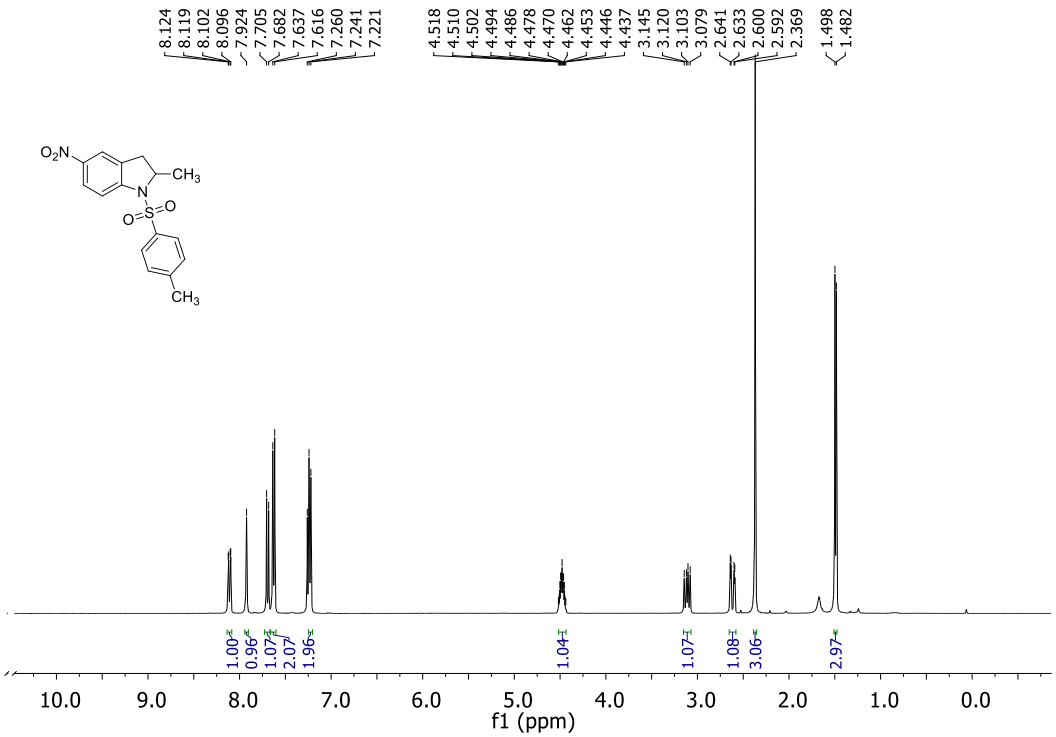

Figure 2.34. ^{1}H NMR of 2-Methyl-5-nitro-1-tosylindoline (**2n**)

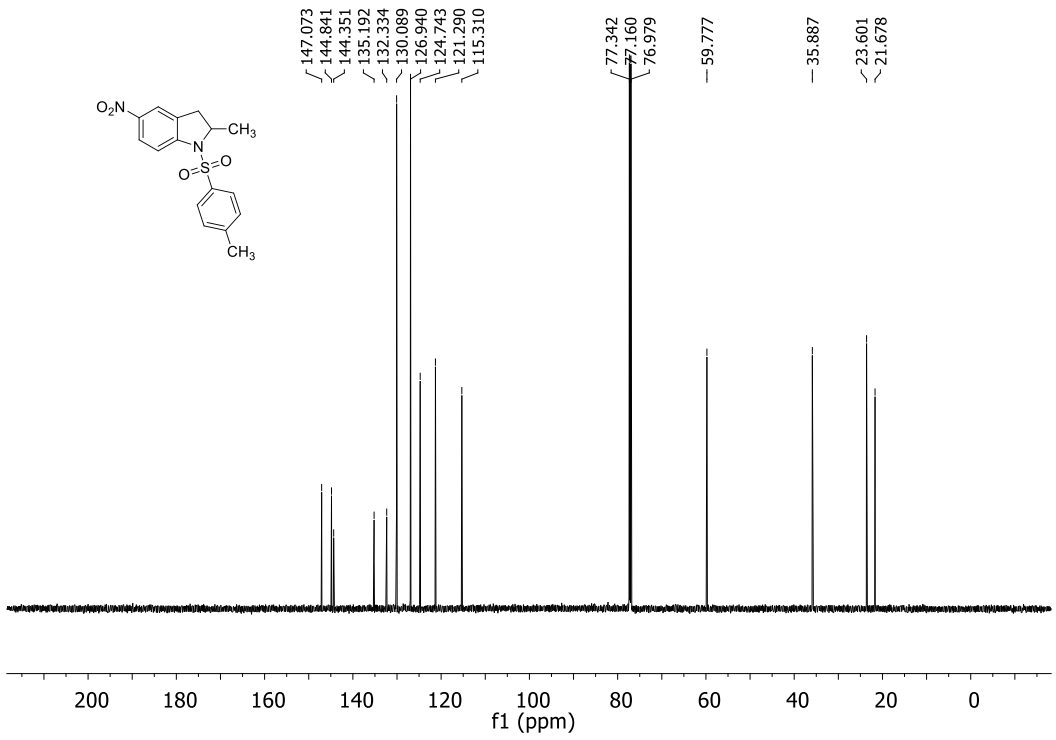

Figure 2.35. ^{13}C NMR of 2-Methyl-5-nitro-1-tosylindoline (**2n**)

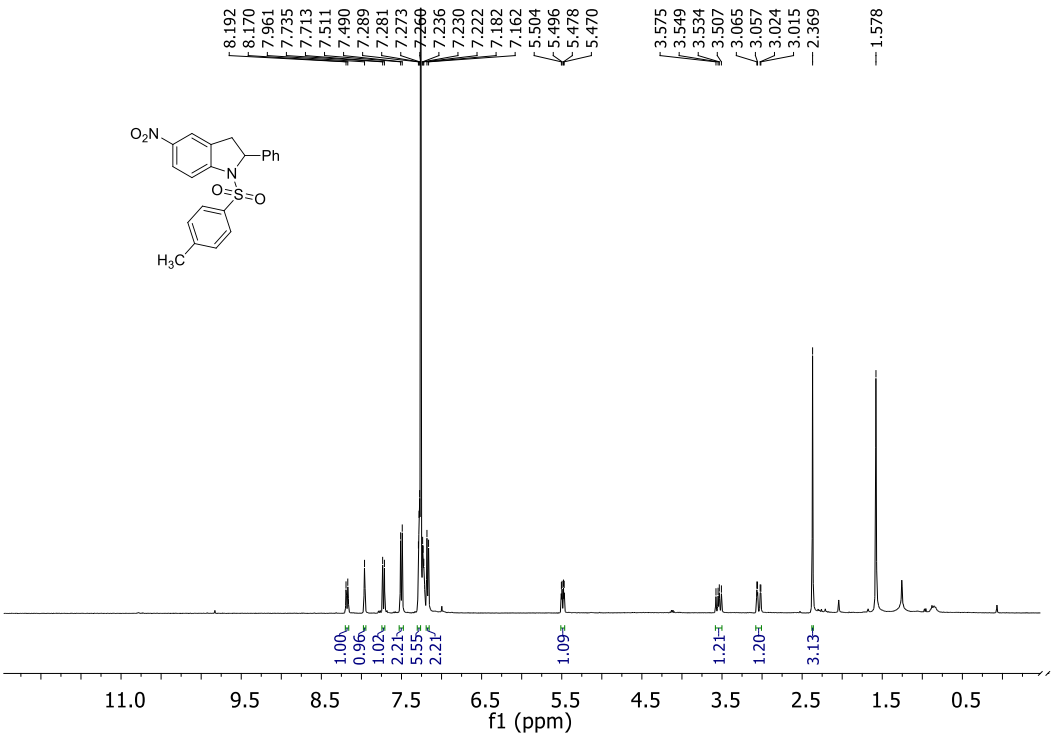

Figure 2.36. ^{1}H NMR of 5-Nitro-2-phenyl-1-tosylindoline (**2o**)

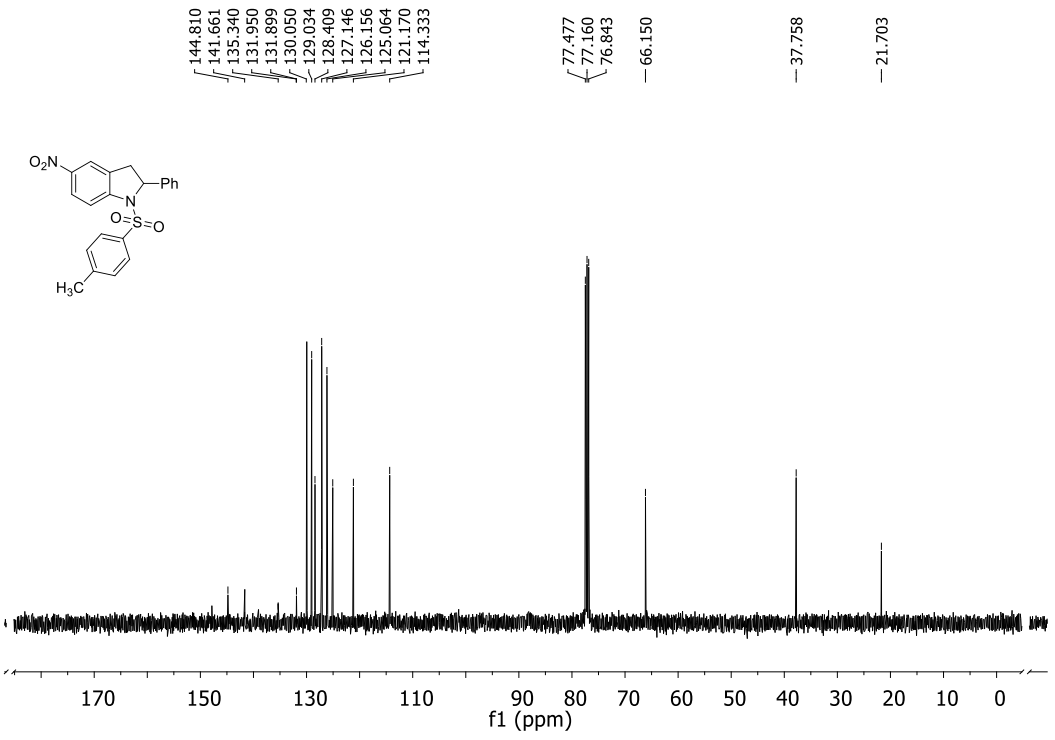

Figure 2.37.^{13}C NMR of 5-Nitro-2-phenyl-1-tosylindoline (**2o**)

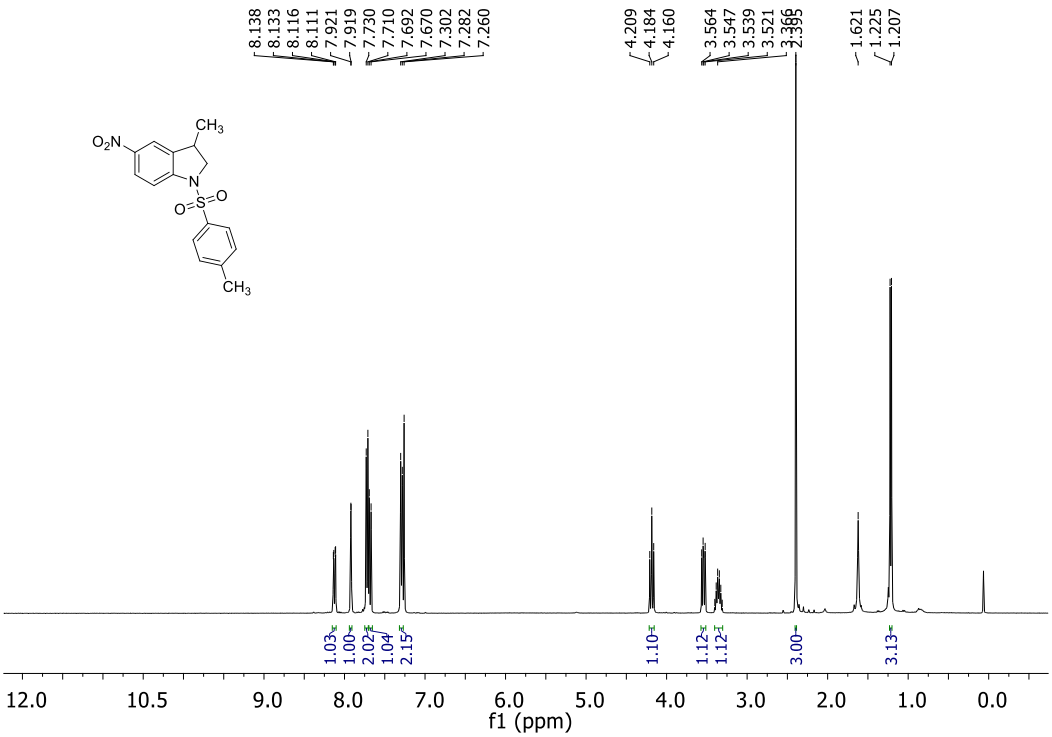

Figure 2.38. ^{1}H NMR of 3-Methyl-5-nitro-1-tosylindoline (**2p**)

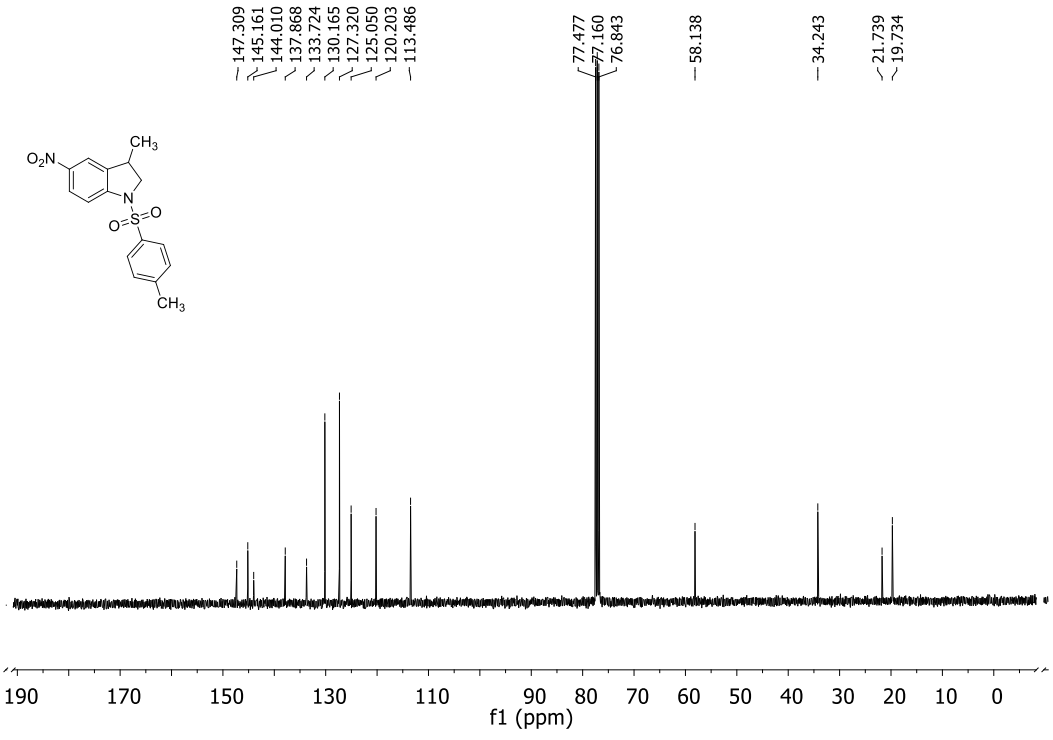

Figure 2.39. ^{13}C NMR of 3-Methyl-5-nitro-1-tosylindoline (**2p**)

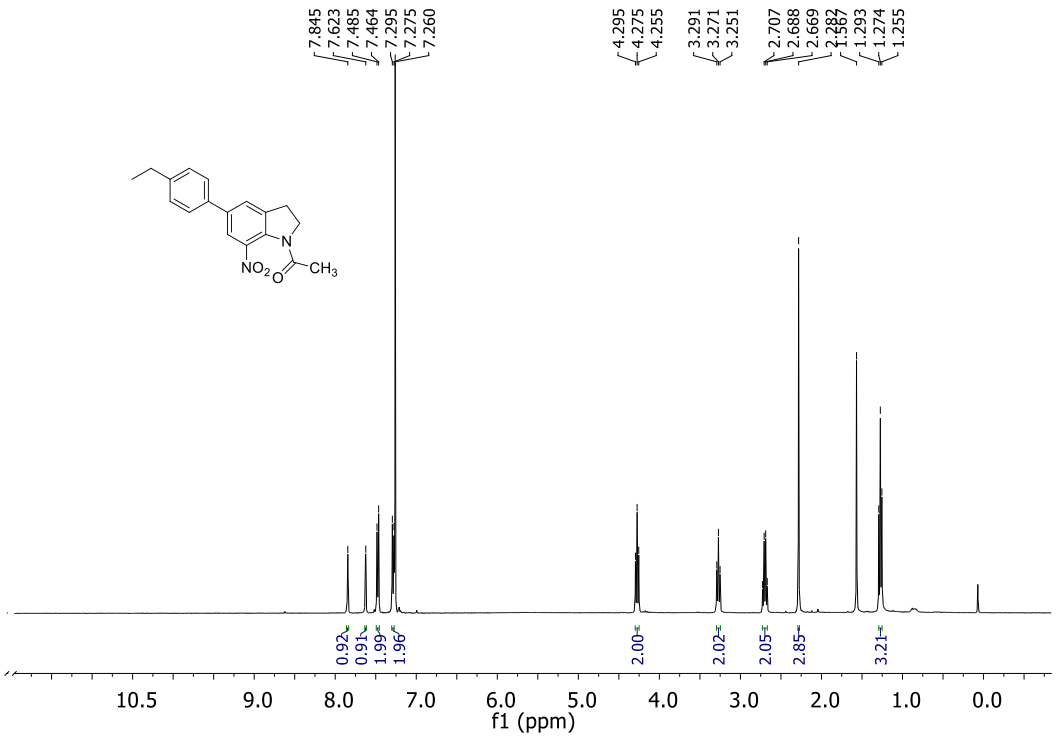

Figure 2.40. ^{1}H NMR of 1-(5-(4-Ethylphenyl)-7-nitroindolin-1-yl)ethanone (**2q**)

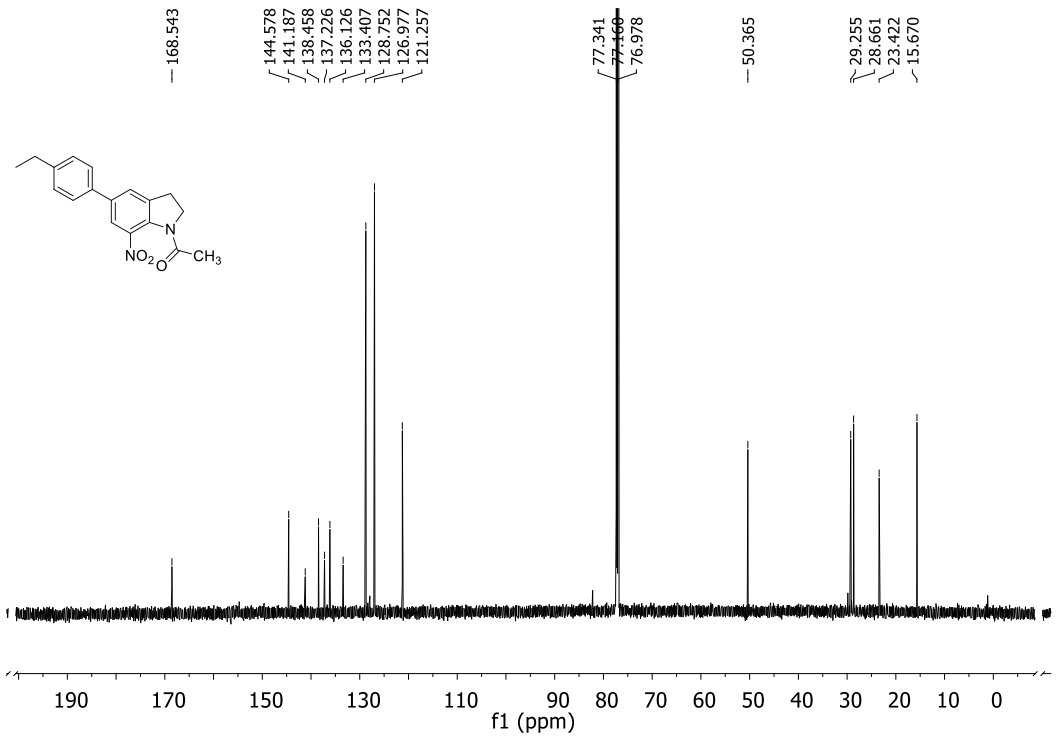

Figure 2.41. ^{13}C NMR of 1-(5-(4-Ethylphenyl)-7-nitroindolin-1-yl)ethanone (**2q)**

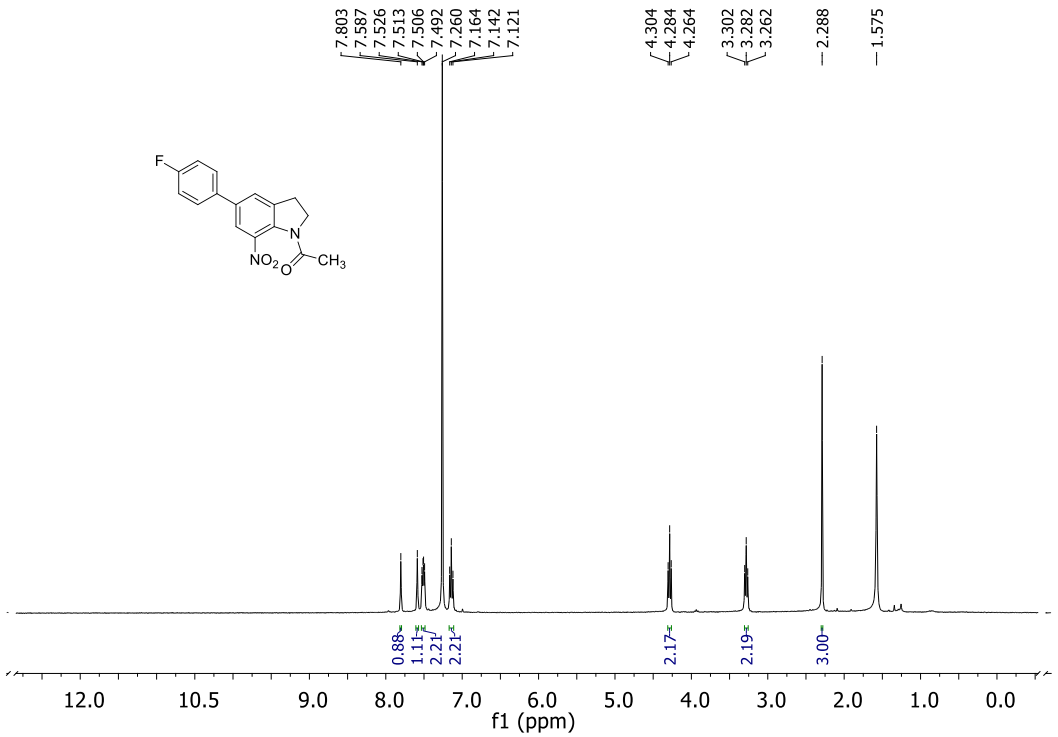

Figure 2.42. ^{1}H NMR of 1-(5-(4-Fluorophenyl)-7-nitroindolin-1-yl)ethanone (**2r**)

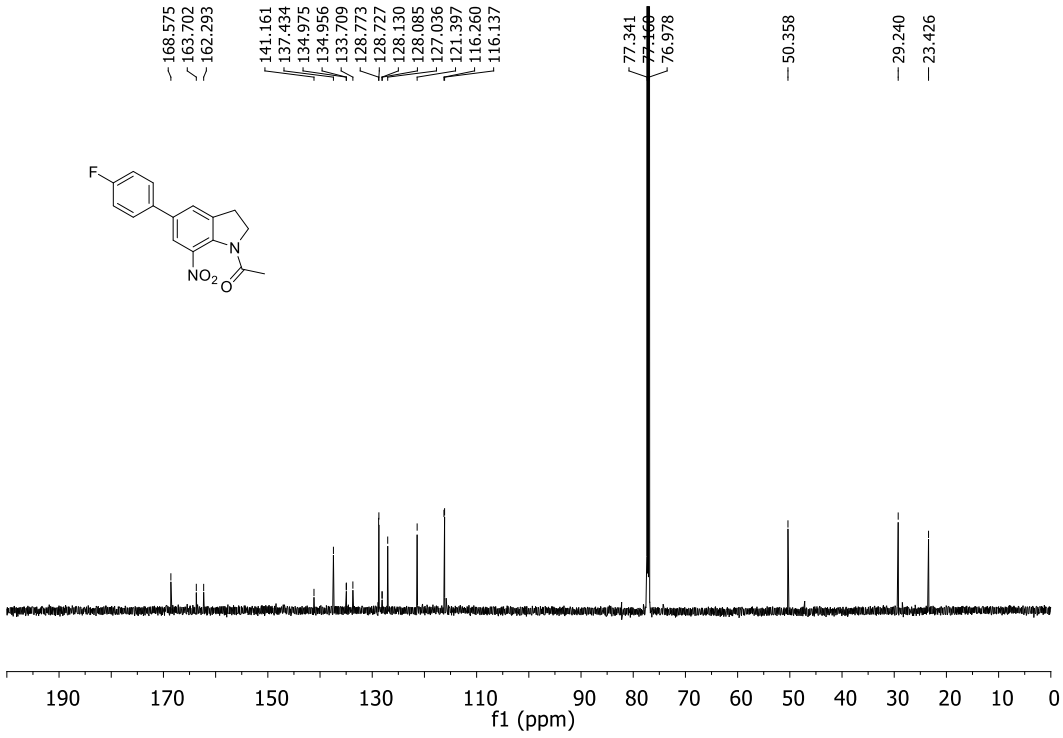

Figure 2.43. ^{13}C NMR of 1-(5-(4-Fluorophenyl)-7-nitroindolin-1-yl)ethanone (**2r**)

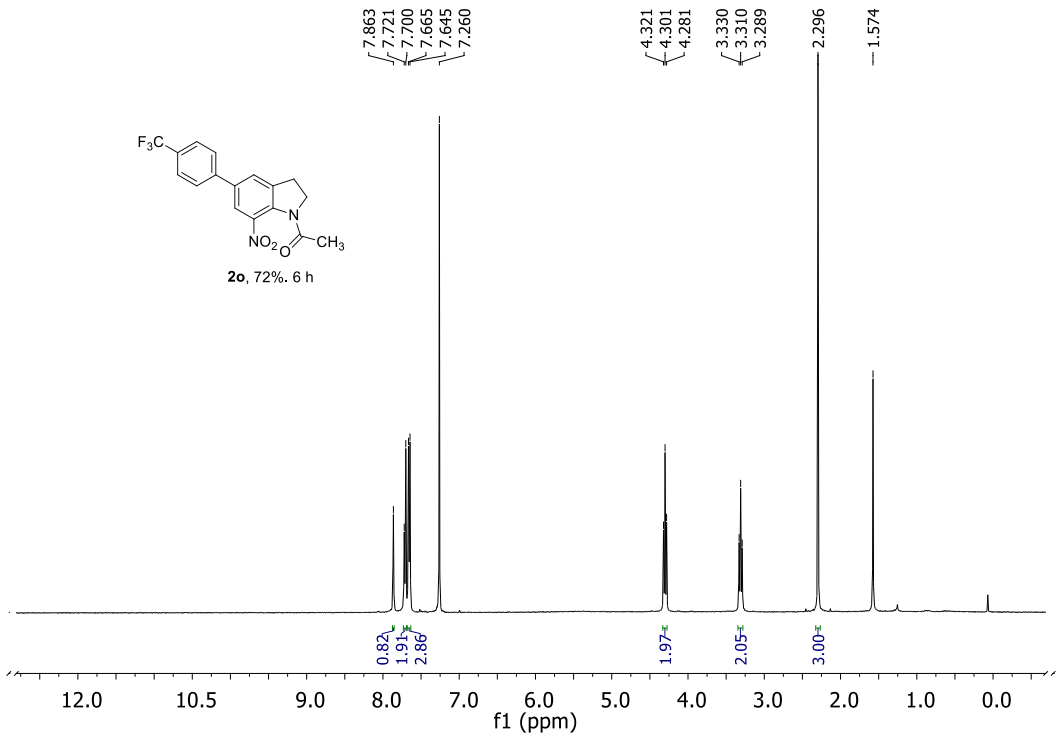

Figure 2.44. ^{1}H NMR of 1-(7-Nitro-5-(4-(trifluoromethyl)phenyl)indolin-1-yl)ethanone (**2s**)

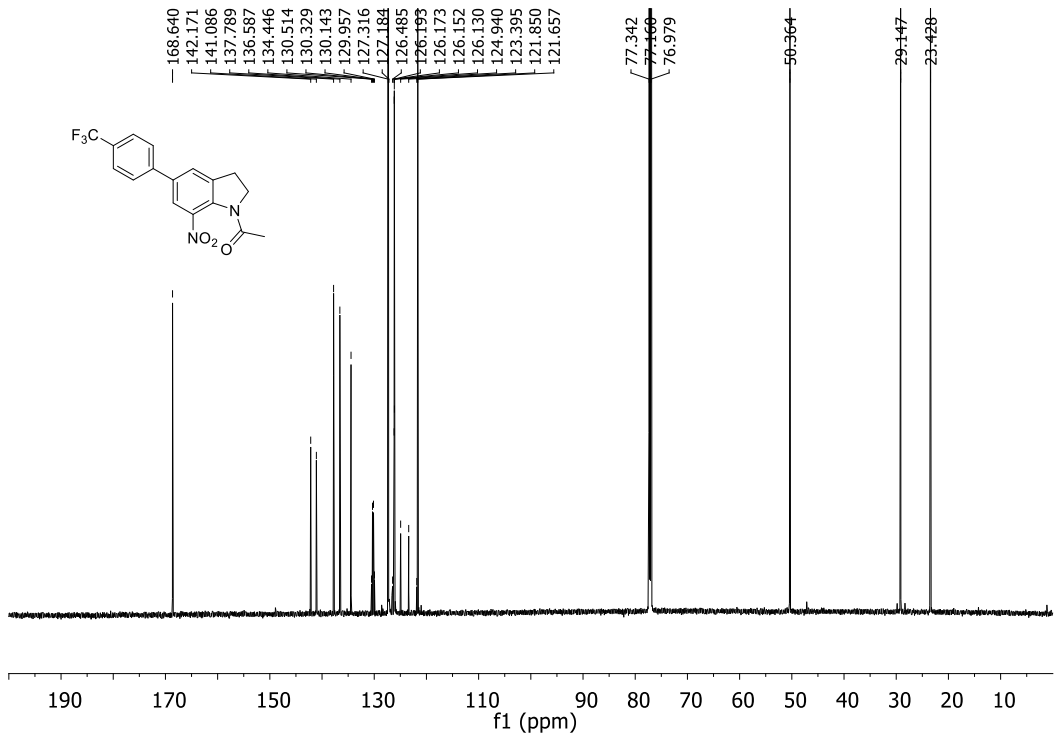

Figure 2.45. ^{13}C NMR of 1-(7-Nitro-5-(4-(trifluoromethyl)phenyl)indolin-1-yl)ethanone (**2s**)

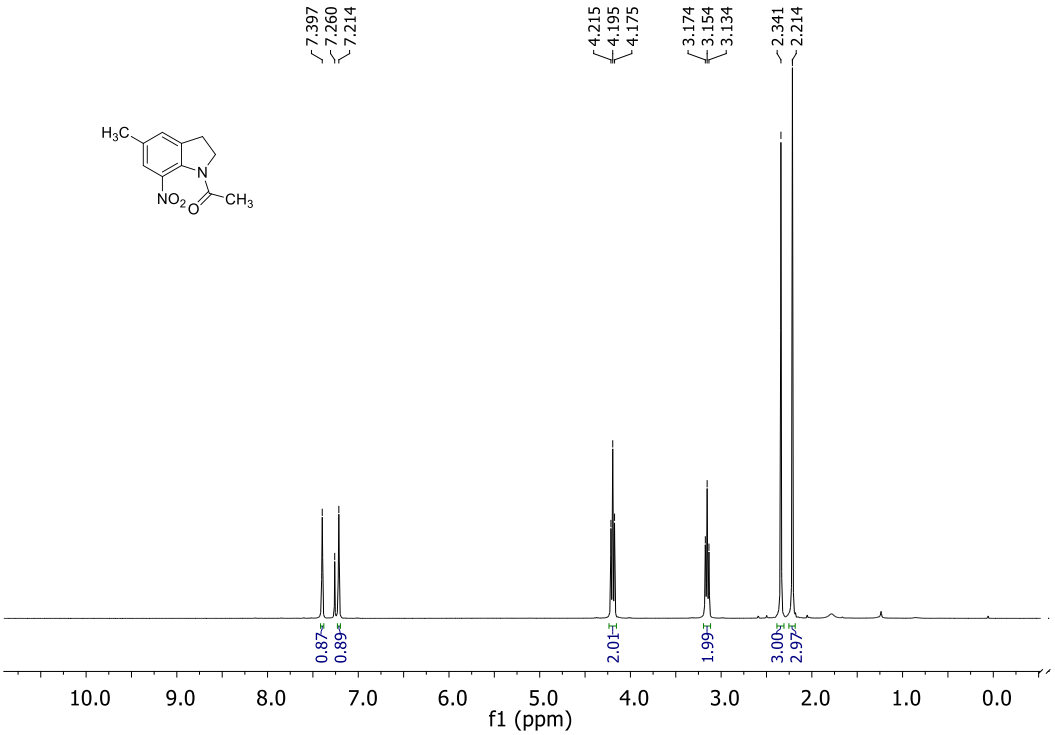

Figure 2.46. ^{1}H NMR of 1-(5-Methyl-7-nitroindolin-1-yl)ethanone (**2t**)

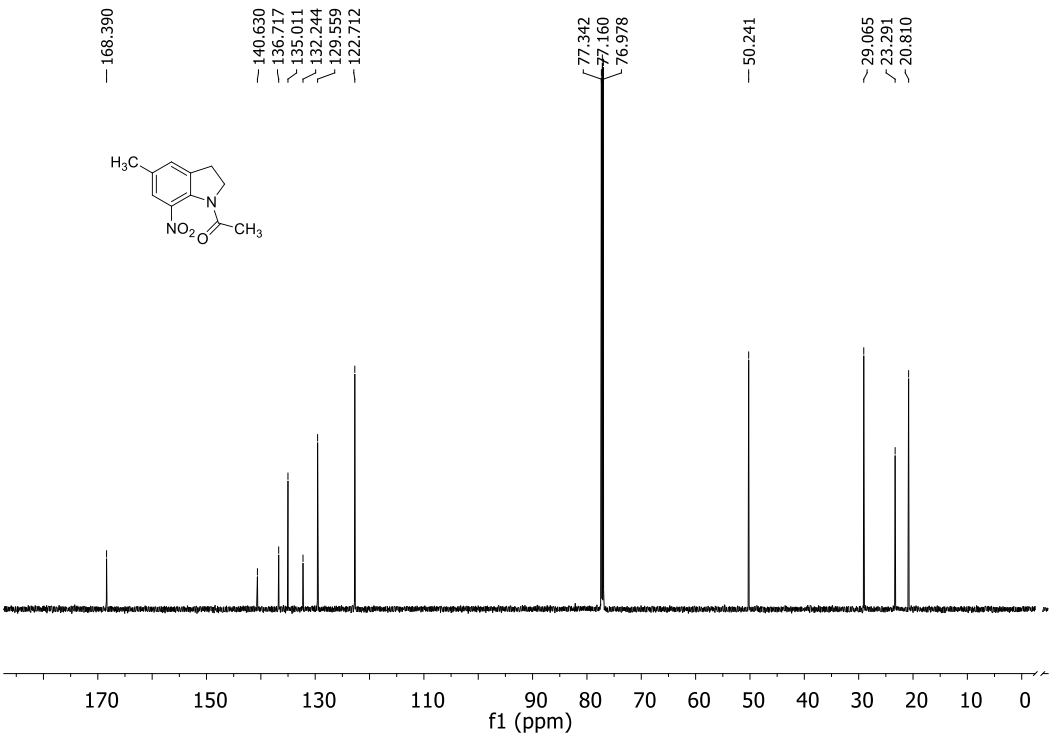

Figure 2.47. ^{13}C NMR of 1-(5-Methyl-7-nitroindolin-1-yl)ethanone (**2t**)

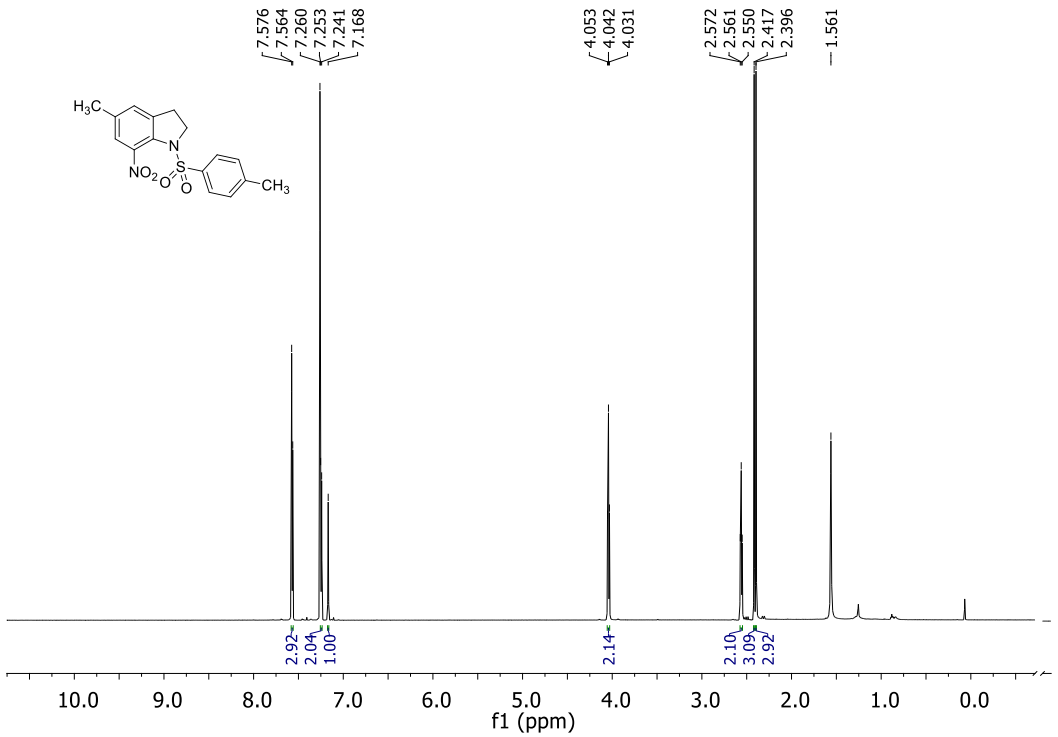

Figure 2.48. ^{1}H NMR of 5-Methyl-7-nitro-1-tosylindoline (**2u**)

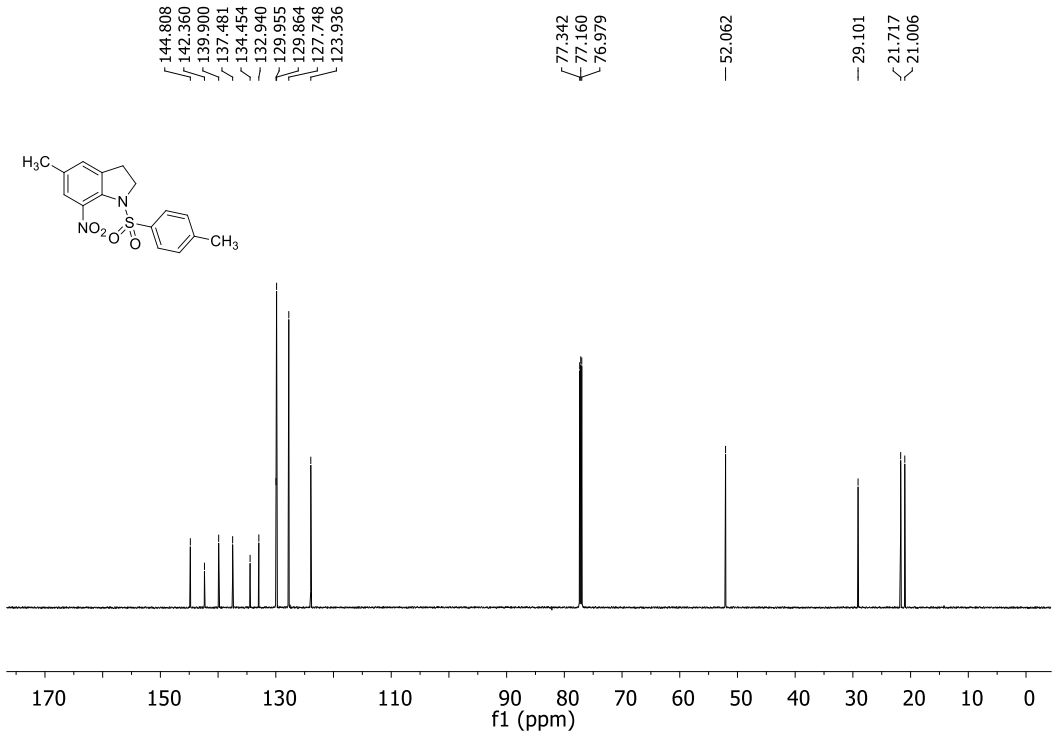

Figure 2.49. ^{13}C NMR of 5-Methyl-7-nitro-1-tosylindoline (**2u)**

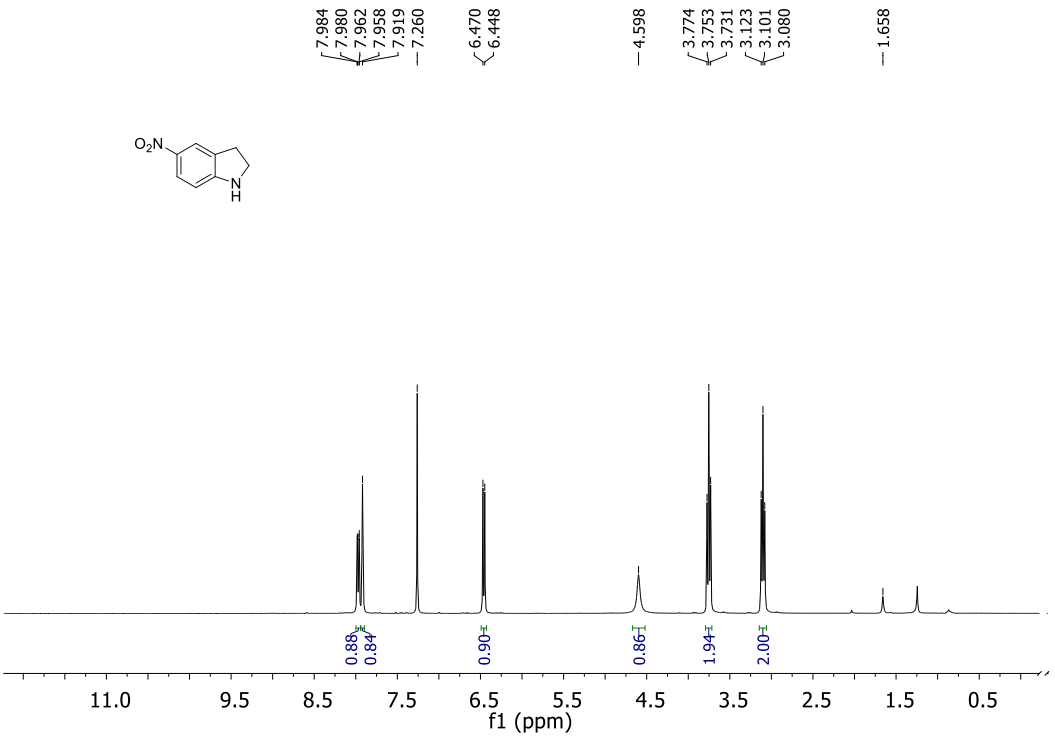

Figure 2.50. ^{1}H NMR 5-Nitroindoline (**3**)

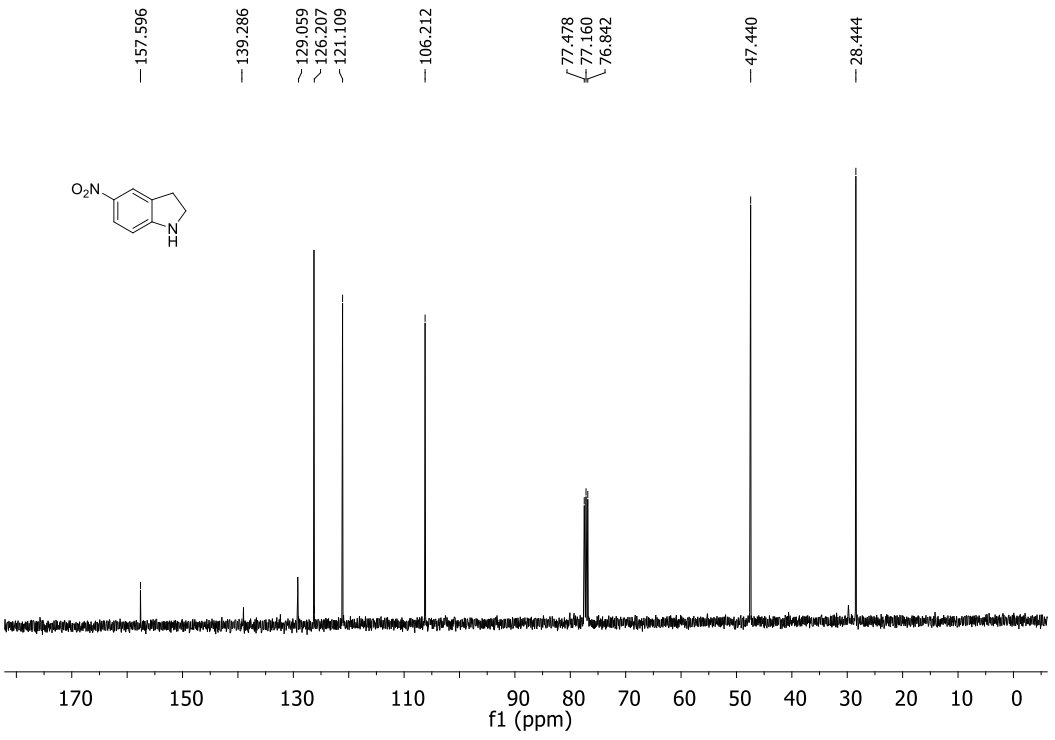

Figure 2.51. ^{13}C NMR 5-Nitroindoline (**3**).

CHAPTER 3

3-Nitro-coumarin Synthesis via Nitrative Cyclization of Aryl Alkynoates using *tert*-Butyl Nitrite

3.1 ABSTRACT

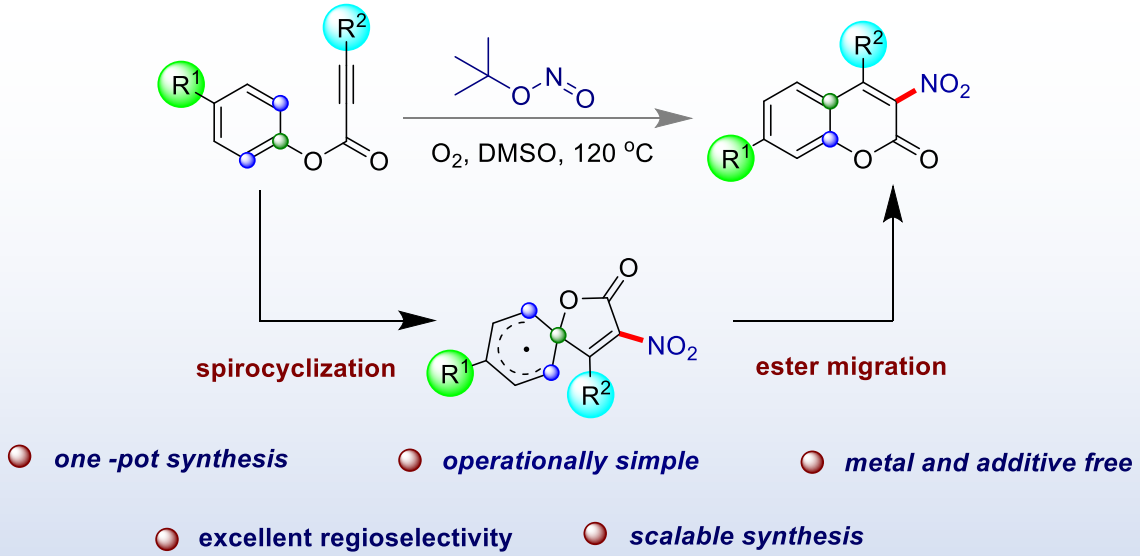

A one-pot metal-free synthesis of 3-nitro-coumarins from aryl alkynoates has been achieved using TBN (*tert*-butyl nitrite) as the sole reagent. We reported a one-pot metal-free synthesis of 3-nitro-coumarins from aryl alkynoates using TBN (*tert*-butyl nitrite) as the sole reagent. The radical triggered cyclization and nitration of the aryl alkynoates proceeded in a cascaded manner *via* nitro radical addition to alkynoates, then 5-exo-trig spirocyclization and ester migration.

3.2 INTRODUCTION

TBN (*tert*-butyl nitrite) has been acknowledged as a multitasking reagent in organic synthesis in the last two decades.[1, 2] Due to the distinct structural features, TBN responds differently depending upon reaction conditions. For example, under an aerobic atmosphere, TBN generates NO radical that captures dioxygen to produce NO_2 radical. The NO_2 radical triggers the reactions like nitration,[3-7] nitrative cyclization,[8-13], etc. For instance, in 2015, Li group established a method for the synthesis of 3-nitro-indole by nitrative cyclization of N-aryl-imines using TBN (Scheme 3.1).[9]

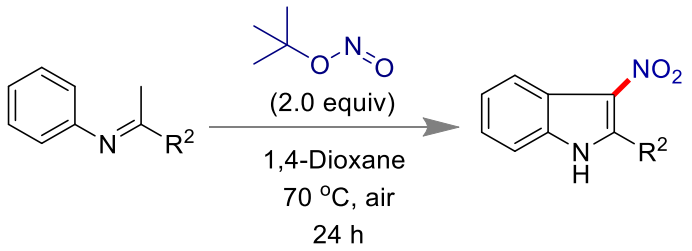

Scheme 3.1. Li's approach for the synthesis of 3-nitro-indole by nitrative cyclization of N-aryl-imines using TBN

In 2018, Wei and co-workers disclosed nitrative cyclization reaction of 1,6-enynes using TBN under metal-free conditions (Scheme 3.2).[8]

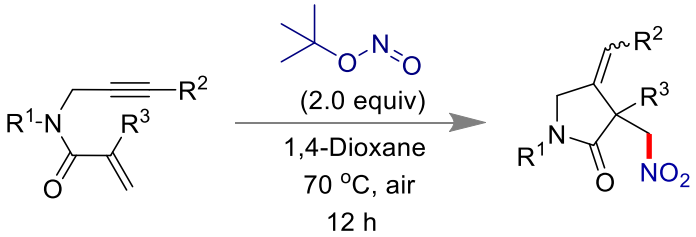

Scheme 3.2. Wei's approach for nitrative cyclization reaction of 1,6-enynes using TBN under the metal-free condition

Radical cascade reactions are eminent tools for synthesizing biologically active structural scaffolds widespread in natural products and pharmaceuticals.[14, 15] Among the radical-induced tandem reactions, the reactions of aryl alkynoates have drawn immense attention to synthetic organic chemists. The aryl alkynoates are easily accessible, and due to the suitable radical accepting properties, they readily undergo cascaded-type cyclization reactions to yield 3-functionalized coumarins.[16, 17] For example, synthesis of various 3-functionalized coumarin through 6-endo-trig cyclization of aryl alkynoates has been cataloged.[16-22] Parallelly, a significant number of reports have appeared in the literatures on the synthesis of 3-functionalized coumarins via 5-exo-trig cyclization of aryl alkynoates.[23-26] In this work we have reported a convenient and metal-free synthesis of 3-nitro-coumarins by radical cascaded cyclization reaction of aryl alkynoates using TBN (Figure 3.1). This reaction proceeded through nitro radical addition to the alkynoates and led to the spirocyclization by 5-exo-trig pathway. Finally, the ester migration led to 3-nitro-coumarin.

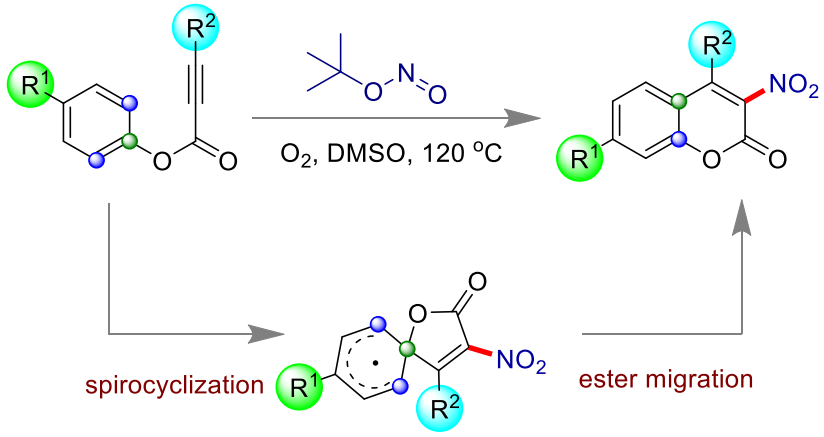

Figure 3.1. Our approach for TBN mediated nitrative cyclization of aryl alkynoates

.The coumarin framework is one of the imperative structural auxiliaries prevalent in bioactive molecules and natural products.[27] These heterocycles furnish a wide array of pharmaceutical properties,[28, 29] and their utilization in materials chemistry is also well documented.[30, 31]

Nitroarenes are also a prominent class of building blocks of many bioactive molecules, pharmaceuticals, and natural products.[32] In addition, nitroarenes are important key intermediates in synthetic organic chemistry.[33, 34] The 3-nitro-coumarin scaffolds are well-known for their bio-antioxidant, neurotropic properties and are used for the treatment of asthma, rhinitis, etc.[35] Nitration of non-prefunctionalized aromatic or heteroaromatic compounds is generally done under harsh conditions and uncontrollable to selective mono-substitution.[36] Recently, several nitration reactions have been established by adopting various mild reaction conditions.[37-39] Significant number of reports on the transition metal-catalyzed C-H nitration have also appeared in literature.[40-43] However, the use of TBN in nitration and nitrative cyclization reactions has several advantages compared to previously mentioned methods as TBN is a mild reagent and after TBN mediated reactions no acidic wastes are produced, only *tert*-Butanol is generated as non-toxic side side product.[1-7]

3.3 RESULT AND DISCUSSION

The compound *p*-tolyl-3-phenylpropiolate (**1a**) was chosen as the model substrate to optimize this nitrative cyclization reaction (Table 3.1). With 4.0 equiv of TBN at 120 ^{o}C under oxygen atmosphere in DMSO after 24 h, the desired product 3-nitro coumarin was obtained with 58% yield (entry 1). When the reaction time was increased to 36 h, the yield was 70% (entry2). However, the reaction yield did not get affected in the increase of reaction time to 48 h (entry 3). The solvents like benzene, toluene, acetone, 1,2-DCB, etc. did not impact the reaction's efficiency (entries 4-7). The reaction failed in EtOH (entry 8). Furthermore, no encouraging results were obtained in the solvents like acetonitrile, DMF, 1,4-dioxane and 1,2-DCE (entries 9-12). The reaction failed at room temperature in DMSO (Table 1, entry 13). The reaction yield was

diminished to 52% and 37% when the TBN loading was 3.0 and 2.0 equiv, respectively (entries 14 and 15). The TBN loading to 5.0 equiv did not have a better result (entry 16). It was observed that there was no notable enhancement of reaction yield when the temperature was increased to 140 ^{o}C (Table 1, entry 17). When the reaction was carried out in air, the desired product was obtained with 31% yield (entry 18). The optimum condition was found to be using 4.0 equiv of TBN, at 120 ^{o}C in O_2 atmosphere and DMSO solvent, with a reaction time of 36 h (entry 2).

Table 3.1. Optimization of reaction parameters[a]

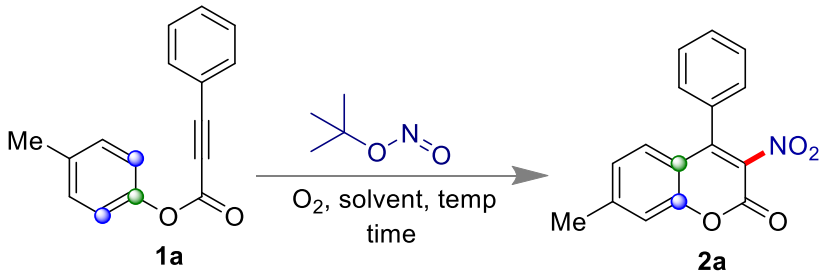

entry	TBN (equiv)	Condition	Time (h)	Yield (%)[b]
1.	4.0	DMSO, 120 ^{o}C	24	58
2.	**4.0**	**DMSO, 120 ^{o}C**	**36**	**70**
3.	4.0	DMSO, 120 ^{o}C	48	68
4.	4.0	Benzene, 80 ^{o}C	36	trace
5.	4.0	Toluene, 110 ^{o}C	36	trace
6.	4.0	Acetone, 60 ^{o}C	36	trace
7.	4.0	1,2-DCB, 120 ^{o}C	36	trace
8.	4.0	EtOH, 90 ^{o}C	36	NR[c]
9.	4.0	ACN, 80 ^{o}C	36	31
10.	4.0	DMF, 100 ^{o}C	36	21
11.	4.0	1,4-dioxane, 90 ^{o}C	36	27
12.	4.0	1,2-DCE, 90 ^{o}C	36	35

13.	4.0	DMSO, rt	36	NR[c]
14.	3.0	DMSO, 120 ^{o}C	36	52
15.	2.0	DMSO, 120 ^{o}C	36	37
16.	5.0	DMSO, 120 ^{o}C	36	67
17.	4.0	DMSO, 140 ^{o}C	36	66
18.	4.0	DMSO, 120 ^{o}C	36	31[d]

[a]Standard conditions: **1a** (0.2 mmol, 1.0 equiv), tert-butyl nitrite (4.0 equiv) in 3 mL of solvent at 120 ^{o}C for 36 h under O_2 atmosphere. [b]Isolated yield. [c]No reaction. [d]Air atmosphere

Under the optimized conditions, the substrate scopes of this nitrative cyclization reaction were verified (Figure 3.2). Different aryl alkynoates containing various electron-donating, electron-withdrawing groups at the phenoxy were examined. Aryl alkynoates with electron-donating groups -Me, -^{t}Bu, -^{i}Pr, -Et, -Ph on the *para*-position of the phenoxy ring led to 3-nitro-coumarins (**2a-2e**) with 68-81% yields. Substrates **1** with halogens (-I, -Br, -Cl, -F) on the *para*-position of phenoxy ring also worked well and the corresponding desired products (**2f-2i**) were obtained with moderate yields (52-63%). Starting compounds containing strong electron-donating substituent (-OMe, -OEt, -OBn) on the para position of phenoxy ring underwent conversion and provided products (**2j-2l**) with fair yields (56-61%). Similarly, with no substituent on phenoxy ring also participated in reaction, and 55% of the product **2m** was obtained. The presence of a naphthyl group responded to optimized reaction condition well and gave desired product **2n** with 63% yield. When substituent was present on the *ortho*-position of phenoxy ring, steric factor played a crucial role, and trace amount products **2o-2p** were identified. The reaction also worked well for the meta-substituted phenoxyl derivatives. The starting compound with substations like –Br, -I and -OMe led to the corresponding products **2q-2s** with 60-64% yields. The electronic effect also played an

important role and substrate **1** containing strong electron-withdrawing groups like -NO_2 on the *para*-position of phenoxy ring did not provide the desired product (**2t**).

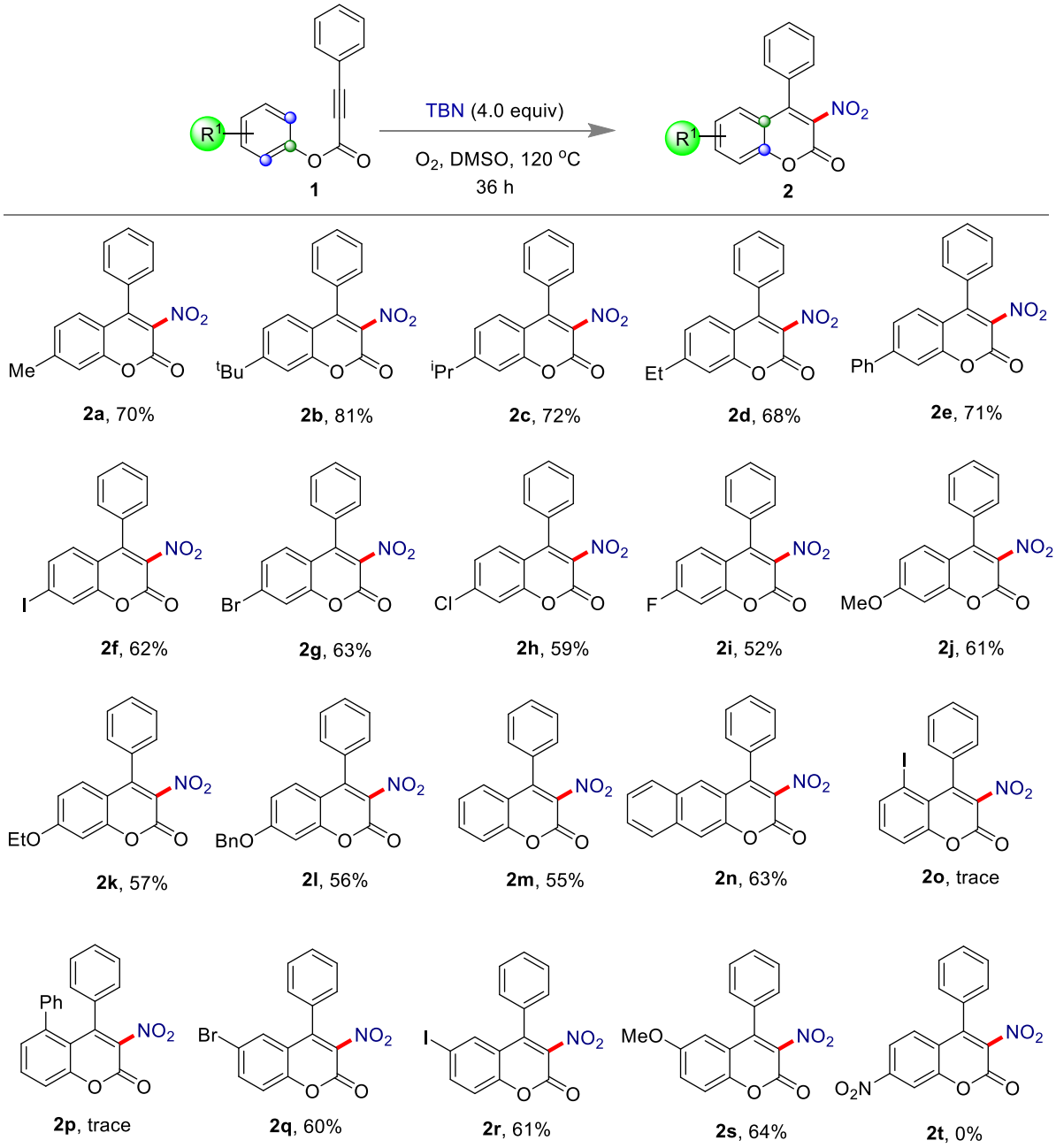

Figure 3.2. Scope of phenols in the nitrative cyclization of aryl alkynoates

Next, we explored the substrate scope with the substitution at the propiolic acids part (Figure 3.3). The reactions were performed for the propiolic acids having electron-donating –Me and –OMe, and electron-withdrawing substituents -Cl, -F and -Br. In both cases, the reaction worked well, and the corresponding 3-nitro-coumarins (**2u-2y**) were obtained in 56-68% yields.

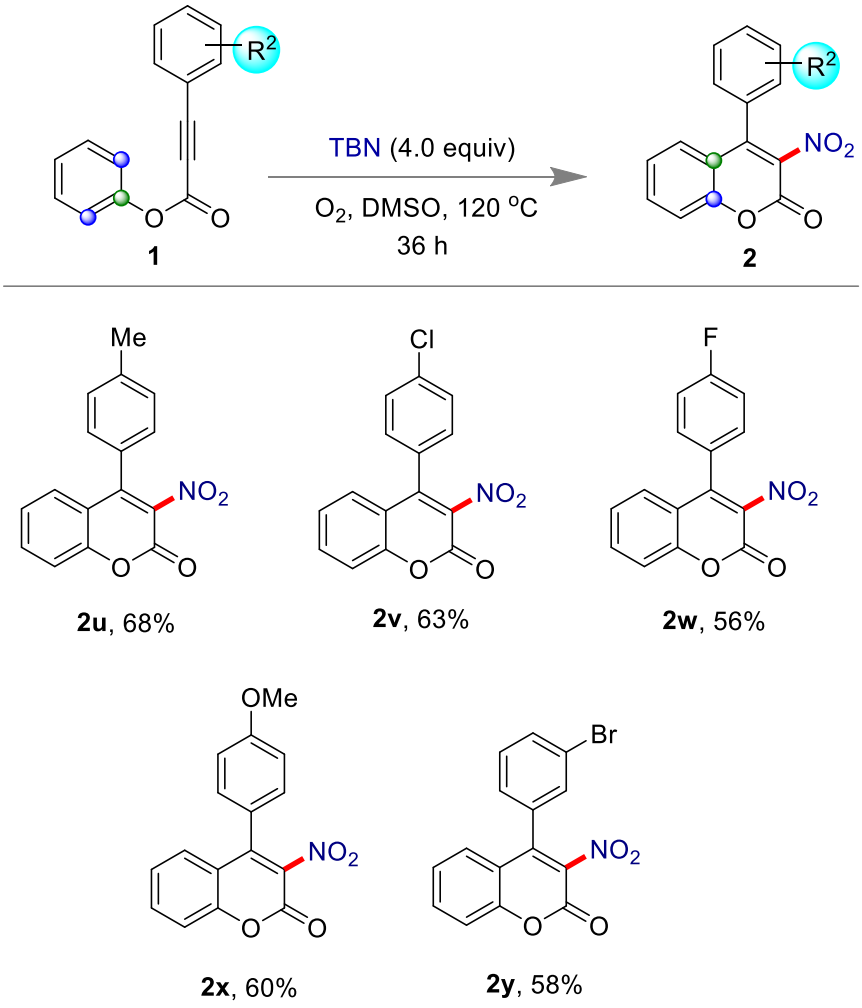

Figure 3.3. Substrate scope with various substitutions at the propiolic acid part.

The synthetic utility of this nitrative cyclization was studied by scaling up the reaction with 7.18 mmol of substrate **1b** (3-(*tert*-butyl)phenyl 3-phenylpropiolate) under the standard condition, and the product **2b** (7-(*tert*-butyl)-3-nitro-4-phenyl-2H-chromen-2-one) was obtained with 59% (1.37 g) yield (Figure 3.4a). Towards post-synthetic application, reduction of 7-Bromo-3-nitro-4-

phenyl-2H-chromen-2-one (**2g**) was carried out with Fe/NH_4Cl[44] and the desired 3-amino-7-bromo-4-phenyl-2H-chromen-2-one (**7**) was isolated with 80% yield (Figure 3.4b).

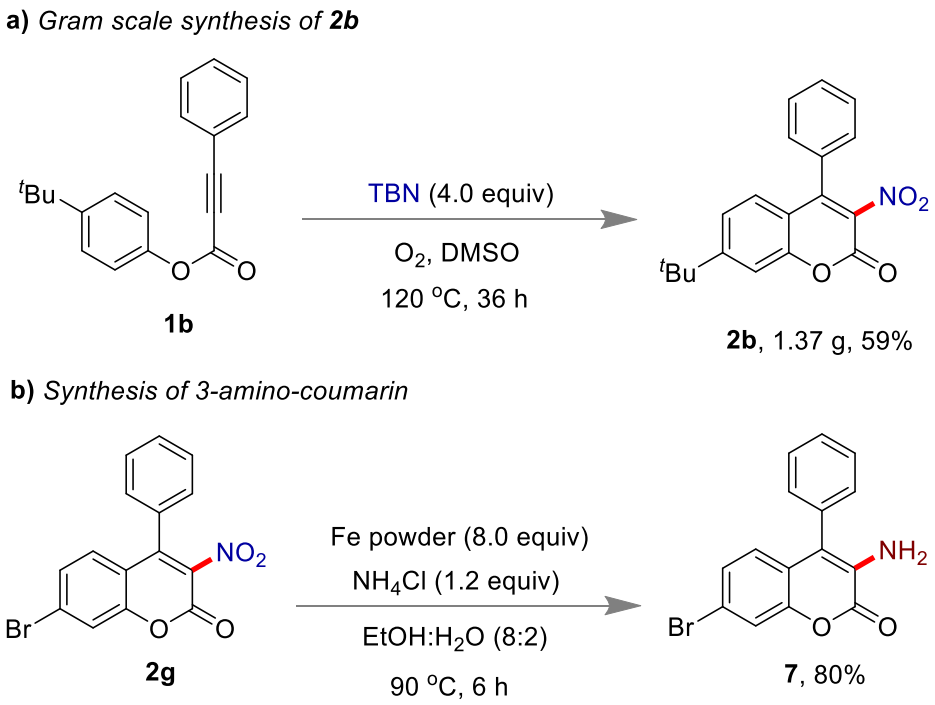

Figure 3.4. Synthetic applications.

The control experiments (Figure 3.5) helped to understand that the reaction proceeded *via* a radial pathway. The reaction of **1a** with the radical scavengers neither TEMPO (2,2,6,6-tetramethylpiperidin-1-yl-oxyl) nor BHT (2,6-di-*tert*-butyl-4-methylphenol) under standard reaction condition did not furnish any product. Therefore, it was expected that the reaction proceeded *via* a radical pathway.

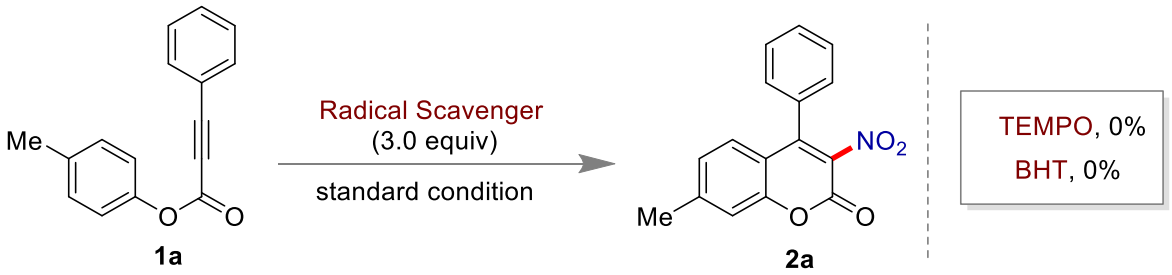

Figure 3.5. Control experiments with radical scavengers.

Based on the literature evidences[1, 23] and control experiments, a plausible mechanism of the nitrative cyclization is proposed in Figure 3.6. In a radical triggered cyclization of aryl alkynoates with TBN, two different modes of cyclization could lead to the products **2** (*via* 5-exo-trig cyclization) or **2'** (*via* 6-endo-trig cyclization). Li and co-workers reported nitrative spirocyclization of *N*-Aryl propiolamides using TBN, TEMPO and water in EtOAc solvent.[13] The conversion finally afforded nitrated spirocycles and the reaction proceeded via 5-exo-trig cyclization. Interestingly, in our case, only **2** was obtained, and the formation of nitrated spirocycles or product **2'** (Figure 3.6a) was not observed. The structure of **2** was confirmed from X-ray crystallography. In the first step, the NO_2 radical[1, 2] was thermally generated from TBN (Figure 3.6b). Next, the NO_2 radical underwent addition to the α-carbon of C=O in **1** and produced the intermediate **3** (Figure 3.6c). After that, intermediate **3** led to the formation of **4** *via* 5-exo-trig cyclization. Subsequently, **4** underwent 1,2-ester migration to generate the intermediate **5** and then cyclization led to another intermediate **6.** Finally, abstraction of H atom by $^{t}BuO^{\bullet}$ radical from intermediate **6** provided the product **2.**

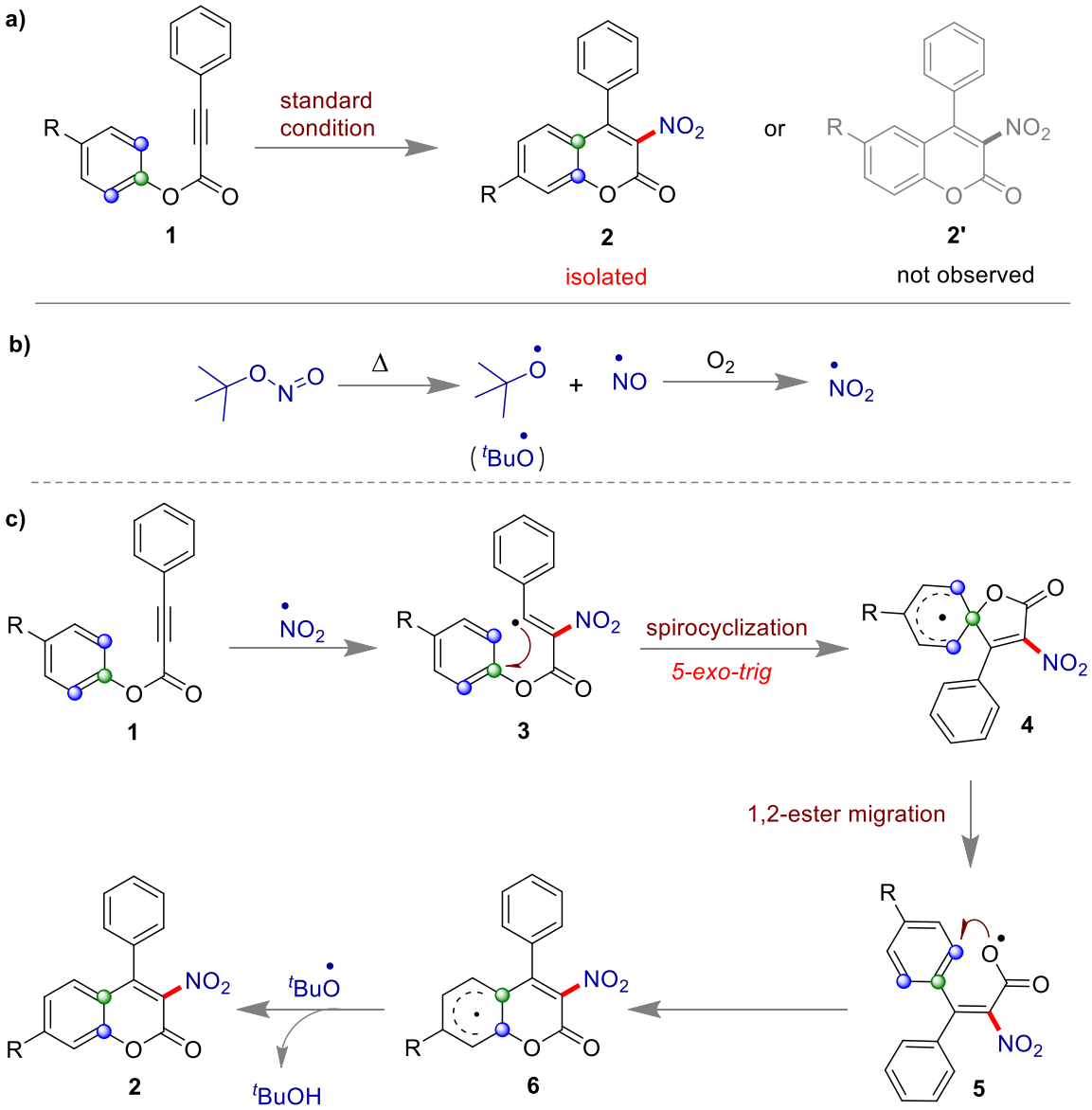

Figure 3.6. Tentative mechanism

3.4 CONCLUSION

In summary, we have developed a metal-free protocol for the 3-nitro-coumarin synthesis via nitrative 5-exo-trig cyclization from easily accessible aryl alkynoates by implementing TBN as the sole reagent without using any additive. With this efficient protocol, a library of 3-nitro coumarins has been synthesized with excellent regioselectivity and tolerance toward a wide spectrum of

functional groups. Furthermore, one-pot synthesis, scalability, and the use of easy handling reagent are the key advantages of this methodology. We anticipate that this simple and convenient protocol will make an important contribution to the research topic of radical cascade cyclization reaction and synthesis of nitro-containing heterocycles.

3.5 EXPERIMENTAL SECTION

Instrumentation and Chemicals: Column chromatography was used for the purification of the compounds using silica gel (with mesh 100-200 or mesh 230-400) and hexane-ethyl acetate mixtures were used as eluent unless otherwise specified. Solvents were purchased from commercially available sources and used in the reaction without further purification. All NMR spectra were recorded in 400 MHz or 700 MHz instruments (Bruker) at room temperature (25 °C). The splitting of the NMR peaks (peak pattern) are represented by s: singlet; d: doublet; t: triplet; q: quartet; m: multiplet; dd: doublet of doublets; td: triplet of doublets; br s: broad singlet. Chemical shift values are reported in parts per million (ppm) with respect to residual trichloromethane (7.26 ppm for ^{1}H and 77.16 ppm for ^{13}C) and dimethyl sulfoxide (2.50 ppm for ^{1}H and 39.52 ppm for ^{13}C). The coupling constant values (*J*) are reported in hertz (Hz). A digital melting point apparatus was used to obtain the melting point of the compounds which were included in the characterization data without any correction. FT-IR spectra were recorded by making a thin film of the compounds on KBr pellets using dichloromethane and IR spectral data are reported in wave number (cm^{-1}). High-resolution mass spectra (HR-MS) were recorded on an ESI-TOF (time of flight) mass spectrometer. The detailed procedure for the preparation of the starting materials and target molecule are described below.

Synthetic procedure for preparation of 7-Methyl-3-nitro-4-phenyl-2H-chromen-2-one (2a). To an oven-dried sealed tube charged with a magnetic stirring bar, *p*-Tolyl 3-phenylpropiolate (81 mg, 0.34 mmol, 1.0 equiv) and 3 mL DMSO were taken. The tube was fitted with a rubber septum and then it was charged with dioxygen. After that TBN (162 µL, 1.37 mmol, 4.0 equiv) was added to it in an oxygen atmosphere, the septum was then replaced by a Teflon screwcap under oxygen flow. The reaction mixture was allowed to stir at 120 ^{o}C in a preheated oil bath for 36 h. After that, the reaction mixture was cooled at room temperature and washed with water. The organic layer was extracted with dichloromethane and was dried over Na_2SO_4, and concentrated under reduced pressure. The crude reaction mixture was purified by silica gel column chromatography using 5% ethyl acetate/hexane. Purification through column chromatography (in 5% ethyl acetate/hexane) yielded 67 mg of 2a (70%).

Procedure for gram-scale synthesis. To an oven-dried sealed tube charged with a magnetic stirring bar, 4-(*tert*-Butyl)phenyl 3-phenylpropiolate (2.0 g, 7.18 mmol, 1.0 equiv) and 25 mL DMSO were taken. The tube was fitted with a rubber septum and then it was charged with dioxygen. After that TBN (3.4 mL, 28.7 mmol, 4.0 equiv) was added to it in an oxygen atmosphere, and the septum was then replaced by a Teflon screwcap under oxygen flow. The reaction mixture was allowed to stir at 120 ^{o}C in a preheated oil bath for 36 h. After that, the reaction mixture was cooled at room temperature and washed with water. The organic layer was extracted with dichloromethane and was dried over Na_2SO_4, and concentrated under reduced pressure. The crude reaction mixture was purified by silica gel column chromatography using 5% ethyl acetate/hexane. Purification through column chromatography (in 5% ethyl acetate/hexane) yielded 1.37 g of **2b** (59%)

Procedure for the radical scavenger experiment with 2,2,6,6-Tetramethylpiperidin-1-yl)oxyl radical (TEMPO). To an oven dried sealed tube charged with a magnetic stirring bar, *p*-Tolyl 3-phenylpropiolate (86.5 mg, 0.37 mmol, 1.0 equiv), TEMPO (228 mg, 1.46 mmol, 3.0 equiv) and 3 mL DMSO were taken. The tube was fitted with a rubber septum and then it was charged with dioxygen. After that TBN (175 µL, 1.47 mmol, 4.0 equiv) was added to it in an oxygen atmosphere, the septum was then replaced by a Teflon screwcap under oxygen flow. The reaction mixture was allowed to stir at 120 ^{o}C in a preheated oil bath for 36 h. After 36 h reaction formation of product, **2a** was not observed.

Synthetic procedure of 3-Amino-7-bromo-4-phenyl-2H-chromen-2-one (7). To an oven-dried sealed tube charged with a magnetic stirring bar, 7-bromo-3-nitro-4-phenyl-2H-chromen-2-one (64.4 mg, 0.186 mmol, 1.0 equiv) was taken and dissolved in EtOH and H_2O (8:2 v/v). To it Fe powder (83.0 mg, 1.488 mmol, 8 equiv), NH_4Cl (12.0 mg, 0.223 mmol, 1.2 equiv), and the resulting mixture were stirred in a preheated oil bath at 90 ^{o}C, for 6 h.[44] Completion of the reaction was confirmed by TLC and the reaction mixture was cooled at room temperature and washed with water. The organic layer was extracted with ethyl acetate and was dried over Na_2SO_4, and concentrated under reduced pressure. The crude reaction mixture was purified by silica gel column chromatography using 5% ethyl acetate/hexane as eluent to get 3-amino-7-bromo-4-phenyl-2H-chromen-2-one as off white solid in 80% yield (48 mg).

Synthetic procedure for preparation of aryl alkynoates.[45] In a round bottom flask equipped with a magnetic stirring bar, phenol (5.5 mmol, 1.0 equiv) and DCM (20 mL) were taken and allowed to stir at 0 ^{o}C for 5 min. Next phenyl propiolic acid (6.1 mmol, 1.1 equiv) was added to it

and allowed to stir at 0 ^{o}C for 5 min. Next, a mixture of dicyclohexylcarbodiimide (8.2 mmol, 1.5 equiv) and 4-dimethylaminopyridine (0.5 mmol, 0.1 equiv) in DCM (10 mL) was added dropwise and the reaction system was allowed to stir at room temperature for 12 h. After the completion of the reaction, the organic layer was extracted with DCM and dried over Na_2SO_4, and concentrated under reduced pressure. Next, the crude reaction mixture was purified by silica gel column chromatography and aryl alkynoates were obtained.

Crystallographic Investigation

The crystals data were collected with Bruker SMART D8 goniometer equipped with an APEX CCD detector and with an INCOATEC micro source (Mo-Kα radiation, λ = 0.71073 Å). SAINT+[46] and SADABS[47] were used to integrate the intensities and to correct the absorption respectively The structure was resolved by direct methods and refined on F^2 with SHELXL-97.[48] Good quality crystals for the compound **2f, 2s** and **2u** were obtained by the slow evaporation of chloroform. ORTEP drawing of the compounds shows ellipsoid contour at the 50% probability level.

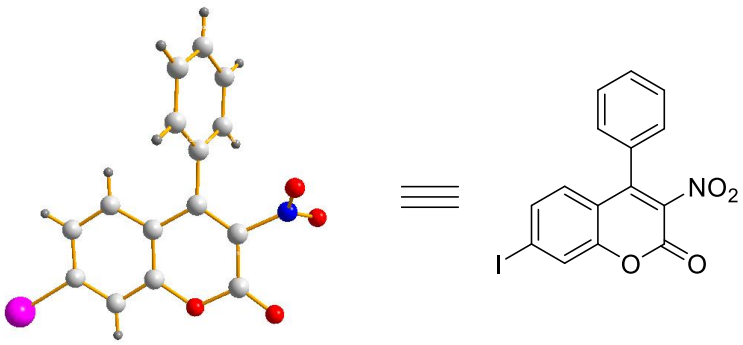

Figure 3.7. Crystal structure of **2f**.

Crystallographic data for 2f.

CCDC number	2064075
Empirical formula	$C_{15}H_8INO_4$
Formula weight	394.63
Temperature/K	100.00(10)
Crystal system	monoclinic
Space group	*P*21/c
a/Å	10.34430(10)
b/Å	15.20400(10)
c/Å	8.99570(10)
α/°	90
β/°	100.7960(10)
γ/°	90
Volume/Å^3	1389.75(2)
Z	4
ρ_{calc}g/cm^3	1.886
μ/mm^{-1}	18.249
F(000)	763
Crystal size/mm^3	0.20 × 0.20 ×0.18
Radiation	CuKα (λ = 1.54184)
2Θ range for data collection/°	8.702 to 150.378
Index ranges	$-12 \le h \le 12$, $-14 \le k \le 19$, $-11 \le l \le 10$
Reflections collected	20661
Independent reflections	2838 [R_{int} = 0.0582, R_{sigma} = 0.0235]
Data/restraints/parameters	2838/0/190
Goodness-of-fit on F^2	1.059

Final R indexes [I>=2σ (I)]	R_1 = 0.0303, wR_2 = 0.0821
Final R indexes [all data]	R_1 = 0.0305, wR_2 = 0.0823
Largest diff. peak/hole / e Å^{-3}	0.96/-1.82

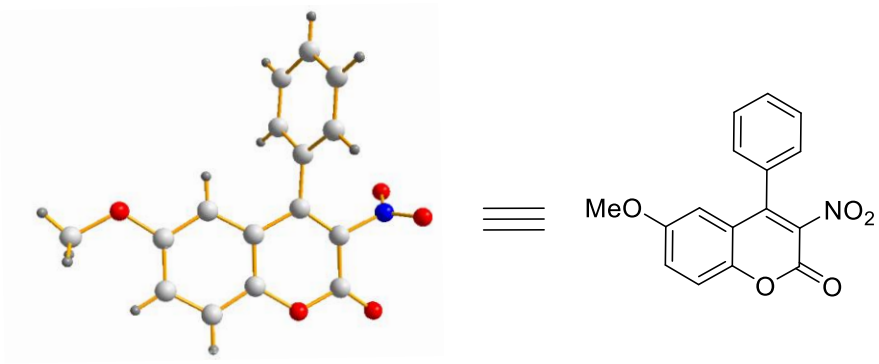

Figure 3.8. Crystal structure of **2s**.

Crystallographic data for 2s.

CCDC number	2076536
Empirical formula	$C_{16}H_{11}NO_5$
Formula weight	297.26
Temperature/K	299.3(6)
Crystal system	orthorhombic
Space group	*P*na2$_1$
a/Å	7.91770(10)
b/Å	16.29580(10)
c/Å	10.82590(10)
α/°	90
β/°	90
γ/°	90
Volume/Å^3	1396.81(2)
Z	4

ρ_{calc}g/cm^3	1.414
μ/mm^{-1}	0.899
F(000)	616
Crystal size/mm^3	0.20 × 0.20 ×0.18
Radiation	CuKα (λ = 1.54184)
2Θ range for data collection/°	4.8770 to 150.094
Index ranges	-8 ≤ h ≤ 9, -20 ≤ k ≤ 20, -13 ≤ l ≤ 13
Reflections collected	37735
Independent reflections	2873 [R_{int} = 0.0561, R_{sigma} = 0.0203]
Data/restraints/parameters	2873/1/200
Goodness-of-fit on F^2	1.072
Final R indexes [I>=2σ (I)]	R_1 = 0.0335, wR_2 = 0.0885
Final R indexes [all data]	R_1 = 0.0353, wR_2 = 0.0901
Largest diff. peak/hole / e Å^{-3}	0.10/-0.13

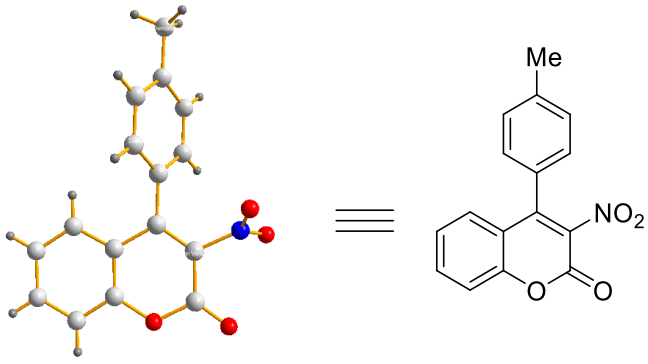

Figure 3.9. Crystal structure of **2u**.

Crystallographic data for 2u.

CCDC number	2064074
Empirical formula	$C_{16}H_{11}NO_4$
Formula weight	281.26
Temperature/K	298.84(10)
Crystal system	triclinic
Space group	*P*-1
a/Å	8.2983(8)
b/Å	9.1387(8)
c/Å	9.6145(7)
α/°	73.544(7)
β/°	72.349(8)
γ/°	82.099(8)
Volume/Å^3	665.27(11)
Z	2
ρ_{calc}g/cm^3	1.404
μ/mm^{-1}	0.852
F(000)	292
Crystal size/mm^3	0.25 × 0.21 ×0.20
Radiation	CuKα (λ = 1.54184)
2Θ range for data collection/°	9.988 to 150.750
Index ranges	-10 ≤ h ≤ 10, -10 ≤ k ≤ 11, -12 ≤ l ≤ 11
Reflections collected	9577
Independent reflections	2670 [R_{int} = 0.0479, R_{sigma} = 0.0245]
Data/restraints/parameters	2670/0/191
Goodness-of-fit on F^2	1.052
Final R indexes [I>=2σ (I)]	R_1 = 0.0708, wR_2 = 0.2122

Final R indexes [all data] $R_1 = 0.0808$, $wR_2 = 0.2247$

Largest diff. peak/hole / e $Å^{-3}$ 0.35/-0.29

Characterization Data

7-Methyl-3-nitro-4-phenyl-2H-chromen-2-one (2a). R_f = 0.5 (10% ethyl acetate/hexane); yellow solid; yield 67 mg (70%); mp: 185-187 ^oC; ^1H NMR (400 MHz, $CDCl_3$) δ 7.56 – 7.52 (m, 3H), 7.37 (dd, *J* = 7.2, 1.6 Hz, 2H), 7.28 (s, 1H), 7.17 (d, *J* = 8.4 Hz, 1H), 7.12 (d, *J* = 8.8 Hz, 1H), 2.50 (s, 3H); ^{13}C NMR (100 MHz, $CDCl_3$) δ 153.8, 153.1, 147.4, 146.3, 136.1, 130.8, 129.3, 129.2, 129.0, 128.0, 127.0, 117.7, 115.5, 22.0; IR (KBr) ῡ 1735, 1616, 1540, 1462, 741 cm^{-1}; HRMS (ESI-TOF) calcd for $C_{16}H_{12}NO_4$ $[M+H]^+$ 282.0761, found 282.0763.

7-(*tert*-Butyl)-3-nitro-4-phenyl-2H-chromen-2-one (2b). R_f = 0.4 (10% ethyl acetate/hexane); yellow liquid; yield 69 mg (81%); ^1H NMR (400 MHz, $CDCl_3$) δ 7.56 – 7.51 (m, 3H), 7.47 (d, *J* = 2.0 Hz, 1H), 7.39 – 7.34 (m, 3H), 7.23 (d, *J* = 8.4 H, 1H), 1.36 (s, 9H); ^{13}C NMR (100 MHz, $CDCl_3$) δ 159.5, 153.9, 153.1, 147.3, 136.2, 130.8, 129.3, 129.2, 128.9, 128.0, 123.4, 115.4, 114.4, 35.7, 31.0; IR (KBr) ῡ 1735, 1635, 1540, 1457, 756 cm^{-1}; HRMS (ESI-TOF) calcd for $C_{19}H_{18}NO_4$ $[M+H]^+$ 324.1230, found 324.1230.

7-Isopropyl-3-nitro-4-phenyl-2H-chromen-2-one (2c). R_f = 0.5 (10% ethyl acetate/hexane); yellow solid; yield 74 mg (72%); mp: 138-140 ^oC; ^1H NMR (400 MHz, $CDCl_3$) δ 7.58 – 7.51 (m, 3H), 7.38 – 7.36 (m, 2H), 7.32 (d, *J* = 0.8 Hz, 1H), 7.23 – 7.17 (m, 2H), 3.03 (h, *J* = 6.8 Hz, 1H), 1.30 (d, *J* = 7.2 Hz, 6H); ^{13}C NMR (100 MHz, $CDCl_3$) δ 157.1, 153.9, 153.3, 147.4, 136.1, 130.8, 129.3, 129.3, 129.2, 128.1, 124.5, 115.8, 115.2, 34.5, 23.6; IR (KBr) ῡ 1738, 1611, 1541, 1421, 744 cm^{-1}; HRMS (ESI-TOF) calcd for $C_{18}H_{15}NNaO_4$ $[M+Na]^+$ 332.0893, found 332.0915

7-Ethyl-3-nitro-4-phenyl-2H-chromen-2-one (2d). R_f = 0.4 (10% ethyl acetate/hexane); light yellow solid; yield 64 mg (68%); mp: 172-175 ºC; ^{1}H NMR (400 MHz, $CDCl_3$) δ 7.59 – 7.51 (m, 3H), 7.39 – 7.36 (m, 2H), 7.30 (d, *J* = 0.8 Hz, 1H), 7.20 (d, *J* = 8.4 Hz, 1H), 7.15 (dd, *J* = 8.4, 1.6 Hz, 1H), 2.79 (q, *J* = 7.6 Hz, 2H), 1.29 (t, *J* = 7.6 Hz, 3H); ^{13}C NMR (100 MHz, $CDCl_3$) δ 153.9, 153.3, 152.5, 147.4, 136.1, 130.8, 129.3, 129.2, 129.1, 128.1, 125.9, 116.5, 115.7, 29.2, 15.1; IR (KBr) ῡ 1738, 1611, 1542, 1421, 760 cm^{-1}; HRMS (ESI-TOF) calcd for $C_{17}H_{13}NNaO_4$ $[M+Na]^+$ 318.0737, found 318.0733.

3-Nitro-4,7-diphenyl-2H-chromen-2-one (2e). R_f = 0.3 (10% ethyl acetate/hexane); yellow solid; yield 64 mg (71%); mp: 182-185 ºC; ^{1}H NMR (400 MHz, $CDCl_3$) δ 7.69 (s, 1H), 7.64 (d, *J* = 6.8 Hz, 2H), 7.58 – 7.47 (m, 7H), 7.42 (d, *J* = 4.8 Hz, 2H), 7.36 (d, *J* = 8.0 Hz, 1H); ^{13}C NMR (100 MHz, $CDCl_3$) δ 153.7, 153.5, 147.6, 147.2, 138.4, 130.9, 129.7 129.5, 129.4, 129.4, 129.1, 129.1, 128.1, 127.5, 124.5, 116.8, 115.6; IR (KBr) ῡ 1739, 1616, 1543, 1421, 760 cm^{-1}; HRMS (ESI-TOF) calcd for $C_{21}H_{14}NO_4$ $[M+H]^+$ 344.0917, found 344.0920.

7-Iodo-3-nitro-4-phenyl-2H-chromen-2-one (2f). R_f = 0.4 (10% ethyl acetate/hexane); yellow solid; yield 37 mg (62%); mp: 220-222 ºC; ^{1}H NMR (700 MHz, $CDCl_3$) δ 7.87 (s, 1H), 7.64 (dd, *J* = 8.4, 0.7 Hz, 1H), 7.59 – 7.54 (m, 3H), 7.36 (d, *J* = 7.0 Hz, 2H), 6.98 (d, *J* = 8.4 Hz, 1H)·; ^{13}C NMR (100 MHz, $CDCl_3$) δ 152.8, 152.5, 146.9, 136.8, 135.1, 131.2, 130.0, 129.5, 128.4, 128.0, 126.8, 117.6, 100.8; IR (KBr) ῡ 1745, 1591, 1546, 1421, 760 cm^{-1}; HRMS (ESI-TOF) calcd for $C_{15}H_9INO_4$ $[M+H]^+$ 393.9571, found 393.9557.

7-Bromo-3-nitro-4-phenyl-2H-chromen-2-one (2g). R_f = 0.3 (10% ethyl acetate/hexane); yellow solid; yield 45 mg (63%); mp: 190-192 ºC; ^{1}H NMR (700 MHz, $CDCl_3$) δ 7.67 (s, 1H), 7.59 – 7.55 (m, 3H), 7.44 (dd, *J* = 8.4, 1.4 Hz, 1H), 7.36 (d, *J* = 7.0 Hz, 2H), 7.16 (d, *J* = 8.4 Hz, 1H); ^{13}C NMR (100 MHz, $CDCl_3$) δ 153.0, 152.9, 146.8, 136.6, 131.2, 130.2, 129.5, 129.3, 128.9, 128.5 128.0, 120.9, 117.1; IR (KBr) ῡ 1745, 1617, 1597, 1545, 1458, 763 cm^{-1}; HRMS (ESI-TOF) calcd for $C_{15}H_8BrNNaO_4$ $[M+Na]^+$ 367.9529 , found 367.9515.

7-Chloro-3-nitro-4-phenyl-2H-chromen-2-one (2h). R_f = 0.4 (10% ethyl acetate/hexane); yellowish white solid; yield 35 mg (59%); mp: 204-206 ºC; ^{1}H NMR (700 MHz, $CDCl_3$) δ 7.60-7.55 (m, 3H), 7.50 (d, *J* = 1.4 Hz, 1H), 7.36 (d, *J* = 7.0 Hz, 2H), 7.29 (dd, *J* = 8.4, 1.4 Hz, 1H), 7.24 (d, *J* = 8.4 Hz, 1H); ^{13}C NMR (100 MHz, $CDCl_3$) δ 153.1, 153.0, 146.7, 140.7, 131.2, 130.2, 129.5, 128.6, 128.0, 126.4, 117.9, 116.7; IR (KBr) ῡ 1744, 1641, 1540, 1461, 752 cm^{-1}; HRMS (ESI-TOF) calcd for $C_{15}H_9ClNO_4$ $[M+H]^+$ 302.0215, found 302.0214.

7-Fluoro-3-nitro-4-phenyl-2H-chromen-2-one (2i). R_f = 0.4 (10% ethyl acetate/hexane); light yellow solid; yield 38 mg (52%); mp: 178-180 ºC; ^{1}H NMR (700 MHz, $CDCl_3$) δ 7.59 – 7.55 (m, 3H), 7.37 (d, *J* = 7.0 Hz, 2H), 7.31 (dd, *J* = 9.1, 6.3 Hz, 1H), 7.21 (dd, *J* = 8.4, 2.1 Hz, 1H), 7.07 – 7.05 (m, 1H); ^{13}C NMR (100 MHz, $CDCl_3$) δ 165.9 (d, $^1J_{C\text{-}F}$ = 257.3 Hz), 154.3, 154.2, 153.2, 147.0, 131.3 (d, $^3J_{C\text{-}F}$ = 10.5 Hz), 131.1, 129.5, 128.8, 128.0, 114.8 (d, $^4J_{C\text{-}F}$ = 2.9 Hz), 114.1 (d, $^2J_{C\text{-}F}$ = 22.5 Hz), 105.3 (d, $^2J_{C\text{-}F}$ = 25.8 Hz); IR (KBr) ῡ 1749, 1616, 1541, 1457, 764 cm^{-1}; HRMS (ESI-TOF) calcd for $C_{15}H_9FNO_4$ $[M+H]^+$ 286.0510, found 286.0512.

7-Methoxy-3-nitro-4-phenyl-2H-chromen-2-one (2j). R_f = 0.3 (10% ethyl acetate/hexane); yellow solid; yield 59 mg (61%); mp: 165-167 ºC; ^{1}H NMR (400 MHz, $CDCl_3$) δ 7.55 – 7.51 (m, 3H), 7.36 (dd, *J* = 7.4, 1.8 Hz, 2H), 7.18 (d, *J* = 8.8 Hz, 1H), 6.94 (d, *J* = 2.4 Hz, 1H), 6.86 (dd, *J* = 8.8, 2.4 Hz, 1H), 3.92 (s, 3H); ^{13}C NMR (100 MHz, $CDCl_3$) δ 164.9, 155.1, 154.0, 148.0, 134.5, 130.8, 130.4, 129.5, 129.3, 128.0, 114.3, 111.1, 101.3, 56.3; IR (KBr) ῡ 1739, 1617, 1540, 1462, 763 cm^{-1}; HRMS (ESI-TOF) calcd for $C_{16}H_{12}NO_5$ $[M+H]^+$ 298.0710, found 298.0716.

7-Ethoxy-3-nitro-4-phenyl-2H-chromen-2-one (2k). R_f = 0.3 (10% ethyl acetate/hexane); yellow solid; yield 42 mg (57%); mp: 175-177 ºC; ^{1}H NMR (400 MHz, $CDCl_3$) δ 7.56 – 7.50 (m, 3H), 7.37 – 7.35 (m, 2H), 7.17 (d, *J* = 9.2 Hz, 1H), 6.91 (d, *J* = 2.4 Hz, 1H), 6.84 (dd, *J* = 8.8, 2.4 Hz, 1H), 4.14 (q, *J* = 7.2 Hz, 2H), 1.48 (t, *J* = 7.2 Hz, 3H); ^{13}C NMR (100 MHz, $CDCl_3$) δ 164.3, 155.2, 154.1, 148.1, 134.4, 130.7, 130.4, 129.5, 129.3, 128.0, 114.6, 110.9, 101.7, 64.9, 14.6; IR (KBr) ῡ 1739, 1610, 1542, 1421, 756 cm^{-1}; HRMS (ESI-TOF) calcd for $C_{17}H_{13}NNaO_5$ $[M+Na]^+$ 334.0686, found 334.0692.

7-(Benzyloxy)-3-nitro-4-phenyl-2H-chromen-2-one (2l). R_f = 0.3 (10% ethyl acetate/hexane); yellow solid; yield 42 mg (56%); mp: 192-194 ºC; ^{1}H NMR (400 MHz, $CDCl_3$) δ 7.55 – 7.50 (m, 3H), 7.43 – 7.34 (m, 7H), 7.19 (d, *J* = 9.2 Hz, 1H), 7.00 (d, *J* = 2.4 Hz, 1H), 6.93 (dd, *J* = 9.2, 2.4 Hz, 1H), 5.18 (s, 2H); ^{13}C NMR (100 MHz, $CDCl_3$) δ 163.9, 155.0, 154.0, 148.0, 135.2, 134.5, 130.7, 130.5, 129.4, 129.3, 129.0, 128.8, 128.0, 127.7, 114.8, 111.3, 102.3, 71.0; IR (KBr) ῡ 1735, 1609, 1539, 1490, 734 cm^{-1}; HRMS (ESI-TOF) calcd for $C_{22}H_{16}NO_5$ $[M+H]^+$ 374.1023, found 374.1008.

3-Nitro-4-phenyl-2H-chromen-2-one (2m).[37] R_f = 0.3 (10% ethyl acetate/hexane); yellow solid; yield 29 mg (55%); mp: 175-177 °C; ^{1}H NMR (400 MHz, $CDCl_3$) δ 7.69 (s, 1H), 7.56 – 7.47 (m, 4H), 7.39-7.32 (m, 4H); ^{13}C NMR (100 MHz, $CDCl_3$) δ 153.6, 153.0, 147.2, 136.8, 134.3, 130.9, 129.3, 128.9, 128.1, 125.7; 118.0, 117.6; IR (KBr) ῡ 1741, 1604, 1543, 1421, 764 cm^{-1}; HRMS (ESI-TOF) calcd for $C_{15}H_9NNaO_4$ $[M+Na]^+$ 290.0424, found 290.0426.

3-Nitro-4-phenyl-2H-benzo[g]chromen-2-one (2n). R_f = 0.3 (10% ethyl acetate/hexane); yellow solid; yield 58 mg (63%); mp: 172-174 °C; ^{1}H NMR (400 MHz, $CDCl_3$) δ 8.59 (dd, *J* = 6.8, 2.8 Hz, 1H), 7.90 (dd, *J* = 6.4, 2.4 Hz, 1H), 7.77 – 7.70 (m, 2H), 7.68 (d, *J* = 8.8 Hz, 1H), 7.58 (dd, *J* = 5.0, 1.8 Hz, 3H), 7.44 – 7.41 (m, 2H), 7.21 (d, *J* = 8.8 Hz, 1H); ^{13}C NMR (100 MHz, $CDCl_3$) δ 153.6, 151.0, 148.5, 136.5, 135.9, 130.8, 130.4, 129.5, 129.4, 128.2, 128.1, 125.7, 123.1, 123.0, 122.8, 113.3; IR (KBr) ῡ 1741, 1636, 1542, 1466, 748 cm^{-1}; HRMS (ESI-TOF) calcd for $C_{19}H_{11}NNaO_4$ $[M+Na]^+$ 340.0580, found 340.0585.

7-Bromo-3-nitro-4-phenyl-2H-chromen-2-one (2q). R_f = 0.3 (10% ethyl acetate/hexane); yellow solid; yield 41 mg (60%); mp: 180-182 °C; ^{1}H NMR (400 MHz, $CDCl_3$) δ 7.77 (dd, *J* = 9.0, 2.2 Hz), 7.61 – 7.55 (m, 3H), 7.39 – 7.36 (m, 4H); ^{13}C NMR (100 MHz, $CDCl_3$) δ 152.9, 151.8, 146.0, 137.3, 137.1 131.4, 131.3, 129.6, 128.2, 128.0, 119.8, 119.3, 118.7; IR (KBr) ῡ 1745, 1621, 1546, 1421, 752 cm^{-1}; HRMS (ESI-TOF) calcd for $C_{15}H_9BrNO_4$ $[M+H]^+$ 345.9709, found 345.9709.

6-Iodo-3-nitro-4-phenyl-2H-chromen-2-one (2r). R_f = 0.3 (10% ethyl acetate/hexane); yellow solid; yield 52 mg (61%); mp: 212-214 °C; ^{1}H NMR (400 MHz, $CDCl_3$) δ 7.95 (dd, *J* = 8.6, 2.2

Hz, 1H), 7.61 – 7.55 (m, 4H), 7.36 (dd, *J* = 7.8, 1.8 Hz, 2H), 7.24 (d, *J* = 8.8 Hz, 1H); ^{13}C NMR (100 MHz, $CDCl_3$) δ 152.9, 152.6, 145.9, 142.9, 137.4, 137.1, 131.3, 129.6, 128.2, 128.0, 120.1, 119.5, 88.8; IR (KBr) ῡ 1742, 1640, 1546, 1420, 763 cm^{-1}; HRMS (ESI-TOF) calcd for $C_{15}H_8INNaO_4$ $[M+Na]^+$ 415.9390, found 415.9376.

6-Methoxy-3-nitro-4-phenyl-2H-chromen-2-one (2s). R_f = 0.2 (10% ethyl acetate/hexane); yellow solid; yield 77 mg (64%); mp: 166-168 ºC; ^{1}H NMR (700 MHz, $CDCl_3$) δ 7.57 – 7.524 (m, 3H), 7.42-7.38 (m, 3H), 7.26-7.24 (m, 1H), 6.68 (d, *J* = 2.8 Hz, 1H), 3.71 (s, 3H); ^{13}C NMR (175 MHz, $CDCl_3$) δ 156.9, 153.7, 147.4, 146.9, 137.2, 131.0, 129.4, 129.0, 128.0, 121.5, 118.6, 118.6, 111.7, 56.0; IR (KBr) ῡ 1737, 1634, 1570, 1543, 1421, 752 cm^{-1}; HRMS (ESI-TOF) calcd for $C_{16}H_{12}NO_5$ $[M+H]^+$ 298.0710, found 298.0707.

3-Nitro-4-(*p*-tolyl)-2H-chromen-2-one (2u). R_f = 0.3 (10% ethyl acetate/hexane); light yellow solid; yield 53 mg (68%); mp: 162-164 ºC; ^{1}H NMR (400 MHz, $CDCl_3$) δ 7.70 – 7.66 (m, 1H), 7.47 (d, *J* = 8.4 Hz, 1H), 7.38 – 7.32 (m, 4H), 7.30 – 7.28 (m, 2H), 2.44 (s, 3H); ^{13}C NMR (100 MHz, $CDCl_3$) δ 153.7, 152.9, 147.4, 141.4, 136.7, 134.2, 130.0, 129.4, 128.0, 125.9, 125.6, 118.1, 117.5, 21.6; IR (KBr) ῡ 1741, 1636, 1543, 1466, 752 cm^{-1}; HRMS (ESI-TOF) calcd for $C_{16}H_{11}NNaO_4$ $[M+Na]^+$ 304.0580, found 304.0579.

4-(4-Chlorophenyl)-3-nitro-2H-chromen-2-one (2v). R_f = 0.6 (10% ethyl acetate/hexane); light yellow solid; yield 59 mg (63%); mp: 182-184 ºC; ^{1}H NMR (400 MHz, $CDCl_3$) δ 7.73 – 7.69 (m, 1H), 7.54 (d, *J* = 8.4 Hz, 2H), 7.49 (d, *J* = 8.0 Hz, 1H), 7.37 – 7.32 (m, 3H), 7.29 (d, *J* = 1.2 Hz, 1H); ^{13}C NMR (100 MHz, $CDCl_3$) δ 153.3, 153.0, 146.1, 137.4, 136.9, 134.6, 129.8, 129.5, 129.0,

127.2, 125.9, 117.8, 117.7; IR (KBr) ῡ 1748, 1616, 1546, 1421, 740 cm^{-1}; HRMS (ESI-TOF) calcd for $C_{15}H_8ClNNaO_4$ $[M+Na]^+$ 324.0034, found 324.0039.

4-(4-Fluorophenyl)-3-nitro-2H-chromen-2-one (2w). R_f = 0.2 (10% ethyl acetate/hexane); yellow solid; yield 48 mg (56%); mp: 172-174 ºC; ^{1}H NMR (400 MHz, $CDCl_3$) δ 7.71 (t, *J* = 7.6 Hz, 1H), 7.49 (d, *J* = 8.0 Hz, 1H), 7.40 – 7.33 (m, 3H), 7.30 – 7.24 (m, 3H); ^{13}C NMR (100 MHz, $CDCl_3$) δ 164.1 (d, $^1J_{C-F}$ = 251.0 Hz), 153.4, 153.0, 146.2, 137.0, 134.5, 130.4 (d, $^3J_{C-F}$ = 8.7 Hz), 129.0, 125.8, 124.8 (d, $^4J_{C-F}$ = 3.6 Hz), 117.9, 117.7, 116.8 (d, $^2J_{C-F}$ = 22.1 Hz); IR (KBr) ῡ 1745, 1598, 1546, 1421, 748 cm^{-1}; HRMS (ESI-TOF) calcd for $C_{15}H_9FNO_4$ $[M+H]^+$ 286.0510, found 286.0511.

4-(4-Methoxyphenyl)-3-nitro-2H-chromen-2-one (2x). R_f = 0.2 (10% ethyl acetate/hexane); yellow solid; yield 51 mg (60%); mp: 172-174 ºC; ^{1}H NMR (400 MHz, $CDCl_3$) δ 7.70 – 7.66 (m, 1H), 7.47 (dd, *J* = 8.4, 0.8 Hz, 1H), 7.40 (dd, *J* = 8.0, 1.6 Hz, 1H), 7.35 – 7.30 (m, 3H), 7.07 – 7.03 (m, 2H), 3.88 (s, 3H); ^{13}C NMR (100 MHz, $CDCl_3$) δ 161.7, 153.7, 153.0, 147.0, 136.9, 134.1, 129.8, 129.3, 125.6, 120.8, 118.3, 117.6, 114.9, 55.6; IR (KBr) ῡ 1738, 1624, 1570, 1537, 756 cm^{-1}; HRMS (ESI-TOF) calcd for $C_{16}H_{12}NO_5$ $[M+H]^+$ 298.0710, found 298.0692.

4-(3-Bromophenyl)-3-nitro-2H-chromen-2-one (2y). R_f = 0.2 (10% ethyl acetate/hexane); yellow solid; yield 52 mg (58%); mp: 182-184 ºC; ^{1}H NMR (400 MHz, $CDCl_3$) δ 7.74 – 7.69 (m, 2H)), 7.54 (dd, *J* = 2.8, 1.6 Hz, 1H), 7.51 – 7.48 (m, 1H), 7.44 (t, *J* = 8.0 Hz, 1H), 7.37 – 7.32 (m, 2H), 7.27 – 7.25 (m, 1H); ^{13}C NMR (100 MHz, $CDCl_3$) δ 153.2, 153.0, 145.5 136.9, 134.6, 134.1,

131.0, 130.9, 130.8, 129.0, 126.8, 125.9, 123.4, 117.8, 117.7; IR (KBr) ῡ 1746, 1624, 1545, 1421, 752 cm^{-1}; HRMS (ESI-TOF) calcd for $C_{15}H_8BrNNaO_4$ $[M+Na]^+$ 367.9529, found 367.9551.

Synthetic procedure of 3-Amino-7-bromo-4-phenyl-2H-chromen-2-one (7). R_f = 0.4 (10% ethyl acetate/hexane); off white solid; yield 48 mg (80%); mp: 138-140 ^oC; ^1H NMR (400 MHz, $CDCl_3$) δ 7.59-7.56 (m, 2H), 7.51 – 7.47 (m, 2H), 7.35 – 7.33 (m, 2H), 7.22 (dd, *J* = 8.4, 1.6 Hz, 1H), 6.86 (d, *J* = 8.4 Hz, 1H), 4.23 (s, 2H); ^{13}C NMR (100 MHz, $CDCl_3$) δ 158.8, 148.7, 132.7, 129.9, 129.3, 129.2, 129.2, 127.8, 125.4, 121.6, 121.1, 119.7, 119.5; HRMS (ESI-TOF) calcd for $C_{15}H_{11}BrNO_2$ $[M+H]^+$ 315.9968, found 315.9928.

***p*-Tolyl 3-phenylpropiolate (1a).[21]** R_f = 0.6 (5% ethyl acetate/hexane); white solid; yield 677 mg (69%); mp: 63-65 ^oC; ^1H NMR (400 MHz, $CDCl_3$) δ 7.64 (d, *J* = 7.2 Hz, 2H), 7.49 (t, *J* = 7.6 Hz, 1H), 7.41 (t, *J* = 7.6 Hz, 2H), 7.22 (d, *J* = 8.8 Hz, 2H), 7.10 – 7.08 (m, 2H), 2.37 (s, 3H); ^{13}C NMR (100 MHz, $CDCl_3$) δ 152.7, 148.0, 136.3, 133.3, 131.1, 130.2, 128.8, 121.2, 119.4, 88.6, 80.4, 21.0; IR (KBr) ῡ 3004, 2234, 1722, 750 cm^{-1}.

4-(*tert*-Butyl)phenyl 3-phenylpropiolate (1b).[21] R_f = 0.8 (5% ethyl acetate/hexane); white solid; yield 750 mg (60%); mp: 88-90 ^oC; ^1H NMR (400 MHz, $CDCl_3$) δ 7.64 – 7.62 (m, 2H), 7.51 – 7.47 (m, 1H), 7.45 – 7.39 (m, 4H), 7.13 – 7.11 (m, 2H), 1.34 (s, 9H); ^{13}C NMR (100 MHz, $CDCl_3$) δ 152.7, 149.4, 147.9, 133.3, 131.1, 128.8, 126.6, 120.9, 119.4, 88.7, 80.5, 34.7, 31.5; IR (KBr) ῡ 2236, 1722, 1604, 737 cm^{-1}.

4-Isopropylphenyl 3-phenylpropiolate (1c).[21] R_f = 0.8 (5% ethyl acetate/hexane); yellowish white solid; yield 650 mg (66%); mp: 66-68 ^oC; ^1H NMR (400 MHz, $CDCl_3$) δ 7.63 – 7.61 (m, 2H), 7.52 – 7.47 (m, 1H), 7.42 – 7.38 (m, 2H), 7.27 (d, *J* = 7.2 Hz, 2H), 7.12 – 7.10 (m, 2H), 2.93 (h, *J* = 6.8 Hz, 1H), 1.26 (d, *J* = 6.8 Hz, 6H); ^{13}C NMR (100 MHz, $CDCl_3$) δ 152.8, 148.2, 147.2, 133.3, 131.1, 128.8, 127.6, 121.3, 119.5, 88.7, 80.5, 33.8, 24.2; IR (KBr) ῡ 2235, 1723, 1603, 754 cm^{-1}.

4-Ethylphenyl 3-phenylpropiolate (1d).[21] R_f = 0.7 (5% ethyl acetate/hexane); yellowish white solid; yield 585 mg (55%); mp: 48-50 ^oC; ^1H NMR (400 MHz, $CDCl_3$) δ 7.64 (d, *J* = 7.2 Hz, 2H), 7.48 (t, *J* = 6.8 Hz, 1H), 7.41 (t, *J* = 6.8 Hz, 2H), 7.25 (d, *J* = 7.2 Hz, 2H), 7.12 (d, *J* = 7.6 Hz, 2H), 2.68 (q, *J* = 7.2 Hz, 2H), 1.26 (t, *J* = 7.2 Hz, 3H); ^{13}C NMR (100 MHz, $CDCl_3$) δ 152.7, 148.1, 142.5, 133.3, 131.1, 129.0, 128.8, 121.3, 119.4, 88.6, 80.4, 28.4, 15.6; IR (KBr) ῡ 2237, 1721, 1635, 758 cm^{-1}.

[1,1'-Biphenyl]-4-yl 3-phenylpropiolate (1e).[21] R_f = 0.6 (5% ethyl acetate/hexane); yellowish white solid; yield 560 mg (68%); mp: 140-142 ^oC; ^1H NMR (400 MHz, $CDCl_3$) δ 7.64 (t, *J* = 7.6 Hz, 4H), 7.58 (d, *J* = 7.6 Hz, 2H), 7.52 – 7.35 (m, 6H), 7.29 –7.26 (m, 2H); ^{13}C NMR (100 MHz, $CDCl_3$) δ 152.6, 149.6, 140.3, 139.7, 133.4, 131.2, 129.0, 128.8, 128.5, 127.6, 127.3, 121.9, 119.4, 89.0, 80.4; IR (KBr) ῡ 2219, 1726, 1644, 760 cm^{-1}.

4-Iodophenyl 3-phenylpropiolate (1f).[21] R_f = 0.7 (5% ethyl acetate/hexane); white solid; yield 698 mg (65%); mp: 81-83 ^oC; ^1H NMR (400 MHz, $CDCl_3$) δ 7.75 – 7.71 (m, 2H), 7.65 – 7.62 (m, 2H), 7.52 – 7.48 (m, 1H), 7.43 – 7.39 (m, 2H), 7.00 – 6.96 (m, 2H); ^{13}C NMR (100 MHz, $CDCl_3$)

δ 152.0, 150.1, 138.8, 133.4, 131.3, 128.8, 123.7, 119.2, 90.7, 89.3, 80.1; IR (KBr) ῡ 2305, 1726, 1605, 770 cm^{-1}.

4-Bromophenyl 3-phenylpropiolate (1g).[21] R_f = 0.7 (5% ethyl acetate/hexane); white solid; yield 670 mg (68%); mp: 68-70 ºC; ^{1}H NMR (400 MHz, $CDCl_3$) δ 7.64 – 7.62 (m, 2H), 7.55 – 7.48 (m, 3H), 7.43 – 7.39 (m, 2H), 7.12 – 7.08 (m, 2H); ^{13}C NMR (100 MHz, $CDCl_3$) δ 152.0, 149.2, 133.3, 132.7, 131.3, 128.8, 123.4, 119.7, 119.1, 89.3, 80.1; IR (KBr) ῡ 2235, 1726, 1605, 701 cm^{-1}.

4-Chlorophenyl 3-phenylpropiolate (1h).[21] R_f = 0.7 (5% ethyl acetate/hexane); white solid; yield 850 mg (58%); mp: 63-65 ºC; ^{1}H NMR (400 MHz, $CDCl_3$) δ 7.65 – 7.63 (m, 2H), 7.52 – 7.48 (m, 1H) 7.43 – 7.36 (m, 4H), 7.15 (d, J = 8.8 Hz, 2H); ^{13}C NMR (100 MHz, $CDCl_3$) δ 152.1, 148.7, 133.4, 132.0, 131.3, 129.8, 128.9, 123.0, 119.2, 89.3, 80.1; IR (KBr) ῡ 2305, 1727, 1604, 768 cm^{-1}.

4-Fluorophenyl 3-phenylpropiolate (1i).[21] R_f = 0.6 (5% ethyl acetate/hexane); white solid; yield 620 mg (62%); mp: 54-56 ºC; ^{1}H NMR (400 MHz, $CDCl_3$) δ 7.63 (d, J = 7.2 Hz, 2H), 7.50 (t, J = 7.6 Hz, 1H), 7.41 (t, J = 7.6 Hz, 2H), 7.16 (s, 2H), 7.10 (t, J = 8.4 Hz, 2H); ^{13}C NMR (100 MHz, $CDCl_3$) δ 160.6 (d, $^1J_{C\text{-}F}$ = 243.7 Hz), 152.4, 146.0 (d, $^4J_{C\text{-}F}$ = 2.9 Hz), 133.3, 131.3, 128.8, 123.1 (d, $^3J_{C\text{-}F}$ = 8.6 Hz), 119.2, 116.4 ($^2J_{C\text{-}F}$ = 23.5 Hz), 89.1, 80.1; IR (KBr) ῡ 2210, 1724, 1644, 741 cm^{-1}.

4-Methoxyphenyl 3-phenylpropiolate (1j).[21] R_f = 0.5 (5% ethyl acetate/hexane); yellow solid; yield 500 mg (55%); mp: 80-82 ºC; ^{1}H NMR (400 MHz, $CDCl_3$) δ 7.63 (d, J = 7.2 Hz, 2H), 7.49

(t, *J* = 7.2 Hz, 1H), 7.40 (t, *J* = 7.2 Hz, 2H), 7.12 (d, *J* = 8.8 Hz, 2H), 6.93 (d, *J* = 8.8 Hz, 2H), 3.81 (s, 3H); ^{13}C NMR (100 MHz, $CDCl_3$) δ 157.7, 152.9, 143.7, 133.3, 131.1, 128.8, 122.3, 119.4, 114.7, 88.7, 80.4, 55.7; IR (KBr) ῡ 2235, 1724, 1639, 745 cm^{-1}.

4-Ethoxyphenyl 3-phenylpropiolate (1k).[49] R_f = 0.5 (5% ethyl acetate/hexane); yellowish white solid; yield 566 mg (59%); mp: 80-82 ºC; ^{1}H NMR (400 MHz, $CDCl_3$) δ 7.63 (d, *J* = 7.2 Hz, 2H), 7.49 (t, *J* = 7.2 Hz, 1H), 7.40 (t, *J* = 7.2 Hz, 2H), 7.10 (d, *J* = 8.8 Hz, 2H), 6.91 (d, *J* = 8.4 Hz, 2H), 4.03 (q, *J* = 6.8 Hz, 2H), 1.42 (t, *J* = 6.8 Hz, 3H); ^{13}C NMR (100 MHz, $CDCl_3$) δ 157.2, 153.0, 143.6, 133.3, 131.1, 128.8, 122.3, 119.4, 115.2, 88.7, 80.4, 64.0, 14.9; IR (KBr) ῡ 2232, 1723, 1644, 769 cm^{-1}.

4-(Benzyloxy)phenyl 3-phenylpropiolate (1l).[50] R_f = 0.4 (5% ethyl acetate/hexane); yellowish white solid; yield 540 mg (58%); mp: 118-120 ºC; ^{1}H NMR (400 MHz, $CDCl_3$) δ 7.64 (dd, *J* = 8.8, 1.6 Hz, 2H), 7.52 – 7.33 (m, 8H), 7.15 – 7.11 (m, 2H), 7.03 – 6.99 (m, 2H), 5.07 (s, 2H); ^{13}C NMR (100 MHz, $CDCl_3$) δ 157.0, 152.9, 143.9, 136.8, 133.3, 131.1, 128.8, 128.8, 128.2, 127.6, 122.4, 119.4, 115.7, 88.8, 80.4, 70.5.

Phenyl 3-phenylpropiolate (1m).[21] R_f = 0.8 (5% ethyl acetate/hexane); white solid; yield 840 mg (72%); mp: 46-48 ºC; ^{1}H NMR (400 MHz, $CDCl_3$) δ 7.65 – 7.62 (m, 2H), 7.52 – 7.47 (m, 1H), 7.45 – 7.39 (m, 4H), 7.31 – 7.27 (m, 1H), 7.22 – 7.20 (m, 2H); ^{13}C NMR (100 MHz, $CDCl_3$) δ 152.5, 150.3, 133.3, 131.2, 129.7, 128.8, 126.5, 121.6, 119.4, 88.8, 80.4; IR (KBr) ῡ 2116, 1723, 1590, 731 cm^{-1}.

Naphthalen-2-yl 3-phenylpropiolate (1n).[51] R_f = 0.7 (5% ethyl acetate/hexane); yellowish white solid; yield 650 mg (66%); mp: 94-96 ºC; ^{1}H NMR (400 MHz, $CDCl_3$) δ 7.92 – 7.84 (m, 3H), 7.70 (d, *J* = 2.4 Hz, 1H), 7.67 – 7.65 (m, 2H), 7.56 – 7.48 (m, 3H), 7.44 – 7.40 (m, 2H), 7.35 (dd, *J* = 8.8, 2.4 Hz, 1H); ^{13}C NMR (100 MHz, $CDCl_3$) δ 152.6, 147.8, 133.8, 133.3, 131.8, 131.2, 129.8, 128.8, 127.9, 127.9, 126.9, 126.2, 120.8, 119.32, 118.7, 89.0, 80.4; IR (KBr) ῡ 2230, 1720, 1630, 748 cm^{-1}.

2-Iodophenyl 3-phenylpropiolate (1o).[52] R_f = 0.5 (5% ethyl acetate/hexane); yellowish white solid; yield 600 mg (67%); mp: 85-87 ºC; ^{1}H NMR (400 MHz, $CDCl_3$) δ 7.88 (dd, *J* = 8.0, 1.6 Hz, 1H), 7.67-7.65 (m, 2H), 7.52-7.48 (m, 1H), 7.44 – 7.39 (m, 3H), 7.20 (dd, *J* = 8.0, 1.2 Hz, 1H), 7.05-7.01 (m, 1H); ^{13}C NMR (100 MHz, $CDCl_3$) δ 151.6, 150.8, 139.9, 133.5, 131.3, 129.7, 128.8, 128.3, 123.2, 119.3, 90.3, 89.6, 80.3; IR (KBr) ῡ 2233, 1727, 1490, 739 cm^{-1}.

[1,1'-Biphenyl]-2-yl 3-phenylpropiolate (1p).[53] R_f = 0.7 (5% ethyl acetate/hexane); yellowish white solid; yield 549 mg (62%); mp: 93-95 ºC; ^{1}H NMR (700 MHz, $CDCl_3$) δ 7.55 (d, *J* = 7.7 Hz, 2H), 7.48 – 7.40 (m, 7H), 7.39-7.35 (m, 4H), 7.24 (d, *J* = 8.4 Hz, 1H); ^{13}C NMR (100 MHz, $CDCl_3$) δ 152.5, 147.3, 137.2, 135.1, 133.3, 131.3, 131.1, 129.1, 128.8, 128.7, 128.6, 127.8, 127.1, 122.9, 119.4, 88.8, 80.2; IR (KBr) ῡ 3052, 2205, 1723, 748 cm^{-1}.

3-Bromophenyl 3-phenylpropiolate (1q).[54] R_f = 0.7 (5% ethyl acetate/hexane); white solid; yield 652 mg (51%); mp: 54-56 ºC; ^{1}H NMR (400 MHz, $CDCl_3$) δ 7.64 (d, *J* = 7.2 Hz, 2H), 7.50 (t, *J* = 7.2 Hz, 1H), 7.44 – 7.40 (m, 4H), 7.30 (d, *J* = 8.0 Hz, 1H), 7.16 (d, *J* = 8.0 Hz, 1H); ^{13}C NMR

(100 MHz, $CDCl_3$) δ 151.9, 150.6, 133.4, 131.4, 130.8, 129.7, 128.8, 125.1, 122.6, 120.5, 119.2, 89.4, 80.0;. IR (KBr) ῡ 3053, 2211, 1726, 1585, 737 cm^{-1}.

3-Iodophenyl 3-phenylpropiolate (1r).[55] R_f = 0.6 (5% ethyl acetate/hexane); white solid; yield 422 mg (62%); mp: 61-63 ºC; ^1H NMR (700 MHz, $CDCl_3$) δ 7.64-7.61 (m, 3H), 7.58 (s, 1H), 7.50 (t, *J* = 7.7 Hz, 1H), 7.41 (t, *J* = 7.7 Hz, 2H), 7.20 – 7.19 (m, 1H), 7.15-7.13 (m, 1H); ^{13}C NMR (100 MHz, $CDCl_3$) δ 152.0, 150.4, 135.7, 133.4, 131.4, 131.0, 130.8, 128.9, 121.2, 119.2, 93.7, 89.4, 80.0; IR (KBr) ῡ 2237, 1724, 1638, 748 cm^{-1}.

3-Methoxyphenyl 3-phenylpropiolate (1s).[54] R_f = 0.6 (5% ethyl acetate/hexane); colorless liquid; yield 729 mg (61%); ^1H NMR (400 MHz, $CDCl_3$) δ 7.66 – 7.61 (m, 2H), 7.52 – 7.46 (m, 1H), 7.41 (t, *J* = 7.4 Hz, 2H), 7.32 (t, *J* = 8.2 Hz, 1H), 6.86 – 6.78 (m, 2H), 6.75 (t, *J* = 2.2 Hz, 1H), 3.82 (s, 3H); ^{13}C NMR (101 MHz, $CDCl_3$) δ 160.7, 152.4, 151.2, 133.3, 131.2, 130.1, 128.8, 119.4, 113.8, 112.4, 107.6, 88.8, 80.4, 55.6; IR (KBr) ῡ 2216, 1723, 1610, 763 cm^{-1}.

4-Nitrophenyl 3-phenylpropiolate (1t).[54] R_f = 0.4 (5% ethyl acetate/hexane); yellowish white solid; yield 652 mg (63%); mp: 96-98 ºC; ^1H NMR (400 MHz, $CDCl_3$) δ 8.31 (d, *J* = 9.2 Hz, 2H), 7.67 – 7.65 (m, 2H), 7.55 – 7.51 (m, 1H), 7.45 – 7.38 (m, 4H); ^{13}C NMR (101 MHz, $CDCl_3$) δ 154.8, 151.2, 145.8, 133.5, 131.6, 128.9, 125.5, 122.5, 118.9, 90.2, 79.7; IR (KBr) ῡ 2304, 1732, 1616, 764 cm^{-1}.

Phenyl 3-(*p*-tolyl)propiolate (1u).[18] R_f = 0.6 (5% ethyl acetate/hexane); yellow solid; yield 315 mg (51%); mp: 79-81 ºC; ^1H NMR (400 MHz, $CDCl_3$) δ 7.53 (d, *J* = 8.0 Hz, 2H), 7.44 – 7.40 (m,

2H), 7.29 (d, *J* = 7.2 Hz, 1H), 7.21 (t, *J* = 7.4 Hz, 4H), 2.40 (s, 3H); ^{13}C NMR (100 MHz, $CDCl_3$) δ 152.6, 150.3, 142.0, 133.3, 129.7, 129.6, 126.5, 121.6, 116.2, 89.5, 80.1, 21.9; IR (KBr) ῡ 2236, 1723, 1636, 779 cm^{-1}.

Phenyl 3-(4-chlorophenyl)propiolate (1v).[18] R_f = 0.8 (5% ethyl acetate/hexane); yellowish white solid; yield 249 mg (55%); mp: 94-96 ºC; ^{1}H NMR (400 MHz, $CDCl_3$) δ 7.58 – 7.55 (m, 2H), 7.45 – 7.38 (m, 4H), 7.31 – 7.28 (m, 1H), 7.20 – 7.18 (m, 2H); ^{13}C NMR (100 MHz, $CDCl_3$) δ 152.3, 150.2, 137.7, 134.5, 129.8, 129.3, 126.6, 121.6, 117.9, 87.5, 81.2; IR (KBr) ῡ 2242, 1730, 1650, 758 cm^{-1}.

Phenyl 3-(4-fluorophenyl)propiolate (1w).[18] R_f = 0.6 (5% ethyl acetate/hexane); white solid; yield 398 mg (51%); mp: 80-82 ºC; ^{1}H NMR (700 MHz, $CDCl_3$) δ 7.66 – 7.60 (m, 2H), 7.42 (t, *J* = 7.7 Hz, 2H), 7.28 (t, *J* = 7.7 Hz, 1H), 7.19 (d, *J* = 8.4 Hz, 2H), 7.11 (t, *J* = 8.4 Hz, 2H); ^{13}C NMR (100 MHz, $CDCl_3$) δ 164.3 (d, $^1J_{C\text{-}F}$ = 252.4 Hz), 152.4, 150.2, 135.7 (d, $^3J_{C\text{-}F}$ = 8.9 Hz), 129.8, 126.6, 121.6, 116.4 (d, $^2J_{C\text{-}F}$ = 22.2 Hz), 115.5 (d, $^4J_{C\text{-}F}$ = 3.5 Hz), 87.8, 80.3; IR (KBr) ῡ 2214, 1726, 1644, 752 cm^{-1}.

Phenyl 3-(4-methoxyphenyl)propiolate (1x).[18] R_f = 0.6 (5% ethyl acetate/hexane); yellowish white solid; yield 527 mg (44%); mp: 70-72 ºC; ^{1}H NMR (400 MHz, $CDCl_3$) δ 7.59 – 7.56 (m, 2H), 7.44 – 7.39 (m, 2H), 7.30 – 7.27 (m, 1H), 7.21 – 7.18 (m, 2H), 6.93 – 6.89 (m, 2H), 3.85 (s, 3H); ^{13}C NMR (100 MHz, $CDCl_3$) δ 162.0 , 152.8, 150.4, 135.4, 129.7, 126.5, 121.7, 114.6, 111.2, 89.9, 80.0, 55.6; IR (KBr) ῡ 2215, 1725, 1609, 763 cm^{-1}.

Phenyl 3-(3-bromophenyl)propiolate (1y).[18] R_f = 0.7 (5% ethyl acetate/hexane); yellow solid; yield 106 mg (51%); mp: 60-62 ^oC; ^1H NMR (400 MHz, $CDCl_3$) δ 7.73 (s, 1H), 7.58 (d, *J* = 8.4 Hz, 1H), 7.51 (d, *J* = 8.4 Hz, 1H), 7.38 (t, *J* = 8.0 Hz, 2H), 7.25 (d, *J* = 7.6 Hz, 2H), 7.16 (t, *J* = 8.0 Hz, 2H); ^{13}C NMR (100 MHz, $CDCl_3$) δ 152.1, 150.2, 135.9, 134.4, 131.8, 130.3 129.8, 126.7, 122.6, 121.5, 121.4, 86.6, 81.2; IR (KBr) ῡ 2236, 1728, 1648, 766 cm^{-1}.

3.6 NOTES AND REFERENCES

1. A. Dahiya, A. K. Sahoo, T. Alam and B. K. Patel, *Chem. Asian J.*, 2019, **14**, 4454-4492.
2. X. Jia and P. Li, *Synthesis*, 2017, **50**, 711-722.
3. P. Chaudhary, S. Gupta, N. Muniyappan, S. Sabiah and J. Kandasamy, *J. Org. Chem.*, 2019, **84**, 104-119.
4. Y. Chen, Y. Ma, L. Li, H. Jiang and Z. Li, *Org. Lett.*, 2019, **21**, 1480-1483.
5. S. Mondal, S. Samanta and A. Hajra, *Adv. Synth. Catal.*, 2018, **360**, 1026-1031.
6. S. Maity, T. Naveen, U. Sharma and D. Maiti, *Org. Lett.*, 2013, **15**, 3384-3387.
7. B. Kilpatrick, M. Heller and S. Arns, *Chem. Commun.*, 2013, **49**, 514-516.
8. W.-T. Wei, W.-W. Ying, W.-H. Bao, L.-H. Gao, X.-D. Xu, Y.-N. Wang, X.-X. Meng, G.-P. Chen and Q. Li, *ACS Sustainable Chem. Eng.*, 2018, **6**, 15301-15305.
9. G. B. Deng, J. L. Zhang, Y. Y. Liu, B. Liu, X. H. Yang and J. H. Li, *Chem. Commun.*, 2015, **51**, 1886-1888.
10. T. Feng, Y. He, X. Zhang and X. Fan, *Adv. Synth. Catal.*, 2019, **361**, 1271-1276.
11. M. Hu, B. Liu, X.-H. Ouyang, R.-J. Song and J.-H. Li, *Adv. Synth. Catal.*, 2015, **357**, 3332-3340.
12. T. Shen, Y. Yuan and N. Jiao, *Chem. Commun.*, 2014, **50**, 554-556.

13. X.-H. Yang, X.-H. Ouyang, W.-T. Wei, R.-J. Song and J.-H. Li, *Adv. Synth. Catal.*, 2015, **357**, 1161-1166.

14. B. Zhang and A. Studer, *Chem. Soc. Rev.*, 2015, **44**, 3505-3521.

15. D. Ravelli, S. Protti and M. Fagnoni, *Chem. Rev.*, 2016, **116**, 9850-9913.

16. W. Fu, M. Zhu, G. Zou, C. Xu, Z. Wang and B. Ji, *J. Org. Chem.*, 2015, **80**, 4766-4770.

17. K. Yan, D. Yang, W. Wei, F. Wang, Y. Shuai, Q. Li and H. Wang, *J. Org. Chem.*, 2015, **80**, 1550-1556.

18. D. Liu, J.-Q. Chen, X.-Z. Wang and P.-F. Xu, *Adv. Synth. Catal.*, 2017, **359**, 2773-2777.

19. W. Wei, J. Wen, D. Yang, M. Guo, Y. Wang, J. You and H. Wang, *Chem. Commun.*, 2015, **51**, 768-771.

20. S. Yang, H. Tan, W. Ji, X. Zhang, P. Li and L. Wang, *Adv. Synth. Catal.*, 2017, **359**, 443-453.

21. W. Yang, S. Yang, P. Li and L. Wang, *Chem. Commun.*, 2015, **51**, 7520-7523.

22. Y.-F. Zeng, D.-H. Tan, Y. Chen, W.-X. Lv, X.-G. Liu, Q. Li and H. Wang, *Org. Chem. Front.*, 2015, **2**, 1511-1515.

23. Q. Wang, C. Yang and C. Jiang, *Org. Biomol. Chem.*, 2018, **16**, 8196-8204.

24. K. Kawaai, T. Yamaguchi, E. Yamaguchi, S. Endo, N. Tada, A. Ikari and A. Itoh, *J. Org. Chem.*, 2018, **83**, 1988-1996.

25. D. Zheng, J. Yu and J. Wu, *Angew. Chem. Int. Ed.*, 2016, **55**, 11925-11929.

26. T. Liu, Q. Ding, Q. Zong and G. Qiu, *Org. Chem. Front.*, 2015, **2**, 670-673.

27. X. Y. Huang, Z. J. Shan, H. L. Zhai, L. Su and X. Y. Zhang, *Chem. Biol. Drug Des.*, 2011, **78**, 651-658.

28. A. Thakur, R. Singla and V. Jaitak, *Eur. J. Med. Chem.*, 2015, **101**, 476-495.

29. S. R. Trenor, A. R. Shultz, B. J. Love and T. E. Long, *Chem. Rev.*, 2004, **104**, 3059-3078.

30. Y. Xiao, X. Tan, W. Xing, K. Zhao, B. Zhang and X. Cheng, *J. Mater. Chem. C*, 2018, **6**, 10782-10792.

31. D. Cao, Z. Liu, P. Verwilst, S. Koo, P. Jangjili, J. S. Kim and W. Lin, *Chem. Rev.*, 2019, **119**, 10403-10519.

32. G. Yan, A. J. Borah and L. Wang, *Org. Biomol. Chem.*, 2014, **12**, 6049-6058.

33. Y. Gao, S. Yang, Y. Huo and X.-Q. Hu, *Adv. Synth. Catal.*, 2020, **362**, 3971-3986.

34. G. Romanazzi, V. Petrelli, A. M. Fiore, P. Mastrorilli and M. M. Dell'Anna, *Molecules*, 2021, **26**.

35. K. N. Venugopala, V. Rashmi and B. Odhav, *BioMed Res. Int.*, 2013, DOI: 10.1155/2013/963248, 963248.

36. G. Koleva, B. Galabov, B. Hadjieva, H. F. Schaefer III and P. v. R. Schleyer, *Angew. Chem. Int. Ed.*, 2015, **54**, 14123-14127.

37. W. Liu, Y. Zhang and H. Guo, *J. Org. Chem.*, 2018, **83**, 10518-10524.

38. A. Bose and P. Mal, *Chem. Commun.*, 2017, **53**, 11368-11371.

39. B. P. Fors and S. L. Buchwald, *J. Am. Chem. Soc.*, 2009, **131**, 12898-12899.

40. Y. Zhou, Z. Tang and Q. Song, *Chem. Commun.*, 2017, **53**, 8972-8975.

41. Y. He, N. Zhao, L. Qiu, X. Zhang and X. Fan, *Org. Lett.*, 2016, **18**, 6054-6057.

42. Z. Fan, J. Ni and A. Zhang, *J. Am. Chem. Soc.*, 2016, **138**, 8470-8475.

43. W. Zhang, S. Ren, J. Zhang and Y. Liu, *J. Org. Chem.*, 2015, **80**, 5973-5978.

44. A. Bose, S. Maiti, S. Sau and P. Mal, *Chem. Commun.*, 2019, **55**, 2066-2069.

45. W. Yang, S. Yang, P. Li and L. Wang, *Chem. Commun.*, 2015, **51**, 7520-7523.

46. SAINT+, Bruker AXS Inc., Madison, Wisconsin, USA, 1999 (Program for Reduction of Data collected on Bruker CCD Area Detector Diffractometer V. 6.02.)

47. G. Sheldrick, 1996.

48. G. Sheldrick, *Acta Crystallogr. Sect. A*, 2008, **64**, 112-122.

49. M. Zhu, W. Fu, Z. Wang, C. Xu and B. Ji, *Org. Biomol. Chem.*, 2017, **15**, 9057-9060.

50. A. H. Bansode, S. R. Shaikh, R. G. Gonnade and N. T. Patil, *Chem. Commun.*, 2017, **53**, 9081-9084.

51. S. Feng, J. Li, Z. Liu, H. Sun, H. Shi, X. Wang, X. Xie and X. She, *Org. Biomol. Chem.*, 2017, **15**, 8820-8826.

52. H.-L. Hua, Y.-T. He, Y.-F. Qiu, Y.-X. Li, B. Song, P. Gao, X.-R. Song, D.-H. Guo, X.-Y. Liu and Y.-M. Liang, *Chem. Eur. J.*, 2015, **21**, 1468-1473.

53. W.-C. Gao, T. Liu, B. Zhang, X. Li, W.-L. Wei, Q. Liu, J. Tian and H.-H. Chang, *J. Org. Chem.*, 2016, **81**, 11297-11304.

54. Z. Wang, X. Li, L. Wang and P. Li, *Tetrahedron*, 2019, **75**, 1044-1051.

55. W. Zhang, C. Yang, Y.-L. Pan, X. Li and J.-P. Cheng, *Org. Biomol. Chem.*, 2018, **16**, 5788-5792.

Copies of ^{1}H and ^{13}C NMR Spectra of selected compounds

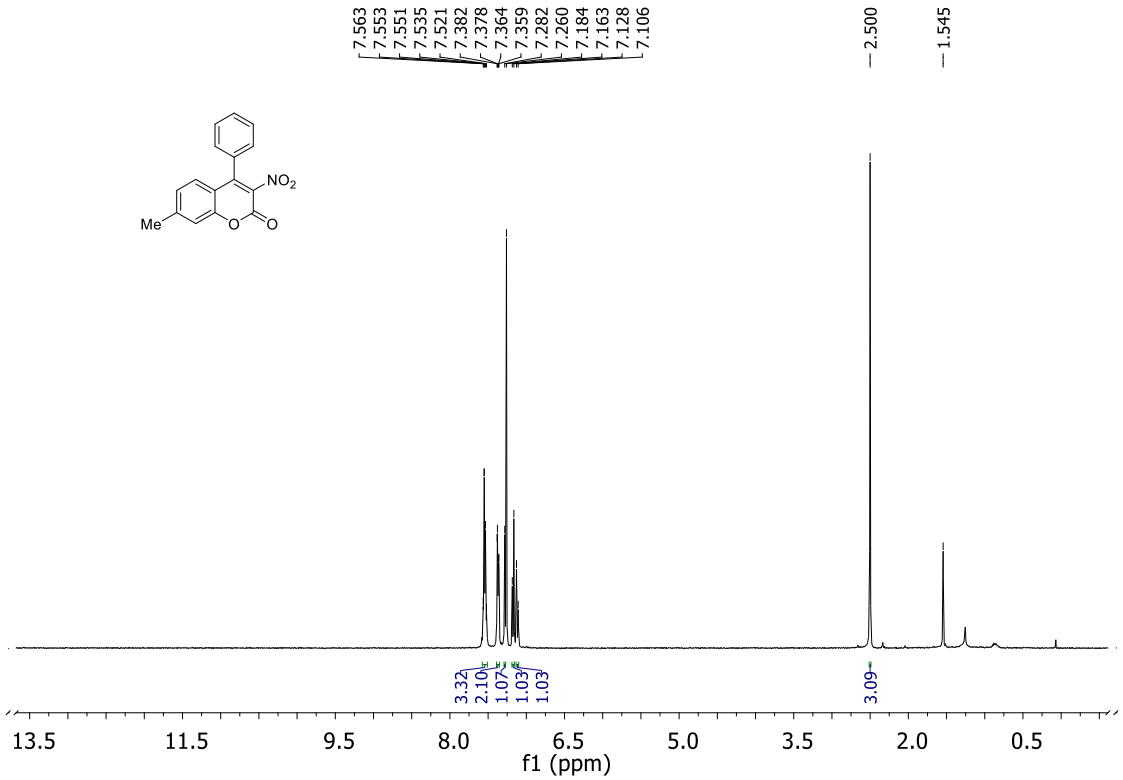

Figure 3.10. ^{1}H NMR of 7-Methyl-3-nitro-4-phenyl-2H-chromen-2-one **(2a).**

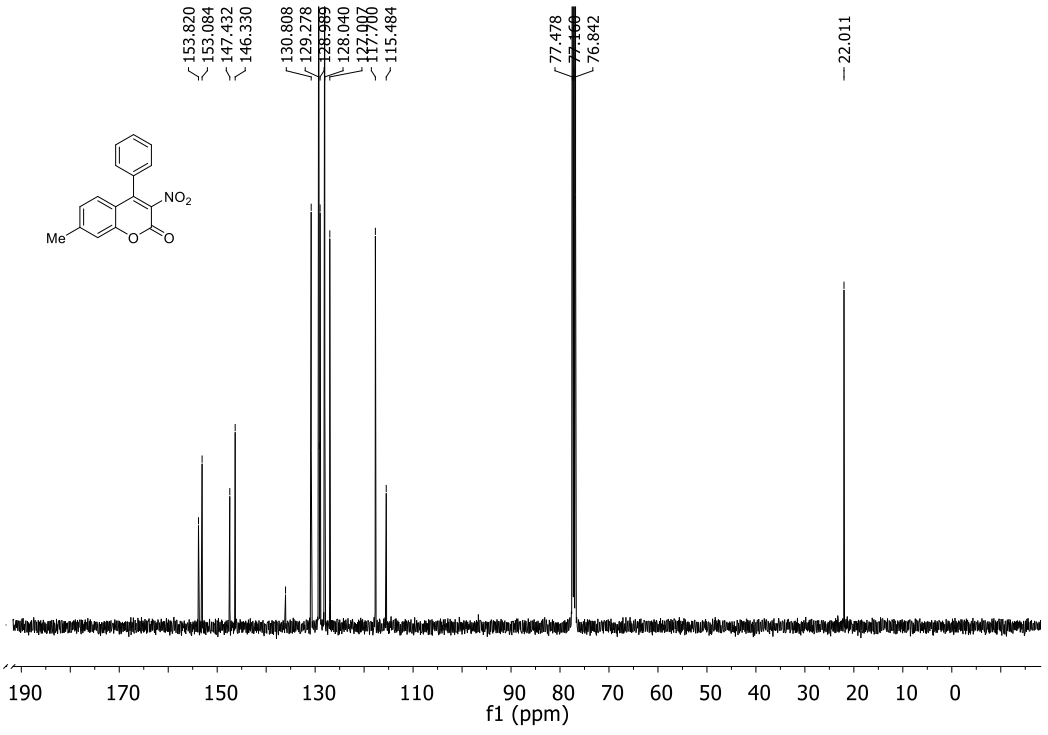

Figure 3.11. ^{13}C NMR of 7-Methyl-3-nitro-4-phenyl-2H-chromen-2-one **(2a).**

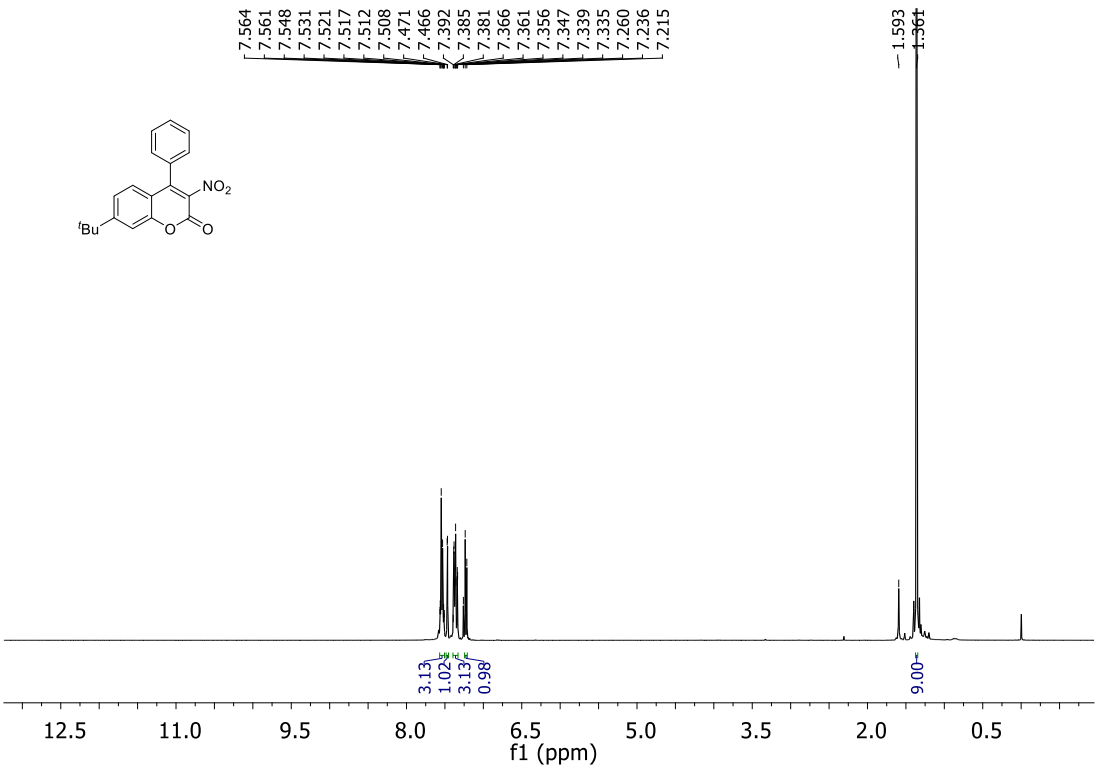

Figure 3.12. ^{1}H NMR of 7-(*tert*-Butyl)-3-nitro-4-phenyl-2H-chromen-2-one **(2b).**

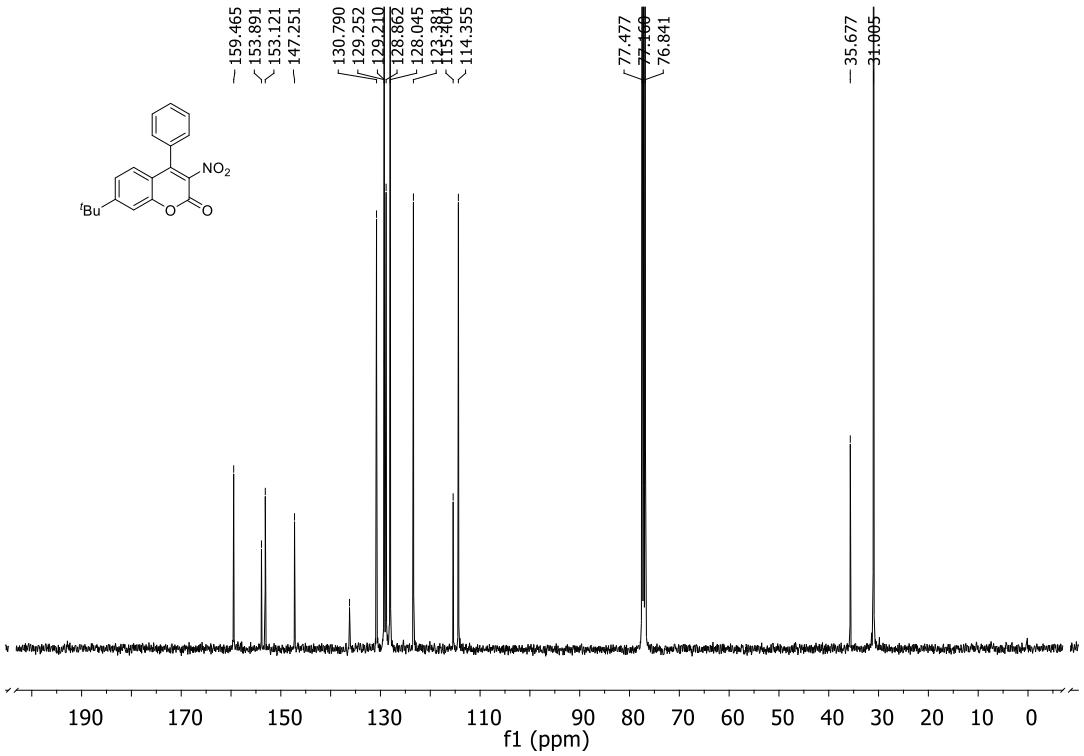

Figure 3.13. ^{13}C NMR of 7-(*tert*-Butyl)-3-nitro-4-phenyl-2H-chromen-2-one **(2b).**

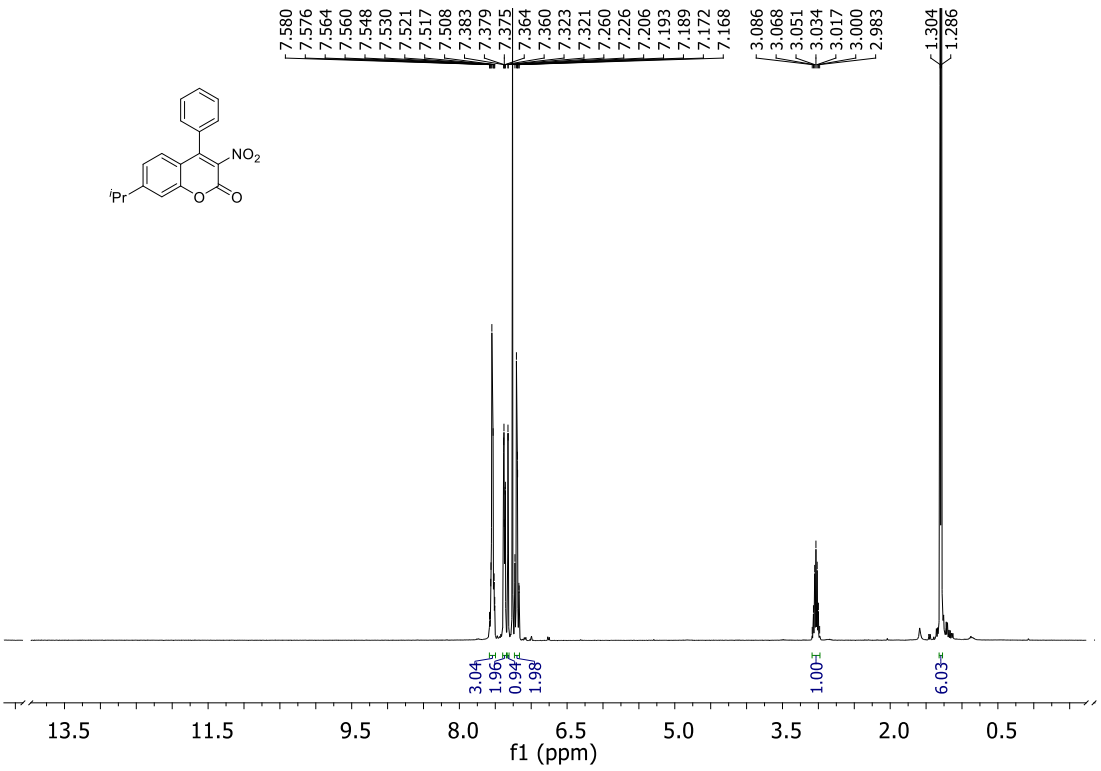

Figure 3.14. ^{1}H NMR of 7-Isopropyl-3-nitro-4-phenyl-2H-chromen-2-one **(2c).**

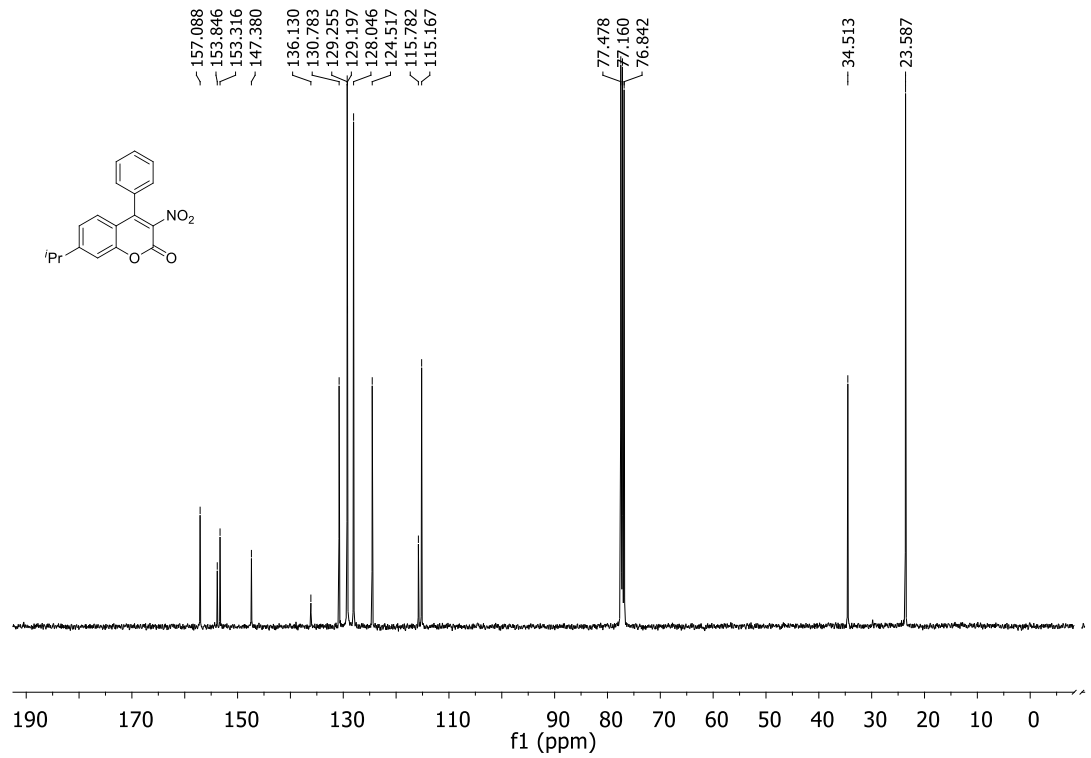

Figure 3.15. ^{13}C NMR of 7-Isopropyl-3-nitro-4-phenyl-2H-chromen-2-one **(2c).**

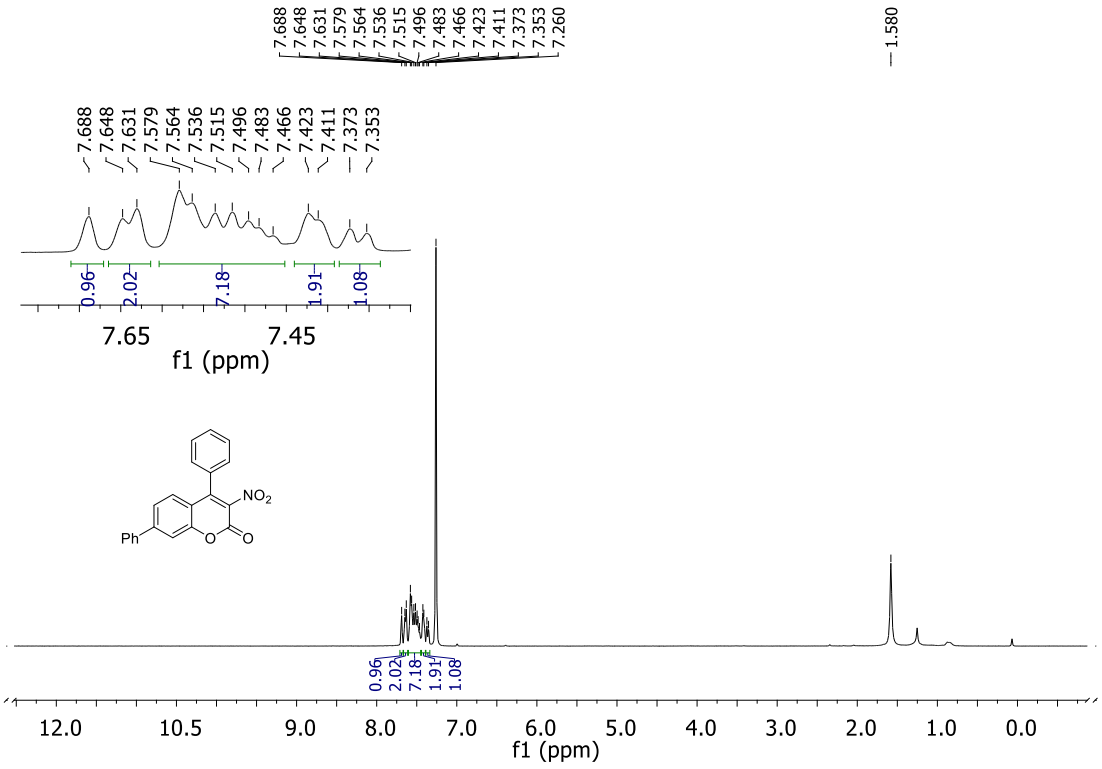

Figure 3.16. ^{1}H NMR of 3-Nitro-4,7-diphenyl-2H-chromen-2-one **(2e).**

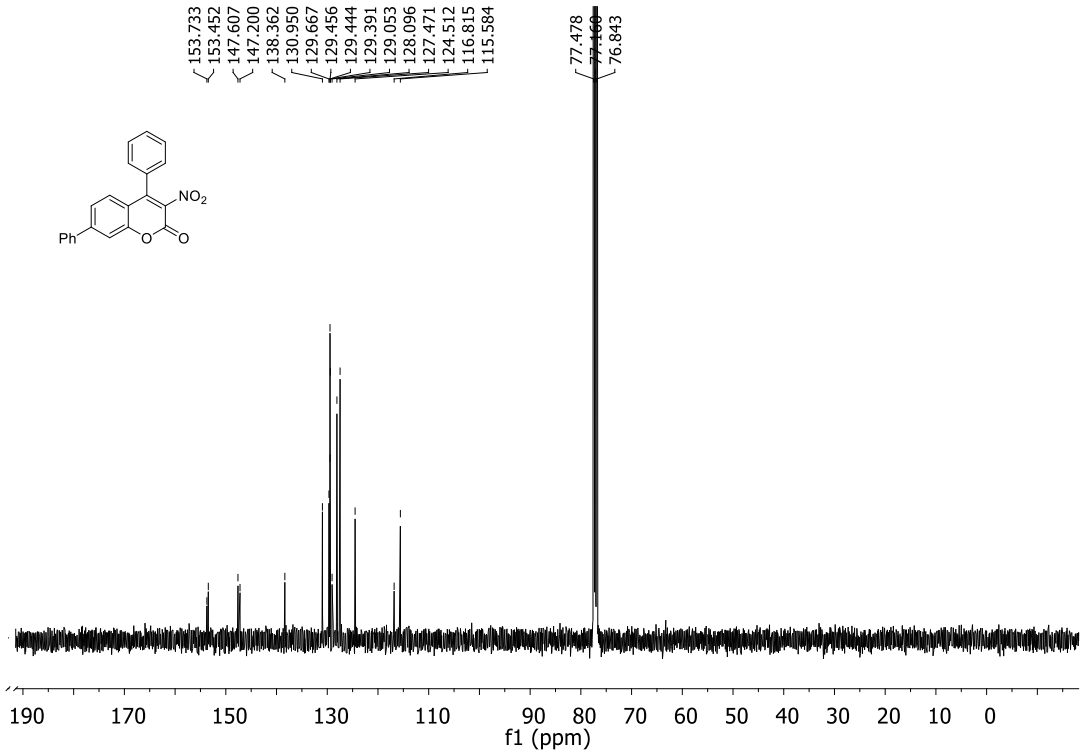

Figure 3.17. ^{13}C NMR of 3-Nitro-4,7-diphenyl-2H-chromen-2-one **(2e).**

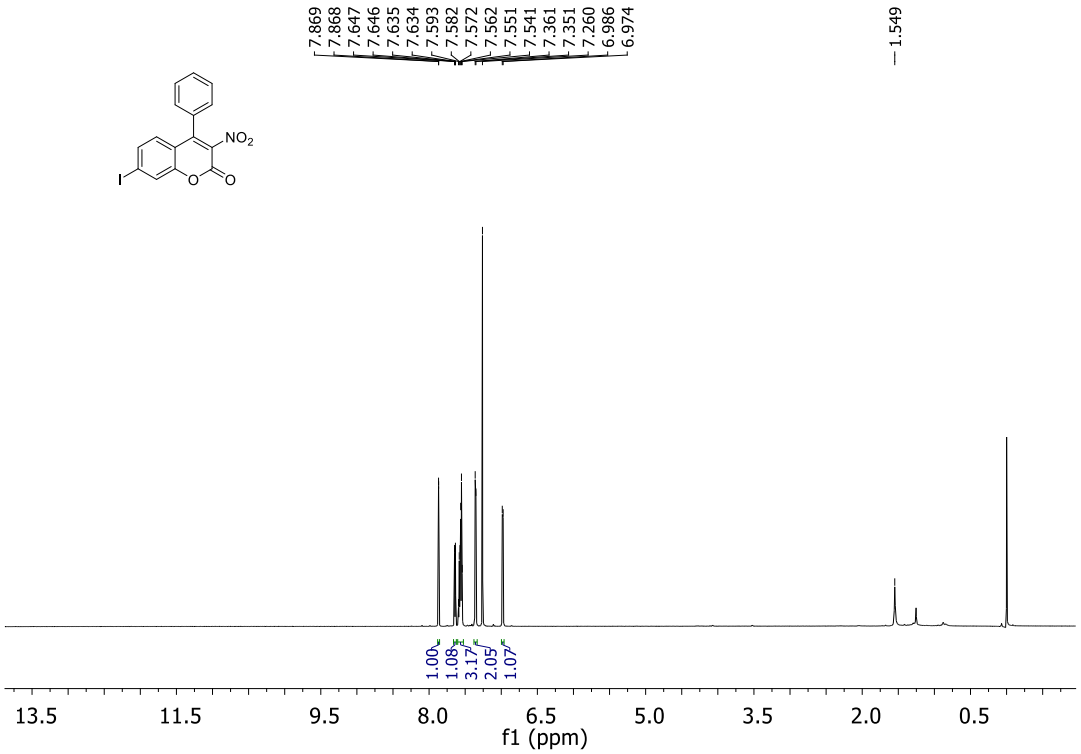

Figure 3.18. ^{1}H NMR of 7-Iodo-3-nitro-4-phenyl-2H-chromen-2-one **(2f).**

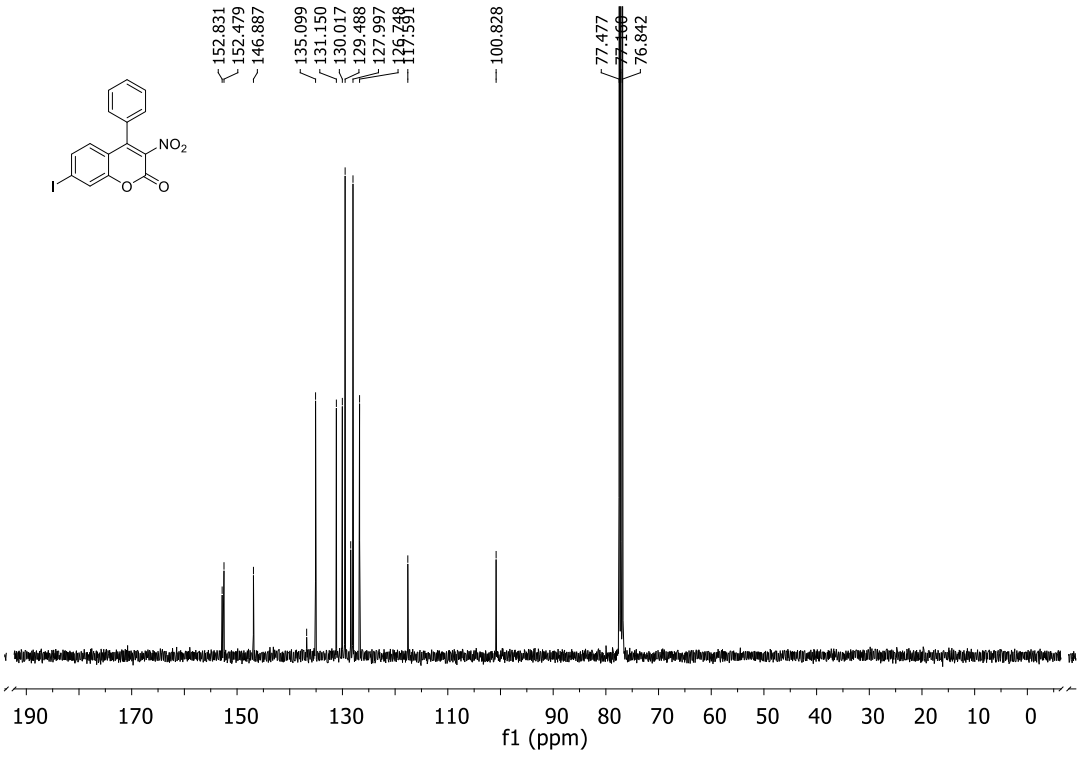

Figure 3.19. ^{13}C NMR of 7-Iodo-3-nitro-4-phenyl-2H-chromen-2-one **(2f).**

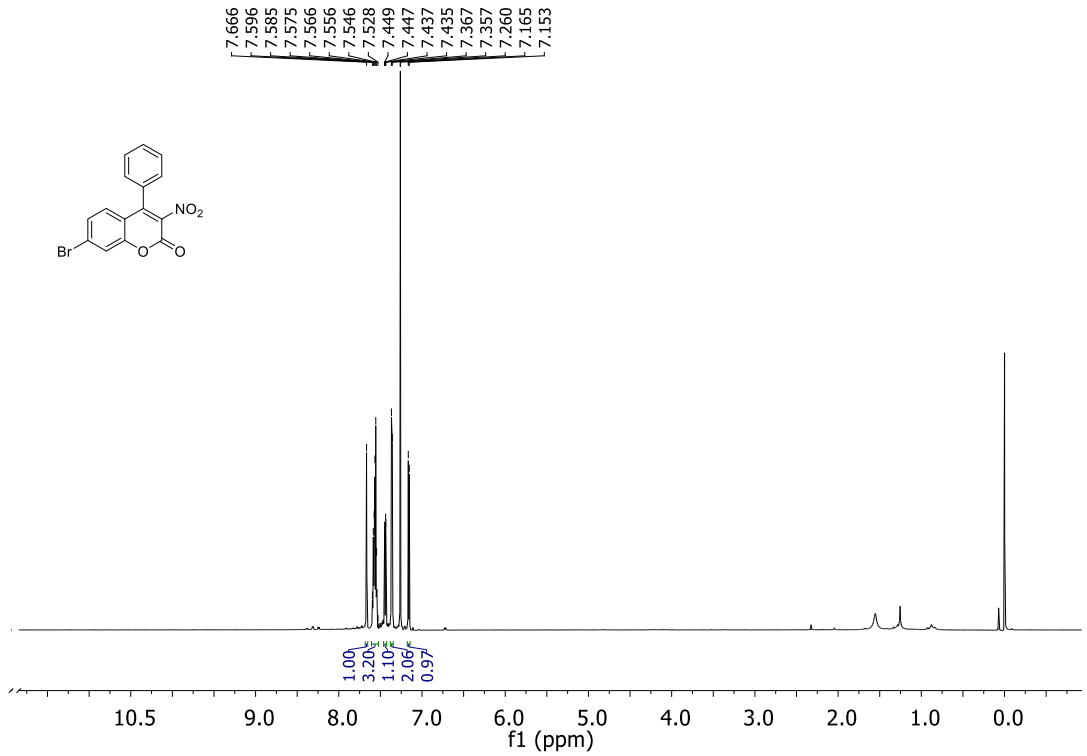

Figure 3.20. ^{1}H NMR of 7-Bromo-3-nitro-4-phenyl-2H-chromen-2-one **(2g).**

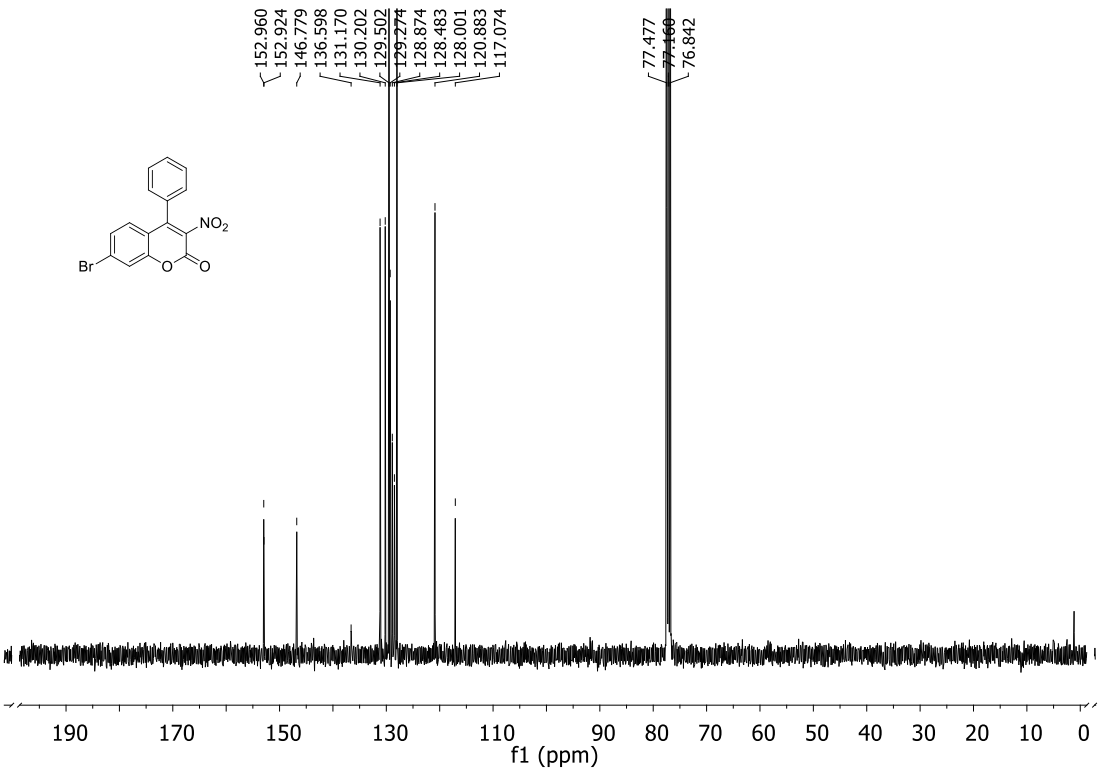

Figure 3.21. ^{13}C NMR of 7-Bromo-3-nitro-4-phenyl-2H-chromen-2-one **(2g).**

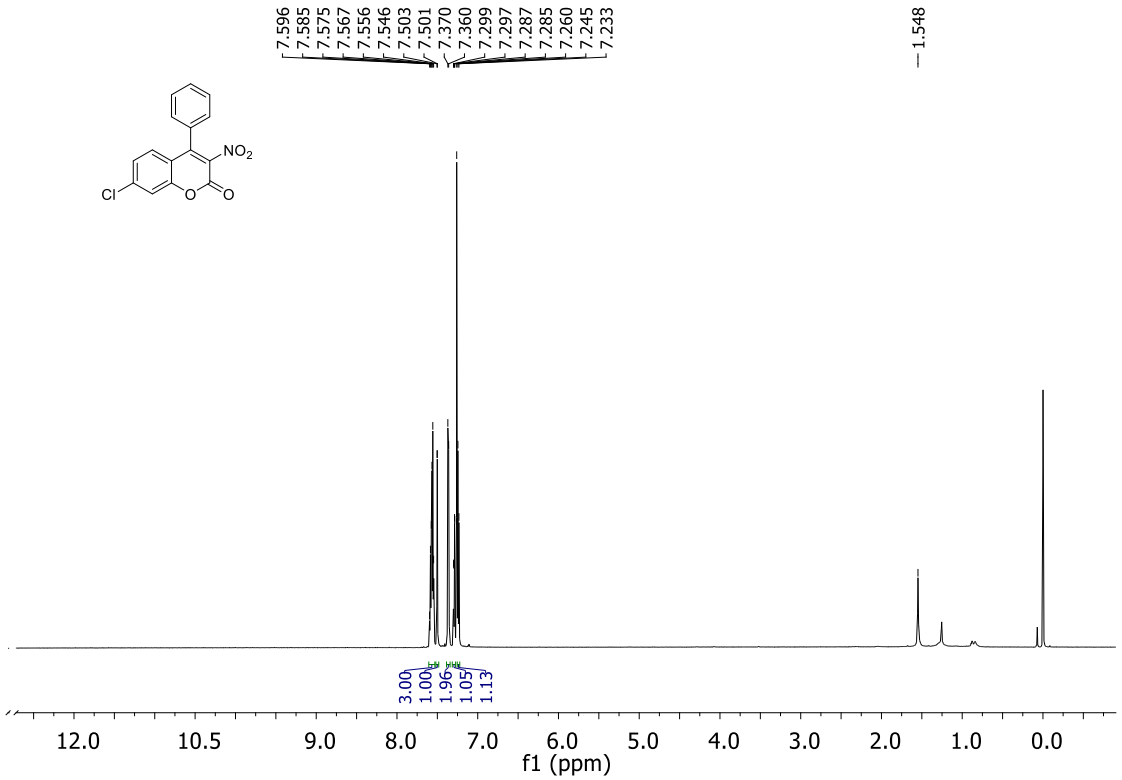

Figure 3.22. ^{1}H NMR of 7-Chloro-3-nitro-4-phenyl-2H-chromen-2-one **(2h).**

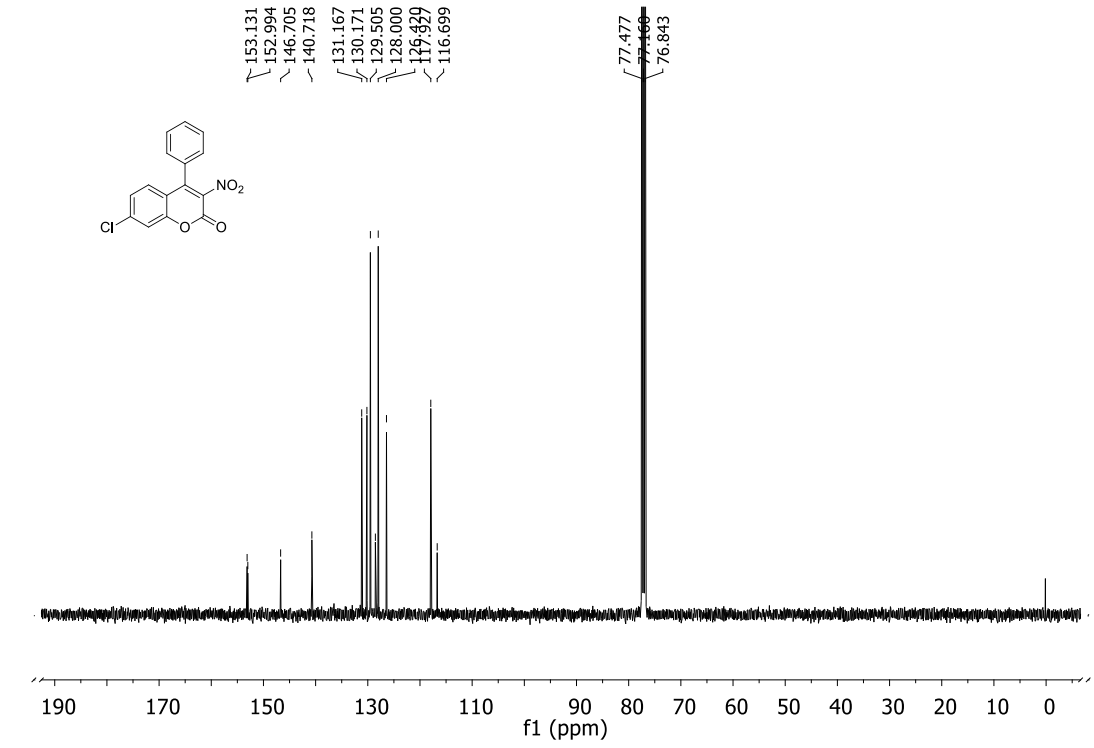

Figure 3.23. ^{13}C NMR of 7-Chloro-3-nitro-4-phenyl-2H-chromen-2-one **(2h)**

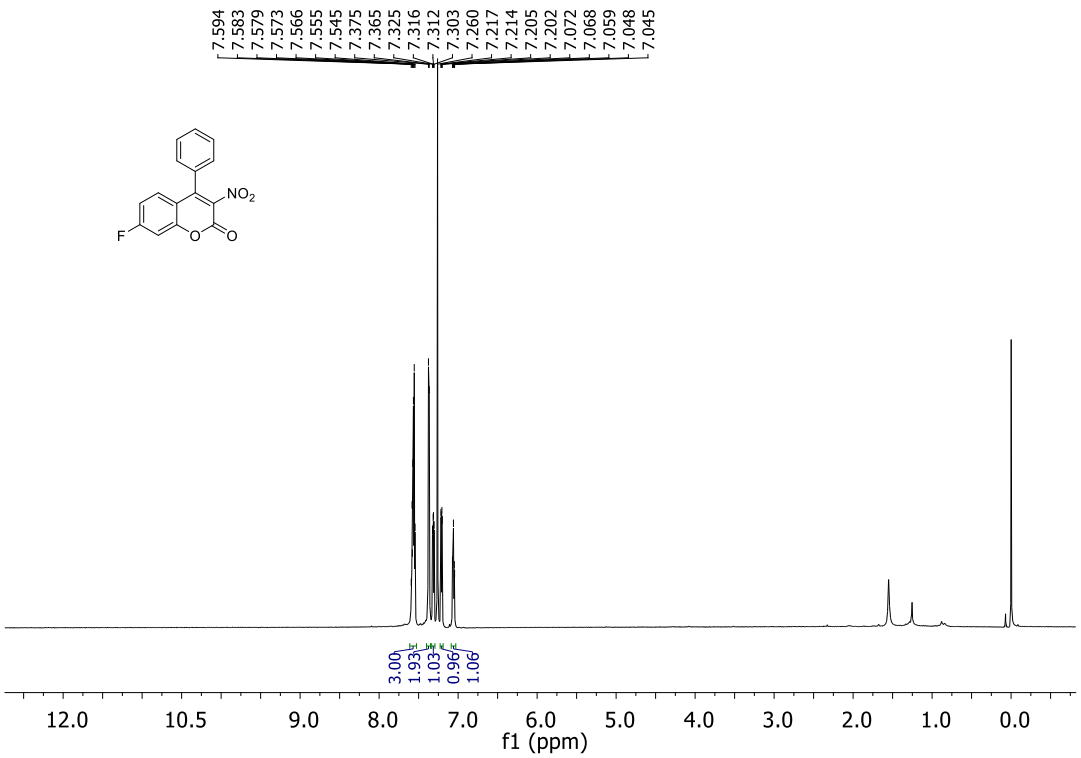

Figure 3.24. ^{1}H NMR of 7-Fluoro-3-nitro-4-phenyl-2H-chromen-2-one **(2i).**

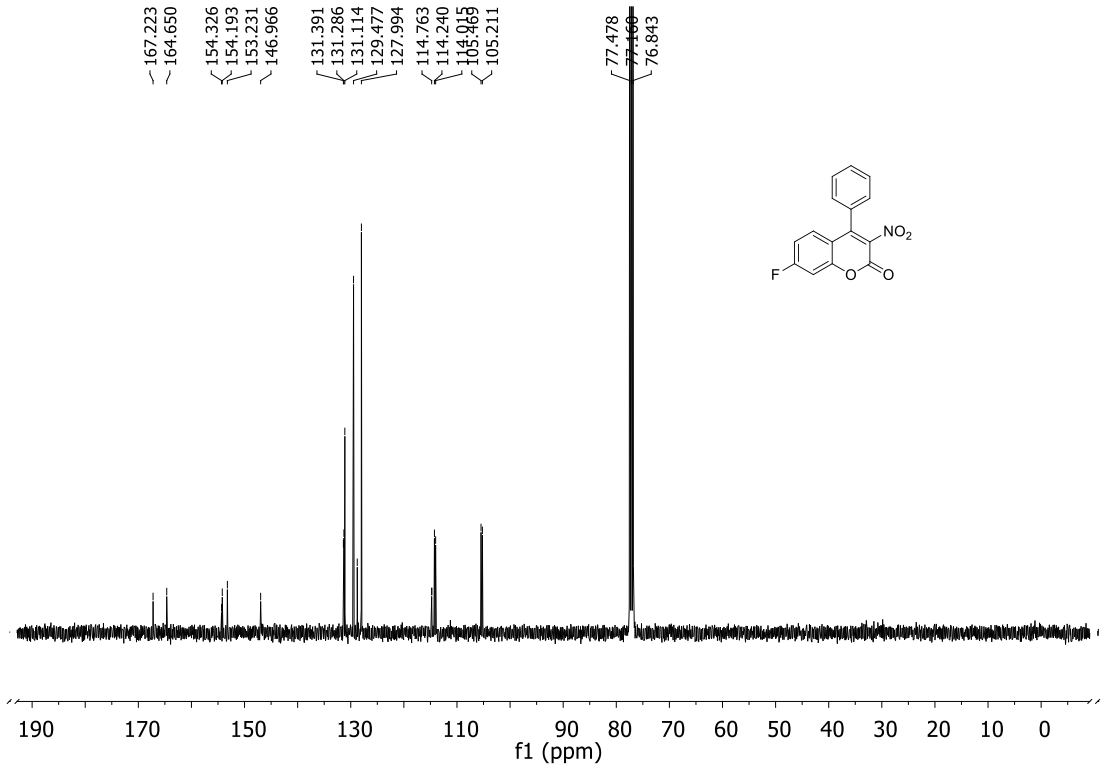

Figure 3.25. ^{13}C NMR of 7-Fluoro-3-nitro-4-phenyl-2H-chromen-2-one **(2i).**

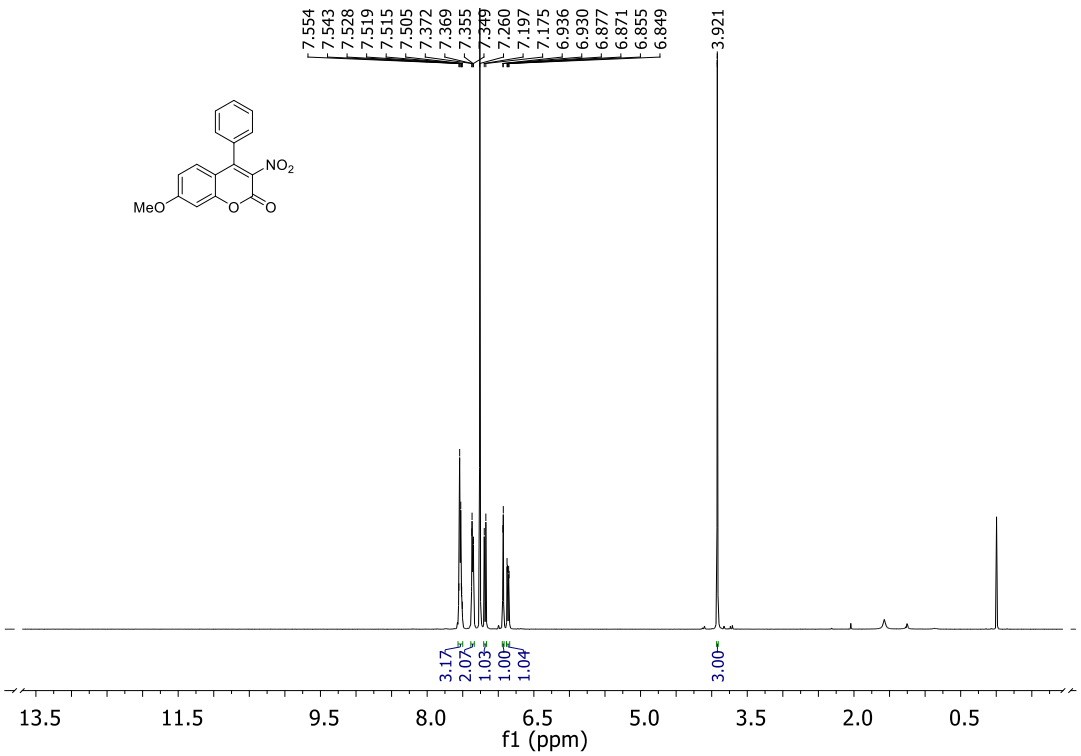

Figure 3.26. [1]H NMR of 7-Methoxy-3-nitro-4-phenyl-2H-chromen-2-one **(2j).**

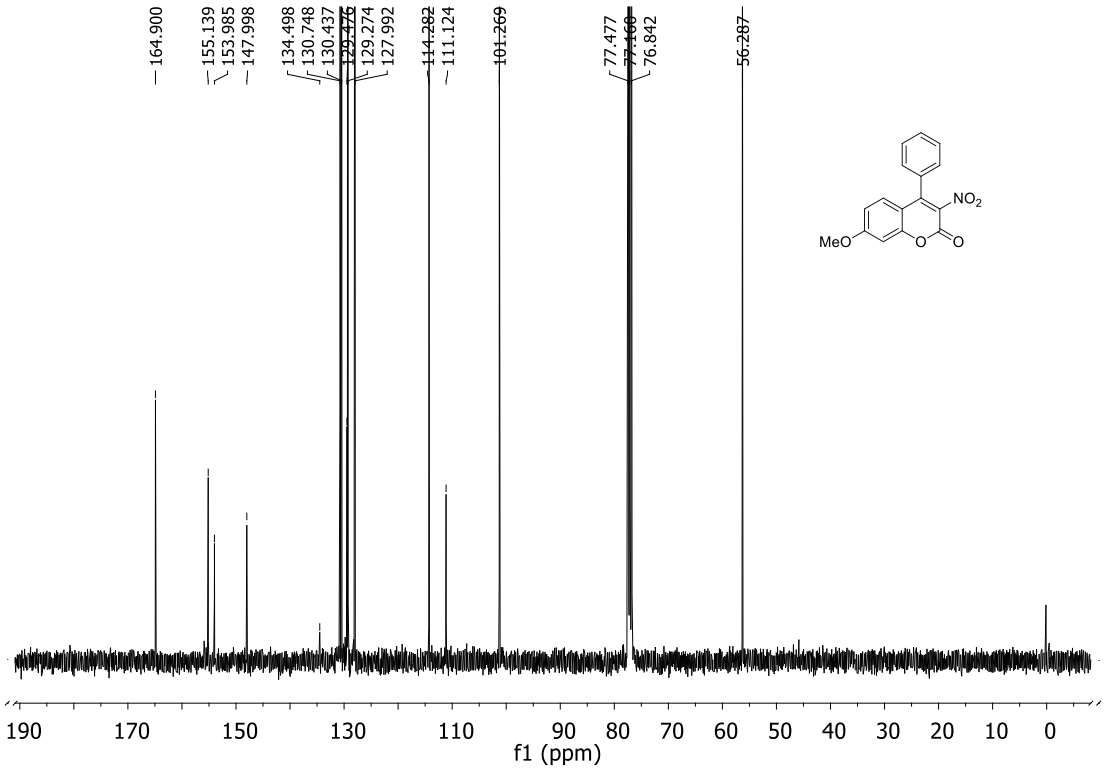

Figure 3.27. [13]C NMR of 7-Methoxy-3-nitro-4-phenyl-2H-chromen-2-one **(2j).**

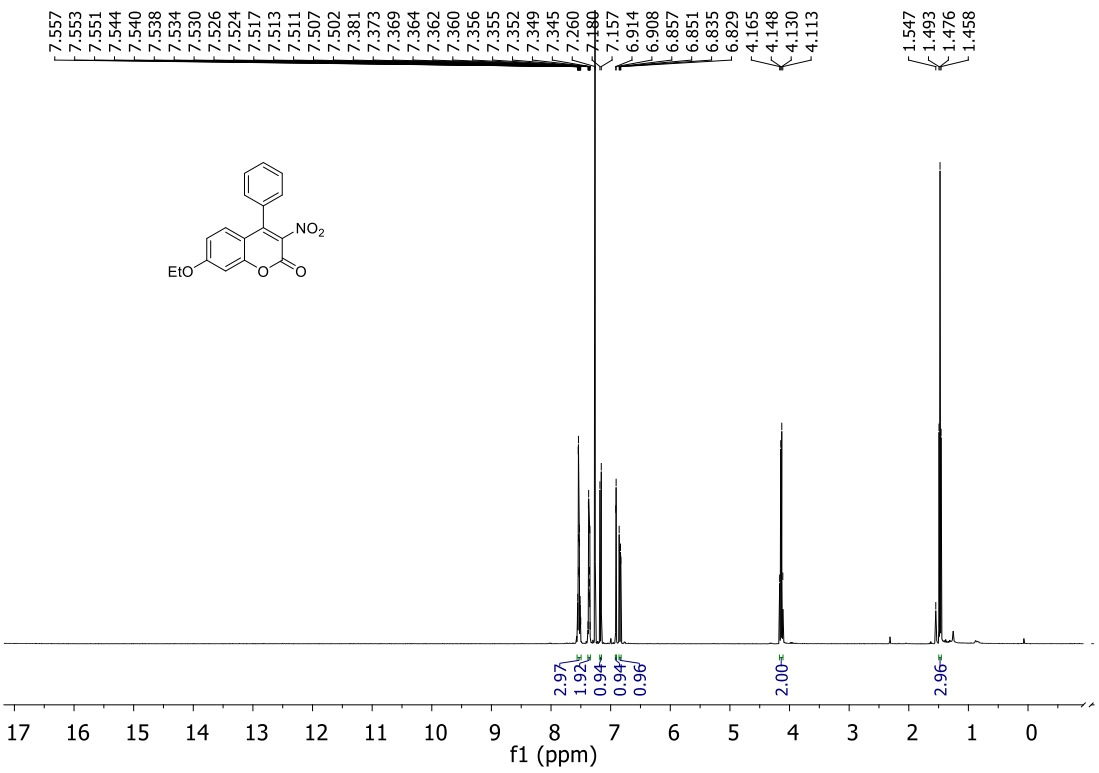

Figure 3.28. [1]H NMR of 7-Ethoxy-3-nitro-4-phenyl-2H-chromen-2-one **(2k).**

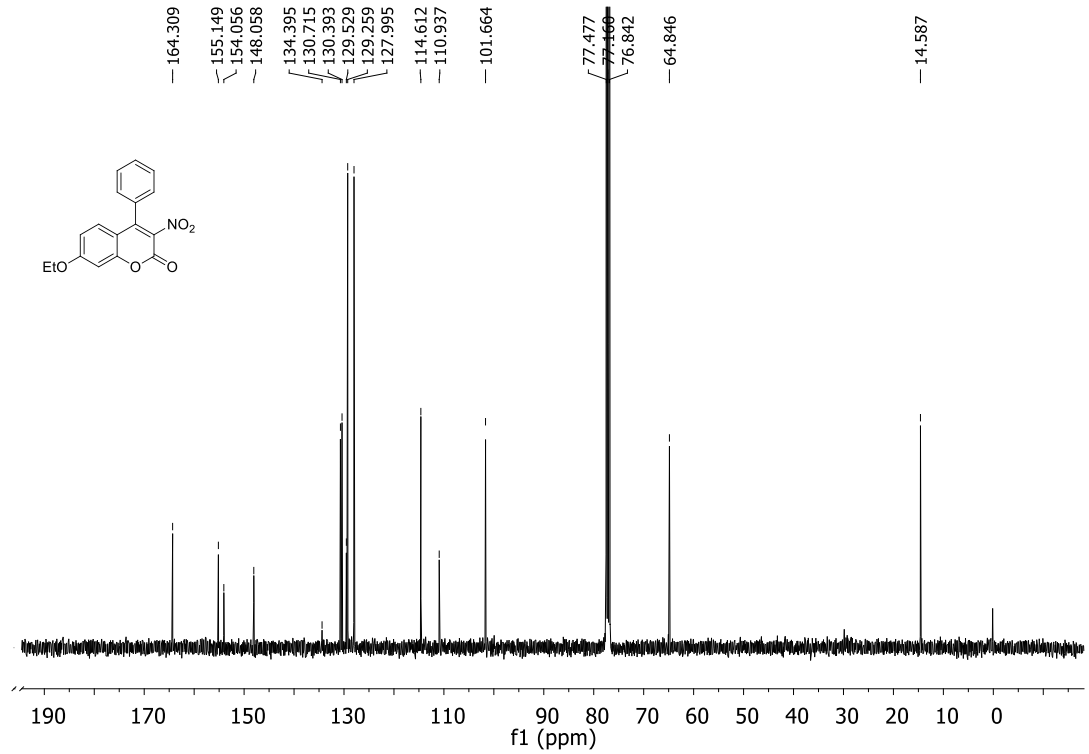

Figure 3.29. [13]C NMR of 7-Ethoxy-3-nitro-4-phenyl-2H-chromen-2-one **(2k).**

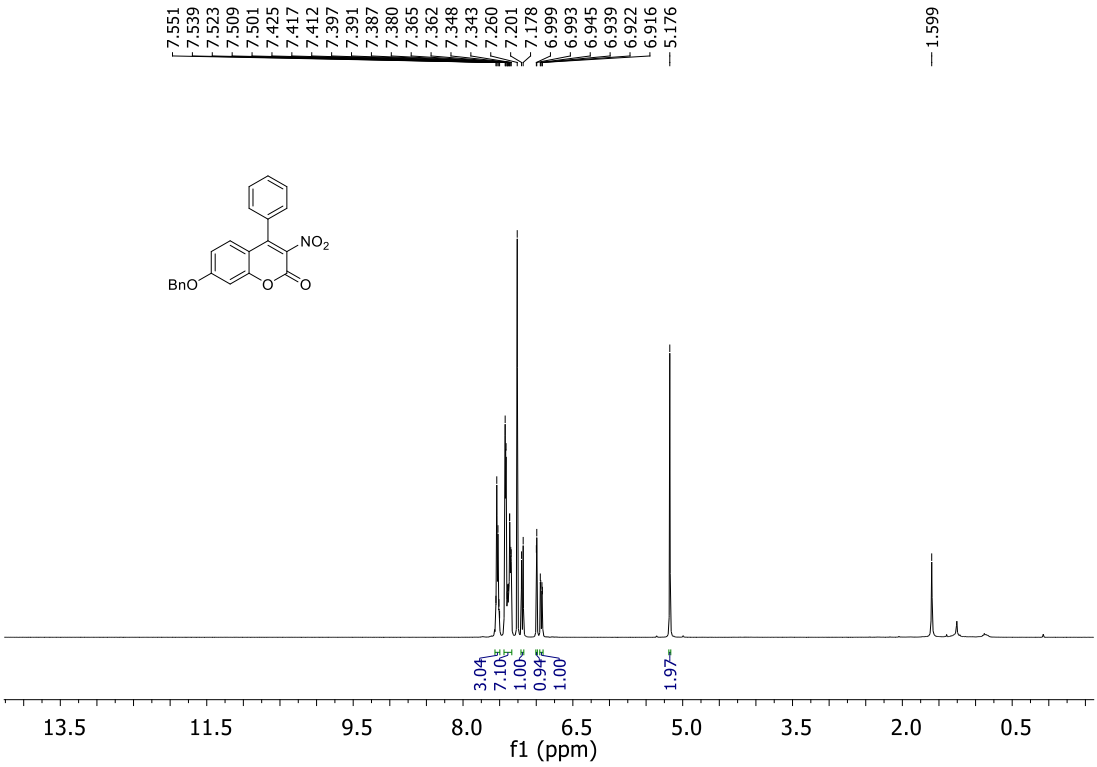

Figure 3.30. ^{1}H NMR of 7-Benzyloxy-3-nitro-4-phenyl-2H-chromen-2-one **(2l).**

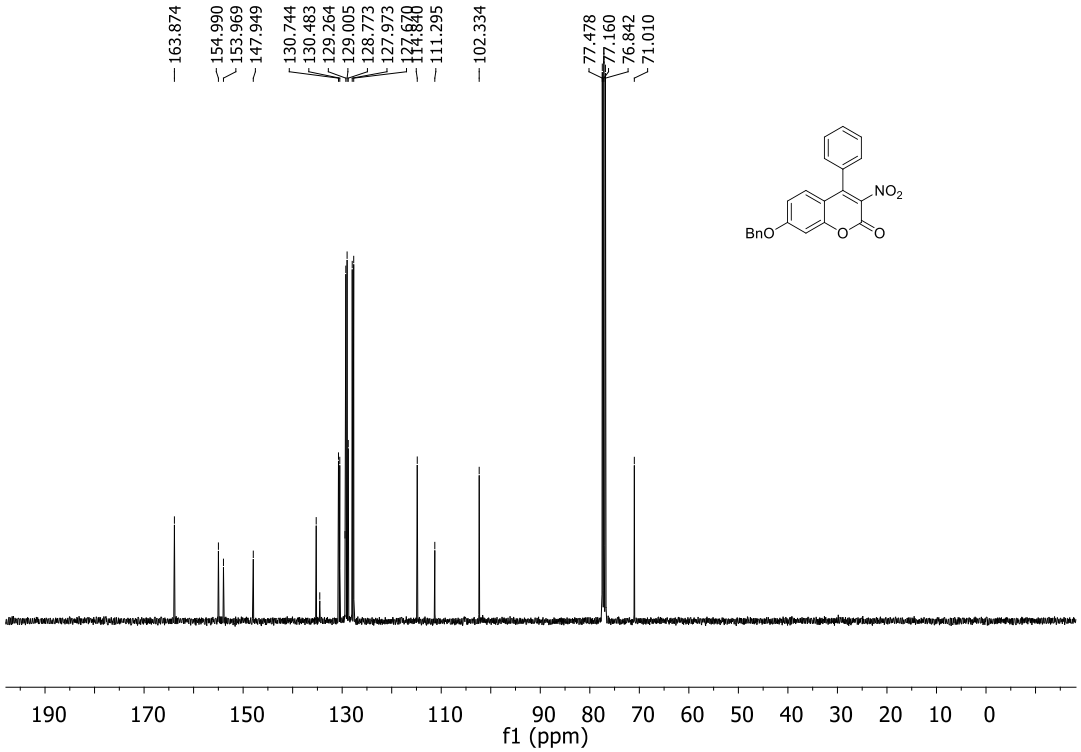

Figure 3.31.^{13}C NMR of 7-Benzyloxy-3-nitro-4-phenyl-2H-chromen-2-one **(2l).**

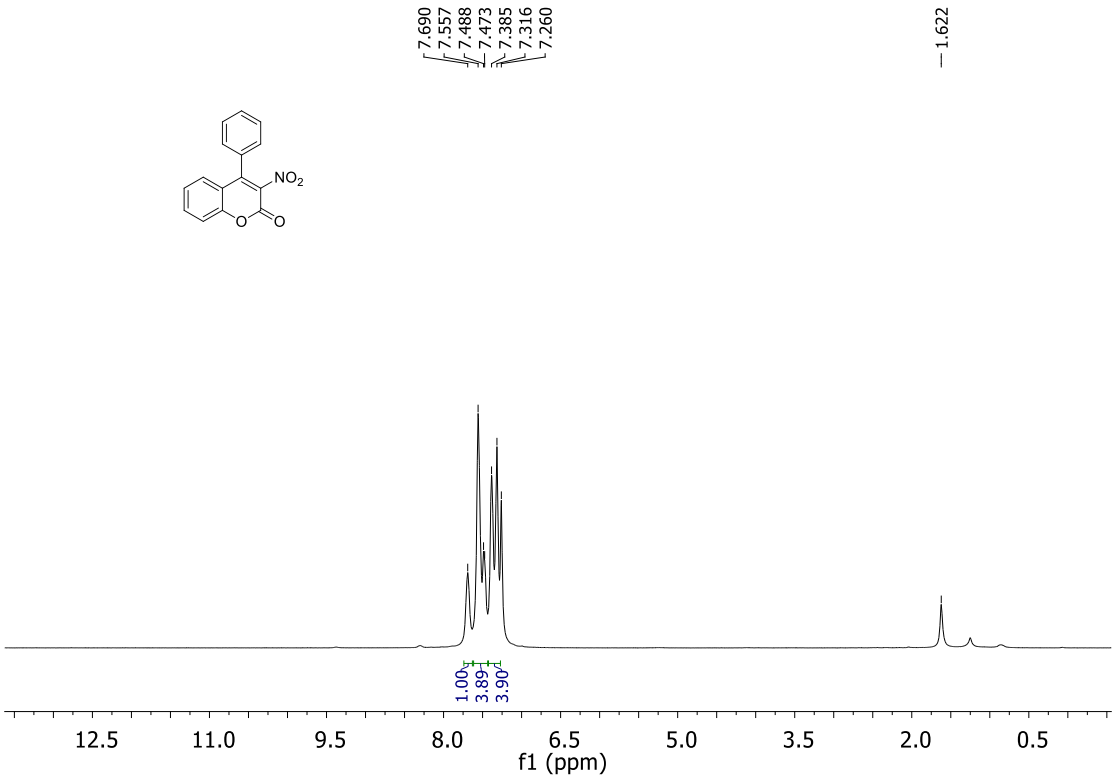

Figure 3.32. ^{1}H NMR of 3-Nitro-4-phenyl-2H-chromen-2-one **(2m).**

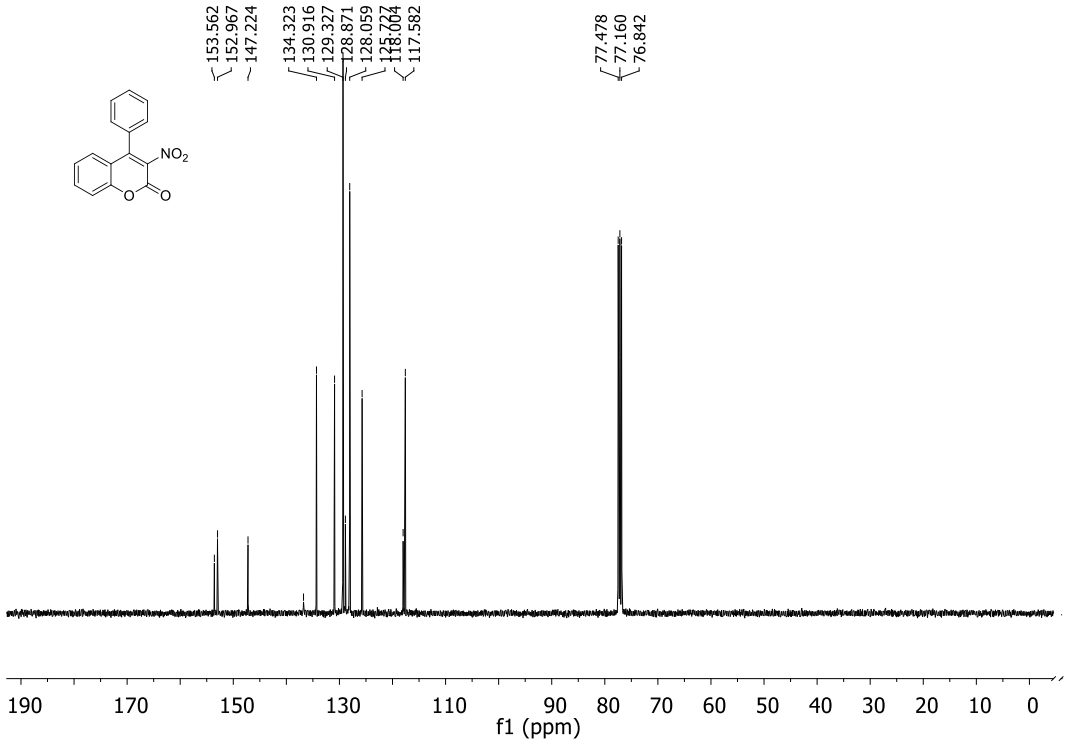

Figure 3.33. ^{13}C NMR of 3-Nitro-4-phenyl-2H-chromen-2-one **(2m).**

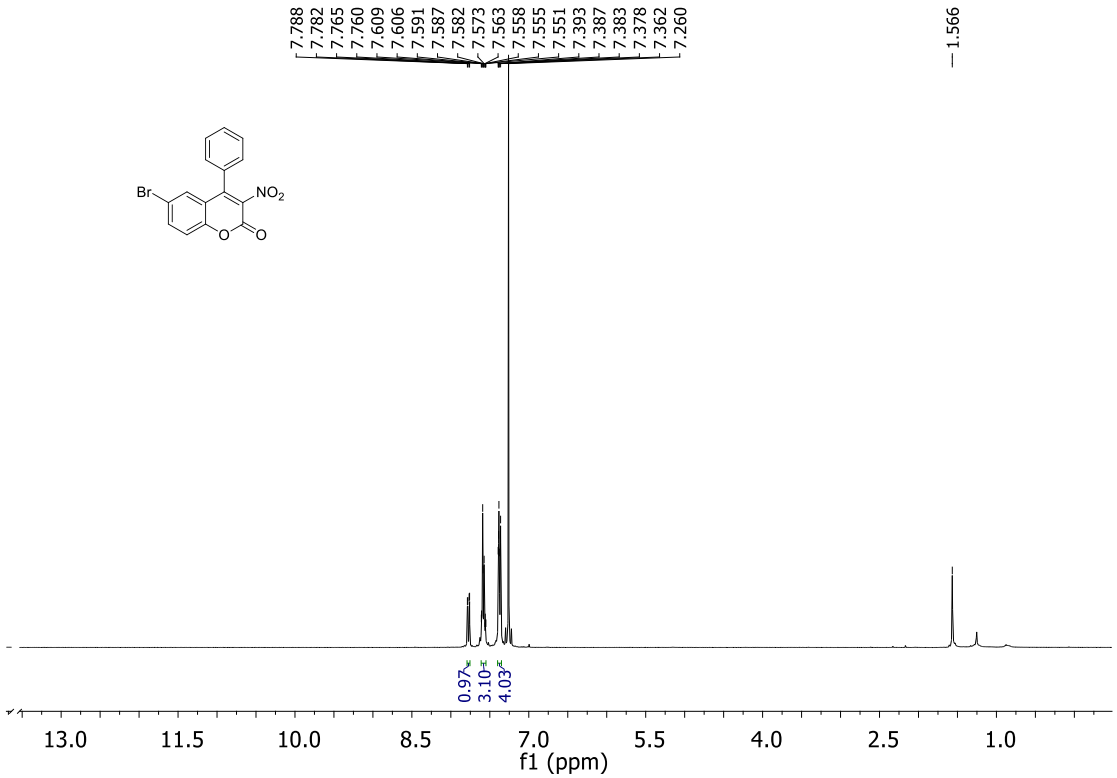

Figure 3.34. [1]H NMR of 6-Bromo-3-nitro-4-phenyl-2H-chromen-2-one **(2q).**

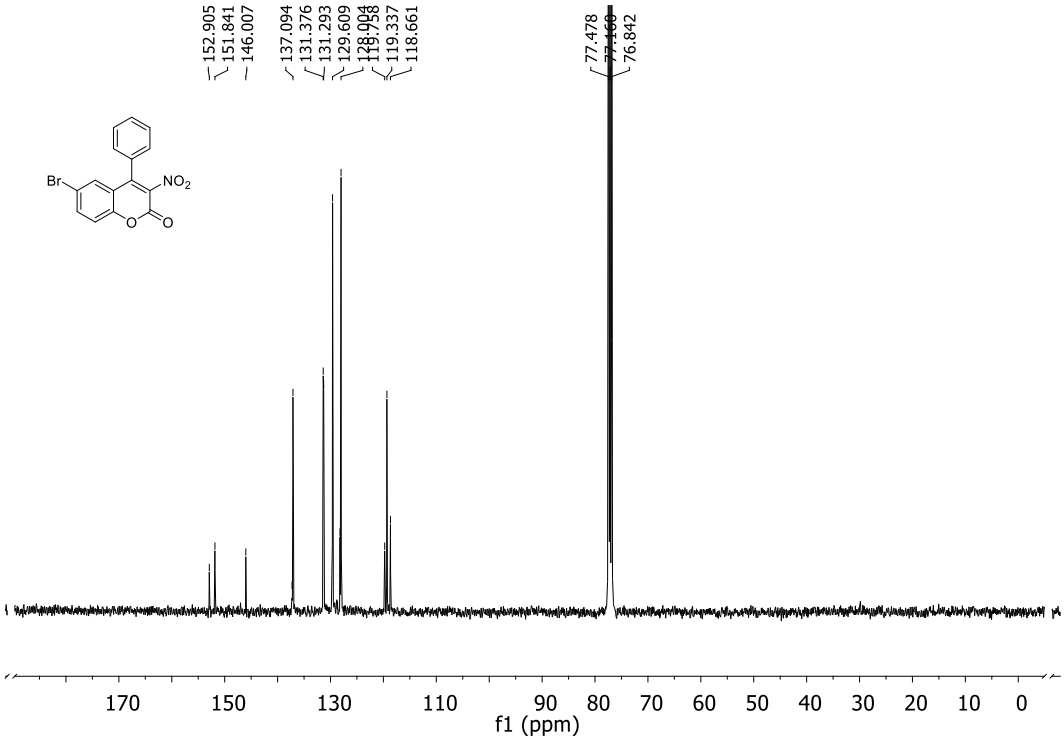

Figure 3.35. [13]C NMR of 6-Bromo-3-nitro-4-phenyl-2H-chromen-2-one **(2q).**

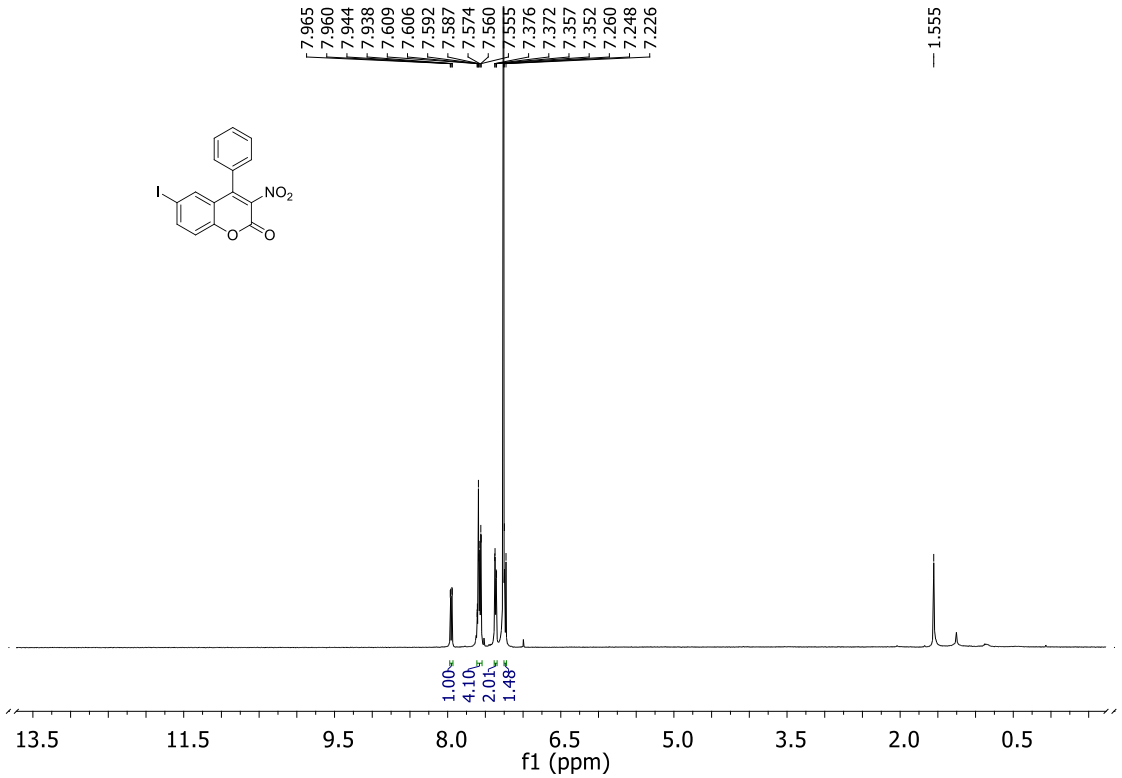

Figure 3.36. ^{1}H NMR of 6-Iodo-3-nitro-4-phenyl-2H-chromen-2-one **(2r).**

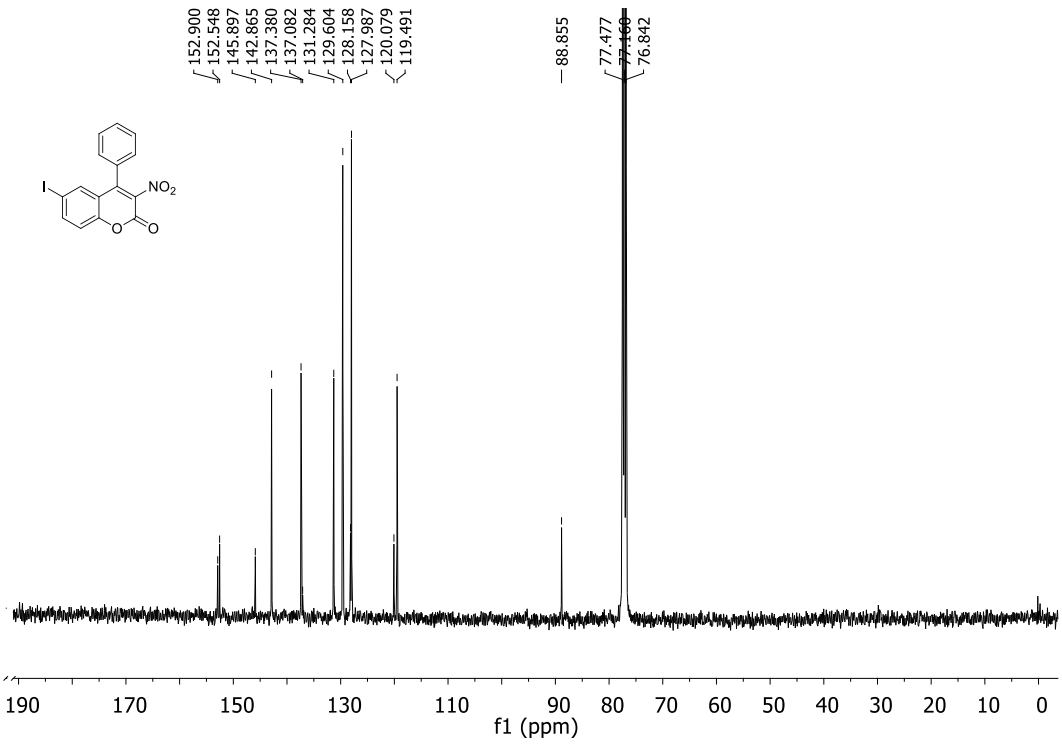

Figure 3.37. ^{13}C NMR of 6-Iodo-3-nitro-4-phenyl-2H-chromen-2-one **(2r).**

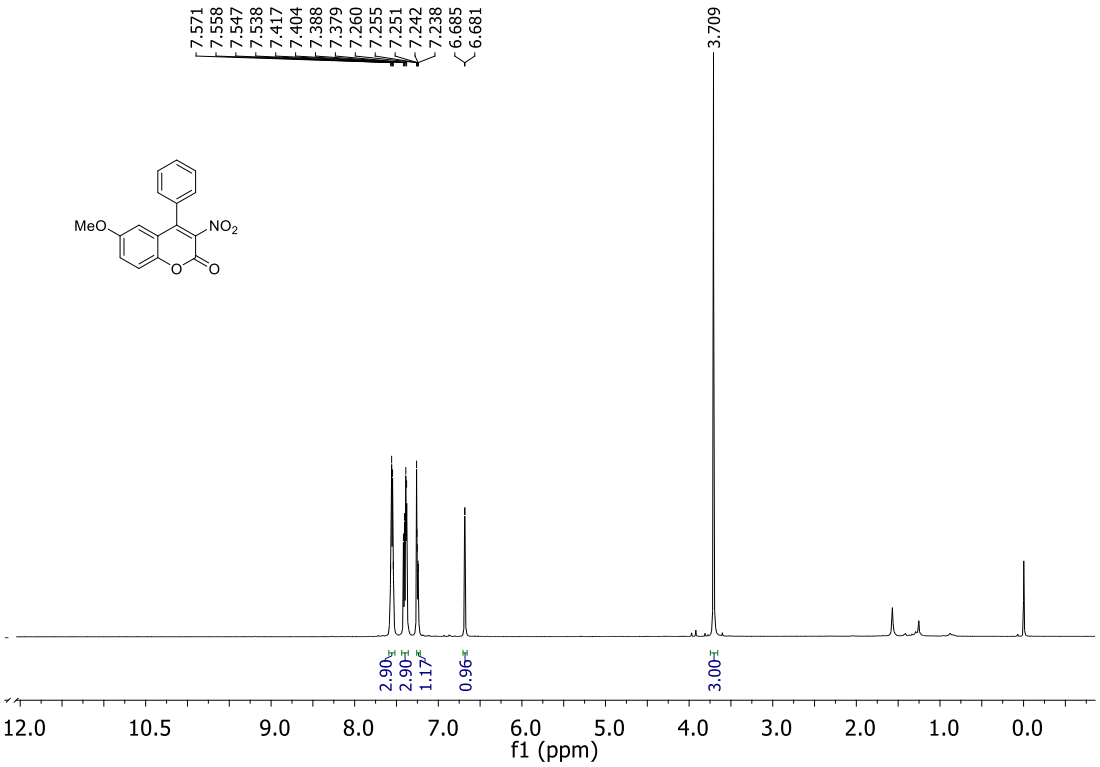

Figure 3.38. ^{1}H NMR of 6-Methoxy-3-nitro-4-phenyl-2H-chromen-2-one **(2s).**

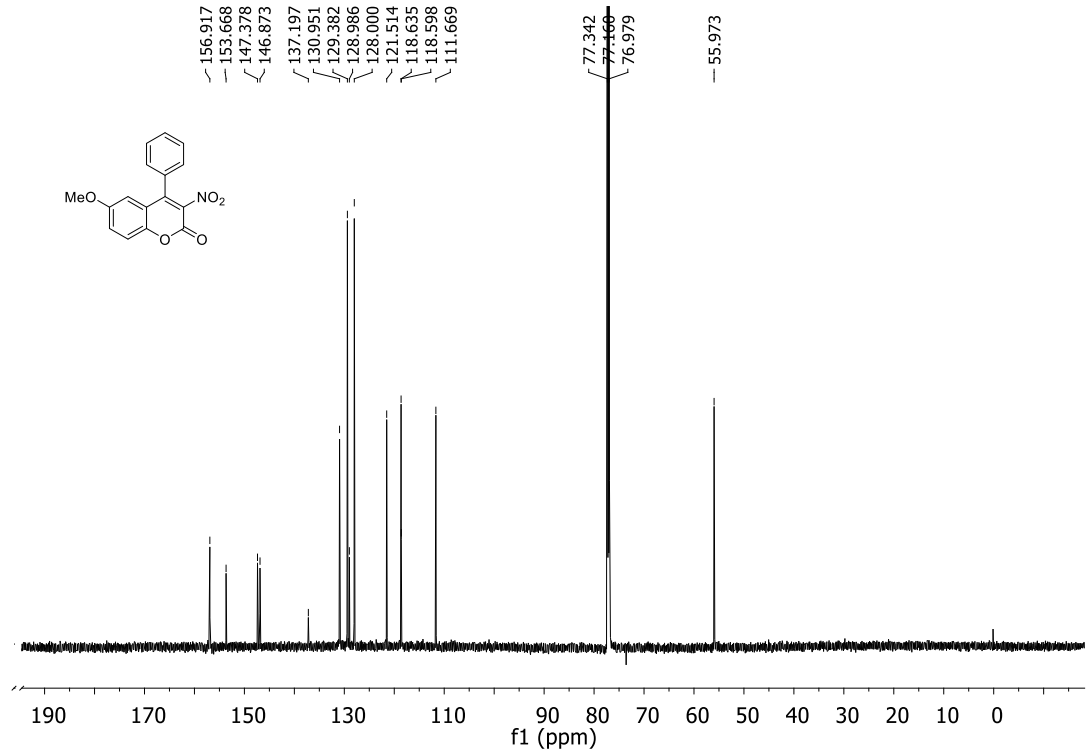

Figure 3.39. ^{13}C NMR of 6-Methoxy-3-nitro-4-phenyl-2H-chromen-2-one **(2s).**

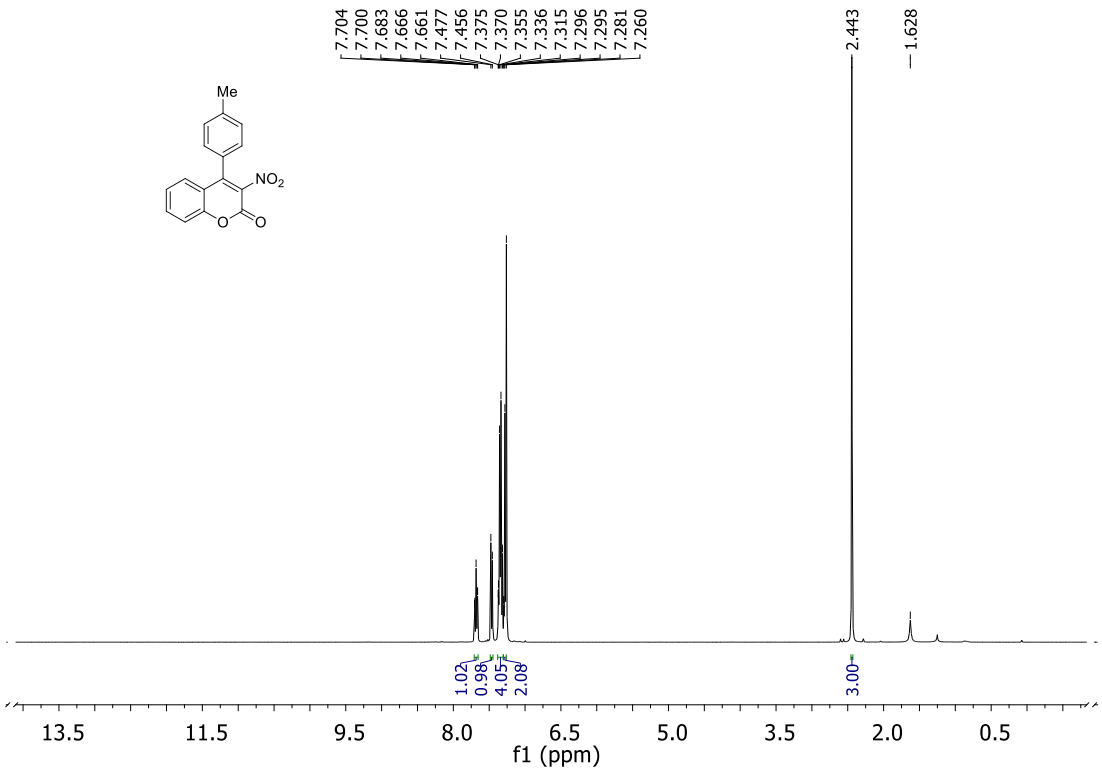

Figure 3.40. ^{1}H NMR of 3-Nitro-4-(*p*-tolyl)-2H-chromen-2-one **(2u).**

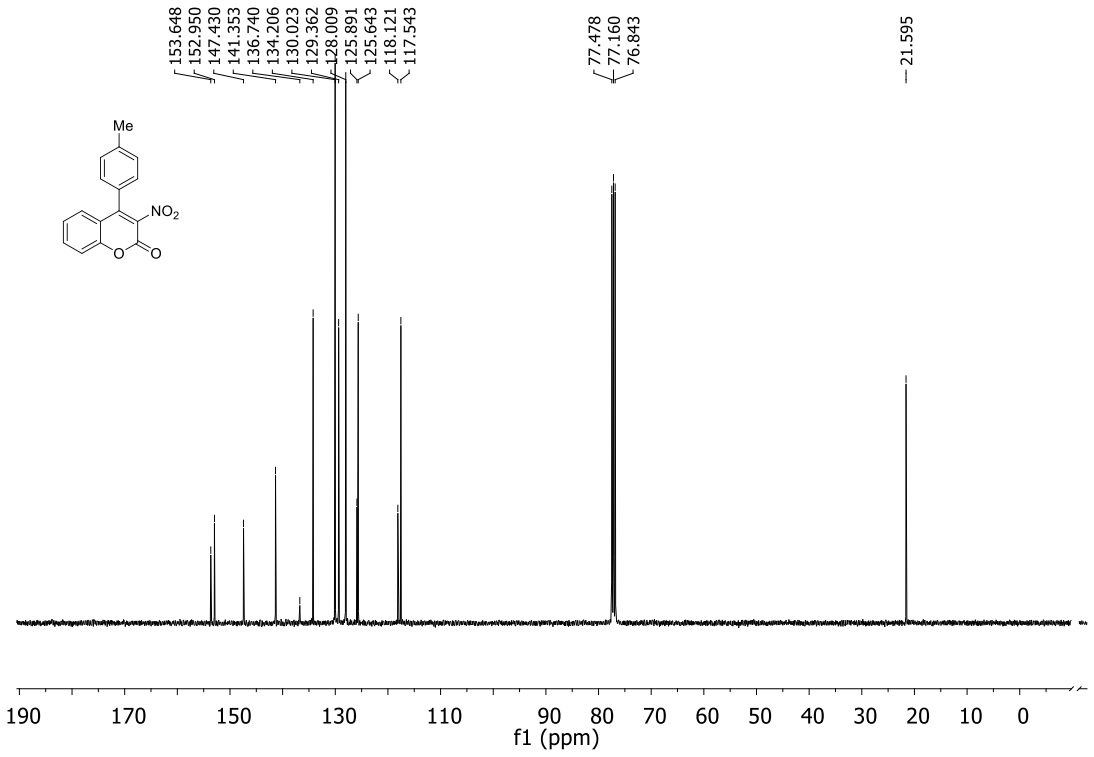

Figure 3.41. ^{13}C NMR of 3-Nitro-4-(*p*-tolyl)-2H-chromen-2-one **(2u).**

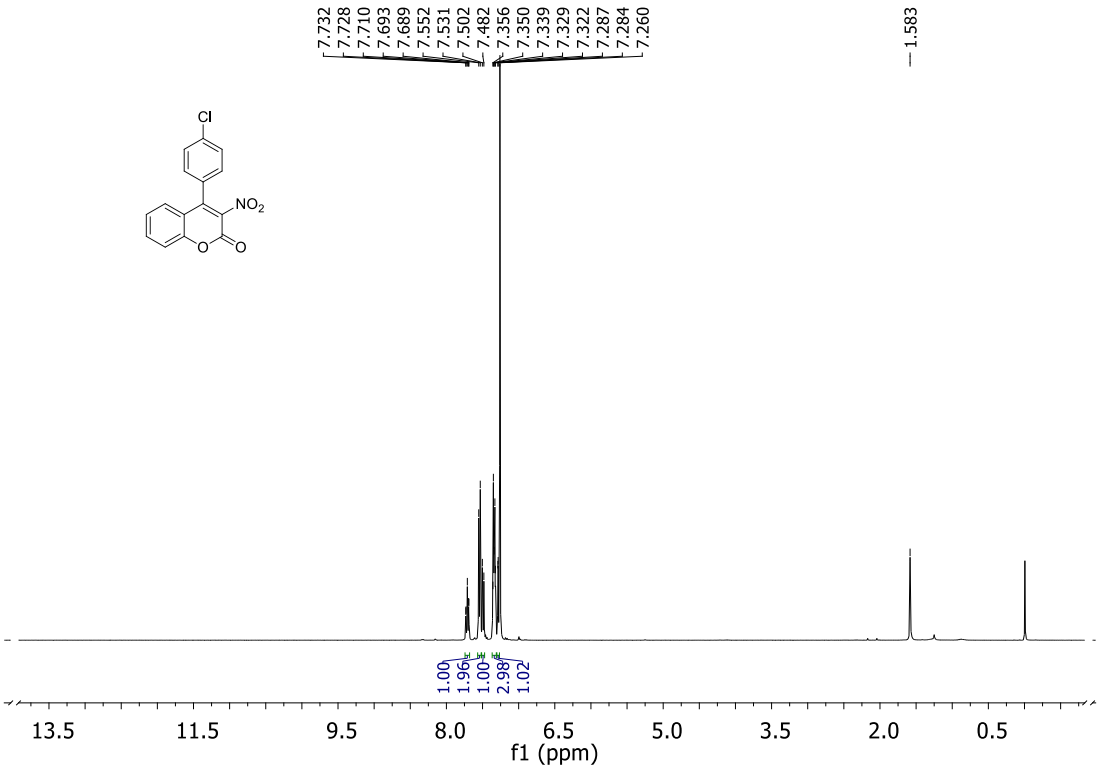

Figure 3.42. ^{1}H NMR of 4-(4-Chlorophenyl)-3-nitro-2H-chromen-2-one **(2v).**

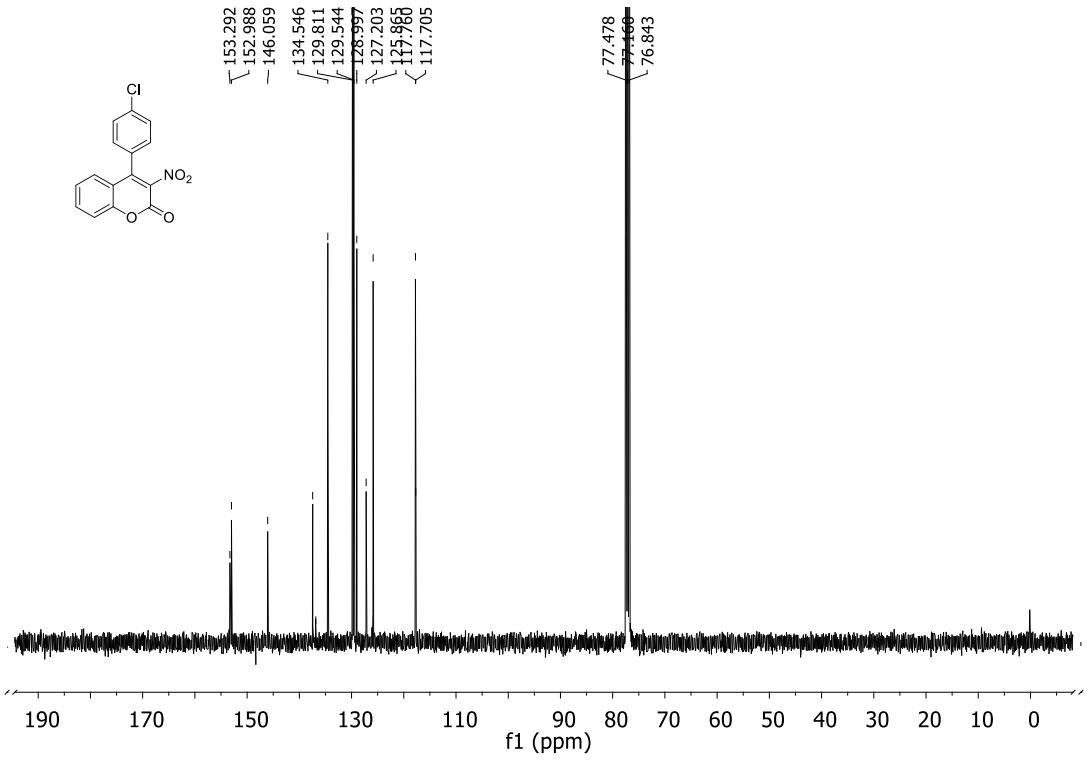

Figure 3.43. ^{13}C NMR of 4-(4-Chlorophenyl)-3-nitro-2H-chromen-2-one **(2v).**

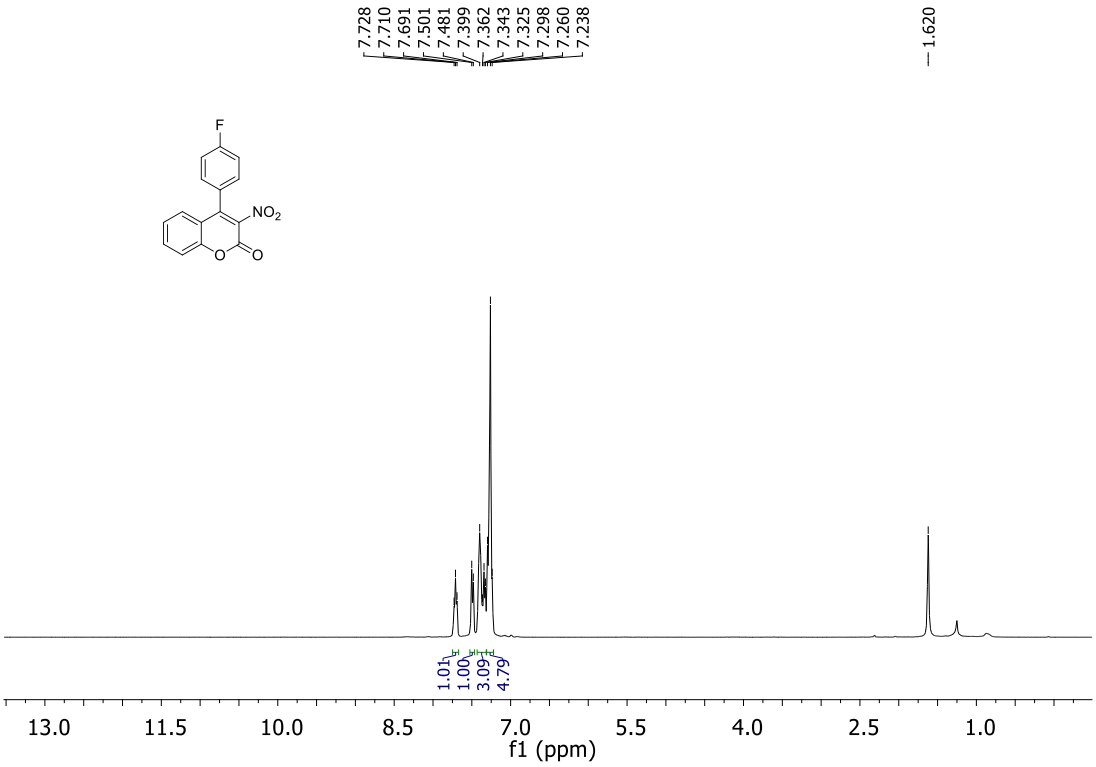

Figure 3.44. [1]H NMR of 4-(4-Fluorophenyl)-3-nitro-2H-chromen-2-one **(2w).**

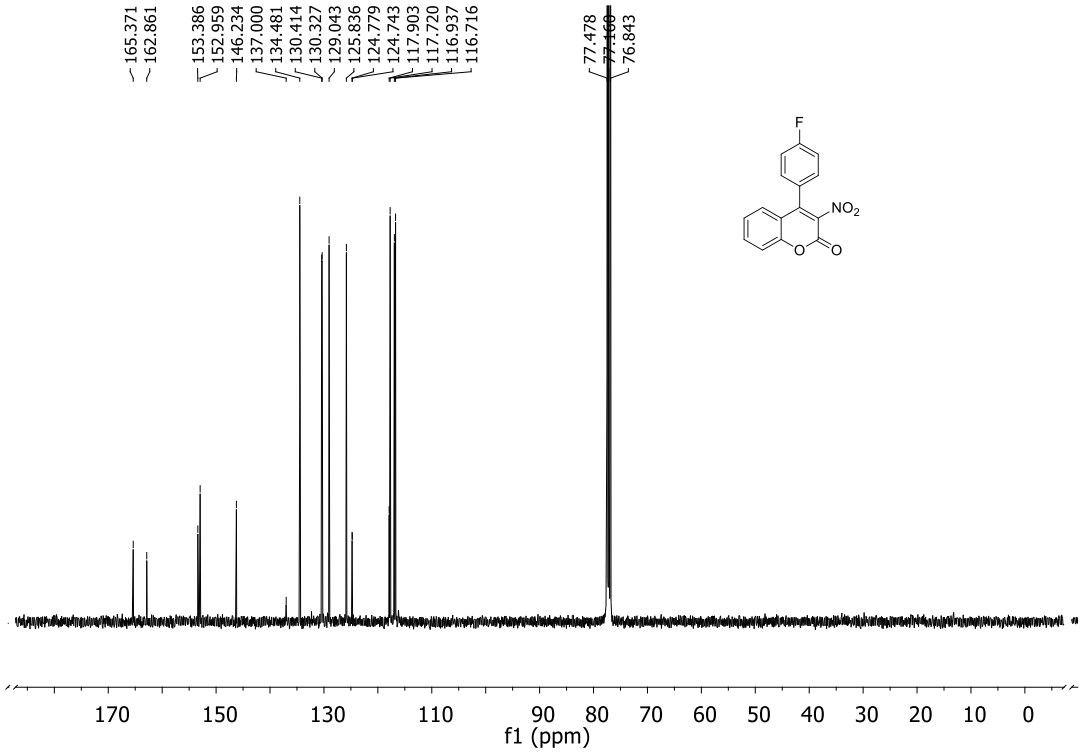

Figure 3.45.[13]C NMR of 4-(4-Fluorophenyl)-3-nitro-2H-chromen-2-one **(2w).**

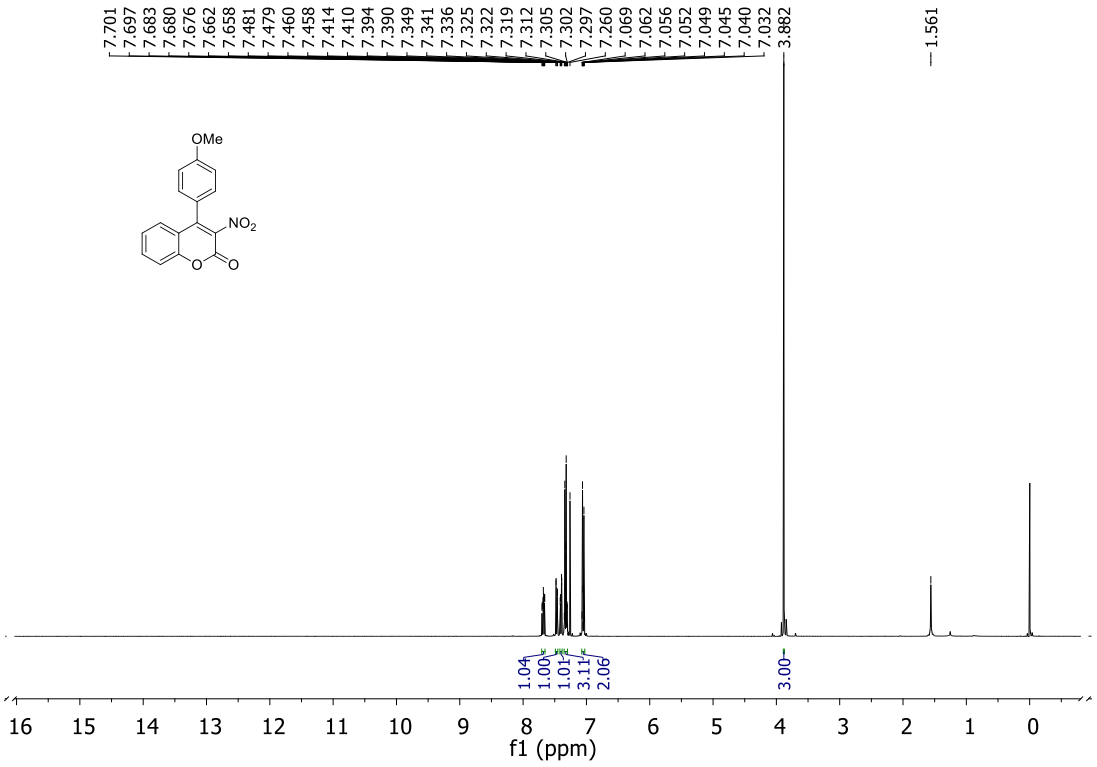

Figure 3.46. [1]H NMR of 4-(4-Methoxyphenyl)-3-nitro-2H-chromen-2-one **(2x).**

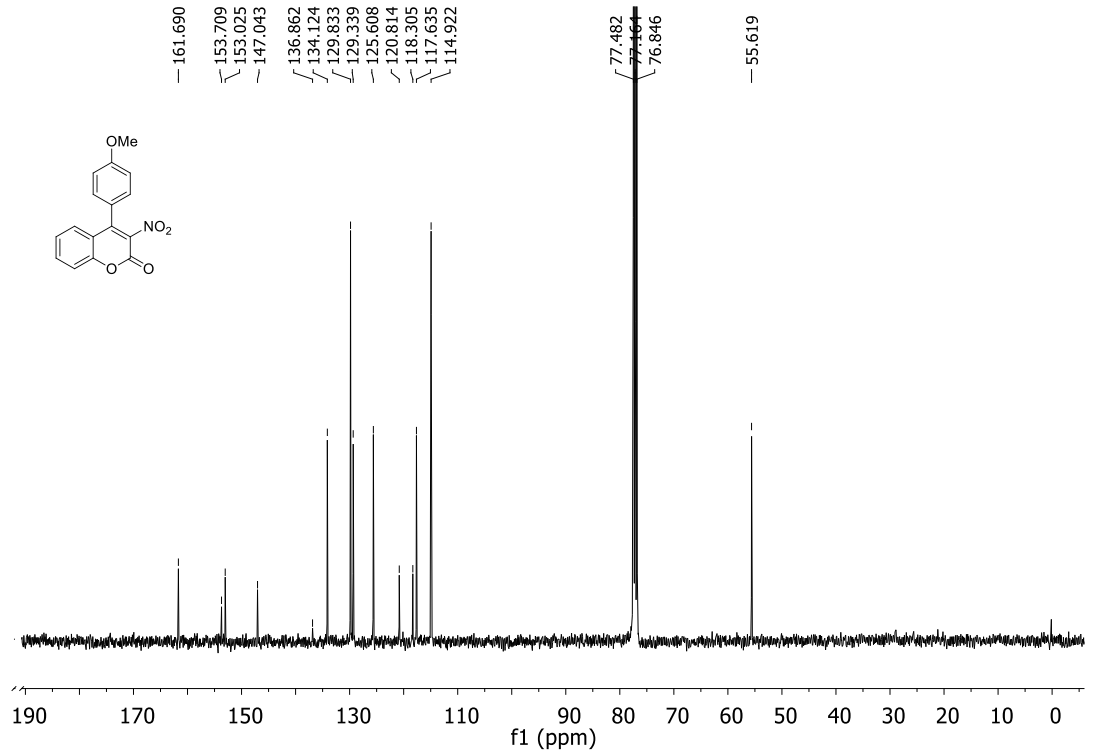

Figure 3.47. [13]C NMR of 4-(4-Methoxyphenyl)-3-nitro-2H-chromen-2-one **(2x).**

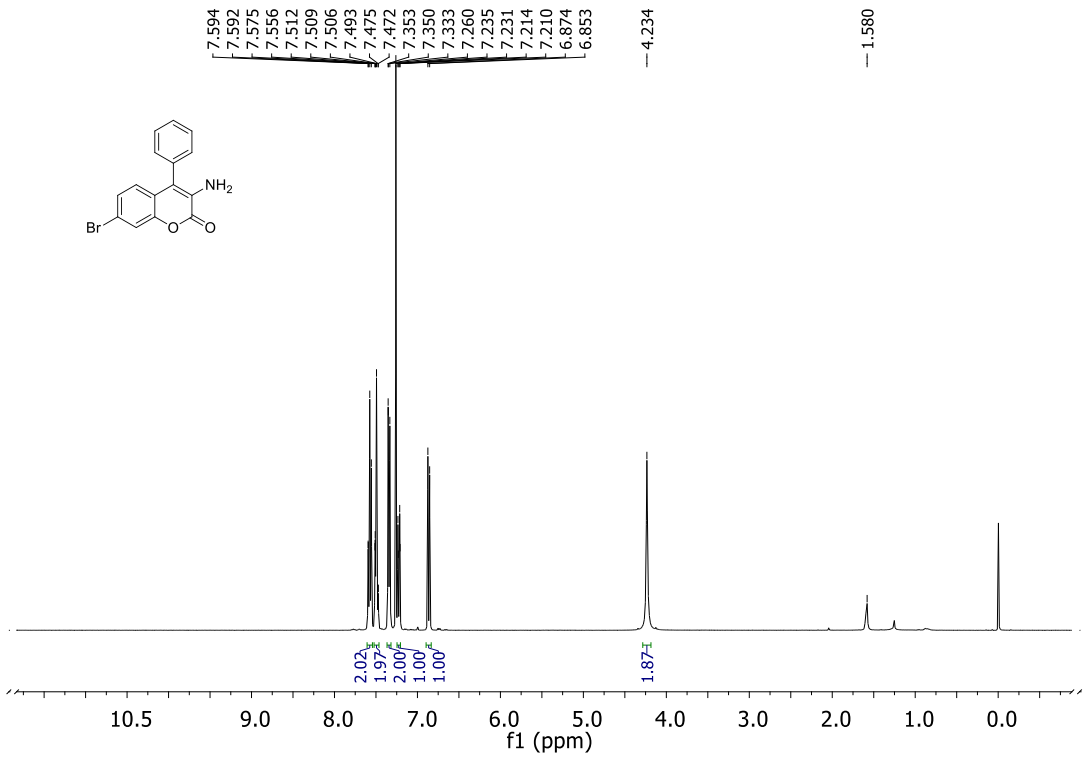

Figure 3.48. [1]H NMR of 3-Amino-7-bromo-4-phenyl-2H-chromen-2-one **(7).**

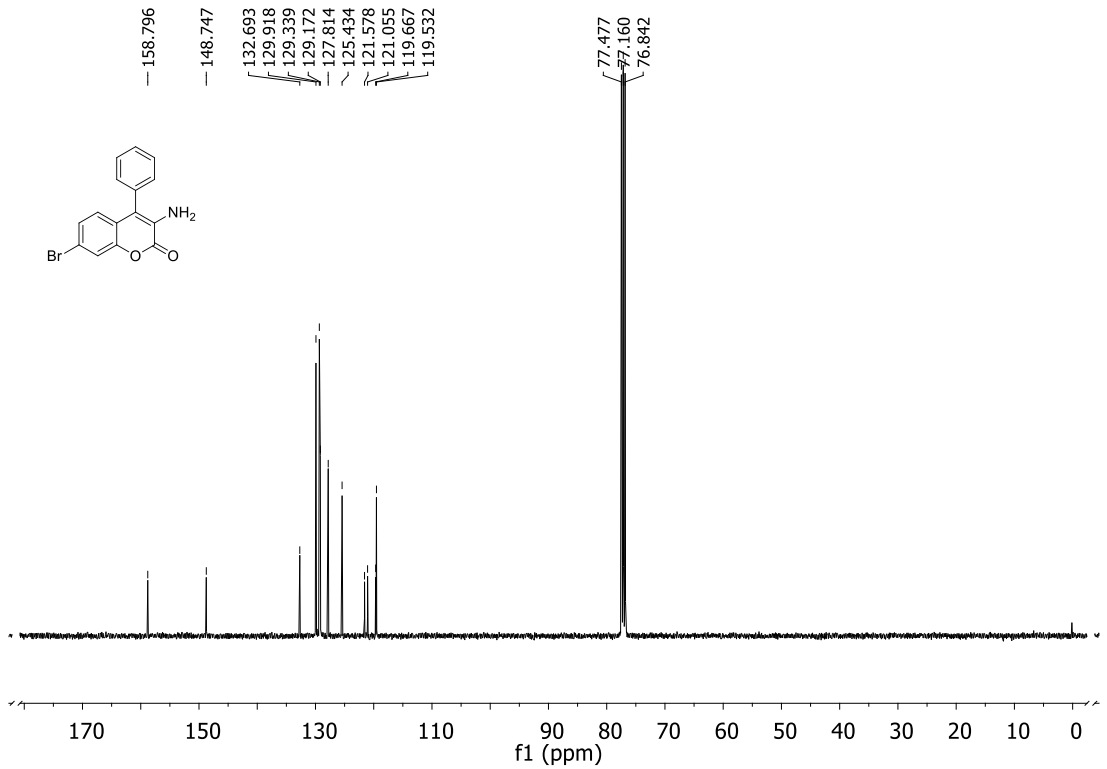

Figure 3.49. [13]C NMR of 3-Amino-7-bromo-4-phenyl-2H-chromen-2-one **(7)**

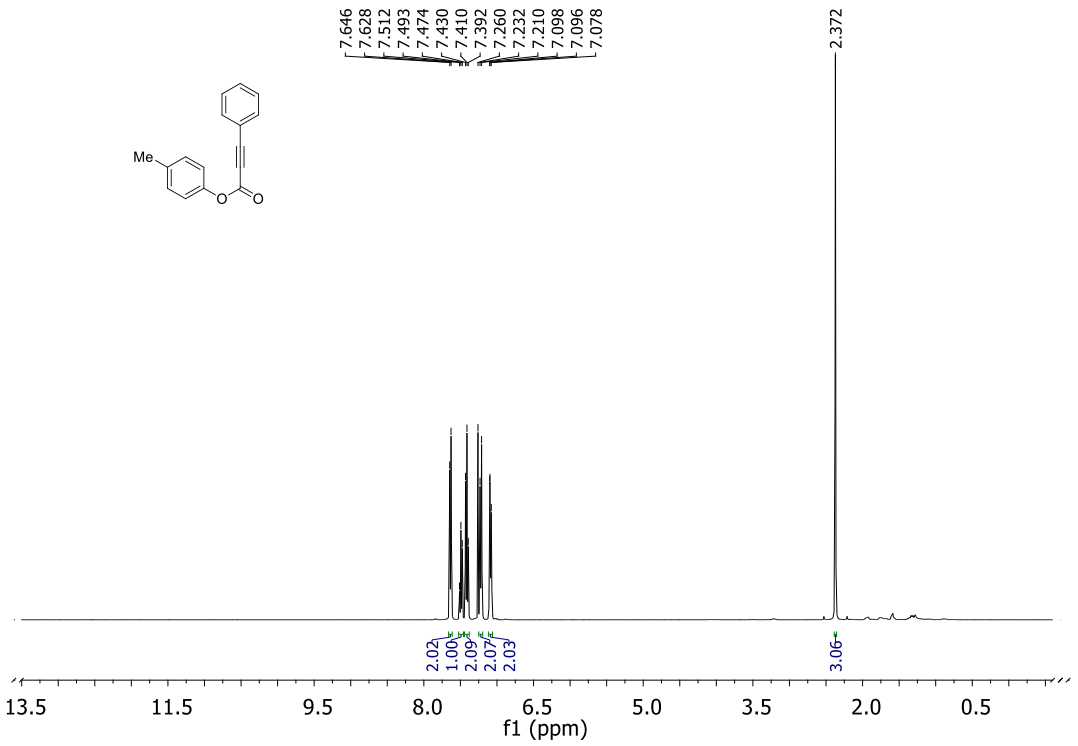

Figure 3.50. ^{1}H NMR of *p*-tolyl 3-phenylpropiolate **(1a).**

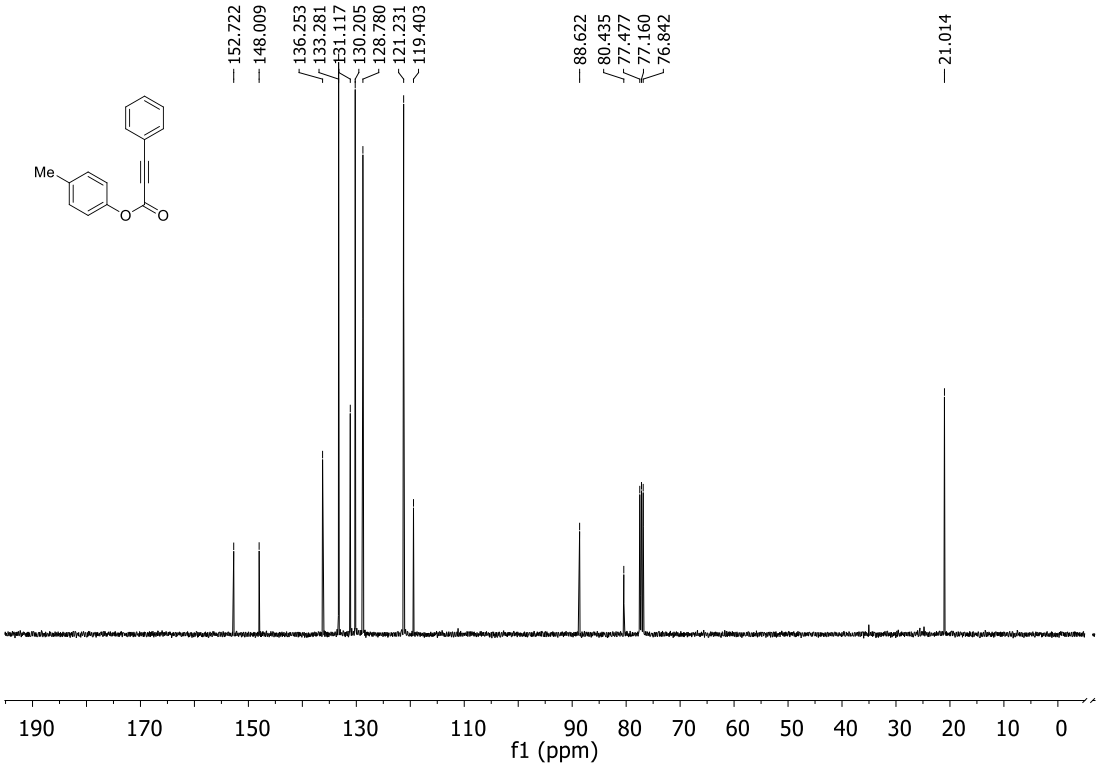

Figure 3.51. ^{13}C NMR of *p*-tolyl 3-phenylpropiolate **(1a).**

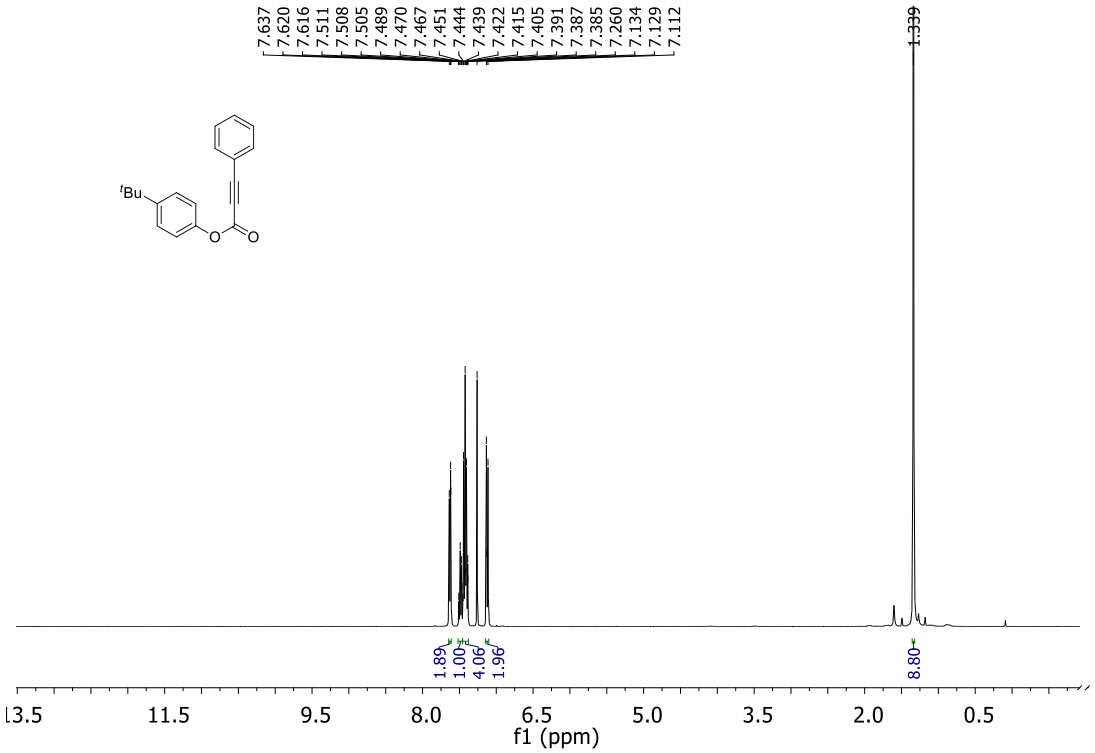

Figure 3.52. ^{1}H NMR of 4-(*tert*-butyl)phenyl 3-phenylpropiolate **(1b).**

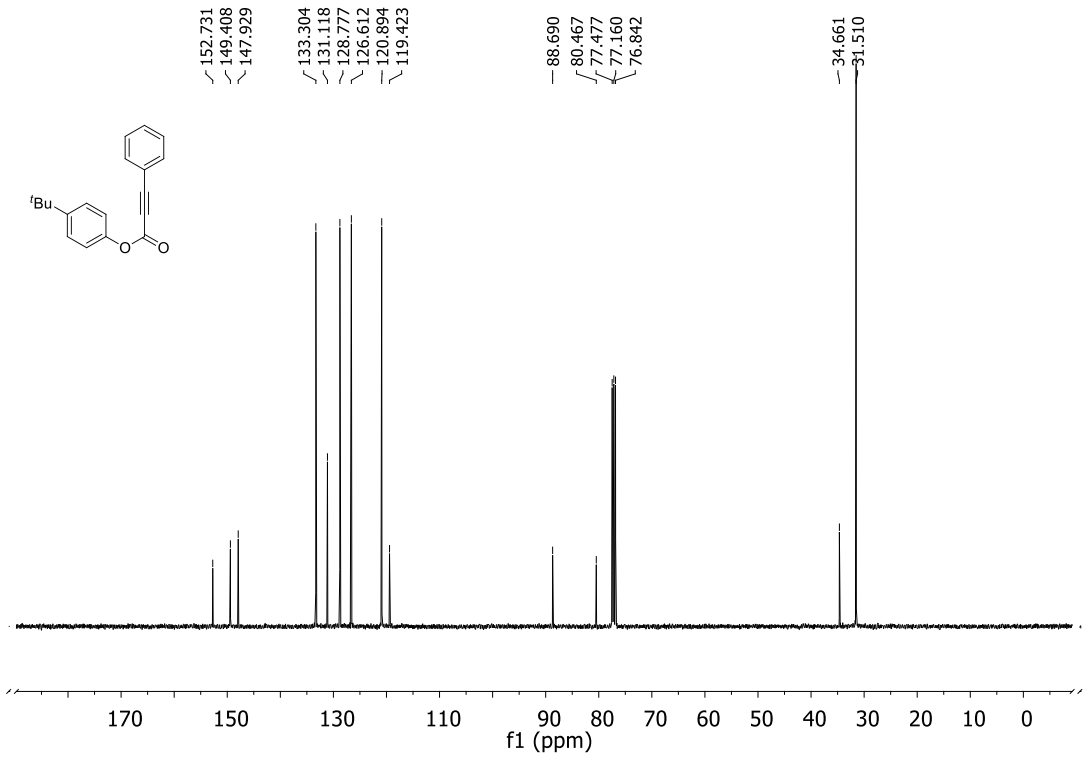

Figure 3.53. ^{13}C NMR of 4-(*tert*-butyl)phenyl 3-phenylpropiolate **(1b).**

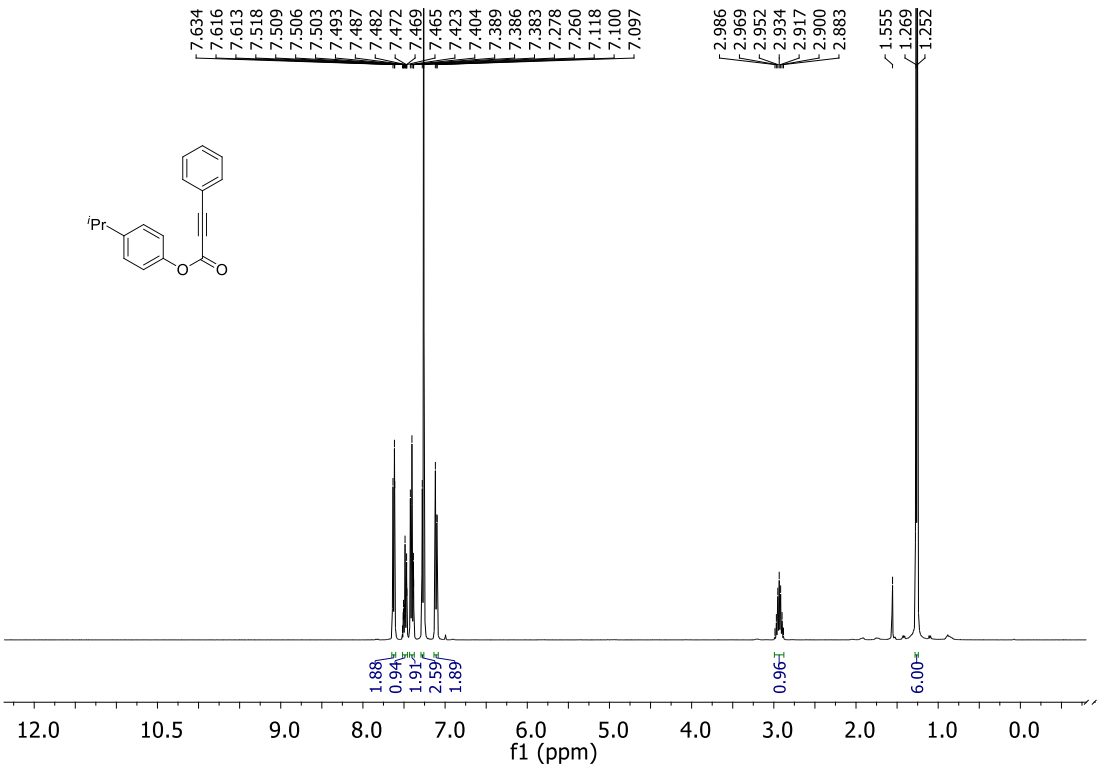

Figure 3.54. ^{1}H NMR of 4-isopropylphenyl 3-phenylpropiolate **(1c).**

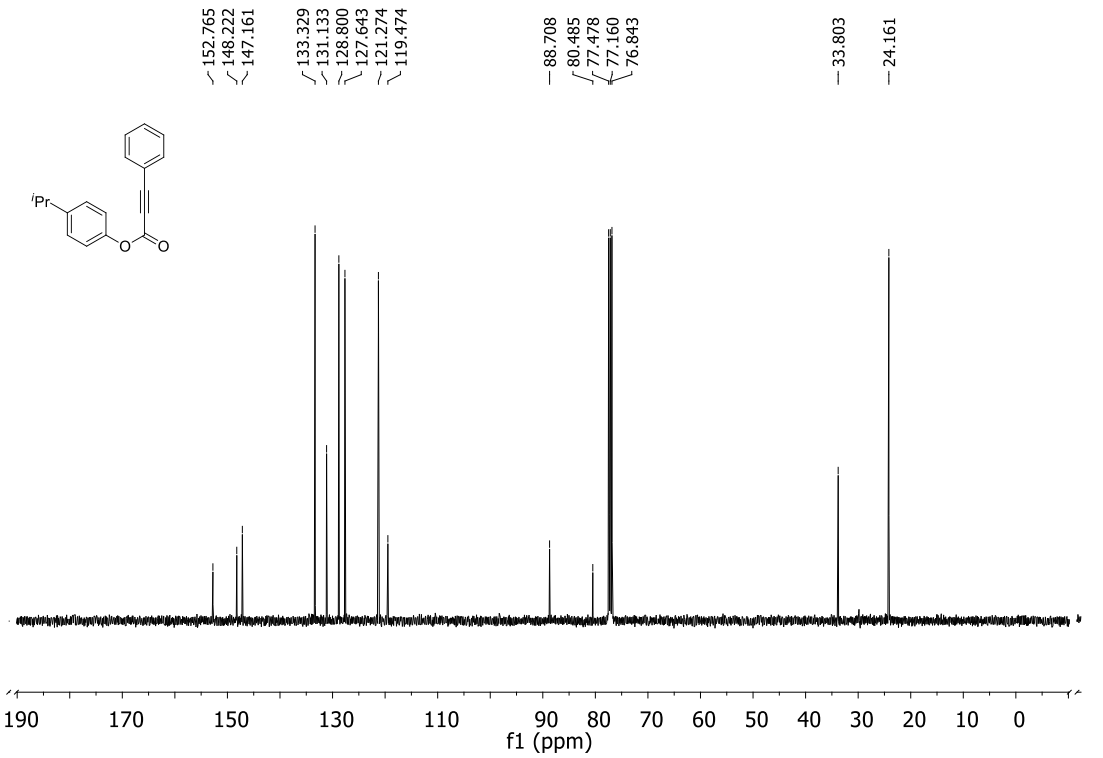

Figure 3.55. ^{13}C NMR of 4-Isopropylphenyl 3-phenylpropiolate **(1c).**

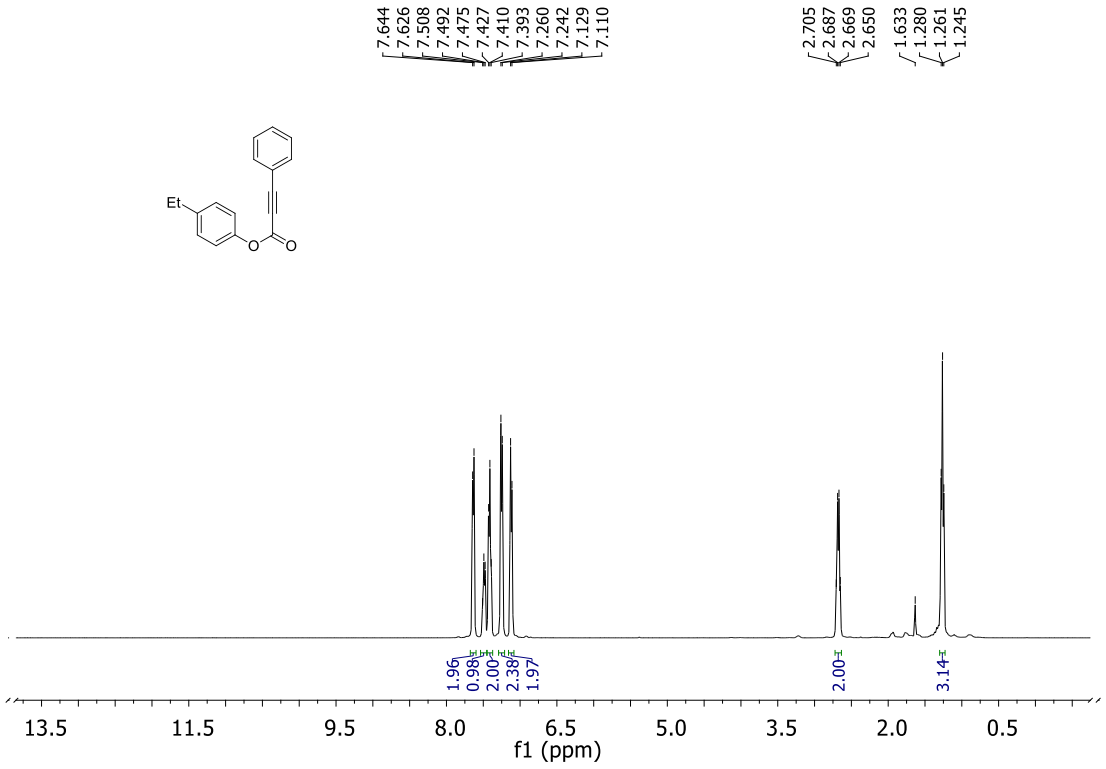

Figure 3.56. ^{1}H NMR of 4-Ethylphenyl 3-phenylpropiolate **(1d).**

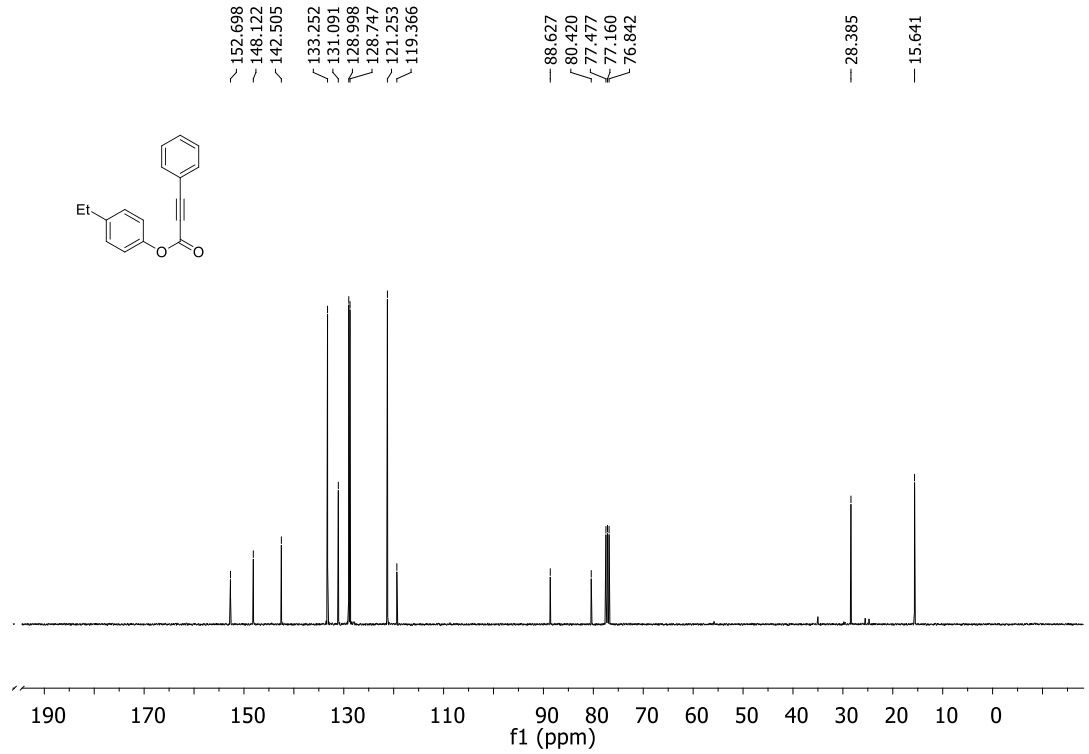

Figure 3.57. ^{13}C NMR of 4-Ethylphenyl 3-phenylpropiolate **(1d)**

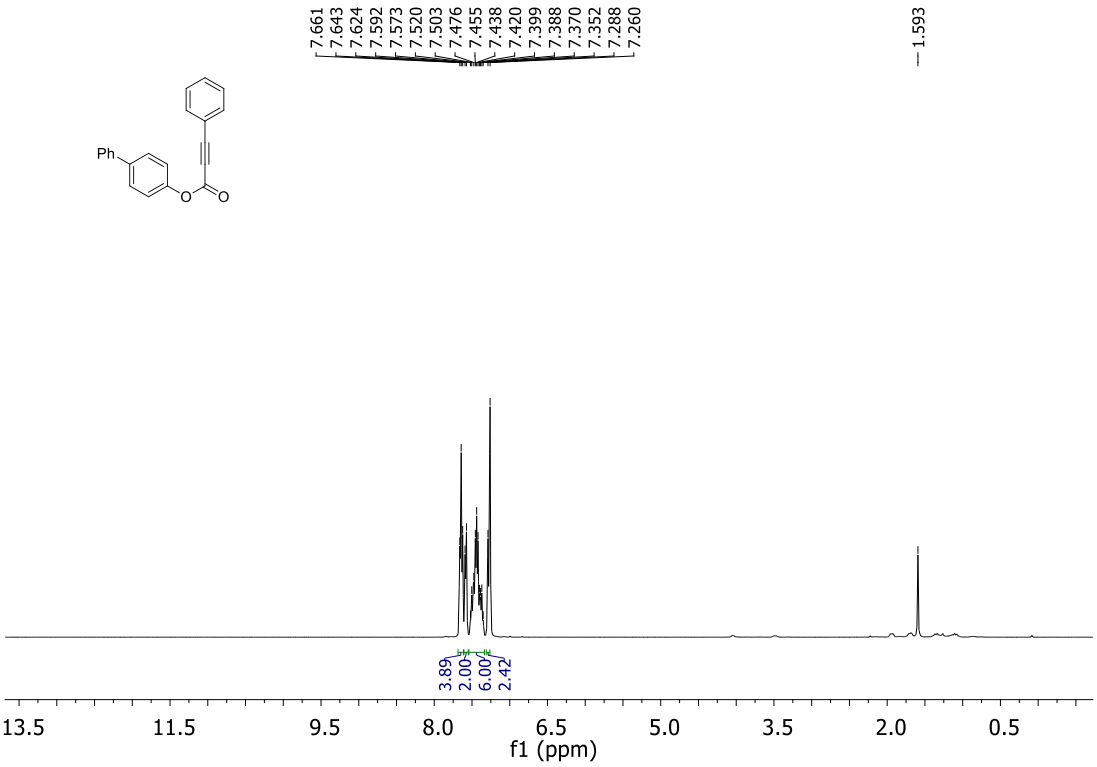

Figure 3.58. ^{1}H NMR of [1,1'-Biphenyl]-4-yl 3-phenylpropiolate **(1e).**

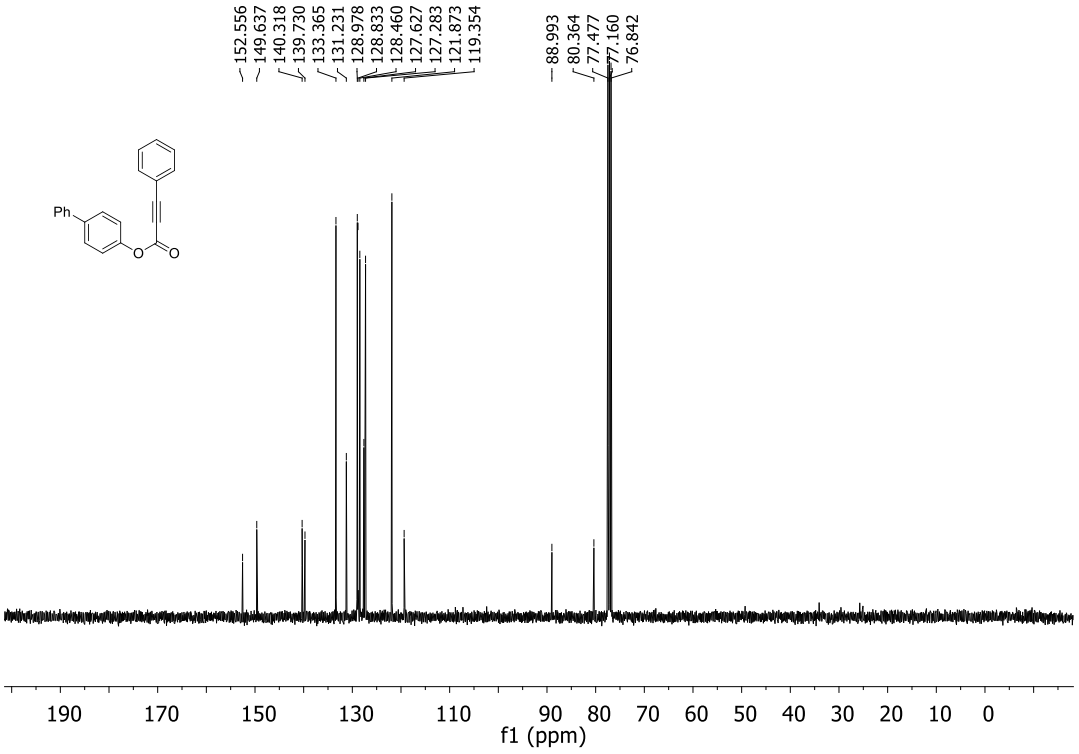

Figure 3.59. ^{13}C NMR of [1,1'-Biphenyl]-4-yl 3-phenylpropiolate **(1e).**

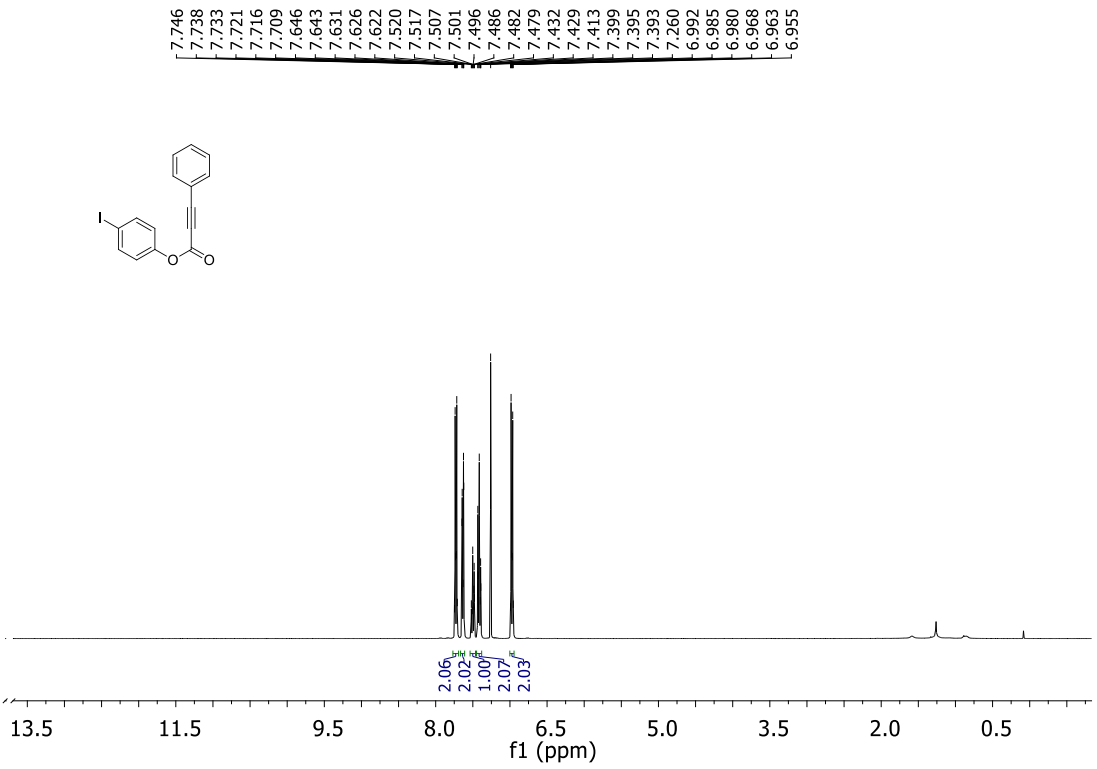

Figure 3.60. ^{1}H NMR of 4-Iodophenyl 3-phenylpropiolate **(1f).**

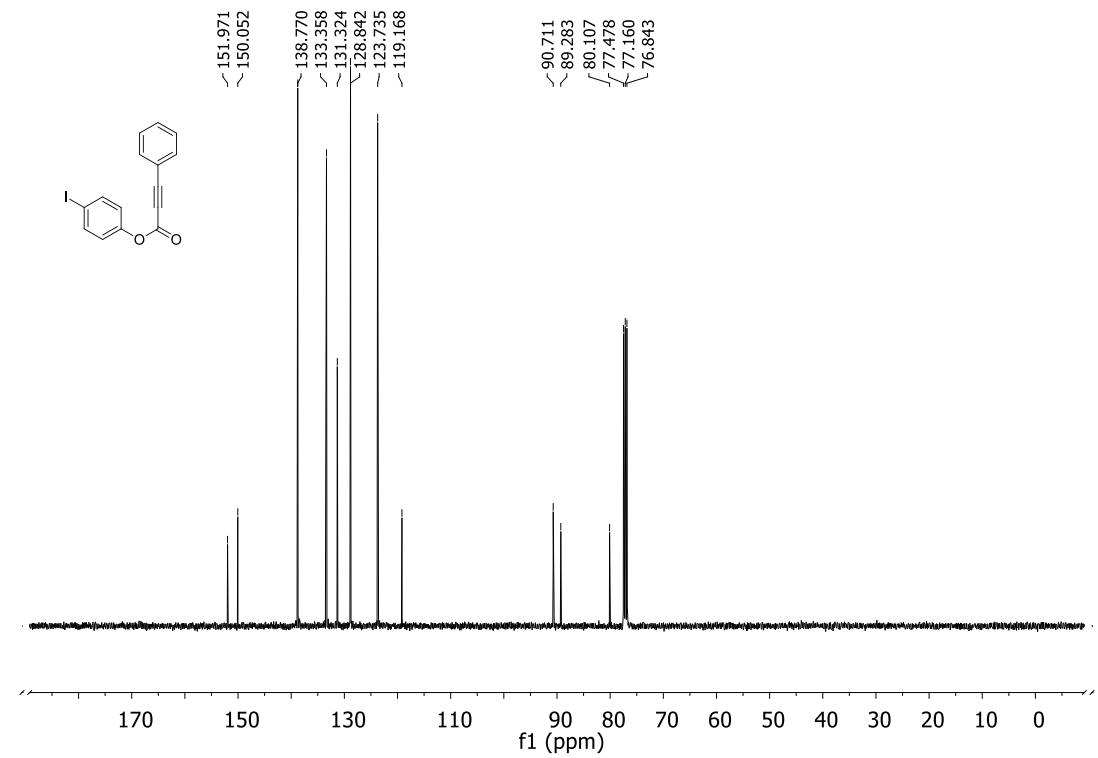

Figure 3.61. ^{13}C NMR of 4-Iodophenyl 3-phenylpropiolate **(1f).**

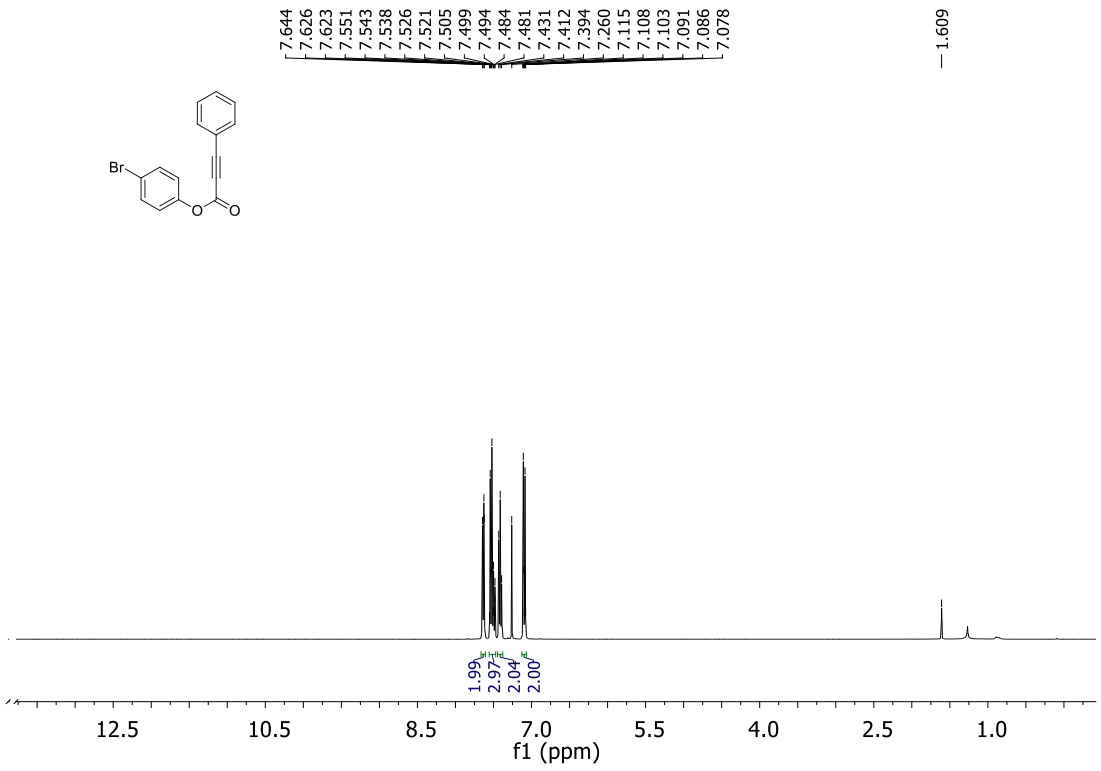

Figure 3.62. ^{1}H NMR of 4-Bromophenyl 3-phenylpropiolate **(1g).**

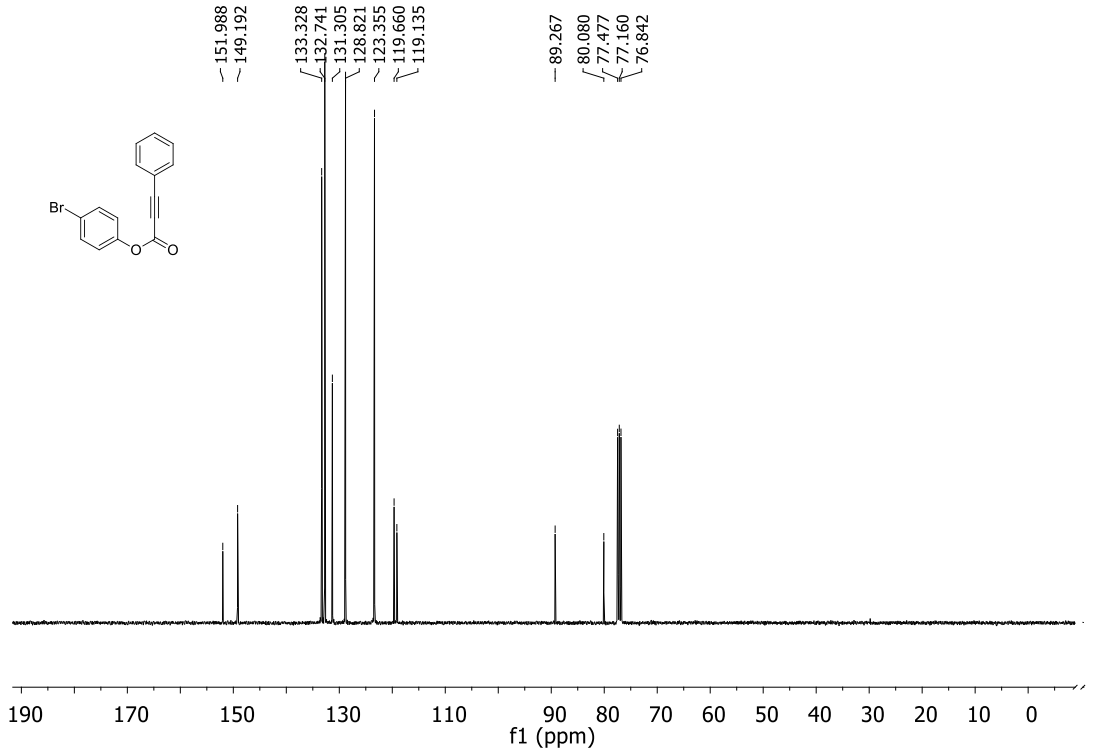

Figure 3.63. ^{13}C NMR of 4-Bromophenyl 3-phenylpropiolate **(1g).**

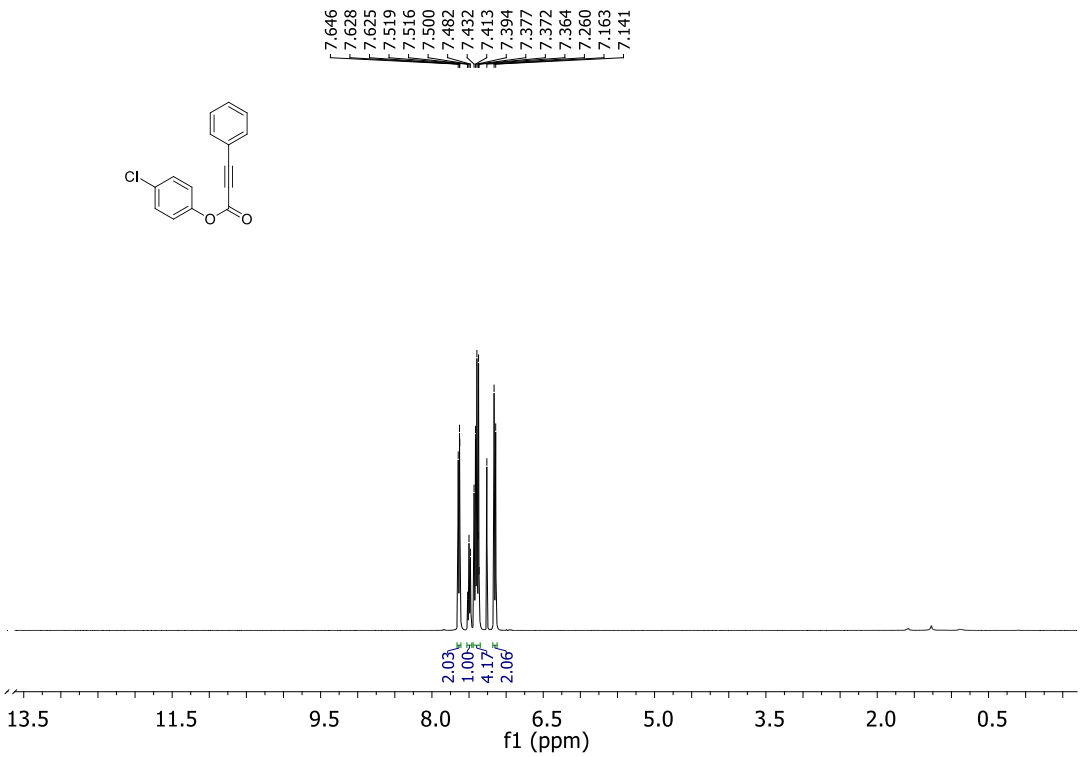

Figure 3.64. ^{1}H NMR of 4-Chlorophenyl 3-phenylpropiolate **(1h).**

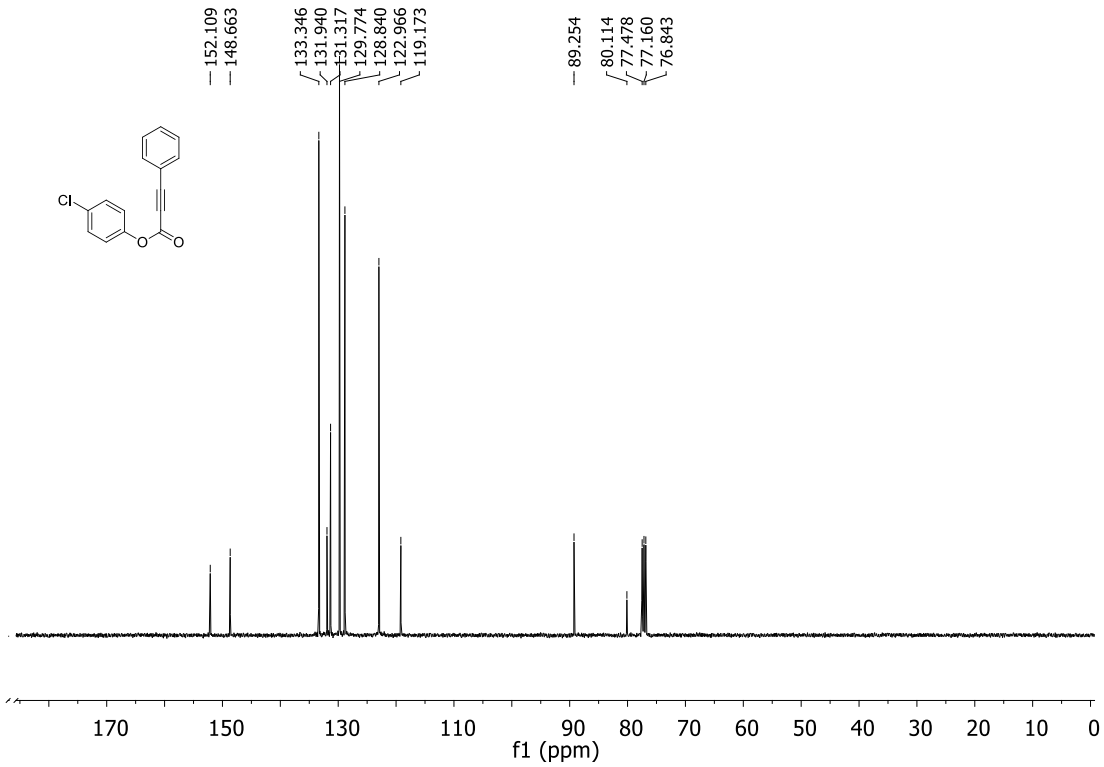

Figure 3.65. ^{13}C NMR of 4-Chlorophenyl 3-phenylpropiolate **(1h).**

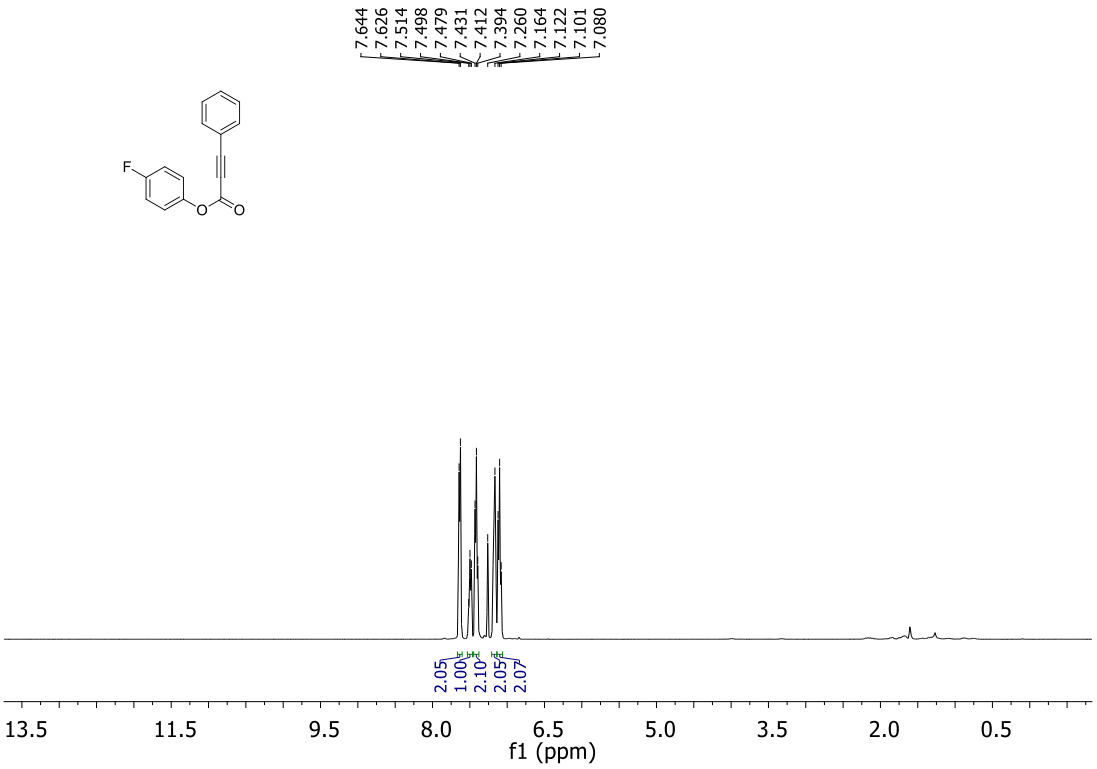

Figure 3.66. ^{1}H NMR of 4-Fluorophenyl 3-phenylpropiolate **(1i).**

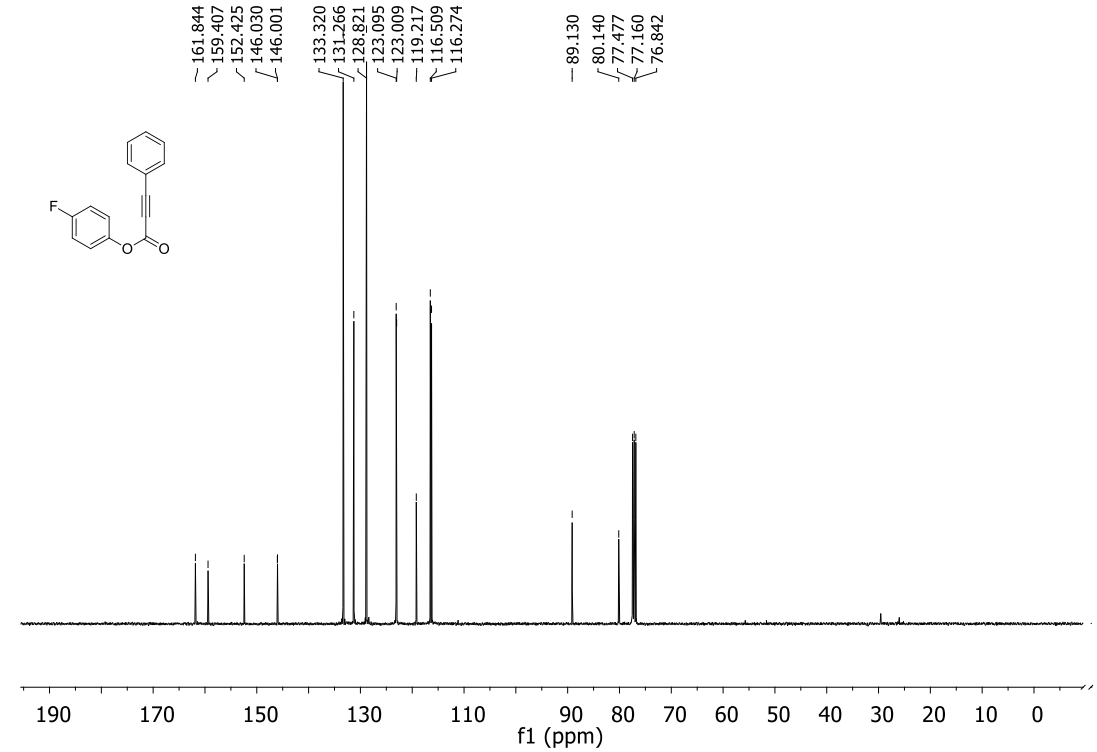

Figure 3.67. ^{13}C NMR of 4-Fluorophenyl 3-phenylpropiolate **(1i).**

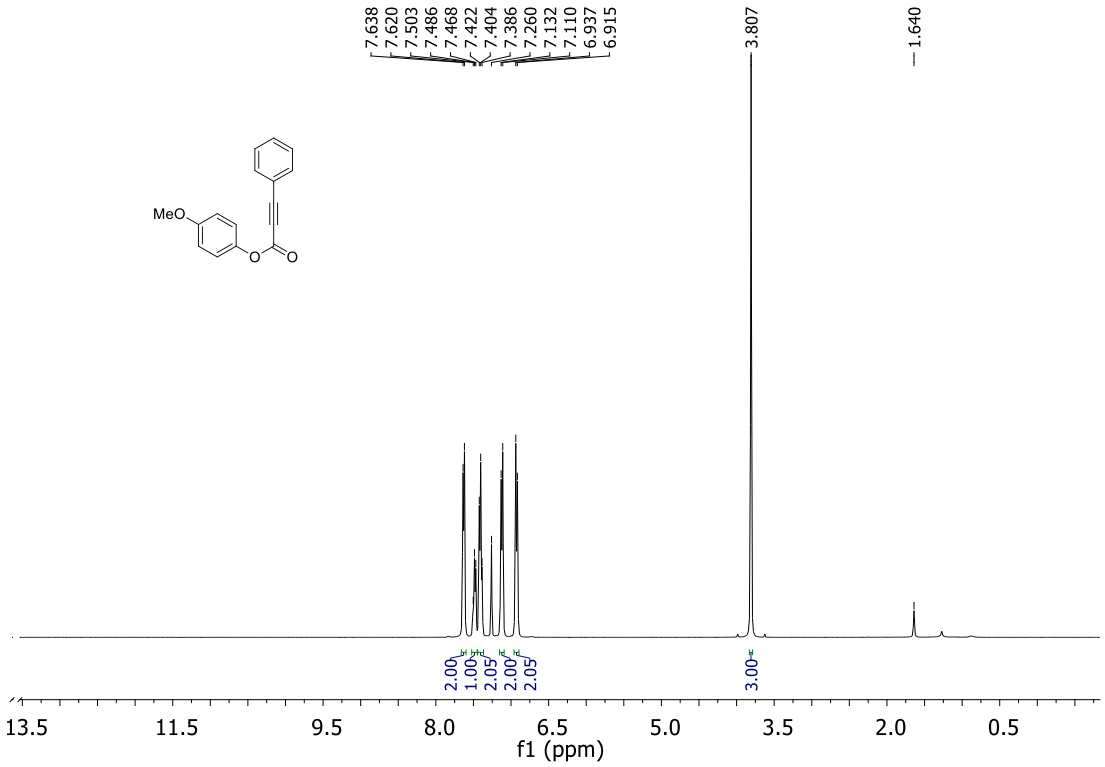

Figure 3.68. ^{1}H NMR of 4-Methoxyphenyl 3-phenylpropiolate **(1j).**

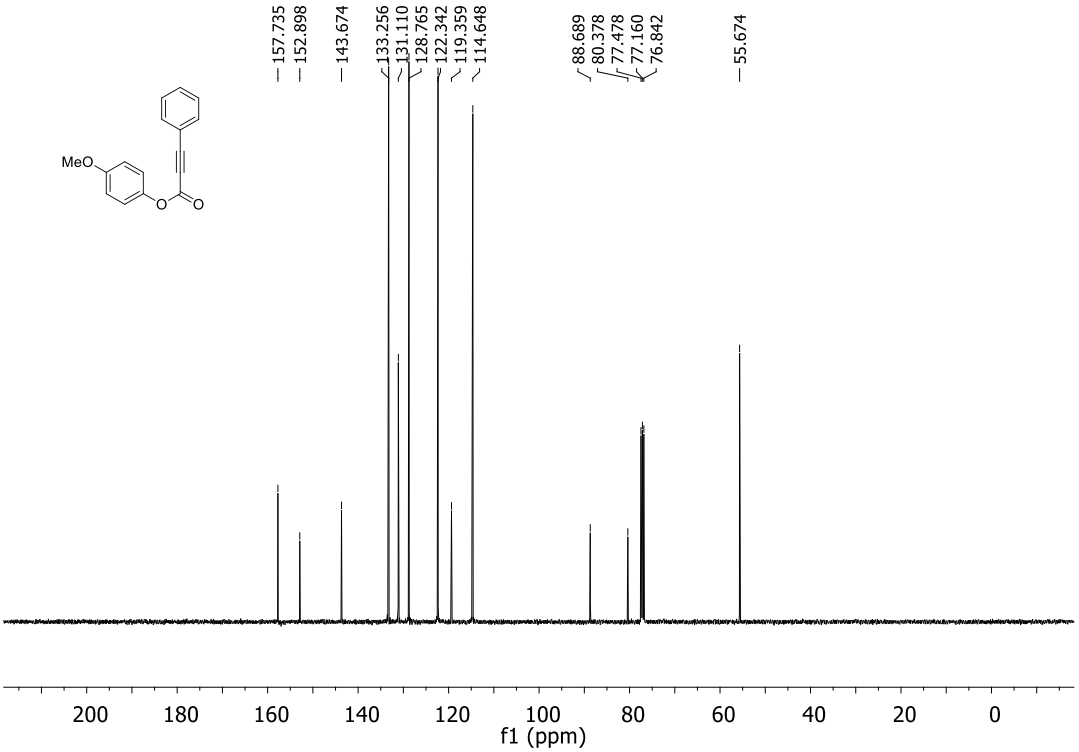

Figure 3.69. ^{13}C NMR of 4-Methoxyphenyl 3-phenylpropiolate **(1j).**

CHAPTER 4

C-H Hydroxylation of Quinoxalin-2(1*H*)-ones through *ipso*-Substitution using *tert*-Butyl Nitrite

4.1 ABSTRACT

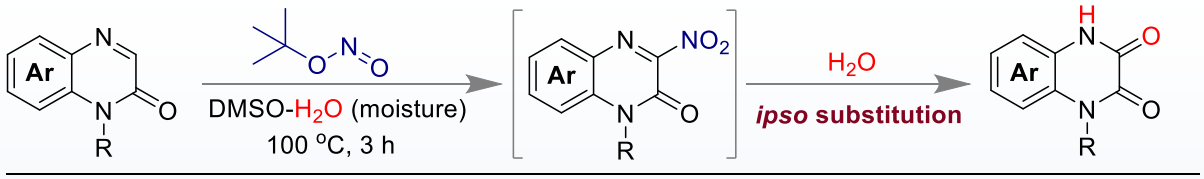

- *30 examples, up to 98 % yield*
- *one -pot synthesis*
- excellent regioselectivity
- *metal and additive free*
- *scalable synthesis*
- *operationally simple*

A convenient one-pot synthesis of quinoxaline-2,3-dione has been developed via C-H hydroxylation of quinoxalin-2(1*H*)-one using TBN (*tert*-butyl nitrite) as a reaction promoter in DMSO solvent. This protocol proceeded through radical-mediated C_3-nitration followed by hydroxylation with water (moisture) via *ipso*-substitution. Following this methodology, a library of quinoxaline-2,3-diones has been synthesized with good to excellent yields. In addition, high regioselectivity, and good functional group tolerance are the key advantages of this protocol.

4.2 INTRODUCTION

Over the last two decades, *tert* Butyl nitrite (TBN) has been admired for its versatility and multitasking nature.[1, 2] Its unique structural characteristic results in its variable behavior depending upon reaction condition and structure of reactant. For example, TBN produces NO radical under

aerobic conditions, capturing dioxygen to generate NO_2 radical. The NO_2 radical is popularly known to trigger nitration,[3-5] nitrative cyclization, and so forth.[6-10]

ipso-substitution is one of the eminent tools to introduce important functionalities into aromatics and hetero-aromatics.[11] Different protocols have been documented which adopt *ipso*-substitution strategy towards desired product formation.[12] For example, *ipso*-nitration of aryl boronic acids,[13-16], and carboxylic acids[16, 17] has been achieved by utilizing suitable nitro sources. Parallelly, *ipso*-nitrosation of trimethylsilyl benzene has been cataloged (Scheme 4.1).[18] The key advantage of the *ipso*-substitution strategy is to overcome the regioselectivity issues. Therefore, the *ipso*-substitution strategy has also become an important research topic in synthetic organic chemistry.[19]

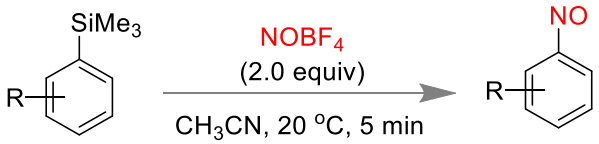

Scheme 4.1. Hilt's approach on Nitrosodesilylation through Electrophilic *ipso*-Substitution.

Direct hydroxylation of C(sp^2)-H bonds is considered as one of the reasonable strategies for synthesizing hydroxylated organic compounds.[20, 21] Hydroxylated compounds have many applications in the pharmaceutical and agrochemical industries.[22] Significant efforts have been made to develop convenient protocols for direct hydroxylation reactions using either transition metal catalysis[23-25] or metal-free reagents.[22, 26, 27] In addition, the strategies using directing groups are also popular in the literature.[28-30] In the development of sustainable methodology for hydroxylation reaction, Hajra's group demonstrated C-5 hydroxylation of 8-aminoquinoline amides using $PhI(OAc)_2$ (Scheme 4.2).[22]

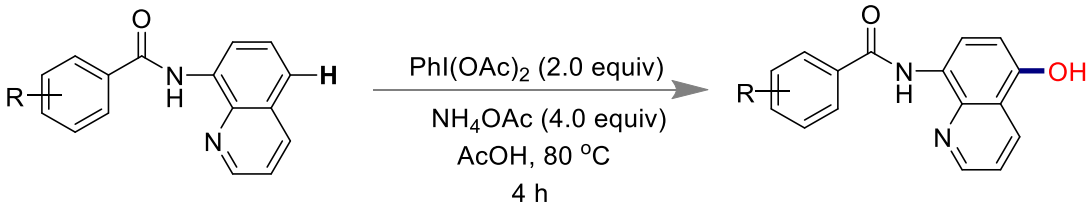

Scheme 4.2. Hajra's approach on C-5 hydroxylation of 8-aminoquinoline amide

Muthukrishnan's group disclosed a convenient approach for direct C-H hydroxylation of chromanones using $PhI(OAc)_2$ as an oxidant (Scheme 4.3).[26]

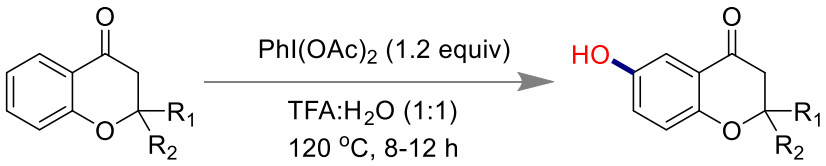

Scheme 4.3. Muthukrishnan's approach for C-H hydroxylation of chromanones

Quinoxalin-2(1*H*)-ones represent one important class of privileged heterocycles omnipresent in bioactive molecules and natural products.[31, 32] They also have pharmaceutical and therapeutic uses as antitumor agents,[33] inhibitors against Hepatitis C virus,[34] etc. In the last two decades, the direct installation of various functionalities at the C-3 position of quinoxalin-2(1*H*)-ones has become a popular research topic.[31] The reactions include C-3 acylation,[35] arylation,[36] benzylation,[37] cyanation,[38] amidation,[39] hydroxylation,[40] phosphonation,[41] alkoxylation,[42] trifluoromethylation,[43] etc.

In our work, we have developed a convenient approach towards the synthesis of quinoxaline-2,3-diones via C-3 hydroxylation of quinoxalin-2(1*H*)-ones using TBN in DMSO, and the reaction time was 3 h at 100 °C (Figure 4.1). The first step proceeded through nitration at C-3 of quinoxalin-2(1*H*)-ones and followed by *ipso*-substitution with water. Quinoxaline-2,3-diones and its

derivatives furnish many applications in material science, organic synthesis, and pharmaceutics.[44-46] They also have broad-ranging applications in fields like bacteriocides and insecticides.[47]

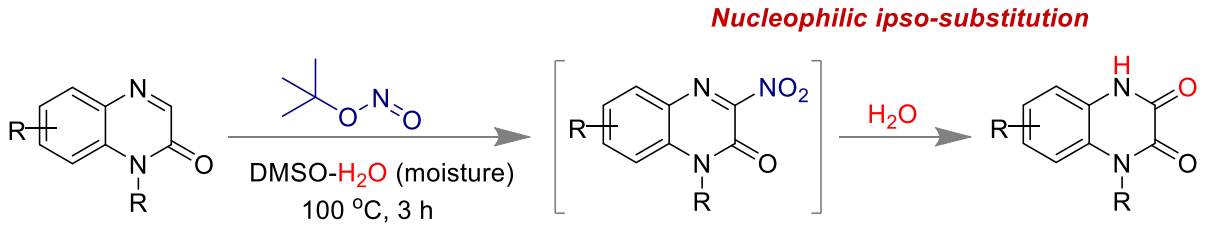

Figure 4.1. Our work on TBN mediated C-3 Hydroxylation of quinoxalin-2(1*H*)-ones via *ipso*-substitution.

4.3 RESULT AND DISCUSSION

To find the optimum reaction condition, we initiated our experiment by choosing 1-benzylquinoxalin-2(1*H*)-one as the model substrate (Table 4.1). We carried out the reaction with 3.0 equiv of TBN in DMSO at 100 ºC for 12 h, and the product 1-benzyl-1,4-dihydroquinoxaline-2,3-dione was obtained in 96% yield (entry 1). Operating the reaction at room temperature with 3.0 equiv TBN in DMSO for 18 h resulted in a 31% product yield (entry 2). When the reaction time was lowered to 3 h with the exact equivalence of TBN loading at 100 ºC in DMSO, the desired product was isolated in a 95% yield (entry 3). Next, we performed the reaction with 2.0 equiv of TBN, by keeping identical conditions, and 98% yield of the desired product was obtained after a reaction time of 3 h (entry 4). Lowering the reaction temperature to 60 ºC resulted in the formation of **2a** in a 65% yield (entry 5). The reaction yield was diminished to 74% when 1.0 equiv of TBN was used (entry 6). Next, we explored the effect of solvents on product formation. Performing the reaction in solvents like DCM, DCE, EtOH, toluene, and THF resulted in a trace amount of product formation (entry 7-11) and a 20% yield of **2a** was obtained in the case of ACN solvent (entry 12). When 1,4-dioxane and DMF were employed as solvents, the reaction yielded 62% and 51% of

desired products, respectively (entry 13-14). Furthermore, the reaction afforded **2a** in 47% yield under an argon atmosphere (entry 15). No product was detected when the reaction was performed in the absence of TBN (entry 16). The optimum condition for the reaction was achieved with 2.0 equiv of TBN at 100 ºC in DMSO at 3 h.

Table 4.1. Screening for optimum reaction conditions[a]

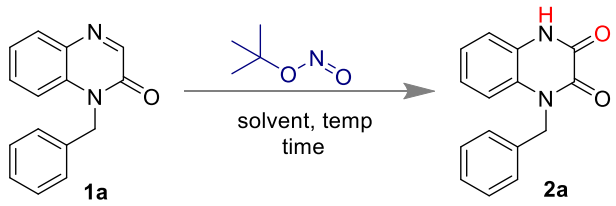

entry	TBN (equiv)	Condition	Time (h)	Yield (%)[b]
1.	3.0	DMSO, 100 ºC	12	96
2.	3.0	DMSO, rt	18	31
3.	3.0	DMSO, 100 ºC	3	95
4.	**2.0**	**DMSO, 100 ºC**	**3**	**98**
5.	2.0	DMSO, 60 ºC	3	65
6.	1.0	DMSO, 100 ºC	3	74
7.	2.0	DCM, 60 ºC	3	trace
8.	2.0	DCE, 90 ºC	3	trace
9.	2.0	EtOH, 90 ºC	3	trace
10.	2.0	Toluene, 100 ºC	3	trace
11.	2.0	THF, 80 ºC	3	trace
12.	2.0	ACN, 80 ºC	3	20
13.	2.0	1,4-dioxane, 90 ºC	3	62
14.	2.0	DMF, 100 ºC	3	51
15.	2.0	DMSO, 100 ºC	3	47[c]
16.	----	DMSO, 100 ºC	3	NR[d]

[a]Standard conditions: **1a** (0.26 mmol), TBN (2.0 equiv) in 2 mL of solvent at 100 °C for 3 h. [b]Isolated yield. [c]Ar atmosphere. [d]No reaction.

We explored the substrate scopes of this protocol using the optimized condition. First, we investigated the scope quinoxalin-2(1*H*)-ones with different substituents at *N*-1 position (Figure 4.2). Quinoxalin-2(1*H*)-ones with different electron-donating substituents -Me, -^{i}Pr, -^{t}Bu at *N*-benzyl part were subjected to standard reaction conditions. The substrates underwent smooth conversion, and the corresponding quinoxaline-2,3-diones (**2b-2d**) were obtained with 86-92% yield. Likewise, substrates with electron-withdrawing groups –CN, -Br, -I, -F, -CF_3, 3,5-difluoro, -NO_2 at *N*-benzyl part worked well under the standard condition, and the desired products (**2e-2k**) were obtained in 84-97% yield. When alkyl groups –Me, -Et, n-butyl, -phenylethyl were present at *N*-1 position of quinoxalin-2(1*H*)-ones, the corresponding substrates responded well and furnished the products (**2l-2o**) with 87-95% yields. Substrates containing phenacyl group at *N*-1 position also underwent conversion and the corresponding quinoxaline-2,3-dione (**2p**) was obtained in 70% yield. In addition, ester functionalities -COOEt, -COO^{i}Pr, -COO^{t}Bu present in substrates were also well tolerated under the optimum reaction condition and delivered the expected products (**2q-2s**) in excellent yields. Moreover, this protocol also exhibited good tolerance towards substrate bearing alkynyl substitution at *N*-1 position and led to the desired products (**2t**) in 88% yield.

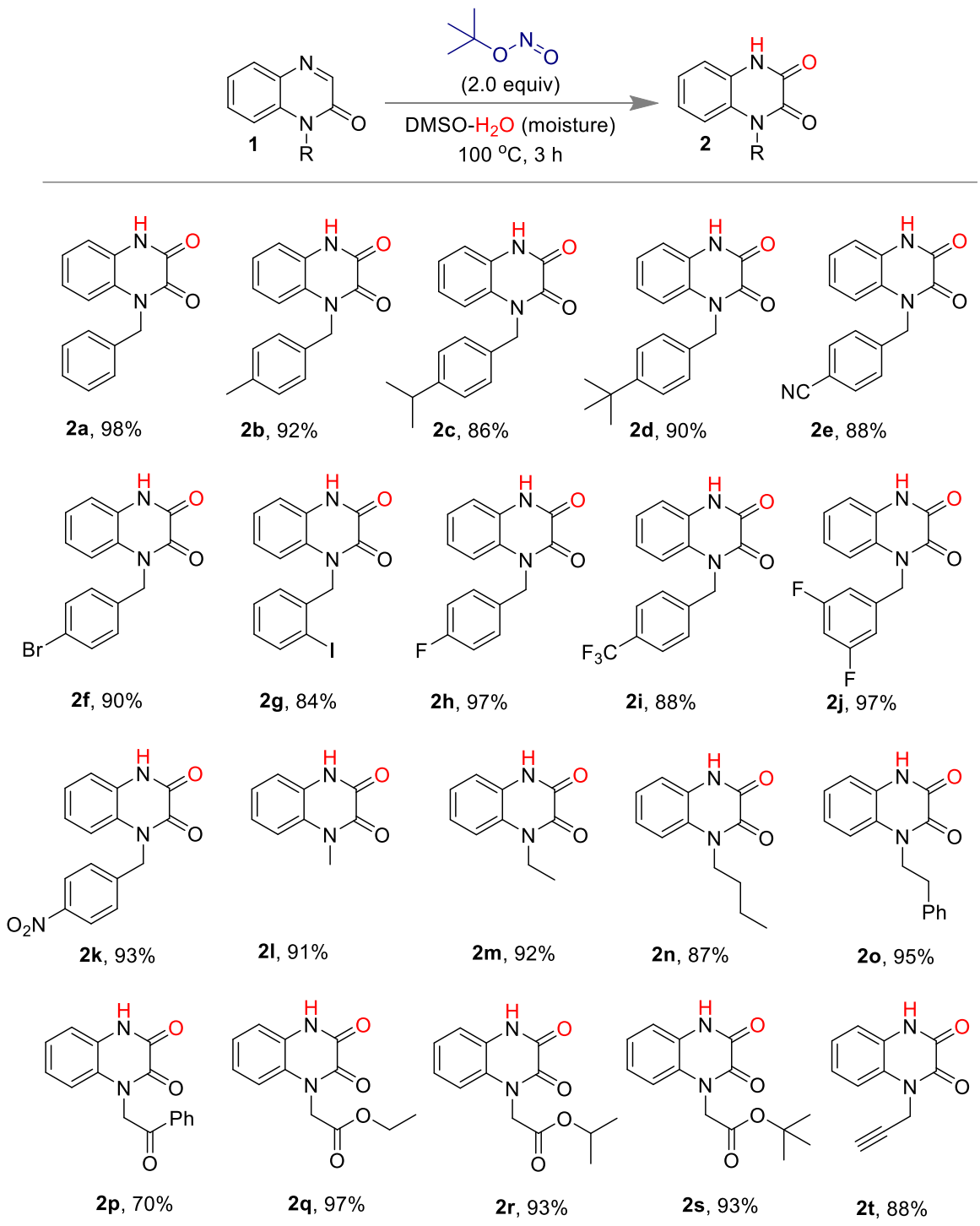

Figure 4.2. Scope of substrates with different substituents at *N*-1 position.

Next, we explored the scopes of *o*-phenylene diamine in substrates (Figure 4.3). Polyaromatic quinoxalin-2(1*H*)-ones with different substituents at *N*-1 position afforded the expected products (**4a** and **4b)** in excellent yields. It was observed that monosubstituted quinoxalin-2(1*H*)-ones with –Me and –Br substitution resulted in 5:3 mixtures of regioisomers **4c** and **4d** with 87% and 91% yields under optimized reaction conditions. Similarly, monosubstituted quinoxalin-2(1*H*)-ones with –Cl substitution provided 3:1 mixture of regioisomers **4e** with excellent yield. Disubstituted quinoxalin-2(1*H*)-ones with alkyl and halogen substituents also successfully participated in the reaction and resulted in the product formation (**4f-4j)** with 79-94% yields.

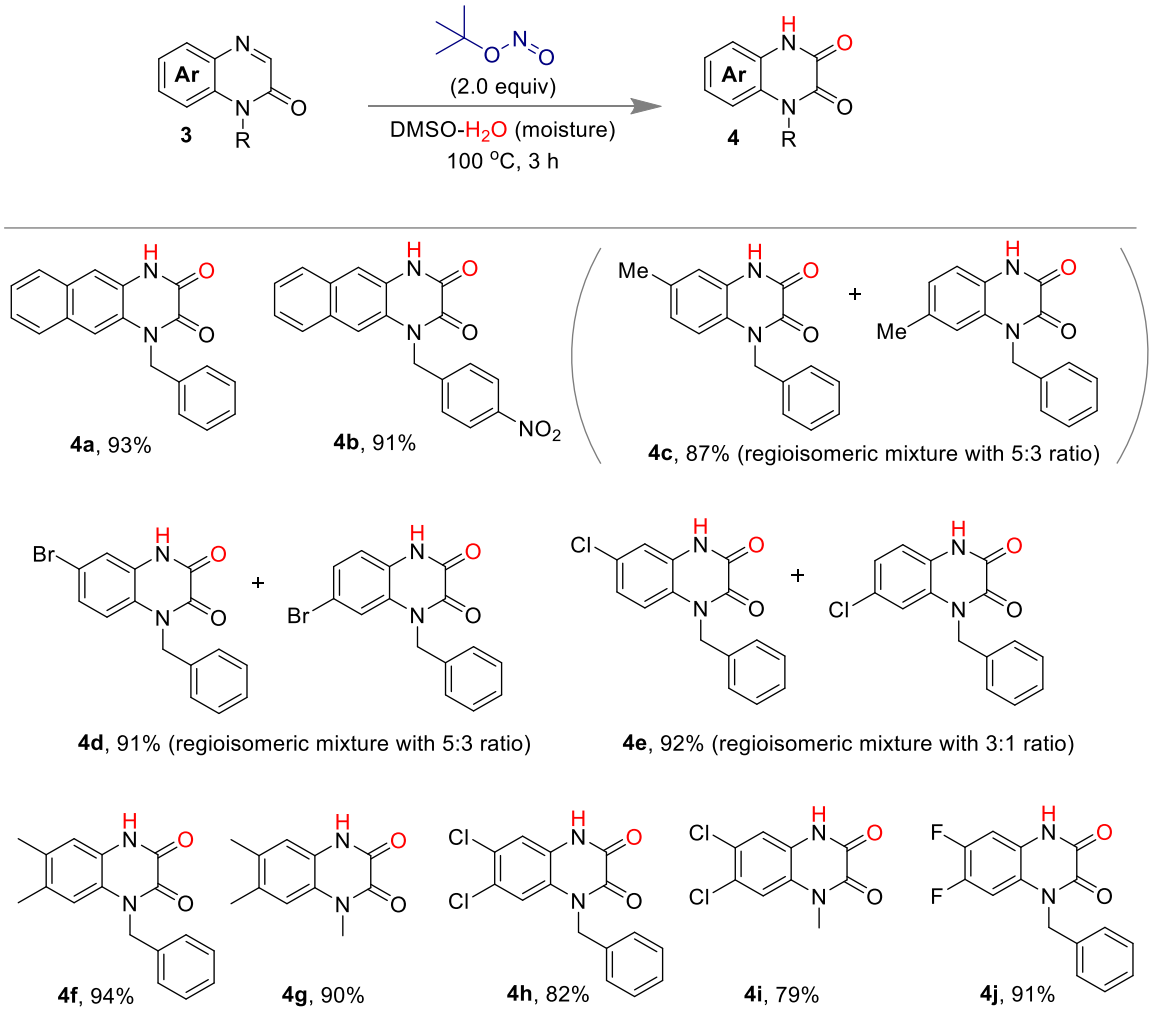

Figure 4.3. Substrates scope with different substitutions in *o*-phenylene diamine.

Control experiments helped to understand the mechanism of the reaction. The reaction was failed in the presence of radical scavengers like TEMPO (2,2,6,6- tetramethylpiperidin-1-yl-oxyl) or BHT (2,6-di-*tert*-butyl-4-methylphenol) under standard reaction condition (Figure 4.4a). This observation suggested that a radical-mediated pathway might be operative in the reaction. Next, to investigate the source of oxygen at the C-3 position of **2a**, O^{18} isotope labeling experiment was performed using H_2O^{18} (Figure 4.4b). After the reaction, O^{18} isotope-labeled product was detected through GC-MS analysis. From O^{18} isotope labeling experiment, it was evident that water (from moisture) served as the source of oxygen at C-3 position of **2a**. To confirm the involvement of NO_2 radical in the reaction pathway, we carried out a reaction with quinoxalin-2(1*H*)-one (**8**) under standard reaction conditions, and the corresponding product 1,4-dihydroquinoxaline-2,3-dione (**9**) was obtained with 75% yield (Figure 4.4c). If NO radial was involved in the reaction pathway, there was a possibility of *N*-nitroso product formation (nitrosation of secondary amine)[48] but that was not observed. So, this result, confirmed that the reaction was NO_2 radical-mediated, and involvement of NO radical in the reaction pathway was ruled out.

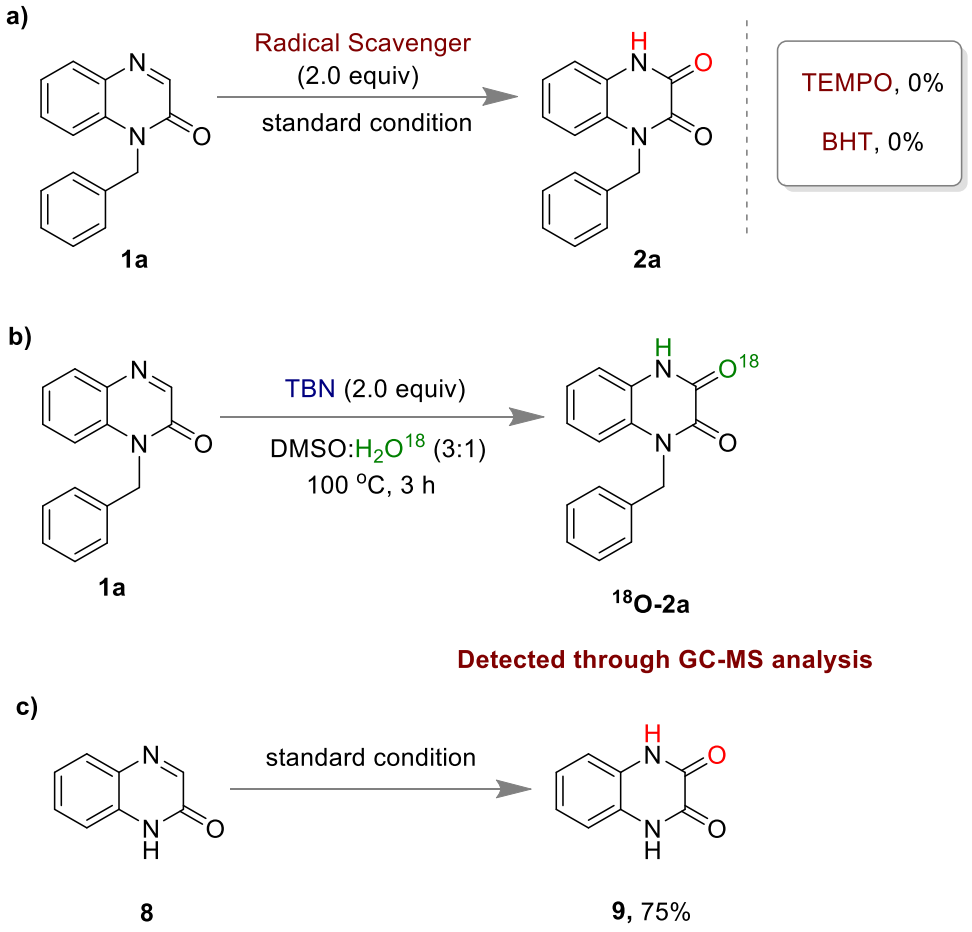

Figure 4.4. Control experiments

A plausible mechanism has been proposed based on the literature report[1] and control experiments (Figure 4.5). In the first step, $^{\bullet}NO_2$ radical was produced from TBN in the presence of aerial oxygen.[1] Subsequently, $^{\bullet}NO_2$ radical underwent addition at C-3 position of **1,** and intermediate **5** was generated. After that, $^{t}BuO^{\bullet}$ radical generated from TBN abstracted C_3-H from **5,** and provided intermediate **6** with the release of *tert*-butanol. Next, the moisture (H_2O nucleophile) of DMSO led to a nucleophilic attack at C-3 of **6**, leading to intermediate **7**. Due to the electron-withdrawing group (carbonyl) or electronegative atoms attached at C-3, the carbon

become highly electrophilic in nature. This was the key requirement for the *ipso*-substitution. Finally, **7** was converted into desired product **2** *via* tautomerization.

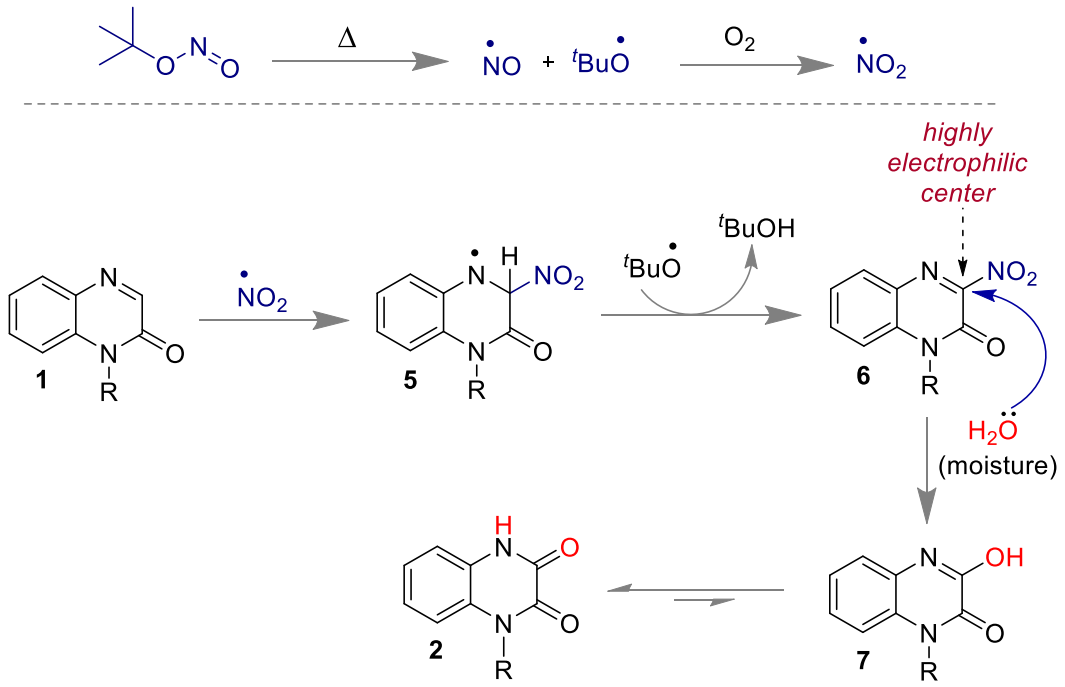

Figure 4.5. Plausible reaction mechanism

To explore the synthetic utility of the methodology, we performed a gram-scale synthesis with 4.62 mmol of **1a** (1-benzylquinoxalin-2(1*H*)-one) under standard reaction conditions, and the corresponding product **2a** (1-benzyl-1,4-dihydroquinoxaline-2,3-dione) was obtained in 91% (1.05 g) yield (Figure 4.6a). Towards post-synthetic application, Sonogashira coupling reaction of **2t** (1-(prop-2-yn-1-yl)-1,4-dihydroquinoxaline-2,3-dione) with 4-iodo toluene was carried out, and the desired product 1-(3-(*p*-tolyl)prop-2-yn-1-yl)-1,4-dihydroquinoxaline-2,3-dione (**10**) was isolated in 85% yield (Figure 4.6b).

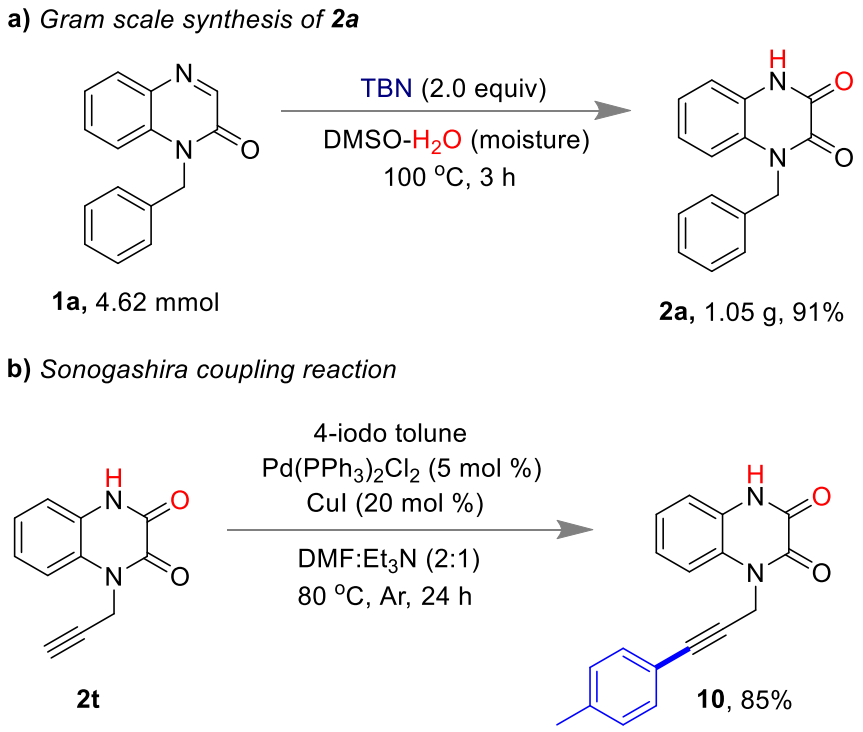

Figure 4.6. Synthetic applications.

4.4 CONCLUSION

In conclusion, we have developed a sustainable approach towards synthesizing quinoxaline-2,3-diones by NO_2 radical triggered C-3 hydroxylation of quinoxalin-2(1*H*)-ones. The reaction proceeded via *ipso*-substitution, where TBN was the promoter of the reaction. The protocol followed mild reaction conditions and the use of any additives or any strong oxidants could be avoided. We anticipate that this operationally simple and highly efficient methodology can be helpful in organic synthesis for the development of *ipso*-substitution reactions.

4.5 EXPERIMENTAL SECTION

Instrumentation and Chemicals: Column chromatography was used for the purification of the compounds using silica gel (with mesh 100-200 or mesh 230-400) and hexane-ethyl acetate mixtures were used as eluent unless otherwise specified. Solvents were purchased from commercially available sources and used in the reaction without further purification. All NMR spectra were recorded in 400 MHz or 700 MHz instruments (Bruker) at room temperature (25 °C). The splitting of the NMR peaks (peak pattern) are represented by s: singlet; d: doublet; t: triplet; q: quartet; m: multiplet; dd: doublet of doublets; td: triplet of doublets; br s: broad singlet. Chemical shift values are reported in parts per million (ppm) with respect to residual trichloromethane (7.26 ppm for ^{1}H and 77.16 ppm for ^{13}C) and dimethyl sulfoxide (2.50 ppm for ^{1}H and 39.52 ppm for ^{13}C). The coupling constant values (*J*) are reported in hertz (Hz). A digital melting point apparatus was used to obtain the melting point of the compounds which were included in the characterization data without any correction. FT-IR spectra were recorded by making a thin film of the compounds on KBr pellets using dichloromethane and IR spectral data are reported in wave number (cm^{-1}). High-resolution mass spectra (HR-MS) were recorded on an ESI-TOF (time of flight) mass spectrometer. The detailed procedure for the preparation of the starting materials and target molecule are described below.

Procedure for the synthesis of 1-benzyl-1,4-dihydroquinoxaline-2,3-dione (2a). To an oven-dried sealed tube charged with a magnetic stirring bar and 1-benzylquinoxalin-2(1*H*)-one (62 mg, 0.264 mmol, 1.0 equiv), TBN (63 µL, 0.530 mmol, 2.0 equiv) in 2 mL DMSO solvent was stirred at 100 ºC for 3 h. After that, the reaction mixture was cooled at room temperature and washed with water. The organic layer was extracted with dichloromethane, dried over Na_2SO_4, and concentrated

under reduced pressure. The resulting mixture was purified using hexane/ethyl acetate mixture as an eluent by silica gel column chromatography.

Gram scale synthesis. To an oven-dried sealed tube charged with a magnetic stirring bar and 1-benzylquinoxalin-2(1*H*)-one (1092 mg, 4.62 mmol, 1.0 equiv), TBN (1102 µL, 9.24 mmol, 2.0 equiv) in 15 mL DMSO solvent was stirred at 100 ºC for 3 h. After that, the reaction mixture was cooled at room temperature and washed with water. The organic layer was extracted with dichloromethane and was dried over Na_2SO_4, and concentrated under reduced pressure. The resulting mixture was purified by silica gel column chromatography using hexane/ethyl acetate mixture as an eluent to obtain 1-benzyl-1,4-dihydroquinoxaline-2,3-dione (**2a**) as a yellow solid in 91% yield.

Procedure for the radical scavenger experiment with 2,2,6,6-Tetramethylpiperidin-1-yl)oxyl radical (TEMPO). To an oven-dried sealed tube charged with a magnetic stirring bar, 1-benzylquinoxalin-2(1*H*)-one (64 mg, 0.270 mmol, 1.0 equiv), TEMPO (84 mg, 0.540 mmol, 2.0 equiv) were dissolved in 2 mL DMSO. To it, TBN (65 µL, 0.540 mmol, 2.0 equiv) was added. The mixture was stirred in a preheated oil bath of 100 ºC for 3 h. After 3 h reaction formation of product **2a** was not observed.

Synthesis of 1-(3-(p-tolyl)prop-2-yn-1-yl)-1,4-dihydroquinoxaline-2,3-dione (10): To an oven-dried sealed tube charged with a magnetic stirring bar and 4-iodo toluene (40 mg, 0.180 mmol, 1.0 equiv), $PdCl_2(PPh_3)_2$ (6 mg, 0.009 mmol, 5 mol %), and CuI (7 mg, 0.036 mmol, 20 mol %) in 2 mL of anhydrous DMF and 1 mL of Et_3N mixture was added 1-(prop-2-yn-1-yl)-1,4-dihydroquinoxaline-2,3-dione **2t** (54 mg, 0.270 mmol, 1.5 equiv) and it was stirred at 80 ºC for 24

h under argon atmosphere.[49] After completion, the reaction mixture was cooled to room temperature and washed with brine solution. The organic layer was extracted with ethyl acetate, dried over Na_2SO_4, and concentrated under reduced pressure. Column purification provided the desired product 1-(3-(p-tolyl)prop-2-yn-1-yl)-1,4-dihydroquinoxaline-2,3-dione (**10**) in 85% yield.

H_2O^{18} labeling experiment for detection of oxygen source at C-3 position of the product. To an oven-dried sealed tube charged with a magnetic stirring bar was added sequentially 1-benzylquinoxalin-2(1*H*)-one (41 mg, 0.174 mmol, 1.0 equiv), DMSO (1.5 mL), TBN (42 µL, 0.347 mmol, 2.0 equiv) and H_2O^{18} (0.5 mL). The mixture was stirred in a preheated oil bath of 100 ^oC for 3 h. After that**,** the reaction mixture was cooled at room temperature and washed with water. The organic layer was extracted with dichloromethane and was dried over Na_2SO_4, and concentrated under reduced pressure. To identify O^{18} labeled product GC-MS experiment was performed.

Representative Procedure for quinoxalin-2(1H)-one synthesis.[50] To an oven dried sealed tube charged with a magnetic stirring bar, 1,2-phenylenediamines (5.5 mmol, 1.0 equiv) was taken in 20 mL of EtOH. It was stirred at room temperature for 5 mins. Next ethyl glyoxylate (6.6 mmol, 1.2 equiv) was added to it and the mixture was allowed to stir at 80 ^oC for 1 h then overnight at room temperature. After the completion of the reaction, the reaction mixture was filtered and washed with EtOH and then the residue on the filter paper was dried and directly used for the next step. For alkylation, in a round bottom flask, quinoxalin-2(1*H*)-one (4.1 mmol, 1.0 equiv) and DMF (20 mL) were taken and allowed to stir at room temperature. Next, to that suspension K_2CO_3

(4.9 mmol, 1.2 equiv) was added and stirred at room temperature for 5 min. After that halogenalkane (6.6 mmol, 1.6 equiv) was added to the suspension and allowed to stir at room temperature until the raw material disappeared. After completion of the reaction, saturated ammonium chloride solution (7 mL) was added to the reaction mixture and the organic layer was extracted with ethyl acetate and dried over Na_2SO_4 and concentrated under reduced pressure. Next, column purification provided our desired N-alkylated quinoxalin-2(1*H*)-one.

Crystallographic Investigation

The crystals data were collected with Bruker SMART D8 goniometer equipped with an APEX CCD detector and with an INCOATEC micro source (Mo-Kα radiation, λ = 0.71073 Å). SAINT+[51] and SADABS[52] were used to integrate the intensities and to correct the absorption respectively The structure was resolved by direct methods and refined on F^2 with SHELXL-97.[53]

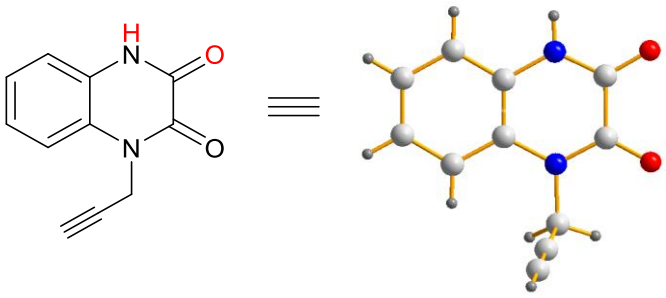

Fig. 4.7. Crystal structure of **2t**.

Crystallographic data for 2t.

CCDC number	2130674
Empirical formula	$C_{11}H_8N_2O_2$
Formula weight	200.19

Temperature/K	100.01(10)
Crystal system	triclinic
Space group	P-1
a/Å	4.4858(3)
b/Å	7.2509(6)
c/Å	14.2632(11)
α/°	103.003(7)
β/°	94.661(6)
γ/°	99.758(6)
Volume/Å^3	442.03(6)
Z	2
ρ_{calc}g/cm^3	1.504
μ/mm^{-1}	0.107
F(000)	208.0
Crystal size/mm^3	0.2 × 0.2 × 0.18
Radiation	MoKα (λ = 0.71073)
2Θ range for data collection/°	7.192 to 61.044
Index ranges	-5 ≤ h ≤ 5, -10 ≤ k ≤ 9, -18 ≤ l ≤ 20
Reflections collected	8153
Independent reflections	2161 [R_{int} = 0.0604, R_{sigma} = 0.0503]
Data/restraints/parameters	2161/0/136
Goodness-of-fit on F^2	1.023

Final R indexes [I>=2σ (I)] $R_1 = 0.0562$, $wR_2 = 0.1528$

Final R indexes [all data] $R_1 = 0.0732$, $wR_2 = 0.1660$

Largest diff. peak/hole / e Å-3 0.43/-0.30

Characterization Data.

1-Benzyl-1,4-dihydroquinoxaline-2,3-dione (2a).[40] R_f = 0.3 (50% ethyl acetate/hexane); yellow solid; yield 65 mg (98%); mp 296-298 ºC; ^{1}H NMR (700 MHz, DMSO-d_6) δ 12.11 (s, 1H), 7.31 (q, *J* = 7.0 Hz, 4H), 7.25 (t, *J* = 7.0 Hz, 1H), 7.21-7.17 (m, 2H), 7.13 (t, *J* = 7.7 Hz, 1H), 7.06 (t, *J* = 7.7 Hz, 1H), 5.38 (s, 2H); ^{13}C{1H} NMR (175 MHz, DMSO-d_6) δ 155.7, 153.7, 135.8, 128.7, 127.2, 126.7, 126.3, 125.9, 123.7, 123.1, 115.7, 115.5, 45.6; IR (KBr) ῡ 1673, 1599, 1439, 710 cm^{-1}.

1-(4-Methylbenzyl)-1,4-dihydroquinoxaline-2,3-dione (2b).[40] R_f = 0.3 (50% ethyl acetate/hexane); yellow solid; yield 70 mg (92%); mp > 300 ºC; ^{1}H NMR (400 MHz, DMSO-d_6) δ 12.10 (s, 1H), 7.18 (t, *J* = 7.8 Hz, 4H), 7.12 (t, *J* = 7.0 Hz, 3H), 7.06 (t, *J* = 7.8 Hz, 1H), 5.33 (s, 2H), 2.25 (s, 3H); ^{13}C{1H} NMR (100 MHz, DMSO-d_6) δ 155.5, 153.5, 136.2, 132.5, 129.0, 126.5, 126.0, 125.7, 123.4, 122.9, 115.5, 115.3, 45.1, 20.4; IR (KBr) ῡ 1667, 1601, 1438, 711 cm^{-1}.

1-(4-Isopropylbenzyl)-1,4-dihydroquinoxaline-2,3-dione (2c). R_f = 0.2 (50% ethyl acetate/hexane); yellow solid; yield 62 mg (86%); mp 268-270 ºC; ^{1}H NMR (400 MHz, DMSO-d_6) δ 12.12 (s, 1H), 7.21 – 7.01 (m, 8H), 5.33 (s, 2H), 2.92 – 2.73 (m, 1H), 1.15 (d, *J* = 6.0 Hz, 6H); ^{13}C{1H} NMR (100 MHz, DMSO-d_6) δ 155.7, 153.7, 147.4, 133.1, 126.8, 126.5, 126.3,

125.9, 123.6, 123.1, 115.7, 115.5, 45.3, 33.1, 23.8; IR (KBr) ῡ 1668, 1600, 1440, 711 cm^{-1}; HRMS (ESI-TOF) calcd for $C_{18}H_{19}N_2O_2$ $[M+H]^+$ 295.1441, found 295.1458.

1-(4-(*tert*-Butyl)benzyl)-1,4-dihydroquinoxaline-2,3-dione (2d). R_f = 0.2 (50% ethyl acetate/hexane; yellow solid; yield 66 mg (90%); mp > 300 ºC; ^1H NMR (400 MHz, DMSO-d_6) δ 12.12 (s, 1H), 7.34 -7.08 (m, 8H), 5.34 (s, 2H), 1.23 (s, 9H); $^{13}C\{1H\}$ NMR (175 MHz, DMSO-d_6) δ 155.7, 153.7, 149.7, 132.8, 126.5, 126.4, 125.9, 125.4, 123.7, 123.2, 115.7, 115.5, 45.3, 34.2, 31.1; IR (KBr) ῡ 1671, 1599, 1383, 712 cm^{-1}; HRMS (ESI-TOF) calcd for $C_{19}H_{21}N_2O_2$ $[M+H]^+$ 309.1598, found 309.1605.

4-((2,3-Dioxo-3,4-dihydroquinoxalin-1(2H)-yl)methyl)benzonitrile (2e). R_f = 0.2 (50% ethyl acetate/hexane); light yellow solid; yield 65 mg (88%); mp > 300 ºC; ^1H NMR (400 MHz, DMSO-d_6) δ 12.10 (s, 1H), 7.79 (d, J = 8.0 Hz, 2H), 7.52 (d, J = 8.0 Hz, 2H), 7.22 – 7.03 (m, 4H), 5.45 (s, 2H); $^{13}C\{1H\}$ NMR (175 MHz, DMSO-d_6) δ 156.5, 154.5, 142.1, 133.3, 128.2, 126.6, 126.3, 124.8, 124.3, 119.4, 116.7, 115.9, 110.7, 46.3; IR (KBr) ῡ 2227, 1692, 1677, 1393, 711 cm^{-1}; HRMS (ESI-TOF) calcd for $C_{16}H_{12}N_3O_2$ $[M+H]^+$ 278.0924, found 278.0944.

1-(4-Bromobenzyl)-1,4-dihydroquinoxaline-2,3-dione (2f). R_f = 0.2 (50% ethyl acetate/hexane); light yellow solid; yield 76 mg (90%); mp 282-284 ºC; ^1H NMR (175 MHz, DMSO-d_6) δ 12.10 (s, 1H), 7.51 (d, J = 8.4 Hz, 2H), 7.29 (d, J = 8.4 Hz, 2H), 7.20 (d, J = 7.7 Hz, 1H), 7.15-7.13 (m, 2H), 7.06 (t, J = 7.7 Hz, 1H), 5.34 (s, 2H); $^{13}C\{1H\}$ NMR (175 MHz, DMSO-d_6) δ 155.8, 153.7, 135.3, 131.5, 129.1, 126.2, 126.0, 123.7, 123.1, 120.3, 115.7, 115.3, 45.1; IR

(KBr) ῡ 1696, 1655, 1395, 708 cm^{-1}; HRMS (ESI-TOF) calcd for $C_{15}H_{12}BrN_2O_2$ $[M+H]^+$ 333.0056, found 333.0041.

1-(2-Iodobenzyl)-1,4-dihydroquinoxaline-2,3-dione (2g). R_f = 0.3 (50% ethyl acetate/hexane); light yellow solid; yield 59 mg (84%); mp > 300 ºC; ^{1}H NMR (400 MHz, DMSO-d_6) δ 12.14 (s, 1H), 7.95 (d, *J* = 7.6 Hz, 1H), 7.24 (d, *J* = 8.0 Hz, 2H), 7.15 (t, *J* = 7.6 Hz, 1H), 7.08 – 7.05 (m, 2H), 6.93 (d, *J* = 7.6 Hz, 1H), 6.81 (d, *J* = 8.0 Hz, 1H), 5.17 (s, 2H); ^{13}C{1H} NMR (100 MHz, DMSO-d_6) δ 155.7, 153.7, 139.3, 136.5, 129.4, 128.7, 126.6, 126.3, 126.1, 123.8, 123.3, 115.9, 115.1, 97.9 51.8; IR (KBr) ῡ 1690, 1659, 1384, 711 cm^{-1}; HRMS (ESI-TOF) calcd for $C_{15}H_{11}IN_2NaO_2$ $[M+Na]^+$ 400.9757, found 400.9778.

1-(4-Fluorobenzyl)-1,4-dihydroquinoxaline-2,3-dione (2h).[40] R_f = 0.2 (50% ethyl acetate/hexane); pale yellow solid; yield 68 mg (97%); mp > 300 ºC; ^{1}H NMR (400 MHz, DMSO-d_6) δ 12.10 (s, 1H), 7.39 – 7.36 (m, 2H), 7.21 – 7.14 (m, 5H), 7.09 – 7.07 (m, 1H), 5.36 (s, 2H); ^{13}C{1H} NMR (100 MHz, DMSO-d_6) δ 161.35 (d, $^1J_{C\text{-}F}$ = 241.5 Hz), 155.8, 153.7, 132.0 (d, $^4J_{C\text{-}F}$ = 2.8 Hz), 128.9 (d, $^3J_{C\text{-}F}$ = 8.1 Hz), 126.2, 126.0, 123.7, 123.1, 115.7, 115.4, 115.4 (d, $^2J_{C\text{-}F}$ = 21.2 Hz), 44.9; IR (KBr) ῡ 1672, 1599, 1443, 711 cm^{-1}.

1-(4-(Trifluoromethyl)benzyl)-1,4-dihydroquinoxaline-2,3-dione (2i). R_f = 0.3 (50% ethyl acetate/hexane); pale yellow solid; yield 66 mg (88%); mp 270-272 ºC; ^{1}H NMR (700 MHz, DMSO-d_6) δ 12.13 (s, 1H), 7.68 (d, *J*= 8.4 Hz, 2H), 7.54 (d, *J*= 7.7 Hz, 2H), 7.22 – 7.05 (m, 4H), 5.47 (s, 2H); ^{13}C{1H} NMR (175 MHz, DMSO-d_6) δ 155.8, 153.7, 140.7, 127.9 (q, $^2J_{C\text{-}F}$ = 31.5 Hz) 127.5, 126.3, 126.0, (q, $^3J_{C\text{-}F}$ = 3.5 Hz), 124.2 (q, $^1J_{C\text{-}F}$ = 270.4 Hz) 123.8, 123.2, 115.8, 115.3,

45.4; IR (KBr) ῡ 1668, 1619, 1383, 680 cm^{-1}; HRMS (ESI-TOF) calcd for $C_{16}H_{11}F_3N_2NaO_2$ $[M+Na]^+$ 343.0665, found 343.0689.

1-(3,5-Difluorobenzyl)-1,4-dihydroquinoxaline-2,3-dione (2j). R_f = 0.2 (50% ethyl acetate/hexane); pale yellow solid; yield 76 mg (97%); mp 275-277 ºC; ^{1}H NMR (400 MHz, DMSO-d_6) δ 12.04 (s, 1H), 7.21 – 7.07 (m, 7H), 5.37 (s, 2H); ^{13}C{1H} NMR (100 MHz, DMSO-d_6) δ 162.6 (dd, J = 244.4, 13.0 Hz), 156.0, 153.8, 140.7 (t, J = 9.4 Hz), 126.3, 126.2, 123.7, 123.0, 115.7, 115.1, 110.7 – 109.4 (m), 102.7 (t, J = 25.8 Hz), 45.2; IR (KBr) ῡ 1670, 1624, 1441, 712 $cm^{-1;}$ HRMS (ESI-TOF) calcd for $C_{15}H_{10}F_2N_2NaO_2$ $[M+Na]^+$ 311.0603, found 311.0604.

1-(4-Nitrobenzyl)-1,4-dihydroquinoxaline-2,3-dione (2k). R_f = 0.2 (50% ethyl acetate/hexane); pale yellow solid; yield 59 mg (93%); mp 276-278 ºC; ^{1}H NMR (700 MHz, $CDCl_3$) δ 12.04 (s, 1H), 7.98 (d, J = 8.4 Hz, 2H), 7.28 – 7.26 (m, 3H), 7.11 – 7.08 (m, 1H), 6.94 (t, J = 7.7 Hz, 1H), 6.86 (t, J = 7.7 Hz, 1H), 6.79 (d, J = 8.4 Hz, 1H), 5.35 (s, 2H); ^{13}C{1H} NMR (175 MHz, $CDCl_3$) δ 155.9, 153.8, 147.1, 142.4, 127.4, 125.6, 125.6, 124.2, 123.8, 123.5, 116.5, 114.4, 45.8; IR (KBr) ῡ 1702, 1651, 1428, 703, 669 cm^{-1}; HRMS (ESI-TOF) calcd for $C_{15}H_{11}N_3NaO_4$ $[M+Na]^+$ 320.0642, found 320.0644.

1-Methyl-1,4-dihydroquinoxaline-2,3-dione (2l).[40] R_f = 0.2 (50% ethyl acetate hexane); pale yellow solid, yield 51 mg (91%); mp 280-282 ºC; ^{1}H NMR (700 MHz, DMSO-d_6) δ 12.01 (s, 1H), 7.35 (d, J = 6.3 Hz, 1H), 7.17 (s, 3H), 3.51 (s, 3H); ^{13}C{1H} NMR (175 MHz, DMSO-d_6) δ 155.7, 153.6, 127.2, 125.6, 123.5, 123.2, 115.4, 115.0, 29.7; IR (KBr) ῡ 1665, 1605, 1387, 729 cm^{-1}.

1-Ethyl-1,4-dihydroquinoxaline-2,3-dione (2m).[40] R_f = 0.1 (50% ethyl acetate1/hexane) pale yellow solid; yield 76 mg (92%); mp 284-286 ºC; ^{1}H NMR (700 MHz, DMSO-d_6) δ 12.01 (s, 1H), 7.40 (d, *J* = 7.7 Hz, 1H), 7.20-7.15 (m, 3H), 4.14 (q, *J* = 7.0 Hz, 2H), 1.21 (t, *J* = 7.0 Hz, 3H); ^{13}C{1H} NMR (175 MHz, DMSO-d_6) δ 154.8, 153.6, 125.9, 125.8, 123.4, 123.3, 115.8, 114.8, 37.3, 12.0; IR (KBr) ῡ 1657, 1595, 1433, 709 cm^{-1}.

1-Butyl-1,4-dihydroquinoxaline-2,3-dione (2n). R_f = 0.2 (50% ethyl acetate/hexane); yellow solid; yield 74 mg (87%); mp 182-184 ºC; ^{1}H NMR (700 MHz, DMSO-d_6) δ 12.02 (s, 1H), 7.37 (d, *J* = 8.4 Hz, 1H), 7.18 – 7.15 (m, 3H), 4.10 – 4.08 (m, 2H), 1.61-1.57 (m, 2H), 1.40-1.35 (m, 2H), 0.92 (t, *J* = 7.0 Hz, 3H); ^{13}C{1H} NMR (175 MHz, DMSO-d_6) δ 155.1, 153.6, 126.2, 125.8, 123.5, 123.4, 115.8, 115.0, 41.9, 28.7, 19.6, 13.7; IR (KBr) ῡ 1685, 1665, 1459, 708 cm^{-1} HRMS (ESI-TOF) calcd for $C_{12}H_{14}N_2NaO_2$ $[M+Na]^+$ 241.0947, found 241.0940.

1-Phenethyl-1,4-dihydroquinoxaline-2,3-dione (2o). R_f = 0.1 (50% ethyl acetate/hexane); pale yellow solid; yield 74 mg (95%); mp 225-227 ºC; ^{1}H NMR (700 MHz, DMSO-d_6) δ 12.04 (s, 1H), 7.46 (d, *J* = 7.7 Hz, 1H), 7.32 – 7.20 (m, 7H), 4.30 (s, 2H), 2.92 (s, 2H); ^{13}C{1H} NMR (175 MHz, DMSO-d_6) δ 154.9, 153.5, 138.2, 128.8, 128.5, 126.5, 126.0, 125.7, 123.5, 123.4, 115.8, 114.9, 43.5, 32.5; IR (KBr) ῡ 1675, 1601, 1390, 696 cm^{-1}; HRMS (ESI-TOF) calcd for $C_{16}H_{14}N_2NaO_2$ $[M+Na]^+$ 289.0947, found 289.0953.

1-(2-Oxo-2-phenylethyl)-1,4-dihydroquinoxaline-2,3-dione (2p). R_f = 0.2 (50% ethyl aetate/hexane); pale yellow solid; yield 55 mg (70%); mp 242-244 ºC; ^{1}H NMR (400 MHz, DMSO-d_6) δ 12.24 (s, 1H), 8.13 (d, *J* = 6.8 Hz, 2H), 7.75-7.62 (m, 3H), 7.26 – 7.11 (m, 4H), 5.80

(s, 2H).; ^{13}C{1H} NMR (100 MHz, DMSO-d_6) δ 192.3, 155.3, 153.4, 134.4, 134.3, 129.0, 128.3, 126.8, 125.5, 123.9, 123.5, 115.9, 115.2, 49.6; IR (KBr) ῡ 1690, 1666, 1407, 715 cm^{-1}, HRMS (ESI-TOF) calcd for $C_{16}H_{13}N_2O_3$ $[M+H]^+$ 281.0921, found 281.0927.

Ethyl 2-(2,3-dioxo-3,4-dihydroquinoxalin-1(2H)-yl)acetate (2q).[40] R_f = 0.2 (50% ethyl acetate/hexane); pale yellow solid; yield 75 mg (97%); mp 278-280 ºC; ^{1}H NMR (400 MHz, DMSO-d_6) δ 12.20 (s, 1H), 7.30 (d, *J* = 7.2 Hz, 1H), 7.22-7.17 (m, 3H), 4.98 (s, 2H), 4.17 (q, *J* = 7.2 Hz, 2H), 1.21 (t, *J* = 7.2 Hz, 3H); ^{13}C{1H} NMR (100 MHz, DMSO-d_6) δ 167.6, 155.3, 153.2, 126.4, 125.5, 124.0, 123.4, 115.9, 114.9, 61.3, 44.2, 14.0; IR (KBr) ῡ 1736, 1679, 1418, 711 cm^{-1}.

Isopropyl 2-(2,3-dioxo-3,4-dihydroquinoxalin-1(2H)-yl)acetate (2r). R_f = 0.3 (50% ethyl acetate/hexane); white solid; yield 68 mg (93%); mp 236-238 ºC; ^{1}H NMR (700 MHz, DMSO-d_6) δ 12.19 (s, 1H), 7.27 (d, *J* = 7.7 Hz, 1H), 7.23 – 7.17 (m, 3H), 4.97 (dd, *J* = 12.6, 5.6 Hz, 1H), 4.94 (s, 2H), 1.22 (d, *J* = 5.6 Hz, 6H); ^{13}C{1H} NMR (175 MHz, DMSO-d_6) δ 167.0, 155.2, 153.2, 126.4, 125.4, 123.9, 123.4, 115.8, 114.8, 69.1, 44.3, 21.5; IR (KBr) ῡ 1728, 1665, 1391, 699 cm^{-1}; HRMS (ESI-TOF) calcd for $C_{13}H_{15}N_2O_4$ $[M+H]^+$ 263.1026, found 263.1007.

***tert*-Butyl 2-(2-oxoquinoxalin-1(2H)-yl)acetate (2s).**[40] R_f = 0.3 (50% ethyl acetate/hexane); pale yellow solid; yield 69 mg (93%); mp 262-264 ºC; ^{1}H NMR (700 MHz, DMSO-d_6) δ 12.18 (s, 1H), 7.25-7.18 (m, 4H), 4.87 (s, 2H), 1.42 (s, 9H); ^{13}C{1H} NMR (175 MHz, DMSO-d_6) δ 166.6, 155.2, 153.3, 126.4, 125.4, 124.0, 123.5, 115.9, 114.8, 82.1, 44.8, 27.7; IR (KBr) ῡ 1722, 1671, 1384, 713 cm^{-1}.

1-(Prop-2-yn-1-yl)-1,4-dihydroquinoxaline-2,3-dione (2t).[40] R_f = 0.2 (50% ethyl acetate/hexane); yellow solid; yield 67 mg (88%); mp 280-282 ºC; ^{1}H NMR (400 MHz, DMSO-d_6) δ 12.11 (s, 1H), 7.42 (d, J = 6.4 Hz, 1H), 7.21 (s, 3H), 4.95 (s, 2H); ^{13}C{1H} NMR (100 MHz, DMSO-d_6) δ 154.6, 153.3, 125.7, 125.6, 124.0, 123.2, 115.7, 115.3, 78.1, 75.1, 31.9; IR (KBr) ϋ 3287, 1673, 1598, 1389, 688 cm^{-1}.

1-Benzyl-1,4-dihydrobenzo[g]quinoxaline-2,3-dione (4a). R_f = 0.4 (50% ethyl acetate/hexane); yellow solid; yield 69 mg (93%); mp > 300 ºC; ^{1}H NMR (400 MHz, DMSO-d_6) δ 12.29 (s, 1H), 7.83-7.76 (m, 2H), 7.68-7.60 (m, 2H), 7.39 – 7.25 (m, 7H), 5.48 (s, 2H); ^{13}C{1H} NMR (100 MHz, DMSO-d_6) δ 155.4, 153.5, 135.7, 129.3, 129.2, 128.6, 127.3, 127.2, 126.8, 126.4, 126., 125.7, 125.1, 112.2, 111.4, 45.8; IR (KBr) ϋ 1674, 1634, 1444, 692 cm^{-1}; HRMS (ESI-TOF) calcd for $C_{19}H_{15}N_2O_2$ $[M+H]^+$ 303.1128, found 303.1124.

1-(4-Nitrobenzyl)-1,4-dihydrobenzo[g]quinoxaline-2,3-dione (4b). R_f = 0.3 (50% ethyl acetate/hexane); yellow solid; yield 68 mg (91%); mp > 300 ºC; ^{1}H NMR (700 MHz, DMSO-d_6) δ 12.29 (s, 1H), 8.18 (d, J = 7.7 Hz, 2H), 7.83 (d, J = 7.7 Hz, 1H), 7.75 (d, J = 7.7 Hz, 1H), 7.69 (d, J = 7.7 Hz, 2H), 7.62 (d, J = 8.4 Hz, 2H), 7.39 (dd, J = 23.1, 7.0 Hz, 2H), 5.60 (s, 2H); ^{13}C{1H} NMR (175 MHz, DMSO-d_6) δ 155.5, 153.5, 146.8, 143.8, 129.4, 129.1, 128.1, 127.3, 126.8, 126.4, 126.3, 125.7, 125.1, 123.7, 111.9, 111.5, 45.6; IR (KBr) ϋ 1678, 1637, 1439, 702 cm^{-1}; HRMS (ESI-TOF) calcd for $C_{19}H_{14}N_3O_4$ $[M+H]^+$ 348.0978, found 348.0957.

1-Benzyl-6-methyl-1,4-dihydroquinoxaline-2,3-dione and 1-Benzyl-7-methyl-1,4-dihydroquinoxaline-2,3-dione (4c). R_f = 0.4 (50% ethyl acetate/hexane); pale yellow solid; yield

65 mg (87%); mp 260-262 ºC; Two regioisomers with 62:38 Ratio; ^{1}H NMR (400 MHz, DMSO-d_6) δ 12.07 (s, 1.6H), 7.32 – 7.25 (m, 8H), 7.11-7.05 (m, 2.2H), 6.99 – 6.95 (m, 1.6H), 6.88 (d, *J* = 8.0 Hz, 1H), 5.36 (s, 3.2H), 2.26 (s, 3H), 2.22 (s, 1.8H); ^{13}C{1H} NMR (100 MHz, DMSO-d_6) δ 155.8, 155.5, 153.8, 153.5, 135.8, 135.8, 133.1, 132.4, 128.6, 127.2, 126.7, 126.6, 126.2, 125.7, 124.4, 124.1, 123.9, 123.5, 115.8, 115.6, 115.6, 115.7, 45.5, 20.8, 20.3; IR (KBr) ῡ 1687, 1657, 1442, 695 cm^{-1}; HRMS (ESI-TOF) calcd for $C_{16}H_{14}N_2NaO_2$ $[M+Na]^+$ 289.0947, found 289.0941.

1-Benzyl-6-bromo-1,4-dihydroquinoxaline-2,3-dione and 1-Benzyl-7-bromo-1,4-dihydroquinoxaline-2,3-dione (4d). R_f = 0.4 (50% ethyl acetate/hexane); pale yellow solid; yield 78 mg (91%); mp 253-255 ºC; Two regioisomers with 62:38 Ratio; ^{1}H NMR (400 MHz, DMSO-d_6) δ 12.16 (s, 1.6H), 7.32-7.21 (m, 11.2H), 7.13-7.08 (1.6H); 5.38 (s, 1.2H), 5.35 (s, 2H); ^{13}C{1H} NMR (100 MHz, DMSO) δ 155.6, 155.4, 153.6, 153.4, 135.4, 128.7, 128.6, 127.8, 127.5, 127.3, 127.3, 126.6, 126.2, 125.9, 125.4, 125.4, 117.8, 117.7, 117.3, 115.1, 114.6, 45.7, 45.6; IR (KBr) ῡ 1705, 1676, 1392, 700 cm^{-1}; HRMS (ESI-TOF) calcd for $C_{15}H_{11}BrN_2NaO_2$ $[M+Na]^+$ 352.9896, found 352.9881.

1-Benzyl-6-chloro-1,4-dihydroquinoxaline-2,3-dione and 1-Benzyl-7-chloro-1,4-dihydroquinoxaline-2,3-dione (4e). R_f = 0.3 (50% ethyl acetate/hexane); play yellow solid; yield 84 mg (92%); mp 250-252 ºC; Two regioisomers with 74:26 Ratio; ^{1}H NMR (400 MHz, DMSO-d_6) δ 12.17 (s, 1.3H), 7.33 – 7.27 (m, 7H), 7.19 (t, *J* = 7.2 Hz, 2.7H), 7.15 – 7.10 (m, 2.4H), 5.38 (s, 0.7H), 5.35 (s, 2H).; ^{13}C{1H} NMR (175 MHz, DMSO-d_6) δ 155.6, 155.4, 153.6, 153.4, 135.4, 135.4, 128.7, 128.7, 127.6, 127.4, 127.3, 127.3, 126.9, 126.6, 125.5, 125.1, 123.4, 122.6,

117.1, 115.1, 114.9, 45.8, 45.6; IR (KBr) ῡ 1705, 1678, 1435, 701 cm^{-1}, HRMS (ESI-TOF) calcd for $C_{15}H_{12}ClN_2O_2$ $[M+H]^+$ 243.0740, found 243.0746.

1-Benzyl-6,7-dimethyl-1,4-dihydroquinoxaline-2,3-dione (4f). R_f = 0.2 (50% ethyl acetate/hexane); pale yellow solid; yield 72 mg (94%); mp > 300 ºC; ^{1}H NMR (400 MHz, DMSO-d_6) δ 12.00 (s, 1H), 7.33 – 7.24 (m, 5H), 7.02 (s, 1H), 6.95 (s, 1H), 5.35 (s, 2H), 2.15 (s, 3H), 2.12 (s, 3H); ^{13}C{1H} NMR (100 MHz, DMSO-d_6) δ 155.6, 153.7, 135.9, 131.9, 131.3, 128.6, 127.2, 126.7, 124.1, 123.5, 116.3, 116.1, 45.4, 19.2, 18.7; IR (KBr) ῡ 1669, 1603, 1441, 729 cm^{-1}; HRMS (ESI-TOF) calcd for $C_{17}H_{17}N_2O_2$ $[M+H]^+$ 281.1285, found 281.1282.

1,6,7-Trimethyl-1,4-dihydroquinoxaline-2,3-dione (4g).[40] R_f = 0.2 (50% ethyl acetate/hexane); yellow solid; yield 71 mg (90%); mp > 300 ºC; ^{1}H NMR (700 MHz, DMSO-d_6) δ 11.88 (s, 1H), 7.14 (s, 1H), 6.92 (s, 1H), 3.48 (s, 3H), 2.25 (s, 3H), 2.19 (s, 3H); ^{13}C{1H} NMR (175 MHz, DMSO-d_6) δ 155.2, 153.6, 131.6, 131.4, 125.0, 123.2, 116.0, 115.8, 29.6, 19.2, 18.8; IR (KBr) ῡ 1682, 1613, 1449, 739 cm^{-1}

1-Benzyl-6,7-dichloro-1,4-dihydroquinoxaline-2,3-dione (4h). R_f = 0.4 (50% ethyl acetate/hexane); pale yellow solid; yield 53 mg (82%); mp > 300 ºC; ^{1}H NMR (400 MHz, DMSO-d_6) δ 12.22 (s, 1H), 7.38 (s, 1H), 7.33 – 7.30 (m, 5H), 7.28 -7.26 (m, 1H), 5.37 (s, 2H); ^{13}C{1H} NMR (100 MHz, DMSO-d_6) δ 155.4, 153.4, 135.2, 128.7, 127.4, 126.8, 126.7, 126.4, 125.3, 124.6, 116.9, 116.4, 45.8; IR (KBr) ῡ 1709, 1662, 1484, 696 cm^{-1}, HRMS (ESI-TOF) calcd for $C_{15}H_{10}Cl_2NaN_2O_2$ $[M+Na]^+$ 343.0012, found 343.0008.

6,7-dichloro-1-methyl-1,4-dihydroquinoxaline-2,3-dione (4i).[40] R_f = 0.3 (50% ethyl acetate/hexane); yellow solid; yield 58 mg (79%); mp > 300 ºC; ^{1}H NMR (700 MHz, DMSO-d_6) δ 12.11 (s, 1H), 7.61 (s, 1H), 7.28 (s, 1H), 3.48 (s, 3H); ^{13}C{1H} NMR (175 MHz, DMSO-d_6) δ 154.9, 153.2, 127.7, 125.9, 125.0, 124.8, 116.6, 116.0, 30.0.

1-Benzyl-6,7-difluoro-1,4-dihydroquinoxaline-2,3-dione (4j). R_f = 0.3 (50% ethyl acetate/hexane); pale yellow solid; yield 71 mg (91%); mp 272-274 ºC; ^{1}H NMR (700 MHz, DMSO-d_6) δ 12.15 (s, 1H), 7.32 (s, 5H), 7.27 (d, J = 5.6 Hz, 1H), 7.16 – 7.14 (m, 1H), 5.35 (s, 2H); ^{13}C{1H} NMR (175 MHz, DMSO-d_6) δ 155.4, 153.4, 145.1 (dd, J = 239.2, 12.2 Hz), 144.9 (dd, J = 237.6, 12.6 Hz) 135.2, 128.7, 127.4, 126.8, 123.2 (d, J = 8.2 Hz), 122.7 (d, J = 7.9 Hz), 105.0 (d, J = 23.5 Hz), 104.1 (d, J = 22.1 Hz), 45.9; IR (KBr) ῡ 1709, 1682, 1401, 715 cm^{-1}; HRMS (ESI-TOF) calcd for $C_{15}H_{10}F_2NaN_2O_2$ $[M+Na]^+$ 311.0603, found 311.0599.

1,4-dihydroquinoxaline-2,3-dione (9).[54] R_f = 0.2 (50% ethyl acetate/hexane); yellow solid; yield 54 mg (75%); mp >300 ºC; ^{1}H NMR (700 MHz, DMSO-d_6) δ 11.90 (s, 2H), 7.13 – 7.12 (m, 2H), 7.09 – 7.07 (m, 2H); ^{13}C{1H} NMR (175 MHz, DMSO-d_6) δ 155.2, 125.6, 123.0, 115.1; IR (KBr) ῡ 1723, 1654, 1439, 718 cm^{-1}

1-(3-(*p*-Tolyl)prop-2-yn-1-yl)-1,4-dihydroquinoxaline-2,3-dione (10). R_f = 0.3 (50% ethyl acetate/hexane); pale yellow solid; yield 45 mg (85%); mp 290-292 ºC, ^{1}H NMR (700 MHz, DMSO-d_6) δ 12.11 (s, 1H), 7.52 (d, J = 7.7 Hz, 1H), 7.31 – 7.20 (m, 5H), 7.15 (d, J = 7.0 Hz, 2H), 5.19 (s, 2H), 2.28 (s, 3H); ^{13}C{1H} NMR (175 MHz, DMSO-d_6) δ 154.8, 153.5, 138.8, 131.5, 129.4, 125.8, 125.8, 124.0, 123.4, 118.6, 115.8, 115.5, 83.5, 83.2, 32.8, 21.0; HRMS (ESI-TOF)

calcd for $C_{18}H_{15}N_2O_2$ $[M+H]^+$ 291.1128, found 291.1142; IR (KBr) ῡ 1668, 1601, 1385, 712 cm^{-1}.

1-Benzylquinoxalin-2(1*H*)-one (1a).[38] R_f = 0.3 (20% ethyl acetate/hexane); pale yellow solid; yield 82% (401 mg); mp 115-117 ºC; ^{1}H NMR (400 MHz, $CDCl_3$) δ 8.41 (s, 1H), 7.89 (dd, *J* = 8.0, 1.2 Hz, 1H), 7.49 – 7.44 (m, 1H), 7.33 – 7.26 (m, 6H), 7.23 (s, 1H), 5.49 (s, 2H). ^{13}C{1H} NMR (100 MHz, $CDCl_3$) δ 155.3, 150.4, 135.1, 133.8, 132.7, 131.2, 130.7, 129.1, 127.9, 126.9, 123.9, 114.8, 45.7.

1-(3-Methylbenzyl)quinoxaline-2(1*H*)-one (1b).[55] R_f = 0.6 (20% ethyl acetate/hexane); pale yellow solid; yield 71% (631 mg); mp 162-164 ºC; ^{1}H NMR (400 MHz, $CDCl_3$) δ 8.40 (s, 1H), 7.90 – 7.88 (m, 1H), 7.49 – 7.44 (m, 1H), 7.33-7.29 (t, *J* = 7.2 Hz, 2H), 7.16 – 7.11 (m, 4H), 5.45 (s, 2H), 2.30 (s, 3H). ^{13}C{1H} NMR (100 MHz, $CDCl_3$) δ 155.3, 150.5, 137.7, 133.8, 132.7, 132.1, 131.1, 130.7, 129.8, 127.0, 123.9, 114.8, 45.5, 21.2.

1-(4-Isopropyl benzyl)quinoxalin-2(1*H*)-one (1c). R_f = 0.3 (20% ethyl acetate/hexane); dark brown solid; yield 70% (695 mg); mp 128-130 ºC; ^{1}H NMR (400 MHz, CDCl3) δ 8.41 (s, 1H), 7.90 (d, *J* = 8.0 Hz, 1H), 7.50 – 7.46 (m, 1H), 7.34-7.30 (m, 2H), 7.17 (s, 4H), 5.46 (s, 2H), 2.90-2.83 (m, 1H), 1.20 (d, *J* = 6.8 Hz, 6H). ^{13}C{1H} NMR (100 MHz, $CDCl_3$) δ 155.3, 150.5, 148.7, 133.8, 132.8, 132.4, 131.2, 130.7, 127.2, 127.0, 123.9, 114.9, 45.5, 33.9, 24.0; IR (KBr) ῡ 1657, 1600, 1460, 754 cm^{-1} HRMS (ESI-TOF) calcd for $C_{18}H_{18}NaN_2O$ $[M+Na]^+$ 301.1311, found 301.1307.

1-(4-(*tert*-Butyl)benzyl)quinoxalin-2(1*H*)-one (1d).[38] R_f = 0.3 (20% ethyl acetate/hexane); dark brown solid; yield 76% (788 mg); mp 134-136 ºC; ^{1}H NMR (400 MHz, CDCl3) δ 8.40 (s, 1H), 7.89 (d, *J* = 8.0 Hz, 1H), 7.51 – 7.46 (m, 1H), 7.32 (t, *J* = 8.0 Hz, 4H), 7.18 (d, *J* = 8.0 Hz, 2H), 5.46 (s, 2H), 1.27 (s, 9H); ^{13}C{1H} NMR (100 MHz, $CDCl_3$) δ 155.3, 150.9, 150.5, 133.7, 132.8, 132.0, 131.2, 130.7, 126.8, 126.0, 123.9, 114.8, 45.4, 34.6, 31.4.

((2-Oxoquinoxaline-1(2*H*)-yl)methyl)benzonitrile (1e).[56] R_f = 0.2 (20% ethyl acetate/hexane); white solid; yield 70% (648 mg); mp 162-164 ºC; ^{1}H NMR (400 MHz, $CDCl_3$) δ 8.41 (s, 1H), 7.93 (d, *J* = 8.0 Hz, 1H), 7.63 (d, *J* = 8.0 Hz, 2H), 7.51 – 7.47 (m, 1H), 7.38-7.34 (m, 3H), 7.14 (d, *J* = 8.4 Hz, 1H), 5.53 (s, 2H). ^{13}C{1H} NMR (100 MHz, $CDCl_3$) δ 155.0, 150.3, 140.5, 133.8, 133.0, 132.3, 131.5, 131.1, 127.7, 124.4, 118.5, 114.2, 112.1, 45.3.

1-(4-Bromobenzyl)quinoxalin-2(1*H*)-one (1f).[57] R_f = 0.4 (20% ethyl acetate/hexane); light yellow solid; yield 69% (825 mg); mp 170-172 ºC; ^{1}H NMR (700 MHz, $CDCl_3$) δ 8.40 (s, 1H), 7.90 (dd, *J* = 8.4, 1.4 Hz, 1H), 7.59 – 7.47 (m, 1H), 7.44 (d, *J* = 8.4 Hz, 2H), 7.35 – 7.32 (m, 1H), 7.22 (d, *J* = 8.4 Hz, 1H), 7.13 (d, *J* = 8.4 Hz, 2H), 5.43 (s, 2H); ^{13}C{1H} NMR (175 MHz, $CDCl_3$) δ 155.2, 150.4, 134.2, 133.8, 132.5, 132.3, 131.3, 130.9, 128.8, 124.1, 121.9, 114.5, 45.1.

1-(2-Iodobenzyl)quinoxalin-2(1*H*)-one (1g). R_f = 0.3 (20% ethyl acetate/hexane); black solid; yield 51% (655 mg); mp 166-168 ºC; ^{1}H NMR (700 MHz, $CDCl_3$) δ 8.58 (s, 1H), 8.05 (d, *J* = 7.7 Hz, 1H), 7.91 (d, *J* = 7.7 Hz, 1H), 7.50 (t, *J* = 7.7 Hz, 1H), 7.36 (t, *J* = 7.7 Hz, 1H), 7.18 (t, *J* = 7.7 Hz, 1H), 7.02 – 6.97 (m, 2H), 6.64 (d, *J* = 7.7 Hz, 1H), 5.45 (s, 2H); ^{13}C{1H} NMR (175 MHz, $CDCl_3$) δ 155.3, 150.5, 140.0, 135.9, 133.4, 132.4, 131.9, 130.6, 129.7, 129.0, 126.4, 124.7, 115.2,

97.5, 77.3, 51.5; IR (KBr) ῡ 1650, 1600, 1459, 748 cm^{-1}; HRMS (ESI-TOF) calcd for $C_{15}H_{12}IN_2O$ $[M+H]^+$ 362.9989, found 362.9965.

1-(4-Fluorobenzyl)quinoxalin-2(1*H*)-one (1h).[56] R_f = 0.5 (20% ethyl acetate/hexane); pale yellow solid; yield 53% (458 mg); mp 110-112 ºC; ^{1}H NMR (700 MHz, $CDCl_3$) δ 8.40 (s, 1H), 7.90 (dd, *J* = 7.7, 1.4 Hz, 1H), 7.50 – 7.47 (m, 1H), 7.34-7.32 (m, 1H), 7.25 – 7.23 (m, 3H), 7.02-7.00 (m, 2H), 5.45 (s, 2H); ^{13}C{1H} NMR (175 MHz, $CDCl_3$) δ 162.40 (d, $^1J_{C\text{-}F}$ = 246.7 Hz), 155.2, 150.4, 133.8, 132.5, 131.2, 130.9, 130.9, 128.86 (d, $^3J_{C\text{-}F}$ = 8.2 Hz), 124.1, 116.1 (d, $^2J_{C\text{-}F}$ = 21.7 Hz), 114.5, 45.0.

1-(4-(Trifluoromethyl)benzyl)quinoxalin-2(1*H*)-one (1i).[56] R_f = 0.2 (20% ethyl acetate/hexane); dark brown; yield 70% (747 mg); mp 106-108 ºC; ^{1}H NMR (700 MHz, $CDCl_3$) δ 8.41 (d, *J* = 4.2 Hz, 1H), 7.92 (d, *J* = 8.4 Hz, 1H), 7.58 (d, *J* = 7.7 Hz, 2H), 7.49 (t, *J* = 7.7 Hz, 1H), 7.36-7.34 (m, 3H), 7.19 (d, *J* = 8.4 Hz, 1H), 5.54 (s, 2H); ^{13}C{1H} NMR (175 MHz, $CDCl_3$) δ 155.1, 150.3, 139.1, 133.8 , 132.4, 131.4, 131.0, 130.3 (q, $^2J_{C\text{-}F}$ = 32.5 Hz), 127.3, 126.15 (q, $^3J_{C\text{-}F}$ = 3.6 Hz), 124.0 (q, $^1J_{C\text{-}F}$ = 270.4 Hz), 124.3, 114.4, 45.3.

1-(3,5-Difluorobenzyl)quinoxalin-2(1*H*)-one (1j). R_f = 0.2 (20% ethyl acetate/hexane); light brown solid; yield 72% (668 mg); mp 138-140 ºC; ^{1}H NMR (700 MHz, $CDCl_3$) δ 8.41 (s, 1H), 7.93 (dd, *J* = 7.7, 0.7 Hz, 1H), 7.52 – 7.50 (m, 1H), 7.36 (t, *J* = 7.7 Hz, 1H), 7.18 (d, *J* = 8.4 Hz, 1H), 6.76 (t, *J* = 6.3 Hz, 1H), 6.74-6.71 (m, 1H), 5.45 (s, 2H); ^{13}C{1H} NMR (175 MHz, $CDCl_3$) δ 125.9 (dd, *J* = 248.6, 12.7 Hz), 117.4, 112.7, 101.4 (t, *J* = 9.0 Hz), 96.1, 94.7, 93.8, 93.4, 86.7,

76.6, 72.4 (dd, *J* = 20.8, 4.9 Hz), 66.0 (t, *J* = 24.8 Hz), 39.7; IR (KBr) ῡ 1656, 1627, 1457, 753 cm^{-1}; HRMS (ESI-TOF) calcd for $C_{15}H_{10}F_2NaN_2O$ $[M+Na]^+$ 295.0653, found 295.0657.

1-(4-Nitrobenzyl)quinoxalin-2(1*H*)-one (1k).[56] R_f = 0.2 (20% ethyl acetate/hexane); pale yellow solid; yield 62% (620 mg); mp 155-157 ºC; ^{1}H NMR (400 MHz, $CDCl_3$) δ 8.42 (s, 1H), 8.18 (d, *J* = 8.0 Hz, 2H), 7.93 (d, *J* = 8.0 Hz, 1H), 7.49 (t, *J* = 7.6 Hz, 1H), 7.42 – 7.34 (m, 3H), 7.14 (d, *J* = 8.4 Hz, 1H), 5.57 (s, 2H). ^{13}C{1H} NMR (100 MHz, $CDCl_3$) δ 155.0, 150.2, 147.7, 142.5, 133.8, 132.2, 131.5, 131.2, 127.8, 124.4, 114.1, 45.1.

1-Methylquinoxalin-2(1*H*)-one (1l).[38] R_f = 0.3 (20% ethyl acetate/hexane); light pink solid; yield 64% (212 mg); mp 130-132 ºC; ^{1}H NMR (400 MHz, $CDCl_3$) δ 8.31 (s, 1H), 7.89 (dd, *J* = 78.0, 1.2 Hz, 1H), 7.62 – 7.58 (m, 1H), 7.39 – 7.34 (m, 2H), 3.70 (s, 3H); ^{13}C{1H} NMR (100 MHz, $CDCl_3$) δ 155.2, 150.3, 133.5, 133.9, 131.2, 130.6, 123.9, 113.9, 28.9.

1-Ethylquinoxalin-2(1*H*)-one (1m).[38] R_f = 0.4 (20% ethyl acetate/hexane); pinkish white solid; yield 71% (467 mg); mp 76-78 ºC; ^{1}H NMR (700 MHz, $CDCl_3$) δ 8.29 (d, *J* = 7.0 Hz, 1H), 7.88 (t, *J* = 7.0 Hz, 1H), 7.58 (t, *J* = 7.7 Hz, 1H), 7.38 – 7.33 (m, 2H), 4.32-4.29 (m, 2H), 1.39-1.36 (m, 3H); ^{13}C{1H} NMR (175 MHz, $CDCl_3$) δ 154.7, 150.4, 133.8, 132.3, 131.1, 130.9, 123.7, 113.8, 37.1, 12.5.

1-Butylquinoxalin-2(1*H*)-one (1n).[58] R_f = 0.3 (20% ethyl acetate/hexane); pale yellow liquid; yield 68% (627 mg); ^{1}H NMR (700 MHz, $CDCl_3$) δ 8.30 (s, 1H), 7.89 (d, *J* = 8.4 Hz, 1H), 7.60 – 7.57 (m, 1H), 7.36 – 7.34 (m, 2H), 4.25 – 4.23 (m, 2H), 1.77 – 1.72 (m, 2H), 1.52 – 1.46 (m, 2H),

1.00 (t, *J* = 7.7 Hz, 3H); $^{13}C\{1H\}$ NMR (175 MHz, $CDCl_3$) δ 155.0, 150.5, 133.8, 132.6, 131.1, 130.9, 123.7, 114.0, 42.0, 29.5, 20.4, 13.9.

1-Phenethylquinoxalin-2(1*H*)-one (1o).[38] R_f = 0.5 (20% ethyl acetate/hexane); yellow solid; yield 67% (635 mg); mp 130-132 ºC; ^1H NMR (700 MHz, $CDCl_3$) δ 8.31 (s, 1H), 7.90 (d, *J* = 7.7 Hz, 1H), 7.58 (t, *J* = 7.7 Hz, 1H), 7.37-7.30 (m, 6H), 7.27 – 7.25 (m, 1H), 4.46 (t, *J* = 8.4 Hz, 2H), 3.04 (t, *J* = 8.4 Hz, 2H); $^{13}C\{1H\}$ NMR (175 MHz, $CDCl_3$) δ 154.8, 150.4, 137.7, 133.8, 132.5, 131.2, 131.0, 128.9, 128.9, 127.1, 123.8, 113.7, 43.5, 33.5.

1-(2-Oxo-2-phenylethyl)quinoxalin-2(1*H*)-one (1p).[38] R_f = 0.3 (20% ethyl acetate/hexane); pale yellow solid; yield 64% (530 mg); mp 188-190 ºC; ^1H NMR (700 MHz, $CDCl_3$) δ 8.37 (s, 1H), 8.07 (d, *J* = 7.7 Hz, 2H), 7.92 (d, *J* = 7.7 Hz, 1H), 7.68 (t, *J* = 7.7 Hz, 1H), 7.56 (t, *J* = 7.7 Hz, 2H), 7.49 (t, *J* = 7.7 Hz, 1H), 7.35 (t, *J* = 7.7 Hz, 1H), 6.98 (d, *J* = 8.4 Hz, 1H), 5.73 (s, 2H); $^{13}C\{1H\}$ NMR (175 MHz, $CDCl_3$) δ 190.9, 154.9, 150.0, 134.6, 134.6, 133.7, 132.8, 131.3, 130.9, 129.2, 128.3, 124.0, 113.8, 48.2.

Ethyl 2-(2-oxoquinoxalin-1(2*H*)-yl)acetate (1q).[56] R_f = 0.4 (20% ethyl acetate/hexane); pale yellow solid; yield 65% (531 mg); mp 128-130 ºC; ^1H NMR (700 MHz, $CDCl_3$) δ 8.34 (s, 1H), 7.91 (dd, *J* = 7.7, 1.4 Hz, 1H), 7.57 – 7.55 (m, 1H), 7.38 – 7.36 (m, 1H), 7.10 (d, *J* = 7.7 Hz, 1H), 5.02 (s, 2H), 4.25 (q, *J* = 7.0 Hz, 2H), 1.27 (t, *J* = 7.0 Hz, 3H); $^{13}C\{1H\}$ NMR (175 MHz, $CDCl_3$) δ 167.0, 154.7, 150.1, 133.5, 132.5, 131.4, 131.0, 124.2, 113.4, 62.3, 43.3, 14.2.

Isopropyl 2-(2-oxoquinoxalin-1(2*H*)-yl)acetate (1r).[38] R_f = 0.5 (20% ethyl acetate/hexane); white solid; yield 67% (654 mg); mp 148-150 ºC; ^{1}H NMR (700 MHz, $CDCl_3$) δ 8.35 (s, 1H), 7.91 (d, *J* = 7.7 Hz, 1H), 7.56 (t, *J* = 7.7 Hz, 1H), 7.37 (t, *J* = 7.7 Hz, 1H), 7.09 (d, *J* = 8.4 Hz, 1H), 5.12-5.08 (m, 1H), 4.99 (s, 2H), 1.25 (d, *J* = 6.3 Hz, 6H); ^{13}C{1H} NMR (175 MHz, $CDCl_3$) δ 166.5, 154.7, 150.1, 133.6, 132.6, 131.3, 131.0, 124.2, 113.4, 70.3, 43.5, 21.8.

***tert*-Butyl 2-(2-oxoquinoxalin-1(2*H*)-yl)acetate (1s).[38]** R_f = 0.5 (20% ethyl acetate/hexane); white solid; yield 67% (654 mg); mp 165-167 ºC; ^{1}H NMR (700 MHz, $CDCl_3$) δ 8.34 (s, 1H), 7.90 (d, *J* = 7.7 Hz, 1H), 7.57 (t, *J* = 7.7 Hz, 1H), 7.37 (t, *J* = 7.7 Hz, 1H), 7.10 (d, *J* = 8.4 Hz, 1H), 4.93 (s, 2H), 1.45 (s, 9H); ^{13}C{1H} NMR (175 MHz, $CDCl_3$) δ 165.90, 154.5, 150.0, 133.4, 132.5, 131.1, 130.8, 124.0, 113.3, 83.4, 43.9, 28.0.

1-(Prop-2-yn-1-yl)quinoxalin-2(1*H*)-one (1t).[38] R_f = 0.2 (20% ethyl acetate/hexane); light brown solid; yield 78% (510 mg); mp 175-177 ºC; ^{1}H NMR (400 MHz, $CDCl_3$) δ 8.30 (s, 1H), 7.89 (d, *J* = 8.0 Hz, 1H), 7.63 (dd, *J* = 11.4, 4.2 Hz, 1H), 7.49 (d, *J* = 8.2 Hz, 1H), 7.38 (t, *J* = 7.6 Hz, 1H), 5.03 (d, *J* = 2.4 Hz, 2H), 2.30 (t, *J* = 2.4 Hz, 1H); ^{13}C{1H} NMR (100 MHz, $CDCl_3$) δ 154.1, 150.1, 133.7, 131.8, 131.3, 130.8, 124.3, 114.5, 76.7, 73.5, 31.3.

1-Benzylbenzo[g]quinoxalin-2(1*H*)-one (3a).[59] R_f = 0.4 (20% ethyl acetate/hexane); brown solid; yield 72% (527 mg); mp 194-196 ºC; ^{1}H NMR (700 MHz, $CDCl_3$) δ 8.41 (d, *J* = 7.7 Hz, 2H), 7.96 (d, *J* = 8.4 Hz, 1H), 7.78 (d, *J* = 8.4 Hz, 1H), 7.58 (s, 1H), 7.53 (t, *J* = 7.0 Hz, 1H), 7.47 (t, *J* = 7.0 Hz, 1H), 7.34 – 7.31 (m, 4H), 7.28 (s, 1H), 5.56 (s, 2H); ^{13}C{1H} NMR (175 MHz,

$CDCl_3$) δ 155.1, 151.0, 135.2, 134.1, 133.0, 130.7, 130.3, 129.7, 129.2, 128.7, 128.3, 127.9, 127.5, 127.0, 125.7, 111.4, 77.3, 77.2, 77.0, 45.8.

1-(4-Nitrobenzyl)benzo[g]quinoxalin-2(1*H*)-one (3b). R_f = 0.3 (20% ethyl acetate/hexane); yellow solid; yield 73% (615 mg); mp 210-212 ºC; ^{1}H NMR (700 MHz, $CDCl_3$) δ 8.45-8.43 (m, 2H), 8.20 (d, *J* = 8.4 Hz, 2H), 7.99 (d, *J* = 7.7 Hz, 1H), 7.76 (d, *J* = 8.4 Hz, 1H), 7.57 – 7.55 (m, 1H), 7.50 (t, *J* = 7.7 Hz, 1H), 7.47 (d, *J* = 8.4 Hz, 2H), 7.43 (s, 1H), 5.65 (s, 2H); ^{13}C{1H} NMR (175 MHz, $CDCl_3$) δ 154.9, 150.7, 147.7, 142.6, 134.1, 132.8, 130.9, 130.3, 129.9, 128.8, 128.7, 127.8, 127.3, 126.1, 124.5, 123.9, 45.2.

1-Benzyl-6-methylquinoxalin-2(1*H*)-one and 1-Benzyl-7-methylquinoxalin-2(1*H*)-one (3c).[60] R_f = 0.3 (20% ethyl acetate/hexane); grey solid; yield 72% (560 mg); mp 110-112 ºC; Two regioisomers with 62:38 Ratio ^{1}H NMR (400 MHz, $CDCl_3$) δ 8.39 (s, 1H), 8.34 (s, 0.6H), 7.77 (d, *J* = 8.0 Hz, 0.6H), 7.68 (s, 1H), 7.34 – 7.29 (m, 4H), 7.25 – 7.21 (m, 4H), 7.17-7.12 (m, 2H), 7.07 (s, 0.6H), 5.47 (s, 3.2H), 2.40 (s, 4.8H); ^{13}C{1H} NMR (100 MHz, $CDCl_3$) δ 155.4, 155.2, 150.3, 149.2, 142.1, 135.2, 135.1, 133.9, 133.7, 132.6, 132.4, 132.0, 130.5, 130.4, 129.1, 129.1, 127.9, 126.9, 125.3, 114.7, 114.5, 45.6, 45.6, 22.3, 20.7.

1-Benzyl-6-bromoquinoxalin-2(1*H*)-one and 1-Benzyl-7-bromoquinoxalin-2(1*H*)-one (3d).[61] R_f = 0.4 (20% ethyl acetate/hexane); light pink solid; yield 46% (256 mg); mp 148-150 ºC; Two regio-isomers with 52:48 ratio, ^{1}H NMR (400 MHz, $CDCl_3$) δ 8.40 (s, 1H), 8.38 (s, 1H), 8.03 (d, *J* = 2.0 Hz, 1H), 7.73 (d, *J* = 8.4 Hz, 1H), 7.55-7.52 (m, 1H), 7.45 – 7.41 (m, 2H), 7.35-7.31 (m, 6H), 7.24 – 7.20 (m, 3H), 7.14 (d, *J* = 8.8 Hz, 1H), 5.46 (s, 2H), 5.43 (s, 1.8H); ^{13}C{1H} NMR

(100 MHz, $CDCl_3$) δ 154.9, 151.6, 150.6, 134.7, 134.6, 133.9, 133.8, 133.1, 132.6, 131.9, 131.8, 129.3, 129.2, 128.2, 128.1, 127.3, 127.0, 126.9, 125.5, 117.7, 116.6, 116.2, 45.8.

1-Benzyl-6-chloroquinoxalin-2(1*H*)-one and 1-Benzyl-7-chloroquinoxalin-2(1*H*)-one (3e).[61] R_f = 0.5 (20% ethyl acetate/hexane); brown solid; yield 53% (398 mg); Two regio-isomers with 69:31 ratio; mp 136-138 ºC; ^{1}H NMR (700 MHz, $CDCl_3$) δ 8.41 (d, *J* = 6.3 Hz, 1H), 8.36 (d, *J* = 6.3 Hz, 0.4H), 7.87 (s, 1H), 7.80 (d, *J* = 8.4 Hz, 0.4H), 7.40 (d, *J* = 9.1 Hz, 1H), 7.35 – 7.30 (m, 3H), 7.28 – 7.24 (m, 3H), 7.20 (t, *J* = 8.4 Hz, 3H), 5.46 (s, 2H), 5.43 (s, 0.9H); ^{13}C{1H} NMR (175 MHz, $CDCl_3$) δ 154.9, 155.0, 151.6, 150.4, 137.2, 134.7, 134.5, 134.3, 133.6, 132.3, 131.8, 131.4, 131.2, 130.0, 129.3, 129.3, 129.2, 128.2, 128.1, 127.0, 126.9, 124.4, 115.9, 114.7, 45.8.

1-Benzyl-6,7-dimethylquinoxalin-2(1*H*)-one (3f).[62] R_f = 0.3 (20% ethyl acetate/hexane); white solid; yield 61% (467 mg); mp 176-178 ºC; ^{1}H NMR (700 MHz, $CDCl_3$) δ 8.32 (s, 1H), 7.63 (s, 1H), 7.31 (t, *J* = 7.7 Hz, 2H), 7.24 (d, *J* = 7.7 Hz, 3H), 7.04 (s, 1H), 5.46 (s, 2H), 2.31 (s, 3H), 2.30 (s, 3H); ^{13}C{1H} NMR (175 MHz, $CDCl_3$) δ 155.4, 149.2, 141.1, 135.4, 133.0, 132.3, 130.7, 130.7, 129.1, 127.8, 127.0, 115.2, 45.6, 20.8, 19.3.

1,6,7-Trimethylquinoxalin-2(1*H*)-one (3g).[40] R_f = 0.2 (20% ethyl acetate/hexane); white solid; yield 67% (438 mg); mp 180-182 ºC; ^{1}H NMR (700 MHz, $CDCl_3$) δ 8.22 (s, 1H), 7.61 (s, 1H), 7.09 (s, 1H), 3.66 (s, 3H), 2.42 (s, 3H), 2.35 (s, 3H); ^{13}C{1H} NMR (175 MHz, $CDCl_3$) δ 155.3, 149.1, 141.2, 132.9, 132.0, 131.4, 130.6, 114.5, 28.8, 20.8, 19.3.

1-Benzyl-6,7-dichloroquinoxalin-2(1*H*)-one (3h).[62] R_f = 0.4 (20% ethyl acetate/hexane); pink solid; yield 56% (395 mg); mp 175-177 ºC; ^{1}H NMR (400 MHz, $CDCl_3$) δ 8.37 (s, 1H), 7.97 (s, 1H), 7.39 – 7.28 (m, 3H), 7.25 – 7.21 (m, 3H), 5.41 (s, 2H); ^{13}C{1H} NMR (100 MHz, $CDCl_3$) δ 154.6, 151.6, 135.5, 134.3, 132.8, 132.1, 131.5, 129.4, 128.3, 127.9, 127.0, 116.2, 46.0.

6,7-Dichloro-1-methylquinoxalin-2(1*H*)-one (3i).[40] R_f = 0.3 (20% ethyl acetate/hexane); light pink solid; yield 73% (389 mg); mp 218-220 ºC; ^{1}H NMR (700 MHz, $CDCl_3$) δ 8.28 (s, 1H), 7.97 (s, 1H), 7.44 (s, 1H), 3.65 (s, 3H); ^{13}C{1H} NMR (175 MHz, $CDCl_3$) δ 154.5, 151.6, 135.5, 132.8, 132.6, 131.5, 127.9, 115.5, 29.1.

1-Benzyl-6,7-difluoroquinoxalin-2(1*H*)-one (3j). R_f = 0.7 (20% ethyl acetate/hexane); light pink solid; yield 63% (450 mg); mp 146-148 ºC; ^{1}H NMR (700 MHz, $CDCl_3$) δ 8.37 (s, 1H), 7.69 (t, *J* = 9.1 Hz, 1H), 7.34 (t, *J* = 7.7 Hz, 2H), 7.30 (t, *J* = 7.0 Hz, 1H), 7.22 (d, *J* = 7.7 Hz, 2H), 7.06 (dd, *J* = 11.2, 7.0 Hz, 1H), 5.42 (s, 2H); ^{13}C{1H} NMR (175 MHz, $CDCl_3$) δ 154.8, 152.0 (dd, *J* = 254.8, 14.2 Hz), 150.8 (d, *J* = 3.5 Hz), 146.9 (dd, *J* = 246.7, 14.0 Hz), 134.3, 130.1 (dd, *J* = 14.8, 5.7 Hz), 129.4, 128.3, 126.9, 118.3 (dd, *J* = 18.1, 2.1 Hz), 103.5 (d, *J* = 23.3 Hz), 46.3; IR (KBr) ῡ 1668, 1590, 1450, 724 cm^{-1}; HRMS (ESI-TOF) calcd for $C_{15}H_{10}F_2NaN_2O$ $[M+Na]^+$ 295.0653, found 295.0674.

4.6 NOTES AND REFERENCES

1. A. Dahiya, A. K. Sahoo, T. Alam and B. K. Patel, *Chem. Asian J.*, 2019, **14**, 4454-4492.
2. X. Jia and P. Li, *Synthesis*, 2018, **50**, 711-722.
3. S. Mondal, S. Samanta and A. Hajra, *Adv. Synth. Catal.*, 2018, **360**, 1026-1031.

4. S. Maity, T. Naveen, U. Sharma and D. Maiti, *Org. Lett.*, 2013, **15**, 3384-3387.

5. P. Chaudhary, S. Gupta, N. Muniyappan, S. Sabiah and J. Kandasamy, *J. Org. Chem.*, 2019, **84**, 104-119.

6. X.-H. Yang, X.-H. Ouyang, W.-T. Wei, R.-J. Song and J.-H. Li, *Adv. Synth. Catal.*, 2015, **357**, 1161-1166.

7. W.-T. Wei, W.-W. Ying, W.-H. Bao, L.-H. Gao, X.-D. Xu, Y.-N. Wang, X.-X. Meng, G.-P. Chen and Q. Li, *ACS Sustainable Chem. Eng.*, 2018, **6**, 15301-15305.

8. T. Shen, Y. Yuan and N. Jiao, *Chem. Commun.*, 2014, **50**, 554-556.

9. S. Sau and P. Mal, *Chem. Commun.*, 2021, **57**, 9228-9231.

10. M. Hu, B. Liu, X.-H. Ouyang, R.-J. Song and J.-H. Li, *Adv. Synth. Catal.*, 2015, **357**, 3332-3340.

11. C. L. Perrin, *J. Org. Chem.*, 2021, **86**, 14245-14249.

12. S. M. Bonesi and M. Fagnoni, *Chem. Eur. J.*, 2010, **16**, 13572-13589.

13. S. Manna, S. Maity, S. Rana, S. Agasti and D. Maiti, *Org. Lett.*, 2012, **14**, 1736-1739.

14. X.-F. Wu, J. Schranck, H. Neumann and M. Beller, *Chem. Commun.*, 2011, **47**, 12462-12463.

15. J. I. Murray, M. V. Silva Elipe, K. D. Baucom, D. B. Brown, K. Quasdorf and S. Caille, *J. Org. Chem.*, 2021, DOI: 10.1021/acs.joc.1c00886.

16. M. Zarei, E. Noroozizadeh, A. R. Moosavi-Zare and M. A. Zolfigol, *J. Org. Chem.*, 2018, **83**, 3645-3650.

17. P. Natarajan, R. Chaudhary and P. Venugopalan, *J. Org. Chem.*, 2015, **80**, 10498-10504.

18. C. Kohlmeyer, M. Klüppel and G. Hilt, *J. Org. Chem.*, 2018, **83**, 3915-3920.

19. T. K. Achar, P. K. Sahoo and P. Mal, *ChemistrySelect*, 2017, **2**, 1944-1949.

20. Q.-Q. Kang, W. Wu, Q. Li and W.-T. Wei, *Green Chem.*, 2020, **22**, 3060-3068.

21. H.-Z. Wang, J.-Z. Li, Z. Guo, H. Zheng and W.-T. Wei, *ChemSusChem*, 2021, **14**, 4658-4670.

22. S. Mondal and A. Hajra, *J. Org. Chem.*, 2018, **83**, 11392-11398.

23. S. Duan, Y. Xu, X. Zhang and X. Fan, *Chem. Commun.*, 2016, **52**, 10529-10532.

24. J. Dong, P. Liu and P. Sun, *J. Org. Chem.*, 2015, **80**, 2925-2929.

25. W. Liu and L. Ackermann, *Org. Lett.*, 2013, **15**, 3484-3486.

26. N. Viswanadh, G. S. Ghotekar, M. B. Thoke, R. Velayudham, A. C. Shaikh, M. Karthikeyan and M. Muthukrishnan, *Chem. Commun.*, 2018, **54**, 2252-2255.

27. L.-Y. Xie, Y. Duan, L.-H. Lu, Y.-J. Li, S. Peng, C. Wu, K.-J. Liu, Z. Wang and W.-M. He, *ACS Sustainable Chem. Eng.*, 2017, **5**, 10407-10412.

28. B. K. Singh and R. Jana, *J. Org. Chem.*, 2016, **81**, 831-841.

29. K. Seth, M. Nautiyal, P. Purohit, N. Parikh and A. K. Chakraborti, *Chem. Commun.*, 2015, **51**, 191-194.

30. X. Li, Y.-H. Liu, W.-J. Gu, B. Li, F.-J. Chen and B.-F. Shi, *Org. Lett.*, 2014, **16**, 3904-3907.

31. Q. Ke, G. Yan, J. Yu and X. Wu, *Org. Biomol. Chem.*, 2019, **17**, 5863-5881.

32. J. A. Pereira, A. M. Pessoa, M. N. D. S. Cordeiro, R. Fernandes, C. Prudêncio, J. P. Noronha and M. Vieira, *Eur. J. Med. Chem.*, 2015, **97**, 664-672.

33. S. Piras, M. Loriga, A. Carta, G. Paglietti, M. Paola Costi and S. Ferrari, *J. Heterocycl. Chem.*, 2006, **43**, 541-548.

34. R. Liu, Z. Huang, M. G. Murray, X. Guo and G. Liu, *J. Med. Chem.*, 2011, **54**, 5747-5768.

35. K. C. C. Aganda, B. Hong and A. Lee, *Adv. Synth. Catal.*, 2021, **363**, 1443-1448.

36. L.-Y. Xie, S. Peng, L.-H. Yang, C. Peng, Y.-W. Lin, X. Yu, Z. Cao, Y.-Y. Peng and W.-M. He, *Green Chem.*, 2021, **23**, 374-378.

37. L. Hu, J. Yuan, J. Fu, T. Zhang, L. Gao, Y. Xiao, P. Mao and L. Qu, *Eur. J. Org. Chem.*, 2018, **2018**, 4113-4120.

38. J. Wang, B. Sun, L. Zhang, T. Xu, Y. Xie and C. Jin, *Org. Chem. Front.*, 2020, **7**, 113-118.

39. J. Yuan, S. Liu, Y. Xiao, P. Mao, L. Yang and L. Qu, *Org. Biomol. Chem.*, 2019, **17**, 876-884.

40. S. Peng, D. Hu, J. L. Hu, Y. W. Lin, S. S. Tang, H. S. Tang, J. Y. He, Z. Cao and W. M. He, *Adv. Synth. Catal.*, 2019, **361**, 5721-5726.

41. M. Gao, Y. Li, L. Xie, R. Chauvin and X. Cui, *Chem. Commun.*, 2016, **52**, 2846-2849.

42. Q. Yang, X. Han, J. Zhao, H. Y. Zhang and Y. Zhang, *J. Org. Chem.*, 2019, **84**, 11417-11424.

43. L. Wang, Y. Zhang, F. Li, X. Hao, H.-Y. Zhang and J. Zhao, *Adv. Synth. Catal.*, 2018, **360**, 3969-3977.

44. D. Dewangan, K. Nakhate, A. Mishra, A. S. Thakur, H. Rajak, J. Dwivedi, S. Sharma and S. Paliwal, *J. Heterocycl. Chem.*, 2019, **56**, 566-578.

45. Q.-H. Xia, W. Hu, C. Li, J.-F. Wu, L. Yang, X.-M. Han, Y.-M. Shen, Z.-Y. Li and X. Li, *Eur. J. Med. Chem.*, 2016, **124**, 311-325.

46. W. Xie, Y. Wu, J. Zhang, Q. Mei, Y. Zhang, N. Zhu, R. Liu and H. Zhang, *Eur. J. Med. Chem.*, 2018, **145**, 35-40.

47. M. G. Moloney, *Natural Product Reports*, 2002, **19**, 597-616.

48. P. Chaudhary, S. Gupta, N. Muniyappan, S. Sabiah and J. Kandasamy, *Green Chem.*, 2016, **18**, 2323-2330.

49. A. Bose, S. Sau and P. Mal, *Eur. J. Org. Chem.*, 2019, **2019**, 4105-4109.

50. K.-J. Li, Y.-Y. Jiang, K. Xu, C.-C. Zeng and B.-G. Sun, *Green Chem.*, 2019, **21**, 4412-4421.

51. SAINT+, Bruker AXS Inc., Madison, Wisconsin, USA, 1999 (Program for Reduction of Data collected on Bruker CCD Area Detector Diffractometer V. 6.02.)

52. SADABS, Bruker AXS, Madison, Wisconsin, USA, 2004

53. G. Sheldrick, *Acta Crystallogr. Sect. A*, 2008, **64**, 112-122.

54. M. M. Alanazi, H. A. Mahdy, N. A. Alsaif, A. J. Obaidullah, H. M. Alkahtani, A. A. Al-Mehizia, S. M. Alsubaie, M. A. Dahab and I. H. Eissa, *Bioorg. Chem.*, 2021, **112**, 104949.

55. J. Xu, H. Yang, L. He, L. Huang, J. Shen, W. Li and P. Zhang, *Org. Lett.*, 2021, **23**, 195-201.

56. S. Liu, Y. Huang, F.-L. Qing and X.-H. Xu, *Org. Lett.*, 2018, **20**, 5497-5501.

57. J. Xu, H. Cai, J. Shen, C. Shen, J. Wu, P. Zhang and X. Liu, *J. Org. Chem.*, 2021, **86**, 17816-17832.

58. K. Niu, L. Ding, P. Zhou, Y. Hao, Y. Liu, H. Song and Q. Wang, *Green Chemistry*, 2021, **23**, 3246-3249.

59. S. Paul, J. H. Ha, G. E. Park and Y. R. Lee, *Adv. Synth. Catal.*, 2017, **359**, 1515-1521.

60. D. Chen, Z.-J. Wang and W. Bao, *J. Org. Chem.*, 2010, **75**, 5768-5771.

61. K. D. Mane, R. B. Kamble and G. Suryavanshi, *New J. Chem.*, 2019, **43**, 7403-7408.

62. X. Zeng, C. Liu, X. Wang, J. Zhang, X. Wang and Y. Hu, *Org. Biomol. Chem.*, 2017, **15**, 8929-8935.

Copies of ^{1}H and ^{13}C NMR Spectra of selected compounds

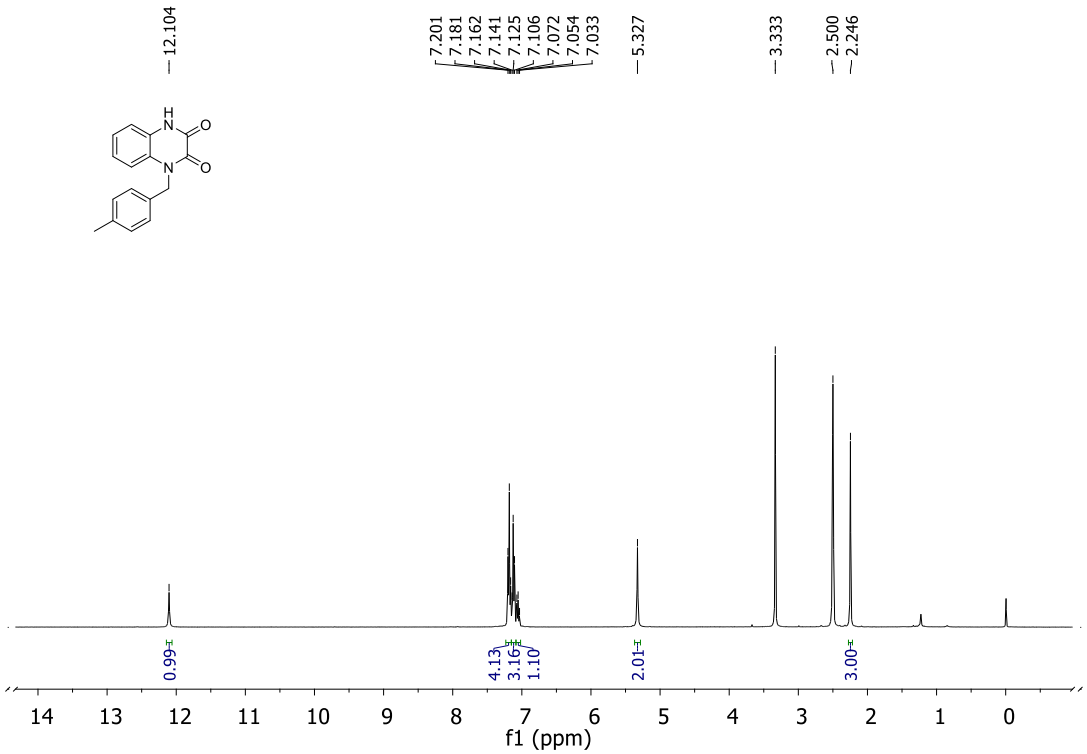

Figure 4.8. ^{1}H NMR of 1-(4-Methylbenzyl)-1,4-dihydroquinoxaline-2,3-dione (**2b**).

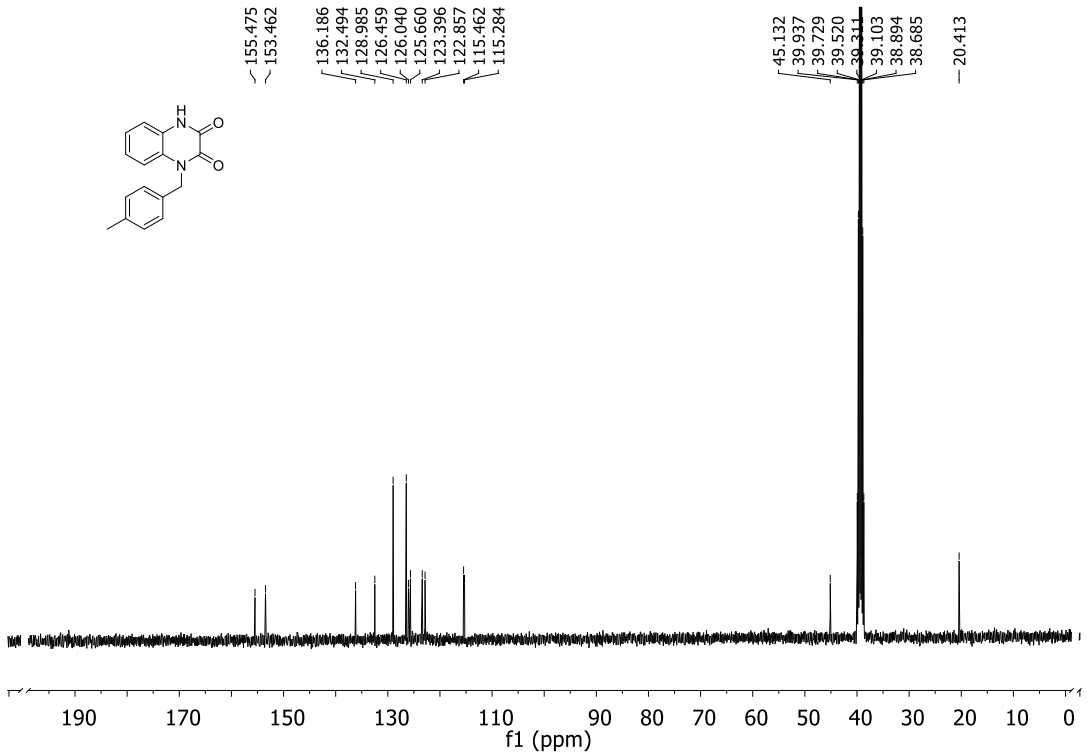

Figure 4.9. ^{13}C NMR of 1-(4-Methylbenzyl)-1,4-dihydroquinoxaline-2,3-dione (**2b**).

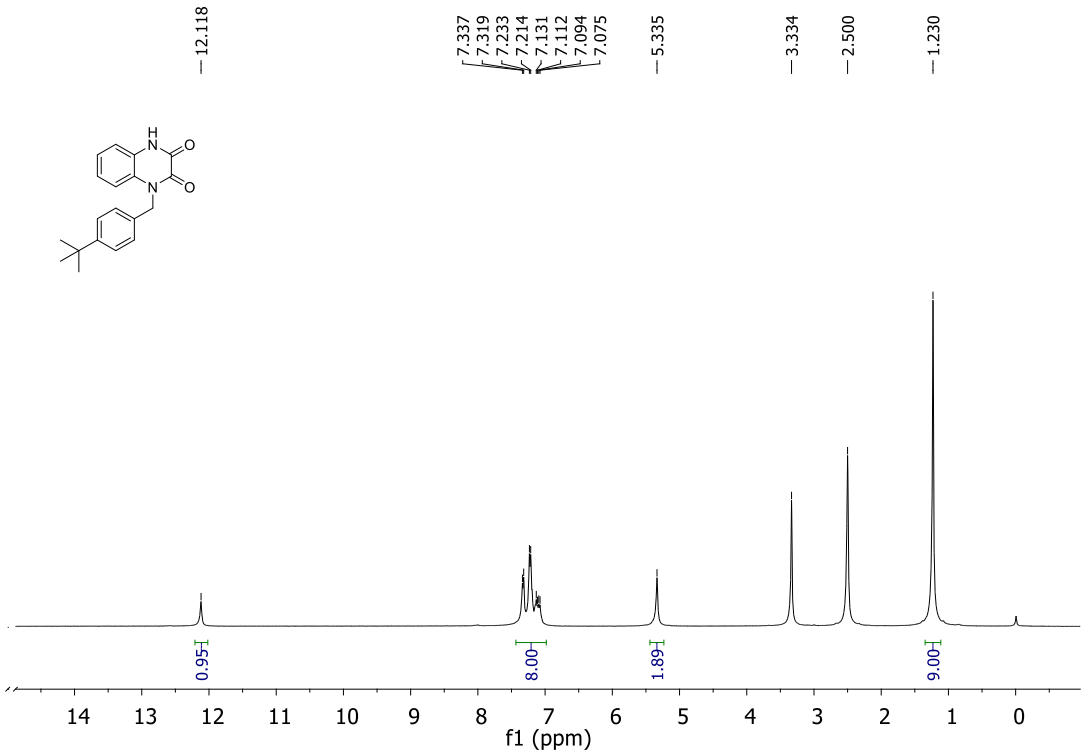

Figure 4.10. ^{1}H NMR of 1-(4-(tert-Butyl)benzyl)-1,4-dihydroquinoxaline-2,3-dione (**2d**).

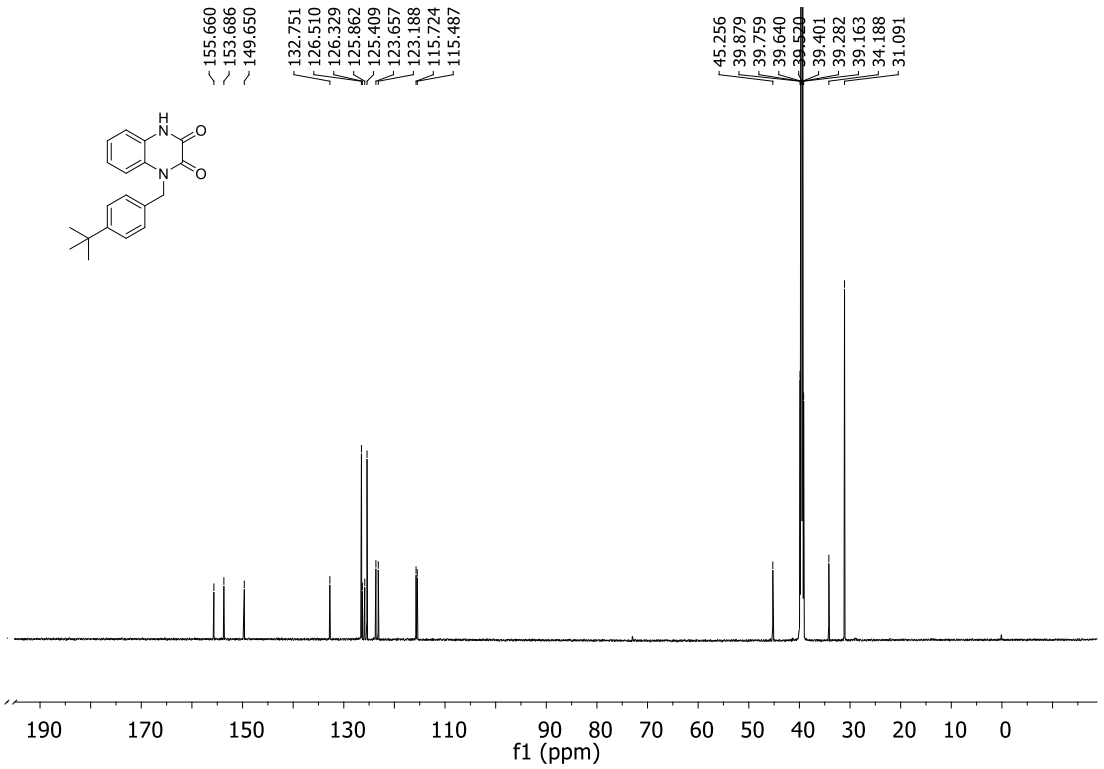

Figure 4.11. ^{13}C NMR of 1-(4-(*tert*-Butyl)benzyl)-1,4-dihydroquinoxaline-2,3-dione (**2d**).

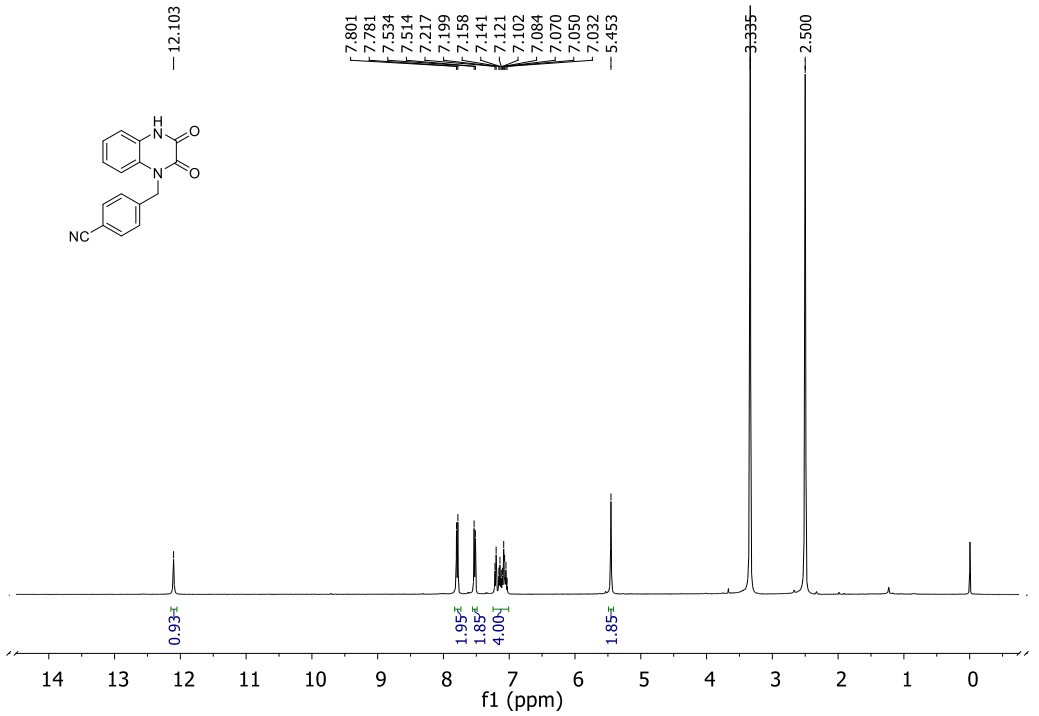

Figure 4.12. ^{1}H NMR of 4-((2,3-Dioxo-3,4-dihydroquinoxalin-1(2H)-yl)methyl)benzonitrile (**2e**)

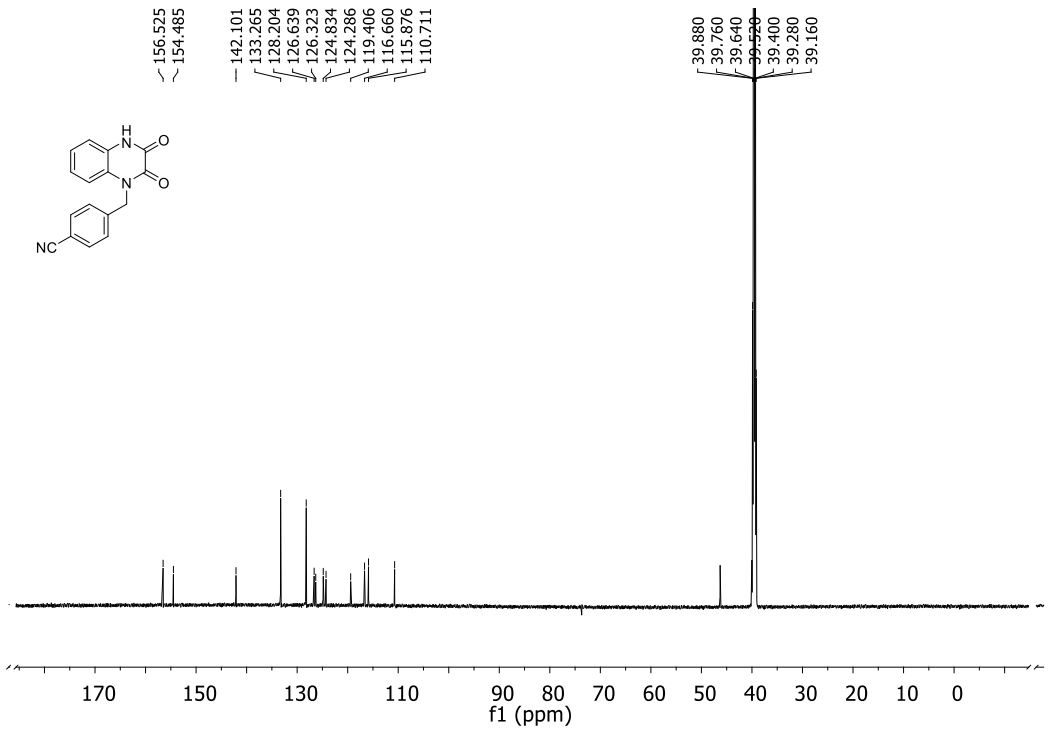

Figure 4.13. ^{13}C NMR of 4-((2,3-Dioxo-3,4-dihydroquinoxalin-1(2H)-yl)methyl)benzonitrile (**2e**).

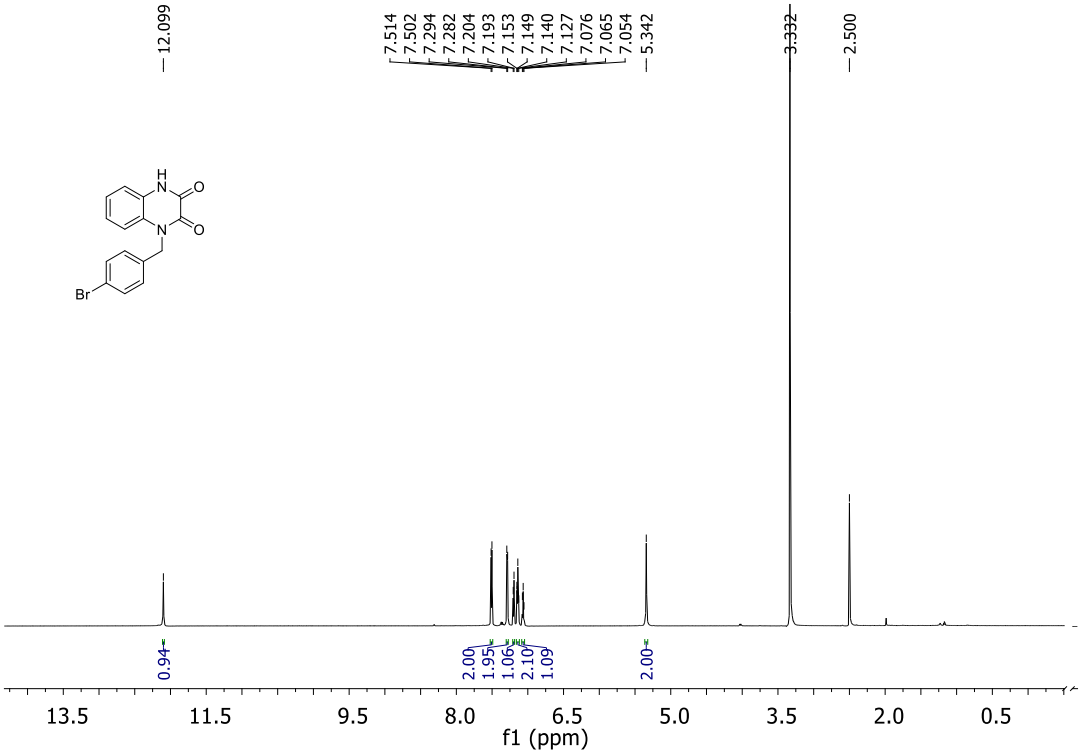

Figure 4.14.. ^{1}H NMR of 1-(4-bromobenzyl)-1,4-dihydroquinoxaline-2,3-dione (**2f**).

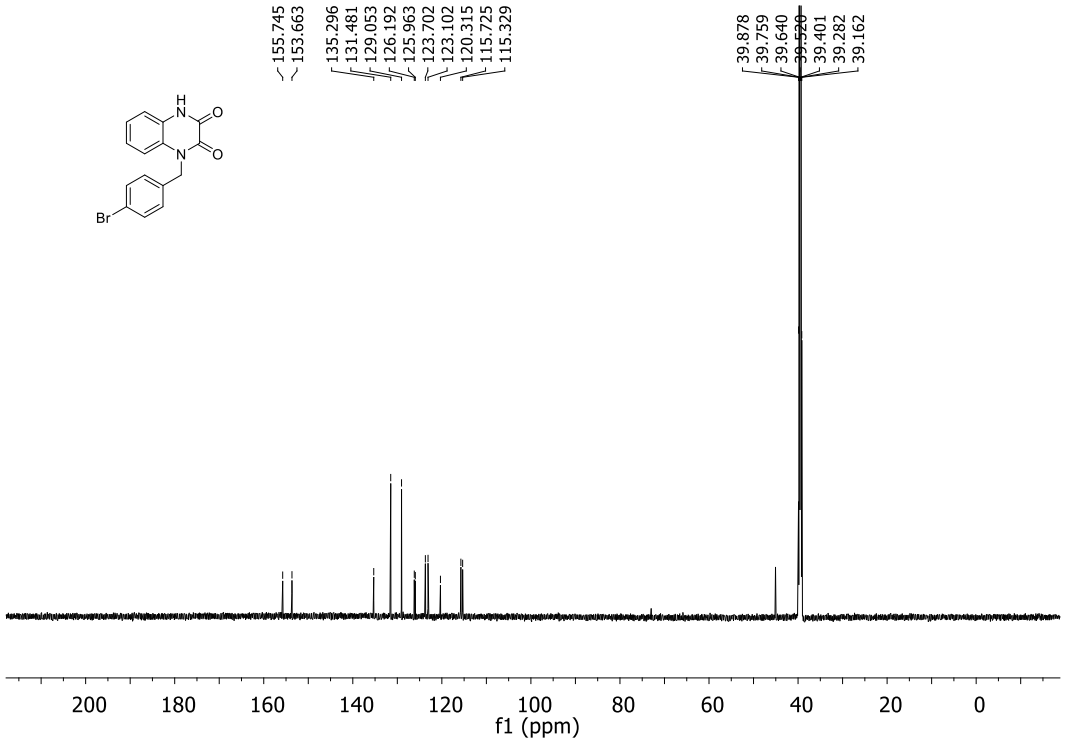

Figure 4.15. ^{13}C NMR of 1-(4-bromobenzyl)-1,4-dihydroquinoxaline-2,3-dione (**2f**).

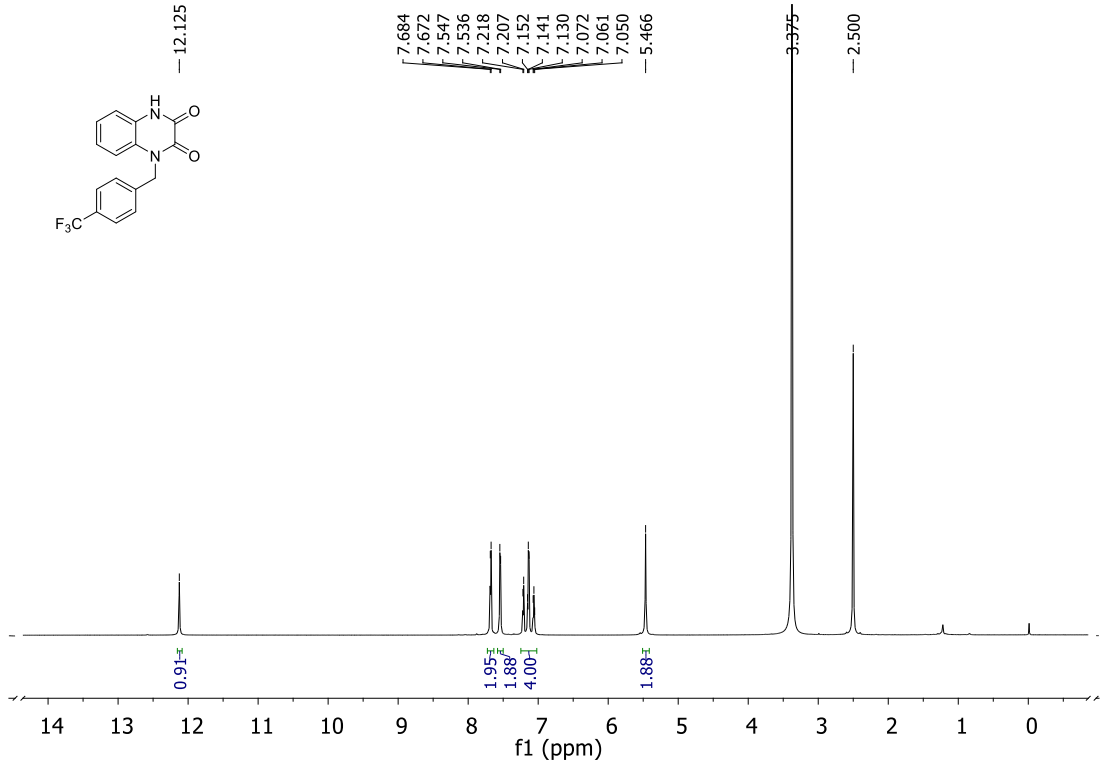

Figure 4.16. ^{1}H NMR of 1-(4-(Trifluoromethyl)benzyl)-1,4-dihydroquinoxaline-2,3-dione (**2i**).

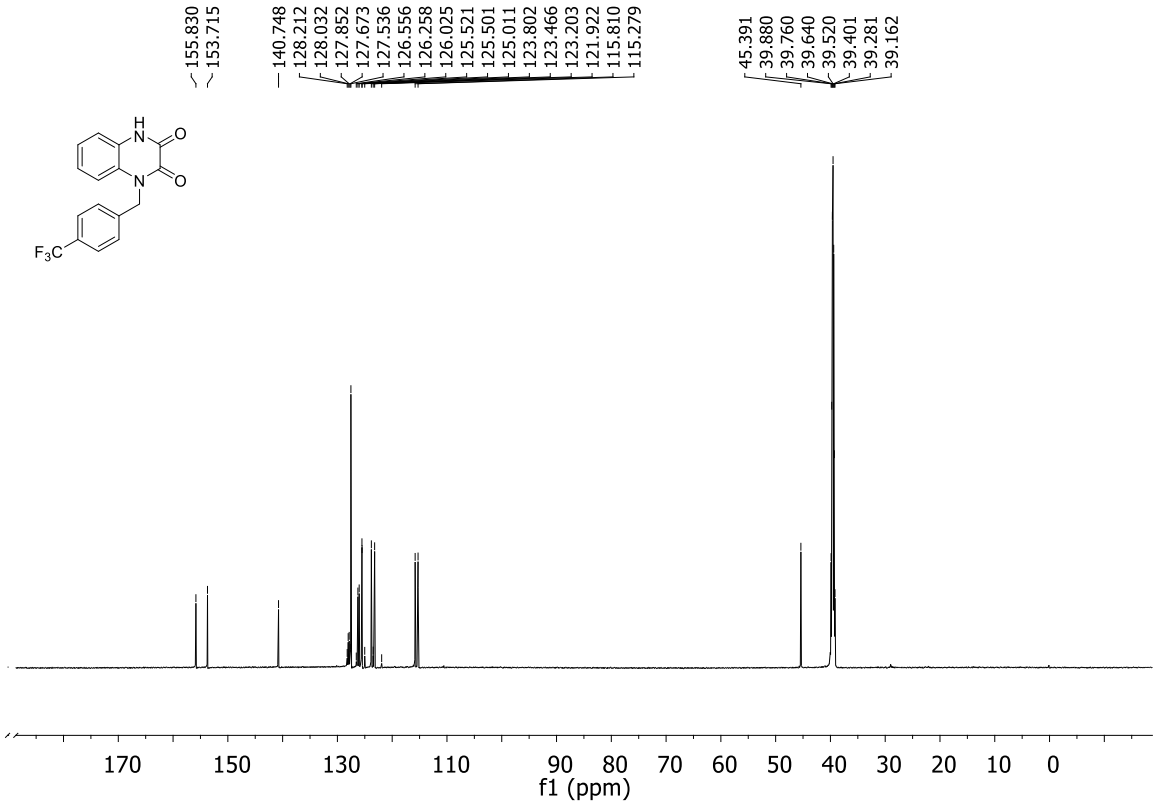

Figure 4.17. ^{13}C NMR of 1-(4-(Trifluoromethyl)benzyl)-1,4-dihydroquinoxaline-2,3-dione (**2i**).

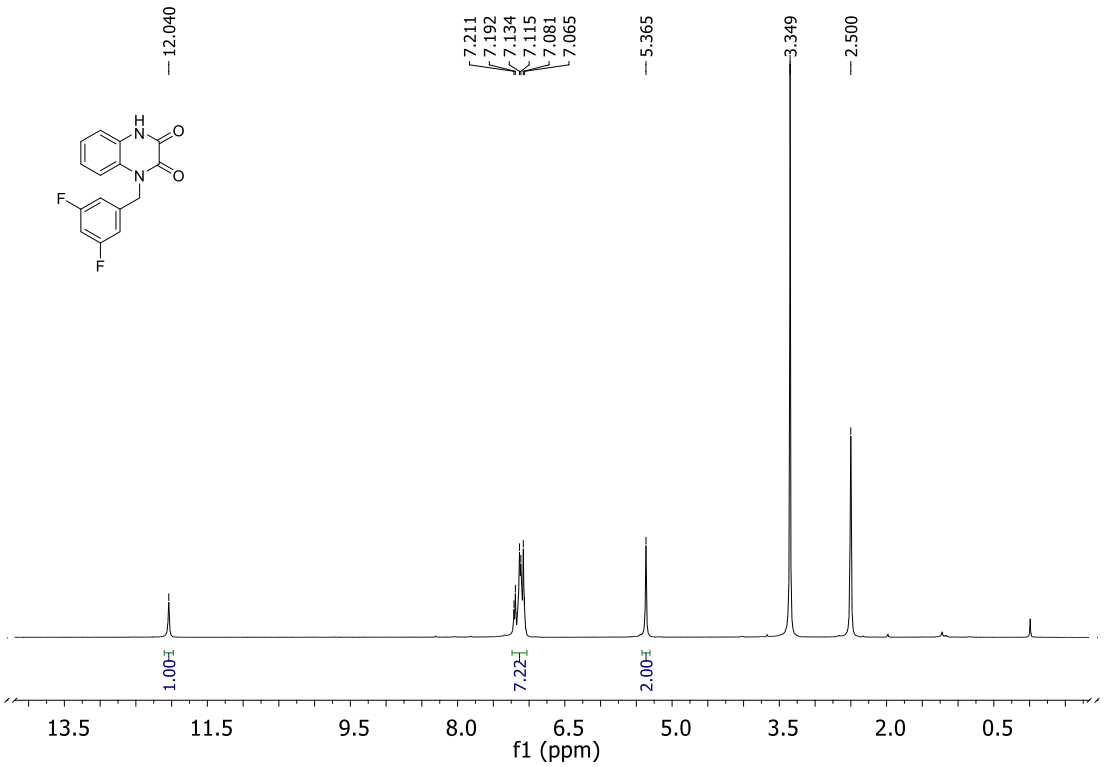

Figure 4.18. ^{1}H NMR of 1-(3,5-Difluorobenzyl)-1,4-dihydroquinoxaline-2,3-dione (**2j**).

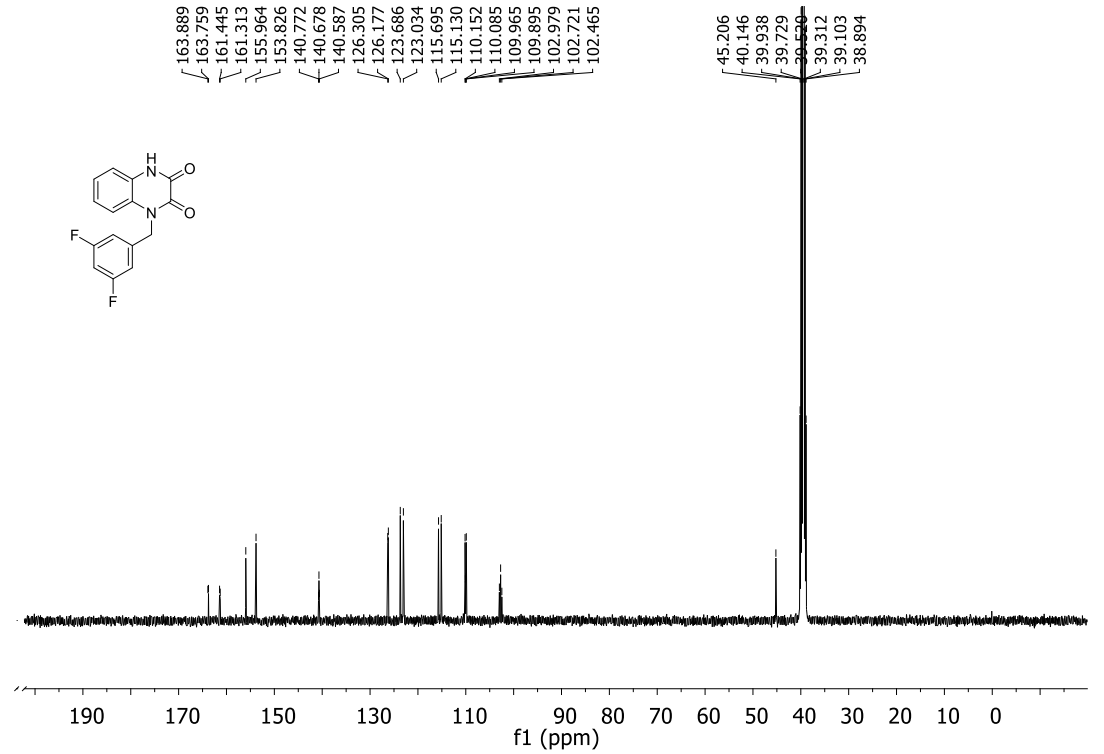

Figure 4.19. ^{13}C NMR of 1-(3,5-Difluorobenzyl)-1,4-dihydroquinoxaline-2,3-dione (**2j**).

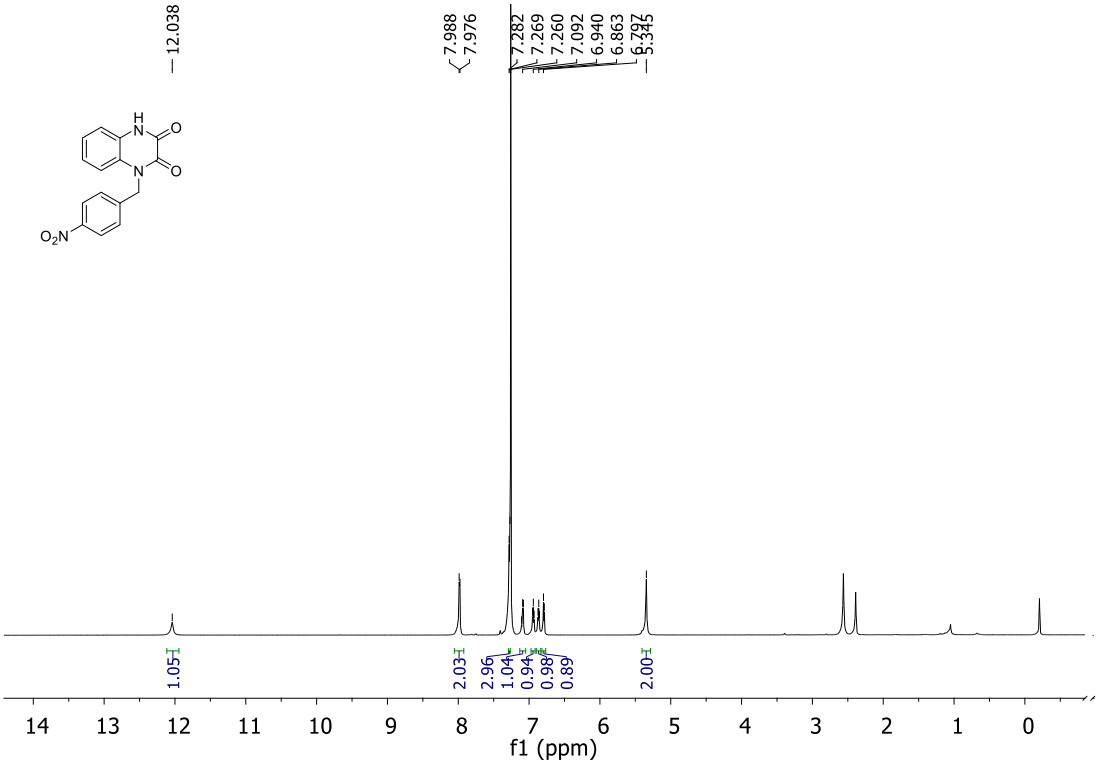

Figure 4.20. [1]H NMR of 1-(4-Nitrobenzyl)-1,4-dihydroquinoxaline-2,3-dione (**2k**).

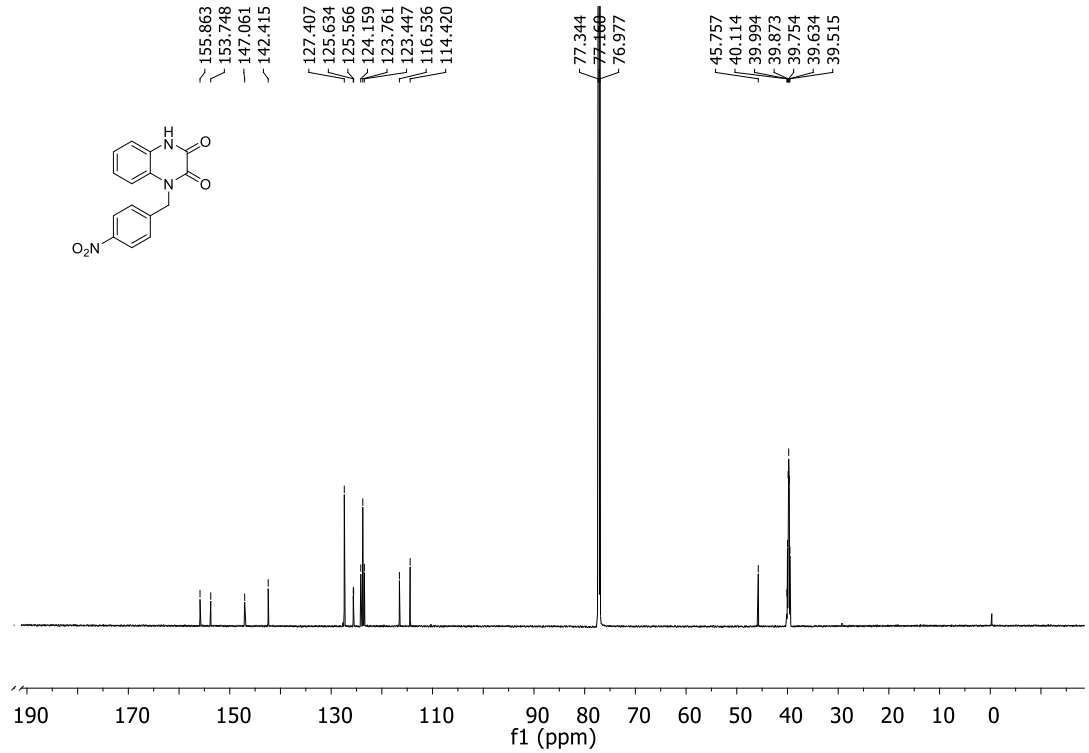

Figure 4.21. [13]C NMR of 1-(4-Nitrobenzyl)-1,4-dihydroquinoxaline-2,3-dione (**2k**).

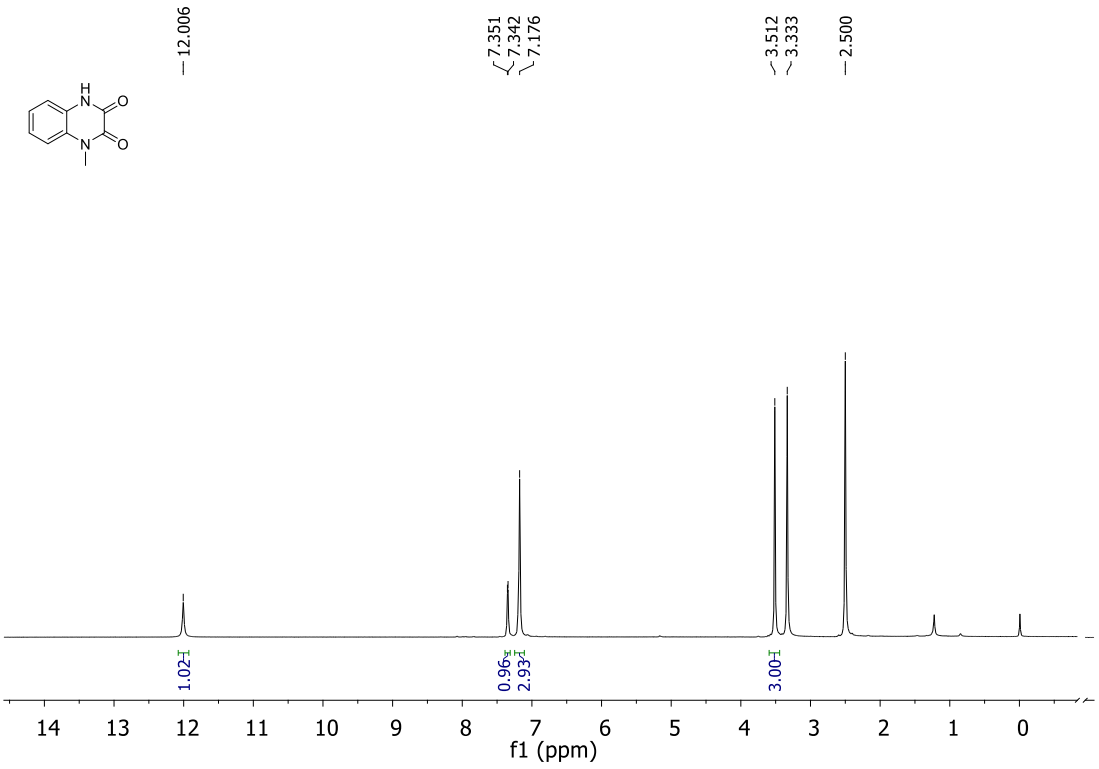

Figure 4.22. ^{1}H NMR of 1-Methyl-1,4-dihydroquinoxaline-2,3-dione (**2l**).

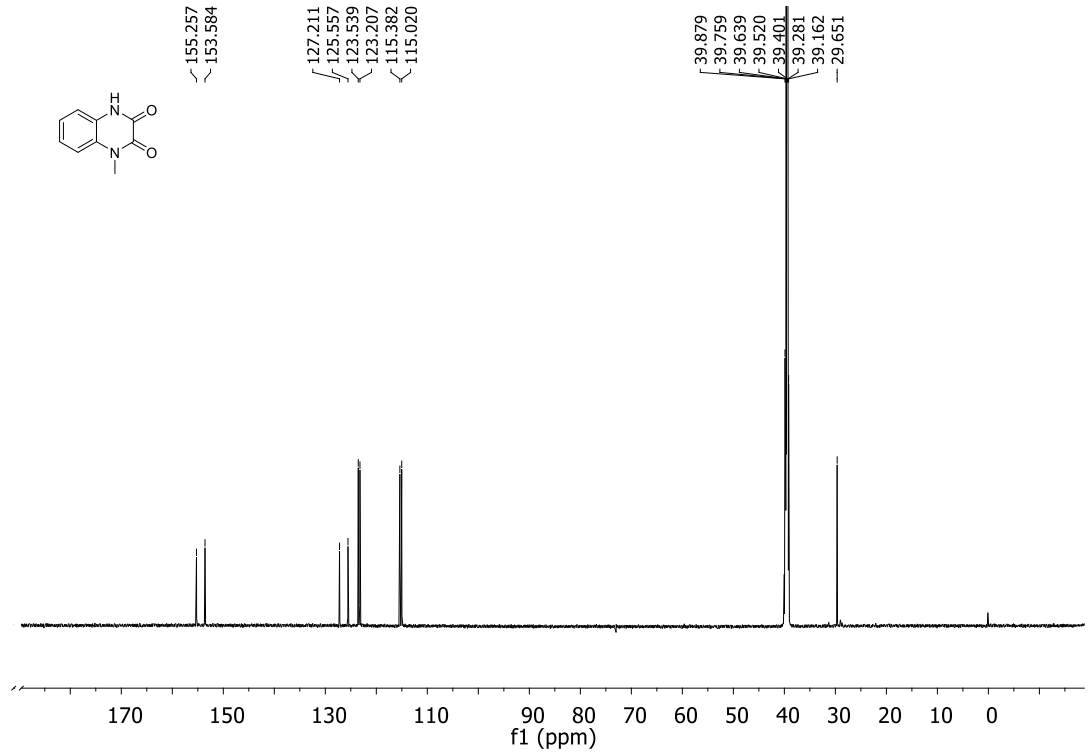

Figure 4.23. ^{13}C NMR of 1-Methyl-1,4-dihydroquinoxaline-2,3-dione (**2l**).

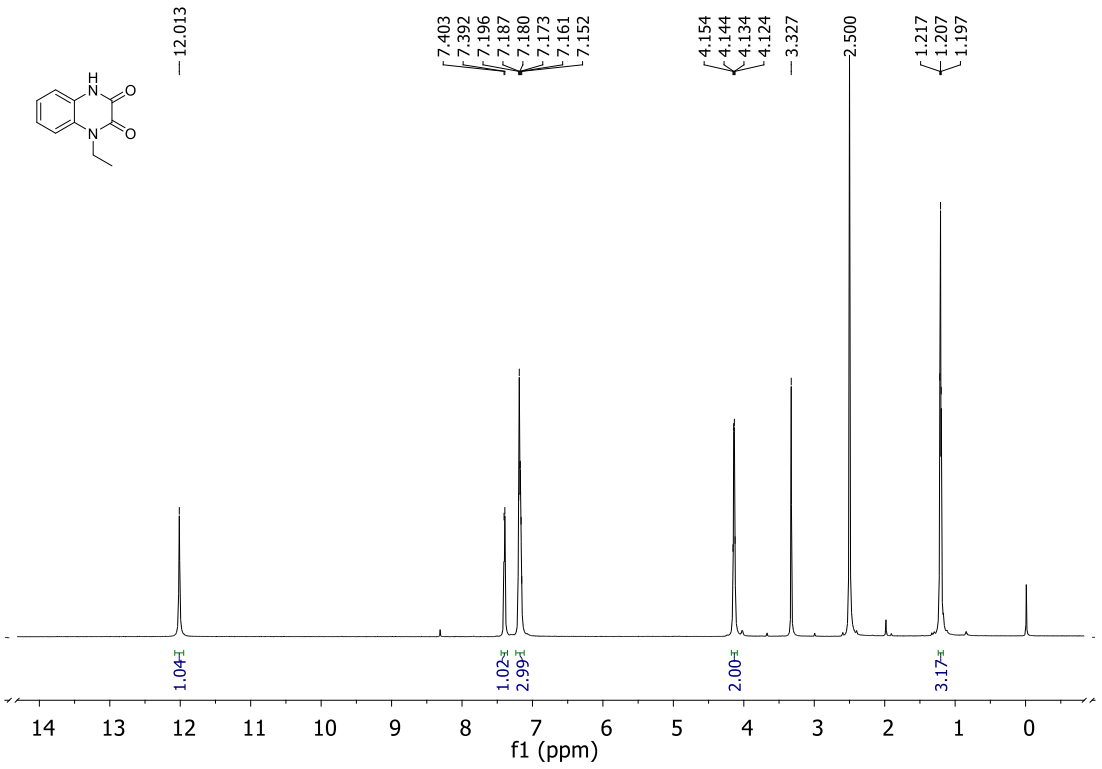

Figure 4.24. ^{1}H NMR of 1-Ethyl-1,4-dihydroquinoxaline-2,3-dione (**2m**).

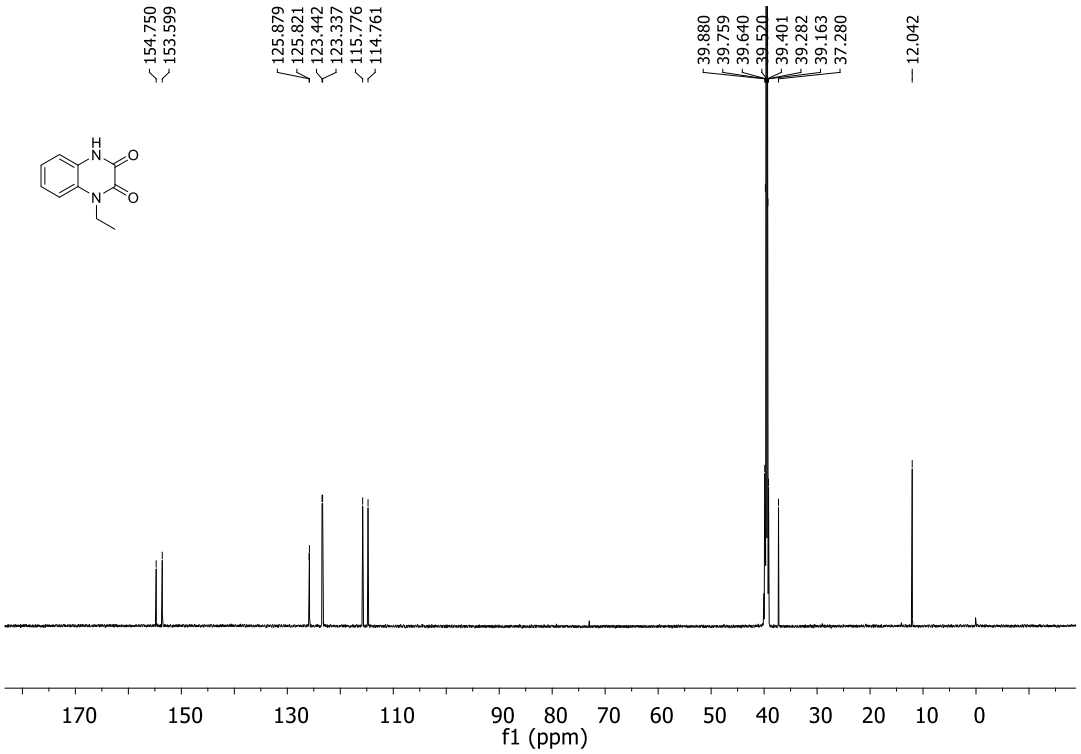

Figure 4.25. ^{13}C NMR of 1-Ethyl-1,4-dihydroquinoxaline-2,3-dione (**2m**).

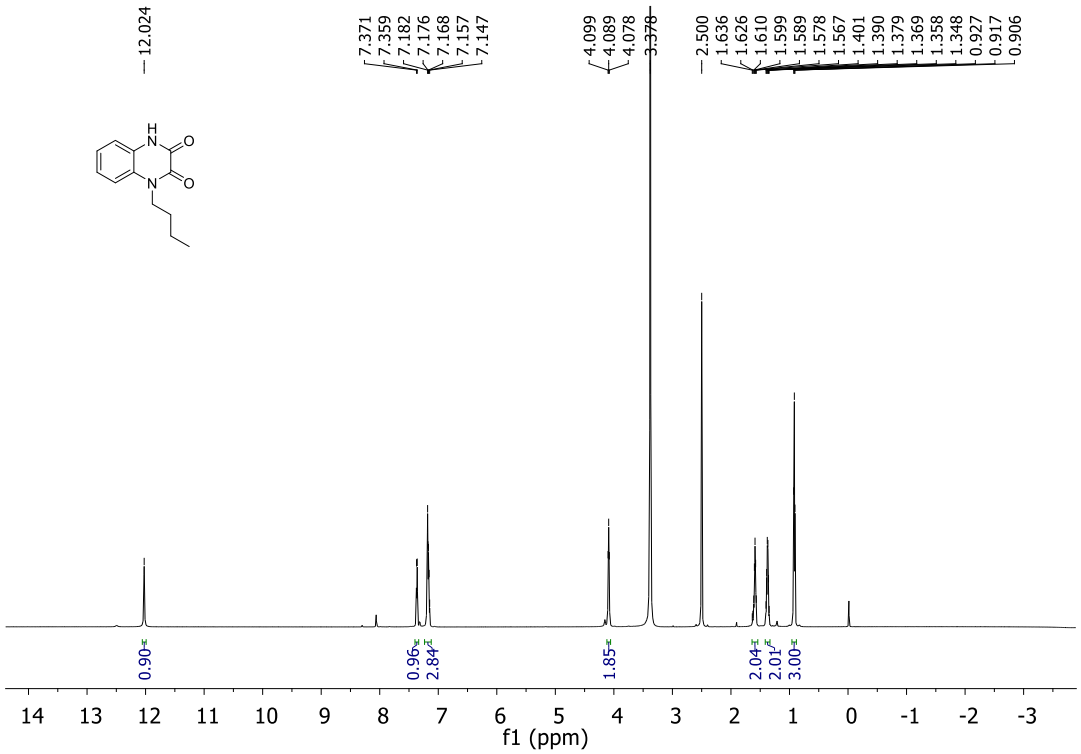

Figure 4.26. ^{1}H NMR of 1-Butyl-1,4-dihydroquinoxaline-2,3-dione (**2n**).

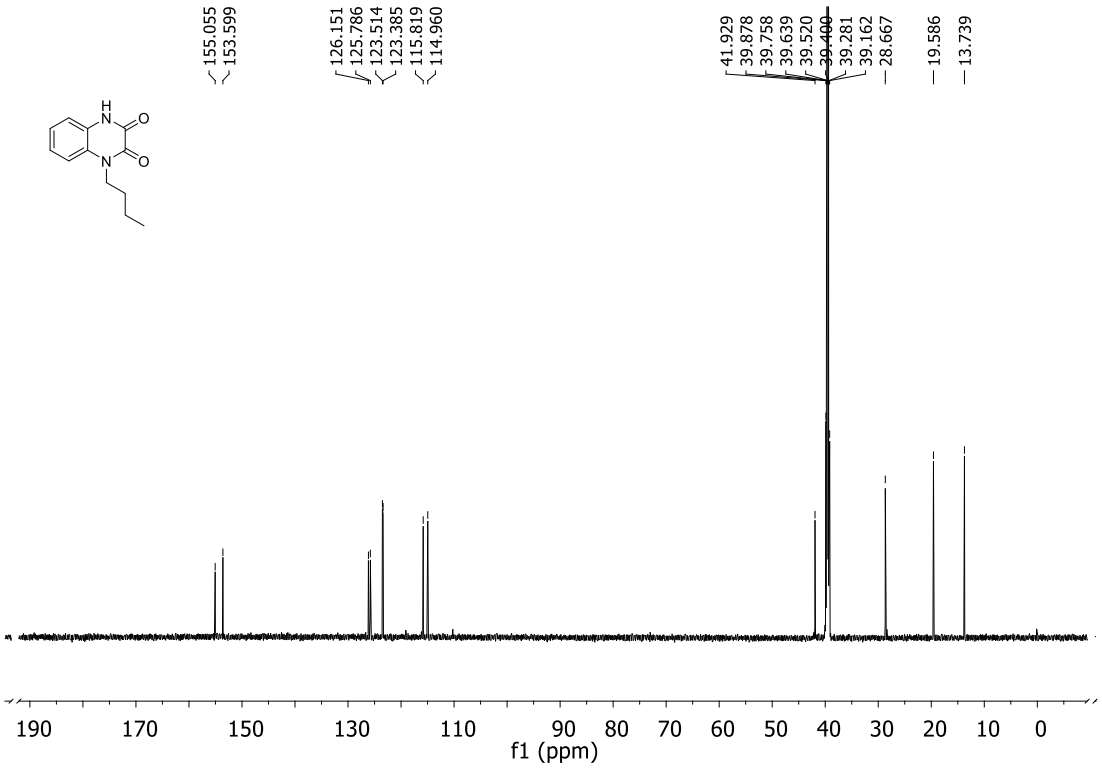

Figure 4.27. ^{13}C NMR of 1-Butyl-1,4-dihydroquinoxaline-2,3-dione (**2n**).

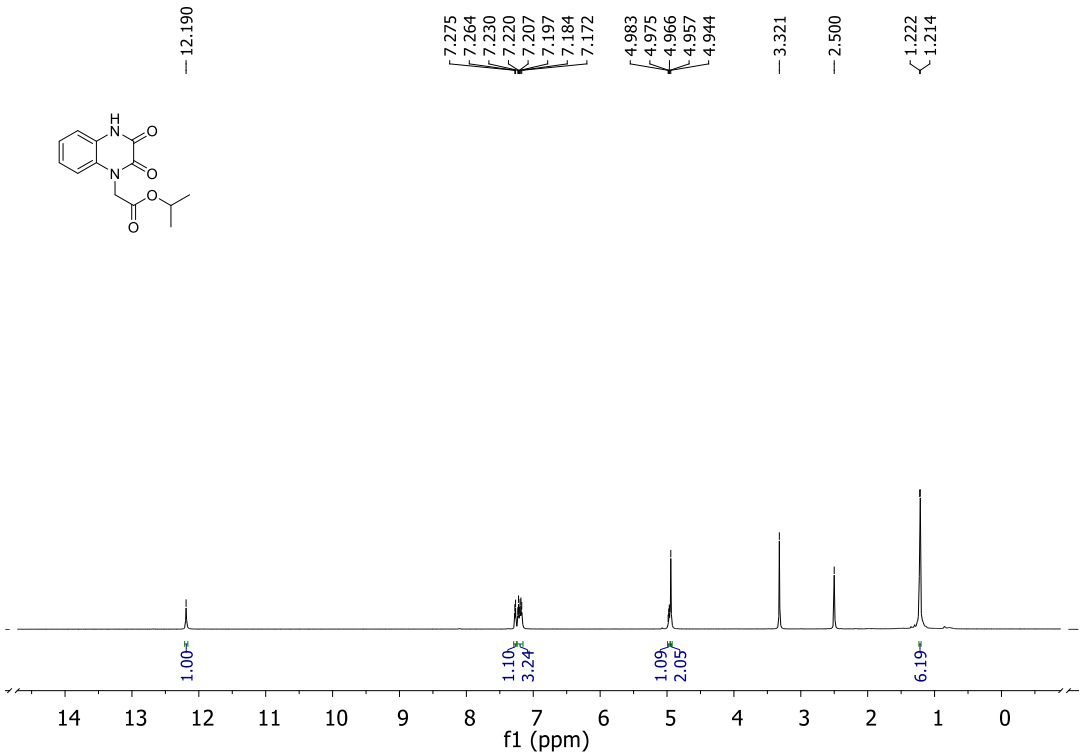

Figure 4.28. [1]H NMR of isopropyl 2-(2,3-dioxo-3,4-dihydroquinoxalin-1(2H)-yl)acetate (**2r**).

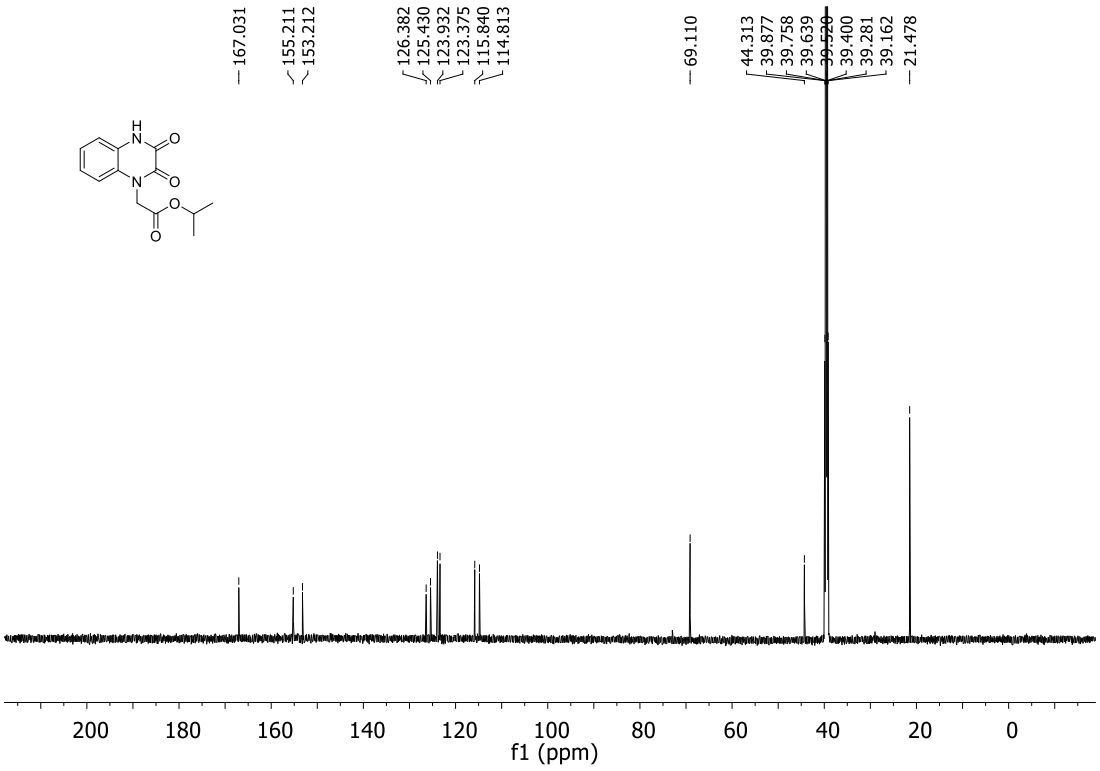

Figure 4.29. [13]C NMR of isopropyl 2-(2,3-dioxo-3,4-dihydroquinoxalin-1(2H)-yl)acetate (**2r**).

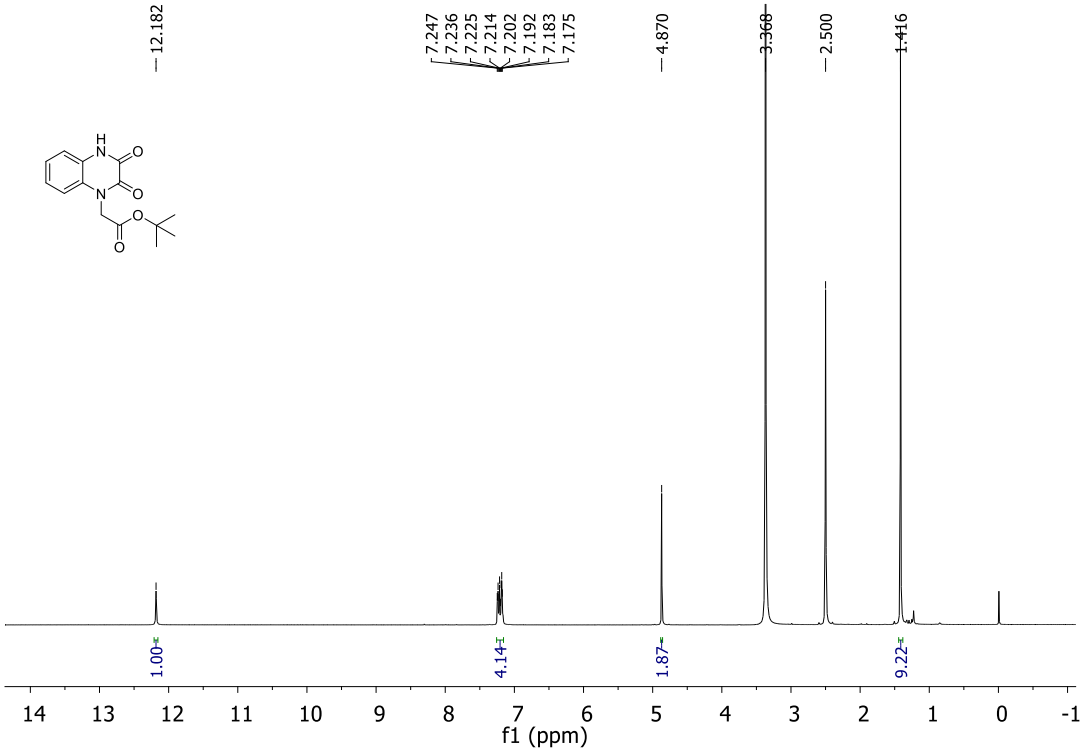

Figure 4.30. [1]H NMR of *tert*-Butyl 2-(2,3-dioxo-3,4-dihydroquinoxalin-1(2H)-yl)acetate (**2s**).

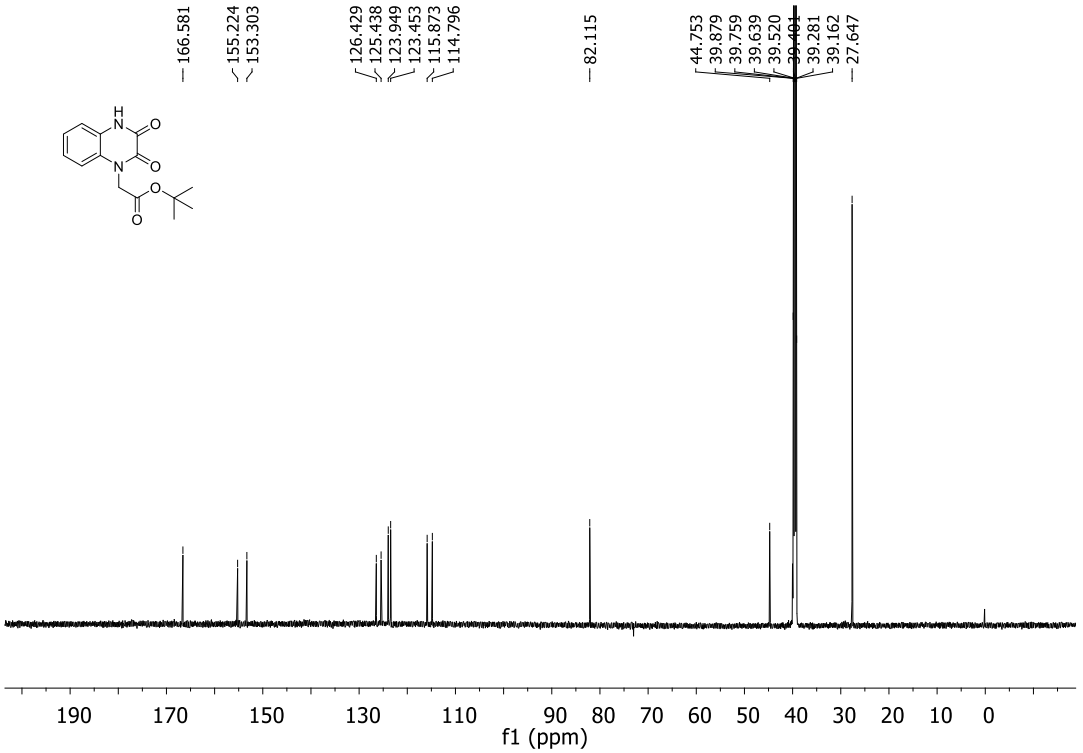

Figure 4.31. [1]H NMR of *tert*-Butyl 2-(2,3-dioxo-3,4-dihydroquinoxalin-1(2H)-yl)acetate **(2s).**

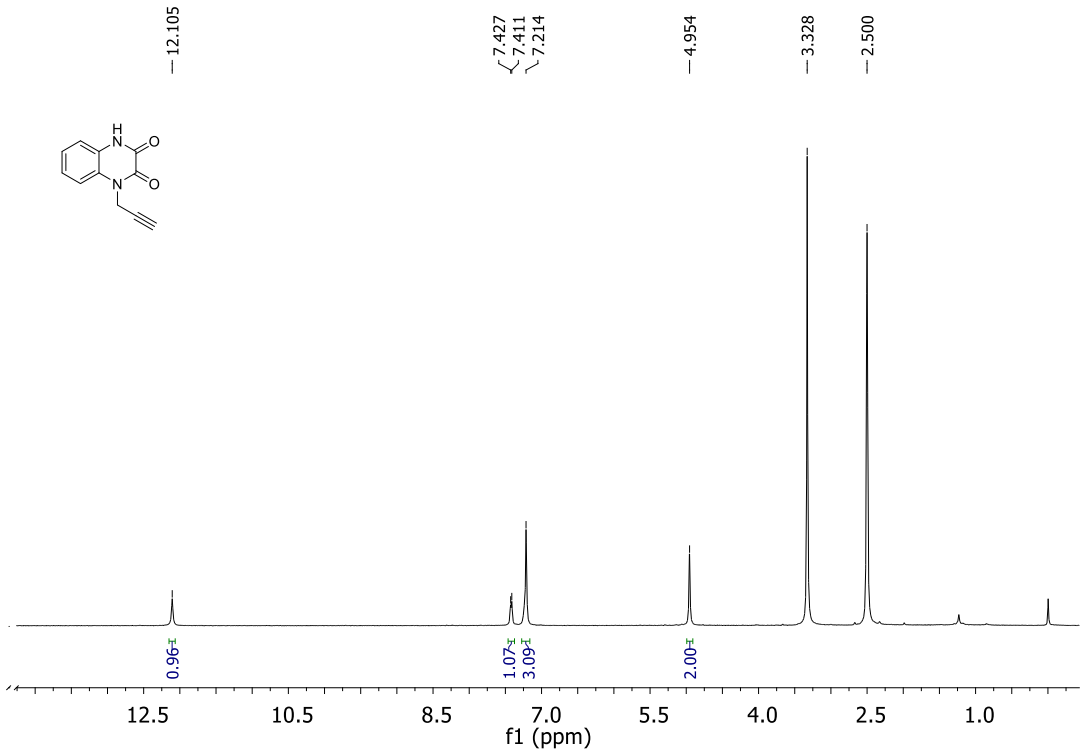

Figure 4.32. [1]H NMR of 1-(Prop-2-yn-1-yl)-1,4-dihydroquinoxaline-2,3-dione (**2t**).

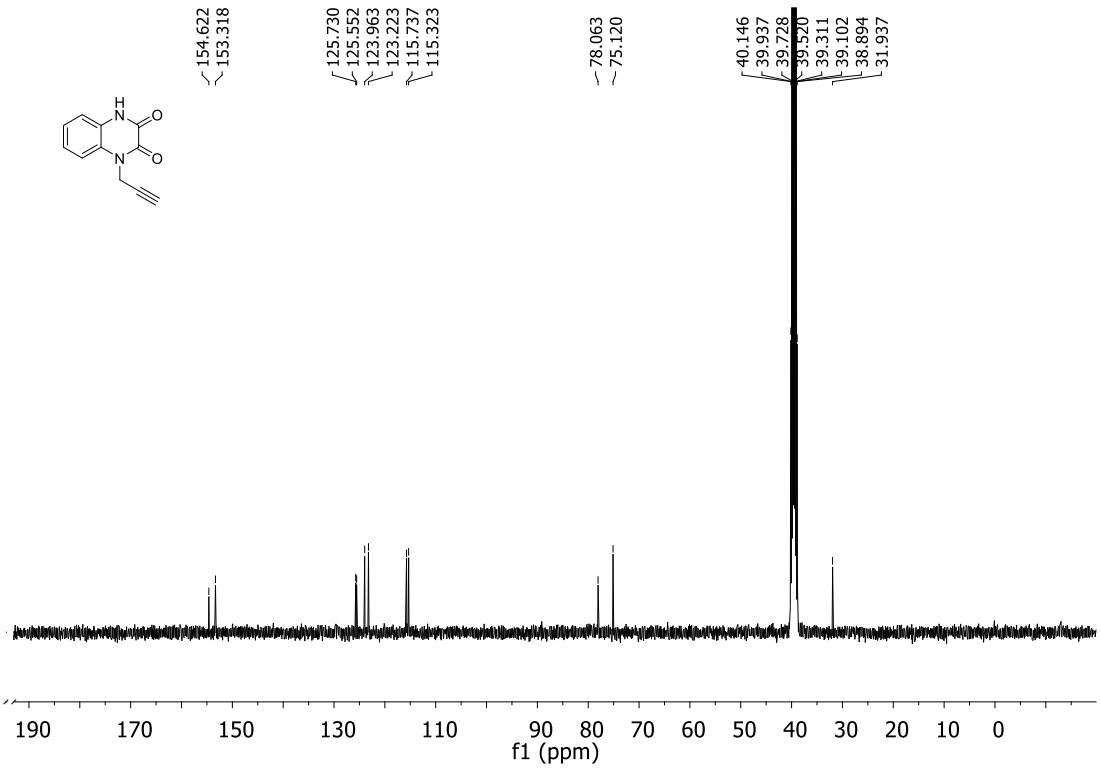

Figure 4.33. [13]C NMR of 1-(Prop-2-yn-1-yl)-1,4-dihydroquinoxaline-2,3-dione (**2t**).

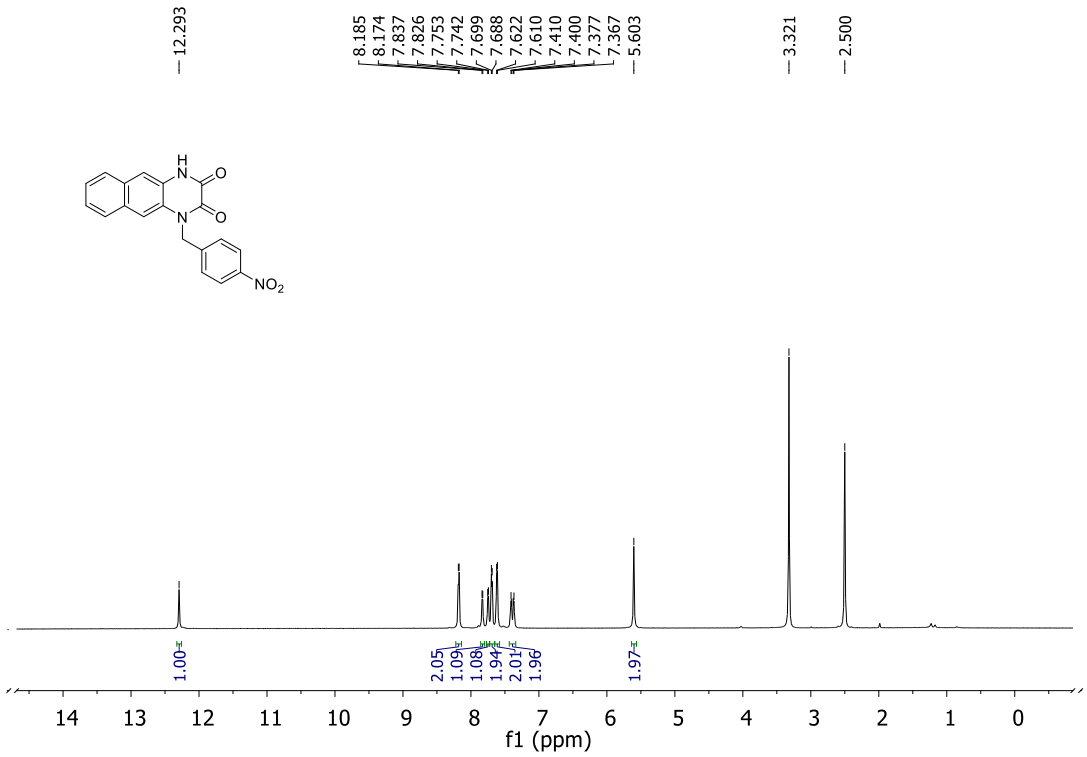

Figure 4.34. ^{1}H NMR of 1-(4-Nitrobenzyl)-1,4-dihydrobenzo[g]quinoxaline-2,3-dione (**4b**).

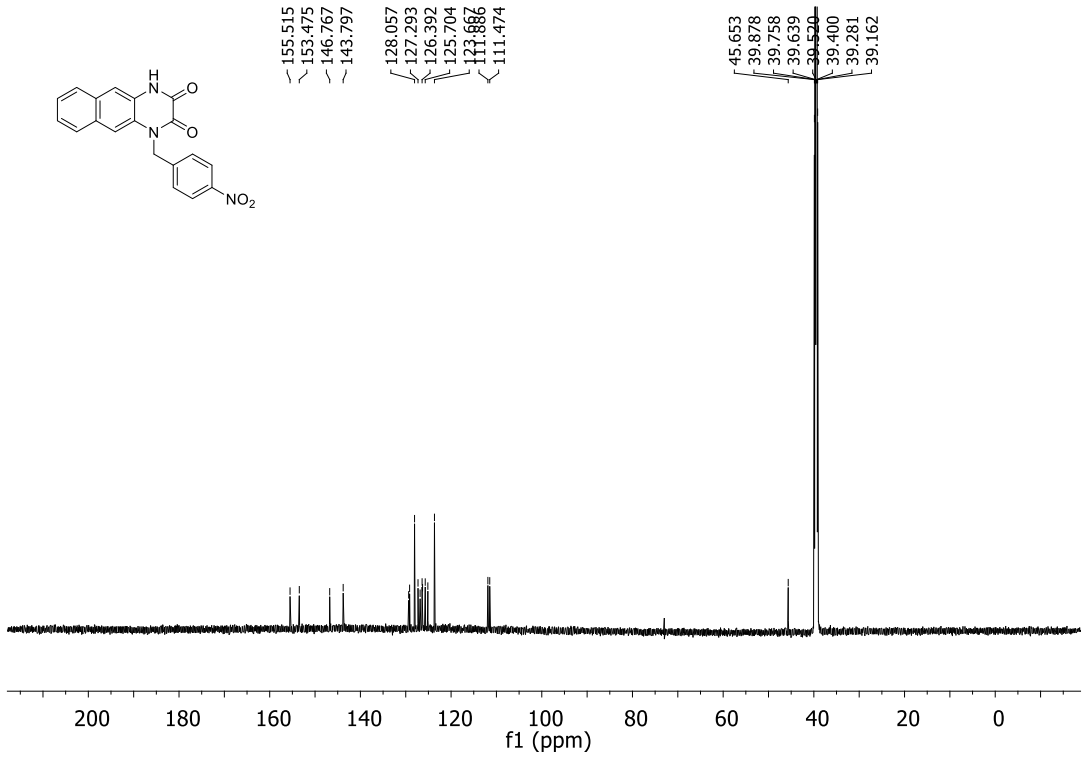

Figure 4.35. ^{13}C NMR of 1-(4-Nitrobenzyl)-1,4-dihydrobenzo[g]quinoxaline-2,3-dione (**4b**).

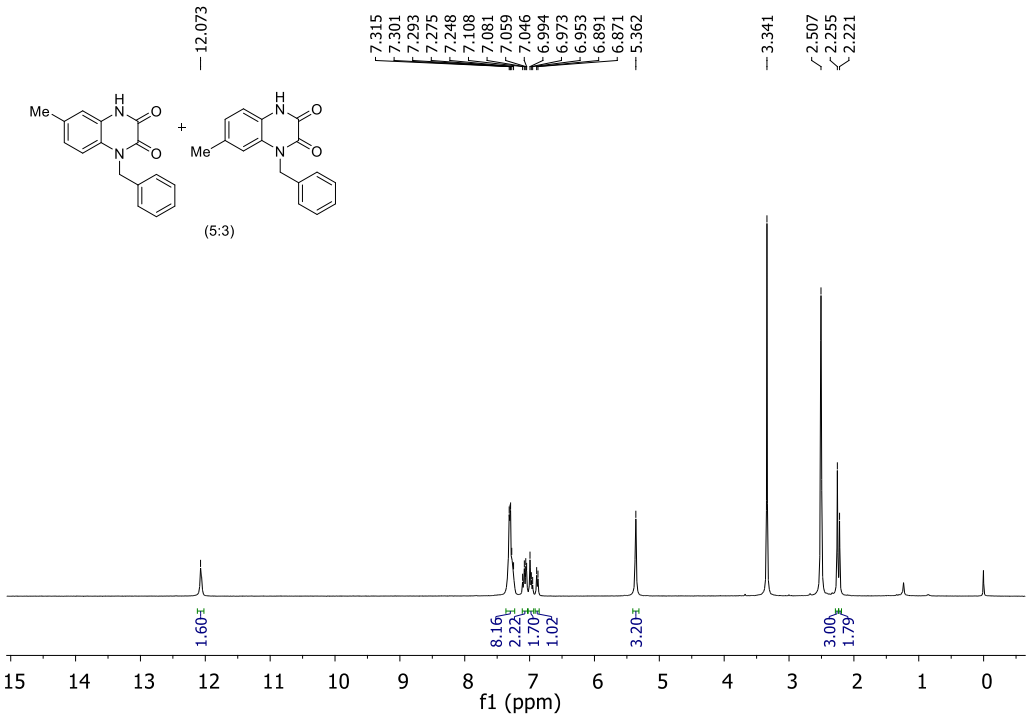

Figure 4.36. [1]H NMR of 1-Benzyl-6-methyl-1,4-dihydroquinoxaline-2,3-dione and 1-Benzyl-7-methyl-1,4-dihydroquinoxaline-2,3-dione (**4c**).

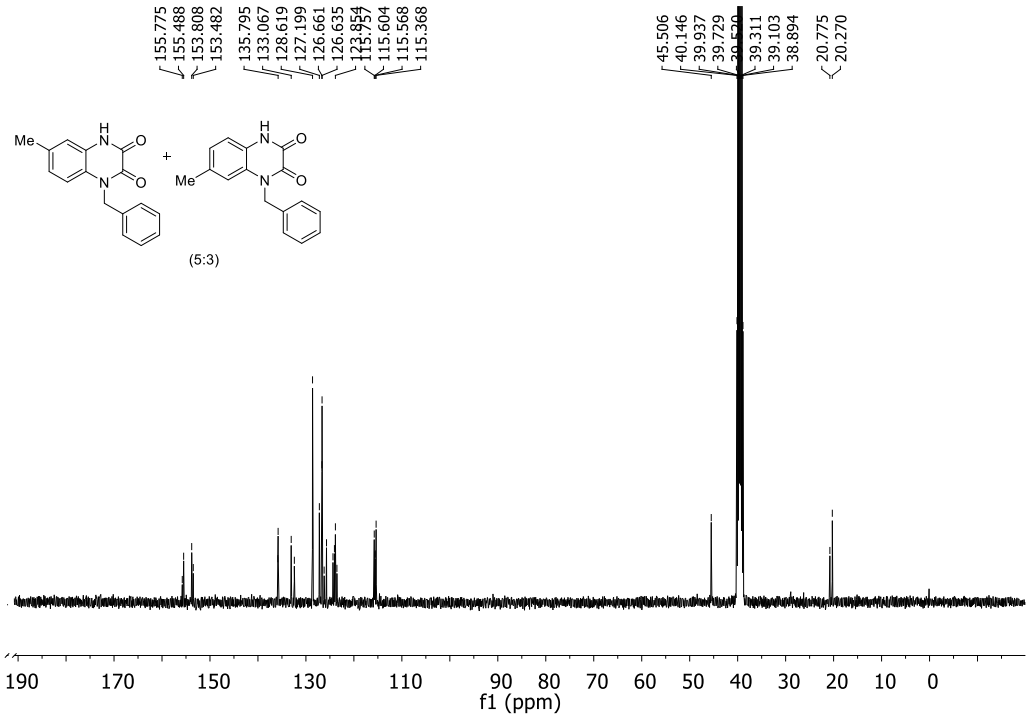

Figure 4.37. [13]C NMR of 1-Benzyl-6-methyl-1,4-dihydroquinoxaline-2,3-dione and 1-Benzyl-7-methyl-1,4-dihydroquinoxaline-2,3-dione (**4c**).

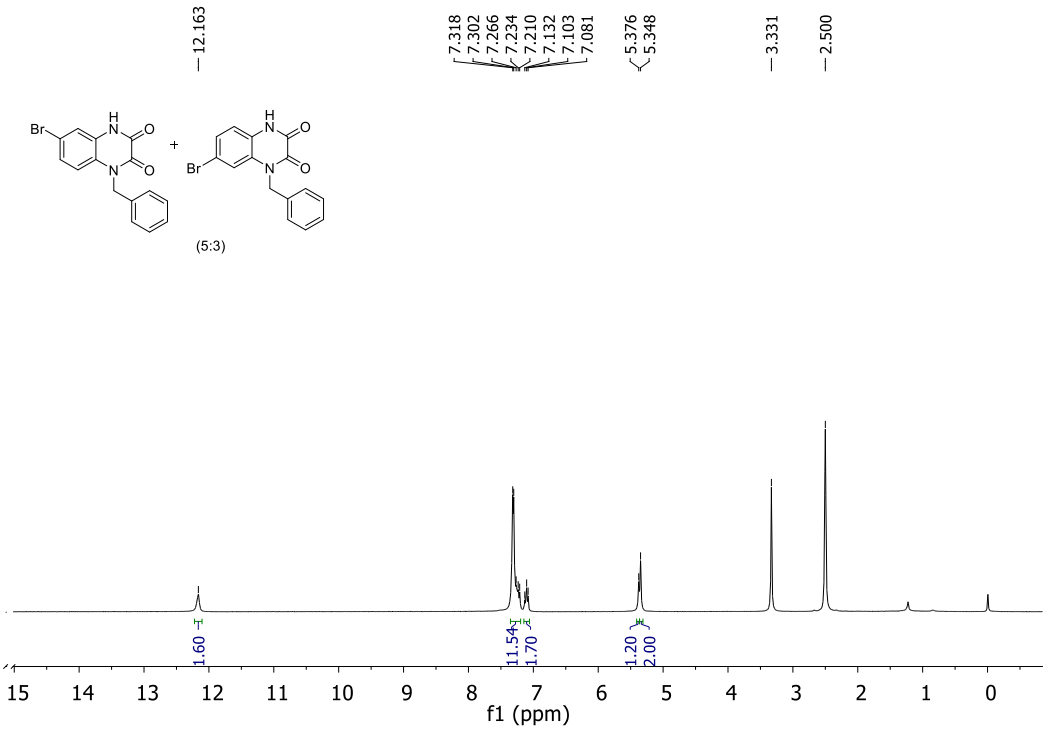

Figure 4.38. ^{1}H NMR of 1-Benzyl-6-bromo-1,4-dihydroquinoxaline-2,3-dione and 1-Benzyl-7-bromo-1,4-dihydroquinoxaline-2,3-dione (**4d**).

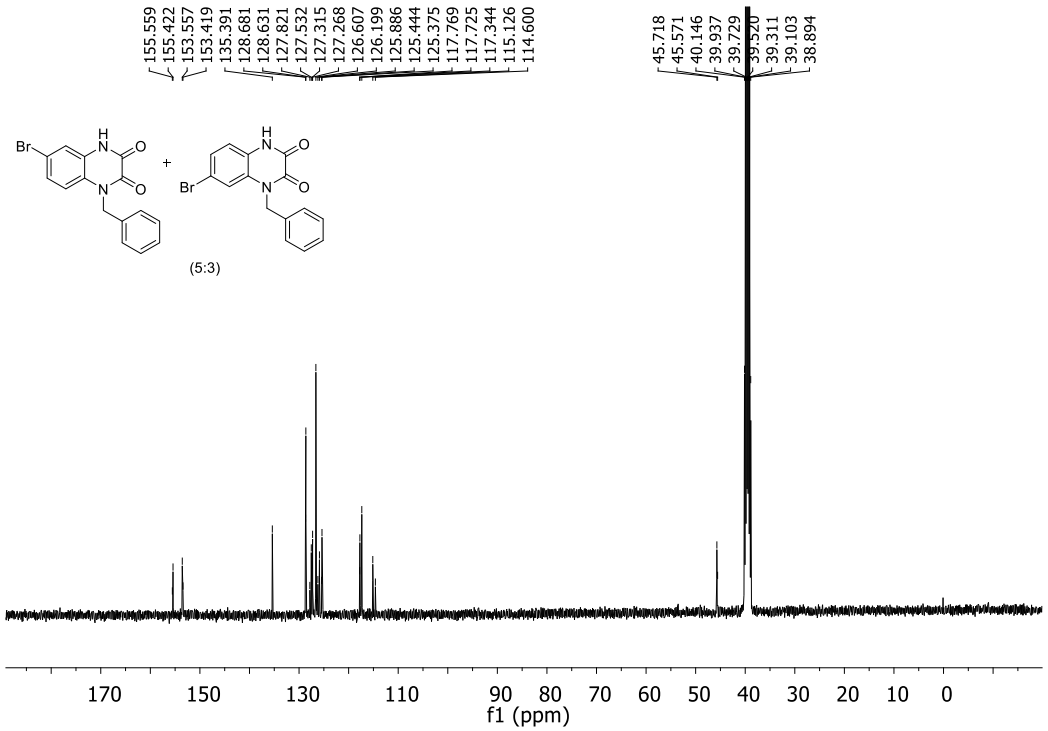

Figure 4.39. ^{13}C NMR of 1-Benzyl-6-bromo-1,4-dihydroquinoxaline-2,3-dione and 1-Benzyl-7-bromo-1,4-dihydroquinoxaline-2,3-dione (**4d**).

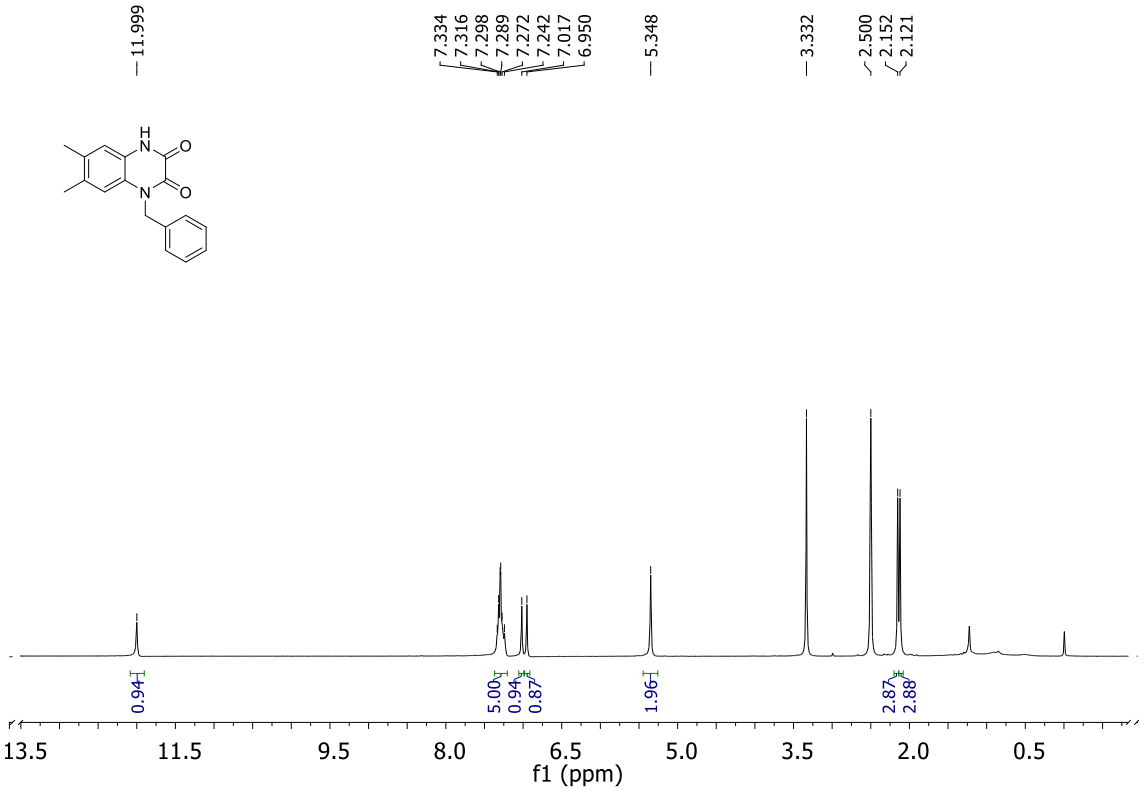

Figure 4.40. ^{1}H NMR of 1-Benzyl-6,7-dimethyl-1,4-dihydroquinoxaline-2,3-dione **(4f).**

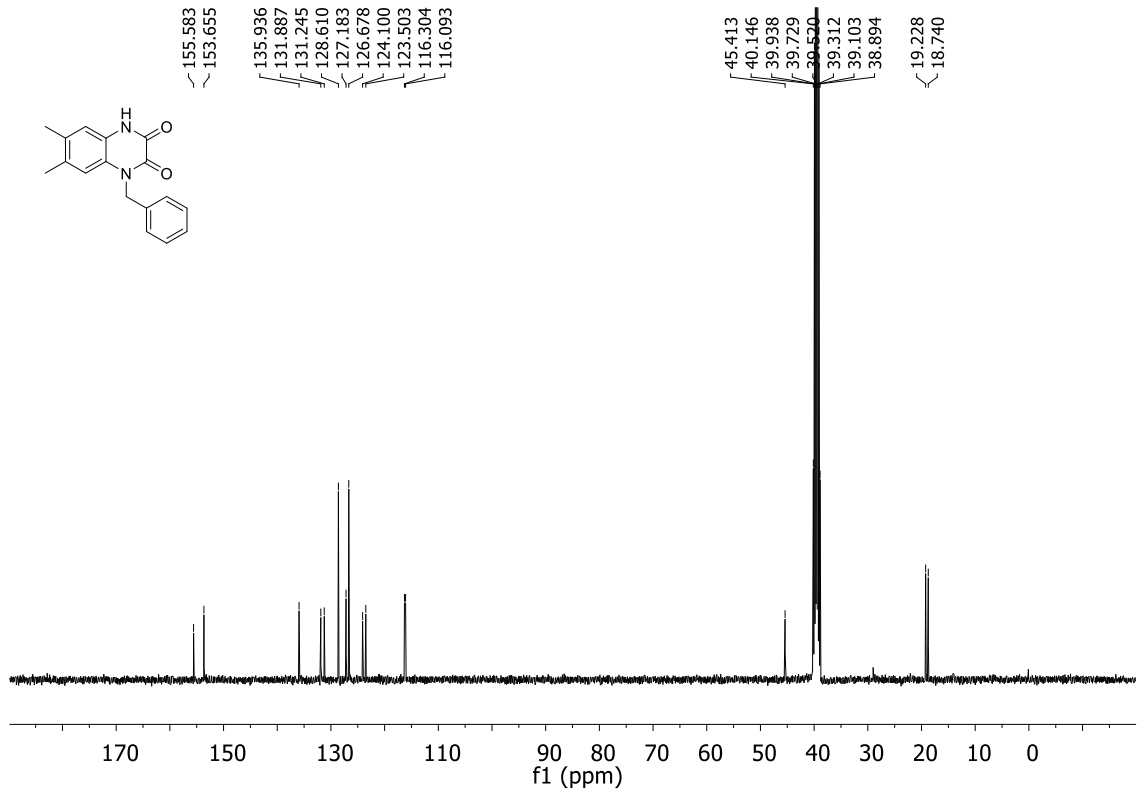

Figure 4.41. ^{13}C NMR of 1-Benzyl-6,7-dimethyl-1,4-dihydroquinoxaline-2,3-dione **(4f).**

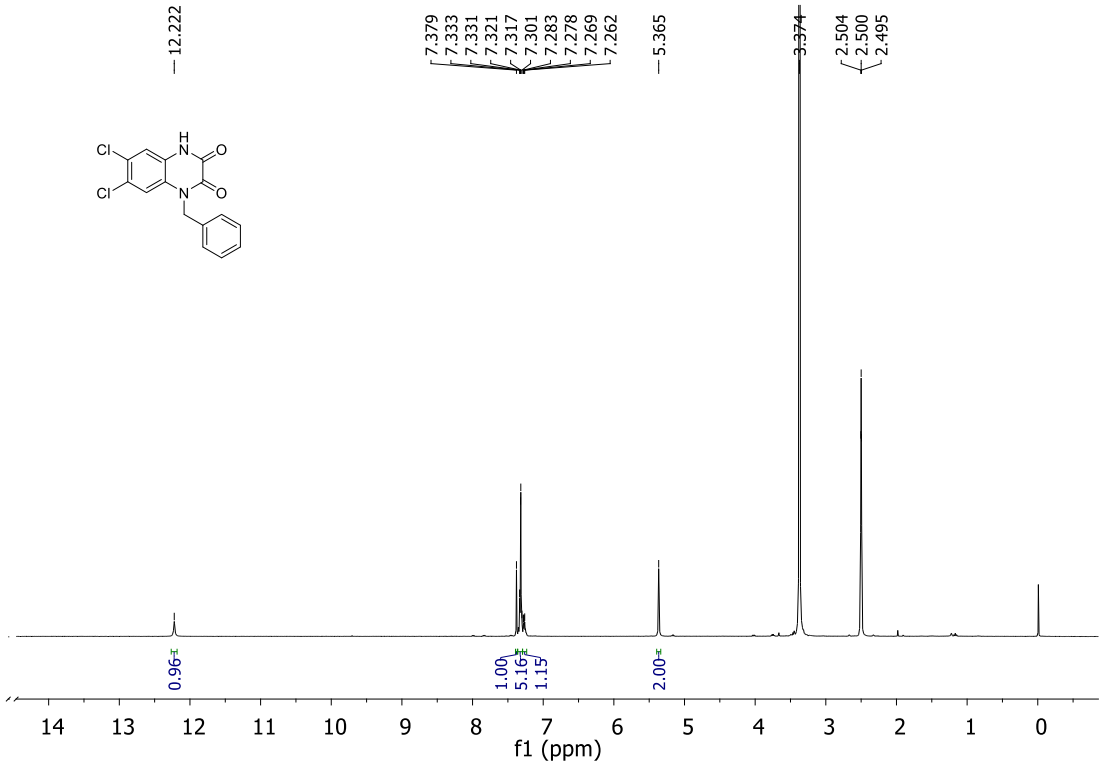

Figure 4.42. [1]H NMR of 1-Benzyl-6,7-dichloro-1,4-dihydroquinoxaline-2,3-dione (**4h**).

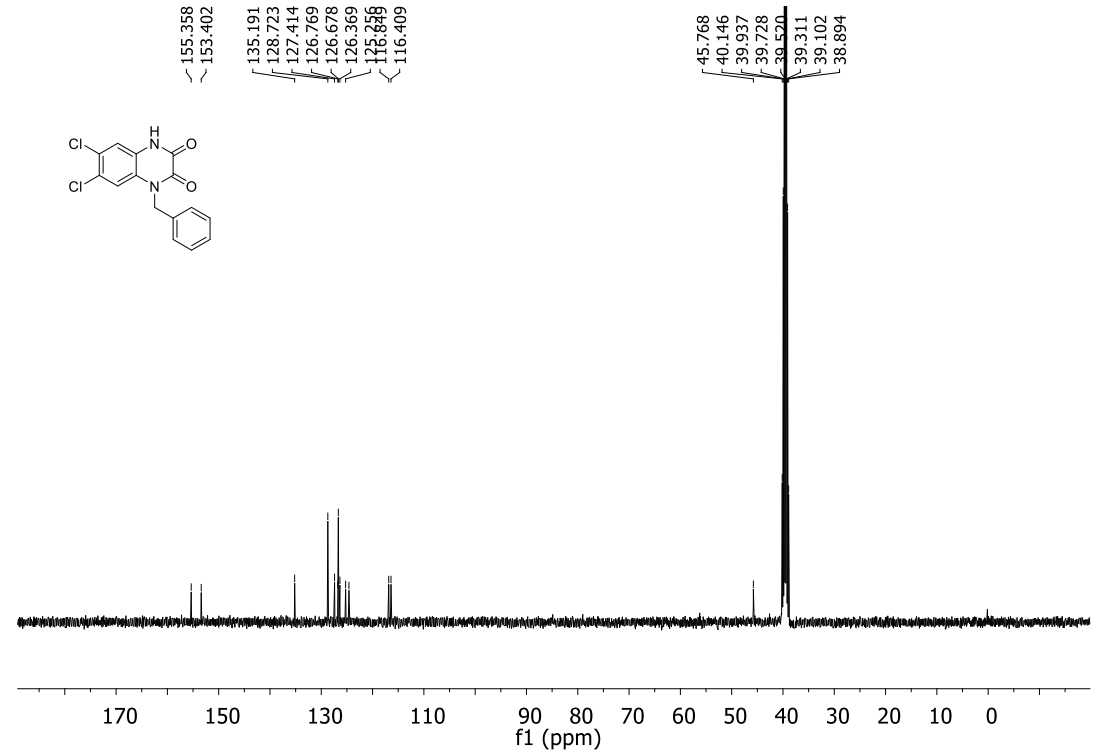

Figure 4.43. [13]C NMR of 1-Benzyl-6,7-dichloro-1,4-dihydroquinoxaline-2,3-dione (**4h**).

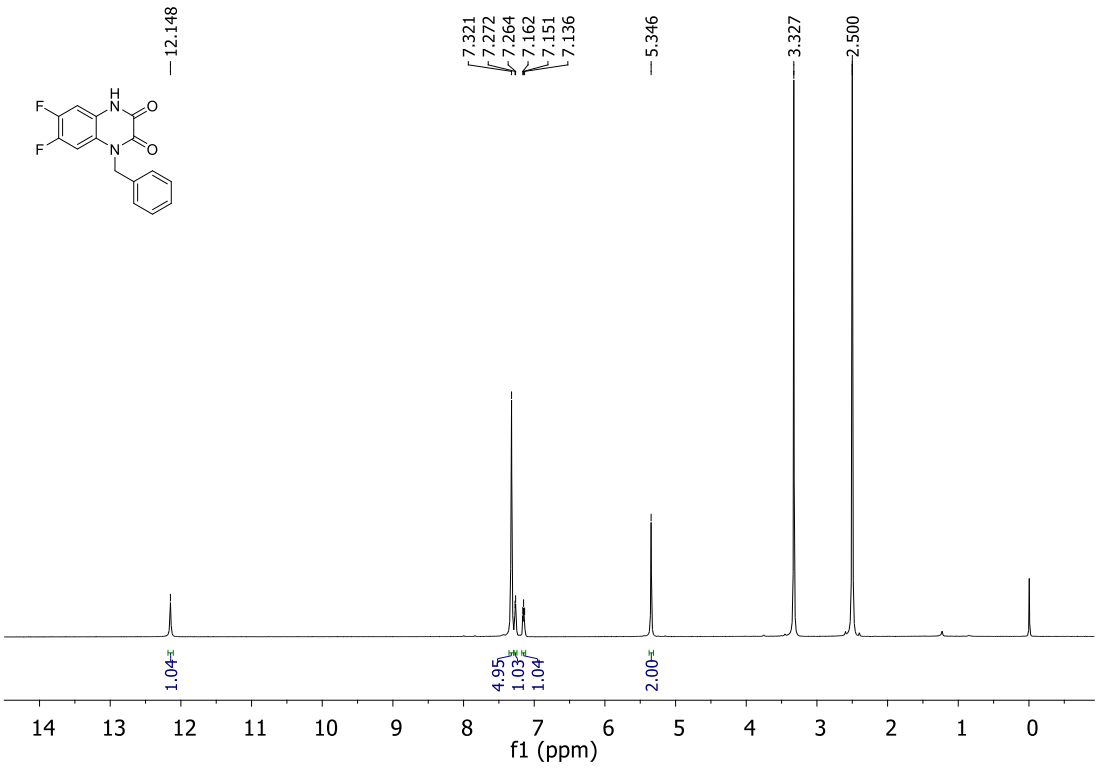

Figure 4.44. ^{1}H NMR of 1-Benzyl-6,7-fluoro-1,4-dihydroquinoxaline-2,3-dione (**4j**).

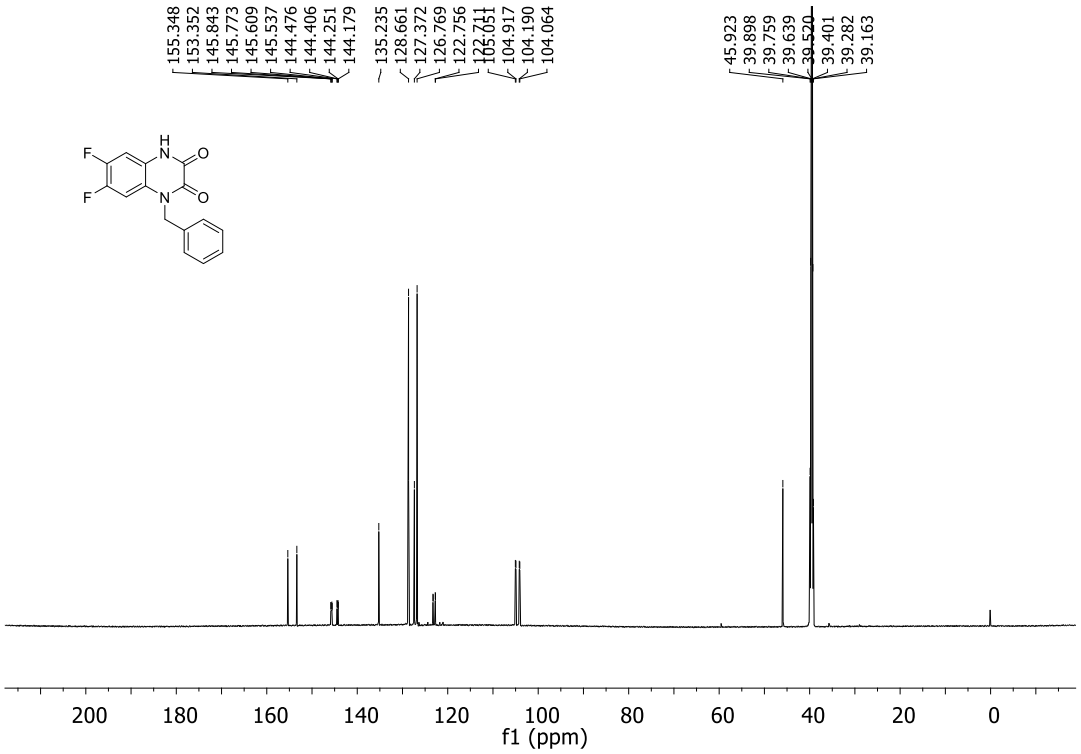

Figure 4.45. ^{13}C NMR of 1-Benzyl-6,7-fluoro-1,4-dihydroquinoxaline-2,3-dione (**4j**).

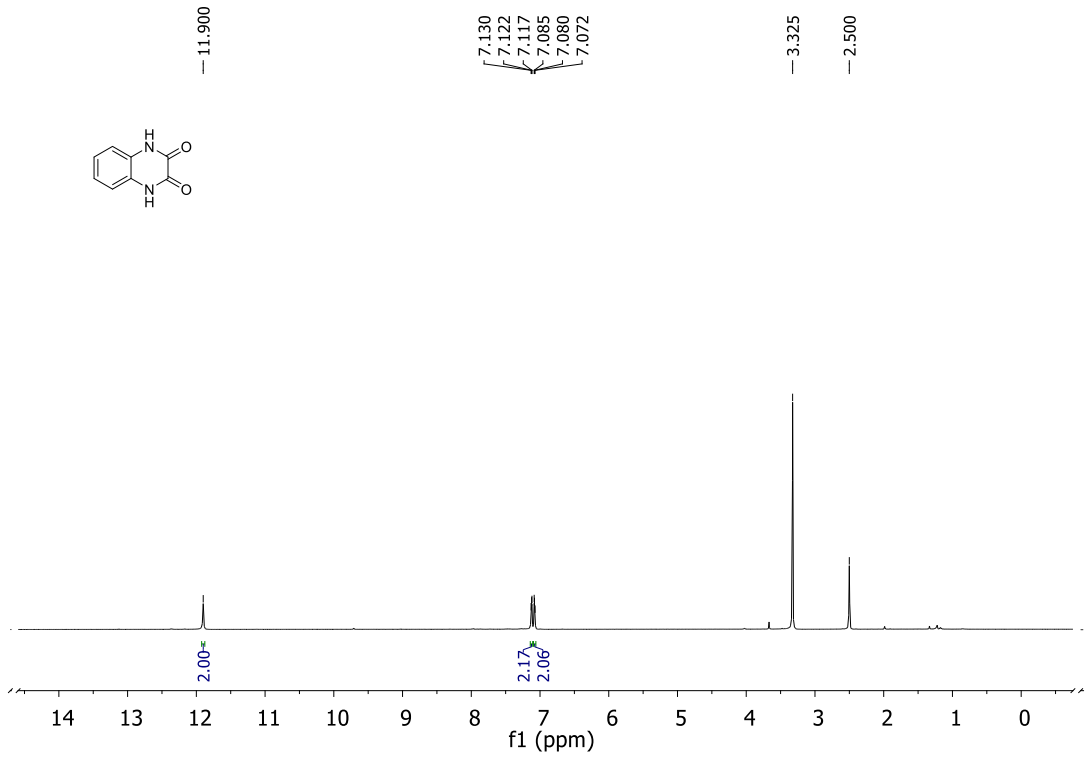

Figure 4.46. ^{1}H NMR of 1,4-dihydroquinoxaline-2,3-dione (**9**).

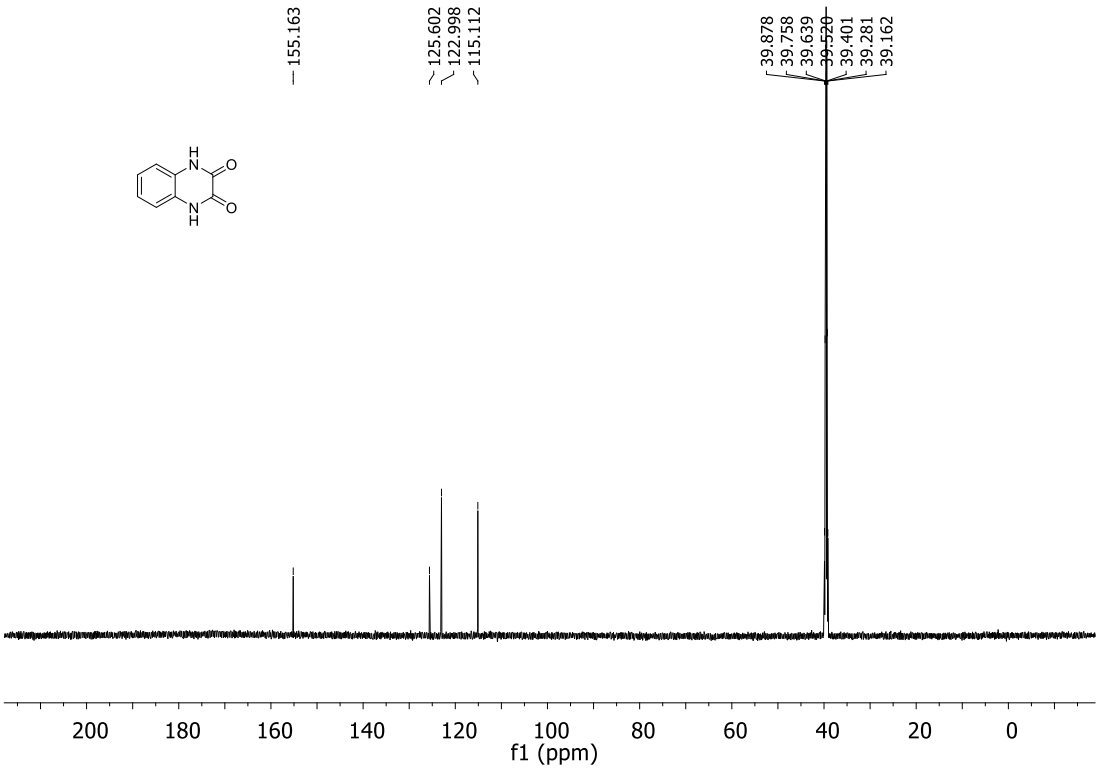

Figure 4.47. ^{13}C NMR of 1,4-dihydroquinoxaline-2,3-dione (**9**).

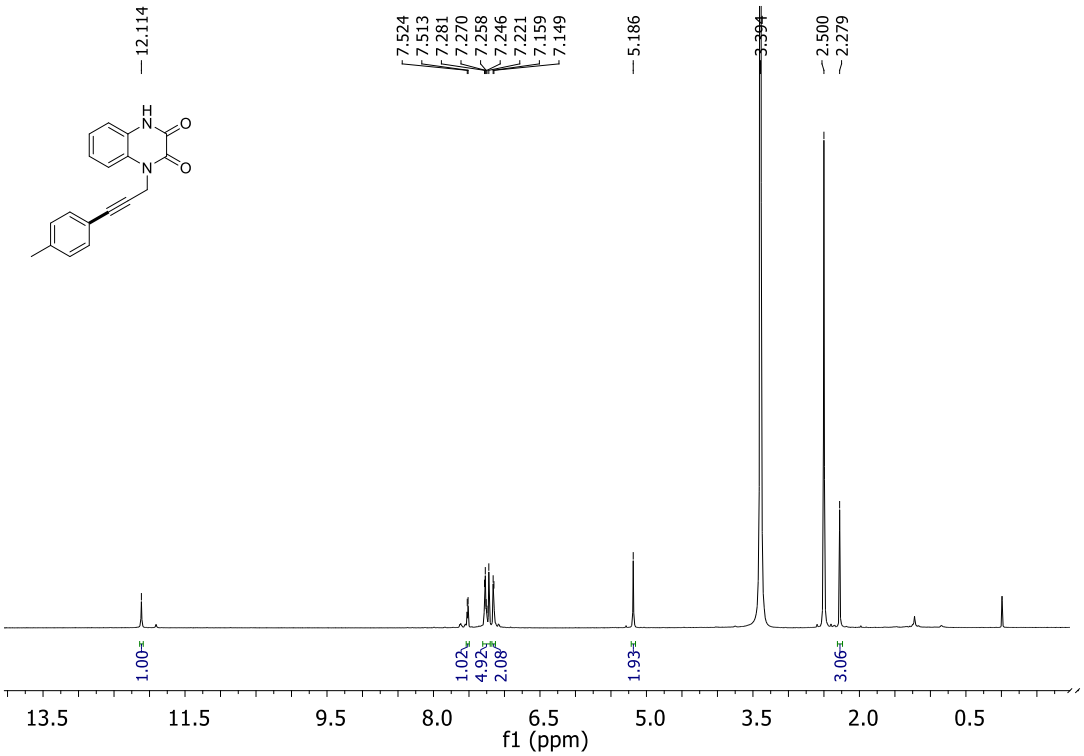

Figure 4.48. ^{1}H NMR of 1-(3-(p-tolyl)prop-2-yn-1-yl)-1,4-dihydroquinoxaline-2,3-dione (**10**).

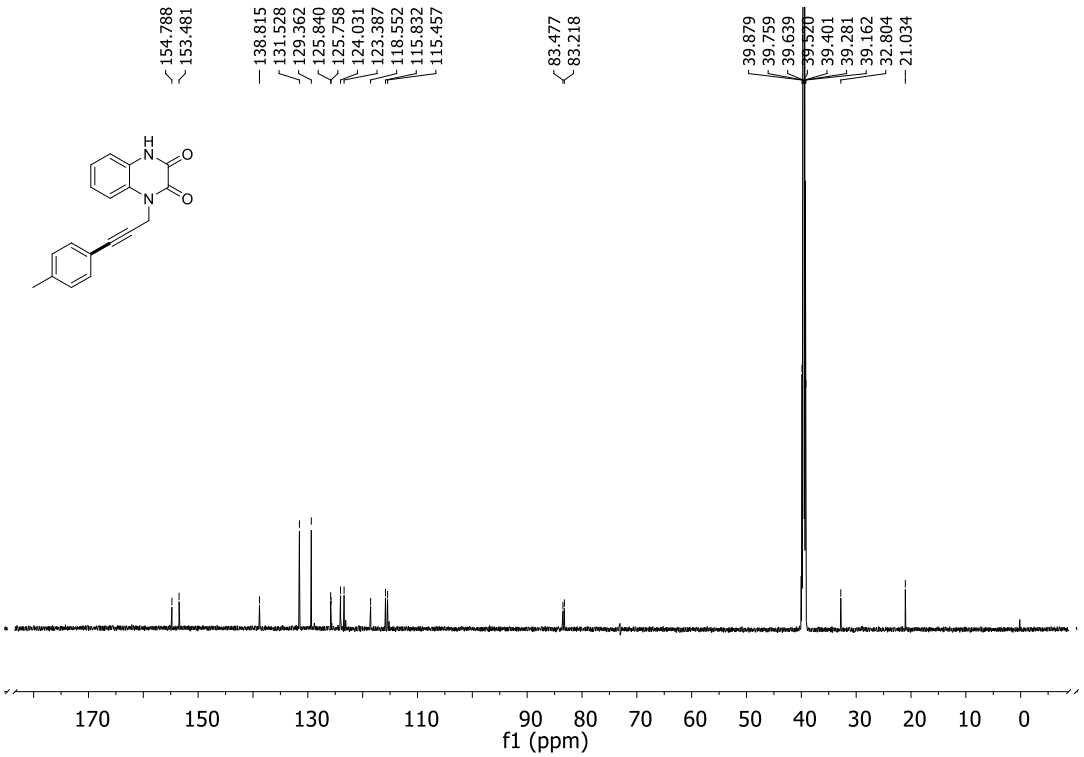

Figure 4.49. ^{13}C NMR of 1-(3-(*p*-tolyl)prop-2-yn-1-yl)-1,4-dihydroquinoxaline-2,3-dione **(10).**

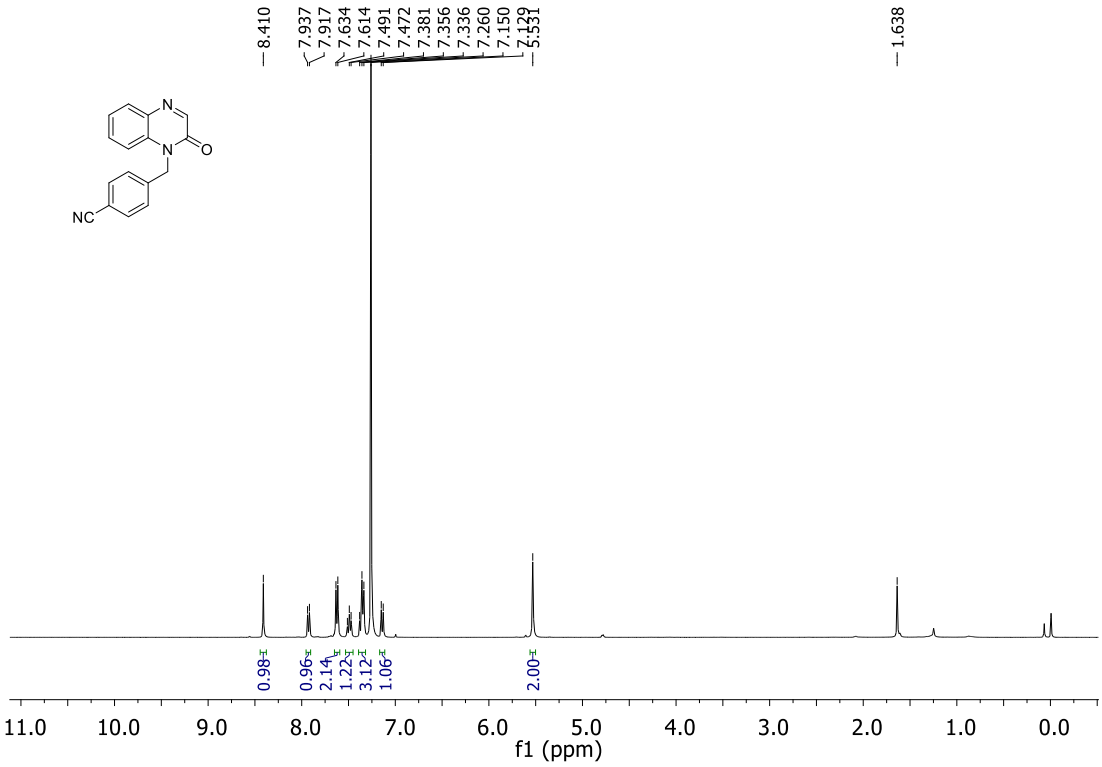

Figure 4.50. ^{1}H NMR of 4-((2-Oxoquinoxalin-1(2*H*)-yl)methyl)benzonitrile **(1e).**

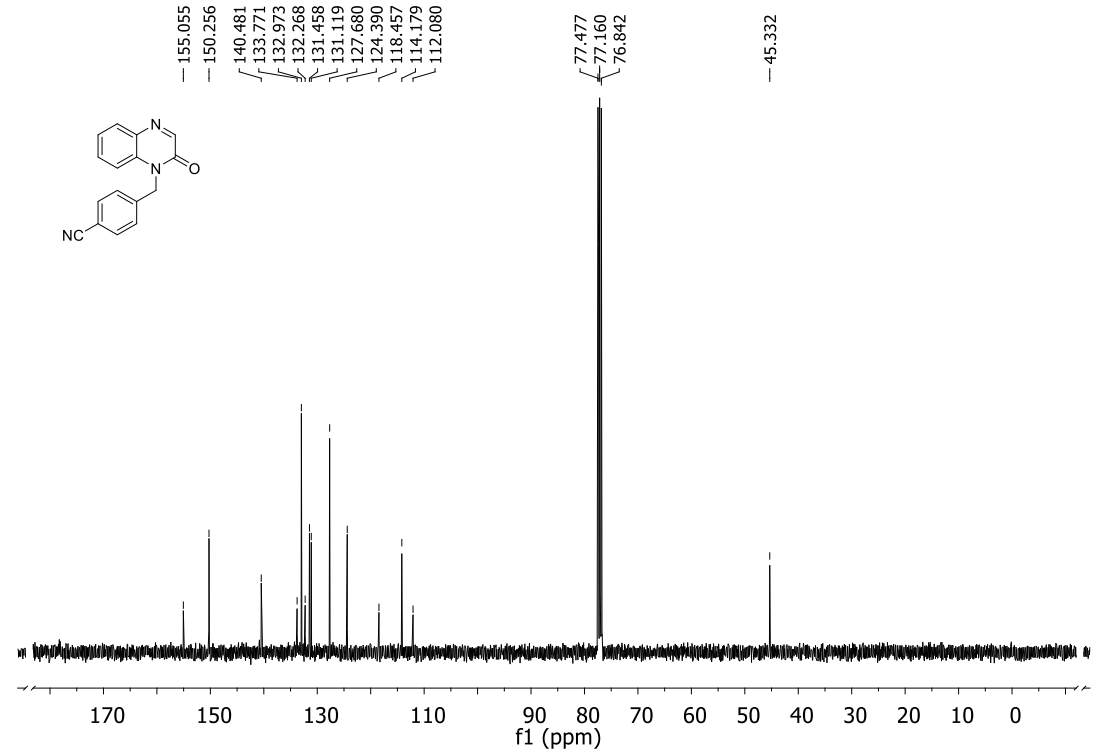

Figure 4.51. ^{13}C NMR of 4-((2-Oxoquinoxalin-1(2*H*)-yl)methyl)benzonitrile **(1e).**

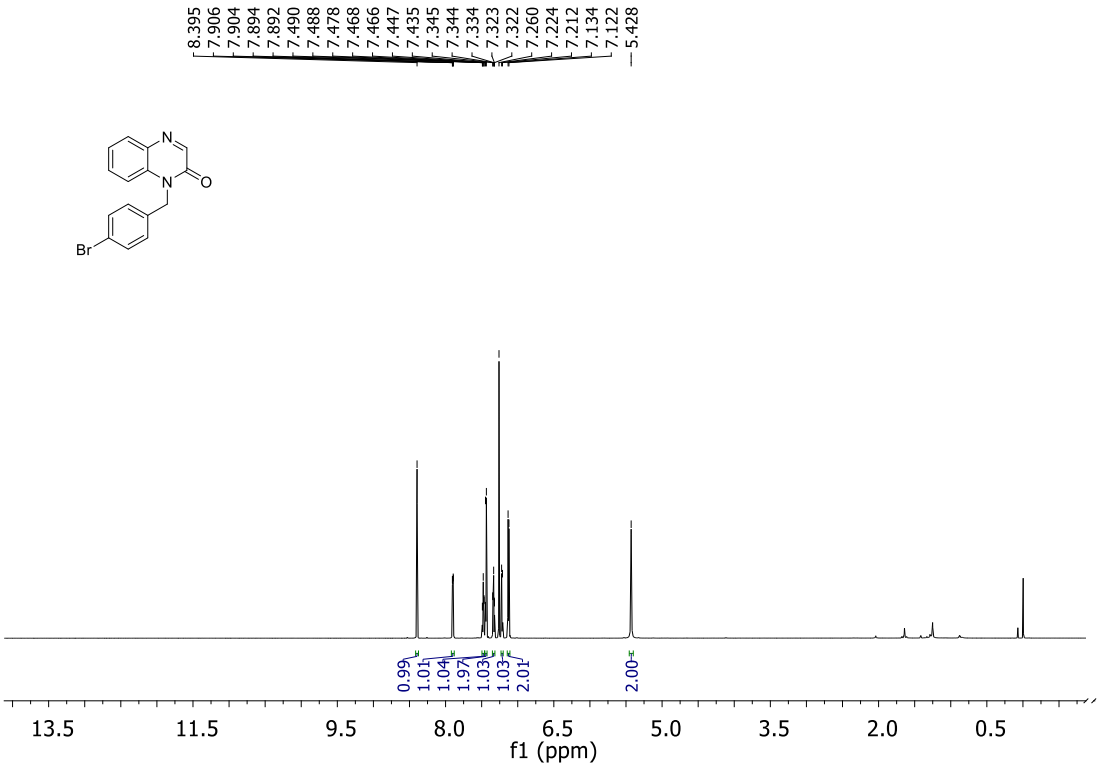

Figure 4.52. ^{1}H NMR of 1-(4-bromobenzyl)quinoxalin-2(1*H*)-one **(1f).**

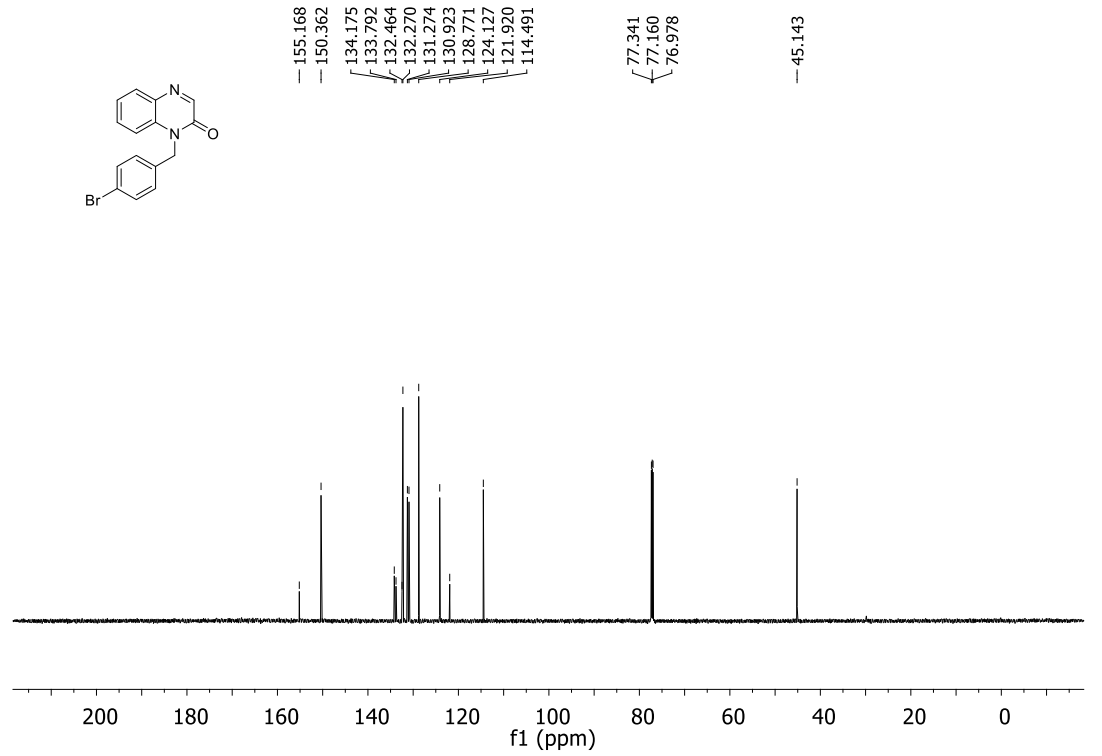

Figure 4.53. ^{13}C NMR of 1-(4-bromobenzyl)quinoxalin-2(1*H*)-one **(1f).**

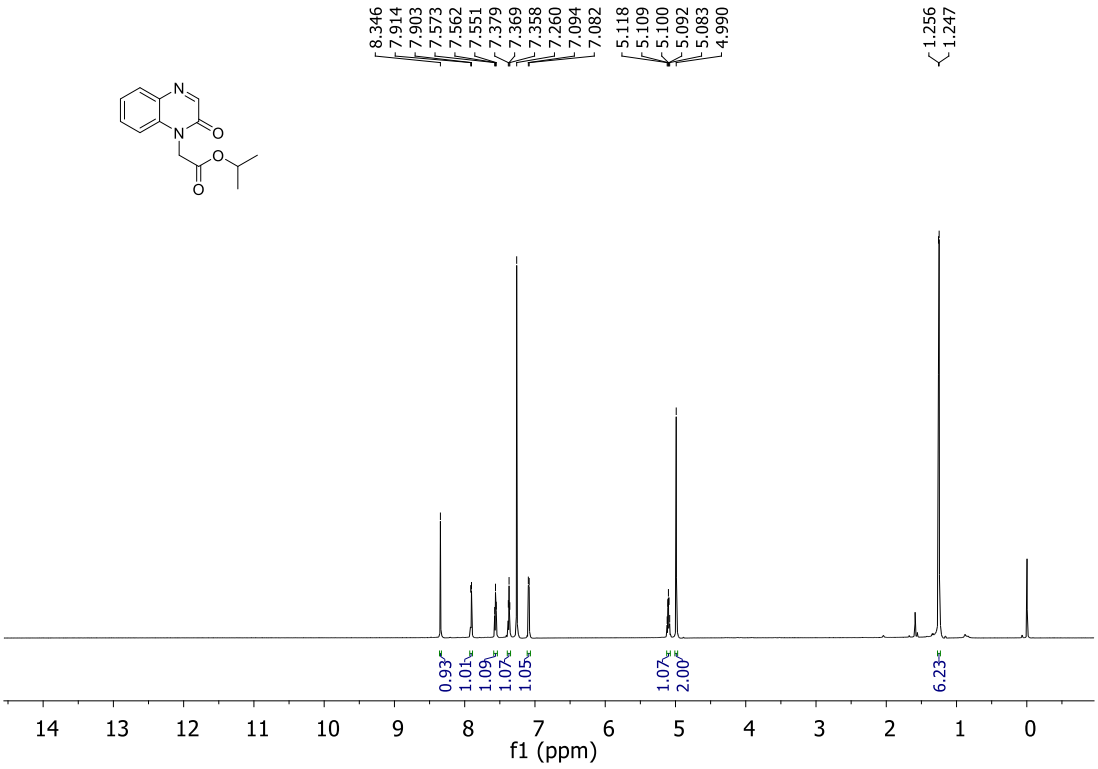

Figure 4.54. ^{1}H NMR of isopropyl 2-(2-oxoquinoxalin-1(2*H*)-yl)acetate **(1r).**

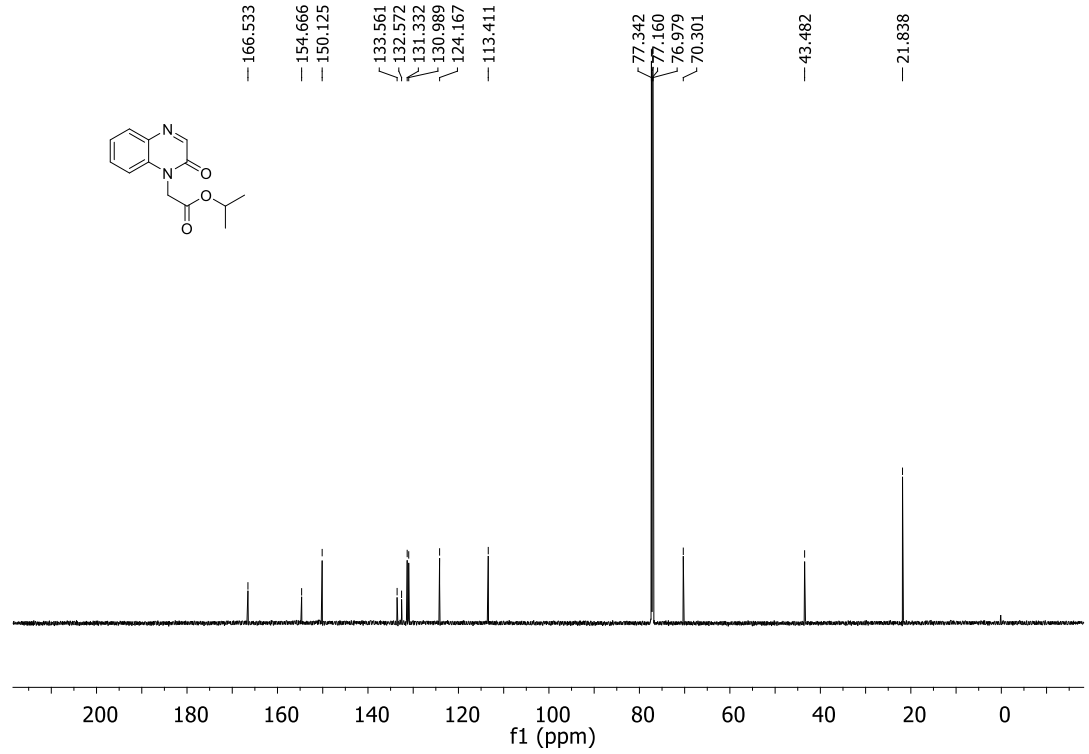

Figure 4.55. ^{13}C NMR of isopropyl 2-(2-oxoquinoxalin-1(2*H*)-yl)acetate **(1r).**

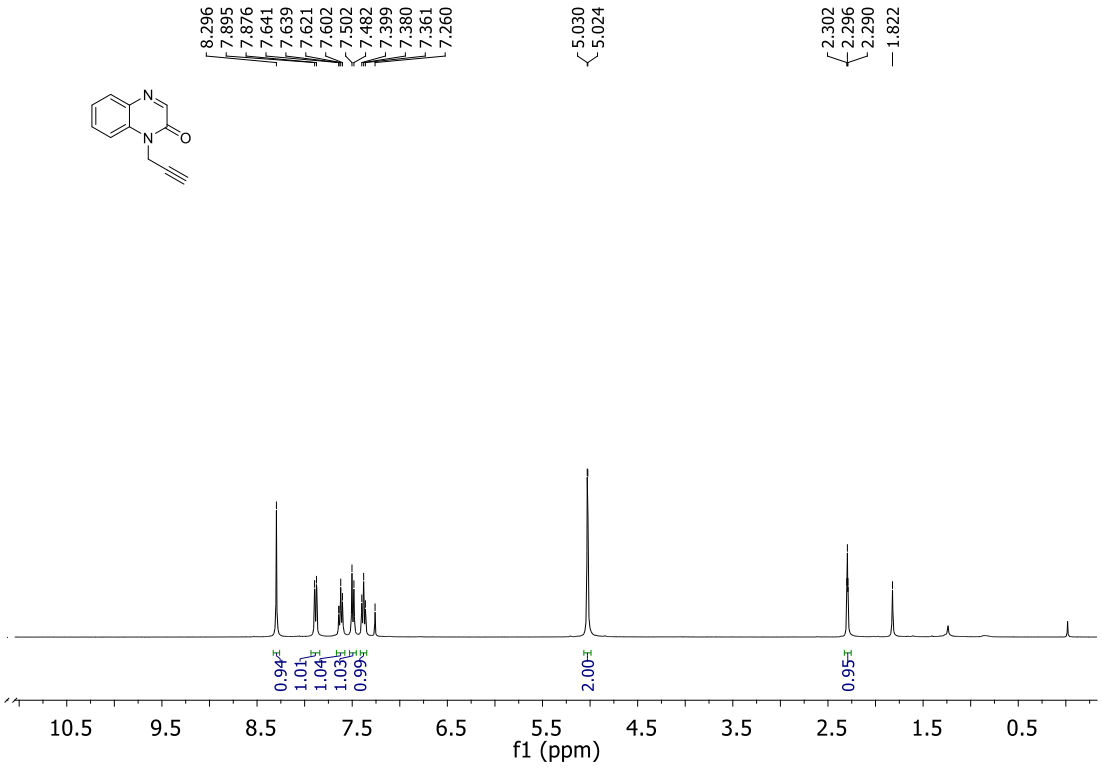

Figure 4.56. ^{1}H NMR of 1-(Prop-2-yn-1-yl)quinoxalin-2(1*H*)-one **(1t).**

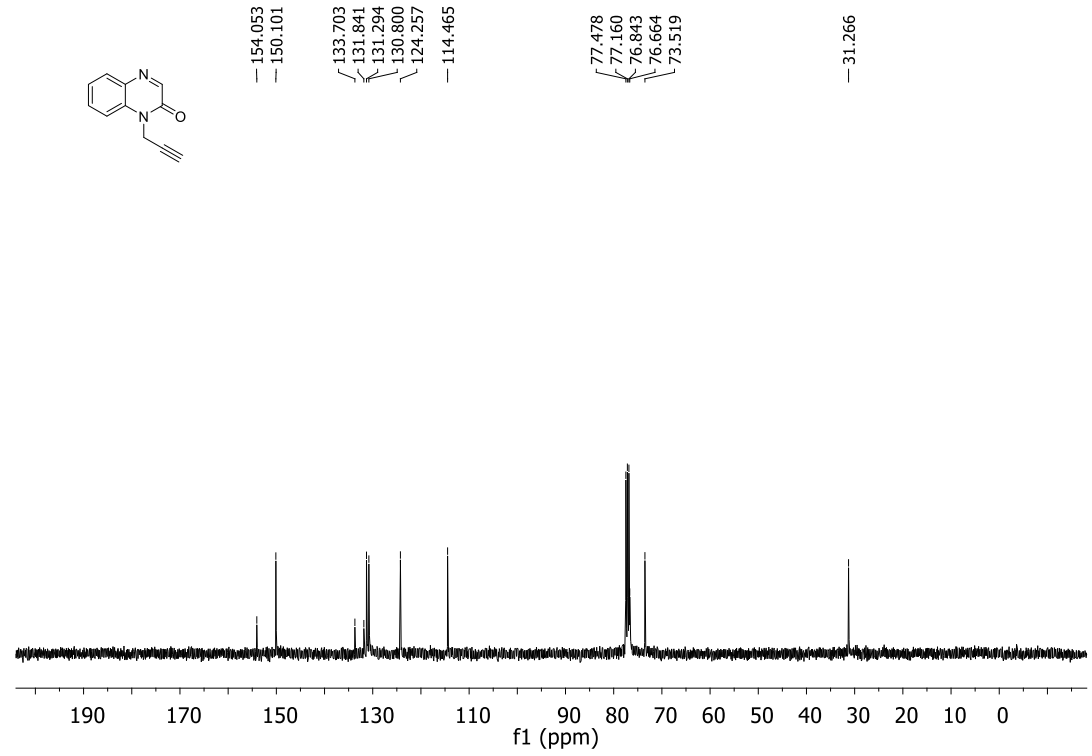

Figure 4.57. ^{13}C NMR of 1-(Prop-2-yn-1-yl)quinoxalin-2(1*H*)-one **(1t).**

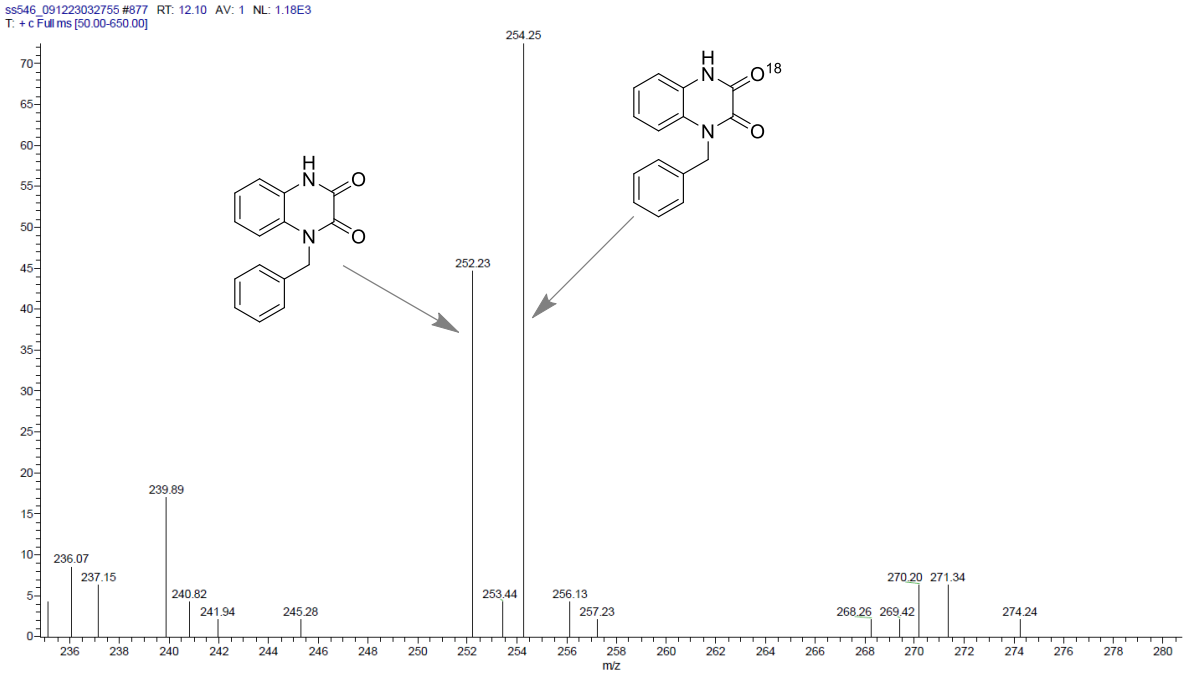

Figure 4.58. GC-MS analysis of O^{18} isotope labelling experiment.

CHAPTER 5

Visible-light Promoted Regioselective Oxygenation of Quinoxalin-2(1*H*)-ones using O_2 as an Oxidant

5.1 ABSTRACT

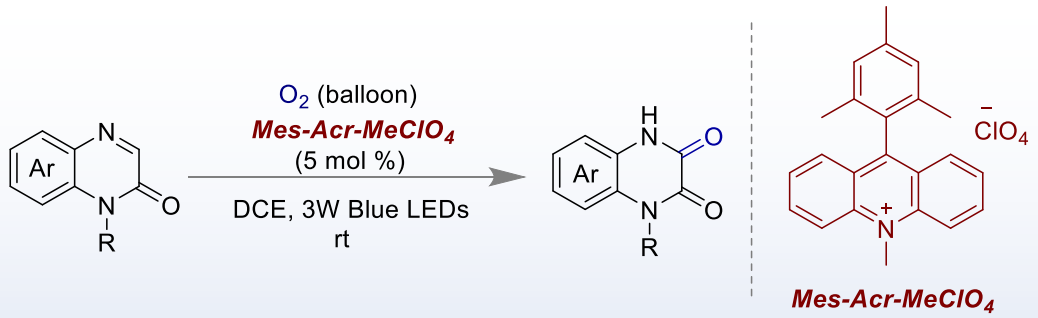

Visible-light photocatalysis Metal-free oxygenation O_2 as the green oxidant Regioselective

A visible-light mediated sustainable approach for metal-free oxygenation of quinoxalin-2(1*H*)-one has been achieved by employing Mes-Acr-MeClO$_4$ as a photocatalyst without using any additive or co-catalyst. O_2 served as the eco-friendly and green oxidant source for this conversion. In addition, the protocol exhibited high regioselectivity and tolerance towards a wide spectrum of functional groups to furnish quinoxaline-2,3-diones in good to excellent yields.

5.2 INTRODUCTION

Finding the sustainable and step-economic strategies for the synthesis and functionalization of organic compounds has recently become a trending topic of research in synthetic organic

chemistry.[1] From this perspective, visible-light photocatalysis[2-4] represents one of the important cutting-edge techniques which has gained significant popularity. Photocatalysts, due to their single-electron transfer capability can trigger diverse chemical transformations.[5-10] Among the photocatalysts used for organic transformations, metal-free organic dyes[4, 11, 12] are inexpensive and easy to handle compared to highly expensive and relatively toxic transition-metal based photocatalysts.[13]

Oxygenation reaction is one of the important and powerful tools to synthesize oxygen-containing molecular scaffolds which are prevalent in bioactive and natural products.[14-16] Oxygen-containing organic compounds have a wide array of industrial and pharmaceutical applications such as cosmetics, anticoagulants, antibiotics, nutrients, etc.[14, 15] Therefore, relentless efforts have been paid toward the development of sustainable strategies for oxygenation reactions.[14, 15] Oxygenation by utilizing molecular oxygen as an eco-friendly and green oxidant under the domain of visible-light photocatalysis is the most convenient and sustainable strategy among various protocols reported.[14, 15] For instance, in 2018, Das and co-workers disclosed α-oxygenation of tertiary amines[17] under visible light irradiation using Rose Bengal as a photocatalyst and O_2 as the oxidant (Scheme 5.1).

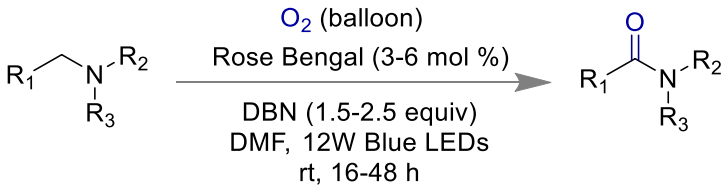

Scheme 5.1. Das's approach for photocatalytic α-oxygenation of tertiary amines

In 2020, the same group revealed dearomatization of indoles[18] in presence of oxygen using Rose Bengal as a visible-light photocatalyst (Scheme 5.2).

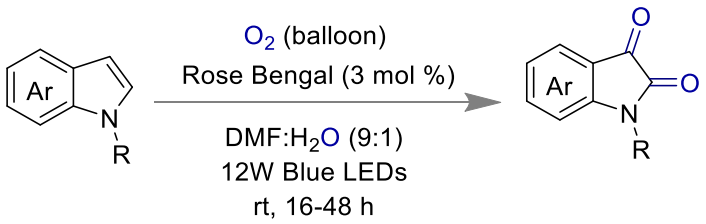

Scheme 5.2. Das's report on dearomatization of indoles using visible-light photocatalysis

Quinoxaline-2,3-diones belong to the category of important heterocyclic skeletons and furnish extensive applications in areas of organic synthesis and material sciences and their substantial utilization is also found in industry and pharmaceutics.[19-22] Due to their salient applications, development of convenient protocols for the synthesis of quinoxaline-2,3-dione and their derivatives has become an important topic of research. Moreover, quinoxalin-2(1*H*)-one is also an important synthetic block in organic chemistry and furnishes a wide array of applications in pharmaceutics and therapeutics.[23-26] Therefore, several protocols have been introduced to synthesize C-3 substituted quinoxalin-2(1*H*)-ones with diverse functionalities via direct C-3 functionalization.[23, 26-32]

Classical synthesis of N-functionalised quinoxaline-2,3-dione utilizes base mediated reaction of mono N-substituted 1,2-diamino benzenes and oxalyl chloride (or ethyl chloroglyoxylate).[33, 34] But disadvantage of classical method lies in use of strong base, toxic oxalyl chloride, and difficulties in synthesis and isolation of mono N-substituted substrates.[33, 34] To overcome the drawbacks of classical method, He and co-workers disclosed the synthesis of quinoxaline-2,3-diones via C-3 hydroxylation of quinoxalin-2(1*H*)-ones using $(NH_4)_2S_2O_8$[35] . Parallelly, our group reported C-3 hydroxylation of quinoxalin-2(1*H*)-ones to access quinoxaline-2,3-diones using tert-butyl nitrite (TBN)[36] via *ipso*-substitution strategy. But stoichiometric amount of oxidants and heating conditions were required in these protocols.[35, 36] According to our knowledge, photocatalytic

synthesis of quinoxaline-2,3-diones from quinoxalin-2(1*H*)-ones using molecular oxygen has not been explored. Herein we reveal visible-light mediated C-3 oxygenation of quinoxalin-2(1*H*)-ones using O_2 as an oxidant and only 5 mol % of Mes-Acr-$MeClO_4$ photocatalyst at room temperature to access quinoxaline-2,3-diones (Figure 5.1).

Figure 5.1. Our approach for photocatalytic oxygenation of quinoxalin-2(1*H*)-ones

5.3 RESULT AND DISCUSSION

1-Benzylquinoxalin-2(1*H*)-one (**1a**) was chosen as the dummy substrate to find the optimum condition for this photocatalytic oxygenation reaction as showcased in Table 5.1. First, we performed the reaction with **1a** under 3 W blue LED irradiation using Eosin Y (5 mol %) in ACN solvent under an O_2 (balloon) atmosphere but the desired product formation was not observed after 24 h (entry 1). Next, we carried out the reaction using Rose Bengal as photocatalyst keeping other parameters the same and after 24 h reaction time, the expected product was not obtained (entry 2). When $Ru(bpy)_3(PF_6)_2$ and $Ru(bpy)_3Cl_2{\cdot}6H_2O$ were employed as photocatalysts, the reactions failed to furnish our target product **2a** (entry 3-4). Executing the reaction using $CeCl_3{\cdot}7H_2O$ as the photocatalyst, also could not provide us with any positive results (entry 5). Then the reaction was accomplished by implementing 9-mesityl-10-methylacridinium perchlorate (Mes-Acr-$MeClO_4$) as the photocatalyst in ACN solvent and interestingly after 24 h, the desired product **2a** was isolated in 31% yield (entry 6). Changing the solvent to DCE, helped to improve the reaction yield and 89% of **2a** was delivered after 24 h (entry 7). Lowering the reaction time to 12 h didn't affect

reaction yield (entry 8). Moreover, when EtOAc and 1,4-dioxane were enrolled as solvents, product **2a** was obtained with 28% and 43% yields respectively (entry 9-10). Utilizing acetone as a solvent for the reaction also did not lead to product formation with a satisfactory yield (entry 11). In addition, the reaction afforded only a trace amount of product in solvents like DCM and THF (entry 12-13). Starting materials were fully unreacted in DMSO and DMF solvents and resulted in no product formation (entry 14-15). When 26W green LED light source was used, only a trace amount of desired product formation was observed (entry 16). Moreover, the reaction was performed under an air atmosphere instead of O_2 (balloon) for 24 h in DCE, and **2a** was obtained with 38% yield (entry 17). From optimization experiments, the ideal condition of the reaction was derived with irradiation of 3W blue LED, 5 mol % of Mes-Acr-MeClO_4 loading under an O_2 (balloon) atmosphere in DCE solvent with a reaction period of 12 h.

Table 5.1. Condition optimization[a]

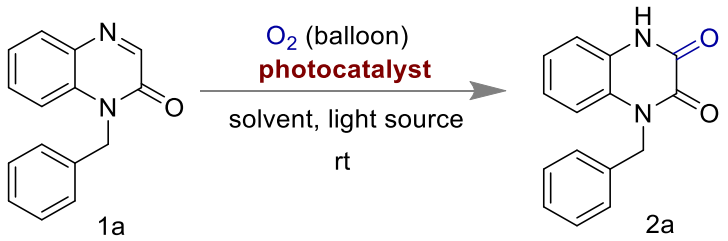

entry	Photocatalyst	Solvent	Light Source	Time (h)	Yield (%)[b]
1	Eosin Y	ACN	Blue LED (3W)	24	0
2	Rose Bengal	ACN	Blue LED (3W)	24	0
3	$Ru(bpy)_3(PF_6)_2$	ACN	Blue LED (3W)	24	0
4	$Ru(bpy)_3Cl_2{\cdot}6H_2O$	ACN	Blue LED (3W)	24	0
5	$CeCl_3{\cdot}7H_2O$	ACN	Blue LED (3W)	24	0

6	Mes-Acr-MeClO$_4$	ACN	Blue LED (3W)	24	31
7	Mes-Acr-MeClO$_4$	DCE	Blue LED (3W)	24	89
8	Mes-Acr-MeClO$_4$	DCE	Blue LED (3W)	12	88
9	Mes-Acr-MeClO$_4$	EtOAc	Blue LED (3W)	24	28
10	Mes-Acr-MeClO$_4$	1,4-dioxane	Blue LED (3W)	24	43
11	Mes-Acr-MeClO$_4$	Acetone	Blue LED (3W)	24	40
12	Mes-Acr-MeClO$_4$	DCM	Blue LED (3W)	24	trace
13	Mes-Acr-MeClO$_4$	THF	Blue LED (3W)	24	trace
14	Mes-Acr-MeClO$_4$	DMSO	Blue LED (3W)	24	NR[c]
15	Mes-Acr-MeClO$_4$	DMF	Blue LED (3W)	24	NR[c]
16	Mes-Acr-MeClO$_4$	DCE	Green LED (26W)	24	trace
17	Mes-Acr-MeClO$_4$	DCE	Blue LED (3W)	24	38[d]

[a]Standard conditions: **1a** (0.254 mmol), Mes-Acr-MeClO$_4$ (5 mol %, 0.0126 mmol) in 2 mL of solvent at O_2 (balloon) atmosphere. [b]Isolated yield. [c]No reaction. [d]Under air atmosphere.

Next, we surveyed the substrate scopes for this protocol applying the optimum condition derived from the optimization study. The scope of different *N*-1 substitutions containing quinoxalin-2(1*H*)-ones has been showcased in Figure 5.2. Quinoxalin-2(1*H*)-ones carrying electron-withdrawing groups –CN, -NO_2, -CF_3, 3,5-difluoro, -F, -Br at *N*-benzyl part responded well under our imposed reaction condition and delivered our desired products (**2b**-**2g**) with 85-98% yields. Next, when electron-donating groups -^{t}Bu, -^{i}Pr, -Me were present as substituents at *N*-benzyl part of quinoxalin-2(1*H*)-ones; the corresponding starting materials promptly participated in the reaction, and the desired products (**2h**-**2j**) were obtained with 83-86% yields. Furthermore, the scope of

substrates with different alkyl groups n-butyl, -phenylethyl, -Et, at *N*-1 position of quinoxalin-2(1H)-ones were also verified and the corresponding products (**2k-2m**) were isolated with 84-90% yields. Substrate with alkynyl functionality at N-1 position underwent conversion and furnished **2n** in good yield. This methodology well tolerated the ester functionalities -COO^{t}Bu, -COO^{i}Pr, –COOEt present in substrates and afforded the expected products (**2o-2q**) with 85-95% yields.

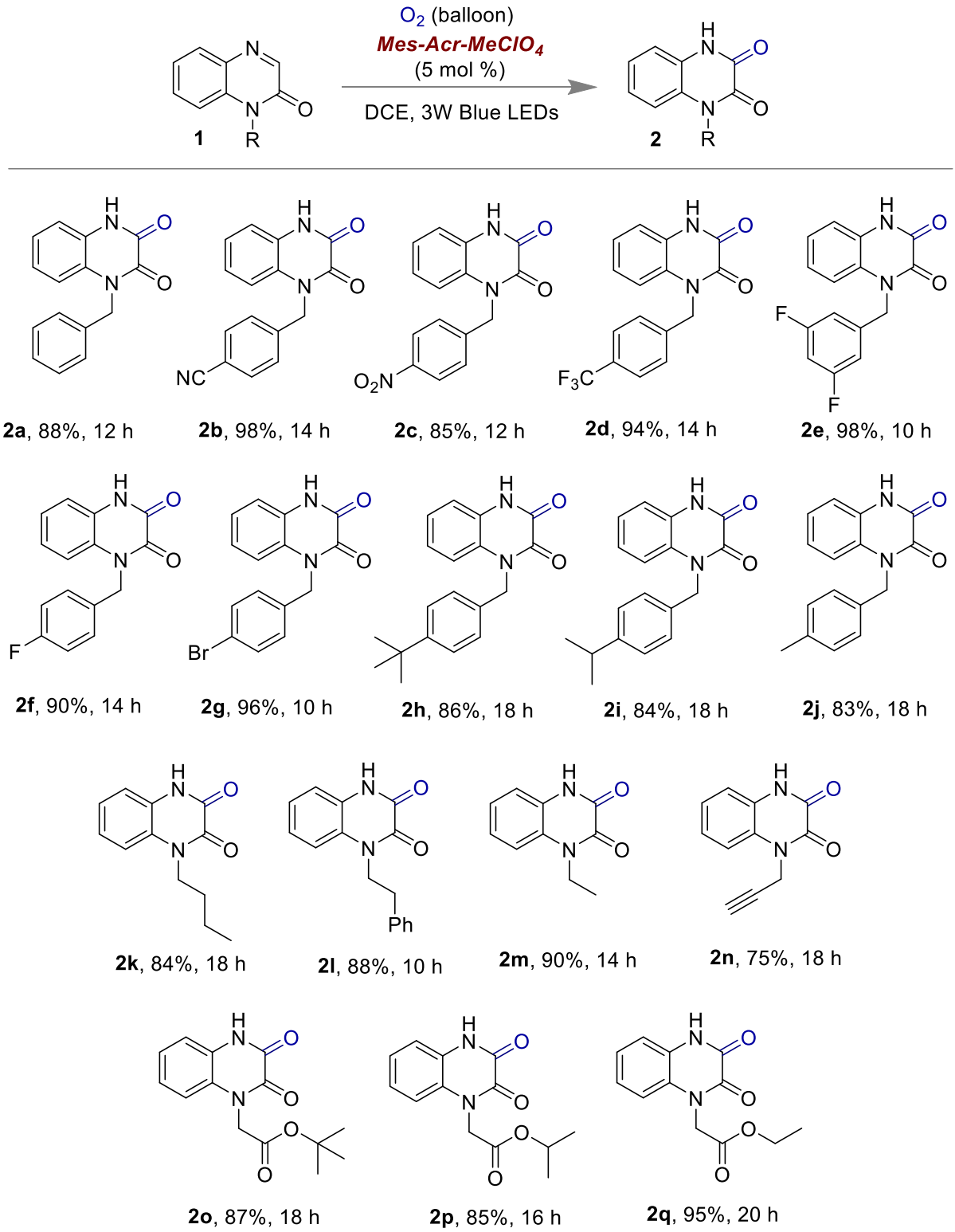

Figure 5.2. Substrate scopes with different substituents at *N*-1 position.

Next, substrate scopes with different o-phenylene diamines were explored (Figure 5.3). Quinoxalin-2(1*H*)-ones containing mono substitution with alkyl and halogen substituents underwent conversion and led to desired product formation (**4a**-**4c**). Quinoxalin-2(1*H*)-one monosubstituted by –Cl, delivered the expected product **4a** in 88% yield with a 3:1 regioisomeric ratio.

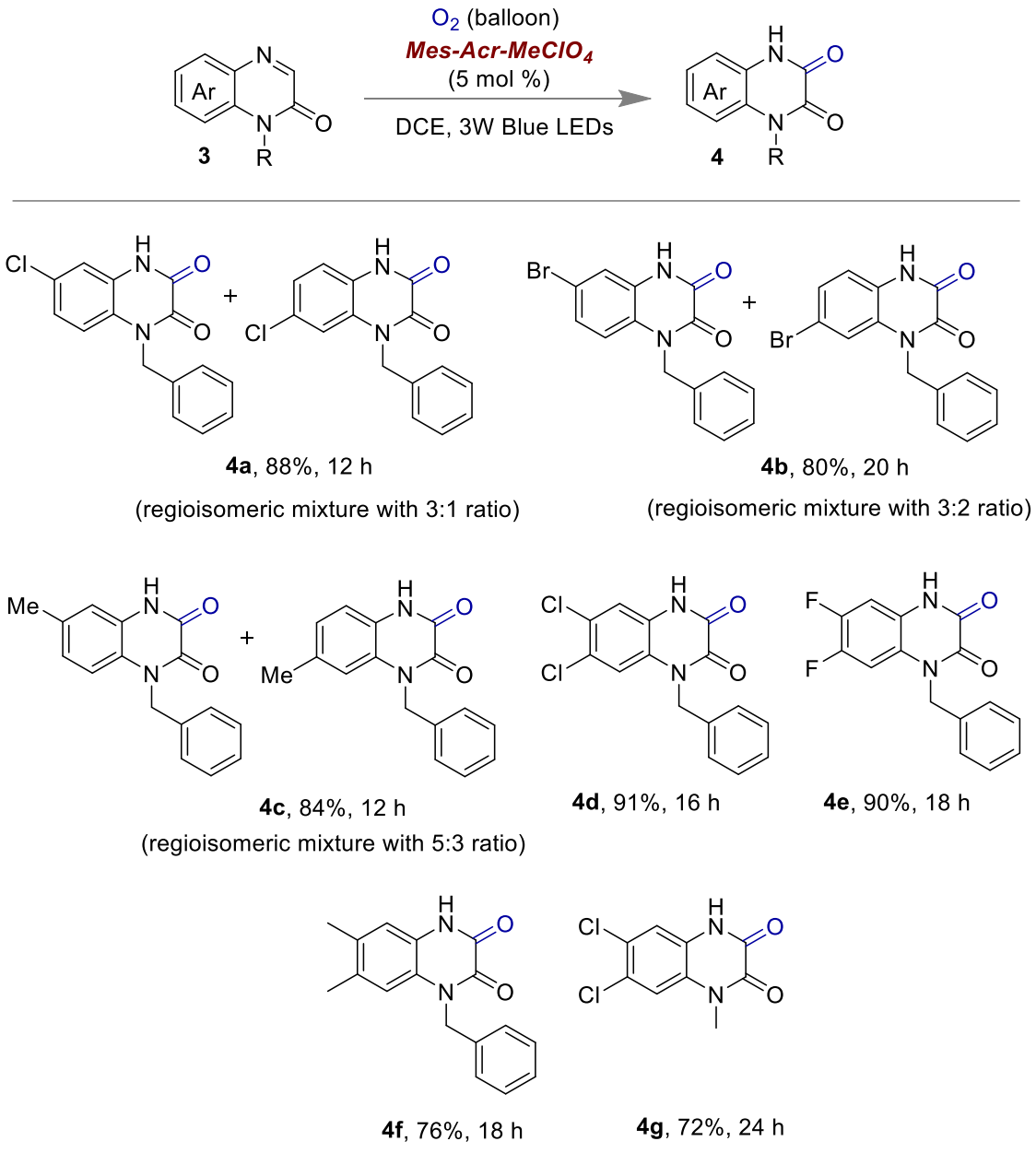

Figure 5.3. Substrates scope with different substitutions in *o*-phenylene diamine.

Starting compound monosubstituted by –Br, led to the formation of corresponding final product **4b** with 80% yield in a 3:2 regioisomeric ratio. Likewise, when –Me was present as monosubstituent, the reaction yielded the product **4c** in a 5:3 regioisomeric ratio. For the substrates containing disubstitutions with alkyl and halogen substituents, the reaction worked well, and the corresponding quinoxaline-2,3-diones (**4d-4g**) were obtained in 72-91% yields.

Control experiments were executed to get a mechanistic insight into the reaction. When no light source was used and the reaction was carried out under dark condition; the reaction did not proceed and starting compound **1a** was fully unreacted (Figure 5.4a). Next, an experiment was conducted without using photocatalyst Mes-Acr-MeClO_4, and in this case, also the desired product formation (**2a**) was not observed (Figure 5.4a). Similarly, executing the reaction in an argon atmosphere resulted in no product formation (**2a**) (Figure 5.4a). These control experiments verified that the implementation of a photocatalyst, visible-light source, and an oxygen atmosphere was necessary for the reaction to proceed towards the formation of **2a**. Under standard reaction condition, radical scavengers like TEMPO (2,2,6,6- tetramethylpiperidin-1-yl-oxyl) (Figure 5.4b, entry 1) or BHT (2,6-di-*tert*-butyl-4-methylphenol) (Figure 5.4b, entry 2) fully inhibited the reaction. These radical scavenger experiments demonstrated that a radical-mediated pathway might be operational in reaction. Execution of the reaction in presence of $CuCl_2$, fully quenched the formation of **2a** suggesting that single electron interplay was involved in the photocatalytic reaction course (Figure 5.4b, entry 3). Further quenching experiments were performed to observe the effect of different quenchers on possible reactive oxygen species in the reaction system. Formation of **2a** was not observed in presence of *p*-benzoquinone under standard reaction conditions (Figure 5.4b, entry 4). This result validated the participation of superoxide radical anion in reaction. When sodium azide was used under optimum reaction conditions, formation of **2a** was experienced in 17% yield;

indicating the presence of singlet oxygen in the reaction system (Figure 5.4b, entry 5). The reaction furnished 81% of **2a** when it was accomplished in presence of *tert*-butanol under optimum reaction conditions, which nullified the involvement of hydroxyl radical in the reaction (Figure 5.4b, entry 6).

a)

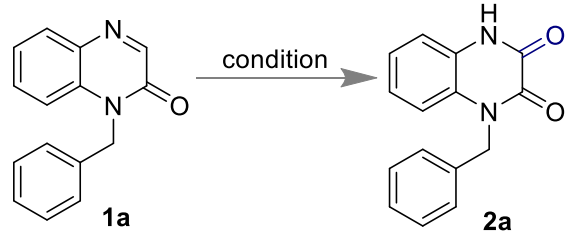

controlled reaction parameter	Yield (%)[b]
standard conditions	88
In darkness	0
No photocatalyst	0
Ar atmosphere	0

b)

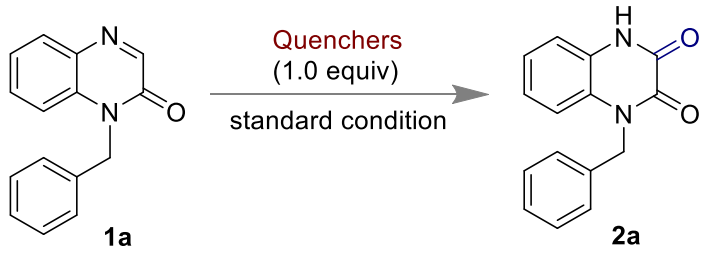

Entry	Quencher	Yield (%)[b]	Role
1	TEMPO	0	radical scavenger
2	BHT	0	radical scavenger
3	$CuCl_2$	0	electron scavenger
4	*p*-benzoquinone	0	superoxide radical anion scavenger
5	sodium azide	17	singlet oxygen scavenger
6	*tert*-butanol	81	hydroxide radical scavenger

Figure 5.4. a) Control experiments with different reaction parameters. b) control experiments in presence of different quenchers.

Furthermore, fluorescence quenching experiment (Figure 5.5a) and Stern-Volmer plot (Figure 5.5c) helped to clarify the reaction mechanism. A gradual decrease of fluorescence intensity of

Mes-Acr-MeClO$_4$ was observed upon addition of 1-benzylquinoxalin-2(1*H*)-one (**1a**), and no change was detected with solution of photocatalyst saturated with oxygen. From these results it was evident that the excited state of Mes-Acr-MeClO$_4$ was quenched by 1-benzylquinoxalin-2(1H)-one (**1a**), not by oxygen. Light ON-OFF-ON experiment was performed to understand the reaction course from time to time in presence of light and absence of light accordingly (Figure 5.5b).

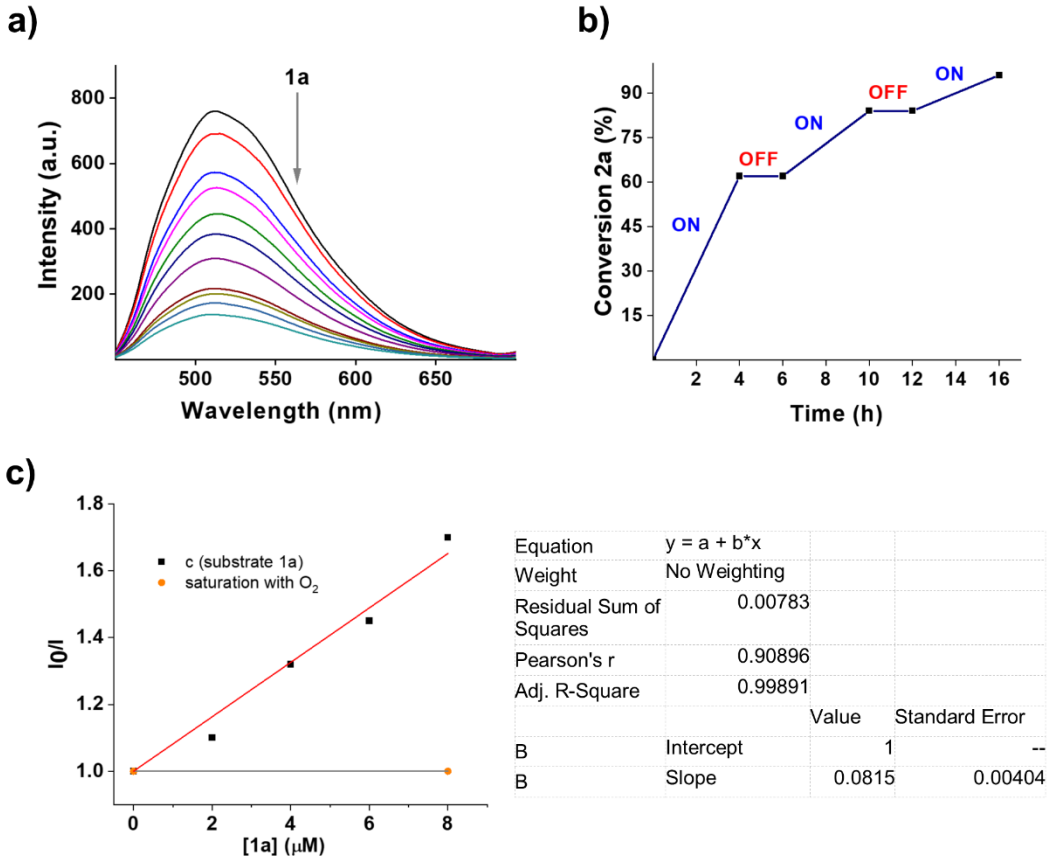

Figure 5.5. a) Fluorescence quenching experiment. b) Light ON-OFF-ON experiment. c) Stern-Volmer plot

A plausible mechanism has been portrayed based on previous literature reports[12, 16, 37], and control experiments performed (Figure 5.6). At first, under the visible light irradiation Mes-Acr-MeClO$_4$

(**PC**) photocatalyst was promoted to its excited state. The excited state photocatalyst (**PC***) then underwent a single electron transfer with **1** and corresponding radical cation **I** was generated. Consequently, **PC*** was itself reduced to **PC**$^{\bullet-}$. Parallelly, O_2 was converted into singlet oxygen ($^1O_2$) *via* sensitization with **PC***[38]. Next, the generated singlet oxygen ($^1O_2$) promptly reacted with **PC**$^{\bullet-}$ and led to the formation of superoxide radical anion **(**$O_2^{\bullet-}$**)**[39] and **PC** was regenerated.[37] Following, superoxide radical anion **(**$O_2^{\bullet-}$**)** underwent addition to the C-3 position of **I** and afforded intermediated **II**. After that, intermediate **II** was converted to intermediate **III** via 1,2-HAT. Finally, two molecules of **III** reacted to furnish molecular oxygen and two molecules of our desired product **2**.[16]

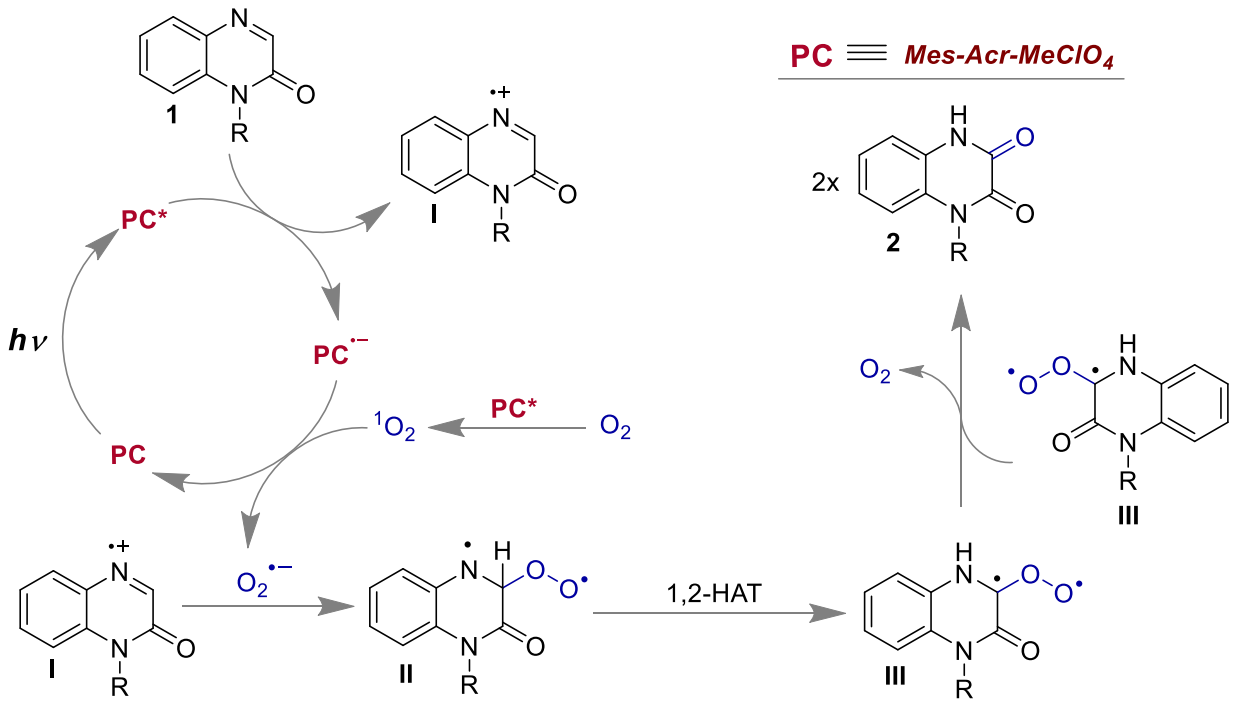

Figure 5.6. Plausible mechanistic pathway

Post-synthetic applications were performed to verify the supremacy of our protocol (Figure 5.7). Sonogashira coupling reaction of **2g** (1-(4-bromobenzyl)-1,4-dihydroquinoxaline-2,3-dione) with

phenyl acetylene was accomplished which resulted in the desired product 1-(4-(phenylethynyl)benzyl)-1,4-dihydroquinoxaline-2,3-dione (**5**) with 82% yield (Figure 5.7a). Parallelly, Suzuki coupling reaction of **2g** (1-(4-bromobenzyl)-1,4-dihydroquinoxaline-2,3-dione) with phenylboronic acid was carried out and the coupled product 1-([1,1'-biphenyl]-4-ylmethyl)-1,4-dihydroquinoxaline-2,3-dione (**6**) was obtained with 84% yield (Figure 5.7b). Gram scale synthesis was performed with 4.66 mmol of **1a** (1-benzylquinoxalin-2(1*H*)-one), and the corresponding product **2a** (1-benzyl-1,4-dihydroquinoxaline-2,3-dione) was obtained in 77% yield (0.91 gm) (Figure 5.7c)

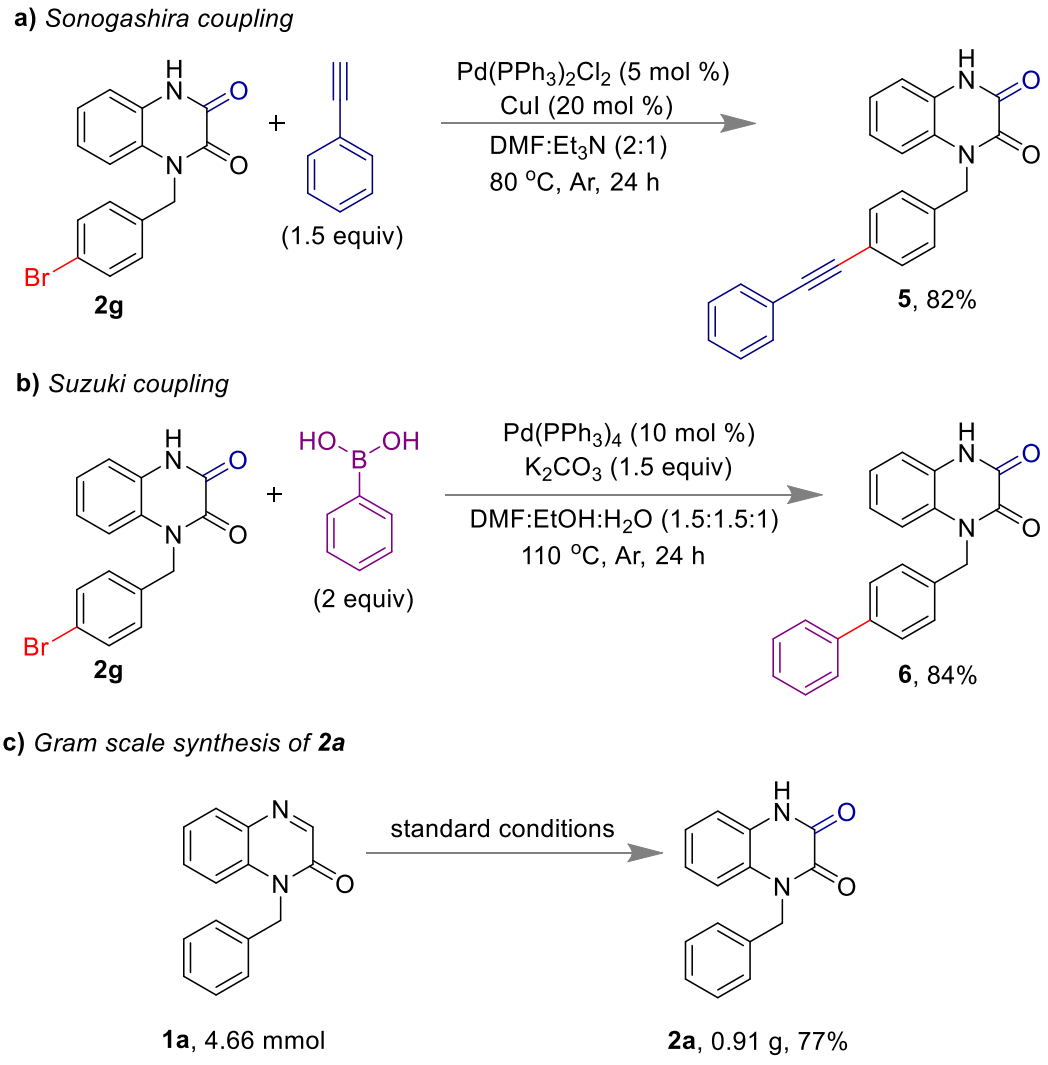

Figure 5.7. Post synthetic applications

5.4 CONCLUSION

In summary, a visible-light mediated metal-free oxygenation protocol of quinoxalin-2(1*H*)-one has been developed by employing Mes-Acr-$MeClO_4$ as a visible-light photocatalyst. In this convenient approach, O_2 served as the green and eco-friendly oxidant source to furnish a library of quinoxaline-2,3-diones from quinoxalin-2(1*H*)-ones. The protocol excluded the use of any strong oxidant, additive, or co-catalyst; exhibited high regioselectivity and good functional group tolerance. We believe that this simple and sustainable protocol will impart a significant contribution to the research areas like visible-light photocatalysis and oxygenation of heterocycles.

5.5 EXPERIMENTAL SECTION

Instrumentation and Chemicals: Column chromatography was used for the purification of the compounds using silica gel (with mesh 100-200 or mesh 230-400) and hexane-ethyl acetate mixtures were used as eluent unless otherwise specified. Solvents were purchased from commercially available sources and used in the reaction without further purification. All NMR spectra were recorded in 400 MHz or 700 MHz instruments (Bruker) at room temperature (25 °C). The splitting of the NMR peaks (peak pattern) are represented by s: singlet; d: doublet; t: triplet; q: quartet; m: multiplet; dd: doublet of doublets; td: triplet of doublets; br s: broad singlet. Chemical shift values are reported in parts per million (ppm) with respect to residual trichloromethane (7.26 ppm for ^{1}H and 77.16 ppm for ^{13}C) and dimethyl sulfoxide (2.50 ppm for ^{1}H and 39.52 ppm for ^{13}C). The coupling constant values (*J*) are reported in hertz (Hz). A digital melting point apparatus was used to obtain the melting point of the compounds which were included in the characterization data without any correction. FT-IR spectra were recorded by making a thin film of the compounds on KBr pellets using dichloromethane and IR spectral data

are reported in wave number (cm^{-1}). High-resolution mass spectra (HR-MS) were recorded on an ESI-TOF (time of flight) mass spectrometer. The detailed procedure for the preparation of the starting materials and target molecule are described below.

Description of Light Source. 3W Blue LEDs were purchased from commercially available source (Murphy). The wavelength was 450-455 nm. Quartz glass (brand name: Luzchem) was used as a reaction vessel. The distance between light source and quartz tube was approximately 4 cm and no filter was used for the reaction. High-speed electric fans were used to maintain the room temperature.

Synthetic procedure for preparation of 1-benzyl-1,4-dihydroquinoxaline-2,3-dione (2a). In an oven-dried quartz tube charged with a magnetic stirring bar, 1-benzylquinoxalin-2(1*H*)-one (60 mg, 0.254 mmol, 1.0 equiv) and Mes-Acr-MeClO_4 (5.3 mg, 0.013 mmol, 5 mol %) were added and dissolved in 2.0 mL dichloroethane (DCE) solvent under an O_2 (balloon) atmosphere. After that, the reaction mixture was irradiated by 3W Blue LEDs (3W×4) light (wavelength 450-455 nm) for 12 h in the presence of an O_2 (balloon). After completion of the reaction, DCE was removed under reduced pressure. Then, the crude mixture was washed with water and extracted with EtOAc. The resulting organic solution was dried over anhydrous sodium Na_2SO_4 and concentrated under reduced pressure. The resulting mixture was purified by silica gel column chromatography using hexane/ethyl acetate mixture as an eluent.

Procedure for the control experiments in presence of different quenchers. In an oven-dried quartz tube charged with a magnetic stirring bar, 1-benzylquinoxalin-2(1*H*)-one (60 mg, 0.254

mmol, 1.0 equiv) and Mes-Acr-$MeClO_4$ (5.3 mg, 0.0123 mmol, 5 mol %) and quencher (1.0 equiv) were added and dissolved in 2.0 mL dichloroethane (DCE) solvent under an O_2 (balloon) atmosphere. After that, the reaction mixture was irradiated by 3W Blue LEDs (3W×4) light for 24 h in the presence of an O_2 (balloon). The reaction was monitored by TLC. After 24 h, DCE was removed under reduced pressure. Then the crude mixture was washed with water and extracted with EtOAc. The resulting organic solution was dried over anhydrous sodium Na_2SO_4 and concentrated under reduced pressure. According to observation, formation of **2a** was not observed when the reaction was carried out in presence of quenchers like TEMPO, BHT, $CuCl_2$, *p*-benzoquinone. Only 17% of product formation was observed in the case of sodium azide as quencher. The reaction delivered the expected product **2a** with 81% yield when executed in presence of *tert*-butanol as quencher.

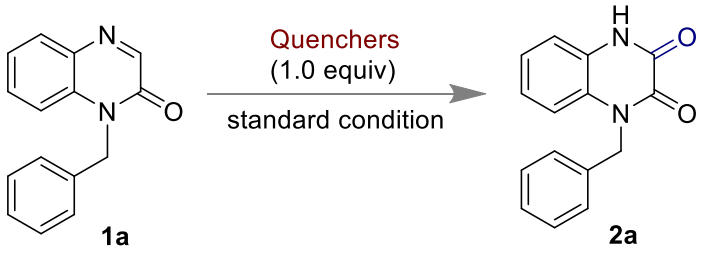

Entry	Quencher	Yield (%)[b]	Role
1	TEMPO	0	radical scavenger
2	BHT	0	radical scavenger
3	$CuCl_2$	0	electron scavenger
4	*p*-benzoquinone	0	superoxide radical anion scavenger
5	sodium azide	17	singlet oxygen scavenger
6	*tert*-butanol	81	hydroxide radical scavenger

Figure 5.8. Control experiments in presence of different quenchers ([b]Isolated yield).

Synthesis of 1-(4-(phenylethynyl)benzyl)-1,4-dihydroquinoxaline-2,3-dione (5). To an oven-dried sealed tube charged with a magnetic stirring bar and 1-(4-bromobenzyl)-1,4-dihydroquinoxaline-2,3-dione (**2g**) (87 mg, 0.264 mmol, 1.0 equiv), $PdCl_2(PPh_3)_2$ (9 mg, 0.013 mmol, 5 mol %), and CuI (10 mg, 0.053 mmol, 20 mol %) in 2 mL of anhydrous DMF and 1 mL of Et_3N mixture was added phenyl acetylene (44 µL, 0.396 mmol, 1.5 equiv) and it was stirred at 80 ºC for 24 h under argon atmosphere.[40] After completion, the reaction mixture was cooled to room temperature and washed with brine solution. The organic layer was extracted with ethyl acetate, dried over Na_2SO_4 and concentrated under reduced pressure. Column purification provided the desired product 1-(4-(phenylethynyl)benzyl)-1,4-dihydroquinoxaline-2,3-dione (**5**) in 82% yield.

Synthesis of 1-([1,1'-biphenyl]-4-ylmethyl)-1,4-dihydroquinoxaline-2,3-dione (6). To an oven-dried sealed tube charged with a magnetic stirring bar and 1-(4-bromobenzyl)-1,4-dihydroquinoxaline-2,3-dione (**2g**) (82 mg, 0.249 mmol, 1.0 equiv), $Pd(PPh_3)_4$ (29 mg, 0.0249 mmol, 10 mol %), and K_2CO_3 (52 mg, 0.373 mmol, 1.5 equiv) in a 4 mL mixture of DMF, EtOH and H_2O (1.5:1.5:1) was added phenyl boronic acid (61 mg, 0.498 mmol, 2.0 equiv) and it was stirred at 100 ºC for 24 h under argon atmosphere.[40] After completion, the reaction mixture was cooled to room temperature and washed with brine solution. The organic layer was extracted with ethyl acetate, dried over Na_2SO_4 and concentrated under reduced pressure. Column purification provided the desired product 1-([1,1'-biphenyl]-4-ylmethyl)-1,4-dihydroquinoxaline-2,3-dione (**6**) in 84% yield.

Gram scale synthesis of 2a. In an oven-dried quartz tube charged with a magnetic stirring bar, 1-benzylquinoxalin-2(1*H*)-one (1.1 g, 4.66 mmol, 1.0 equiv) and Mes-Acr-$MeClO_4$ (96.0 mg, 0.233 mmol, 5 mol %) were added and dissolved in 10.0 mL dichloroethane (DCE) solvent under an O_2 (balloon) atmosphere. After that, the reaction mixture was irradiated by 3W Blue LEDs (3W×4) light (wavelength 450-455 nm) for 30 h in the presence of an O_2 (balloon). After completion of the reaction, DCE was removed under reduced pressure. Then, the crude mixture was washed with water and extracted with EtOAc. The resulting organic solution was dried over anhydrous sodium Na_2SO_4 and concentrated under reduced pressure. The resulting mixture was purified by silica gel column chromatography using hexane/ethyl acetate mixture as eluent.

Light ON-OFF-ON Experiment. In an oven dried quartz tube charged with a magnetic stirring bar, 1-benzylquinoxalin-2(1*H*)-one (60 mg, 0.254 mmol, 1.0 equiv) and Mes-Acr-$MeClO_4$ (5.3 mg, 0.013 mmol, 5 mol %) were added and dissolved in 2.0 mL dichloroethane (DCE) solvent under an O_2 (balloon) atmosphere. After that, the reaction mixture was irradiated by 3W Blue LEDs (3W×4) light for 12 h in the presence of an O_2 (balloon). The progress of the reaction was monitored every 4 h and 2 h in the presence of light and absence of light by ^{1}H NMR experiment.

Fluorescence quenching experiment. The maximum emission of the photocatalyst Mes-Acr-$MeClO_4$ (2×10^{-5} M in DCE) was observed at 512 nm at the excitation wavelength of 360 nm. Addition of 1a (2×10^{-3} M in DCE) in an incremental way led to the gradual decrease of fluorescence intensity of the photocatalyst.

Synthesis of starting materials. Starting material preparation has been discussed in chapter 4.[36]

Characterization Data

1-Benzyl-1,4-dihydroquinoxaline-2,3-dione (2a).[36] R_f = 0.3 (50% ethyl acetate/hexane); yellow solid; yield 56 mg (88%); mp 294-296 ºC; ^{1}H NMR (700 MHz, DMSO-d_6) δ 12.12 (s, 1H), 7.34 – 7.28 (m, 4H), 7.25 (t, *J* = 7.0 Hz, 1H), 7.20 (d, *J* = 7.0 Hz, 1H), 7.17 (d, *J* = 8.4 Hz, 1H), 7.13 (t, *J* = 7.0 Hz, 1H), 7.06 (t, *J* = 7.7 Hz, 1H), 5.37 (s, 2H); ^{13}C{1H} NMR (100 MHz, DMSO-d_6) δ 155.8, 153.8, 135.8, 128.7, 127.3, 126.7, 126.3, 125.9, 123.7, 123.2, 115.8, 115.5, 45.7.

4-((2,3-Dioxo-3,4-dihydroquinoxalin-1(2*H*)-yl)methyl)benzonitrile (2b).[36] R_f = 0.2 (50% ethyl acetate/hexane); light yellow solid; yield 68 mg (98%); mp > 300 ºC; ^{1}H NMR (700 MHz, DMSO-d_6) δ 12.10 (s, 1H), 7.79 (d, *J* = 8.4 Hz, 2H), 7.52 (d, *J* = 8.4 Hz, 2H), 7.21 (d, *J* = 7.0 Hz, 1H), 7.14 (t, *J* = 7.7 Hz, 1H), 7.09 (d, *J* = 7.7 Hz, 1H), 7.05 (t, *J* = 7.7 Hz, 1H), 5.45 (s, 2H); ^{13}C{1H} NMR (175 MHz, DMSO-d_6) δ 157.3, 155.5, 142.4, 133.9, 128.6, 127.0, 126.4, 125.9, 125.5, 120.1, 117.5, 116.6, 111.3, 47.1.

1-(4-Nitrobenzyl)-1,4-dihydroquinoxaline-2,3-dione (2c).[36] R_f = 0.2 (50% ethyl acetate/hexane); pale yellow solid; yield 54 mg (85%); mp 277-279 ºC; ^{1}H NMR (700 MHz, DMSO-d_6) δ 12.12 (s, 1H), 8.17 (d, *J* = 8.4 Hz, 2H), 7.60 (d, *J* = 8.4 Hz, 2H), 7.21 (d, *J* = 7.7 Hz, 1H), 7.15 (t, *J* = 7.7 Hz, 1H), 7.11 (d, *J* = 7.7 Hz, 1H), 7.05 (t, *J* = 7.7 Hz, 1H), 5.51 (s, 2H); ^{13}C{1H} NMR (175 MHz, DMSO-d_6) δ 155.8, 153.7, 146.8, 143.8, 128.0, 126.2, 126.1, 123.8, 123.7, 123.1, 115.8, 115.2, 45.4.

1-(4-(Trifluoromethyl)benzyl)-1,4-dihydroquinoxaline-2,3-dione (2d).[36] R_f = 0.3 (50% ethyl acetate/hexane); pale yellow solid; yield 62 mg (94%); mp 265-267 ºC; ^{1}H NMR (700 MHz,

DMSO-d_6) δ 12.12 (s, 1H), 7.68 (d, J = 8.4 Hz, 2H), 7.54 (d, J = 8.4 Hz, 2H), 7.21 (d, J = 8.4 Hz, 1H), 7.15 – 7.13 (m, 2H), 7.07 – 7.05 (m, 1H), 5.47 (s, 2H); ^{13}C{1H} NMR (175 MHz, DMSO-d_6) δ 156.0, 153.9, 140.8, 128.2 (q, $^2J_{C\text{-}F}$ = 31.7 Hz), 127.7, 126.4, 126.1, 125.7 (q, $^3J_{C\text{-}F}$ = 3.5 Hz), 124.4 (q, $^1J_{C\text{-}F}$ = 270.4 Hz), 124.1, 123.5, 116.1, 115.5, 45.6.

1-(3,5-Difluorobenzyl)-1,4-dihydroquinoxaline-2,3-dione (2e).[36] R_f = 0.2 (50% ethyl acetate/hexane); pale yellow solid; yield 65 mg (98%); mp 276-278 ºC; ^{1}H NMR (700 MHz, DMSO-d_6) δ 12.03 (s, 1H), 7.20 (d, J = 7.7 Hz, 1H), 7.16 – 7.04 (m, 6H), 5.37 (s, 2H); ^{13}C{1H} NMR (175 MHz, DMSO-d_6) δ 162.57 (dd, J = 244.6, 13.1 Hz), 155.9, 153.8, 140.7 (t, J = 9.1 Hz), 126.3, 126.2, 123.7, 123.0, 115.7, 115.1, 110.00 (dd, J = 21.0, 4.5 Hz), 102.70 (t, J = 25.2 Hz), 45.2.

1-(4-Fluorobenzyl)-1,4-dihydroquinoxaline-2,3-dione (2f).[36] R_f = 0.2 (50% ethyl acetate/hexane); pale yellow solid; yield 61 mg (90%); mp > 300 ºC; ^{1}H NMR (700 MHz, DMSO-d_6) δ 12.09 (s, 1H), 7.37 (dd, J = 8.2, 5.6 Hz, 2H), 7.19 (t, J = 7.7 Hz, 2H), 7.16 – 7.13 (m, 3H), 7.07 (t, J = 7.7 Hz, 1H), 5.36 (s, 2H); ^{13}C{1H} NMR (175 MHz, DMSO-d_6) δ 161.3 (d, $^1J_{C\text{-}F}$ = 243.1 Hz), 155.7, 153.7, 131.9 (d, $^4J_{C\text{-}F}$ = 2.8 Hz), 128.9 (d, $^3J_{C\text{-}F}$ = 8.2 Hz), 126.2, 126.0, 123.7, 123.1, 115.7, 115.4 (d, $^2J_{C\text{-}F}$ = 21.3 Hz) , 115.3, 44.9.

1-(4-Bromobenzyl)-1,4-dihydroquinoxaline-2,3-dione (2g).[36] R_f = 0.2 (50% ethyl acetate/hexane); light yellow solid; yield 61 mg (96%); mp 279-281 ºC; ^{1}H NMR (700 MHz, DMSO-d_6) δ 12.10 (s, 1H), 7.51 (d, J = 8.4 Hz, 2H), 7.29 (d, J = 8.4 Hz, 2H), 7.20 (d, J = 7.7 Hz, 1H), 7.15 – 7.13 (m, 2H), 7.06 (t, J = 7.7 Hz, 1H), 5.34 (s, 2H); ^{13}C{1H} NMR (175 MHz, DMSO-d_6) δ 155.7, 153.7, 135.3, 131.5, 129.1, 126.2, 126.0, 123.7, 123.1, 120.3, 115.7, 115.3, 45.1.

1-(4-(*tert*-Butyl)benzyl)-1,4-dihydroquinoxaline-2,3-dione (2h).[36] R_f = 0.2 (50% ethyl acetate/hexane; yellow solid; yield 58 mg (86%); mp > 300 ºC; ^{1}H NMR (700 MHz, DMSO-d_6) δ 12.12 (s, 1H), 7.33 (d, *J* = 8.4 Hz, 2H), 7.22 (d, *J* = 7.0 Hz, 3H), 7.20 (d, *J* = 7.7 Hz, 1H), 7.13 (t, *J* = 7.0 Hz, 1H), 7.08 (t, *J* = 7.7 Hz, 1H), 5.34 (s, 2H), 1.23 (s, 9H); ^{13}C{1H} NMR (175 MHz, DMSO-d_6) δ 155.7, 153.7, 149.6, 132.8, 126.5, 126.3, 125.9, 125.4, 123.6, 123.2, 115.7, 115.5, 45.2, 34.2, 31.1.

1-(4-Isopropylbenzyl)-1,4-dihydroquinoxaline-2,3-dione (2i).[36] R_f = 0.2 (50% ethyl acetate/hexane); yellow solid; yield 54 mg (84%); mp 269-271 ºC; ^{1}H NMR (400 MHz, DMSO-d_6) δ 12.11 (s, 1H), 7.23-7.15 (m, 6H), 7.13 – 7.06 (m, 2H), 5.33 (s, 2H), 2.87-2.80 (m, 1H), 1.15 (d, *J* = 6.8 Hz, 6H); ^{13}C{1H} NMR (100 MHz, DMSO-d_6) δ 155.7, 153.7, 147.4, 133.1, 126.8, 126.5, 126.3, 125.9, 123.6, 123.1, 115.7, 115.5, 45.3, 33.0, 23.8.

1-(4-Methylbenzyl)-1,4-dihydroquinoxaline-2,3-dione (2j).[36] R_f = 0.3 (50% ethyl acetate/hexane); yellow solid; yield 55 mg (83%); mp > 300 ºC; ^{1}H NMR (400 MHz, DMSO-d_6) δ 12.10 (s, 1H), 7.18 (t, *J* = 7.6 Hz, 4H), 7.13 (t, *J* = 6.8 Hz, 3H), 7.06 (t, *J* = 7.6 Hz, 1H), 5.33 (s, 2H), 2.25 (s, 3H); ^{13}C{1H} NMR (100 MHz, DMSO-d_6) δ 155.8, 153.7, 136.4, 132.7, 129.2, 126.7, 126.2, 125.9, 123.6, 123.1, 115.7, 115.5, 45.3, 20.6.

1-Butyl-1,4-dihydroquinoxaline-2,3-dione (2k).[36] R_f = 0.2 (50% ethyl acetate/hexane); yellow solid; yield 57 mg (84%); mp 184-186 ºC, ^{1}H NMR (400 MHz, DMSO-d_6)) δ 12.02 (s, 1H), 7.38 (d, *J* = 8.0 Hz, 1H), 7.18 (brs, 3H), 4.09 (t, *J* = 7.2 Hz, 2H), 1.63-1.56 (m, 2H), 1.43-1.33 (m, 2H),

0.92 (t, *J* = 7.2 Hz, 3H); ; ^{13}C{1H} NMR (100 MHz, DMSO-d_6) δ 155.0, 153.5, 126.1, 125.8, 123.5, 123.3 115.8, 114.9, 41.9, 28.6, 19.5, 13.7.

1-Phenethyl-1,4-dihydroquinoxaline-2,3-dione (2l).[36] R_f = 0.1 (50% ethyl acetate/hexane); pale yellow solid; yield 58 mg (88%); mp 226-228 ºC; ^{1}H NMR (400 MHz, DMSO-d_6) δ 12.03 (s, 1H), 7.47 (d, *J* = 7.6 Hz, 1H), 7.32 (d, *J* = 4.0 Hz, 4H), 7.19 (s, 4H), 4.32 – 4.29 (m, 2H), 2.94 – 2.90 (m, 2H); ^{13}C{1H} NMR (100 MHz, DMSO-d_6) δ 154.9, 153.5, 138.2, 128.8, 128.5, 126.5, 126.0, 125.7, 123.5, 123.4, 115.8, 114.9, 43.5, 32.4.

1-Ethyl-1,4-dihydroquinoxaline-2,3-dione (2m).[36] R_f = 0.1 (50% ethyl acetate1/hexane) pale yellow solid; yield 60 mg (90%); mp 285-287 ºC; ^{1}H NMR (700 MHz, DMSO-d_6) δ 12.02 (s, 1H), 7.40 (d, *J* = 7.7 Hz, 1H), 7.18 (d, *J* = 9.1 Hz, 3H), 4.14 (q, *J* = 7.0 Hz, 2H), 1.22 – 1.20 (m, 3H); ^{13}C{1H} NMR (175 MHz, DMSO-d_6) δ 154.8, 153.6, 125.9, 125.8, 123.5, 123.3, 115.8, 114.8, 37.3, 12.0.

1-(Prop-2-yn-1-yl)-1,4-dihydroquinoxaline-2,3-dione (2n).[36] R_f = 0.2 (50% ethyl acetate/hexane); yellow solid; yield 51 mg (75%); mp 283-285 ºC; ^{1}H NMR (700 MHz, DMSO-d_6) δ 12.10 (s, 1H), 7.42 (d, *J* = 7.7 Hz, 1H), 7.24 – 7.21 (m, 3H), 4.96 (s, 2H); ^{13}C{1H} NMR (175 MHz, DMSO-d_6) δ 154.6, 153.3, 125.7, 125.5, 124.0, 123.2, 115.7, 115.3, 78.1, 75.1, 31.9.

***tert*-Butyl 2-(2-oxoquinoxalin-1(2*H*)-yl)acetate (2o).**[36] R_f = 0.3 (50% ethyl acetate/hexane); pale yellow solid; yield 56 mg (87%); mp 264-266 ºC; ^{1}H NMR (700 MHz, DMSO-d_6) δ 12.18 (s,

1H), 7.25-7.18 (m, 4H), 4.87 (s, 2H), 1.42 (s, 9H); ^{13}C{1H} NMR (175 MHz, DMSO-d_6) δ 166.5, 155.2, 153.3, 126.4, 125.4, 123.9, 123.4, 115.8, 114.8, 82.1, 44.7, 27.6.

Isopropyl 2-(2,3-dioxo-3,4-dihydroquinoxalin-1(2*H*)-yl)acetate (2p).[36] R_f = 0.3 (50% ethyl acetate/hexane); white solid; yield 58 mg (85%); mp 238-240 ºC; ^{1}H NMR (700 MHz, DMSO-d_6) δ 12.19 (s, 1H), 7.27 (d, *J* = 7.7 Hz, 1H), 7.23 – 7.16 (m, 3H), 4.97-4.96 (m, 1H), 4.94 (s, 2H), 1.22 (d, *J* = 6.3 Hz, 6H); ^{13}C{1H} NMR (175 MHz, DMSO-d_6) δ 167.0, 155.2, 153.2, 126.4, 125.4, 124.0, 123.4, 115.9, 114.8, 69.1, 44.3, 21.5.

Ethyl 2-(2,3-dioxo-3,4-dihydroquinoxalin-1(2*H*)-yl)acetate (2q).[36] R_f = 0.2 (50% ethyl acetate/hexane); pale yellow solid; yield 62 mg (95%); mp 280-282 ºC; ^{1}H NMR (700 MHz, DMSO-d_6) δ 12.19 (s, 1H), 7.30 (d, *J* = 8.4 Hz, 1H), 7.23-7.16 (m, 3H), 4.98 (s, 2H), 4.17 (q, *J* = 7.7 Hz, 2H), 1.21 (t, *J* = 7.0 Hz, 3H); ^{13}C{1H} NMR (175 MHz, DMSO-d_6) δ 167.6, 155.2, 153.2, 126.4, 125.5, 124.0, 123.4, 115.8, 114.9, 61.3, 44.2, 14.0.

1-Benzyl-6-chloro-1,4-dihydroquinoxaline-2,3-dione and 1-Benzyl-7-chloro-1,4-dihydroquinoxaline-2,3-dione (4a).[36] R_f = 0.3 (50% ethyl acetate/hexane); pale yellow solid; yield 65 mg (88%); mp 251-253 ºC; Two regioisomers with 74:26 Ratio; ^{1}H NMR (700 MHz, DMSO-d_6) δ 12.19 (s, 0.3H), 12.18 (s, 1H), 7.32-7.29 (m, 5.6H), 7.26 (d, *J* = 7.0 Hz, 1.7H), 7.19 (d, *J* = 7.0 Hz, 2H), 7.15 (d, *J* = 9.1 Hz, 1H), 7.11 (d, *J* = 9.1 Hz, 11H), 5.37 (s, 0.6H), 5.35 (s, 2H); ^{13}C{1H} NMR (175 MHz, DMSO-d_6) δ 156.1, 155.9, 154.1, 153.9, 135.9, 135.8, 129.2, 129.1, 128.0, 127.9, 127.8, 127.8, 127.7, 127.4, 127.1, 126.0, 125.5, 123.8, 123.0, 117.5, 115.6, 115.4, 46.2, 46.1.

1-Benzyl-6-bromo-1,4-dihydroquinoxaline-2,3-dione and 1-Benzyl-7-bromo-1,4-dihydroquinoxaline-2,3-dione (4b).[36] R_f = 0.4 (50% ethyl acetate/hexane); pale yellow solid; yield 58 mg (80%); mp 258-260 ºC; Two regioisomers with 60:40 Ratio; ^{1}H NMR (700 MHz, DMSO-d_6) δ 12.18 (s, 0.7H), 12.16 (s, 1H), 7.36 – 7.28 (m, 9.5H), 7.28-7.25 (m, 2.5H), 7.22 (d, *J* = 8.4 Hz, 2H), 7.13-7.09 (m, 2H), 5.37 (s, 1.4H), 5.35 (s, 2H); ^{13}C{1H} NMR (175 MHz, DMSO-d_6) δ 155.6, 155.4, 153.6, 153.4, 135.4, 128.7, 128.7, 127.8, 127.5, 127.3, 127.3, 126.6, 126.2, 125.9, 125.5, 125.4, 117.8, 117.7, 117.4, 115.1, 114.6, 45.7, 45.6.

1-Benzyl-6-methyl-1,4-dihydroquinoxaline-2,3-dione and 1-Benzyl-7-methyl-1,4-dihydroquinoxaline-2,3-dione (4c).[36] R_f = 0.4 (50% ethyl acetate/hexane); pale yellow solid; yield 57 mg (84%); mp 263-265 ºC; Two regioisomers with 62:38 Ratio; ^{1}H NMR (700 MHz, DMSO-d_6) δ 12.07 (s, 1.6H), 7.33 – 7.23 (m, 8.6H), 7.09 (d, *J* = 7.7 Hz, 0.6H), 7.05 (d, *J* = 8.4 Hz, 1H), 7.02-6.99 (m, 1.6H), 6.95 (d, *J* = 7.7 Hz, 0.6H), 6.87 (d, *J* = 8.4 Hz, 1H), 5.35 (s, 1.2H), 5.34 (s, 2.0H), 2.24 (s, 3H), 2.20 (s, 1.8H); ^{13}C{1H} NMR (175 MHz, DMSO-d_6) δ 156.0, 155.7, 154.0, 153.7, 135.9, 135.9, 133.4, 132.8, 128.9, 128.9, 127.5, 127.5, 126.8, 126.8, 126.3, 125.8, 124.7, 124.2, 123.7, 116.0, 115.9, 115.8, 115.6, 45.8, 45.7, 21.0, 20.4.

1-Benzyl-6,7-dichloro-1,4-dihydroquinoxaline-2,3-dione (4d)[36] R_f = 0.4 (50% ethyl acetate/hexane); pale yellow solid; yield 63 mg (91%); mp > 300 ºC; ^{1}H NMR (700 MHz, DMSO-d_6) δ 12.22 (s, 1H), 7.38 (s, 1H), 7.33 (d, *J* = 6.3 Hz, 5H), 7.27 (d, *J* = 6.3 Hz, 1H), 5.37 (s, 2H); ^{13}C{1H} NMR (175 MHz, DMSO-d_6) δ 155.3, 153.4, 135.2, 128.7, 127.4, 126.8, 126.7, 126.4, 125.2, 124.6, 116.8, 116.4, 45.7.

1-Benzyl-6,7-difluoro-1,4-dihydroquinoxaline-2,3-dione (4e).[36] R_f = 0.3 (50% ethyl acetate/hexane); pale yellow solid; yield 49 mg (90%); mp 270-272 ºC; ^{1}H NMR (700 MHz, DMSO-d_6) δ 12.15 (s, 1H), 7.32 (s, 5H), 7.27 (d, *J* = 6.3 Hz, 1H), 7.16-7.14 (m, 1H), 5.35 (s, 2H); ^{13}C{1H} NMR (175 MHz, DMSO-d_6) δ 155.3, 153.4, 145.1 (dd, *J* = 239.4, 12.4 Hz), 144.9 (dd, *J* = 237.6, 12.6 Hz), 135.2, 128.7, 127.4, 126.8, 123.23 (d, *J* = 7.7 Hz), 122.72 (d, *J* = 9.1 Hz), 105.0 (d, *J* = 23.5 Hz), 104.13 (d, *J* = 21.9 Hz), 45.9.

1-Benzyl-6,7-dimethyl-1,4-dihydroquinoxaline-2,3-dione (4f).[36] R_f = 0.2 (50% ethyl acetate/hexane); pale yellow solid; yield 49 mg (76%); mp > 300 ºC; ^{1}H NMR (700 MHz, DMSO-d_6) δ 12.00 (s, 1H), 7.32 (t, *J* = 7.0 Hz, 2H), 7.28 (d, *J* = 7.7 Hz, 2H), 7.24 (t, *J* = 7.0 Hz, 1H), 7.02 (s, 1H), 6.95 (s, 1H), 5.35 (s, 2H), 2.15 (s, 3H), 2.12 (s, 3H); ^{13}C{1H} NMR (175 MHz, DMSO-d_6) δ 155.6, 153.7, 135.9, 131.9, 131.3, 128.6, 127.2, 126.7, 124.1, 123.5, 116.3, 116.1, 45.4, 19.2, 18.8.

6,7-dichloro-1-methyl-1,4-dihydroquinoxaline-2,3-dione (4g).[36] R_f = 0.3 (50% ethyl acetate/hexane); yellow solid; yield 50 mg (72%); mp > 300 ºC; ^{1}H NMR (700 MHz, DMSO-d_6) δ 12.11 (s, 1H), 7.58 (s, 1H), 7.27 (s, 1H), 3.47 (s, 3H); ^{13}C{1H} NMR (175 MHz, DMSO-d_6) δ 154.9, 153.2, 127.7, 125.9, 125.0, 124.9, 116.6, 116.0, 30.1.

1-(4-(phenylethynyl)benzyl)-1,4-dihydroquinoxaline-2,3-dione (**5**). R_f = 0.3 (50% ethyl acetate/hexane); light yellow solid; yield 76 mg (82%); mp > 300 ºC; ^{1}H NMR (700 MHz, DMSO-d_6) δ 12.12 (s, 1H), 7.54-7.50 (m, 4H), 7.41 (d, *J* = 3.5 Hz, 3H), 7.37 (d, *J* = 7.7 Hz, 2H), 7.21 (d, *J* = 7.7 Hz, 1H), 7.16-7.14 (m, 2H), 7.07 (t, *J* = 7.7 Hz, 1H), 5.41 (s, 2H); ^{13}C{1H} NMR (175

MHz, DMSO-d_6) δ 155.8, 153.7, 136.6, 131.6, 131.4, 128.8, 128.8, 127.1, 126.3, 126.0, 123.7, 123.1, 122.2, 121.1, 115.7, 115.4, 89.3, 89.1, 45.5.

1-([1,1'-biphenyl]-4-ylmethyl)-1,4-dihydroquinoxaline-2,3-dione (**6**). R_f = 0.3 (50% ethyl acetate/hexane); light yellow solid; yield 69 mg (84%); mp > 300 ºC; ^{1}H NMR (700 MHz, DMSO-d_6) δ 12.13 (s, 1H), 7.62 (t, *J* = 8.4 Hz, 4H), 7.44 (t, *J* = 7.7 Hz, 2H), 7.40 (d, *J* = 8.4 Hz, 2H), 7.35 (t, *J* = 7.7 Hz, 1H), 7.25-7.21 (m, 2H), 7.15 (t, *J* = 7.7 Hz, 1H), 7.09 (t, *J* = 7.7 Hz, 1H), 5.43 (s, 2H); ^{13}C{1H} NMR (175 MHz, DMSO-d_6) δ 155.7, 153.7, 139.7, 139.2, 135.0, 128.9, 127.4, 127.3, 126.9, 126.6, 126.3, 125.9, 123.7, 123.1, 115.7, 115.5, 45.3;

5.6 NOTES AND REFERENCES

1. R. H. Verschueren and W. M. De Borggraeve, *Molecules*, 2019, **24**, 2122.
2. N. A. Romero and D. A. Nicewicz, *Chem. Rev.*, 2016, **116**, 10075-10166.
3. L. Marzo, S. K. Pagire, O. Reiser and B. König, *Angew. Chem. Int. Ed.*, 2018, **57**, 10034-10072.
4. S. Fukuzumi and K. Ohkubo, *Org. Biomol. Chem.*, 2014, **12**, 6059-6071.
5. G. Shukla, T. Alam, H. K. Srivastava, R. Kumar and B. K. Patel, *Org. Lett.*, 2019, **21**, 3543-3547.
6. A. K. Sahoo, A. Rakshit, A. Dahiya, A. Pan and B. K. Patel, *Org. Lett.*, 2022, **24**, 1918-1923.

7. S. K. Parida, T. Mandal, S. Das, S. K. Hota, S. De Sarkar and S. Murarka, *ACS Catal.*, 2021, **11**, 1640-1683.

8. J. Singh and A. Sharma, *Adv. Synth. Catal.*, 2021, **363**, 3411-3438.

9. M. Pramanik, A. Mathuri, S. Sau, M. Das and P. Mal, *Org. Lett.*, 2021, **23**, 8088-8092.

10. S. Mitra, M. Ghosh, S. Mishra and A. Hajra, *J. Org. Chem.*, 2015, **80**, 8275-8281.

11. S. Sharma and A. Sharma, *Org. Biomol. Chem.*, 2019, **17**, 4384-4405.

12. R. I. Patel, A. Sharma, S. Sharma and A. Sharma, *Org. Chem. Front.*, 2021, **8**, 1694-1718.

13. C. K. Prier, D. A. Rankic and D. W. C. MacMillan, *Chem. Rev.*, 2013, **113**, 5322-5363.

14. C. Tang, X. Qiu, Z. Cheng and N. Jiao, *Chem. Soc. Rev.*, 2021, **50**, 8067-8101.

15. N. L. Reed and T. P. Yoon, *Chem. Soc. Rev.*, 2021, **50**, 2954-2967.

16. Y. Zhang, S. Qin, N. Claes, W. Schilling, P. K. Sahoo, H. Y. V. Ching, A. Jaworski, F. Lemière, A. Slabon, S. Van Doorslaer, S. Bals and S. Das, *ACS Sustainable Chem. Eng.*, 2022, **10**, 530-540.

17. Y. Zhang, D. Riemer, W. Schilling, J. Kollmann and S. Das, *ACS Catal.*, 2018, **8**, 6659-6664.

18. W. Schilling, Y. Zhang, D. Riemer and S. Das, *Chem. Eur. J.*, 2020, **26**, 390-395.

19. D. Dewangan, K. Nakhate, A. Mishra, A. S. Thakur, H. Rajak, J. Dwivedi, S. Sharma and S. Paliwal, *J. Heterocycl. Chem.*, 2019, **56**, 566-578.

20. Q.-H. Xia, W. Hu, C. Li, J.-F. Wu, L. Yang, X.-M. Han, Y.-M. Shen, Z.-Y. Li and X. Li, *Eur. J. Med. Chem.*, 2016, **124**, 311-325.

21. W. Xie, Y. Wu, J. Zhang, Q. Mei, Y. Zhang, N. Zhu, R. Liu and H. Zhang, *Eur. J. Med. Chem.*, 2018, **145**, 35-40.

22. M. G. Moloney, *Natural Product Reports*, 2002, **19**, 597-616.

23. Q. Ke, G. Yan, J. Yu and X. Wu, *Org. Biomol. Chem.*, 2019, **17**, 5863-5881.

24. S. Piras, M. Loriga, A. Carta, G. Paglietti, M. Paola Costi and S. Ferrari, *J. Heterocycl. Chem.*, 2006, **43**, 541-548.

25. R. Liu, Z. Huang, M. G. Murray, X. Guo and G. Liu, *J. Med. Chem.*, 2011, **54**, 5747-5768.

26. Kiran, P. Rani, S. Chahal, J. Sindhu, S. Kumar, R. S. Varma and R. Singh, *New J. Chem.*, 2021, **45**, 18722-18763.

27. L. Wang, Y. Zhang, F. Li, X. Hao, H.-Y. Zhang and J. Zhao, *Adv. Synth. Catal.*, 2018, **360**, 3969-3977.

28. Q. Yang, X. Han, J. Zhao, H. Y. Zhang and Y. Zhang, *J. Org. Chem.*, 2019, **84**, 11417-11424.

29. M. Gao, Y. Li, L. Xie, R. Chauvin and X. Cui, *Chem. Commun.*, 2016, **52**, 2846-2849.

30. J. Yuan, S. Liu, Y. Xiao, P. Mao, L. Yang and L. Qu, *Org. Biomol. Chem.*, 2019, **17**, 876-884.

31. J. Wang, B. Sun, L. Zhang, T. Xu, Y. Xie and C. Jin, *Org. Chem. Front.*, 2020, **7**, 113-118.

32. L.-Y. Xie, S. Peng, L.-H. Yang, C. Peng, Y.-W. Lin, X. Yu, Z. Cao, Y.-Y. Peng and W.-M. He, *Green Chem.*, 2021, **23**, 374-378.

33. J. Dudash, Y. Zhang, J. B. Moore, R. Look, Y. Liang, M. P. Beavers, B. R. Conway, P. J. Rybczynski and K. T. Demarest, *Bioorg. Med. Chem. Lett.*, 2005, **15**, 4790-4793.

34. B. Loev, J. H. Musser, R. E. Brown, H. Jones, R. Kahen, F. C. Huang, A. Khandwala, P. Sonnino-Goldman and M. J. Leibowitz, *J. Med. Chem.*, 1985, **28**, 363-366.

35. S. Peng, D. Hu, J. L. Hu, Y. W. Lin, S. S. Tang, H. S. Tang, J. Y. He, Z. Cao and W. M. He, *Adv. Synth. Catal.*, 2019, **361**, 5721-5726.

36. S. Sau and P. Mal, *Eur. J. Org. Chem.*, 2022, e202200425.

37. W. Schilling, D. Riemer, Y. Zhang, N. Hatami and S. Das, *ACS Catal.*, 2018, **8**, 5425-5430.

38. G. Liang, J.-H. Wang, T. Lei, Y.-Y. Cheng and L.-Z. Wu, *Org. Lett.*, 2021, **23**, 8082-8087.

39. M. Lanzi, J. Merad, D. V. Boyarskaya, G. Maestri, C. Allain and G. Masson, *Org. Lett.*, 2018, **20**, 5247-5250.

40. A. Bose, S. Sau and P. Mal, *Eur. J. Org. Chem.*, 2019, 4105-4109.

Copies of ^{1}H and ^{13}C NMR Spectra of selected compounds

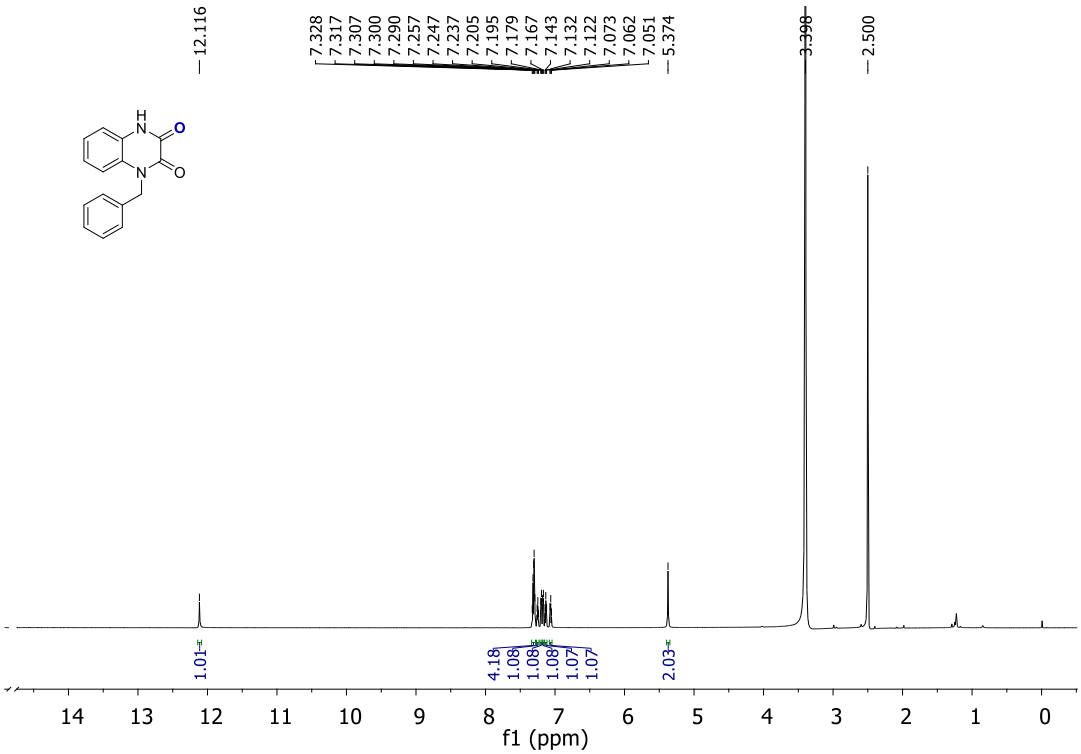

Figure 5.9. ^{1}H NMR of 1-Benzyl-1,4-dihydroquinoxaline-2,3-dione **(2a).**

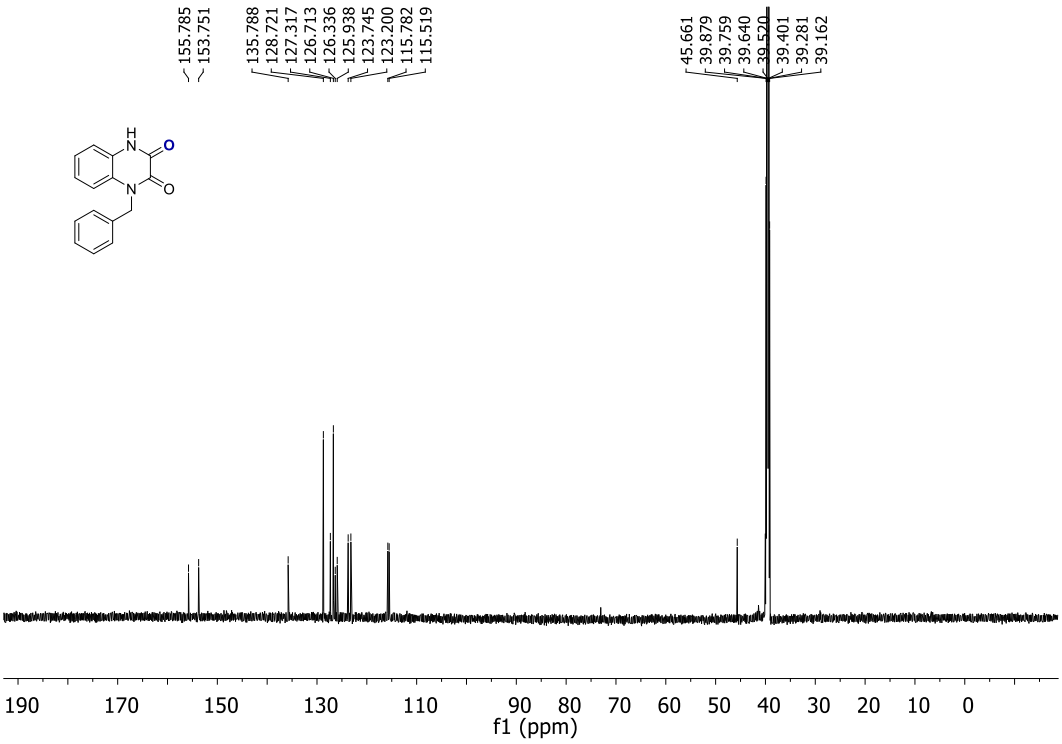

Figure 5.10. ^{13}C NMR of 1-Benzyl-1,4-dihydroquinoxaline-2,3-dione **(2a).**

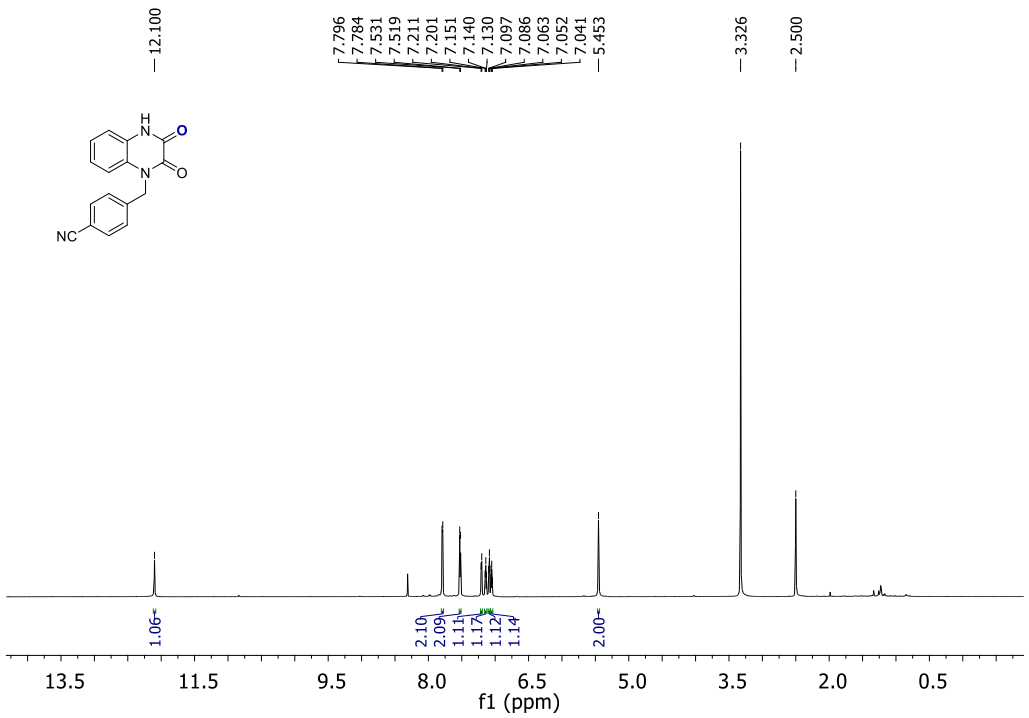

Figure 5.11. [1]H NMR of 4-((2,3-Dioxo-3,4-dihydroquinoxalin-1(2H)-yl)methyl)benzonitrile (**2b**).

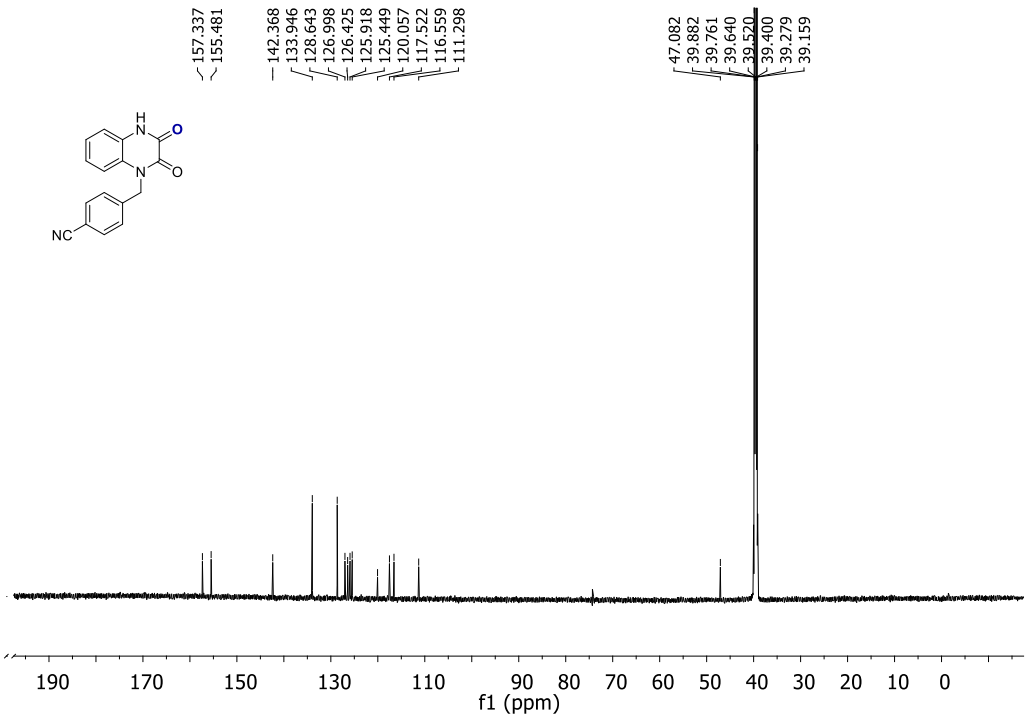

Figure 5.12. [13]C NMR of 4-((2,3-Dioxo-3,4-dihydroquinoxalin-1(2*H*)-yl)methyl)benzonitrile (**2b**).

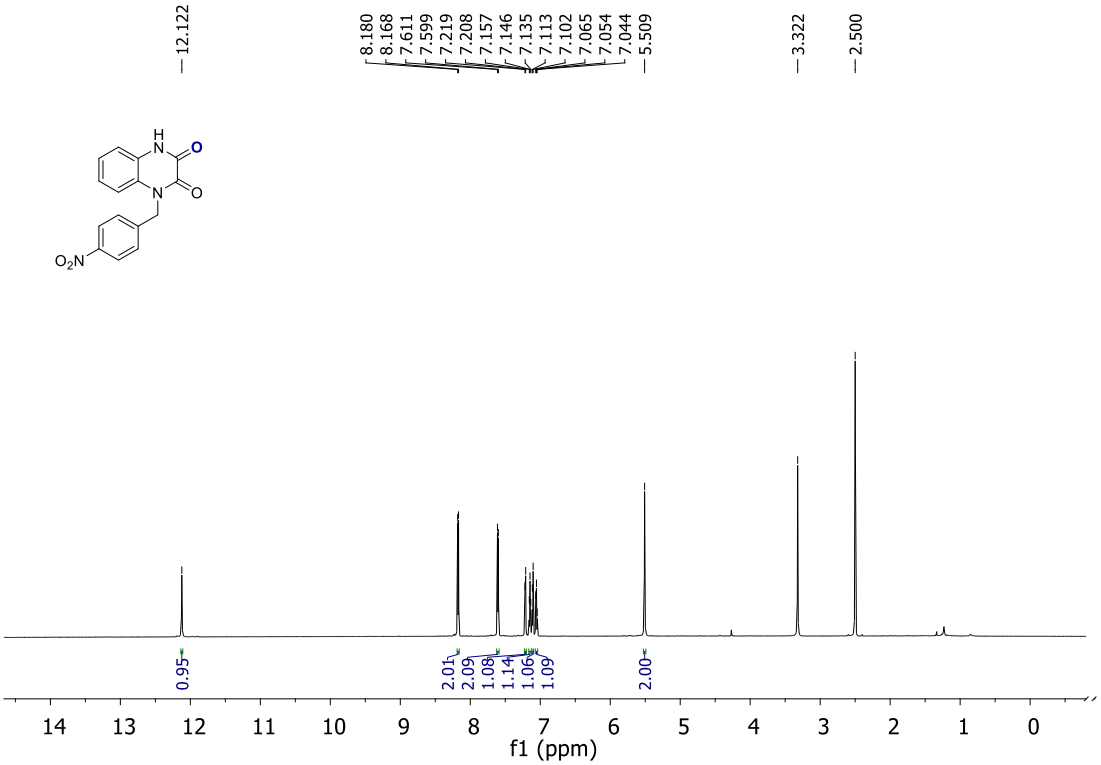

Figure 5.13. ^{1}H NMR of 1-(4-Nitrobenzyl)-1,4-dihydroquinoxaline-2,3-dione (**2c**).

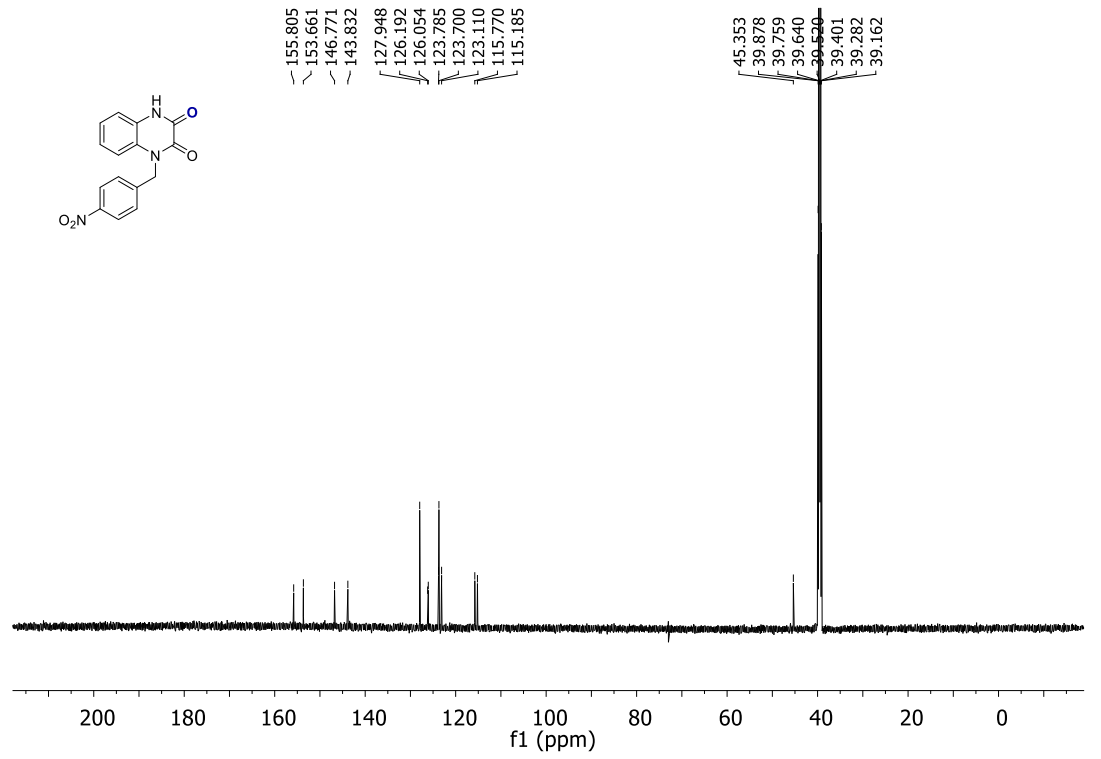

Figure 5.14. ^{13}C NMR of 1-(4-Nitrobenzyl)-1,4-dihydroquinoxaline-2,3-dione (**2c**).

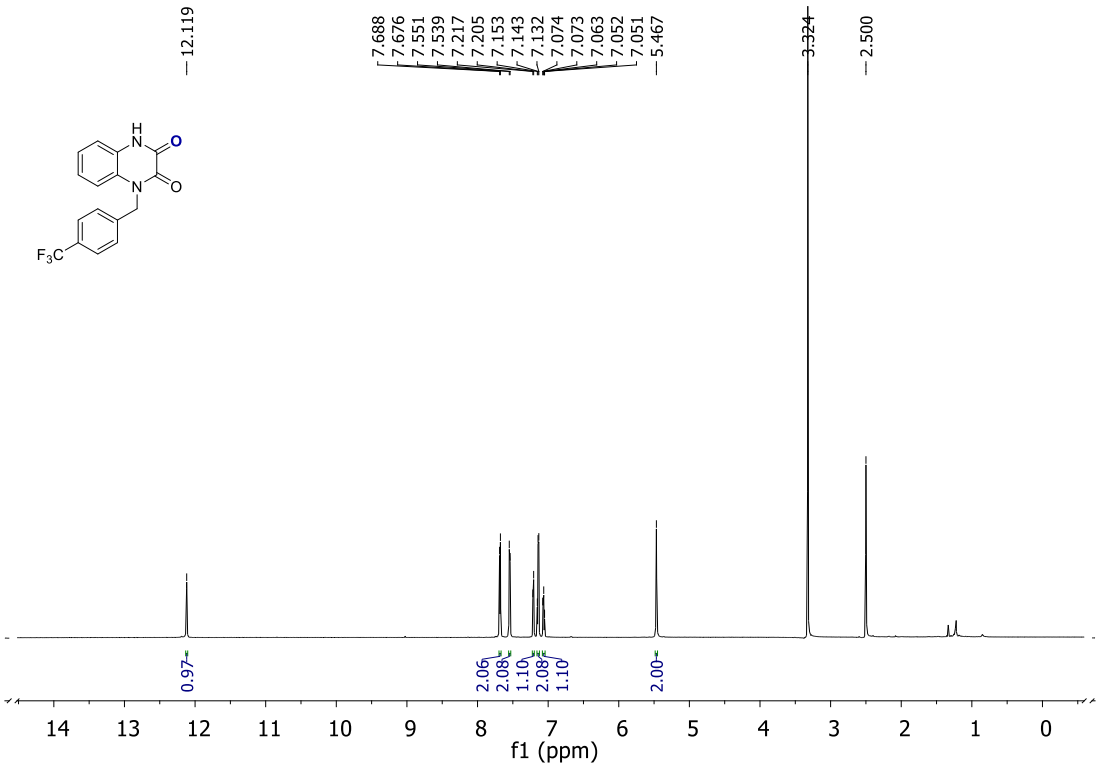

Figure 5.15. ^{1}H NMR of 1-(4-(Trifluoromethyl)benzyl)-1,4-dihydroquinoxaline-2,3-dione (**2d**).

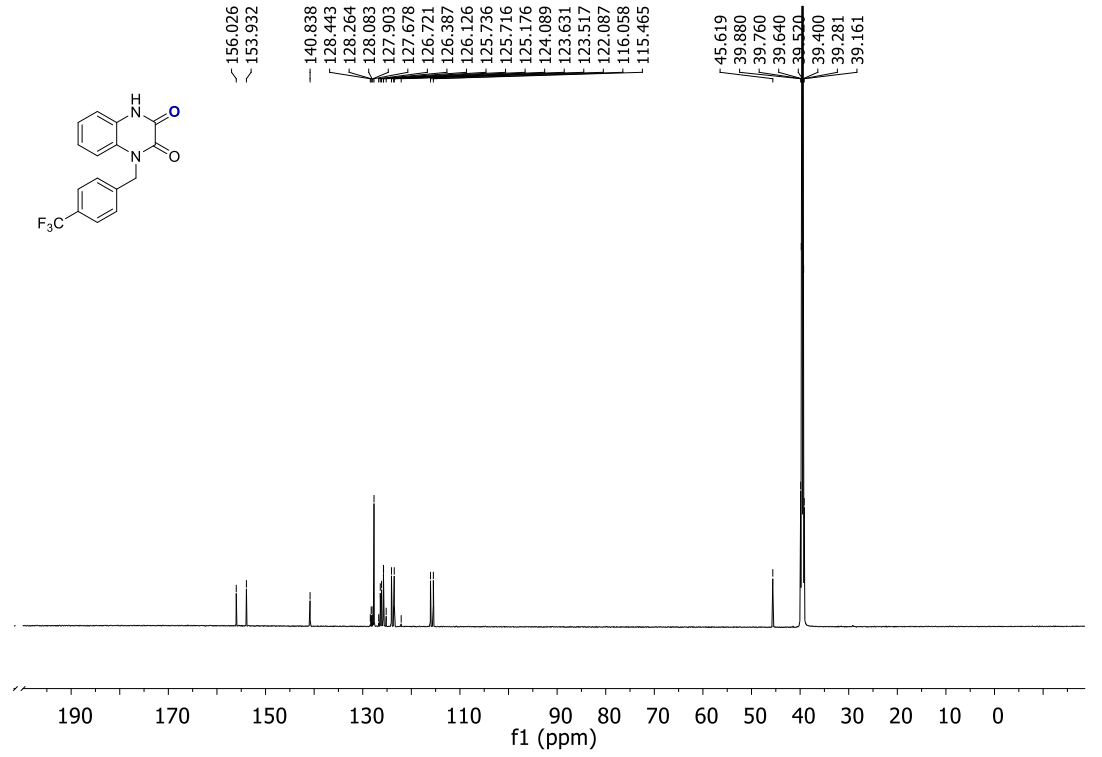

Figure 5.16. ^{13}C NMR of 1-(4-(Trifluoromethyl)benzyl)-1,4-dihydroquinoxaline-2,3-dione (**2d**).

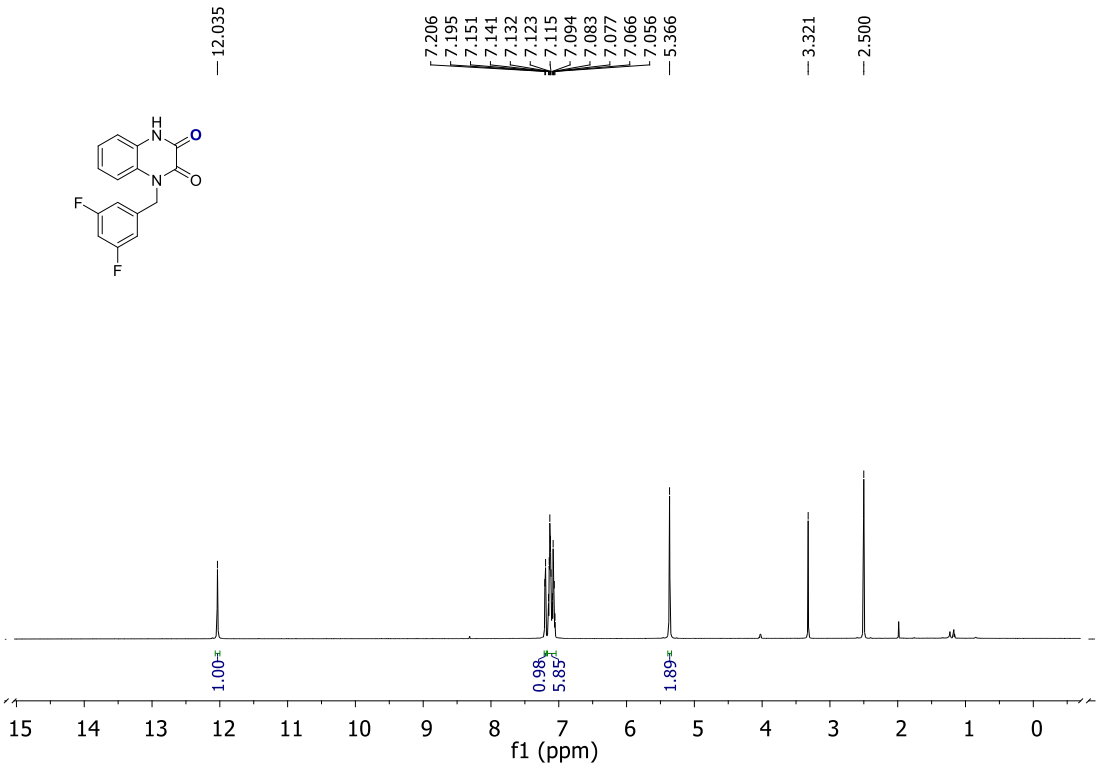

Figure 5.17. ^{1}H NMR of 1-(3,5-Difluorobenzyl)-1,4-dihydroquinoxaline-2,3-dione (**2e**).

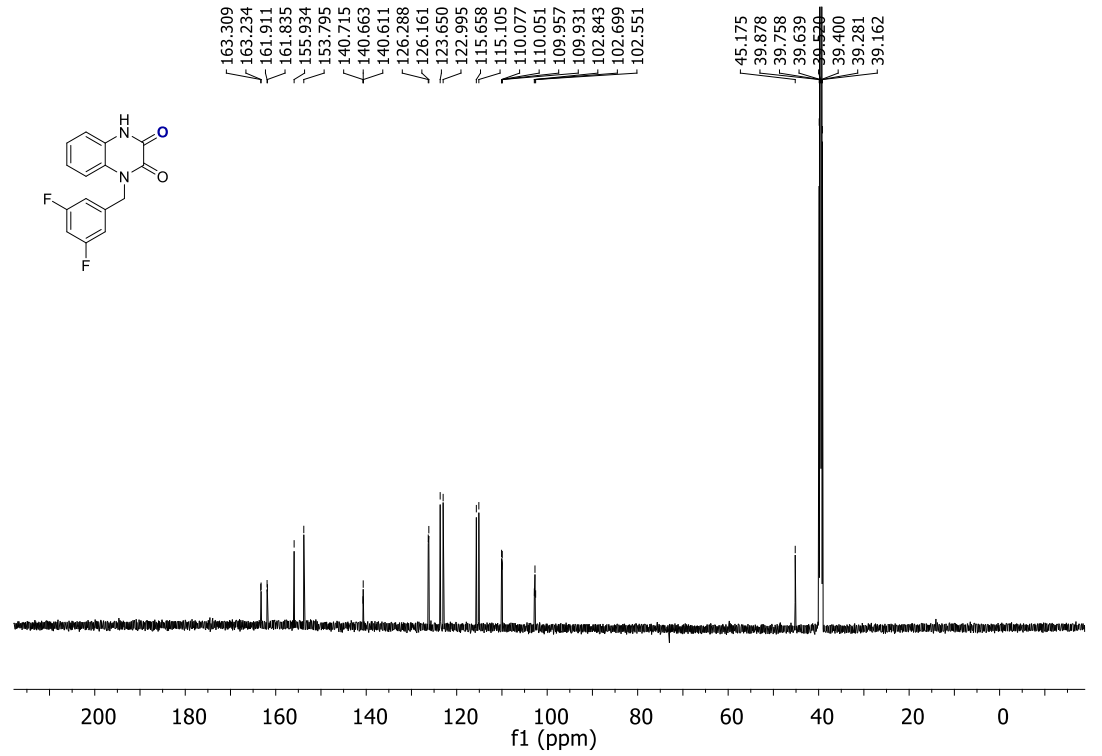

Figure 5.18. ^{13}C NMR of 1-(3,5-Difluorobenzyl)-1,4-dihydroquinoxaline-2,3-dione (**2e**).

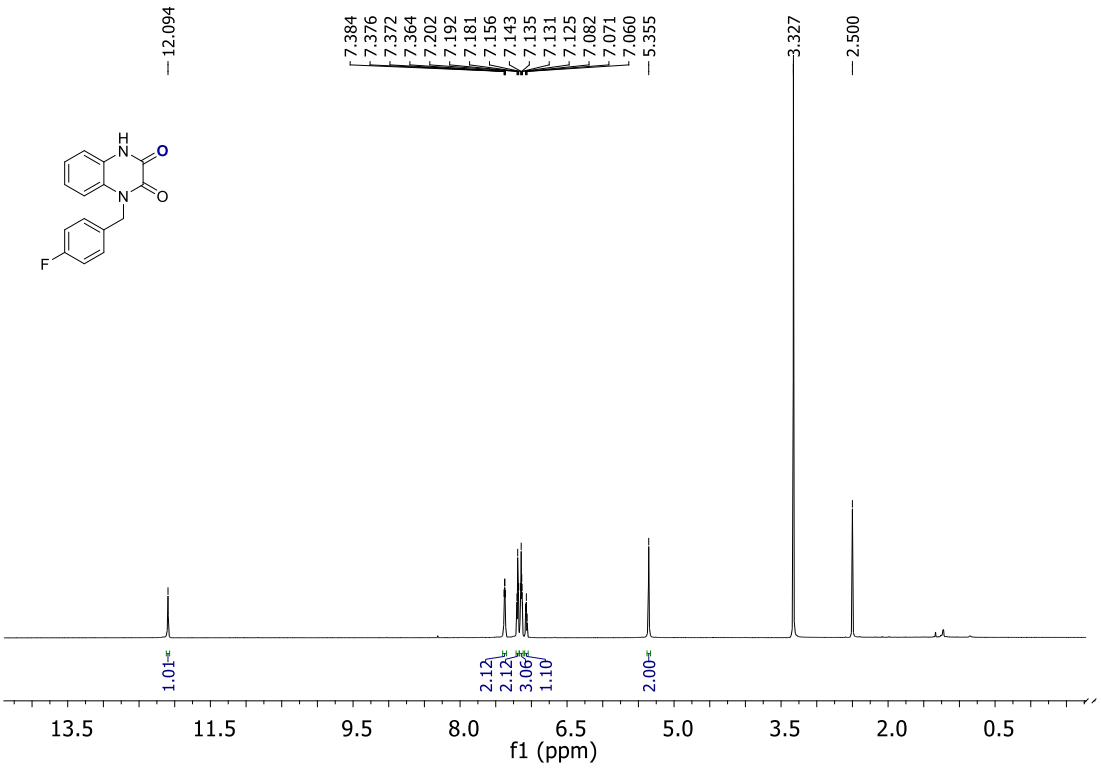

Figure 5.19. ^{1}H NMR of 1-(4-Fluorobenzyl)-1,4-dihydroquinoxaline-2,3-dione (**2f**).

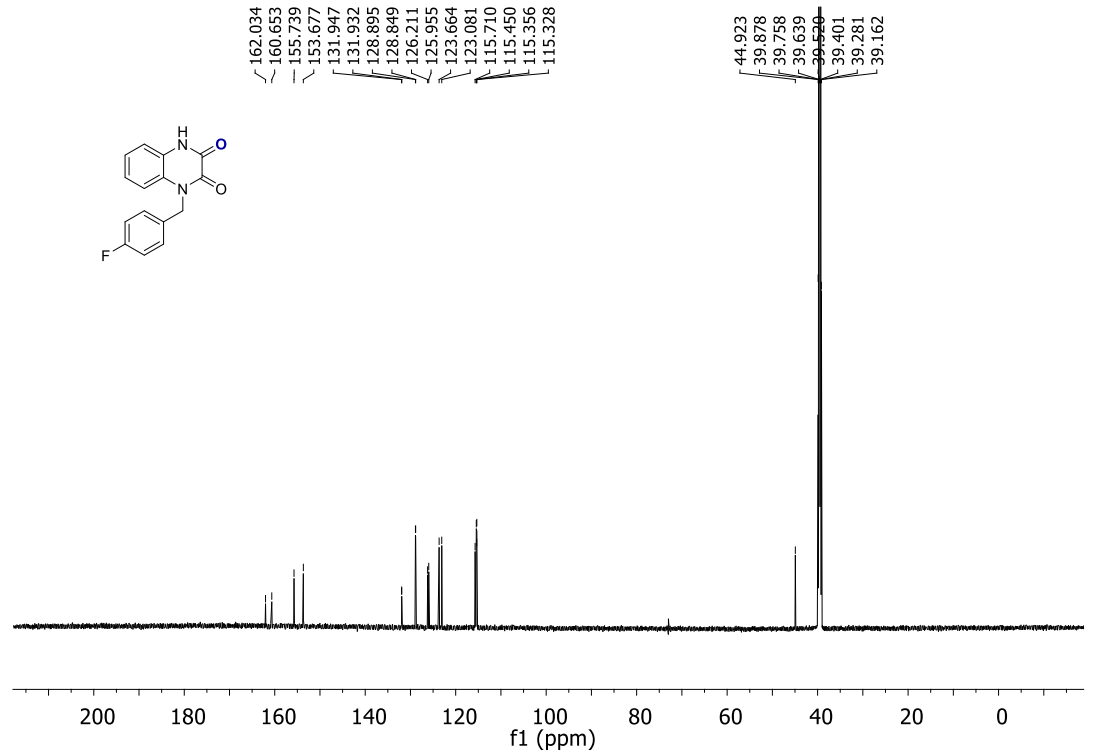

Figure 5.20. ^{13}C NMR of 1-(4-Fluorobenzyl)-1,4-dihydroquinoxaline-2,3-dione (**2f**).

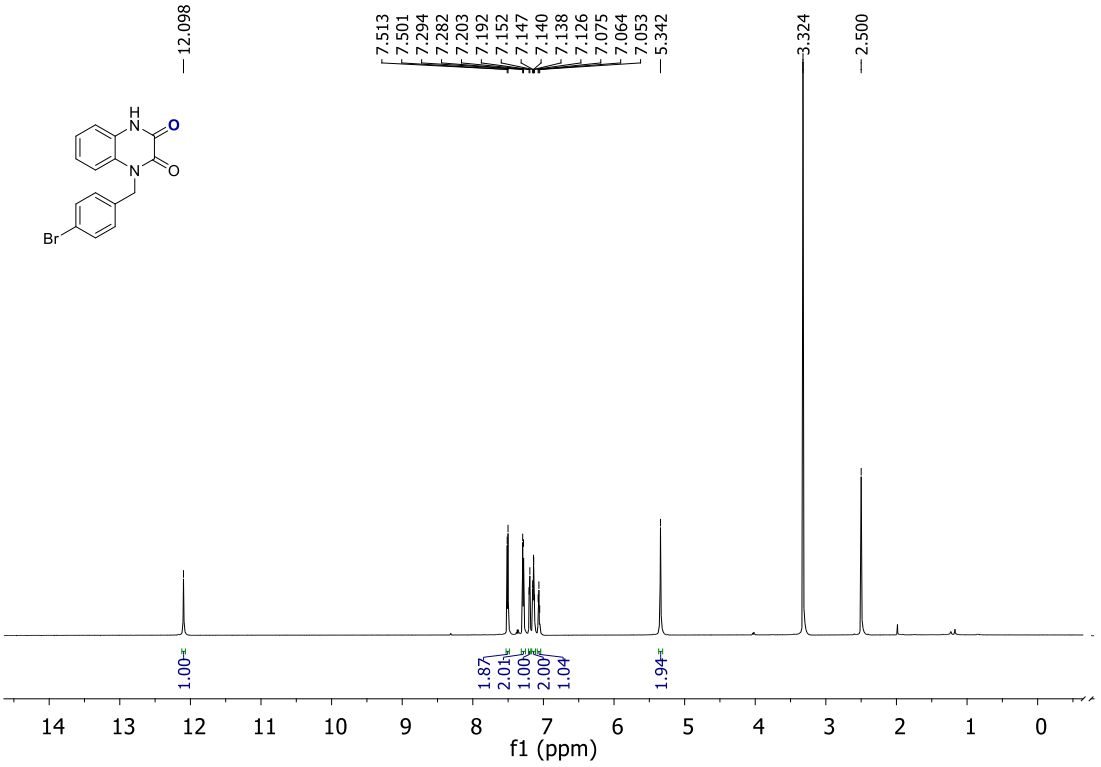

Figure 5.21. ^{1}H NMR of 1-(4-bromobenzyl)-1,4-dihydroquinoxaline-2,3-dione (**2g**).

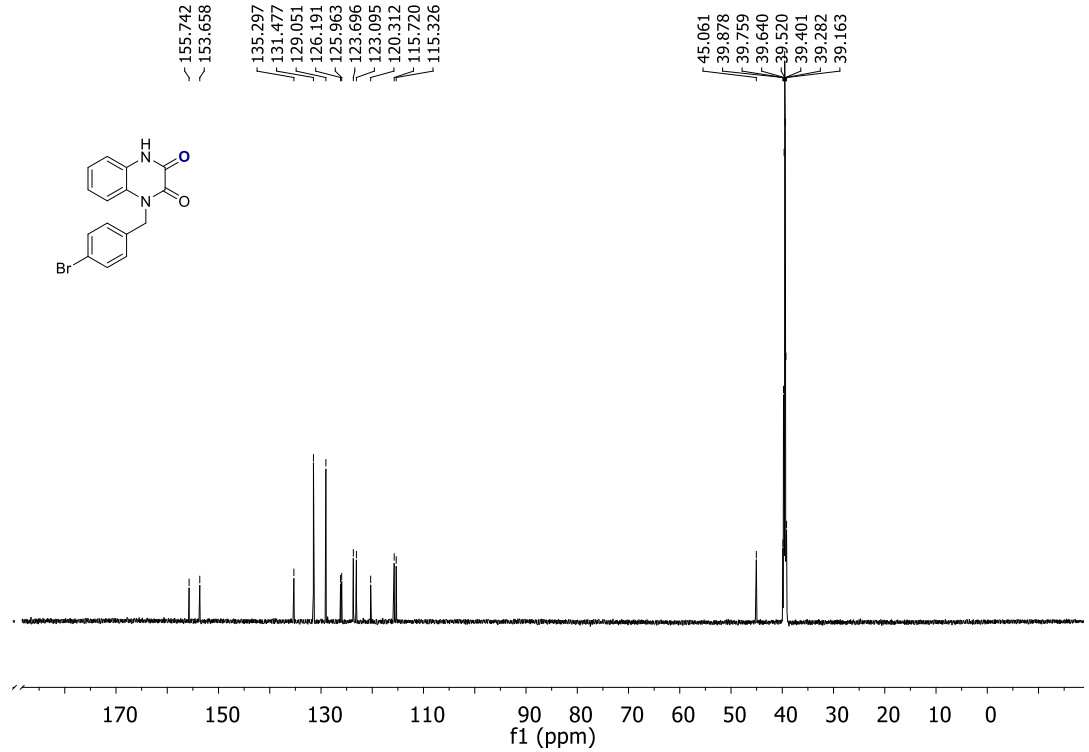

Figure 5.22. ^{13}C NMR of 1-(4-bromobenzyl)-1,4-dihydroquinoxaline-2,3-dione (**2g**).

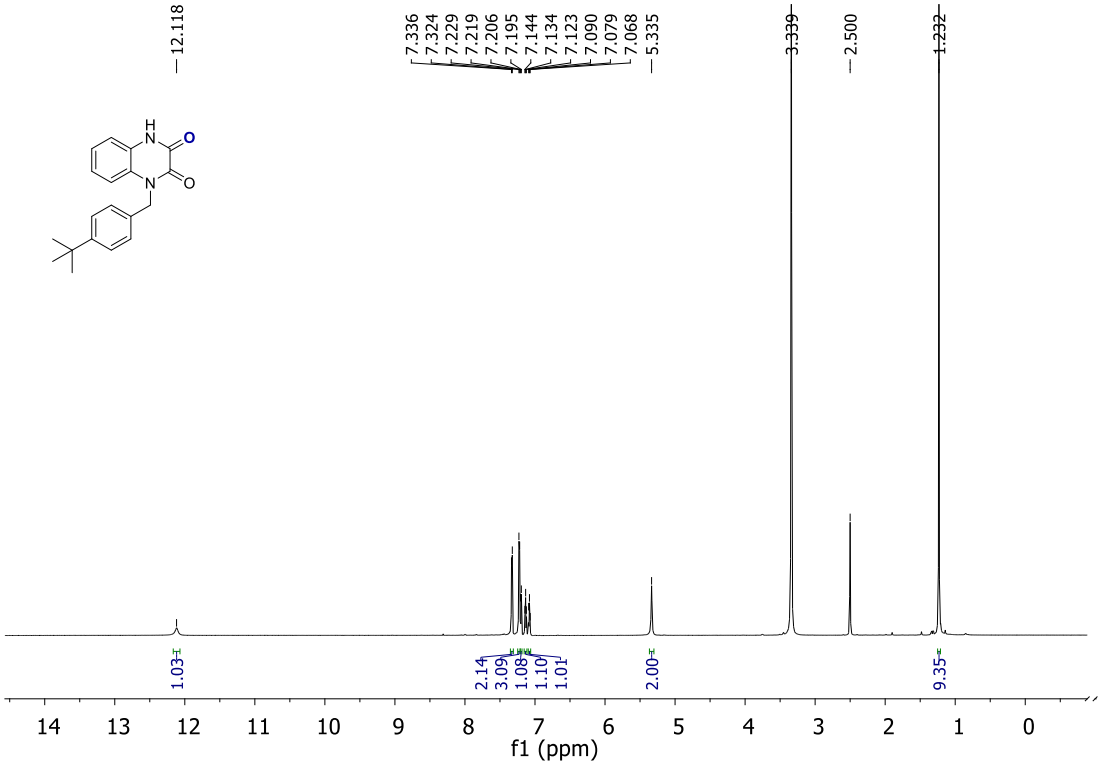

Figure 5.23. ^{1}H NMR of 1-(4-(tert-Butyl)benzyl)-1,4-dihydroquinoxaline-2,3-dione (**2h**).

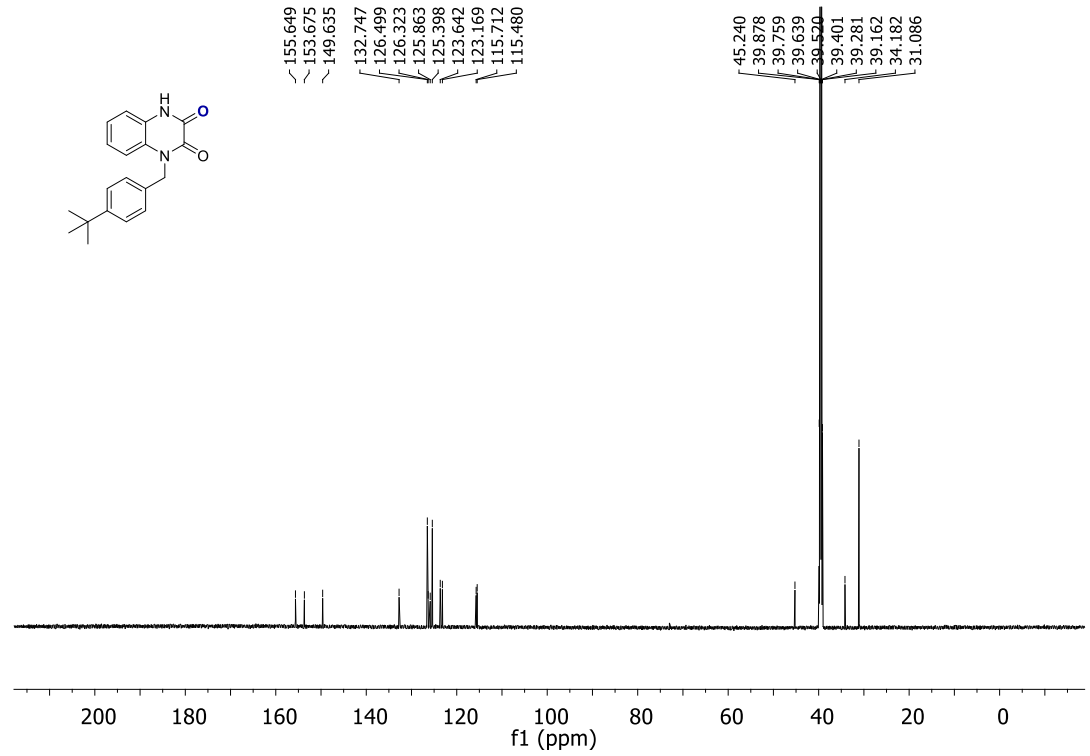

Figure 5.24. ^{13}C NMR of 1-(4-(tert-Butyl)benzyl)-1,4-dihydroquinoxaline-2,3-dione (**2h**).

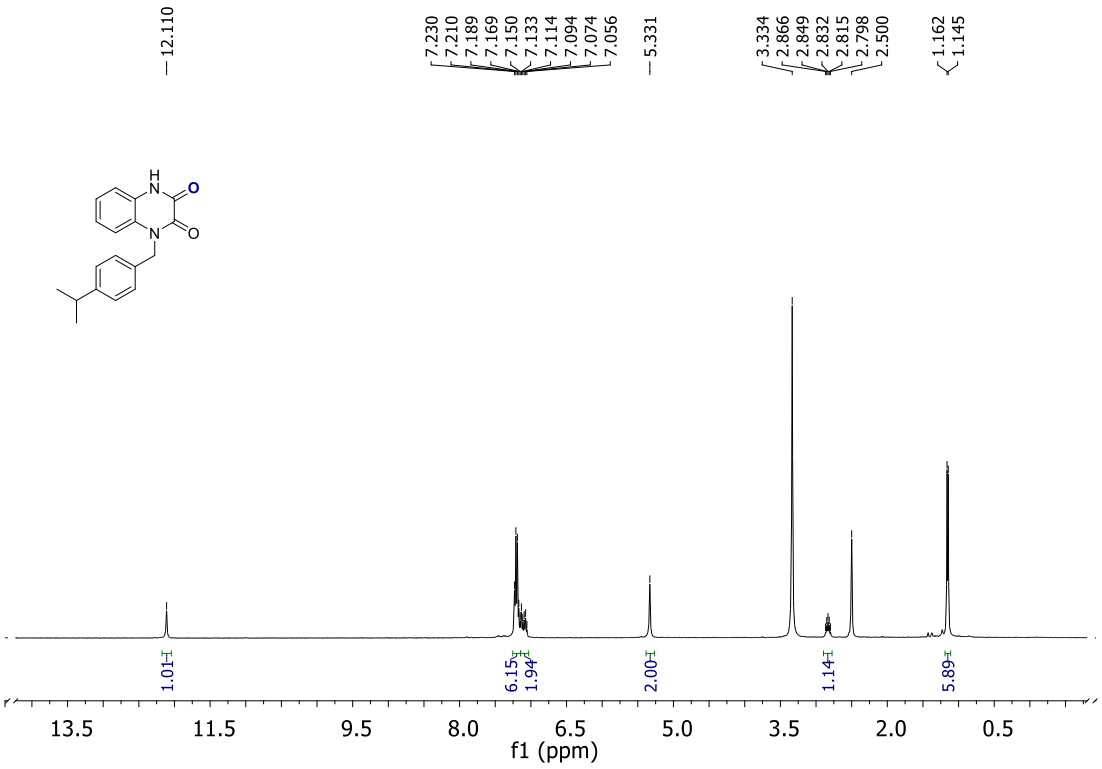

Figure 5.25. ^{1}H NMR of 1-(4-Isopropylbenzyl)-1,4-dihydroquinoxaline-2,3-dione (**2i**).

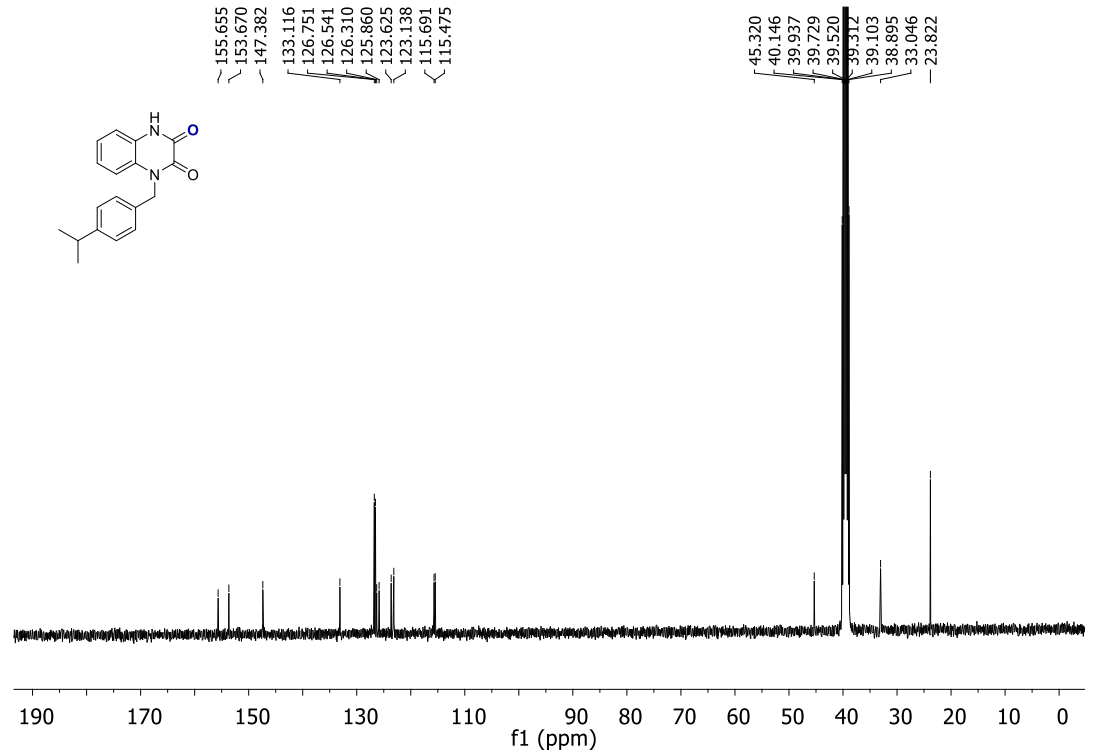

Figure 5.26 ^{13}C NMR of 1-(4-Isopropylbenzyl)-1,4-dihydroquinoxaline-2,3-dione (**2i**).

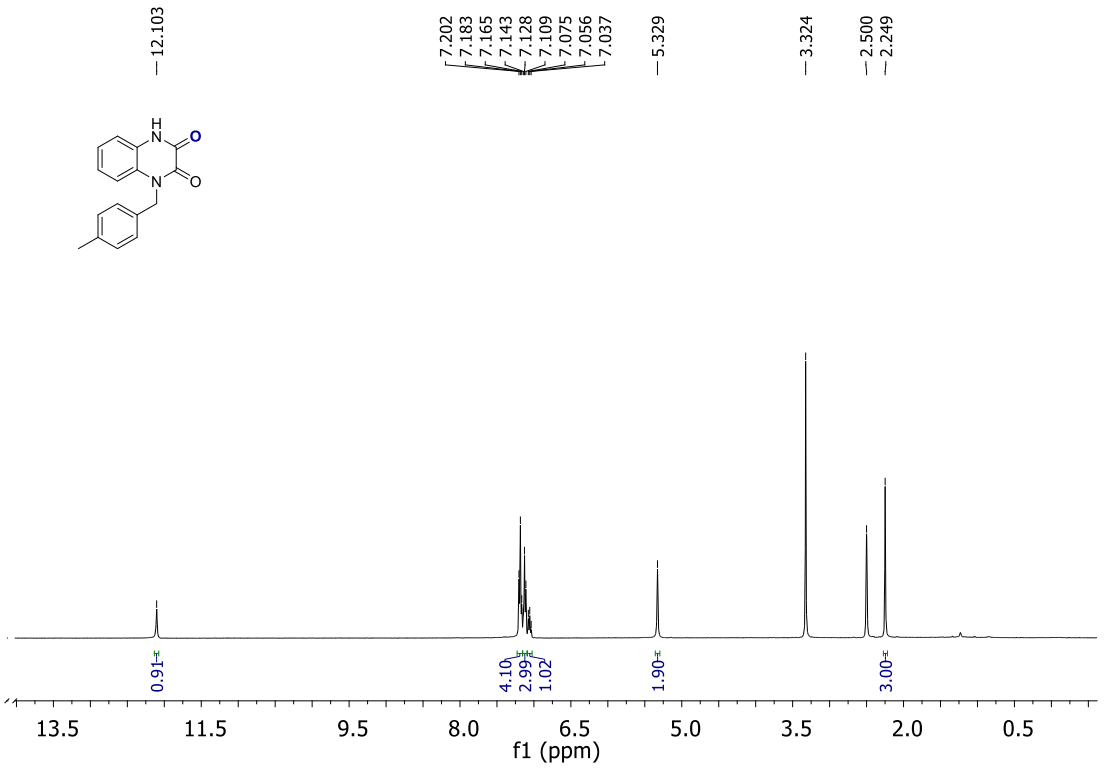

Figure 5.27. ^{1}H NMR of 1-(4-Methylbenzyl)-1,4-dihydroquinoxaline-2,3-dione (**2j**).

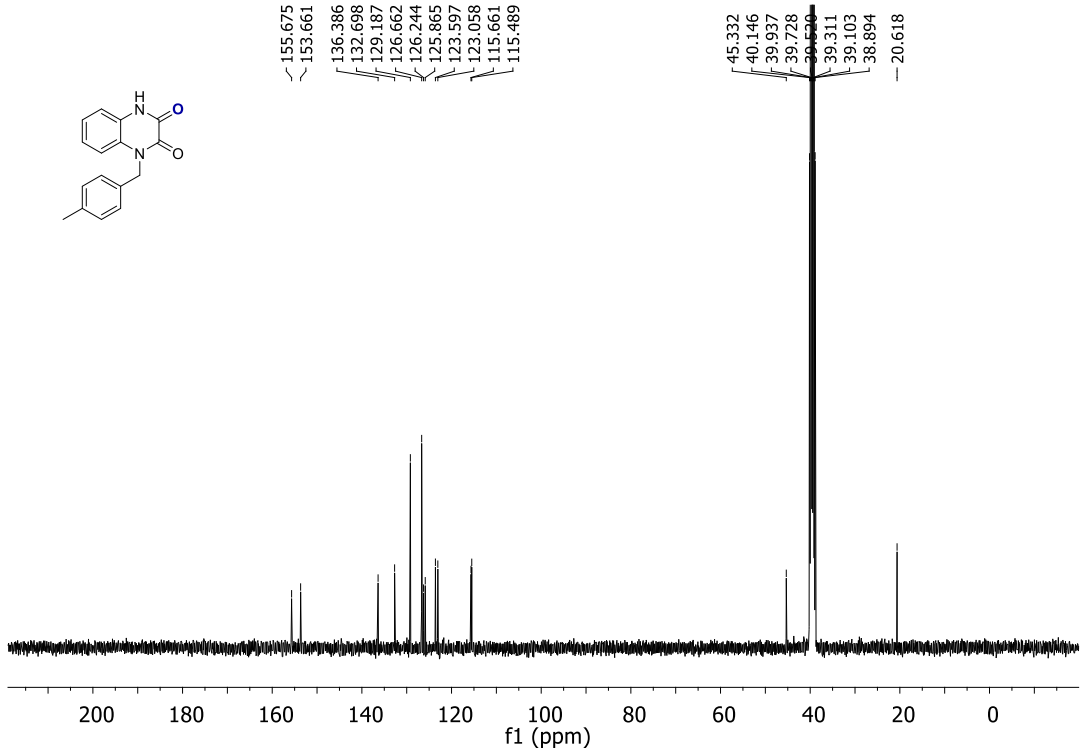

Figure 5.28. ^{13}C NMR of 1-(4-Methylbenzyl)-1,4-dihydroquinoxaline-2,3-dione (**2j**).

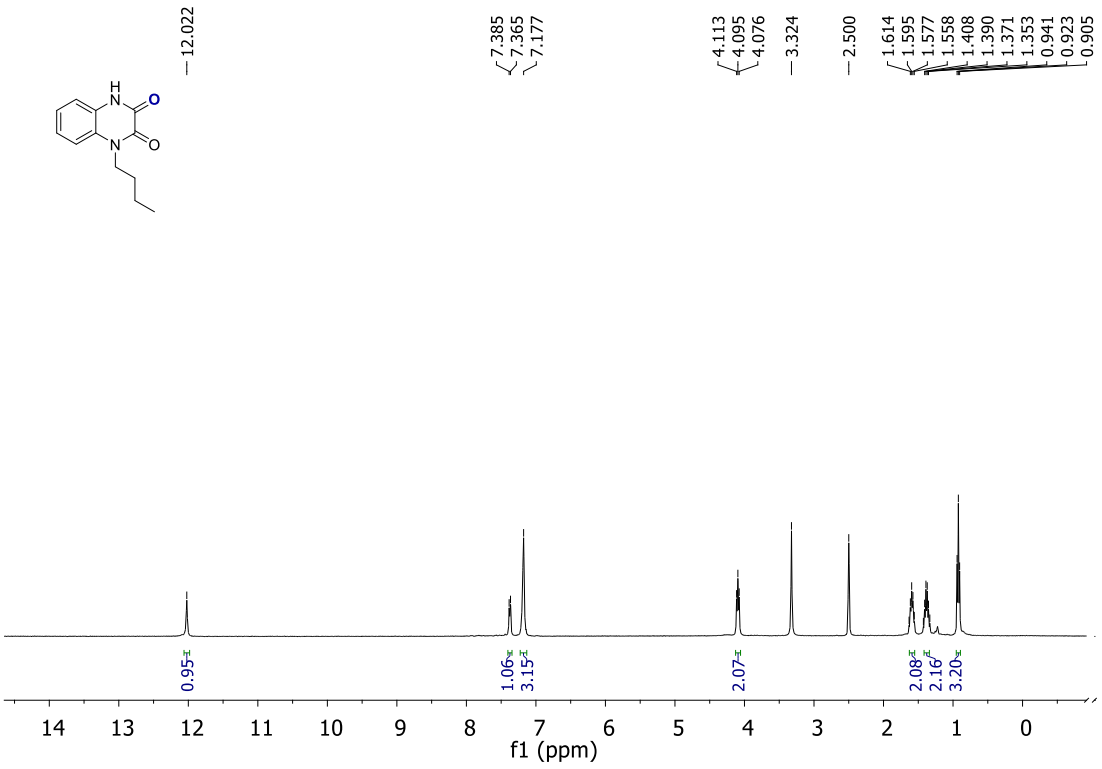

Figure 5.29. [1]H NMR of 1-Butyl-1,4-dihydroquinoxaline-2,3-dione (**2k**).

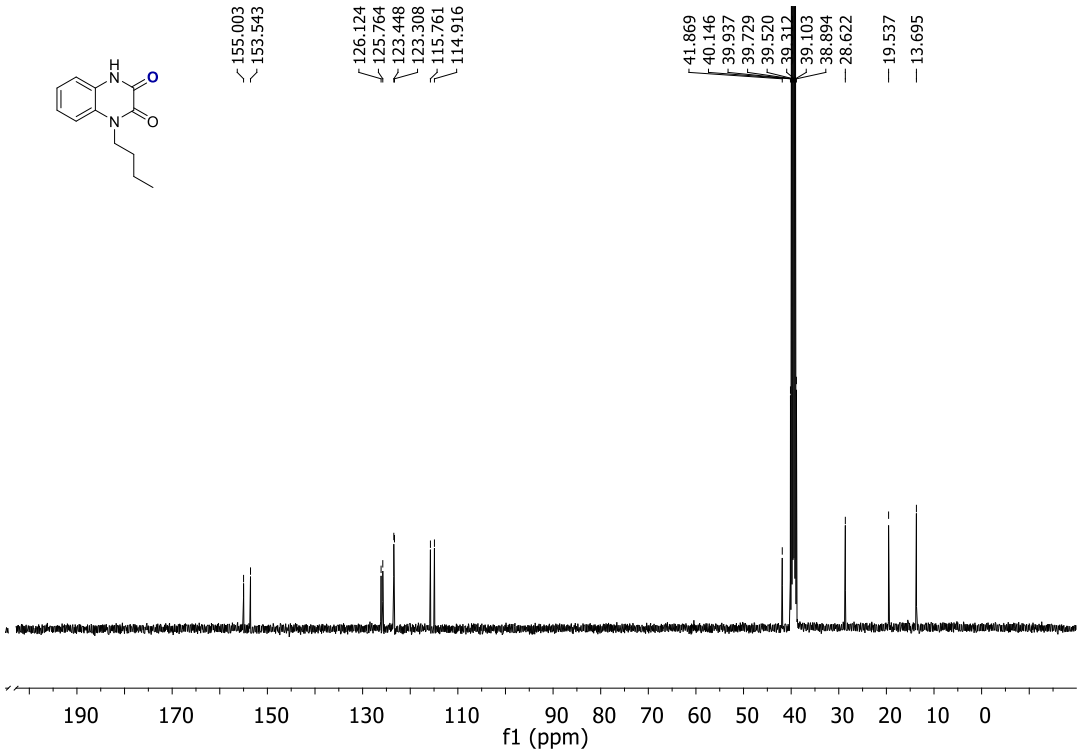

Figure 5.30. [13]C NMR of 1-Butyl-1,4-dihydroquinoxaline-2,3-dione (**2k**).

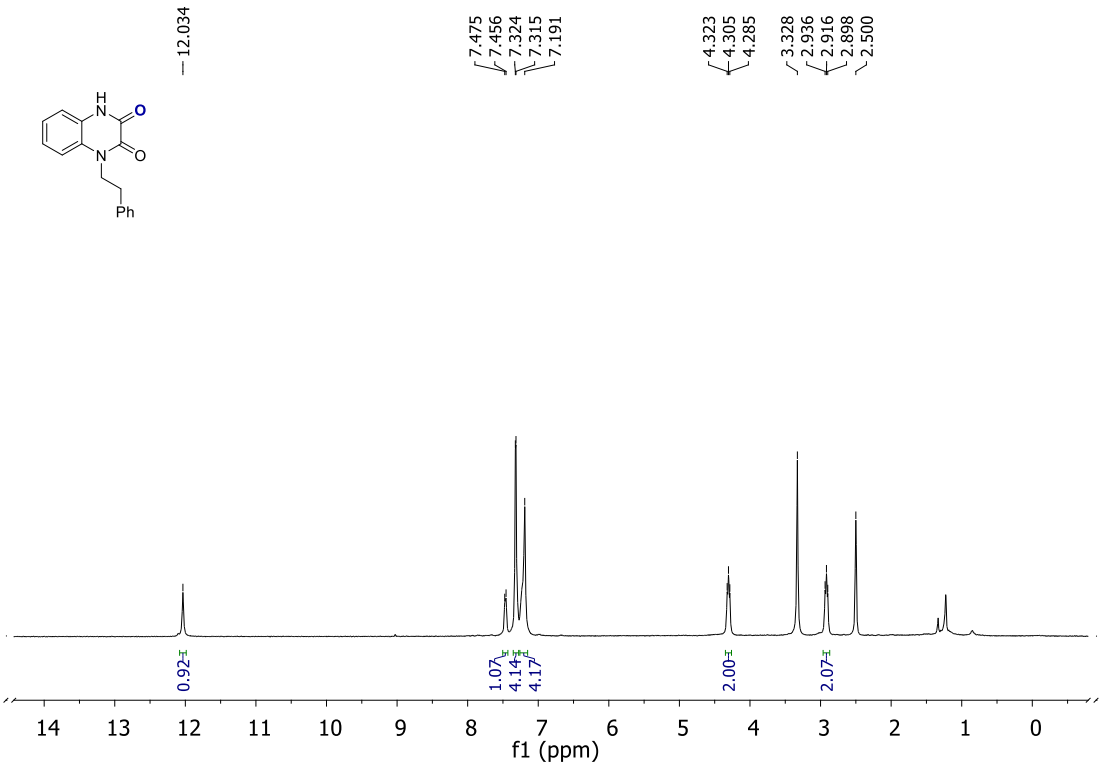

Figure 5.31. ^{1}H NMR of 1-Phenethyl-1,4-dihydroquinoxaline-2,3-dione (**2l**).

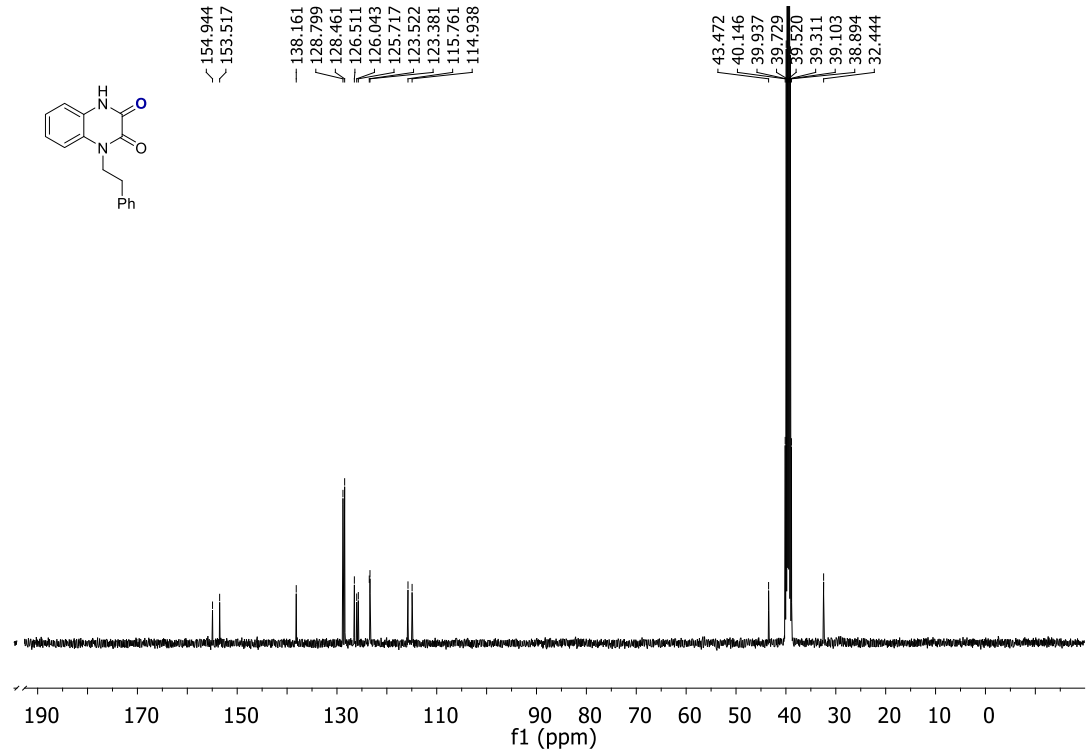

Figure 5.32. ^{13}C NMR of 1-Phenethyl-1,4-dihydroquinoxaline-2,3-dione (**2l**).

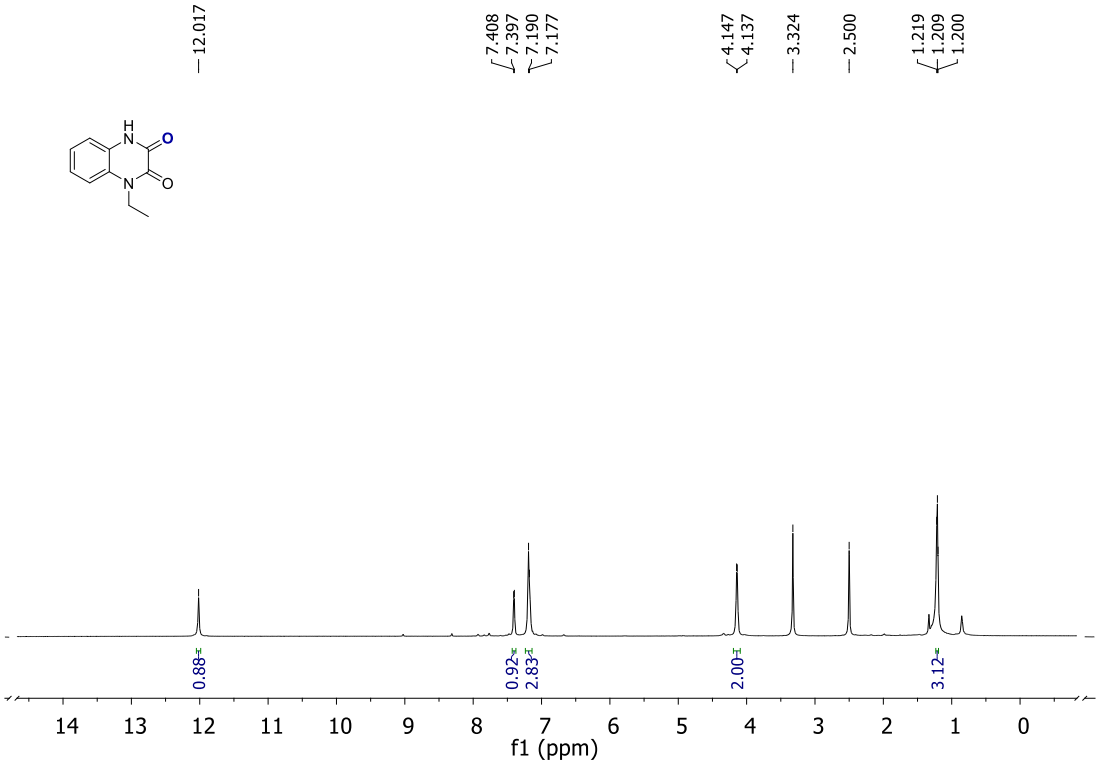

Figure 5.33. ^{1}H NMR of 1-Ethyl-1,4-dihydroquinoxaline-2,3-dione (**2m**).

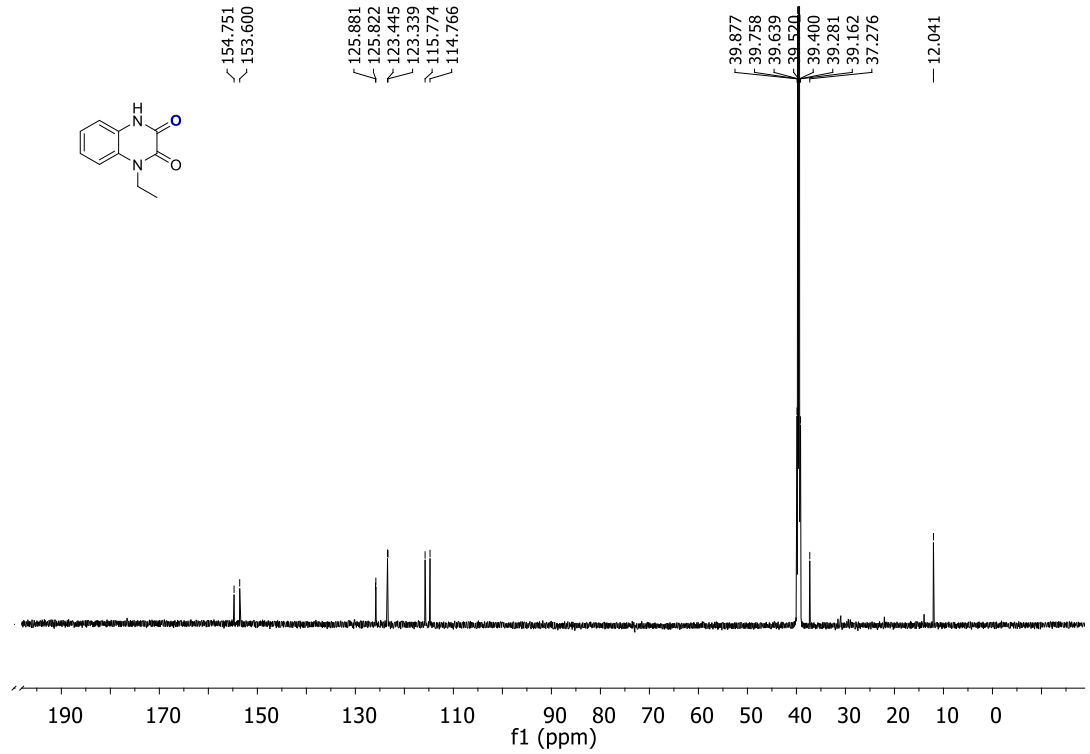

Figure 5.34. ^{13}C NMR of 1-Ethyl-1,4-dihydroquinoxaline-2,3-dione (**2m**).

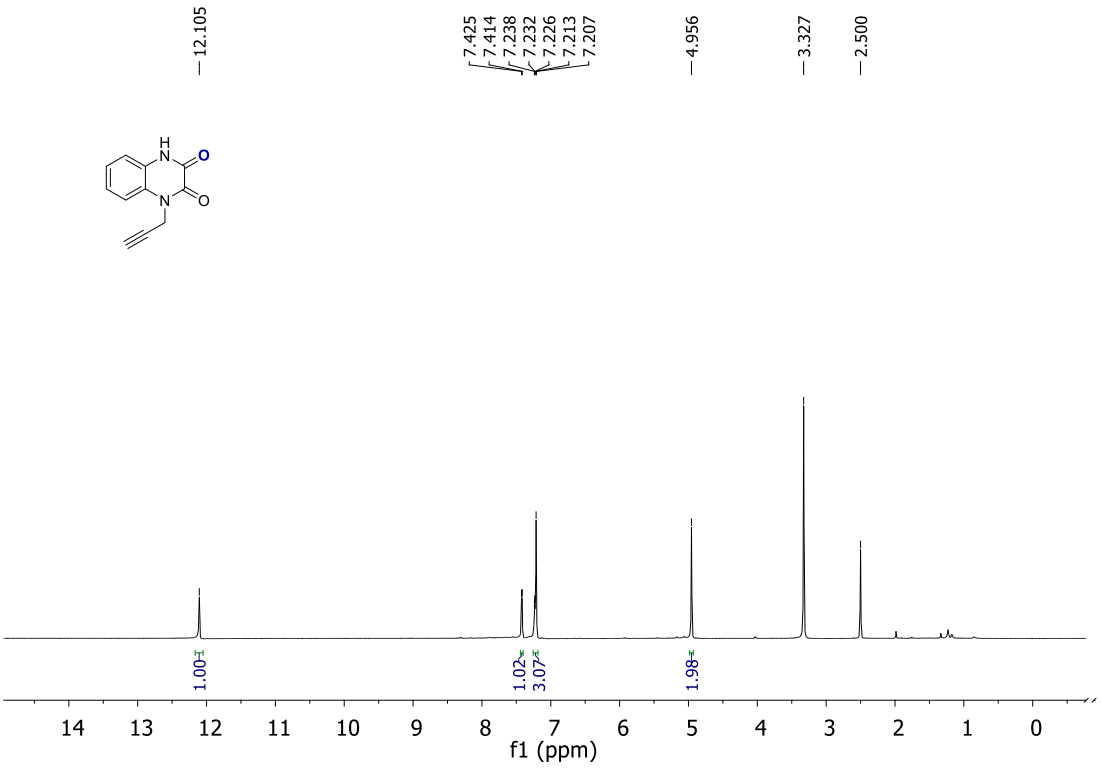

Figure 5.35. ^{1}H NMR of 1-(Prop-2-yn-1-yl)-1,4-dihydroquinoxaline-2,3-dione (**2n**).

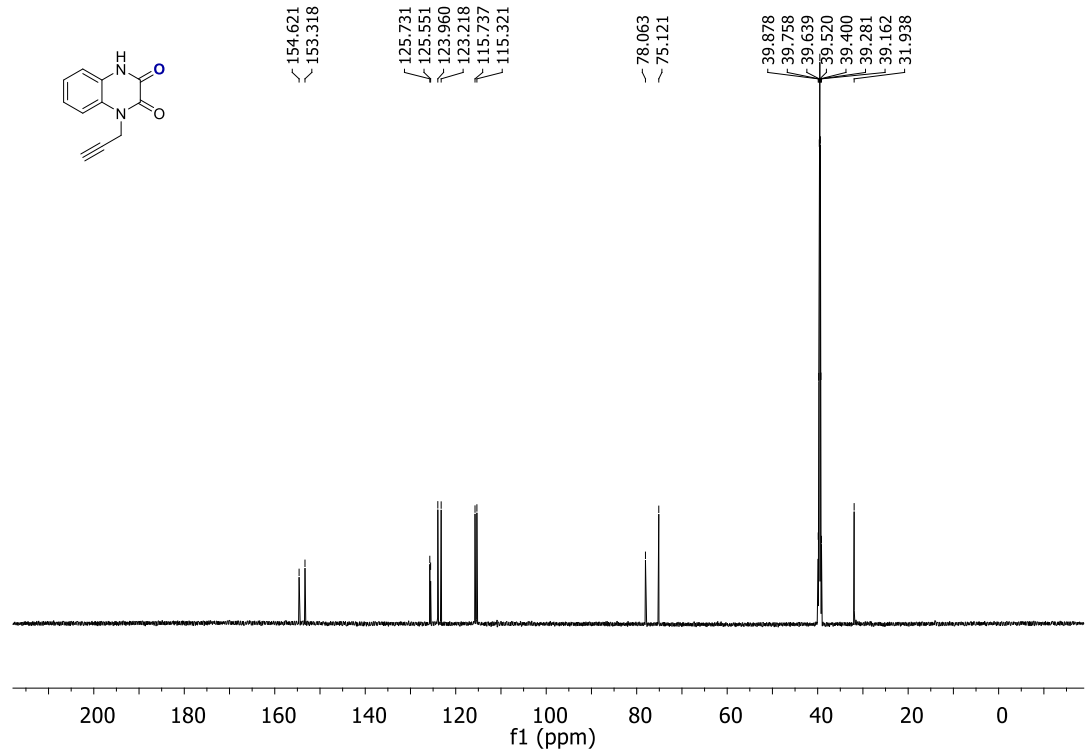

Figure 5.36. ^{13}C NMR of 1-(Prop-2-yn-1-yl)-1,4-dihydroquinoxaline-2,3-dione (**2n**).

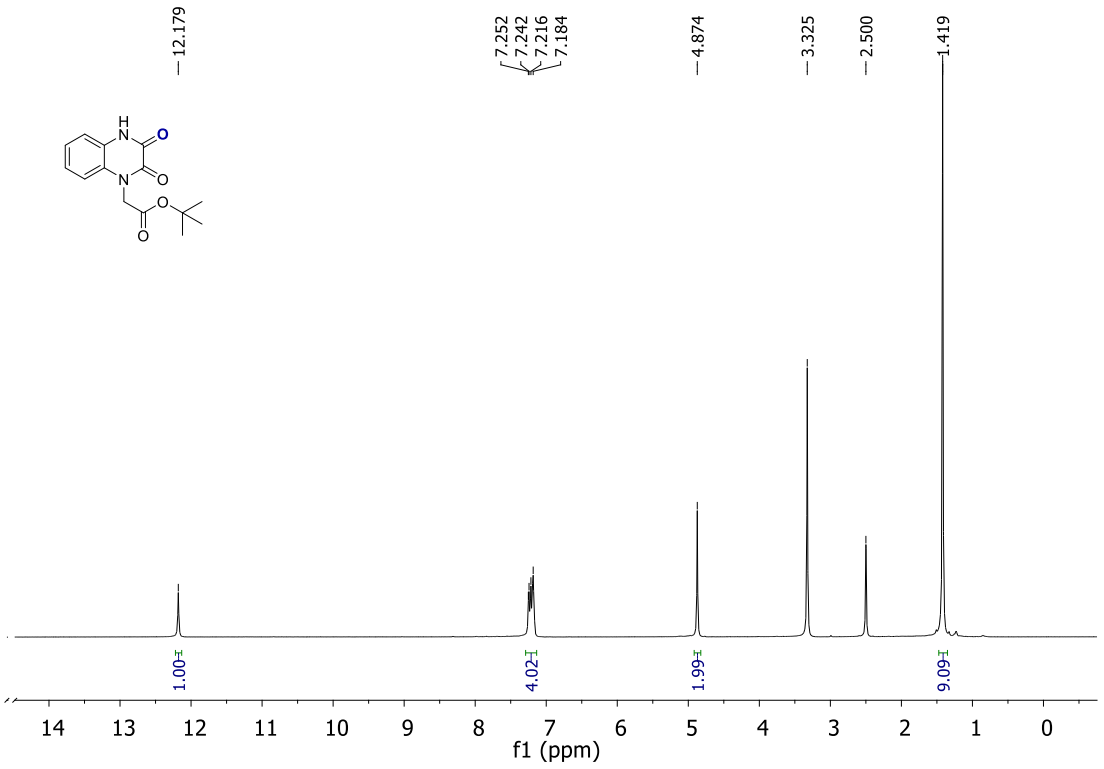

Figure 5.37. [1]H NMR of *tert*-Butyl 2-(2,3-dioxo-3,4-dihydroquinoxalin-1(2*H*)-yl)acetate (**2o**).

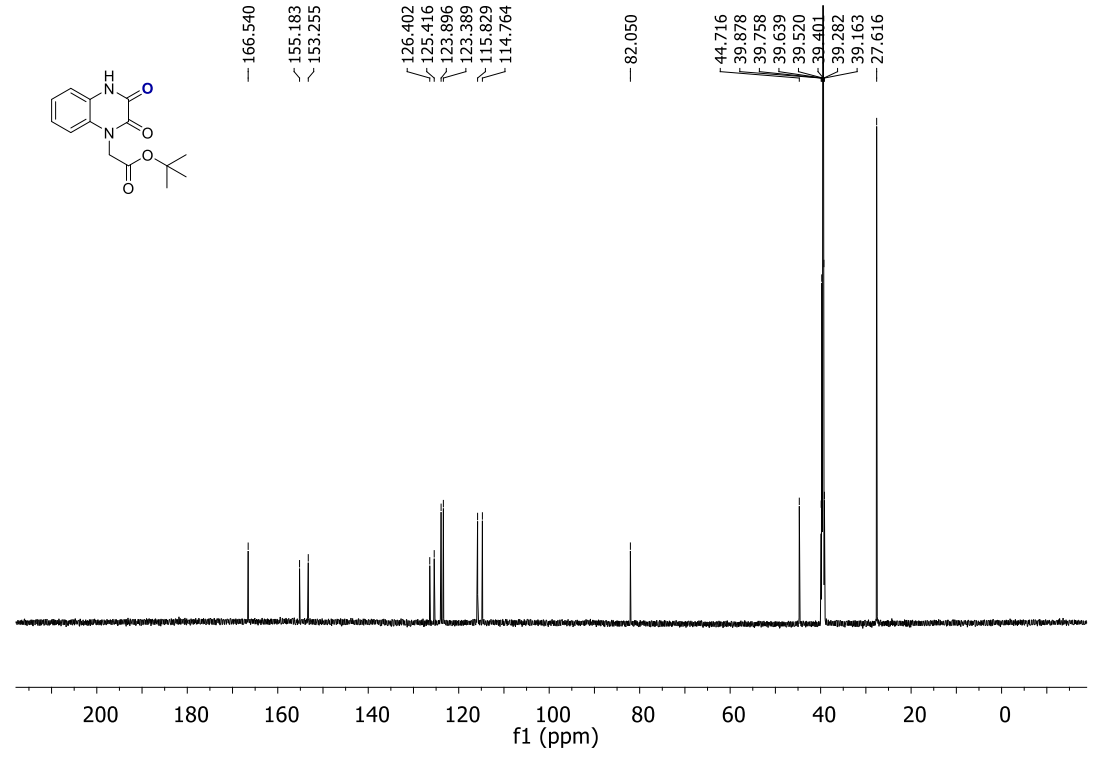

Figure 5.38. [13]C NMR of *tert*-Butyl 2-(2,3-dioxo-3,4-dihydroquinoxalin-1(2*H*)-yl)acetate (**2o**).

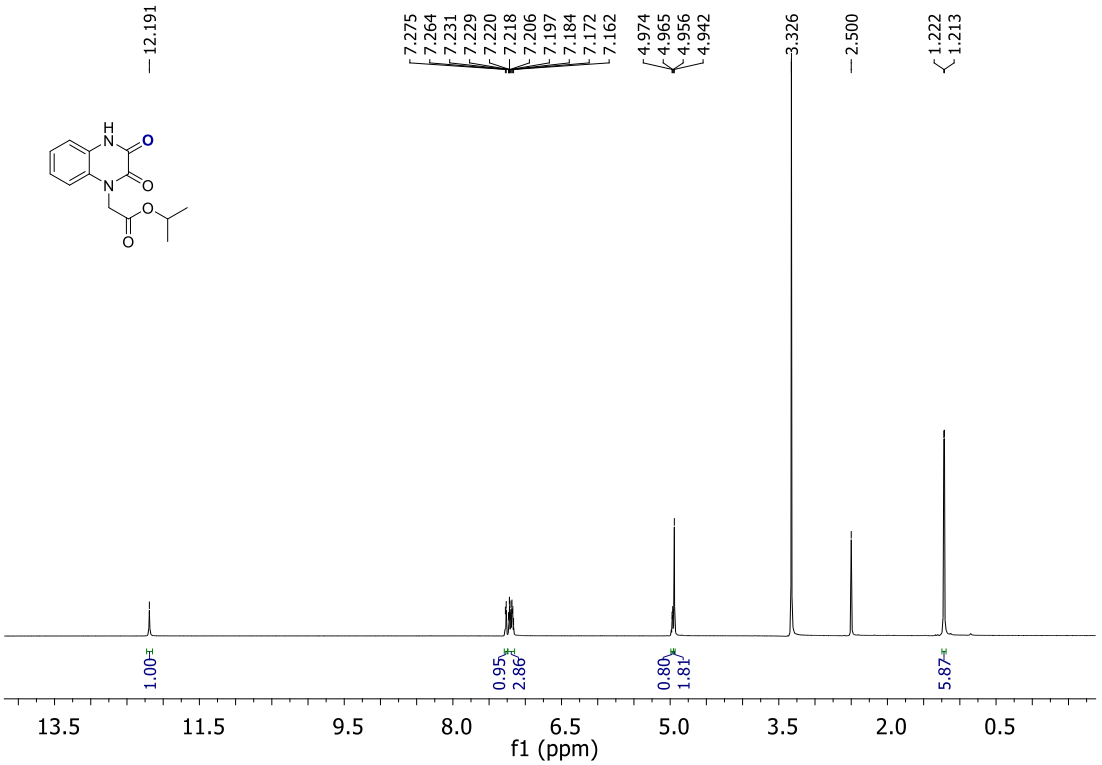

Figure 5.39. [1]H NMR of isopropyl 2-(2,3-dioxo-3,4-dihydroquinoxalin-1(2*H*)-yl)acetate (**2p**).

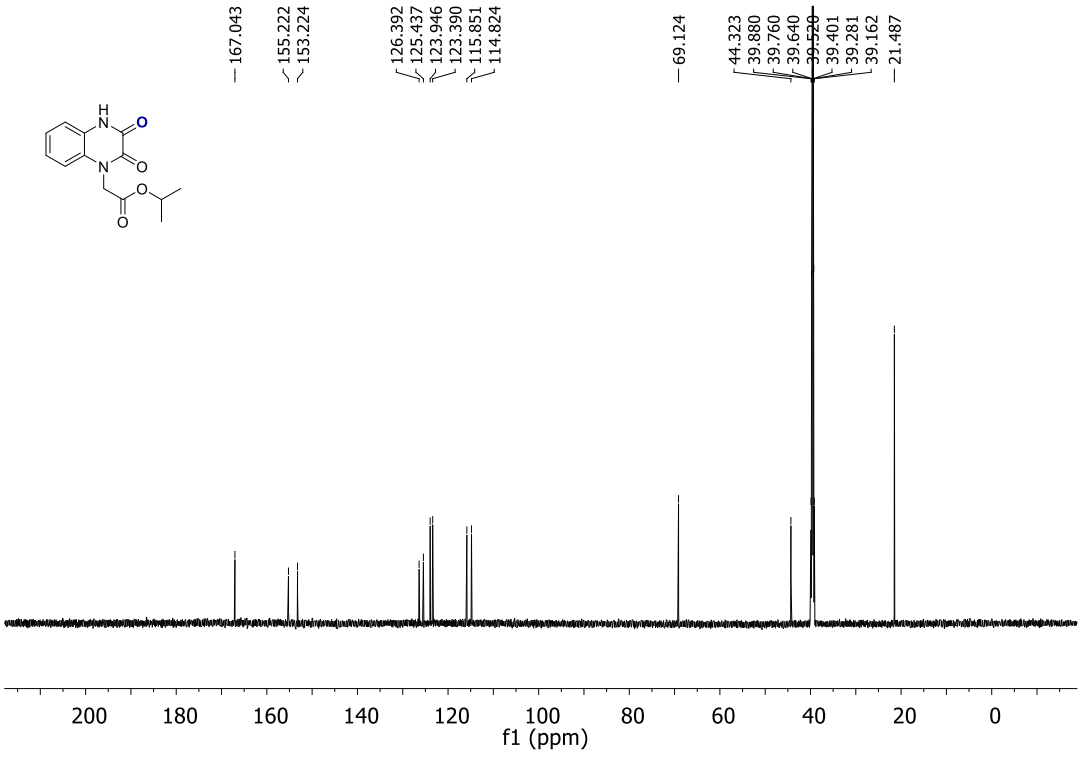

Figure 5.40. [1]H NMR of isopropyl 2-(2,3-dioxo-3,4-dihydroquinoxalin-1(2*H*)-yl)acetate (**2p**).

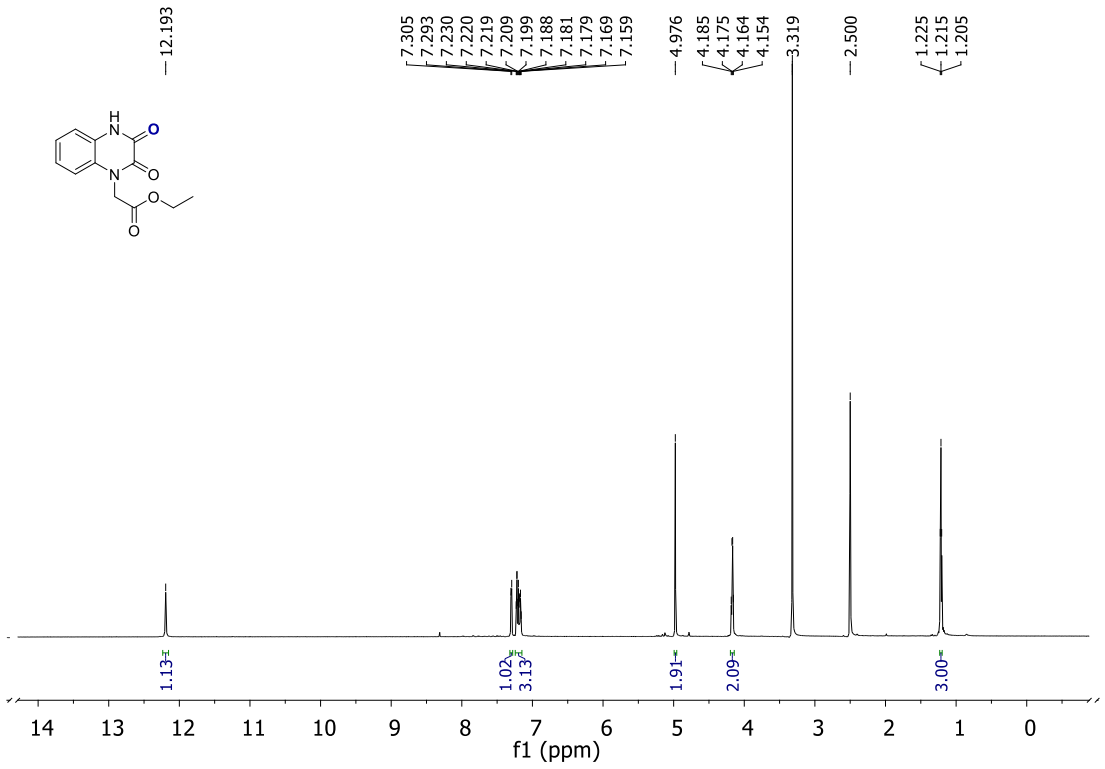

Figure 5.41. ^{1}H NMR of Ethyl 2-(2,3-dioxo-3,4-dihydroquinoxalin-1(2*H*)-yl)acetate (**2q**).

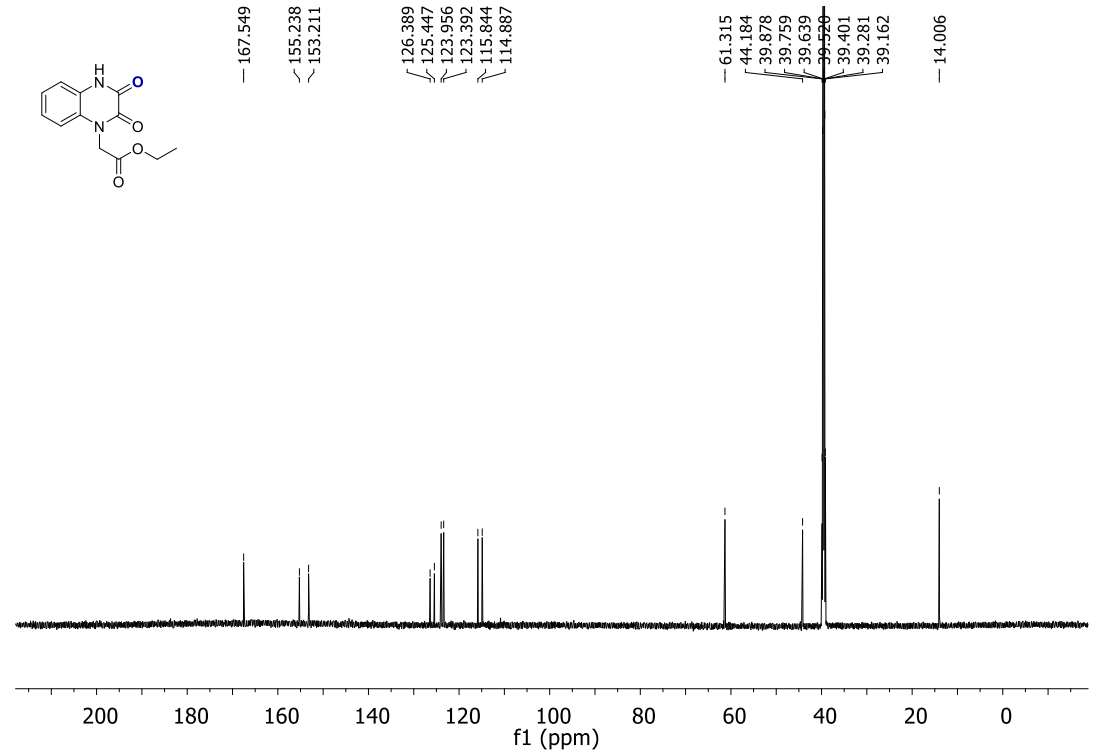

Figure 5.42. ^{13}C NMR of Ethyl 2-(2,3-dioxo-3,4-dihydroquinoxalin-1(2*H*)-yl)acetate (**2q**).

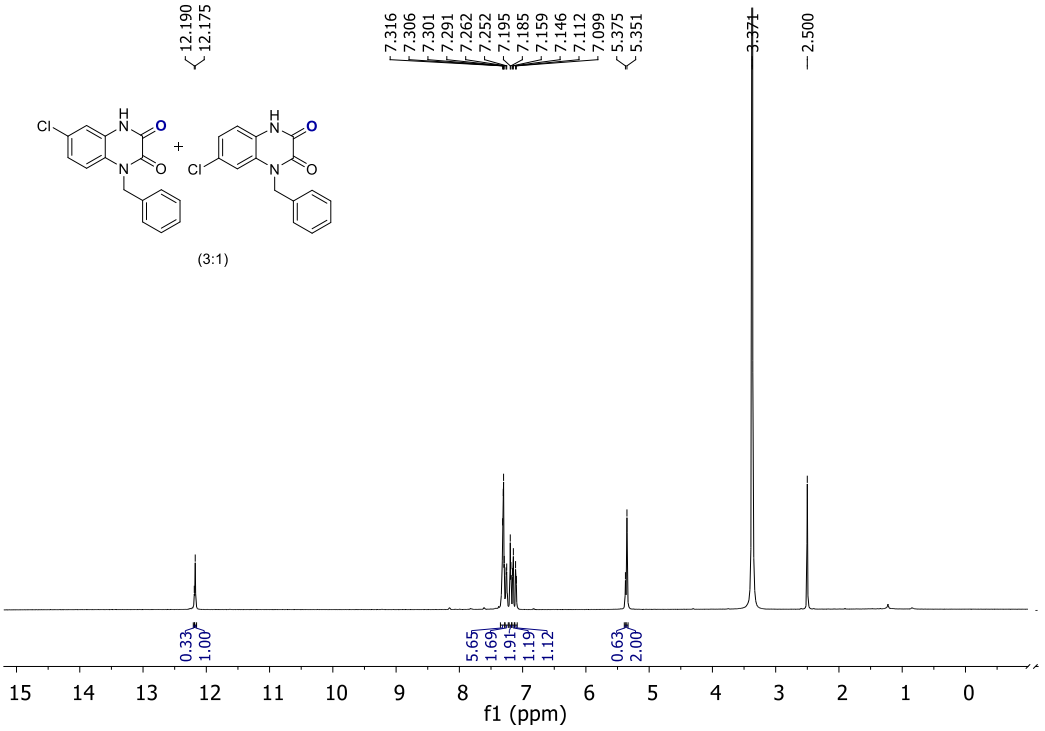

Figure 5.43. ^{1}H NMR of 1-Benzyl-6-chloro-1,4-dihydroquinoxaline-2,3-dione and 1-Benzyl-7-chloro -1,4-dihydroquinoxaline-2,3-dione (**4a**).

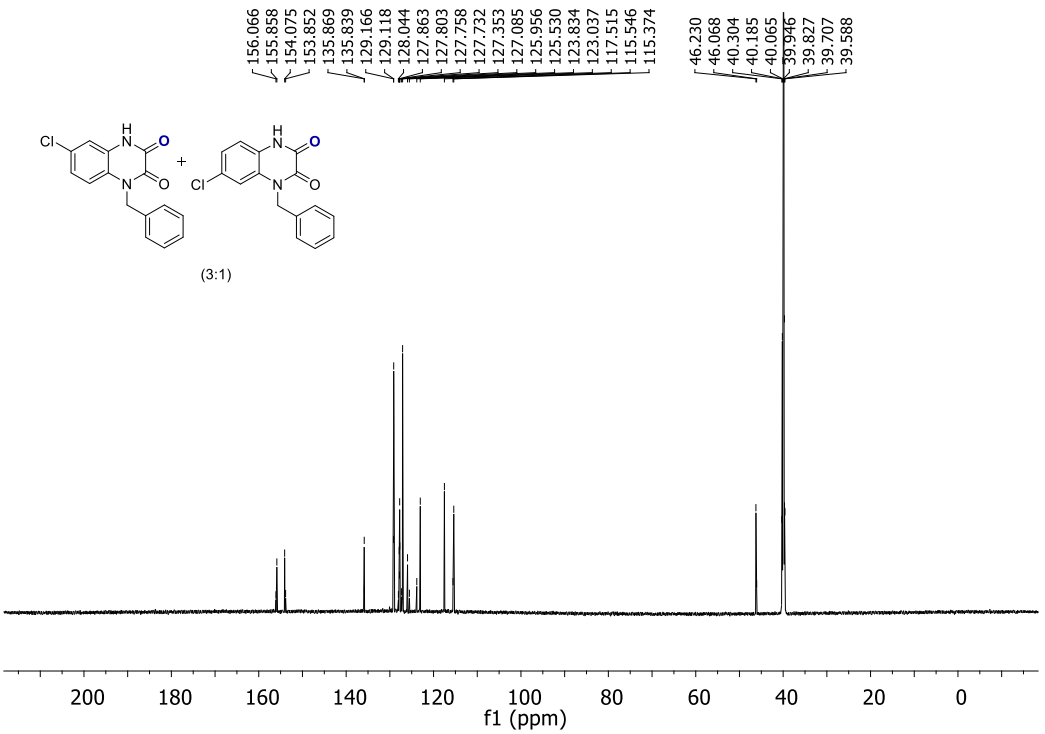

Figure 5.44. ^{13}C NMR of 1-Benzyl-6-chloro-1,4-dihydroquinoxaline-2,3-dione and 1-Benzyl-7-chloro -1,4-dihydroquinoxaline-2,3-dione (**4a**).

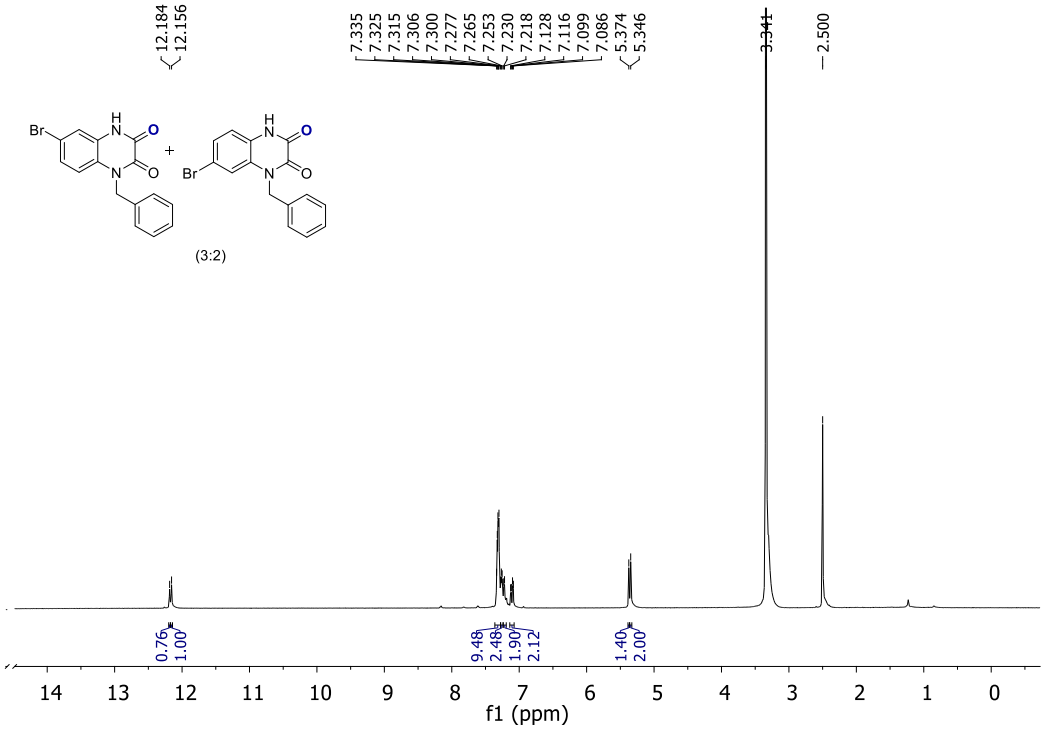

Figure 5.45. [1]H NMR of 1-Benzyl-6-bromo-1,4-dihydroquinoxaline-2,3-dione and 1-Benzyl-7-bromo -1,4-dihydroquinoxaline-2,3-dione (**4b**).

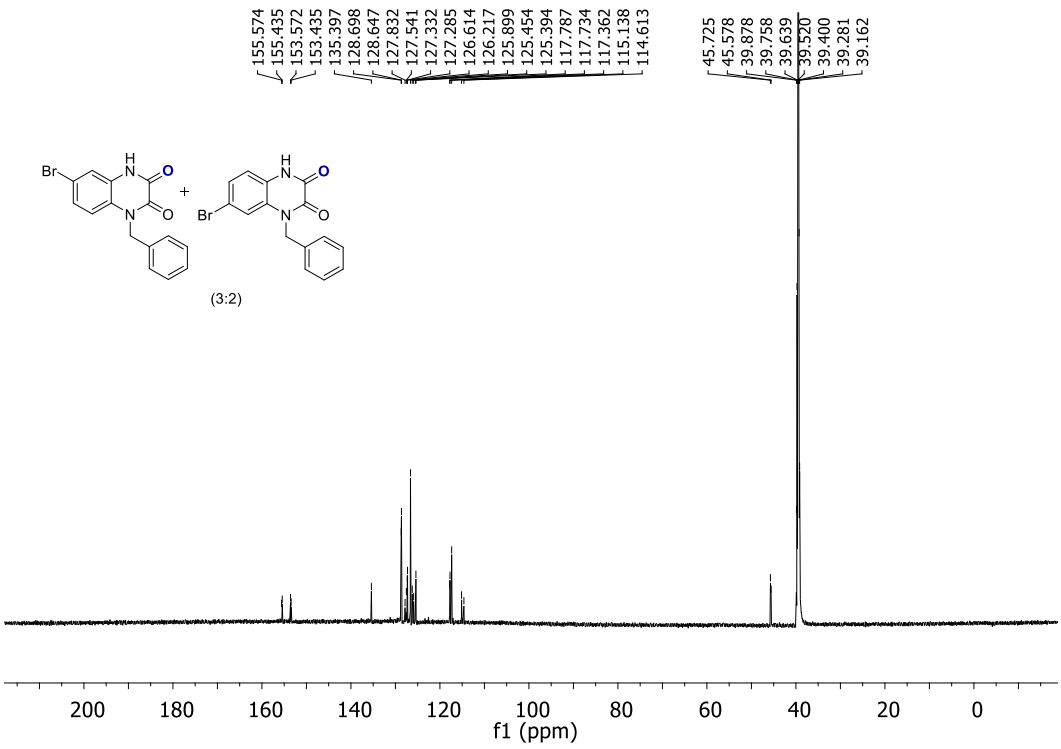

Figure 5.46. [13]C NMR of 1-Benzyl-6-bromo-1,4-dihydroquinoxaline-2,3-dione and 1-Benzyl-7-bromo -1,4-dihydroquinoxaline-2,3-dione (**4b**).

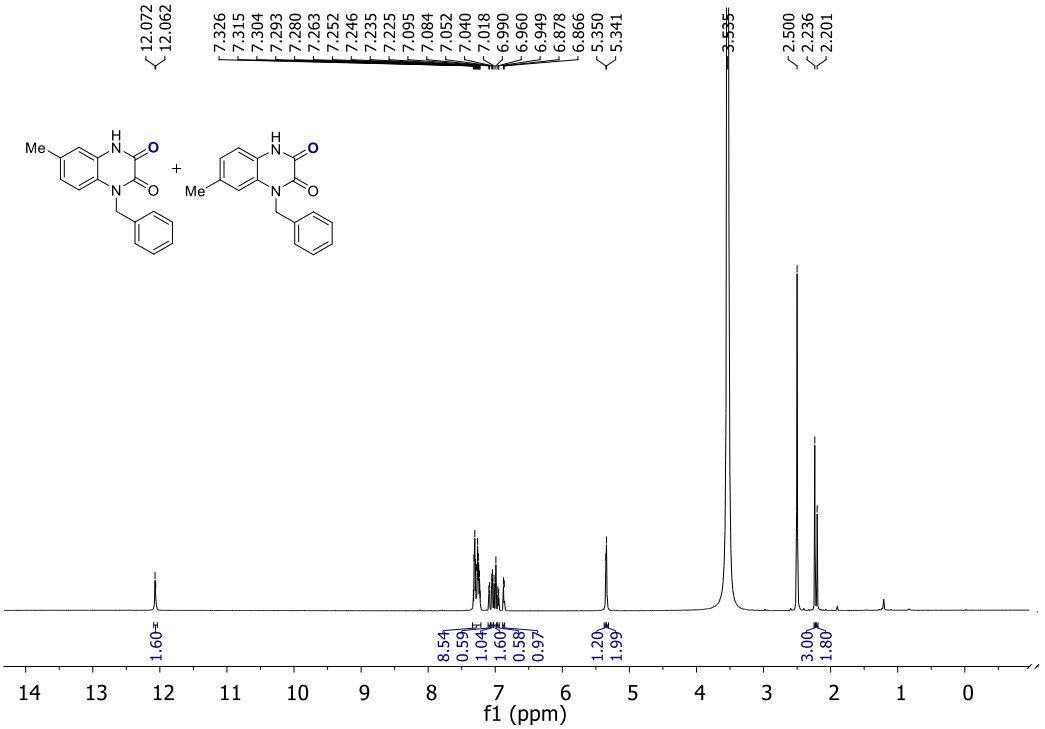

Figure 5.47. [1]H NMR of 1-Benzyl-6-methyl-1,4-dihydroquinoxaline-2,3-dione and 1-Benzyl-7-methyl -1,4-dihydroquinoxaline-2,3-dione (**4c**).

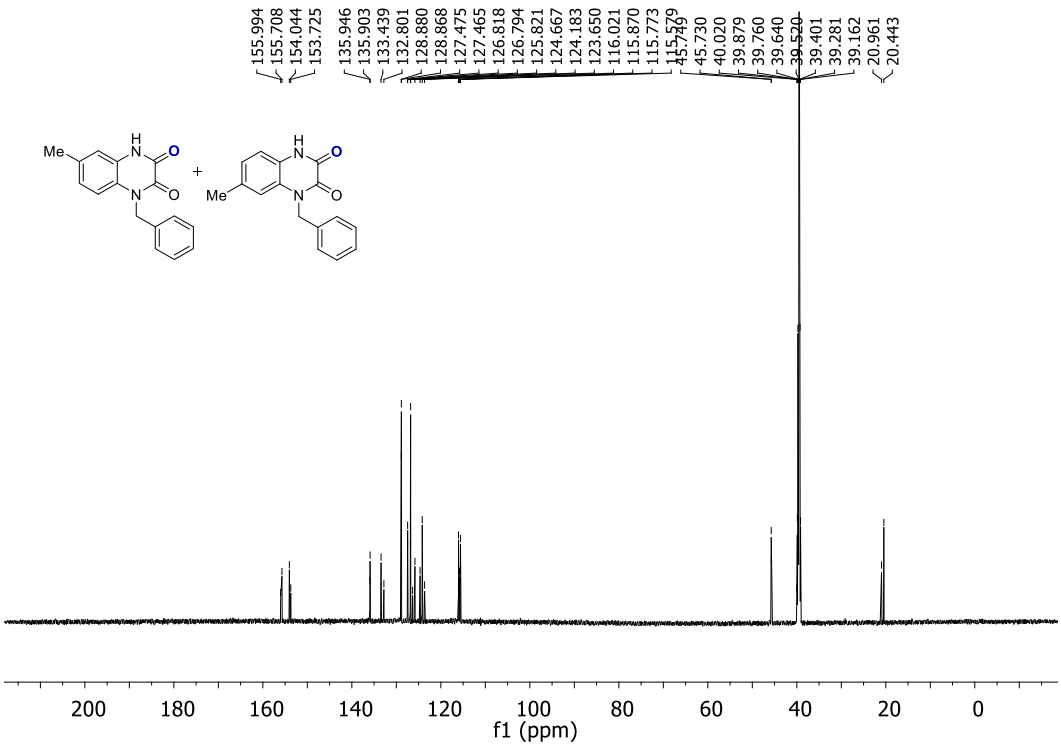

Figure 5.48. [13]C NMR of 1-Benzyl-6-methyl-1,4-dihydroquinoxaline-2,3-dione and 1-Benzyl-7-methyl -1,4-dihydroquinoxaline-2,3-dione (**4c**).

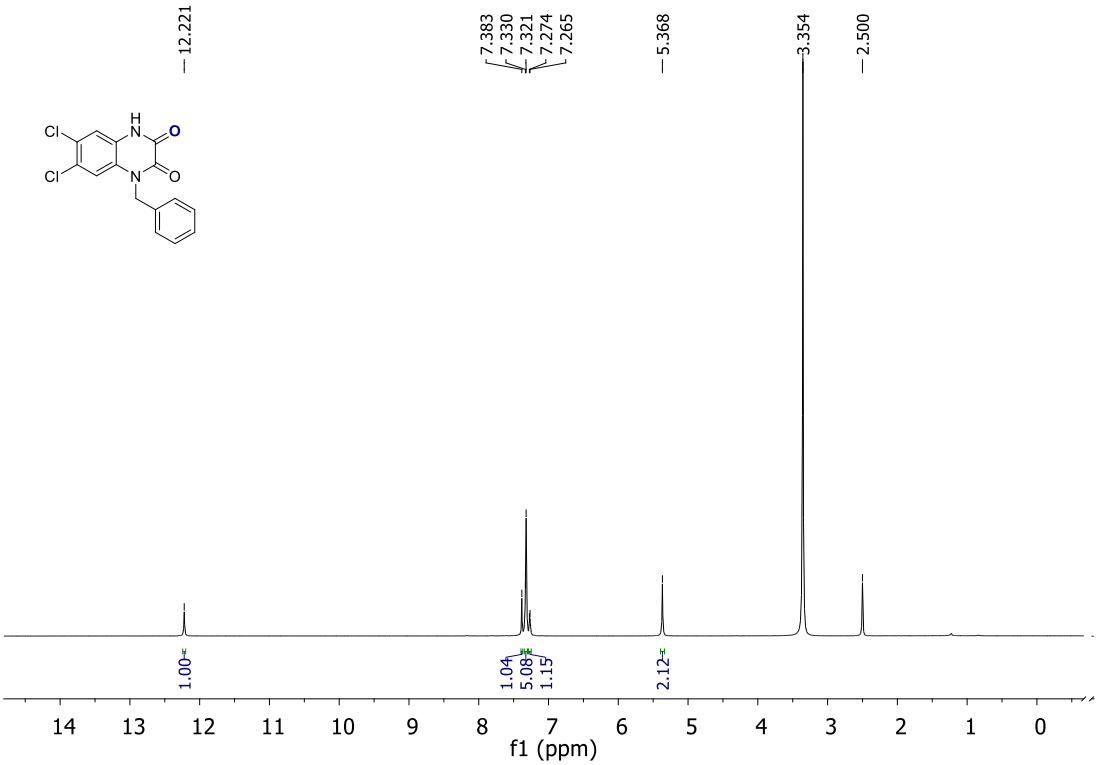

Figure 5.49. ^{1}H NMR of 1-Benzyl-6,7-dichloro-1,4-dihydroquinoxaline-2,3-dione (**4d**).

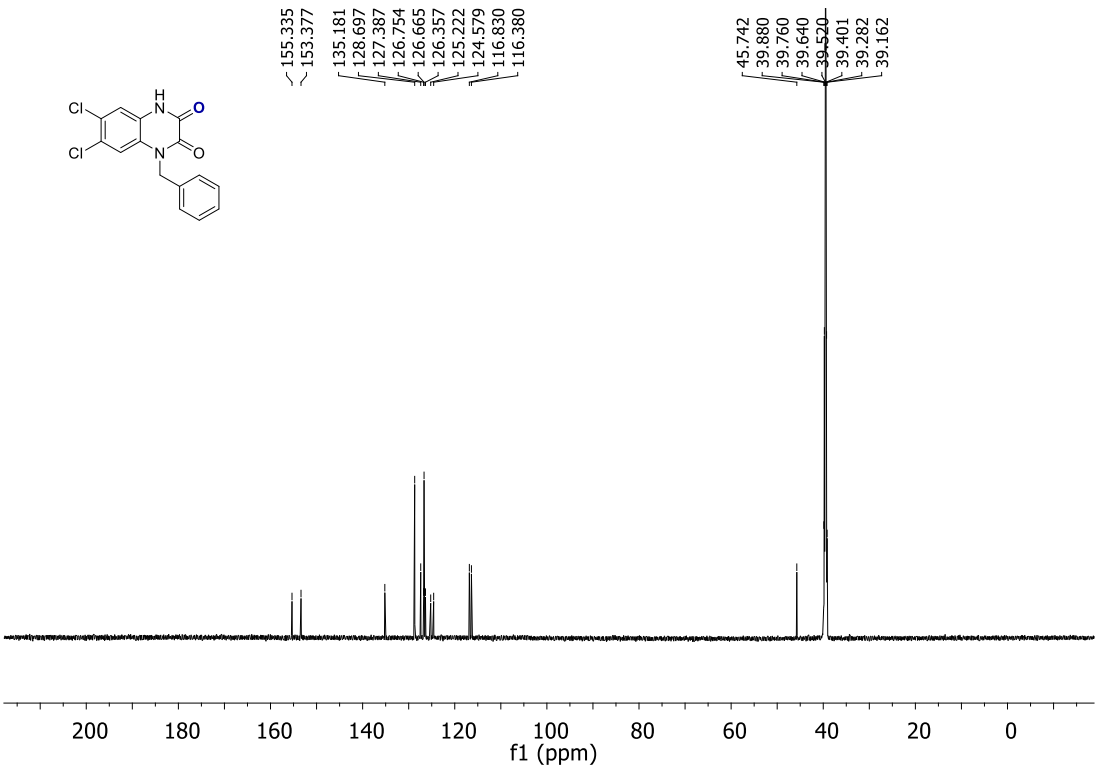

Figure 5.50. ^{13}C NMR of 1-Benzyl-6,7-dichloro-1,4-dihydroquinoxaline-2,3-dione (**4d**).

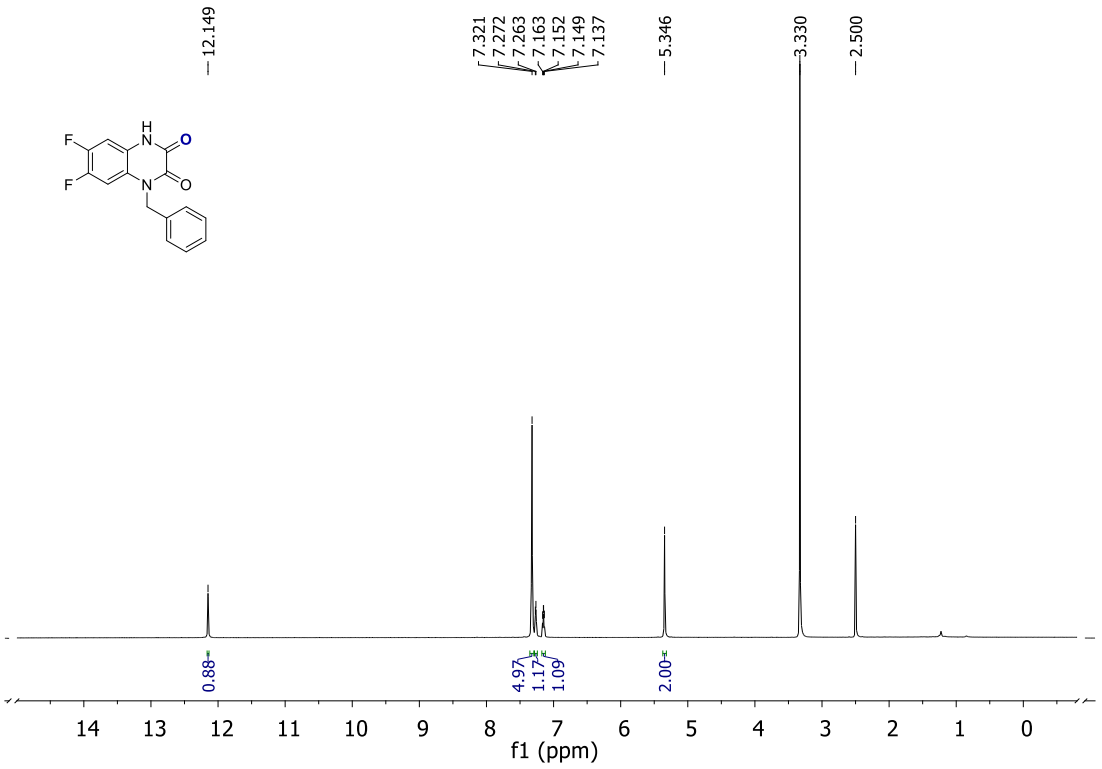

Figure 5.51. ^{1}H NMR of 1-Benzyl-6,7-difluoro-1,4-dihydroquinoxaline-2,3-dione (**4e**).

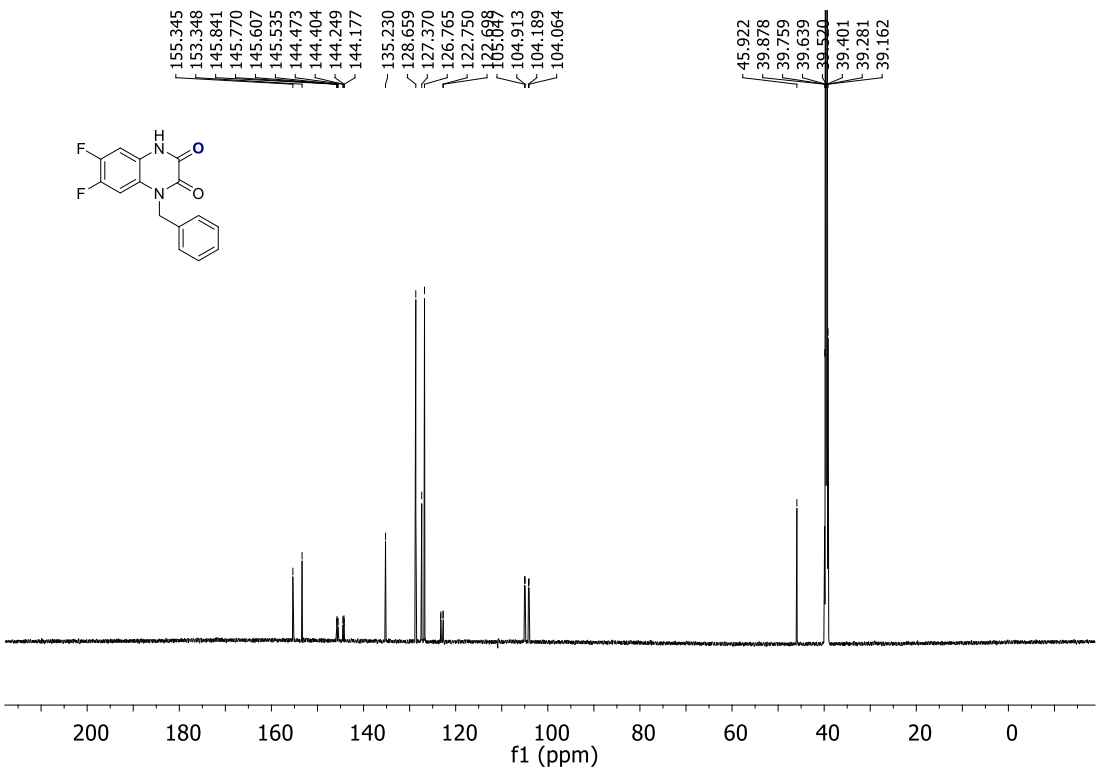

Figure 5.52. ^{13}C NMR of 1-Benzyl-6,7-difluoro-1,4-dihydroquinoxaline-2,3-dione (**4e**).

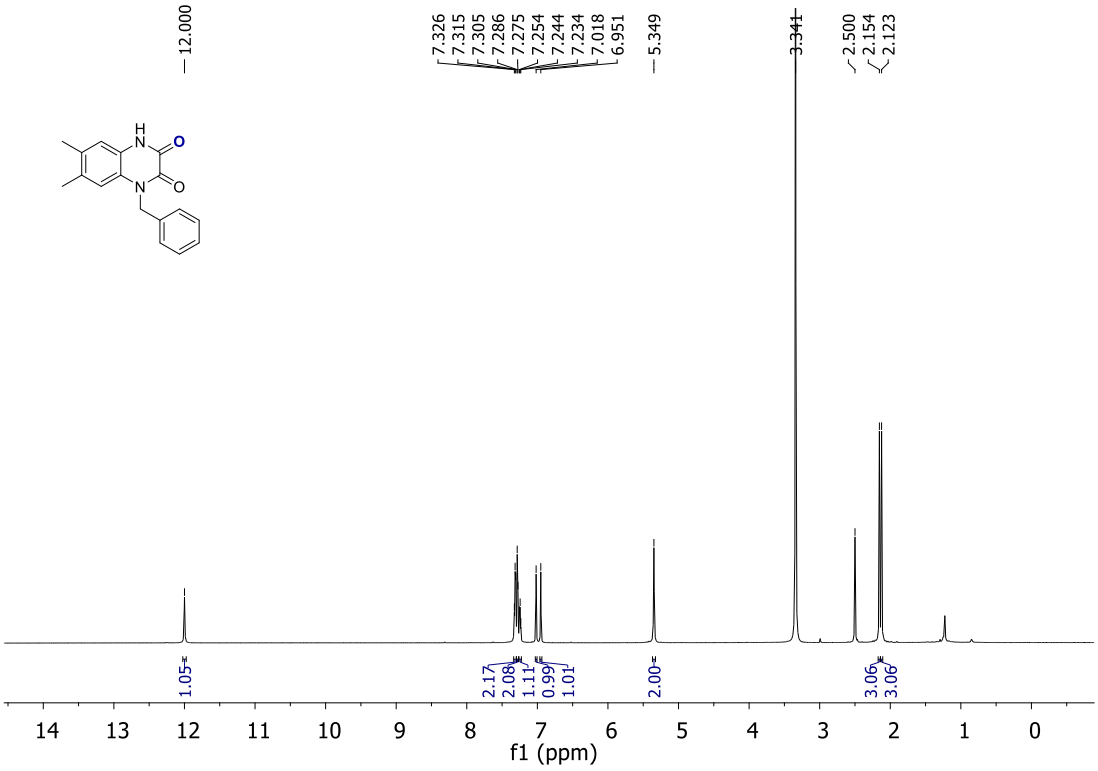

Figure 5.53. [1]H NMR of 1-Benzyl-6,7-dimethyl-1,4-dihydroquinoxaline-2,3-dione (**4f**).

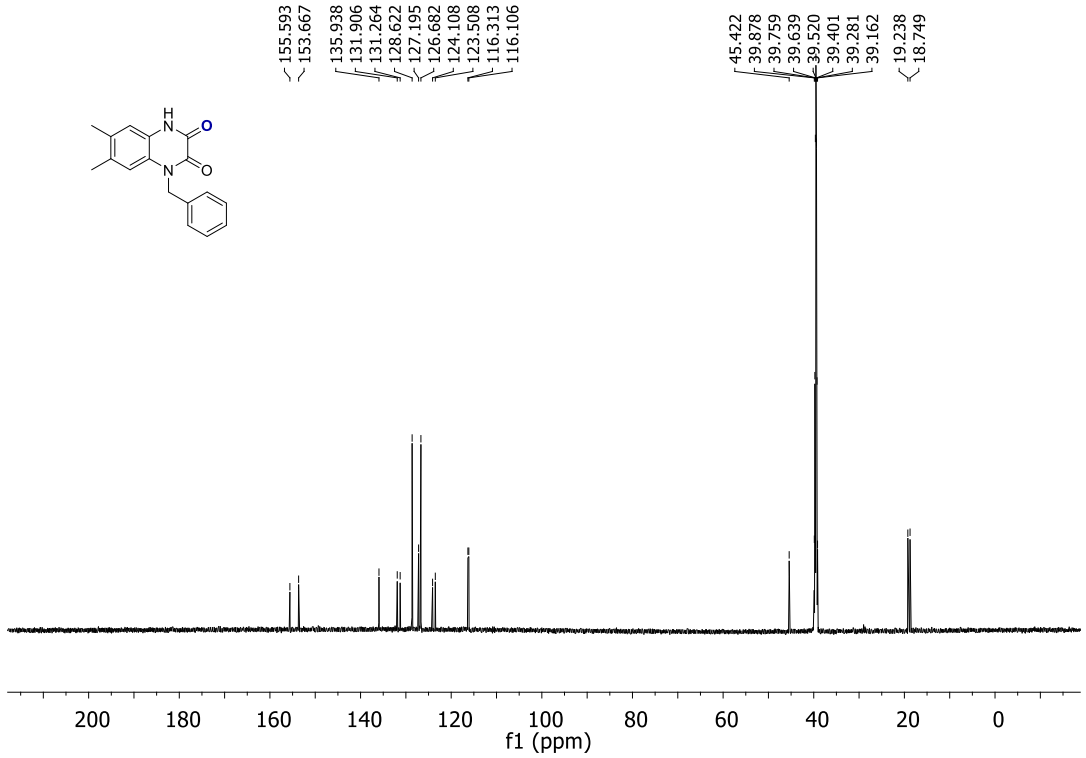

Figure 5.54. [13]C NMR of 1-Benzyl-6,7-dimethyl-1,4-dihydroquinoxaline-2,3-dione (**4f**).

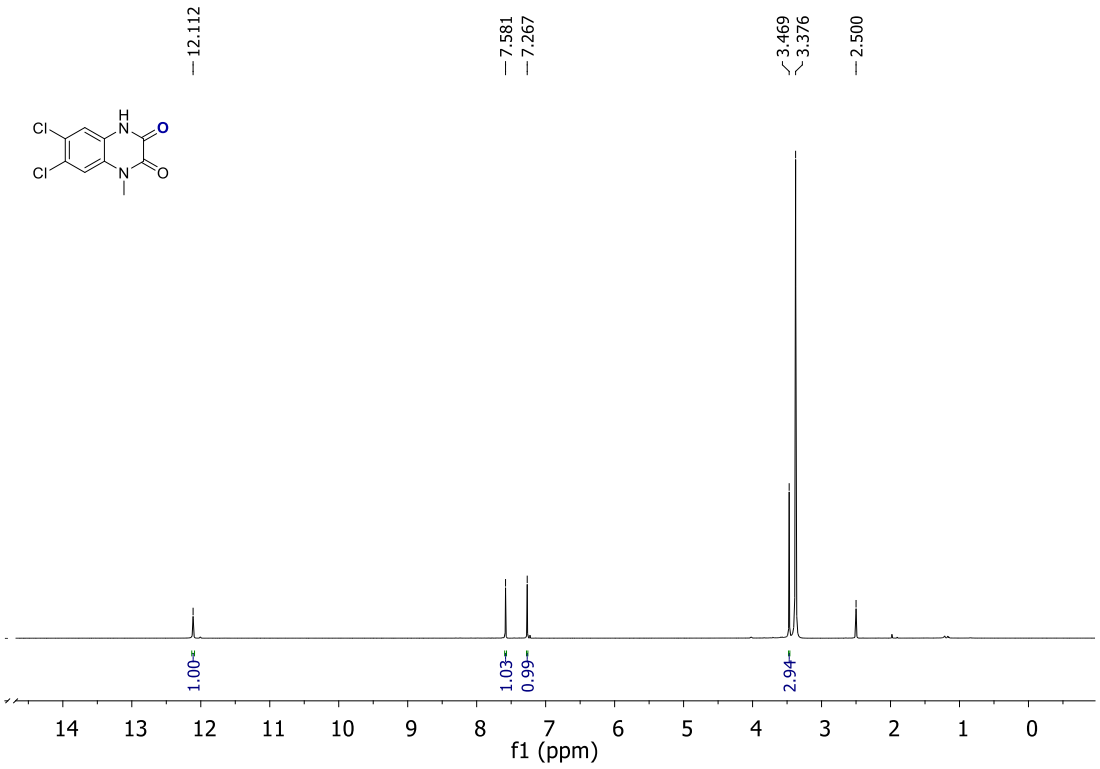

Figure 5.55. ^{1}H NMR of 6,7-dichloro-1-methyl-1,4-dihydroquinoxaline-2,3-dione (**4g**).

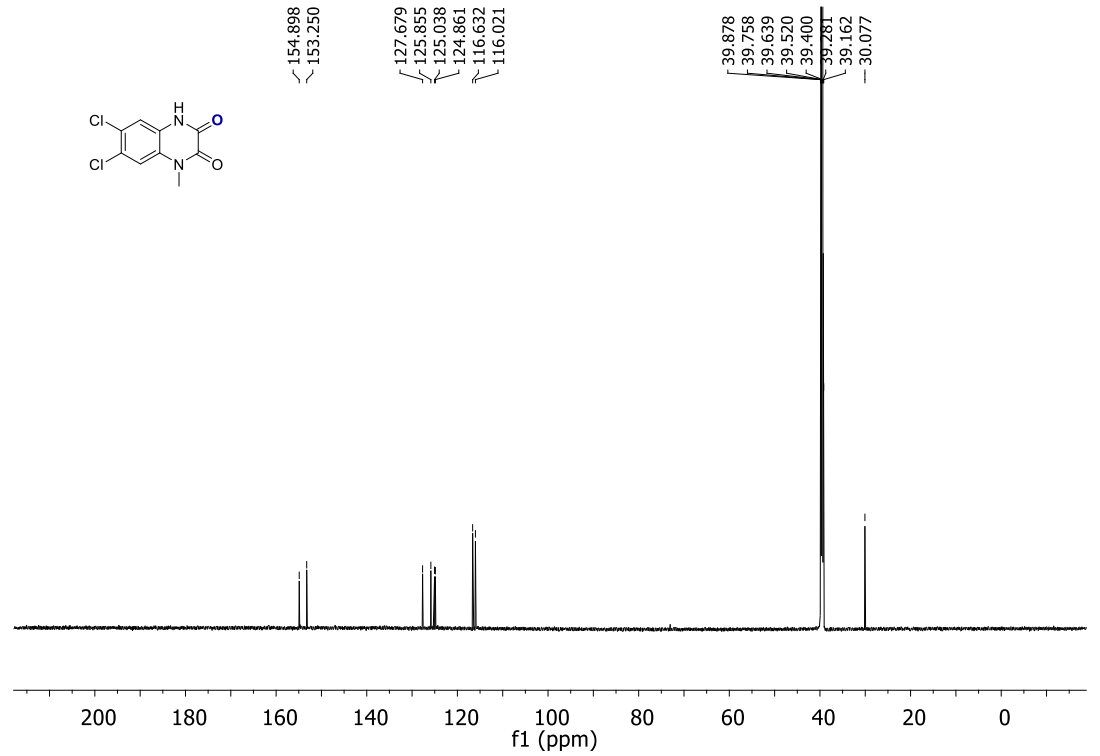

Figure 5.56. ^{13}C NMR of 6,7-dichloro-1-methyl-1,4-dihydroquinoxaline-2,3-dione (**4g**).

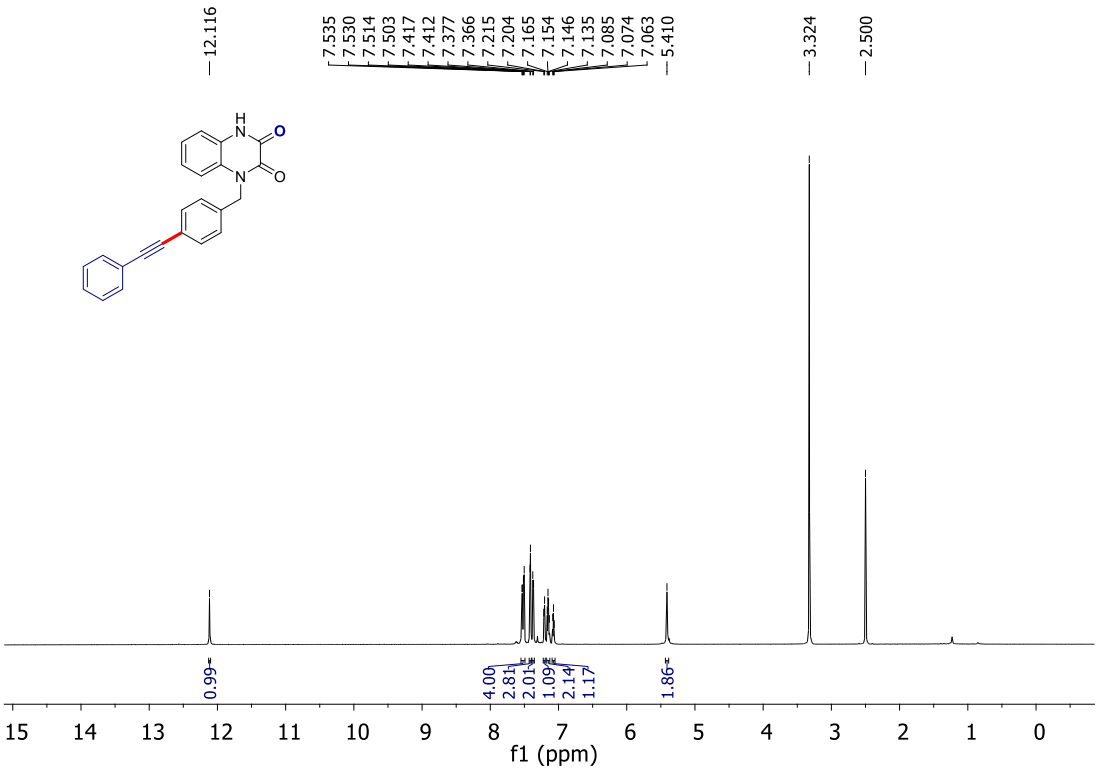

Figure 5.57. ^{1}H NMR of 1-(4-(phenylethynyl)benzyl)-1,4-dihydroquinoxaline-2,3-dione (**5**)

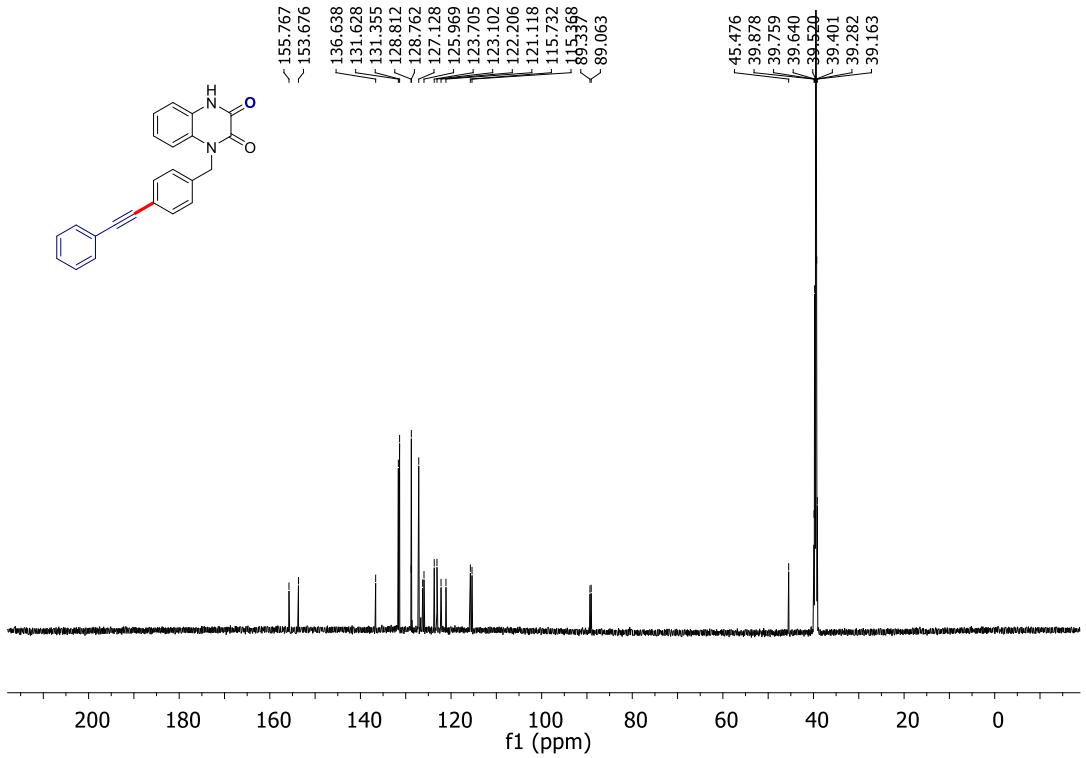

Figure 5.58. ^{13}C NMR of 1-(4-(phenylethynyl)benzyl)-1,4-dihydroquinoxaline-2,3-dione (**5**)

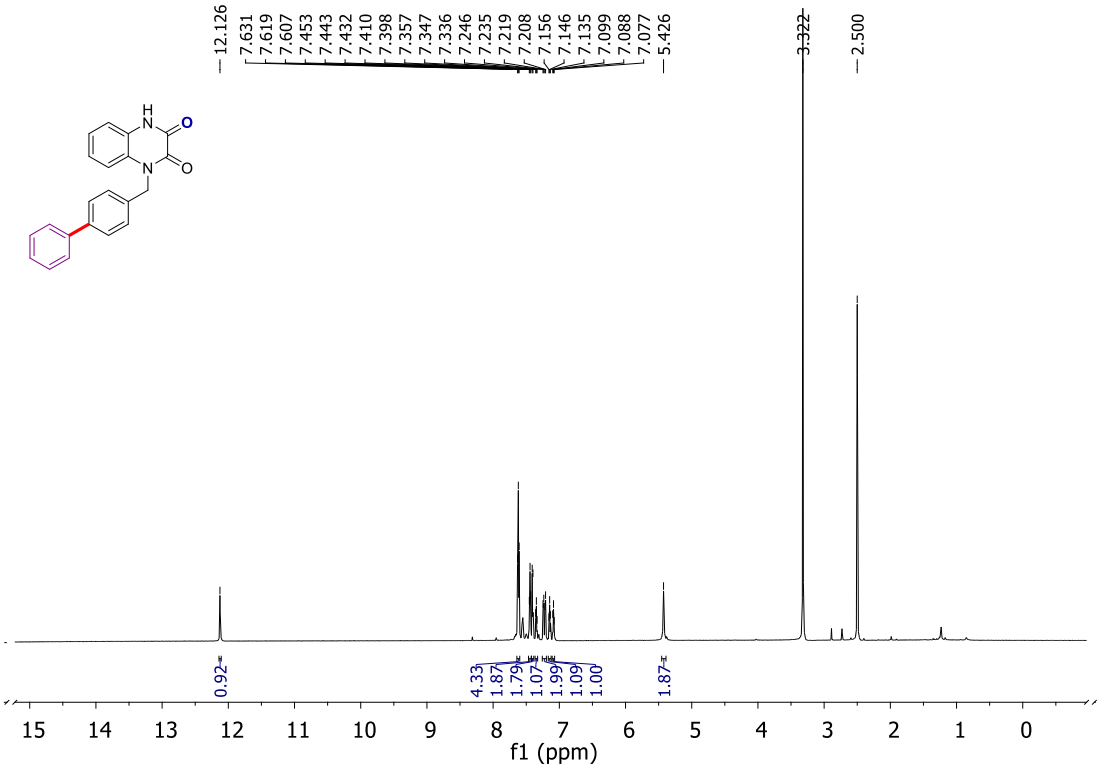

Figure 5.59. ^{1}H NMR of 1-([1,1'-biphenyl]-4-ylmethyl)-1,4-dihydroquinoxaline-2,3-dione (**6**)

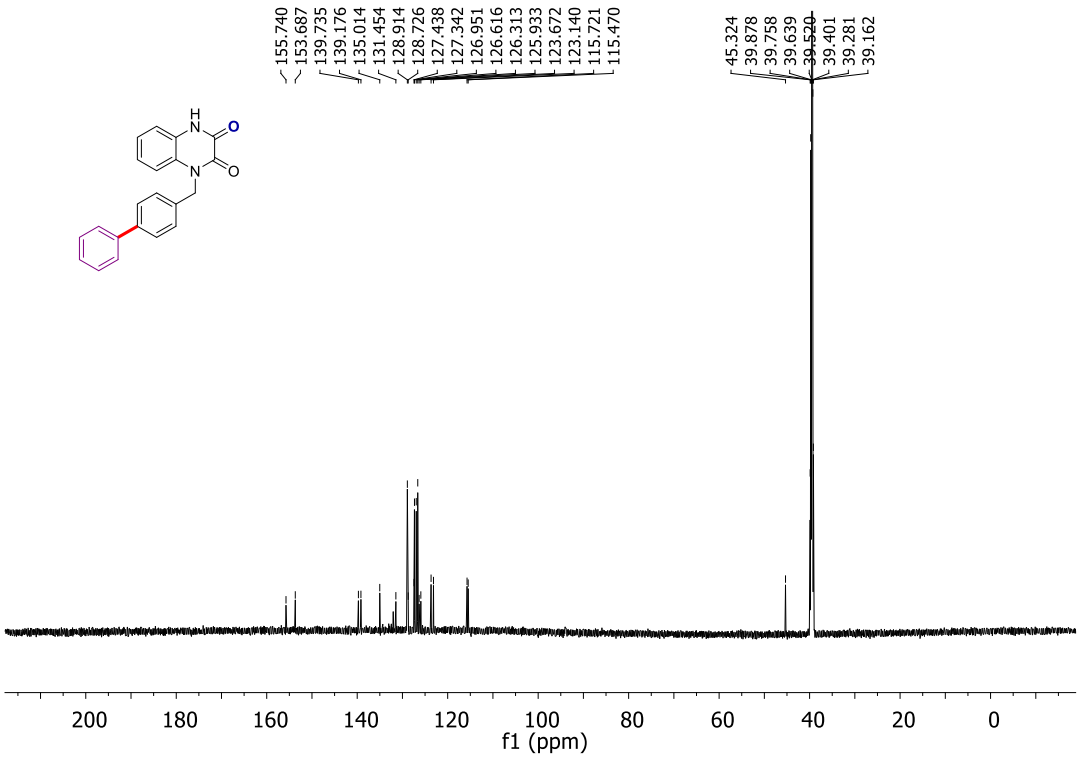

Figure 5.60. ^{13}C NMR of 1-([1,1'-biphenyl]-4-ylmethyl)-1,4-dihydroquinoxaline-2,3-dion (**6**)

Thesis at a Glance

Regioselective C_5 or C_7 nitration of indolines

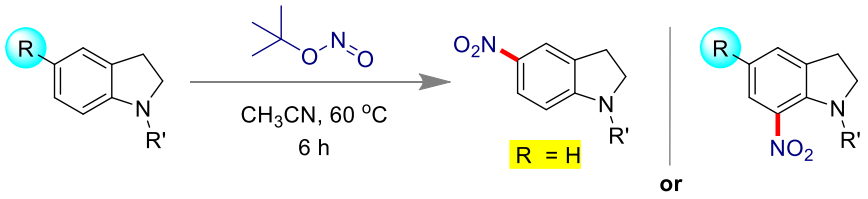

Asian J. Org. Chem., **2019**, *8,* 1854-1857.

Synthesis of 3-Nitro coumarins from Aryl alkynoates

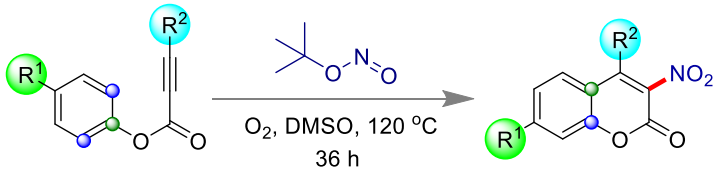

Chem. Commun., **2021**, *57*, 9228-9231.

Regioselective C-H Hydroxylation of Quinoxalin-2(1*H*)-ones

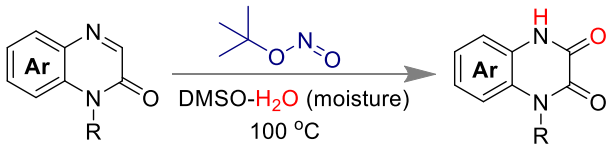

Eur. J. Org. Chem., **2022**, e202200425.

Photocatalytic Oxygenation of Quinoxalin-2(1*H*)-ones

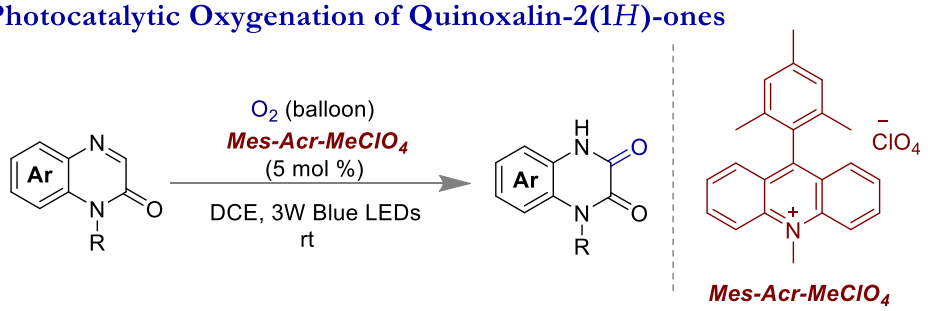

J. Org. Chem., **2022**, *87*, 14565-14579.

Conclusion and Future Prospect

Finding sustainable and step-economic strategies for the synthesis and functionalization of organic compounds is always an important topic of research in synthetic organic chemistry. This thesis is focused on designing and development of mild and sustainable protocols towards C-X (-N, -C, -O) bond formation reaction for the synthesis and functionalization of heterocycles using mild reaction conditions. In this regard, various strategies like utilization of the mild and metal-free reagent *tert*-Butyl Nitrite (TBN) and implementation of visible-light photocatalysis were adopted. Initially, regioselective C_5- or C_7- mono-nitration of indolines was achieved by implementing *tert*-Butyl Nitrite (TBN) as a sole nitrating agent. In continuation, we explored a mild and convenient approach toward nitrative cascade cyclization of aryl alkynoates using *tert*-Butyl Nitrite (TBN) as a sole reagent without using any additive or co-catalyst and a library of 3-nitro coumarins was devised. Next, we developed a protocol for C-H hydroxylation of quinoxalin-2(1*H*)-ones using *tert*-Butyl Nitrite (TBN) through ipso-substitution strategy. This protocol demonstrated a very mild and convenient strategy towards the synthesis of quinoxalin-2,3-diones from quinoxalin-2(1*H*)-ones. We also implemented visible-light photocatalysis in our research. Visible-light mediated approach for regioselective oxygenation of quinoxalin-2(1*H*)-one was achieved with the use of 5 mol % of Mes-Acr-MeClO_4 photocatalyst. O_2 served as the eco-friendly and green oxidant source for this conversion. Overall, we have synthesized important heterocyclic skeletons like 5-nitro indolines, 7-nitro indolines, 3-nitro coumarins, and quinoxalin-2,3-diones. The nitro-substituted organic compounds have widespread applications in industries like pesticides, pharmacology, polymers, agrochemical, and dyes. In addition, some derivatives of nitroindoles have shown anti-tuberculosis activity. The coumarin framework is one of the privileged structural scaffolds prevalent in bioactive molecules and natural products. Coumarin derivatives furnish a

wide array of pharmaceutical properties. For instance, warfarin and acenocoumarin are known to exhibit anticoagulant properties; calanolide A is a recognized anti-HIV agent and carbochromein is a potent vasodilator. Moreover, 3-nitro-coumarin scaffolds are well-known for their bio-antioxidant, and neurotropic properties and are used for the treatment of asthma and rhinitis. Parallelly, quinoxaline-2,3-dione and their derivatives also furnish a wide array of applications in material science and fields like bacteriocides and insecticides. Their applications in pharmaceutics are well documented such as 5-chloro-7-trifluoromethyl-1,4-dihydro-2,3-quinoxalinedione (ACEA-1011) is a potent ionotropic glutamate receptor antagonist. In summary, these simple, cost-effective, and sustainable protocols are anticipated to contribute significantly to the research areas like metal-free nitration of heterocycles, nitrative cyclization reactions, cascade cyclization reactions, metal-free hydroxylation of heterocycles, visible-light photocatalysis and oxygenation of heterocycles. Moreover, we have shown the gram-scale synthesis for each protocol, so the synthesis of these compounds can be scaled up at the industry level and our protocols might get commercial importance and have significant applications in medicinal chemistry, pharmaceutical industries and other fields.